Genetic and Molecular Technologies to Optimise Novel Vaccines for Hepatitis C Virus Infection

Leo Swadling

St. Catherine's College

MRC Industrial CASE studentship



This thesis is submitted for the degree of Doctor of Philosophy in Clinical Medicine, University of Oxford, Michaelmas 2015



Supervised by:

Professor. Eleanor Barnes
Nuffield Department of Clinical Medicine

Professor. Paul Klenerman
Nuffield Department of Clinical Medicine

Dr. Antonella Folgori
Okairos



Genetic and Molecular technologies to optimise novel vaccines for hepatitis C Virus infection

Leo Swadling, St Catherine's College
D.Phil in Clinical Medicine, Michaelmas Term 2015

Analysis of the immune response during spontaneous clearance and protection upon reinfection with hepatitis C (HCV) has highlighted the importance of T-cells in the control of HCV infection. An effective T-cell vaccine for HCV would have a significant effective on the global burden of disease associated with HCV. No clear immune correlates of protection exists for HCV and we lack immunological competent animal models in which to assess candidate HCV vaccines. I have performed in-depth characterisation of the T-cell response to candidate virally vectored HCV vaccines with regard to the T-cell parameters most likely to impact on their efficacy in a prophylactic and therapeutic setting.

I describe here a heterologous prime/boost vaccine regimen of a simian adenoviral vector (ChAd3), boosted with a modified vaccinia Ankara (MVA) encoding the non-structural (NS) proteins of HCV. This regimen elicits an unprecedented magnitude of HCV-specific CD8+ and CD4+ T-cells; which are broadly targeted, durable, and highly functional. ChAd3-NS/MVA-NS vaccination induces a population of persistent effector memory CD8+ T-cells (Tem) similar in phenotype to those induced by infection with CMV. I show that in these diverse settings the functional and phenotypic characteristics of the CD8+ T-cells are highly conserved and are controlled at the level of gene expression. Vaccination of HCV+ patients induced T-cell response that were significantly lower in magnitude, and viral sequencing at key epitopes demonstrates that the T-cells induced by vaccination show weak cross-recognition of the patients circulating virus.

While working with an industrial collaborator, I have developed our understanding of the mechanism of action of the enhancer element, MHC class II invariant chain. I show that tethering antigen to Ii within virally vectored vaccines targets it for rapid degradation by the proteasome, enhancing its presentation on MHC class I molecules and the concomitant CD8+ T-cell response to vaccination.

The work described here is relevant to T-cell vaccine development, in particular for Ad and MVA constructs, and to our understanding of antigen processing and heterogeneity within the CD8+ T-cell compartment.

Thesis contributions by others:

Experiments and analyses presented in this thesis that were performed by those other than myself are as follows:

Chapters 3-6

I performed approximately half of the blood processing, ELISpot assays, and set-up of tritiated thymidine proliferation assays and 3/4 of the ICS presented here, with the rest being performed by Tony Brown, Rachel Townsend and Ayako Kurioka. Development of thymidine proliferation assays was performed by Tony Brown.

Chapters 3

Richard Antrobus – clinical management of healthy volunteer. Safety data (figure 3-1).
Felicity Hartnell – clinical management of healthy volunteers.
Katrin Frohnmuller – Genotypic variance data Table 3-4.

Chapter 4

Evan Newell – reagents, protocols and PCA for CyTOF work.
Jo Fergusson – CyTOF: All experiments were performed in collaboration with Jo.
Microarray, GSEA and PCA in figures 4-12 and 4-13 were performed by Bea Bollinger, Stuart Sims, Emanuele (Manu) Marchi

Chapter 5

All animal handling was performed with the assistance of Morena D'Alise, Maria Luisa Esposito, and Mariarosaria Naddeo (Okairos, Italy).
Morena D'Alise – ELISpot data (figure 5-4)
All Ad constructs generated by Okairos or Peter Holst.
Peter Holst - Antigen presentation blocking experiments described in 5.5.4

Chapter 6 – Therapeutic vaccination

All sequencing data was generated by Christabel Kelly (Table 6-4) and Johnny Halliday (Table 6-6). Cross-reactive ELISpots (figure 6-8) and analysis of genotypic variation (figure 6-10) performed by Christabel Kelly.
Mariarosaria Naddeo – anti Ad-hexon nAb assay (figure 6-6).

Many thanks to the following for their scientific discussion: Evan Newell, Peter Holst, Mark Davis, Adrian Hill, Mariano Stornaiuolo, Nick Haining. D.phil transfer and confirmation assessors: John Frater, Chris Willberg, Antonio Reyes-Sandoval and Helen McShane.

None of this work would have been possible without the co-operation and good will of the volunteers and patients who participated in the clinical trials, and the brilliant nurses and doctors at the gastroenterology dept. JR hospital and CCVTM.

Funding

This D.Phil was funded through an MRC industrial CASE (Collaborative Awards in Science and Engineering) studentship, which provides students with experience of collaborative research with a non-academic partner. 8 months of this D.Phil was spent working at Okairos AG (now part of GSK), a small clinical-stage biopharmaceutical company in Naples, Italy. The work performed at Okairos, under the supervision of Antonella Folgori, Stefania Capone, and Morena D'Alise is described in **chapter 5**.

Clinical trials HCV001, HCV002, HCV003 are funded by the European Union (Framework VI:HEPACIVAC), MRC (UK) and the Oxford National institute for health and research Biomedical Research centre. This work was completed in collaboration with Okairos, Italy.

Acknowledgments

First of all I would like to thank my supervisors, Ellie and Paul, for taking the risk and giving me a job in Oxford in the first place. On a daily basis I was reminded what a great and unique opportunity it was. It is thanks to the calibre of the work your groups produce that I was able to collaborate with such great people at Okairos and at the universities in Stanford, Harvard, and Oxford. It is thanks to the quality of your characters that I have loved virtually every minute of my D.Phil. Every time I had doubts or problems a 5 minute conversation with you Ellie was all I needed to be positive and focused again.

I would also like to thank Antonella, Stefania, and Morena for the huge amount of time and effort they gave to my work at Okairos. I enjoyed our scientific discussions immensely and I continue to be impressed at how quickly you all can interpret and distil out the importance from new data.

I would like to thank the following people for many reasons, but above all for showing me how fantastic research is and for giving me an amazing 4 years:

To Jake for showing me how a PhD is done, and to my family for their support in everything. To Tony for looking after me when I knew nothing, for cleaning up the lab after me, and for playing a part in every experiment the vaccine team does. PMB core team (Alba, Ayako, Matt B, Jaqui, Jo, Ruth and Rachel) for everything! Julia for suffering through the eclipse with me. To the PMB tennis team (Gen, Morgane, Matt), and the rest of the PMB, especially those that come to PMB football!. Namely: Johnny, Christabel, Annette, Emma, Matt P, Flick, Ellen, Chris, Dan, Tianqi, Manu, Emily H and Emily A, Jodi, Tim, Prabh, Bonnie, Tamsin, Senthil, and Dave. To Evan Newell for all the help at Stanford. To Kathleen Yates for all the help at Harvard. To the Okairos Lab for showing me an amazing time in Napoli, especially Fede, Pietro, Angiolo, Ciro and Valentino for keeping me safe and to Morena, Rosie and Marilu for baby sitting me (and my mice) in the lab. And most of all to my personal physician, chauffeur, foreign language, snowboarding and life coach, Maddalena, for making the last year and a half the best yet.

A huge thank you to all who played a part in my doctoral training.

Abbreviations:

aa – amino acids
Ab - antibody
Ad – adenovirus
AE – adverse event
ALT – alanine aminotransferase
APC – antigen presenting cell
APC when used within methods sections - allophycocyanin
BMDC – bone marrow derived DCs
CBF – Oxford universities clinical Biomanufacturing facility
CCVTM – clinical vaccinology and tropical medicine department
CD – cluster of differentiation
ChAd – a chimpanzee-derived adenovirus
conA – concavalin A
COP – correlate of protection
CMV - cytomegalovirus
CLIP - class II-associated invariant chain peptide
CRT - calreticulin
CXN - calnexin
CyTOF – cytometry by time-of-flight
DAA – directly-acting antivirals
DC – dendritic cell
ddH20 – distilled water
DEG – differentially expressed gene
DMSO – dimethyl sulfoxide
DNA – deoxyribonucleic acid
DRiPs – defective ribosomal products
EDTA – ethyl diamine tetra acetic acid
eGFP – enhanced green fluorescent protein
ELISA – enzyme-linked immunoassay
ELISpot – enzyme-linked immunoSpot assay
Eomes - eomesodermin
EOS – end of study
ER – endoplasmic reticulum
ERp57 – endoplasmic reticulum protein 57
ERAP - endoplasmic reticulum aminopeptidase
ESS – endolysosomal sorting sequence
FACS – fluorescence activated cell sorting
FCS – fetal calf serum
FITC - Fluorescein isothiocyanate
Flu - influenza
FMO – fluorescence minus one
FoxP3 – forkheap box P3 protein
GCP – good clinical practice
geoMFI – geometric mean of fluorescence intensity
GFP – green fluorescent protein
GM-CSF - granulocyte macrophage colony-stimulating factor

GMP – good manufacturing practice
GP - glycoprotein
GSEA – gene set enrichment analysis
GWAS – genome wide association studies
GzA –granzyme A
GzB – granzyme B
HAART – highly active antiretroviral therapy
HBV – hepatitis B virus
HCV – hepatitis C virus
HCVcc – cell culture-derived hepatitis C virus
HCVpp – hepatitis C pseudo-particles
HEV – hepatitis E virus
hIi – human major histocompatibility class II invariant chain
HIV – human immunodeficiency virus
HLA – human leukocyte antigen
HPV – human papillomavirus
ICP-TOF-MS – inductively coupled plasma by time-of-flight mass spectrometer
ICS – Intracellular cytokine staining
IFN – interferon
Ii – major histocompatibility class II invariant chain (CD74)
i.m. - intramuscular
IVDU – intravenous drug users
KEY -
KIR – killer-cell immunoglobin like receptors
LCMV - lymphocytic choriomeningitis virus
L/D – live dead
LILR – leukocyte immunoglobin like receptor
l.monocytogenes = *Listeria monocytogenes*
LTNP – long-term non-progressor
MFI – mean fluorescence intensity
MHC – major histocompatibility complex
MHC-1 – major histocompatibility complex class I molecule
MHC-II - major histocompatibility complex class II molecule
MIF – macrophage migration inhibitory factor
MIIC – major histocompatibility complex class II compartment
mIi – murine major histocompatibility class II invariant chain
MOI – multiplicity of infection
MVA – modified vaccinia Ankara
nAb – neutralising antibodies
NFAT – nuclear factor of activated T-cells
NHP – non-human primates
NIR – near-infrared
NK – natural killer Cells
NKT – natural killer T cell
NS – non-structural region of HCV (in this thesis it refers to NS3-5B from BK HCV strain)
NP - nucleoprotein
OVA – ovalbumin
PB – pacific blue

PBMC – peripheral blood mononuclear cells
PCA – principal component analysis
PCR – real time polymerase chain reaction
PE - phycoerythrin
PEG – polyethylene glycol
pfu – plaque forming units
PLC – protein loading complex
PMA – phorbol 12-myristate 12-acetate
PMT – photomultiplier tube
PO – pacific orange
Rib - ribavirin
RLU – relative light units
RNA - ribonucleic acid
rpm – revolution per minute
RSV – respiratory syncytial virus
RT – room temperature
RT-PCR – real time polymerase chain reaction
SEAP – secreted alkaline phosphatase
SFC – spot forming cells (IFNγ producing cells in ELISpot assay)
SIV – simian immunodeficiency virus
SNPs – single nucleotide polymorphisms
SVR – sustained virological response (HCV undetectable [<15 IU/mL HCV RNA] 6 months after completing therapy)
TAP – transporter associated with antigen processing
Tbet - T-box transcription factor TBX21
Tcm – central memory T-cells
TCR – T-cell receptor
Teff – effector T-cells
Tem – effector memory T-cells
Temra – terminal effector memory T-cells
TM - transmembrane
TNFα – tumour necrosis factor alpha
Treg – regulatory T-cell
Tscm – stem cell like memory T-cells
TW – trial week
VLP – virus-like particles
vp – viral particles

First Author publications

Kelly, Swadling *et al*. Chronic HCV infection subverts vaccine induced T cell immunity in humans. **Hepatology. 2015 Oct 16.**

Swadling *et al*. A human vaccine strategy based on chimpanzee adenoviral and MVA vectors that primes, boosts, and sustains functional HCV-specific T cell memory. **Science Translational Medicine. 2014 Nov 5;6(261):261ra153.**

Swadling *et al*. Ever closer to a prophylactic vaccine for HCV. **Expert Opinions on Biological Therapy 2013 Aug;13(8):1109-24.**

Contributing Author publications

Bolinger, Sims, Swadling *et al*. Adenoviral Vector Vaccination Induces a Conserved Program of CD8+ T Cell Memory Differentiation in Mouse and Man. **Cell Reports. 2015 Nov 11. pii: S2211-1247(15)01204-8**

Fergusson *et al*. CD161int CD8+ T cells: a novel population of highly functional, memory CD8+ T cells enriched within the gut. **Mucosal Immunology. 2015 Jul 29.**

Kelly, Swadling *et al*. Cross-reactivity of hepatitis C virus specific vaccine-induced T cells at immunodominant epitopes: Clinical immunology. **European Journal of Immunology. 2015 Jan;45(1):309-16.**

Fergusson *et al*. CD161 Defines a Transcriptional and Functional Phenotype across Distinct Human T Cell Lineages. **Cell Reports. 2014 Nov 6;9(3):1075-88.**

Barnes, Folgori, Capone, Swadling. *et al*. Novel adenovirus-based vaccines induce broad and sustained T cell responses to HCV in man. **Science Translational Medicine. 2012 Jan 4;4(115):115ra1.**

Table of Content

1 INTRODUCTION 20

1.1 HEPATITIS C VIRAL INFECTION 20
1.1.1 A GLOBAL HEALTH PROBLEM 20
1.1.2 THE CLINICAL COURSE OF HCV INFECTION 21
1.1.3 THE VIRUS 23

1.2 TREATMENT OPTIONS FOR HCV AND REINFECTION 26
1.3 THE IMMUNE RESPONSE TO HCV 29
1.3.1 INNATE IMMUNITY 30
1.3.2 HUMORAL IMMUNITY 31
1.3.3 CELLULAR IMMUNITY 34

1.4 WHICH T-CELLS WILL PROTECT AGAINST PERSISTENT HCV INFECTION? 38
1.4.1 MAGNITUDE 39
1.4.2 BREADTH 40
1.4.3 PROLIFERATION AND CYTOKINE PRODUCTION 42
1.4.4 CYTOTOXICITY 44
1.4.5 T-CELL PHENOTYPE 46

1.5 NOVEL TECHNOLOGIES FOR ASSESSING T-CELL QUALITY 48
1.6 CURRENT VACCINE APPROACHES 50
1.6.1 RECOMBINANT PROTEIN VACCINES 50
1.6.2 PEPTIDE VACCINES 54
1.6.3 DNA VACCINES 56
1.6.4 VIRAL VECTORS 56
1.6.5 OXFORD'S HCV VACCINE PROGRAMME - SELECTION OF VECTORS 60

1.7 VACCINE DEVELOPMENT PIPELINE 62
1.7.1 CHALLENGES 63

1.8 A THERAPEUTIC VACCINE 66
1.8.1 ESCAPE 66
1.8.2 REGULATORY T-CELLS 68
1.8.3 T-CELL EXHAUSTION 68
1.8.4 THERAPEUTIC VACCINE TRIALS 72
1.8.5 UTILITY OF A THERAPEUTIC VACCINE 72

1.9 OPTIMISING VIRALLY VECTORED VACCINES 73
1.9.1 IMMUNOGEN 73

1.10 MHC CLASS II INVARIANT CHAIN AS AN ENHANCER OF VACCINE-INDUCED 74
1.11 BACKGROUND OBSERVATIONS 75
1.12 KEY HYPOTHESIS TESTED IN THIS THESIS 76

2 MATERIAL AND METHODS 78

2.1 VACCINE VIRAL CONSTRUCTS & IMMUNOGEN 78
2.1.1 ADENOVIRAL CONSTRUCTS (AD6-NS AND CHAD3-NS) 78
2.1.2 MODIFIED VACCINIA ANKARA CONSTRUCT (MVA-NS) 78
2.1.3 IMMUNOGEN 79

2.2 VACCINE STUDY DESIGNS AND MONITORING 79
2.2.1 CLINICAL TRIALS 79
2.2.2 VACCINATION ROUTE 82
2.2.3 DOSE ESCALATION 82
2.2.4 SAFETY 83
2.2.5 VIRAL LOAD AND FULL BLOOD COUNT (HCV002 AND HCV003 ARM B) 83

2.3 BLOOD PROCESSING 83
2.3.1 PLASMA COLLECTION 83
2.3.2 PERIPHERAL BLOOD MONONUCLEAR CELL ISOLATION, FREEZING, THAWING 83

2.4 PEPTIDES AND ANTIGENS 84
2.5 ENZYME-LINKED IMMUNOSPOT ASSAY 86
2.5.1 ELISPOT ASSAY 86
2.5.2 DEFINING THE POSITIVE CUT-OFF FOR THE ELISPOT ASSAY 87

2.6 FLUORESCENCE ACTIVATED CELL SORTING (FACS) 88
2.6.1 MHC CLASS I PENTAMER STAINING 88
2.6.2 FACS ANTIBODY TITRATION 90
2.6.3 FLUORESCENCE MINUS ONE (FMO) AND ISOTYPE CONTROLS 90
2.6.4 INTRACELLULAR CYTOKINE STAINING (ICS) 92
2.6.5 FACS ANALYSIS 92

2.7 *IN VITRO* T-CELL LINES 95
2.8 THYMIDINE INCORPORATION ASSAY 95
2.9 VIRAL SEQUENCE 95
2.9.1 HCV VIRAL SEQUENCING 95
2.9.2 SEQUENCE VARIABILITY AT T-CELL EPITOPES AT A POPULATION LEVEL 96
2.9.3 IL28B GENOTYPING 97

2.10 REAGENTS 97
2.11 ADENOVIRAL HEXON NEUTRALISING ANTIBODY TITERS 97
2.12 STATISTICAL ANALYSIS 98

3 HETEROLOGOUS PRIME/BOOST VACCINATION STRATEGIES CHAD3-NS/MVA-NS VS. CHAD3-NS/AD6-NS 99

3.1 PRIMARY HYPOTHESIS 99
3.2 INTRODUCTION 99
3.3 KEY QUESTIONS 101
3.4 CHAPTER SPECIFIC MATERIAL & METHODS 102
3.4.1 CLINICAL TRIALS 102
3.4.2 IMMUNOASSAYS 103

3.5 RESULTS 104

3.5.1 VACCINATION WITH CHAD3-NS AND MVA-NS IS SAFE AND WELL TOLERATED 104
3.5.2 MVA-NS OPTIMALLY BOOST HCV-SPECIFIC T-CELL RESPONSES PRIMED BY CHAD3-NS AND INDUCES A HIGHER MAGNITUDE MEMORY T-CELL RESPONSE 105
3.5.3 REGULATORY T-CELLS ARE NOT EXPANDED AFTER CHAD3-NS/MVA-NS VACCINATION 109
3.5.4 MVA-NS BOOSTS A BROADER HCV-SPECIFIC T-CELL RESPONSE 112
3.5.5 VACCINE-INDUCED T-CELLS CROSS-RECOGNISE MULTIPLE HCV GENOTYPES 117
3.5.6 T-CELLS TARGETING 'PROTECTIVE EPITOPES' ARE INDUCED BY VACCINATION 119
3.5.7 T-CELL PROLIFERATIVE CAPACITY IS OPTIMAL LONG-TERM AFTER MVA-NA BOOST 128
3.5.8 MVA-NS BOOST VACCINATION ENHANCES T-CELL POLYFUNCTIONALITY 132
3.5.9 THE CYTOLYTIC POTENTIAL OF MVA-NS INDUCED HCV-SPECIFIC T-CELLS 137
3.5.10 VIRAL VECTOR COMBINATION HAS A PROFOUND EFFECT ON THE T-CELL MEMORY SUBSETS INDUCED BY VACCINATION 141
3.5.11 OPTIMISING REGIMENS – RE-BOOSTING STRATEGIES AND MVA DOSE DE-ESCALATION 143
3.6 DISCUSSION 148
3.7 CONCLUSION 156
3.8 SUMMARY OF RESULTS 158

4 MASS CYTOMETRY – SINGLE CELL ANALYSIS OF THE CD8+ VACCINE-INDUCED T-CELL RESPONSE 160

4.1 PRIMARY HYPOTHESIS 160
4.2 INTRODUCTION 160
4.3 KEY QUESTIONS 164
4.4 CHAPTER SPECIFIC MATERIAL & METHODS 165
4.4.1 HEAVY METAL LABELLING OF ANTIBODIES 165
4.4.2 TETRAMER LOADING AND MULTIPLEXING 166
4.4.3 CYTOF SAMPLE PREPARATION 167
4.4.4 CYTOF ANALYSIS 169
4.5 RESULTS 171
4.5.1 MASS CYTOMETRY: INTRODUCING THE TECHNOLOGY 171
4.5.2 VALIDATION OF CYTOF DATA WITH FACS 172
4.5.3 POLYFUNCTIONALITY OF VACCINE-INDUCED HCV-SPECIFIC T-CELLS 175
4.5.4 A PICTURE OF T-CELL COMPLEXITY – 3D-PCA 178
4.5.5 VACCINE-INDUCED T-CELLS ON THE CONTINUUM 185
4.5.6 A SHARED T-CELL PHENOTYPE BETWEEN CHAD/MVA AND CMV INDUCED T-CELLS. 188
4.5.7 A CONSERVED TRANSCRIPTIONAL PROGRAMME OF PERSISTENT TEM IN MICE AND MAN IS CONTROLLED BY A SUBSET OF KEY TRANSCRIPTION FACTORS 190
4.5.8 T-BOX TRANSCRIPTION FACTOR EXPRESSION IN VACCINE AND CMV-INDUCED CD8+ T-CELLS IN MAN 196
4.6 DISCUSSION 200
4.7 CONCLUSION 206
4.8 SUMMARY OF FINDINGS 209

5 THE MHC CLASS II INVARIANT CHAIN AS A GENETIC ENHANCER OF CD8+ T-CELL RESPONSES 210

5.1 PRIMARY HYPOTHESIS 210
5.2 INTRODUCTION 210
5.3 KEY QUESTIONS 219
5.4 CHAPTER SPECIFIC MATERIAL & METHODS 220
5.4.1 REAGENTS AND CONSUMABLES 220
5.4.2 INVARIANT CHAIN CONTAINING ADENOVIRAL CONSTRUCTS 220
5.4.3 ANIMALS AND *IN VIVO* VACCINATIONS 221
5.4.4 ISOLATION OF MOUSE SPLENOCYTES 222
5.4.5 *EX VIVO* MURINE IFNΓ ELISPOT 222
5.4.6 *EX VIVO* CD74 EXPRESSION ON LEUKOCYTE SUBSETS 223
5.4.7 MHC CLASS I PENTAMER STAINING 225
5.4.8 CELL COUNT AND VIABILITY 227
5.4.9 BONE MARROW DERIVED DENDRITIC CELL (BMDC) CULTURE 227
5.4.10 BMDC – TRANSDUCTION & CD74 SURFACE EXPRESSION 228
5.4.11 BMDC – ANTIGEN PRESENTATION ASSAY 229
5.4.12 JAWSII – CULTURE AND ANTIGEN PRESENTATION 230
5.4.13 THP-1 - CULTURE, MATURATION, AND TRANSDUCTION 231
5.4.14 HELA - CULTURE, MATURATION, AND TRANSDUCTION 232
5.4.15 B3Z T-CELL ACTIVATION ASSAY 232
5.5 RESULTS 233
5.5.1 THE SHORTENED CONSTRUCTS – NARROWING DOWN TO KEY DOMAINS 233
5.5.2 THE MECHANISM – IMPROVED AG PRESENTATION 241
5.5.3 CORRELATING IMPROVED PRESENTATION WITH T-CELL ACTIVATION AND PROLIFERATION 247
5.5.4 HOLST *ET AL* – BLOCKING THE CLASS I AND CLASS II PRESENTATION PATHWAYS 249
5.5.5 TETHERING ANTIGEN TO II LEADS TO RAPID DEGRADATION BY THE PROTEASOME 251
5.5.6 LINKAGE OF ANTIGEN TO II WITHIN AD VECTORS DOES NOT CHANGE THE PHENOTYPE OF ANTIGEN-SPECIFIC T-CELLS INDUCED 254
5.5.7 SURFACE EXPRESSION OF CD74 ON APCS 257
5.5.8 ASSESSING CD74 SURFACE EXPRESSION AFTER TRANSDUCTION: HUMAN MODEL – THP-1 261
5.5.9 ASSESSING CD74 SURFACE EXPRESSION AFTER TRANSDUCTION: MURINE MODEL – BMDC 263
5.6 DISCUSSION 268
5.7 CONCLUSION 278
5.8 SUMMARY OF FINDINGS 280

6 A THERAPEUTIC T-CELL VACCINE FOR HCV 281

6.1 PRIMARY HYPOTHESIS 281
6.2 INTRODUCTION 281
6.3 KEY QUESTIONS 283
6.4 CHAPTER SPECIFIC MATERIAL & METHODS 284
6.4.1 CLINICAL TRIAL PATIENT ENROLMENT 284
6.4.2 HCV002 STUDY DESIGN 284
6.4.3 HCV003 ARMS B AND C STUDY DESIGN 286
6.4.4 IMMUNOASSAYS 287
6.4.5 CD8+ T-CELL DEPLETION ELISPOTS 287
6.5 RESULTS 288
6.5.1 HCV002 TRIAL (CHAD3-NS/AD6-NS) PATIENT CHARACTERISTICS AND OUTCOME 288
6.5.2 VACCINATION WITH AD6-NS AND CHAD3-NS IS WELL TOLERATED 288
6.5.3 HETEROLOGOUS CHAD3-NS PRIME/AD6-NS BOOST INDUCES HCV SPECIFIC T-CELLS 290
6.5.4 VACCINATION AT HIGH OR LOW HCV VIRAL LOAD 292
6.5.5 HCV SPECIFIC T-CELL RESPONSES IN CHRONIC HCV INFECTION, COMPARED TO HEALTHY VOLUNTEERS 294
6.5.6 ANTI-VECTOR IMMUNITY IN RESPONSE TO VACCINATION 295
6.5.7 THE RELATIONSHIP BETWEEN THE SEQUENCE OF THE CIRCULATING VIRUS AND THE VACCINE IMMUNOGEN 299
6.5.8 CROSS-RECOGNITION OF VARIANTS BY VACCINE-INDUCED T-CELLS 304
6.5.9 SEQUENCE VARIATION AT THE POPULATION LEVEL 307
6.5.10 VACCINE-INDUCED T-CELL FUNCTION IN PATIENTS WITH CHRONIC HCV 310
6.5.11 THE MAGNITUDE AND KINETICS OF THE T-CELL RESPONSE IN PATIENTS RECEIVING MVA-NS BOOST VACCINATION 315
6.5.12MVA-NS BOOSTED T-CELLS TARGET SEQUENCES THAT ARE MISMATCHED BETWEEN VACCINE AND CIRCULATING VIRUS 321
6.5.13 FUNCTIONALITY OF THE T-CELL RESPONSE IN PATIENTS RECEIVING MVA-NS BOOST VACCINATION 322
6.5.14 HLA-A2 ALLELE DOES NOT HAVE A DOMINANT IMPACT ON OVERALL RESPONSE 325
6.5.15 CULTURING PRE-VACCINATION HCV-SPECIFIC T-CELLS 326
6.6 DISCUSSION 329
6.7 CONCLUSION 337
6.8 SUMMARY OF FINDINGS 339

7 DISCUSSION 340

7.1 A PROPHYLACTIC VACCINE FOR HCV 340
7.2 SINGLE CELL ANALYSIS OF VACCINE-INDUCED T-CELLS 341
7.3 WHY ARE ADENOVIRUSES SUCH GOOD VECTORS? 343
7.4 II AS A GENETIC ADJUVANT 345
7.5 SUBVERSION OF THE T-CELL RESPONSE BY HCV 347
7.6 VACCINATION AFTER CURE AND T-CELL RECOVERY 348
7.7 NEXT GENERATION IMMUNOGEN DESIGN 350
7.8 THE FUTURE OF OXFORD'S HCV VACCINE PROGRAMME 352

8 APPENDIX 2-1 - INFORMED CONSENT 355

9 APPENDIX 2-2 – PEPTIDES COVERING VACCINE IMMUNOGEN 359

10 APPENDIX 2-3 PCR CONDITIONS FOR VIRAL SEQUENCING 361

11 APPENDIX 5-1 ISOLATING MOUSE SPLENOCYTES 362

12 APPENDIX 5-2 MURINE ELISPOT PROTOCOL 364

13 REFERENCES 367

List of Tables

Table 1-1. Primate and human studies - candidate prophylactic HCV vaccines 53

Table 2-1. HCV vaccine trials described in this thesis 81

Table 2-2. Antibody and fluorochrome/metal ion combinations 89

Table 2-3. to Table 2-7 Antibody panels 91

Table 2-8. Flow cytometer detector set up 94

Table 3-1. Vaccine trials described in chapter 3 103

Table 3-2. Specificity of T-cell response to HCV NS after vaccination 116

Table 3-3. Protective epitopes – variants tested 121

Table 3-4. Frequency of common genotype 1 variant sequences 124

Table 4-1. MHC class I multimer cloud size: FACS vs CyTOF 174

Table 5-1. Evidence of Ii-mediated adjuvanticity 212

Table 5-2. Non-replicative Ad vectors used in murine experiments 221

Table 5-3. FACS reagents used in Chapter 5 224

Table 5-4. Murine CD74 & Table 5-5. Human CD74 surface panels 225

Table 5-6. Mouse pentamer staining panel 226

Table 5-7. Subculturing conditions for cell lines 231

Table 6-1. Therapeutic vaccine trials 286

Table 6-2. HCV002 trial patient demographics and treatment outcome 289

Table 6-3. T-cell responses mapped in HCV+ patients 301

Table 6-4. Circulating HCV sequence at immunogenic T-cell epitopes 302

Table 6-5. HCV Viral sequence in patients who responded to vaccination 304

Table 6-6. Circulating HCV sequence at immunogenic epitopes (HCV003 trial) 322

List of Figures

Figure 1-1 Organisation of the HCV genome 24
Figure 1-2 Relative prevalence of HCV genotypes by 'global burden of disease' region 25
Figure 1-3 Candidate HCV vaccine immunogens 51
Figure 1-4 Peak magnitude of the T-cell response to candidate vaccines 55
Figure 1-5 Progress to an effective prophylactic vaccine against HCV 64

Figure 2-1 Peptide pools and recombinant proteins for immune assays 85

Figure 3-1 Safety data after vaccination 105
Figure 3-2 Magnitude of the T-cell response to HCV NS after ChAd3-NS/MVA-NS vs. after ChAd3-NS/Ad6-NS vaccine regimens 107
Figure 3-3 Magnitude of Flu, EBV and CMV-specific T-cell responses across the trial 109
Figure 3-4. CD4+ Tregs across the vaccine trial 111
Figure 3-5. Breadth of the T-cell responses to HCV NS after vaccination 114
Figure 3-6. The cross-reactivity of ChAd3-NS/MVA-NS induced T-cells 118
Figure 3-7. Induction of T-cells targeting a HLA-B27 restricted protective epitopes 122
Figure 3-8. Induction of T-cells targeting HLA-B15 restricted protective epitopes 127
Figure 3-9. Proliferative capacity of vaccine-induced T-cells 129
Figure 3-10. *In viv*o expansion and activation status of vaccine-induced T-cells 130
Figure 3-11. Cytokine production by vaccine-induced T-cells 134
Figure 3-12. Polyfunctionality of HCV-specific CD4+ and CD8+ T-cells 136
Figure 3-13. Polyfunctional cells make more cytokine per cell 137
Figure 3-14. Cytotoxic potential of vaccine-induced T-cells 139
Figure 3-15. Memory phenotype of vaccine-induced CD8+ T-cells 141
Figure 3-16. Further boosting the magnitude of HCV-specific T-cells 144
Figure 3-17. Memory phenotype of vaccine-induced CD8+ T-cells after re-boosting 147
Figure 3-18. A dose de-escalation of MVA-NS 148

Figure 4-1. Cytometry by time-of-flight (CyTOF) 170
Figure 4-2. CyTOF validation 173
Figure 4-3. Polyfunctionality of HCV-specific CD8+ T-cells analysed by CyTOF 177
Figure 4-4. Principal component analysis (PCA) of T-cell immunity in human vaccinees 179
Figure 4-5. 3D Principle Component Analysis of CD8+ T-cells 181
Figure 4-6. Plotting T-cell memory subsets against principal components 183
Figure 4-7. Cytokine producing CD8+ T-cells 184
Figure 4-8. CD8+ T-cells possessing 8 functions 185
Figure 4-9. 3D Principal Component Analysis of vaccine-induced CD8+ T-cells 186

Figure 4-10. PCA identifies cells recently activated *in vivo* 187
Figure 4-11. Mass cytometry and FACS reveal a shared phenotype of T-cells induced by virally vectored vaccines and CMV 189
Figure 4-12. MCMV- and βgal-specific persistent CD8+ Tem cells share a conserved transcriptional programme 193
Figure 4-13. Tem show a distinct conserved gene expression profile 195
Figure 4-14. Eomes and Tbet expression on bulk and antigen-specific T-cells 197

Figure 5-1. Antigen presentation on MHC class I and MHC class II molecules 214
Figure 5-2. The known functional domains of Ii 217
Figure 5-3. mIi variants 235
Figure 5-4. T-cell responses in mice immunized with Ad5-OVA +/- mIi variants 236
Figure 5-5. Immunogenicity of Ii containing Ad vectors at limiting dose 240
Figure 5-6 Assessing presentation of an immunodominant OVA peptide on murine DCs 242
Figure 5-7. The effect of tethering OVA to mIi and its variants on *in vitro* surface antigen presentation 246
Figure 5-8. Increased presentation correlates with increased proliferation 248
Figure 5-9. eGFP N-terminal linked to mIi within an Ad vector is rapidly degraded 253
Figure 5-10. MHC class I pentamer staining of OVA-specific T-cell populations after transduction with Ad5-mIi(1-105)-OVA or Ad5-mIi(1-50)-OVA 255
Figure 5-11. Phenotyping of OVA-specific T-cells 257
Figure 5-12. Surface expression of Ii (CD74) on murine and human PBMC subsets 259
Figure 5-13. Specificity of human and murine CD74 antibodies on human PBMC 260
Figure 5-14. Specificity of human and murine CD74 antibodies on murine PBMC 261
Figure 5-15. Transduction and surface CD74 staining of human THP-1 cell line 262
Figure 5-16. Surface CD74 staining of murine BMDC transduced with Ad encoding mIi 265
Figure 5-17. Surface CD74 staining of murine BMDC transduced with Ad encoding hIi 267

Figure 6-1. Liver enzymes in relation to vaccination 290
Figure 6-2. Patients on treatment - Magnitude of HCV specific T-cell responses 291
Figure 6-3. The magnitude of non-HCV antiviral T-cells during the study 292
Figure 6-4. Untreated patients - Magnitude of HCV specific T-cell responses 294
Figure 6-5. Magnitude of HCV specific T-cell responses in healthy volunteers compared to HCV infected patients 295
Figure 6-6. Anti-vector immunity – neutralising antibodies and anti-hexon T-cells 298
Figure 6-7. Epitopes mapped to HCV genomic regions 300
Figure 6-8. The cross-reactivity of vaccine induced T-cells to circulating viral antigen 306
Figure 6-9. Cross-reactivity of T-cells targeting HLA-A2 restricted epitopes 307
Figure 6-10. Viral variability at a population level of HCV T-cell epitopes 309

Figure 6-11. Comparison of Phenotype and function of vaccine induced HCV-specific T-cells in patients vs. healthy volunteers 311
Figure 6-12. Cytokine production by vaccine-induced cells in HCV+ patients 313
Figure 6-13. Breath & proliferative capacity of vaccine-induced T-cells HCV+ patients 314
Figure 6-14. Magnitude of HCV specific T-cell responses by peptide pool in IFNα/ribavirin treated HCV+ patients receiving ChAd3-NS/MVA-NS 316
Figure 6-15. Magnitude of HCV specific T-cell responses by peptide pool in untreated HCV+ patients receiving ChAd3-NS/MVA-NS 317
Figure 6-16. Magnitude of HCV specific T-cell responses after ChAd3-NS (prime) and MVA-NS (boost) vaccination in HCV+ patients 318
Figure 6-17. Comparison of the HCV-specific T-cell induction by ChAd3-NS/MVA-NS vs. ChAd3-NS/Ad6-NS vaccine regimens in HCV+ patients 320
Figure 6-18. Functional analysis of MVA-NS boosted HCV-specific T-cells HCV+ patients 323
Figure 6-19. A comparison of Phenotype of vaccine induced HCV-specific T-cells in patients vs. healthy volunteers after Ad6-NS or MVA-NS boost vaccination 324
Figure 6-20. A comparison of the total T-cell response to HCV NS in HCV+ patients with and without the HLA-A2 allele 326
Figure 6-21. CD8+ T-cell responses exist below the limit of detection in HCV+ patients pre-vaccination 328

1 Introduction

1.1 Hepatitis C viral infection

1.1.1 A global health problem

The prevention of persistent hepatitis C virus (HCV) infection is an area of real unmet clinical need. HCV is able to persist in the majority of immune-competent hosts it infects, and this leads to a state of chronic hepatic inflammation, which can progress to fibrosis and cirrhosis of the liver, and ultimately liver failure or hepatocellular carcinoma (**Lavanchy 2011; Lauer & Walker 2001**) . Prevalence estimates from the global burden of disease project suggest more than 180 million people are chronically infected with HCV (**Messina et al. 2014**) and of the estimated 3-4 million new HCV infections per year approximately 70% will result in persistent infection and 10-20% will lead to decompensated liver disease (**Lauer & Walker 2001**)**.** Due to overlapping methods of transmission HCV and human immunodeficiency virus 1 (HIV-1) co-infection is common and the resultant liver disease is now one of the leading causes of death for patients on highly active antiretroviral therapy (HAART; reviewed in (**Chen et al. 2014**)**.** HCV is also the most common indication for liver transplantation in many countries (**Kim et al. 2014**).

It was previously thought that an effective vaccine against HCV would be impossible, however, unlike with HIV-1 infection, we now know that a significant number of individuals spontaneously clear the virus in the setting of an appropriate immune response, and there is evidence of protective

immunological memory against HCV in chimpanzees and humans, where secondary infection is associated with reductions in: peak and duration of viraemia, hepatic inflammation, and an increased rate of viral clearance (**Osburn et al. 2010; Dahari et al. 2010; Mehta et al. 2002**). Immunological memory does not appear as effective as is seen with hepatitis A, B, or E, as it is rarely, if ever, sterilizing (**Mehta et al. 2002; Osburn et al. 2010**); however, an attenuated course of infection associated with early viral clearance can prevent chronicity (**Mehta et al. 2002; Osburn et al. 2010**). The goal for a vaccine against HCV is unusual in that to prevent disease it need only prevent persistence of the virus rather than prevent initial infection.

1.1.2 The clinical course of HCV infection

HCV is primarily a blood-borne or parenterally transmitted infection. In developed countries it is most commonly transmitted by sharing of needles between intravenous drug users (IVDUs), and emerging epidemics of illicit heroin and prescription narcotic abuse are leading to increased incidence among the young (**Suryaprasad et al. 2014**). Despite effective blood screening, HCV is still transmitted through poor blood hygiene in some less developed countries (**Lauer & Walker 2001**). HCV can be spread by sexual contact, and in some HIV-1+ populations the incidence of HCV in men who have sex with men (MSM) has risen sharply in the last decade (**Wandeler et al. 2012**). A smaller number of infectious result from occupational exposure (mainly needle-stick injuries; **Henderson 2003**), perinatal transmission (**Benova et al. 2015**), heterosexual intercourse (**Terrault et al. 2013**), unsterilised tattooing needles (**Tohme &**

Holmberg 2012), and hemodialysis (**Etik et al. 2015**). For approximately 20% of infections the route of transmission is unknown (**Alter et al. 1999**).

Acute HCV infection commonly goes unrecognised and is less well studied because it is often asymptomatic. HCV RNA is detectable from 2 weeks after infection, and it is followed by a relatively delayed seroconversion and/or emergence of HCV-specific T-cells 8-12 weeks later **(Netski et al. 2005; Thimme et al. 2001**). HCV screening is performed by enzyme-linked immunoassay (ELISA) on patient serum or plasma using recombinant HCV proteins to detect anti-HCV antibodies. Positive screenings are confirmed by PCR, which is used to confirm viraemia, quantify viral titer and for genotyping. Fulminant hepatitis with HCV infection has been described (**Farci et al. 1996**) but is extremely rare and when symptomatic acute HCV infection is usually accompanied by jaundice, nausea and fatigue. Most chronic infections will lead to some degree of fibrosis but severe complications and death usually occur only in persons with cirrhosis, which develops in 10-20% of those infected (**Seeff & Hoofnagle 2002**). Progression to cirrhosis is accelerated by certain risk factors such as alcohol use (>20-30 dL/day), male sex, age (>40 years), and comorbid diabetes, obesity, or fatty liver, or co-infection with HIV-1 or hepatitis B virus (HBV)(**Chen & Morgan 2006**). Progressive liver damage can lead to the subsequent development of decompensated liver disease or hepatocellular carcinoma. Chronic HCV infection has also been associated with extrahepatic manifestations such as cryoglobulinemia, membranoproliferative glomerulonephritis, porphyria cutaneous tarda, lichen planus, and vitiligo (**Negro et al. 2015**). Much of the morbidity and mortality caused by HCV occurs due to the long-term persistence of the virus, however, it is still

unclear whether this is caused directly by cytopathic effects of HCV on the cells in which is has infected or is a result of the accompanying inflammation and underlying immune stimulation caused by immune recognition of chronic HCV infection (**Walters et al. 2009**).

1.1.3 The virus

HCV is a single stranded RNA virus with an enveloped virion of the genus Hepacivirus (family Flaviviridae,) identified less than 30 years ago as the main source of non-A non-B viral hepatitis (**Choo et al. 1989**). The positive sense HCV genome is approximately 9600 nucleotides and is translated into a single polyprotein of ~3011 amino acids in length (**figure 1-1**). This polyprotein is cleaved by cellular and viral proteases into structural (core, E1, E2) and non-structural regions (p7, NS2, NS3, NS4A, NS4B, NS5A and NS5B)(**Grakoui et al. 1993**). HCV lipoviral particles gain entry into hepatocytes by clathrin-mediated endocytosis via interactions of their envelope proteins (E1E2 heterodimers) with heparin sulphate proteoglycans (HSPGs), scavenger receptor class B member 1 (SRB1), CD81, low-density-lipoprotein receptor (LDLR) and the two tight-junction proteins claudin 1 and occludin (**Lindenbach & Rice 2013**)

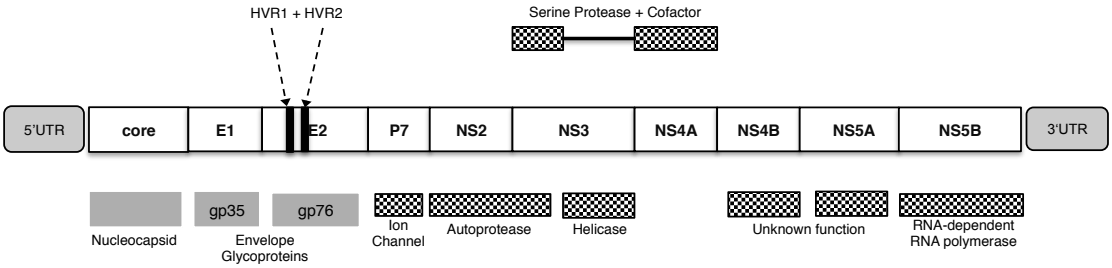


Figure 1-1 Organisation of the HCV genome: HCV, a single-stranded RNA virus of ~ 9.6 kb, consists of a single open-reading frame and two untranslated regions. The HCV genomic RNA serves as an mRNA for the translation of a single polyprotein, which is cleaved by a host signal protease in the structural region and the HCV-encoded serine protease in the non-structural (NS) region. The hypervariable regions of E2 (HVR1 + HVR2) are indicated by dashed arrows. The protein products of cleavage are shown. The structural regions consist of core and the two envelope proteins, gp35 and gp76. The NS proteins are shown and their functions are indicated where known.

The characteristic of HCV that will offer the biggest problem for vaccine design is its sequence diversity, which is ten times more diverse than HIV-1. HCV is classified into 7 genotypes which differ at 31-34% of their nucleotide positions (**figure 1-2**; (**Simmonds et al. 1993; Simmonds et al. 2005**) and ~1-10 trillion viral variants are generated per day per infected individual during chronic infection (**Neumann et al. 1998**). This diversity results from a lack of proof reading capacity of the viral RNA-dependent polymerase (NS5b) used by HCV during replication, combined with a short half-life and rapid turnover of virions (**Bukh et al. 1995**); therefore, HCV exists within a host as a constantly evolving swarm of closely related but diverse quasispecies, giving it the ability to respond instantly to new selection pressures (**Farci et al. 2000**).

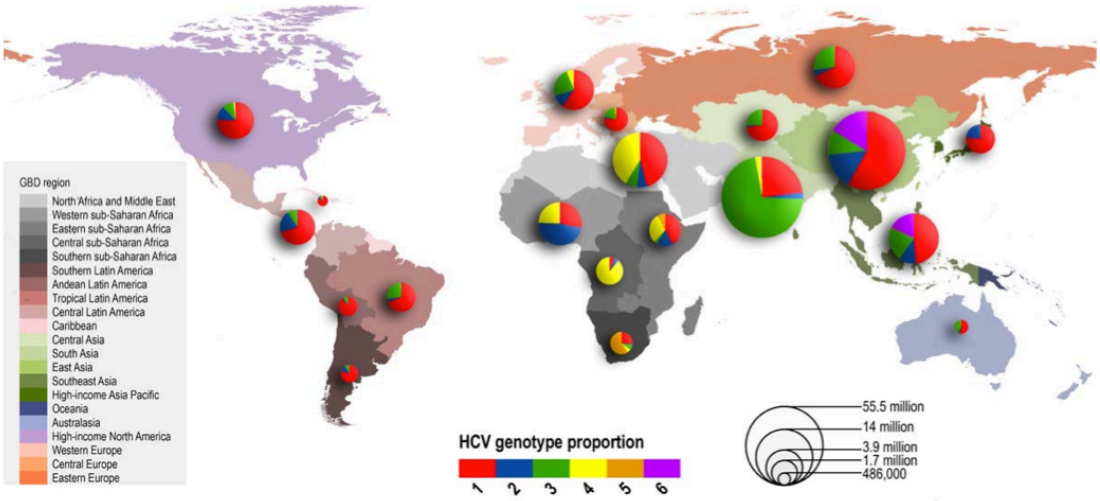


Figure 1-2 Relative prevalence of HCV genotypes by 'global burden of disease' region: Pie size is proportional to seroprevalent cases, slices coloured by genotype (1-6). Image reproduced with permission from (**Messina et al. 2014**).

Over the ~1000yrs HCV has been infecting humans, HCV genotypes have evolved in distinct geographical regions due to 'neutral' sequence drift and by rapid adaptive changes due to immunological selection pressure (**figure 1-2**)(**Pybus et al. 2009; Simmonds 2001**). In recent decades, epidemics of certain genotypes have spread through distinct risk groups, such as the epidemic of genotype 3a HCV amongst IVDUs in the UK, and single source outbreaks due to contaminated blood products (**Lavanchy 2011; Messina et al. 2014**). A globally effective prophylactic vaccine for HCV should aim to account for all levels of HCV variability: within a host, within a cohort, and between isolated (by geography or transmission route) subtypes and genotypes.

1.2 Treatment options for HCV and reinfection

Initial treatment for HCV consisted of injections of the non-specific antiviral interferon-α (IFNα); the rate of sustained virological response (SVR) improved from ~5% to ~50% of those treated by the early 2000s due to optimization of the dose, treatment length, stabilization of IFNα by pegylation (addition of polyethylene glycol), and by the addition of the RNA nucleoside analogue Ribavirin (reviewed in **Lam et al. 2015**). This relatively toxic, prolonged (24-48 weeks) and often ineffective treatment (SVR in approximately 50% of patients) remained until recently the only licensed treatment for HCV; many patients were ineligible for, or intolerant of IFN-based therapies due to side effects – for instance autoimmune disease or mental health problems (reviewed in **Lam et al. 2015**).

Attention switched to two enzymes essential for HCV replication: its serine protease encoded within the NS3-4A protein and its RNA polymerase encoded in NS5b, along with NS5A (a non-enzymatic but essential protein) as attractive HCV-specific targets for limiting viral replication. In 2011 two protease inhibitors were approved for treatment of genotype 1 infections in the US and Europe in combination with pegylated-IFNα/Ribavirin (PEG-IFNα/rib), raising the SVR rates to around 70%, but with significant adverse events and the emergence of viral resistance (**Hézode et al. 2014**). 2013 saw FDA approval of the first all-oral and IFN-free treatment regimen, with or without ribavirin, with SVR rates in excess of 95% 12 weeks after the cessation of treatment (SVR12; **Feld et al. 2014; Afdhal et al. 2014; Sulkowski et al. 2014**). These new

regimens have short durations (with programmes as short as 4 weeks currently being tested), minimal side-effects, low pill burden (often single daily combination pills) and efficacy in excess of 90% even in 'difficult to treat' cohorts (cirrhotic patients, patients that have previously failed treatment, or genotype 3 infections; reviewed in **Lam et al. 2015**).

The effectiveness of these new directly-acting antivirals (DAAs) is yet to be tested in all genotypes and in some key patient groups, such as: children, pregnant women, treatment-experienced patients and patients with decompensated liver disease.

Unlike HIV-1 and HBV a SVR12, defined as undetectable (<15IU/mL) HCV RNA 12 weeks post-treatment cessation, in the vast majority of cases likely reflects a true clinical cure as HCV does not develop a reservoir within the host and does not incorporate into the host's genome. Statistical modelling tools predict that an HCV RNA level close to the limit of detection can still mean up to a million virions being produced daily (**Neumann et al. 1998**), however, SVR at 24 weeks in several cohorts has shown 99% concordance with SVR12 **(Sulkowski et al. 2014**) and even many patients with low level but detectable HCV RNA after treatment do not show viral rebound but go on to clear HCV (**Kohli et al. 2015**; **Sidharthan et al. 2015**), suggesting that the immune system alone can clear remaining virus (as can be seen in rare instances with HIV-1; (**Sáez-Cirión et al. 2013; Conway & Perelson 2015**) or that detected virions are not infectious.

A SVR has been significantly associated with a decrease in all-cause mortality, liver-related mortality, and incidence of hepatocellular carcinoma (**Ng & Saab 2011**), however, long-term follow-up of patients to assess the outcome of DAA-mediated clearance on the progression of disease are needed and a complete resolution of cirrhosis and reversal of liver damage thus far appears rare (**D'Ambrosio et al. 2012; Shiffman et al. 2014**).

Reinfection does occur, particularly in groups of individuals who continue to practice high-risk behaviour such as IVDUs (reviewed in (**Grady et al. 2013**)). The incidence of confirmed reinfections varies widely in the small studies performed so far, with a meta-analysis suggesting anincidence of 2-5 per 100 person-years (**Aspinall et al. 2013**) but rates as high as 28.8 per 100 person-years seen in some studies (**Sacks-Davis et al. 2015; Sacks-Davis et al. 2013**).

Despite continuing improvements in the prevention of HCV transmission and in treatment regimens, HCV is likely to persist in areas with limited access to antivirals and poor blood product hygiene and needle usage. Using real world data of SVR rates for seven sites in the UK and modelling based on >90% SVR rates of IFN-free DAA treatment Martin *et al* (**Martin et al. 2015**) suggest treatment rates with new DAA regimens are unlikely to lead to an observable reduction in prevalence of chronic HCV over the next ten years. Significant reductions in incidence of HCV infection in the UK and globally, particularly for non-genotype 1 strains, are unlikely without significant scale-up of treatment and/or a vaccine (**Van Den Berg et al. 2007; Hahn et al. 2009; Thomas 2013; Bennett et al. 2015**). The cost of treatment and surveillance programmes to

identify largely asymptomatic HCV infections could be prohibitive in many areas and DAA resistance is likely to be a problem. Models incorporating data on the lack of fidelity of HCV's RNA polymerase suggest that variants exist with all viable single and double resistance mutations in every host before treatment, suggesting only treatments with the highest genetic barrier to resistance will lead to sustained viral control (**Rong et al. 2010**); a vaccine targeting multiple sites across the viral genome simultaneously is therefore highly desirable.

Many of these limitations do not apply to an effective prophylactic vaccine and the targeted use of a vaccine in at-risk populations and even in DAA treated patients remains a desirable, realistic, and cost-effective method of reducing the global burden of disease associated with HCV infections (**Krahn et al. 2005; Hahn et al. 2009; Pronker et al. 2013; Scott et al. 2015**).

1.3 The immune response to HCV

Comparative analyses of individuals with distinct clinical outcomes have been performed by several groups, and there is now some consensus on the immune response required to prevent persistence of HCV, but there is no single correlate of protection (COP; reviewed in (**Ishii & Koziel 2008; Cooper et al. 1999; Klenerman & Thimme 2012**). Most simply put, a strong, broad, and persistent HCV-specific adaptive immune response during acute infection is required for clearance (reviewed in (**Bowen & Walker 2005; Lechner, Sullivan, et al. 2000; Klenerman & Thimme 2012**); however, in the face of such adaptive immune responses HCV persists in some patients, which likely reflects the importance of

other antiviral mechanisms (**Ishii & Koziel 2008; Cooper et al. 1999; Lechner, Wong, et al. 2000**).

1.3.1 Innate immunity

As with other viral infections, the innate immune system – broadly mediated by phagocytes, Natural killer (NK) cells, complement, and soluble antiviral factors - has an important role in the control of HCV (reviewed in **(Randall & Goodbourn 2008**)). Accordingly, HCV has been shown to suppress early innate immune responses by multiple mechanisms. For instance, HCV viral proteins can alter the downstream effects of IFN expression and block its production, as well as down-regulate NK activity (**Gale & Foy 2005; Li & Lemon 2012; Cheent & Khakoo 2011; Khakoo et al. 2004; Horner 2014**).

Recent genome wide association studies (GWAS) have highlighted the importance of innate host genes in the clearance of HCV. Single nucleotide polymorphisms (SNPs) linked to the interferon-λ3 and interferon-λ4 genes have been associated with spontaneous clearance of HCV and response to IFN containing therapies; for instance the genotype at these SNPs are the most powerful baseline predictor of a sustained virological response (SVR; undetectable [<15IU/mL] HCV RNA 24 weeks post end of treatment) in genotype 1 patients treated with PEG-IFNα/rib (**Schreiber et al. 2012; Naggie et al. 2012; Kelly et al. 2011**); however, the overall role of IFNs in control of HCV infection remains unclear **(Schreiber et al. 2012; Kelly et al. 2011; Bucci et al. 2013**).

Evidently, the innate immune response is involved in the effective control of HCV, but it is more difficult practically to manipulate for vaccine strategies due to its lack of specificity; nevertheless, it is clear that the use of adjuvants or vectors that elicit an innate response are key to optimising the adaptive immune response to vaccination.

1.3.2 Humoral immunity

Neutralising antibodies (nAb) provide the clearest COP for many viral infections, and generation of such antibodies is the basis of most if not all successful and licensed vaccines (**Burton 2002; Corti & Lanzavecchia 2013**). Furthermore, vaccines that generate protective antibody responses against HPV (human papillomavirus) and HBV demonstrate that prevention of chronic viral infection by antibody inducing vaccination is possible (**Kwak et al. 2011; Zuckerman 2006**). Unfortunately the generation of a protective antibody response for control of HCV has not yet been realised for a variety of reasons.

Circulating antibodies against structural and non-structural regions of HCV develop in all patients, regardless of outcome, and a direct correlation between viral clearance and the rapid induction of high-titer cross-neutralising antibodies has been shown (**de Jong et al. 2014; Lavillette et al. 2005**), however, in most patients antibody responses are not neutralising or are isolate specific (**Freeman et al. 2001; Farci et al. 1994; Logvinoff et al. 2004; Pestka et al. 2007**). Much of the sequence diversity of HCV is concentrated in areas of high

variability, such as the hypervariable regions 1 and 2 (HVR-1, HVR-2) in E2. These are the major antibody targets meaning antibodies often offer protection only against a single HCV strain and are easily evaded by viral mutations (**Simmonds 2004; von Hahn et al. 2007**). Abs targeting the non-structural (NS) regions of HCV have been observed, however, the mechanism by which HCV NS proteins are presented to B-cells is not clear (**Netski et al. 2005**). If vaccine induced immunity to HCV is to be antibody driven a strong and broadly cross-reactive response is needed to account for extensive global diversity and inherent mutability of the virus (**Law et al. 2008; Perotti et al. 2008; Meunier et al. 2008**).

How nAbs contribute to clearance of HCV *in vivo* is unclear (**Farci et al. 1994**). *In vitro* neutralisation of HCV by anti-HCV antibodies has been demonstrated in chimpanzees (**Farci et al. 1996**) but passive transfer of antibodies or serum has shown limited efficacy in the chimpanzee challenge model (**Morin et al. 2012; Krawczynski et al. 1996**) and in the setting of reinfection post liver transplantation (**Chung et al. 2013; Davis et al. 2005; Feray et al. 1998**). Despite induction of broadly neutralizing antibodies some individuals have failed to control secondary infections, suggesting incomplete protection by humoral memory responses (**Osburn et al. 2010**). Typically B-cells produce IgM isotype antibodies on initial recognition of a pathogen, however, HCV-specific IgM and IgG antibodies are almost simultaneously detected in the acute phase of infection (**Chen et al. 1992**) and IgM often remains detectable during chronic infection (**Yamaguchi et al. 2000**); HCV-specific IgM has therefore not proved an accurate marker of acute infection, as it is with other viruses, and the dysregulation of the

early Ab responses may explain why it is less effective against HCV in the acute phase of infection relative to other viruses.

Due to its hepatotropic nature, a mechanism for antibody evasion available to HCV is cell-to-cell spread via tight-junctions, which are common between hepatocytes (**Brimacombe et al. 2011**). It is also likely the glycosylated coating of HCV and its interactions with high-density lipoproteins are not only used in cell entry but also hinder antibody binding (**Logvinoff et al. 2004; Fauvelle et al. 2015**).

A coordinated adaptive immune response involving both antibodies and T-cells is normally required for pathogen control (**Burton 2002**). Conceptually then, is it plausible that a vaccine inducing T-cells alone can prevent persistent HCV infection? Several observations suggest it can: Chimpanzees and humans can clear HCV infection without a detectable antibody response and HCV-specific cellular immune responses can be detected in exposed uninfected persons without seroconversion (**Logvinoff et al. 2004; Post et al. 2004; Abdelwahab et al. 2012; Heller et al. 2013**). It has also been shown that hypogammaglobulinemic patients, deficient in antibody responses, can clear HCV (**Semmo 2006**).

HCV uses multiple mechanisms to avoid antibodies, which can explain why in the face of a detectable antibody responses HCV can persist (**Wahid & Dubuisson 2013**); this, combined with mounting evidence that clearance can occur without the detection of antibodies, suggests that although generation of effective

antibody responses would be ideal, a vaccine against HCV need not necessarily induce HCV-specific antibodies.

1.3.3 Cellular immunity

Comparative studies have shown that a functional early T-cell response of high magnitude, targeted at multiple major histocompatibility complex (MHC) class I and II epitopes is characteristic of effective immunity, and that conversely, the hallmark of persistent infection is a weak, narrowly targeted, and dysfunctional T-cell response (**Zhang et al. 2009; Urbani et al. 2006; Wedemeyer et al. 2002; Diepolder et al. 1995; Gerlach et al. 1999; Lauer et al. 2004**). Patients that go on to be chronically infected often do not lack a cell mediated response initially, but there is evidence that the timing, persistence, and functionality of the response is insufficient to control HCV (**Gerlach et al. 1999; Netski et al. 2005; Lechner, Wong, et al. 2000; Semmo et al. 2005**).

Some of the most convincing evidence for the importance of T-cells in protection against HCV infection comes from chimpanzee studies in which antibody-depletion of CD8+ T-cells leads to prolonged viraemia in convalescent chimpanzees that had previously cleared two rounds of infection (**Shoukry et al. 2003**); subsequent viral clearance was precisely correlated with a recovery of HCV-specific CD8+ T-cells (**Shoukry et al. 2003**). A complementary experiment depleting CD4+ T-cells again led to the abrogation of a previously protective immune response (**Grakoui et al. 2003)**. Retention of an effective population of CD4+ T-helper cells appears to be a pre-requisite for on-going viral control, as

shown by the re-occurrence of viraemia in individuals where CD4+ responses wane, even after several months of apparent control (**Cooper et al. 1999; Lechner, Wong, et al. 2000; Matloubian et al. 1994; Gerlach et al. 1999; Semmo et al. 2005**). Secondary infections of HCV are associated with a lower peak viral load, a quicker adaptive immune response and a higher rate of spontaneous resolution, however, this protection is lost upon reduction of CD4+ T-cells by HIV-1 infection (**Mehta et al. 2002**). Kaplan *et al* showed in their cohort of acutely infected patients that those who cleared HCV had a highly functional virus-specific CD4+ response and broadly targeted IFNγ+ T-cell response, but that patients with CD8+ T-cells or nAb in the absence of a detectable CD4+ T-cell response failed to clear HCV (**Kaplan et al. 2007**). There is also a temporal association between the T-cell response and HCV control. In man, a drop in viral load and a rise in serum transaminase levels is often concurrent with the emergence of HCV-specific T-cells and increased intrahepatic IFNγ expression (**Cooper et al. 1999; Grakoui et al. 2003; Cox et al. 2005; Gerlach et al. 1999**) and in chimpanzees a 90-99% drop in viral titer accompanies the upregulation of CD8β and IFNγ mRNA in the liver (**Shin et al. 2006**).

Natural history studies of single source outbreaks or large cohorts of HCV infected patients have shown a clear relationship between a patient's human leukocyte antigen (HLA) alleles and the outcome of their infection; HLA-B15, HLA-B27, HLA-B57, and HLA-A3 have all been associated with an increased rate of spontaneous clearance of certain HCV genotypes, emphasizing the importance of effective antigen presentation and concomitant T-cell response in the

clearance of HCV (**Fitzmaurice et al. 2011; Dazert et al. 2009; Neumann-Haefelin & Thimme 2007; Kim et al. 2011**).

These alleles could mediate their enhanced protection through a series of diverse mechanisms (**Neumann-Haefelin 2013**). The most common 'virological' mechanisms by which protective HLA alleles mediate their effect on HCV is through the presentation of epitopes with a higher genetic barrier of escape (reviewed in (**Goulder & Walker 2012; Neumann-Haefelin 2013**)). In order to elicit a T-cell response, antigenic fragments from viral proteins are presented bound to MHC molecules on the surface of designated antigen presenting cells (APCs) to T-cells via their highly specific T-cell receptor (TCR). MHC class I and II alleles are highly polymorphic and the repertoire of antigenic peptides that can bind to them and be effectively presented varies between alleles. The viral epitopes that can be targeted by an individual depends, therefore, on the MHC alleles they express. The protective effect of having HLA-B27 or HLA-B15, for example, are linked to immunodominant CD8+ T-cell epitopes (B27:$NS5B_{2841-2849}$; B15: $NS5B_{2466-2474}$ and $NS5B_{2450-2458}$; **Ruhl et al. 2012; Dazert et al. 2009)**. Other 'immunological' mechanisms by which these protective HLA alleles could mediate their protective effects on diverse viral infections are less well defined but include: preferential thymic selection and larger naïve precursor frequencies, looser peptide binding restrictions, and better concordance with antigen processing pathways, different susceptibility to inhibition by regulatory T-cells (Tregs), and interactions with other HLA binding partners – such as killer-cell immunoglobulin like receptors (KIRs) on NK cells, and leukocyte immunoglobulin like receptors (LILRs) on dendritic cells (DCs) (**Goulder &**

Walker 2012; Neumann-Haefelin 2013). Regardless of the mechanisms by which they offer enhanced protection, a T-cell vaccine should aim to induce T-cells targeting viral epitopes associated with clearance in natural infection.

It should be noted that responses of similar breadth and magnitude to those affording protection from persistence in some patients have been seen in patients that go on to be chronically infected with HCV and there have been contrasting results when trying to correlate the magnitude of intra-hepatic HCV-specific T-cells and viraemia or outcome of infection (**Urbani et al. 2006; Rehermann et al. 1996; Freeman et al. 2001**).

As well as a delayed emergence of the adaptive immune response to HCV infection, another unique characteristic of the immune response to HCV is a 'stunned' early response to infection, regardless of outcome, where T-cells initially appear with limited proliferative capacity and effector function, in particular a lack of IFNγ production (**Lechner, Wong, et al. 2000; Thimme et al. 2001; Urbani et al. 2006).** Following this, deletion or loss of T-cell responses (particularly CD4+ T-cells) in those that fail to clear HCV is seen and T-cells which remain detectable are often dysfunctional and show the hallmarks of T-cell exhaustion (**Bengsch et al. 2007; Urbani et al. 2002; Bengsch et al. 2010; Semmo et al. 2005; Rosen 2002; Lauer et al. 2004**). Priming T-cells away from the tolerogenic environment of the liver, in the absence of HCVs immunomodulatory effects and immune activation, should lead to a more functional HCV-specific T-cell response, with the characteristics of T-cell immune memory (i.e. a more rapid and focused response than on initial encounter of

antigen). The accelerated kinetics and increased functionality of the cellular immune response after prophylactic vaccine could tip the balance in favor of the host and lead to a much higher rate of spontaneous resolution, even if sterilizing immunity is not possible.

1.4 Which T-cells will protect against persistent HCV infection?

When a naïve T-cell is primed and activated it undergoes clonal expansion and differentiation, and of the resulting pool of effector T-cells (Teff) a small subset persist as memory T-cells that can respond more rapidly and effectively to further exposure to antigen (**Kaech et al. 2002; Badovinac et al. 2005; Badovinac et al. 2002)**. We now understand that both pools of effector and memory T-cells are highly heterogeneous in terms of their phenotype, functionality, and longevity, and many factors influence the 'quality' of a T-cell response (**Kaech & Wherry 2007; Kaech, Hemby, et al. 2002; Newell et al. 2012; Haining 2012b; Sallusto et al. 2004; Sallusto et al. 1999; Appay et al. 2008**).

By monitoring surface and intracellular proteins on T-cells researchers are beginning to characterize subsets of T-cells at different stages of maturation and have been able to link these phenotypes not only to functionality, but importantly to protective efficacy (**Hansen et al. 2009; Reyes-Sandoval et al. 2011; Northfield et al. 2007**).

As our understanding of T-cell evolution and how these subsets form, function, and persist, increases we are becoming more capable of understanding T-cell mediated immunity and how we can predict, assess, and manipulate vaccine induced T-cell responses in an attempt to align responses to COP and to provide life long T-cell mediated protection against viral infection. Several methodologies are progressing to clinical studies in humans but we know relatively little about the type of immune response offering protection from persistent HCV infection and even more broadly which T-cell parameters are most likely to define a good 'quality' T-cell.

1.4.1 Magnitude

The most fundamental characteristic of a T-cell response is its magnitude, as measured directly by the frequency of antigen-specific T-cells or by the number of T-cells displaying a certain effector function, most commonly production of IFNγ. Although no defined cut-off for a protective response against HCV exists, responses in individuals who clear acute infection are typically in the region of a few hundred IFNγ producing cells per million PBMC, and the responses often remain detectable for many years after infection (**Lechner, Wong, et al. 2000; Spada 2004; Lauer et al. 2004; Folgori et al. 2006a; Kaplan et al. 2007**).

Prospective vaccines against HCV have induced T-cell populations with a wide range of magnitudes, but the largest magnitude HCV-specific T-cell responses seen in animal models and humans thus far have come from regimens using

virally vectored vaccines and these are of the order of magnitude seen in those that spontaneous clear HCV.

Although vaccines that induce high levels of HCV-specific T-cells in animal models have protected against persistent HCV infection, this is not always the case; T-cell responses as high as 2368 SFC/10^6 PBMC in chimpanzees vaccinated with DNA and boosted with MVA were not protective against challenge with a heterologous strain of HCV, highlighting the importance of other factors, in particular the functionality and specificity of the vaccine induced T-cells (**Rollier et al. 2007**).

With the development of viral vectors we now have the means to induce large numbers of antigen-specific and IFNγ producing T-cells. However, it is apparent that the magnitude of the T-cell response alone is a poor predictor of protection for many viral infections and that an understanding of the combination of functions possessed by T-cell populations is needed (**Makedonas & Betts 2010; Darrah et al. 2007; Sallusto et al. 2010; Rollier et al. 2011**). Several T-cell parameters of importance when designing a T-cell mediated HCV vaccine are discussed below.

1.4.2 Breadth

The selection pressure exerted by the adaptive immune response rapidly selects for HCV escape variants, leading to persistence of HCV strains that are unrecognisable by circulating T-cells and antibodies, in both natural infection of

humans and in animal infection models (**Erickson et al. 2001; Puig et al. 2006; von Hahn et al. 2007; Klenerman 2000**). The breadth of a T-cell response has been reproducibly associated with control in human correlative studies and for an effective HCV vaccine, a T-cell response targeting multiple epitopes will be required to limit the possibility of viral escape and to effectively block viral replication (**Lauer et al. 2004; Spada 2004; Urbani et al. 2006; Lechner, Wong, et al. 2000**; **von Delft et al. 2015; Kelly et al. 2015a; Kelly et al. 2015b**).

The breadth of the T-cell response to vaccination is dependent upon the size and specificity of the immunogen, and vaccine studies to date have induced T-cell responses with a wide variation in breadth. The number of epitopes targeted by a peptide vaccine will be restricted by the number of peptide targets included and the HLA repertoire of the vaccinated population, whereas a virally vectored vaccine approach, including larger sections of the HCV sequence, may induce a broadly targeted T-cell response in a diverse HLA background population (**Firbas et al. 2006; Barnes et al. 2012**).

As well as targeting multiple HCV epitopes, an effective global vaccine will likely also need to cross-recognise variant sequences at these epitopes from several viral genotypes (**Simmonds 2004**). Using HCV pseudoparticles recombinant E1E2 protein vaccines induced antibodies with cross-reactivity against genotypes 1a, 1b, and 2a (**Stamataki et al. 2011**). Barnes *et al* showed response to ChAd3-NS/Ad6-NS vaccination containing the NS region from a 1b BK strain recognized peptides of genotypes 1a, and to a more limited extent, 3a sequences,

the most prevalent genotypes in Europe and America (**Barnes et al. 2012; Messina et al. 2014**).

A prophylactic vaccine that can induce T-cells which target a selection of functionally constrained viral epitopes, which are therefore common between genotypes and that can not mutate to viable viral variants, should be effective against HCV.

1.4.3 Proliferation and Cytokine production

A dysfunction in the proliferative capacity of HCV-specific T-cells has been repeatedly identified in patients who fail to control HCV, relative to those who clear infection (**Gerlach et al. 1999; Wedemeyer et al. 2002; Spangenberg et al. 2005; Diepolder et al. 1995**). A strong proliferative capacity is key for memory T-cell responses induced by prophylactic vaccination, as the rapid and large expansion of these to secondary effector T-cells is key for enhanced protection upon reinfection. Lymphoproliferative responses to HCV proteins have been assessed in several HCV vaccine studies (**Folgori et al. 2006b; Leroux-Roels et al. 2004; Frey et al. 2010; Firbas et al. 2006; Elmowalid et al. 2007**).

One of the effector functions available to T-cells for combatting viral infections is the secretion of antiviral and immune-modulatory molecules. Intracellular cytokine staining (ICS) can be used to assess the production of cytokines relevant to viral control by antigen stimulated T-cells. The production of IFNγ

and TNFα is measured, due to their synergistic direct and indirect antiviral effects (**Locksley et al. 2001; Schroder et al. 2004**), as well as IL-2 production, which promotes the clonal expansion of T-cell populations (**Malek 2008**). These cytokines are often measured in combination with CD107α (lysosome-associated membrane protein [LAMP]-1), a marker of T-cell degranulation (**Betts et al. 2003**), and the pro-inflammatory cytokine MIP-1-β (macrophage inflammatory protein-1β; CCL4 (**Florholmen et al. 2011**).

It has been assumed, but not convincingly shown, that a polyfunctional T-cell, with the capacity to carry out multiple antiviral functions, is more effective at clearing a virus than a monofunctional T-cell, or group of monofunctional T-cells that together possess the same combination of functions (**Betts et al. 2006; Makedonas & Betts 2010; Darrah et al. 2007; Kannanganat et al. 2007; Bogdan et al. 1990; Precopio et al. 2007)**; evidence of this came from comparative studies of long-term non-progressors (LTNPs) and progressors in the setting of HIV-1 infection (**Betts et al. 2006**), and mouse studies of *Leishmania major* (**Darrah et al. 2007**). The T-cell population in LTNPs, relative to progressors, is enriched for CD8+ T-cells that can co-produce Mip-1-β, TNFα, IFNγ, and CD107α (**Makedonas & Betts 2010**). But these highly polyfunctional T-cells are lacking in some LTNPs, when present represent a small fraction of the total HIV-specific T-cell population, and could simply be an indicator of low antigenic load in these individuals. Polyfunctionality not only affords a larger repertoire of functions for the individual cell, but it can also mean a larger per-cell production of the cytokine relative to monocytokine producers (e.g. in some studies monocytokine producing T-cells made 10x less IFNγ per cell than

polyfunctional T-cells) (**Kannanganat et al. 2007; Bogdan et al. 1990; Darrah et al. 2007; Precopio et al. 2007**). Nevertheless, polyfunctionality is not a requirement in all settings, for instance, IFNγ monoproducing T-cells are capable of protecting against infection with malaria in chimpanzees and mice **(Ewer et al. 2013; Reyes-Sandoval et al. 2010**).

Evidence of a hierarchy in cytokine production is emerging, where increased antigen exposure and co-stimulation leads to an increase in functions expressed by a T-cell (**Wherry et al. 2003; Seder et al. 2008; La Gruta et al. 2004; Viola & Lanzavecchia 1996**). Viola *et al* showed MIP-1-β and IFNγ are most readily released by T-cells on limited stimulation and that IL-2 production is only triggered when a T-cell has been exposed to high levels of antigen and co-stimulation (**Viola & Lanzavecchia 1996).** The antigenic load resulting from vaccination is highlighted as a key attribute that will affect T-cell quality and vaccine efficacy (**Zheng et al. 2008; Richter et al. 2012**).

1.4.4 Cytotoxicity

The definitive mechanism by which T-cells control HCV *in vivo* has not been conclusively shown, as studies in human populations are correlative and non-mechanistic. One functional attribute of human CD8+ T-cells that unequivocally combats acute viral infections is cytotoxicity (**Lechner, Wong, et al. 2000; Thimme et al. 2002**) and *in vitro* T-cells have been shown to have the capacity to mediate their control over HCV both by direct cytotoxic killing of infected cells

and by the release of antiviral cytokines (**Jo et al. 2009; Frese et al. 2002; Li et al. 2005**).

Direct cytotoxic killing of infected cells is primarily mediated by the activation of apoptotic pathways within the target cell by granzyme cleavage of intracellular caspases. On recognition of an infected cell activated CD8+ (and potentially a small number of CD4+ T-cells; **Soghoian & Streeck 2010**) secrete lysosomes containing the pore-forming protein, perforin, and granzymes, which are delivered to the target cell, inducing its apoptosis **(Bots & Medema 2006; Peters et al. 1991**).

Rather than its *ex vivo* expression, the rapid up-regulation of perforin is a key effector function of T-cells, and one that appears to be lacking in HCV-specific T-cells taken from chronically infected patients (**Makedonas et al. 2009; Makedonas et al. 2010; Jo et al. 2012**). Although it has been shown that during chronic infection HCV-specific CD8+ T-cells are often deficient in perforin expression and up-regulation relative to CMV-specific populations, it remains unclear how much perforin is necessary to initiate granzyme mediated killing (**Jo et al. 2012**).

Surface mobilization of CD107α has been used to identify cells that have degranulated on stimulation and, although this assay does not show killing directly or give information on the content of the granules released, it can be combined with staining for granzymes and perforin to give an indication of the cytolytic potential of a T-cell (**Betts et al. 2003**).

Few trials have assessed the cytolytic capacity of vaccine induced CTL, but it remains a key parameter that should ideally be assessed in any vaccine aiming to mediate protection through the induction of T-cells.

1.4.5 T-cell Phenotype

Research over the last decade has revealed an ever increasing complexity and division of labour within T-cells, particularly within the memory compartment (**Newell et al. 2012; Sallusto et al. 1999; Appay, Douek, et al. 2008; Appay & Rowland-Jones 2004**). Antigen-experienced T-cells in humans express the short, CD45RO, form of the protein tyrosine phosphatase CD45, whereas the long form, CD45RA, is expressed by naïve T-cells and is re-expressed by a subset of memory T-cells (**Merkenschlager et al. 1988**). In combination with the lymph node homing receptor CCR7, four broad populations of T-cells can be described (**Sallusto et al. 1999; Sallusto et al. 2004**): Central memory T-cells (Tcm; CD45RA- CCR7+) that home to the lymph nodes and in most settings have limited immediate effector function, but high proliferative capacity; Effector memory T-cells (Tem; CD45RA-CCR7-) that show immediate effector and cytolytic function and circulate through peripheral tissues; naïve, antigen-inexperienced T-cells (CD45RA+ CCR7+); "terminally differentiated" effector memory T-cells (Temra; CD45RA+ CCR7-) that have re-expressed CD45RA.

Additional complexity has been found in mice studies that have tried to identify precursors of long-lived memory cells in the effector pool. Effector T-cells have been divided into memory precursor effector cells (MPECs) and short lived effector cells (SLECs) by their expression of CD127 (IL-7Rα), and KLRG1 (**Kaech et al. 2003; Kaech & Wherry 2007**) and a population of T-cells with stem cell like properties has been described (Tscm; defined as naïve-like CD45RA+CCR7+ T-cells which express CD95+ and CXCR3, LFA-1, CD122, CD27, CD28 and CD62L) (**Gattinoni et al. 2011; Lugli et al. 2013**).

Rather than being a trivial pursuit, the description of these subsets of T-cells has led to the identification of certain subsets as being the main mediators of protection after vaccination and during the course of natural infection (**Hansen et al. 2009; Ewer et al. 2013; Barouch et al. 2012**). For example effector memory T-cells (Tem) have been shown to mediate protection against challenge with malaria sporozoites after Ad-MVA vaccination (**Reyes-Sandoval et al. 2011**) and in protection against SIV challenge in rhesus cytomegalovirus vector vaccinated rhesus macaques (**Hansen et al. 2011; Hansen et al. 2009**). The absolute number of antigen-specific terminally differentiated effector memory T-cells (Temra) at the time of acute infection has been associated with HIV-1 viral load set point (**Northfield et al. 2007**) and the magnitude of pre-existing Temra correlated with symptom score to pandemic influenza virus (**Sridhar et al. 2013**).

It is now clear T-cells play a key role in clearance of HCV, but we are lacking information about which subsets mediate this control and which subsets we

should aim to elicit by vaccination. It is likely that a mixed population of lymph-node homing Tcm, with the potential to rapidly proliferate and differentiate into effector T-cells, along side a population of Tem, which circulate the periphery and have a more immediate effector function, would in theory be most effective.

The vaccine platform used to deliver an immunogen has a profound influence on the type of T-cell response elicited, due to differences in the innate signalling pathways stimulated and the persistence and quantity of antigen after vaccination (**Casimiro et al. 2003; Flatz et al. 2011; Hansen et al. 2009**).

Clearly, a better understanding of the division of labor between T-cell subsets and the steps involved in T-cell differentiation and memory formation should aid in identification of COPs for viral pathogens. Because of the cost and practical difficulties of efficacy testing of vaccines in humans it is essential that we search for clear COP against HCV infection in several settings and that we use in depth characterization of the immune response to vaccination to predict efficacy.

1.5 Novel technologies for assessing T-cell quality

The use of a small number of classic phenotypic markers to dissect T-cells into functionally discrete subpopulations has under represented the complexity of T-cell phenotypes and has failed to explain some fundamental and emergent properties of T-cells as a whole and their function within the immune system. The complex heterogeneity of immune cells, even within lineages for which we are lucky enough to have relatively well defined lineage-specific markers, such as

CD3, CD4 and CD8 for T lymphocytes, is a major challenge to identifying clinically relevant measurements that reflect the state and capability of the cell population.

Single cells represent discrete and easily identified entities within the immune system on which measurements can be made. The assumption that behaviour and capabilities of groups of cells taken as an average reflect the qualities of each individual within that population has not always been useful in understanding underlying mechanisms in immunology, therefore, a methodological reductionist approach would suggest the obvious next step is to use complementary single-cell analysis to allow a better understanding of the molecular events within a cell and how these influence cell population and system level events.

The advent of sophisticated cytometric techniques (i.e. multiparametric flow cytometry, cytometry by time-of-flight, and gene expression profiling) capable of analysing multiple T-cell parameters simultaneously may enhance the stratification of T-cell subpopulations by function (**Newell et al. 2012; Flatz et al. 2011; Bendall et al. 2012**); for example, a recent study described phenotypically identical T-cell populations induced by different vaccine regimens that were distinct when the cell transcriptome was assessed (**Flatz et al. 2011**), therefore, comparing the magnitude, cytokine production, and classic phenotyping may not be sufficient to identify correlates of protection because they are insensitive to the full extent of heterogeneity in CD8+ responses.

1.6 Current vaccine approaches

Several mechanisms have been investigated for the introduction of HCV specific antigens to induce immunological memory to HCV (**Figure 1-3** & **Table 1-1**).

1.6.1 Recombinant protein vaccines

The HCV viral sequence has been isolated and cloned into bacteria, yeast, and mammalian cells, and the recombinant protein expressed can be purified for use in HCV vaccines. The advantage of recombinant protein vaccines is that they do not contain the pathogen or its genetic material and they do not require cultivation of the organism. Recombinant proteins must be administered with adjuvants, however, to elicit the innate immune response and costimulation that is required to effectively prime or boost an adaptive immune response.

The first prophylactic vaccine candidate tested for HCV, T2S-918/InnoVac-C by Innogenetics, consisted of a c-terminally truncated recombinant E1 protein (**figure 1-3**) with aluminium hydroxide (alum) adjuvant (**Leroux-Roels et al. 2004**). This vaccine elicited antibody titers against E1 in healthy volunteers that were significantly higher than those seen in patients with persistent HCV infection, but Innogenetics ceased work on this vaccine in 2007.

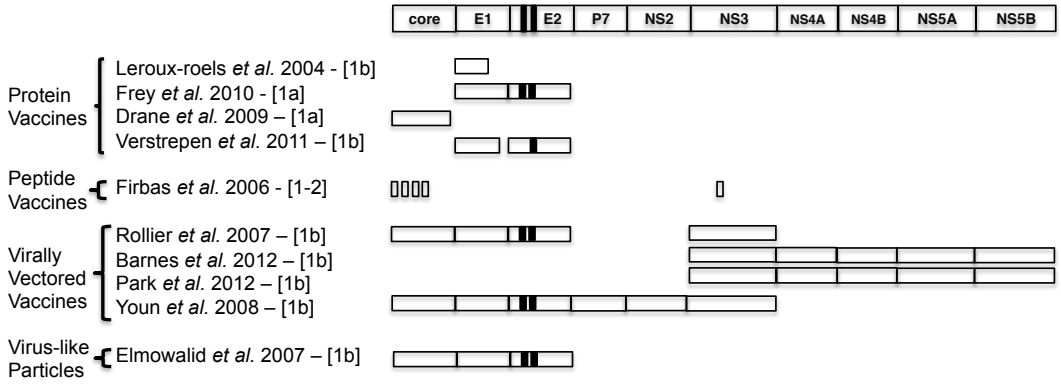


Figure 1-3 Candidate HCV vaccine immunogens: Prophylactic vaccines for HCV tested in primates (including man) are listed according to the lead author of the paper in which they are described. The relative coverage of the HCV genome by vaccine immunogen is shown (not to scale) and the HCV genotype of the immunogen is given in squared brackets.

The immunogenicity of E1 and E2 (with deletion of HVR1; **figure 1-3**) were assessed as separate proteins, potentially uncovering new antibody targets not available in the natural heterodimeric form of E1E2 (**Verstrepen et al. 2011**). After vaccination with either E1 or E2 adjuvanted with alum, antibodies were elicited in four chimpanzees, but only antibodies against E1 were shown to neutralize HCV pseudoparticles (HCVpp) and to offer protection, and antibody titers declined after challenge (**Verstrepen et al. 2011**).

Full length heterodimeric E1E2 has also been tested (**figure 1-3**) as a recombinant peptide vaccine and proved to be highly immunogenic, showing sterilizing immunity in one study against a homologous HCV strain in 5/7 chimpanzees (**Choo et al. 1994**). By combining results from chimpanzee vaccine studies using E1E2 glycoprotein it was shown to offer protection from persistent HCV infection in 10/12 and 8/9 chimpanzees when challenged with homologous or heterologous HCV strains respectively (**Houghton & Abrignani 2005**). When

this vaccine moved into phase-I human trials strong antibodies responses were detected by ELISA and these antibodies could block viral E2 protein binding CD81, a major entry receptor for HCV (**Frey et al. 2010**). Despite these promising results technical difficulties in the manufacturing of E1E2 protein has hampered its use in vaccines. A strong CD4+ T-cell response against the envelope proteins after vaccination had also been noted with this vaccine, however, the relative contributions to protection from HCV persistence by antibody and cellular responses with this vaccine were not determined (**Frey et al. 2010**).

Due to recent developments in cell culture models of HCV, for the first time there is the possibility of using complete inactive HCV as a vaccine (**Houghton et al. 2013)**. A relatively low dose of an inactivated genotype 2a cell culture strain (J6/JFH-1 cultured in Huh7 cells) induced the same level of cross-reactive nAbs as a 200-fold higher yield of recombinant protein (**Akazawa et al. 2013; intraperitoneal vaccination of BALB/c mice**).

Table 1-1 Primate and human studies describing candidate prophylactic HCV vaccines

Type of Vaccine	Investigator	Lead author	Year	Vaccine	Tested in	Adjuvant
Recombinant protein	Innogenetics	Leroux-Roels	2004	recombinant E1 (T2S-918/InnoVac-C)	Human n=20	alum
	Chiron/Novartis	Choo	1994	rE1E2	Chimpanzee n=7	MF59
		Frey	2010	rE1E2	Human n=60	MF59
	CSL Ltd.	Drane	2009	recombinant Core	Human n=30	ISCOMATRIX
	BPRC, Holland	Verstrepen	2011	recombinant E1 or E2	Chimpanzee n=4	alum
Peptide	Intercell AG	Firbas	2006	7 HLA-A2 restricted peptides (IC41)	Human n=128 (HLA-A2)	poly-l-arginine
		Firbas	2010	7 HLA-A2 restricted peptides (IC41)	Human n=54 (HLA-A2)	poly-l-arginine
Virally Vectored	Transgene Co.	Rollier	2007	DNA/MVA	Chimpanzee n=4	-
	Okairos Co.	Folgori	2006	Ad6/Ad24 + electroporated DNA	Chimpanzee n=5	-
		Fattori	2006	Ad6/Ad6/ChAd32	Rhesus Macaque n=3	-
	University of Oxford / Okairos Co.	Barnes	2012	Ad6/ChAd3	Human n=30	-
	NIH / Okairos Co.	Park	2012	Ad/DNA	Chimpanzee n=5	-
	NYC blood center	Youn	2008	recombinat vaccinia	Chimpanzee n=4	-
Other	NIH	Elmowalid	2007	Virus like particles	Chimpanzee n=4	AS01B

Ad: Adenovirus, numbers indicate type; ChAd: Adenoviruses of Chimpanzee origin; BPRC: Biomedical Primate Research HCV genetic material; HLA-A2: Human leukocyte antigen serotype A2; MVA: Non-replicative modified vaccinia ankara rE1 or E2: Chimpanzees were vaccinated either with recombinant E1 protein or with recombinant E2 protein; rE1E2:

Novartis is pursuing a vaccine consisting of recombinant HCV core protein (**figure 1-3**) produced in yeast, administered with a potent T-cell adjuvant immunostimulating complex matrix (IMX) (**Drane et al. 2009**). Promising results in rhesus macaques led to a phase I dose escalation trial in 30 healthy volunteers, where all but one showed vaccine induced antibodies against HCV core protein, but T-cells were detectable in only 2 volunteers receiving a high dose of vaccine (**Drane et al. 2009**). Limited by the amount of vaccine available, higher doses than 50 μg of recombinant core protein have yet to be tested.

The use of whole heat killed recombinant yeast that express targeted molecular immunogens (tarmogens) has also been assessed (**figure 1-3**) (**Habersetzer et al. 2009**). A core-NS3-5 fusion protein is encoded in the vaccine candidate GI-5005a and when combined with IMX and administered to 5 naïve chimpanzees a T-cell response was measurable in the liver and blood. Despite altered viral kinetics during the acute phase of infection in all vaccinated animals relative to controls, none cleared HCV after challenge (**Habersetzer et al. 2009**).

1.6.2 Peptide vaccines

Synthetic HCV peptides have been used to induce T-cell immunity through direct presentation on APCs. Peptide vaccines are HLA-specific and target only a selected subset of epitope sequences within HCV, limiting their breadth and coverage within the population but allowing closer control over the immunodominance hierarchy of the vaccine response.

Five synthetic HCV peptides containing T-cell epitopes (**figure 1-3**), administered with poly-L-arginine, make up the vaccine candidate IC41. When administered to 128 HLA-A2+ healthy volunteers in a phase I study IC41 was shown to be safe and immunogenic (**Firbas et al. 2006**). Few IFNγ producing cells were induced by IC41, as measured by IFNγ ELISpot (enzyme-linked immunoSpot assay; **Figure 1-4**; median of 30 spot-forming cells [SFC] per 10^6 peripheral blood mononuclear cells [PBMCs]). In the setting of chronic infection this vaccine caused a significant 0.47 log10 drop in HCV RNA, but this did not correlate with the size of the T-cell response (**Klade et al. 2012; Klade et al. 2008**).

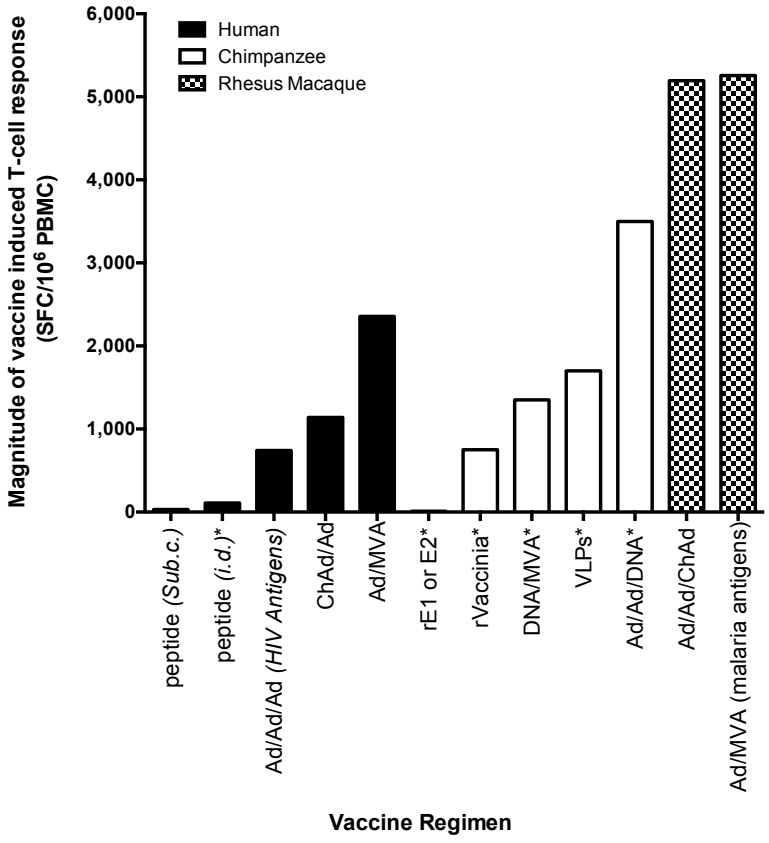


Figure 1-4 Peak magnitude of the T-cell response to candidate vaccines: A comparison of the magnitude of vaccine-induced T-cell responses in primates is shown (median of peak response after vaccination as measured by IFNγ ELISpot). Vaccines contained HCV antigens

unless otherwise stated. Successive vaccinations are separated by a forward slash, e.g., DNA/MVA refers to a vaccine regimen using DNA priming followed by an MVA boost. * Denotes approximation of published values. ChAd: Adenovirus of chimpanzee origin; i.d.: Vaccine was administered intradermally; rE1 or E2: Chimpanzees were vaccinated either with recombinant E1 protein or with Recombinant E1 or E2 protein; rE1E2: recombinant E1E2 heterodimer; Sub.c.: Vaccine administered subcutaneously; rVaccinia: Replication competent recombinant vaccinia vector. Taken from (**Swadling et al. 2013**).

1.6.3 DNA vaccines

Injection of recombinant plasmids has been shown to result in effective protein expression *in vivo* and a subsequent immune response in mice, but this initial success has not yet been translated well into man. DNA uptake and gene expression decreases with the size of the immunized host, however, there has been much development in technologies to improve cell transfection, such as transdermal delivery with the gene gun, and *in vivo* electroporation (**Sällberg et al. 2009**).

Plasmids encoding HCV NS3/4a (ChronVac-c) or core/E1/E2 (CIGB-230) have shown some efficacy as potential therapeutic vaccines for HCV, but there is no published data on their effectiveness as prophylactic vaccines (**Ahlen et al. 2005; Alvarez-Lajonchere et al. 2009**).

1.6.4 Viral Vectors

Over the last decade great advances in molecular virology have enabled the manipulation of viruses for delivery of foreign genetic material to mammalian cells (**figure 1-3; Table 1-1**). Their highly evolved mechanisms of cell entry and

gene expression within the host cell remain intact and viral vectors can be rendered non-pathogenic and non-replicative by deletions at specific locus (**Bråve et al. 2007; Capone et al. 2013**). Viral vectors are also self-adjuvanting and induce much of the acute innate immune response seen with replicative-competent viruses, as is attested by the local and systemic adverse events induced by vaccination. Some viral vectors at the earliest stages of testing as delivery vehicles for HCV genetic material include: alphaviruses, canary pox, ovine atadenovirus, and semliki-like virus (**Lin et al. 2008; Pancholi et al. 2003; Wüest et al. 2004; Brinster et al. 2002**).

Virus like particles (VLPs) are attractive vectors for gene delivery as they mimic the properties of native virions, are safe, and are easily manufactured. VLPs encoding the HCV core-E1E2 genes (**figure 1-3**) induced a large HCV-specific CD4+ T-cell population in chimpanzees (**figure 1-4)** and all four vaccinees cleared challenge with homologous strain of HCV (**Elmowalid et al. 2007**). Surprisingly, no HCV-specific antibody response was detected.

Adenoviral (Ad) vectors are perhaps the best characterized viral vectors and have emerged as the most potent at T-cell priming in non-human primates (NHP) and humans (**Casimiro et al. 2003; Chen et al. 2010; Capone et al. 2013**). Ad-based vaccines are particularly attractive gene vehicles as they can stably express large foreign inserts (~10kbp), they remain epichromosomal, and can be easily rendered replication defective by deletion of the E1 locus (**Bråve et al. 2007**; **Tatsis & Ertl 2004**).

The major limitation with the use of Adenoviruses is that pre-existing immunity to the vector can lead to its clearance before a responses is elicited to the inserted immunogen (**Zak et al. 2012; Casimiro et al. 2004; Lindsay et al. 2010**): this can in part be overcome by the use of rare subtypes that are of low seroprevalence, or the use of adenovirus with altered surface proteins. An extensive study of chimpanzee adenoviruses by researchers at Okairos (Napoli, Italy) isolated over a thousand strains and showed their immunogenicity in mice varied widely (**Colloca et al. 2012**). Chimpanzee adenovirus 3 (ChAd3) and Ad6 were selected for analysis in human and animal trials, with the whole non-structural region (NS) of HCV (genotype 1b, BK strain) due to their consistently strong immunogenicity (equal to that of Ad5) in rodents, NHP, and humans (**Barnes et al. 2012; Capone et al. 2006b; Antonella Folgori et al. 2006b; Quinn et al. 2015**).

Modified vaccinia Ankara (MVA) is another attractive vaccine vector due to its excellent safety record and immunogenicity in man. It has been shown to be particularly effective as a boosting vector, broadening and increasing the magnitude of pre-existing T-cell responses (**Barouch et al. 2012; Reyes-Sandoval et al. 2012; Casimiro et al. 2003; Capone et al. 2010; Stanley et al. 2014**). One of the greatest successes in modern medicine, the eradication of smallpox, using a replication-competent vaccinia virus highlighted it as a candidate vector. To improve safety attenuated vaccinia strains were generated and MVA has proved stably attenuated after serial passage in chicken embryo fibroblasts and six major deletions mean it is no longer replicative in mammalian cell lines. MVA has been widely used and a mass immunization

study in Germany of 120,000 people, including high-risk groups (elderly, alcoholics, those with allergies) showed good safety and tolerability. Viral replication is blocked late during infection of cells but importantly viral and recombinant protein synthesis is unimpaired.

A heterologous prime-boost regimen with DNA and MVA encoding core-E1-E2 (**figure 1-3**) and NS3 was tested in naïve chimpanzees by TRANSGENE (**Rollier et al. 2007**). A large T-cell response was seen post-vaccination by IFNγ and IL-4 ELISpot (**figure 1-4)**, but proliferative responses were transient and a high expression of IDO, CTLA-4 and PD-1 mRNA transcripts in the liver after challenge suggested induced T-cells could have been dysfunctional (**Rollier et al. 2007**). 3/4 went on to be chronically infected when challenged with a heterologous J4 strain of HCV. Using the malaria antigen ME.TRAP, priming vaccination with Ad elicited similar T-cell responses to Ad encoding HCV NS, and these responses were boosted 3-5 fold by vaccination with MVA containing ME.TRAP, showing the effectiveness of MVA as a boost vaccination for Ad-primed T-cell responses (**figure 1-4**)(**Capone et al. 2010**). Durable and uniform protection against Ebola was induced by ChAd3/MVA heterologous prime-boost vaccination, and not by ChAd3 prime or homologous ChAd3/ChAd3 or heterologous ChAd3/ChAd63 prime-boost when assessed in the macaque Ebola challenge model (**Stanley et al. 2014**). Protection by ChAd3/MVA was associated with a higher induction of anti-GP antibodies, and CD4+ and CD8+ T-cell responses and greater polyfunctionality of T-cells.

As discussed earlier, there is some evidence that T-cells alone, in the absence of a humoral response could mediate effective clearance of HCV, however, a cellular and humoral responses combine to control most, if not all viral infections, therefore the possibility of combining antibody and T-cell inducing vaccines should be considered. An adenovirus encoding full length or truncated E1E2 has been tested with a recombinant protein boost in mice and guinea pigs and has shown the induction of antibodies and T-cells which can control HCV pseuoparticles and cell culture-derived HCV (HCVcc) (**Chmielewska et al. 2014**).

1.6.5 Oxford's HCV vaccine programme - selection of vectors

Support for the use of Ad-based vaccines against HCV in man came from a trial in which chimpanzees received heterologous Ad6-Ad24 followed by further boosting with electroporated DNA, all containing the NS region of HCV (**figure 1-3**) (**Folgori et al. 2006b**). All vaccinated chimpanzees produced a high magnitude T-cell response (**figure 1-4;** peak total anti-HCV responses ranged from 615-2509 SFC/10^6 PBMC and 1108-7678 SFC/10^6 PBMC for CD4+ and CD8+ T-cells respectively) and when challenged with a heterologous HCV strain 4/5 cleared the virus (**Folgori et al. 2006b**). Vaccinated animals showed strong anamnestic responses that resulted in a blunted peak viraemia and shorter period of infection relative to controls. Prime-boost vaccination with heterologous adenovirus containing HCV NS also induced a large and broadly targeted HCV-specific T-cell response in rhesus macaques (**figure 1-4)** (**Fattori et al. 2006**).

On the strength of this pre-clinical data Oxford University, in collaboration with Okairos (now park of GSK) aimed to develop an Ad based prophylactic vaccine for HCV. The adenoviral vectors ChAd3 and Ad6 were tested in a phase I clinical trial in healthy volunteers (**Barnes et al. 2012**). All 10 healthy volunteers receiving the highest dose of Ad responded to vaccination, with peak T-cell responses averaging over 1000 SFC/10^6 PBMC (**figure 1-4;** range 443-4263). However, boosting with heterologous Ad in healthy volunteers was not as effective as predicted from the results in rhesus macaques, which is likely due to higher levels of cross-reactive antibodies against the Ads in humans (**Fattori et al. 2006; Barnes et al. 2012**). The major capsid protein in adenoviruses, hexon, is the main target for nAb, and despite ChAd3 being confirmed as a separate serotype to Ad6 (anti-sera against Ad5 and Ad6 were unable to neutralize ChAd3 in vitro), the homology between ChAd3 and Ad5 (both classified in subgroup C) may have lead to a immunogenicity-limiting cross-neutralising antibody response when ChAd3 and Ad6 were used in heterologous Ad/Ad vaccine regimens in humans (**Barnes et al. 2012**).

Building on the results outlined above, a trial to assess the safety and efficacy of a prime-boost regimen using ChAd3-NS boosted with MVA-NS in patients and healthy volunteers was performed (**Swadling et al. 2014**), the results of which are described in this thesis (**Chapters 3 and 4**), with comparisons to the previously tested ChAd3-NS/Ad6-NS regimen.

Both ChAd3-NS/Ad6-NS and ChAd3-NS/MVA-NS vaccine regimens have also been tested in HCV infected patients +/- PEG-IFNα/rib (vaccine trial HCV002; (**Kelly et al. 2015b**) and HCV003 arm B respectively) and the results of these trials will be discussed in **chapter 6**.

The ChAd3-NS/MVA-NS HCV vaccine regime has progressed to a phase II efficacy study, which will take place in an intra-venous drug using community in the US (NCT01436357). This study will be the first double blinded, randomized, placebo-controlled trial of a vaccine to prevent HCV persistence.

1.7 Vaccine Development Pipeline

The average vaccine takes approximately 11 years to develop from pre-clinical studies to licensing and has a market entry probability of just 6%, therefore, it is essential to gain as much information as possible on the potential efficacy of candidate vaccines at an early stage of testing (**Pronker et al. 2013**).

Figure 1-5 summarises how several research paths towards a HCV vaccine can be investigated in parallel, integrating information from basic research, natural history studies, and all phases of vaccine testing. A better understanding of the immune response to vaccination does not just lead to optimisation and assessment of that particular construct, but it can inform our understanding of the immune response to vaccination and HCV in general, and may help to identify correlates of protection (**figure 1-5**). Vaccination also offers a controlled antigen challenge model in which the timing, dose, and route of antigen

exposures is known and, therefore, data from these trials can inform our fundamental understanding of the biology of immunity and provide insight into the evolution of disease and help establish the signatures of effective immune responses.

1.7.1 Challenges

The prospects for a HCV vaccine have improved greatly in the last decade and there is now strong evidence from animal models that HCV is highly amenable to a prophylactic T-cell vaccine. Evidence from secondary infections in patients and from vaccine studies in humans and NHP show immunological memory can protect against persistence of HCV and therefore disease, and this protection appears to be prominently mediated by cellular immunity (**Osburn et al. 2010; Lauer et al. 2004; Dahari et al. 2010; Gerlach et al. 2003; Mehta et al. 2002**).

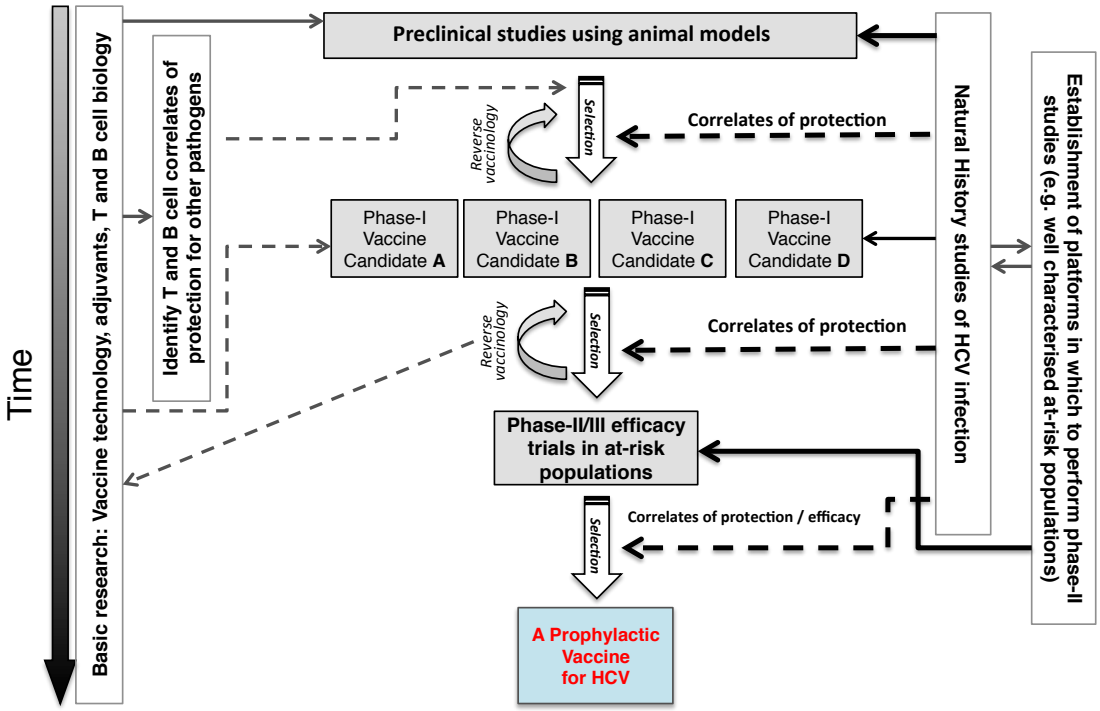


Figure 1-5 Progress to an effective prophylactic vaccine against HCV: A summary of some of the key interactions between basic research and vaccine studies is shown. Natural history studies of HCV infection are used to better understand the immune correlates of protection against HCV infection; the correlates of protection inform all levels of vaccine development, in particular, offering criteria in which to rank the potential of vaccines in preclinical and phase I studies and when selecting vaccines for which efficacy will be tested. Cohorts of at-risk populations need to be assessed in parallel with early-stage vaccine development so that they are well characterised before candidate vaccines can be tested in Phase II/III studies. Vaccine efficacy studies may be required to further define correlates of protection for optimal vaccine generation - a process termed "reverse vaccinology". Basic research into vaccine modalities, adjuvants and the biology of T and B cells can be fed into the process of vaccine development at all stages to allow us to better design, assess, and implement novel vaccines. HCV: Hepatitis C virus. Taken from (**Swadling et al. 2013**).

A major limiting factor when investigating the biology of HCV is its narrow species and tissue tropism, and the subsequent difficulties in developing cell culture or *in vivo* models of HCV (reviewed in (**Catanese & Dorner 2015**)). With

the exception of one genotype 2a HCV (JFH1) isolate, infection with patient-derived isolates does not result in productive infection *in vitro*, meaning opportunities for studying the life cycle of HCV and assessment of candidate vaccines are limited.

Much of our understanding of viral entry and replication and in the effectiveness of humoral and cellular immune responses to HCV is a result of the development of subgenomic replicon systems (**Lohmann et al. 1999**), HCV pseudoparticles (HCVpp)(**Bartosch et al. 2003**), and the first cell culture derived HCV (HCVcc; JFH1) (**Lindenbach & Rice 2005**). Chimpanzees (pan troglodytes) represented the only naturally permissive animal model for HCV and now, due to ethical regions, research using chimpanzees ceased in most countries in 2013, leaving the tree shrew (Tupaia belangeri) (**Xu et al. 2007**) and the pigtailed macaques (Macaca nemestrina) (**Sourisseau et al. 2013**) as the leading immunocompetent animal models available for investigation of HCV infection. Genetically humanised mouse models and human liver chimeric mice, with or without components of the human immune system, have been developed which allow *in vivo* assessment of HCV infection, however, they require much manipulation of the murine immune system (**Dorner et al. 2011; de Jong et al. 2014; Thibault & Wilson 2014**). An effective means to differentiate human embryonic stem cells (hESC) and induced pluripotency stem cells (iPSC) into hepatocyte-like cells, and culture methods for maintaining primary human hepatocytes remain elusive.

Other, non-technical challenges to the assessment of candidate HCV vaccines are

practical, financial, and ethical difficulties associated with characterising and vaccinating cohorts of HCV exposed individuals such as MSM, IVDU and prison inmates (**White et al. 2014**). The power required for assessing the efficacy of candidate prophylactic vaccines means in many developed countries with the infrastructure to monitor the outcome of vaccination incidence may be prohibitively low. Nevertheless, cohorts have been established and proof-of-concept phase II studies of prophylactic vaccines for HCV are underway (NCT01436357)(**White et al. 2014**).

1.8 A therapeutic vaccine

Therapeutic vaccination against chronic viral infections is a complex task because established viral infections may have already attenuated anti-viral immunity to allow viral persistence. Even in the setting of pharmacologically reduced or eradicated viraemia it is unlikely that the adaptive immune system will not bare some effects of the previous infection. Many of the mechanisms HCV uses to evade the T-cell response in primary infection will apply when exposing chronically infected or treated individuals to a vaccination.

There are three main mechanisms by which HCV subverts T-cell responses; i) immune escape, ii) regulation by Tregs, and iii) T-cell exhaustion.

1.8.1 Escape

T-cells recognize short viral peptide sequences (epitopes) presented in the groove of MHC class I and II alleles. Due to the inherent mutability of HCV,

viruses with variant sequences at these epitopes are produced daily, however, only under the selection pressure of the T-cell response do these variants become the dominant viral sequence because these mutations invariably involve a fitness cost to the virus as it is forced to move away from an optimal viral sequence (**Soderholm et al. 2006; Dazert et al. 2009; Neumann-Haefelin & Thimme 2007**). The emergence of viruses with variant sequences that are no longer effectively presented to, or recognized by, T-cells is termed 'immune escape' and it is a common mechanism by which HCV subverts the adaptive immune response (**Bowen & Walker 2005**). Variant epitope sequences can lead to a loss of recognition of infected cells because they are less well: processed to peptides, loaded on MHC molecules, or recognized in the context of peptide-MHC molecules. Nevertheless, T-cells which can effectively recognize the autologous virus within an infected individual do persist (**Cox et al. 2005)** and immune escape has rarely to date been seen in CD4+ T-cell epitopes (**Fleming et al. 2010; Fuller et al. 2010**).

Single source outbreaks involving a known single founding HCV sequence have proved informative in highlighting epitopes for which escape occurs as the 'footprint' of the escape is reproducibly seen in the viral sequence only in individuals with protective HLA alleles (as they can present the epitope and select out the variant sequences (**Fitzmaurice et al. 2011; Merani et al. 2011**). Some sections of the viral sequence are so essential to the functioning of the virus that they remain highly conserved despite being targets for T-cells; in this setting alternative methods for avoiding T-cell mediate clearance may be used by the virus.

1.8.2 Regulatory T-cells

A population of CD4+ regulatory T-cells (Tregs), defined by their expression of the transcription factor Forkhead box P3 (FoxP3) and high affinity IL-2 receptor (CD25) have been shown to have a broad negative regulatory effect on immune responses and are involved in establishing tolerance and preventing autoimmunity, but also in tempering expansion of antigen-specific T-cell responses to infection or vaccination (**Vignali et al. 2008**).

The liver infiltrating lymphocytes are particularly enriched for Tregs in healthy individuals and a number of groups have reported increased numbers of intrahepatic and peripheral Tregs during HCV infection, with associated functional regulation of the antiviral T-cell response (**Boettler et al. 2005; Cabrera et al. 2004; Losikoff et al. 2014; Sturm et al. 2010**). The role of Tregs in disease progression remains to be determined however, as their frequency has not been associated with fibrosis score (**Ward et al. 2007**). Tregs appeared to require cell-contact for inhibition of HCV-specific T-cell proliferation but were also able to secrete TGF-β and IL-10, which inhibit the secretion of IFNγ by stimulated HCV-specific T-cells (**Boettler et al. 2005; Cabrera et al. 2004**). It is not clear whether the functionality and frequency of Tregs normalizes after effective cure of HCV (**Spaan et al. 2015; Boettler et al. 2005**).

1.8.3 T-cell Exhaustion

Once persistent HCV infection is established T-cell responses are generally weak and narrowly focused (**Lauer et al. 2004**) and although they may remain detectable *ex vivo* and can be expanded *in vitro* (**Barnes et al. 2004**), they are generally dysfunctional or in a state of T-cell exhaustion (**Penna et al. 2007; Schulze et al. 2012; Day et al. 2006; Missale et al. 2012**). In particular the CD4+ T-cells are often primed but poorly sustained in those that go on to developed chronic HCV infection **(Schulze et al. 2012; Semmo et al. 2005**).

The key hallmarks of T-cell exhaustion are: i) weak or lacking ability to perform effector functions, in particular lacking the ability to secrete anti-viral cytokines; ii) co-expression of inhibitory receptors, including PD-1, Lag-3, Tim-3, CTLA-4; iii) an altered gene expression profile, particularly for transcription factors that are involved with T-cell differentiation status and functional capacity (e.g. Tbet, Eomes; (**Quigley et al. 2010; Kao et al. 2011; Paley et al. 2012; Doering et al. 2012**); iv) poor proliferative capacity on activation; v) defective homeostatic (antigen-independent) proliferation and extreme exhaustion leads to T-cell deletion (**Wherry & Ahmed 2004; Intlekofer et al. 2005; Shin et al. 2007**).

There appears to be a hierarchical loss of function when T-cells are over-stimulated, analogous to the hierarchical acquisition of functions with increased antigen and co-stimulation during T-cell priming (**Wherry 2011; McKinney et al. 2015; Wherry et al. 2003**). Physical deletion and more extreme exhaustion was observed for T-cells targeting well presented epitopes and a strong correlation between the viral load for a given infection (i.e. antigen levels) and level of exhaustion suggested antigen is the main driver of the loss of function

(**Wherry et al. 2003**). When comparing CD4+ and CD8+ T-cells in HIV-1 infected patients a higher viral load was associated with more extreme exhaustion and T-cells were generally IFNγ monoproducers, whereas T-cells of the same specificity in LTNPs were highly functional (reviewed in (**Seder et al. 2008**)(**Betts et al. 2006**). In patients where HIV-1 viral load and therefore antigen levels are controlled by HAART T-cell functionality was not discernible from T-cells in LTNPs (**Tilton et al. 2007**).

Exhaustion is thought to be driven by prolonged, high level antigen exposure in the context of signals from surface inhibitory receptors (**Wherry 2011**), with different combinations of inhibitory receptors being more or less important in the exhaustion of CD4+ (BTLA, PD-1, CTLA-4) or CD8+ (LAG-3, 2B4, CD160) T-cells, and even in a virus specific manner (**Bengsch et al. 2010; Bengsch et al. 2014**).

The extent to which T-cell exhaustion is reversible is an open question, but it is likely dependent on the severity of exhaustion (**Angelosanto et al. 2012**). Classic treatment of HCV with IFN-based therapy has not consistently been associated with improved T-cell responses (**Schirren et al. 2003; Kamal et al. 2002; Pembroke et al. 2012; Barnes et al. 2009; Burton et al. 2008**), however, recent data suggests that both NK and T-cell function may recover after all oral DAA therapy (**Serti et al. 2015; Martin et al. 2014**).

While some mouse studies demonstrate that exhausted T-cells become "antigen-addicted" and fail to survive upon antigen removal (**Wherry & Ahmed 2004;**

Shin et al. 2007) other studies suggest that on cure of chronic infection, some exhausted T-cells may persist (**Utzschneider et al. 2013; Angelosanto et al. 2012**) and recover functionality. Furthermore, it is clear that exhausted T-cells that persist are not inert, but mediate containment of chronic infections as they drive immune escape and containment of infection is lost on their depletion (**Li et al. 2005**).

The pharmacological reversal of exhaustion by inhibitory receptor blockade has demonstrated some re-invigoration of exhausted T-cells in mice (**Barber et al. 2006**) and humans (**Day et al. 2006; Golden-Mason et al. 2008; Nakamoto et al. 2009; Nakamoto et al. 2008**) and promising clinical trial data are emerging on inhibitory receptor pathway blockade in cancer (**Brahmer et al. 2010; Topalian et al. 2012**) and infectious disease (**Gardiner et al. 2013**). An important study in mice has shown that the window of opportunity for reversal by inhibitory receptor blockade may be relatively narrow, with later blockade in the LCMV exhaustion model being less effective (**Penaloza-MacMaster et al. 2015**); unfortunately late blockade also selectively expanded PD-1+ Tregs and depletion of CD4+ T-cells prior to blockade was needed for effective reinvigoration of T-cells which may not be a viable in humans (**Penaloza-MacMaster et al. 2015**).

Fundamentally, some reversal of T-cell exhaustion is possible but the safety profile of inhibitory receptor blockade may not be acceptable in the context of HCV infection.

1.8.4 Therapeutic vaccine trials

Immunotherapeutic vaccine approaches (reviewed in (**Halliday et al. 2011**)) have included HCV peptide vaccines (**Klade et al. 2012**) recombinant yeast expressing an HCV NS3-core fusion protein (**Habersetzer et al. 2009**), autologous dendritic cells loaded *ex vivo* with lipopeptides (**Gowans et al. 2010**) and DNA vaccines (**Alvarez-Lajonchere et al. 2009**). In each case only transient very low-level effects were seen on T-cell induction or HCV viral load. More recently repeated vaccination in HCV infected patients with MVA encoding HCV NS proteins in combination with PEG-IFNα/rib was associated with the induction of HCV-specific T-cells at low levels with a non-significant increase in SVR in the vaccinated group (**Di Bisceglie et al. 2014; Habersetzer et al. 2011**). However, studies of HCV immunotherapy have not evaluated the effect of vaccination in the context of the circulating viral sequence. Because of the inherent ability of HCV to mutate and escape T-cell immunity it is essential to assess whether T-cells induced by vaccination effectively recognise a patients autologous viral sequence.

1.8.5 Utility of a therapeutic vaccine

The utility of an immunotherapeutic approach for HCV can be debated. Recently licensed DAA therapies will transform our capacity to treat patients, with phase-IIb/III studies consistently showing viral clearance rates of >90% (**Afdhal et al. 2014**). However, impacting on the HCV epidemic may require the treatment of IVDUs who frequently live in chaotic social settings (**Martin et al. 2013**) –

therefore, vaccines administered as adjuvant immunotherapy that markedly shorten therapy duration, or the vaccination of cured individuals at risk of becoming reinfected would be beneficial.

In addition, the development of a prophylactic HCV vaccine remains an important goal and the assessment of T-cell induction in the presence of circulating viral variants may be readily assessed through therapeutic vaccine strategies, and so inform rational vaccine design.

1.9 Optimising virally vectored vaccines

1.9.1 Immunogen

The choice of immunogen is critical to the success of a vaccine, never more so than when targeting a highly variable pathogen such as HCV. The NS region is relatively well conserved across genotypes, it does not include the hypervariable regions in E1 and E2, and it represents approximately 2/3rds of the HCV genome. Such a broad approach increases the chances of including regions that are targeted by all HLA-alleles and which are cross-reactive between the genotype 1b vaccine sequence and other genotype and subtype HCV sequences.

Nearly half of the HCV infections worldwide are by genotype 1 viruses, and it is the dominant genotype in 85/117 countries where genotypic data is available (**figure 1-2**). 68% of the genotype 1 infections are attributable to subtype 1b (**Messina et al. 2014**), making it a good basis for a global vaccine. More than 90 CD4+ and 70 CD8+ T-cell epitopes have been identified within the NS region of

HCV (**Kuiken et al. 2005; Kim et al. 2012**) including several which have been directly associated with protection (**Fitzmaurice et al. 2011; Kim et al. 2011; Neumann-Haefelin & Thimme 2007; Dazert et al. 2009**). The NS region from NS3-NS5b from genotype 1b BK strain was selected for use in the virally vectored vaccines discussed in this thesis.

1.10 MHC class II invariant chain as an enhancer of vaccine-induced T-cells

Although robust immunity can be generated by current viral vectors approaches, the ability to enhance the magnitude of the T-cell response, to uniquely enrich responses for CD4+ or CD8+ T-cells, to adjust the differentiation status of the T-cells induced or to simply reduce the number of vaccinations needed would improve the versatility of viral vectors and could lead to improvements in efficacy of the plethora of virally vectored vaccines currently in development.

Many approaches have been taken in an attempt to improve T-cell response to genetic vaccines (DNA and virally vectored vaccines), such as the co-administration of potential adjuvants or the inclusion of genetic adjuvants encoded within the vector's genome. The inclusion of classic co-stimulatory molecules (4-1BBL, CD80. CD27L; **Kanagavelu et al. 2014; Gilligan et al. 1998; Bukczynski et al. 2004; Ohs et al. 2013**) and cytokines (IL-2, IL-7, IL-12, IL-15, GM-CSF; **Moore et al. 2002; Kanagavelu et al. 2014**) have had little if any effect on T-cell responses – in particular when progressing from murine models to testing in NHP, most likely due to the already adequate innate immune

activation afforded by viral vectors. The genetic adjuvant that has consistently shown the potential to enhance antigen-specific T-cell responses when linked to a transgene is MHC class II invariant chain (Ii or CD74).

It has recently been shown with DNA vaccines, lentiviral vectors, and both adenoviral and modified Vaccina Ankara vectors that linking the inserted immunogen to Ii can enhance the transgene-specific T-cell response (**Jensen et al. 2013; Holst et al. 2008; Holst et al. 2010; Capone et al. 2014**). This effect of encoded Ii has been seen with several antigens and in mice and NHP, showing it works by a highly conserved mechanism **(Capone et al. 2014; Holst et al. 2011; Mikkelsen et al. 2011**). Although initially included in DNA plasmid vaccines as a means for enhancing CD4+ T-cell responses, the effect of tethering Ii to an antigen is more pronounced on the CD8+ T-cell response to vaccination, by an unknown mechanism. In **chapter 5** I investigate the functional domains of Ii that are involved in this adjuvant effect and assess changes in intracellular antigen stability, processing, and presentation in an attempt to elucidate a mechanism for Ii as a genetic enhancer.

1.11 Background observations

This thesis is concerned with the detailed characterization of the immune response to vaccination with ChAd3-NS and MVA-NS in the immunologically diverse settings of healthy volunteers and chronic HCV infected patients. It also involved the continuing analysis of vaccination regimens using ChAd3-NS and Ad6-NS (in healthy volunteers; HCV001: in patients; HCV002). New technologies

for assessing the immune response in humans to a greater depth and resolution were assessed and optimized. A novel genetic adjuvant (the MHC class II invariant chain) - with the potential to enhance T-cell responses to all existing viral vectors, regardless of the antigens they encode - was investigated. Virally vectored vaccine were viewed as controlled antigen exposures and the immune response elicited was used to inform our basic understanding of the evolution of a T-cell response in man and the complexities within this response.

1.12 Key hypothesis tested in this Thesis

I tested the following hypotheses, with the ultimate goal of assessing and optimising the immunogenicity of HCV vaccines:

(1) Heterologous prime-boost vaccination with ChAd3-NS followed by MVA-NS can safely induce high magnitude, functional HCV-specific CD4+ and CD8+ T-cell memory responses in healthy volunteers, overcoming the limitations of vaccination with ChAd3-NS/Ad6-NS.

(2) Single cell analysis by mass cytometry and polychromatic fluorescence activated cell sorting will allow informative in-depth characterization of the T-cell response to vaccination and will show that ChAd3-NS/MVA-NS prime-boost vaccination induces CD8+ T-cells of high quality.

(3) Linking antigen to MHC class II invariant chain (Ii) within T-cell vaccines can enhance the magnitude, kinetics, and breadth of the CD8+ T-cell response without affecting T-cell phenotype or function. Tethering to Ii stabilises antigen or allows antigen to persist within APCs, allowing prolonged presentation and enhanced T-cell activation.

(4) Virally vectored vaccines can safely induce functional HCV-specific T-cells in patients with chronic HCV infection.

2 Material and Methods

Chapter 2 describes the materials and methods that are common to multiple chapters. Specific material and methods can also be found in each chapter.

2.1 Vaccine viral constructs & Immunogen

2.1.1 Adenoviral constructs (Ad6-NS and ChAd3-NS)

Non-replicative human Ad6 and chimpanzee-derived ChAd3 adenoviral vaccine vectors encoding the NS3-5B (NS) region of BK strain HCV have been described previously (**Folgori et al. 2006b; Colloca et al. 2012; Capone et al. 2006a; Fattori et al. 2006; Barnes et al. 2012**) and were manufactured at the Clinical BioManufacturing Facility (CBF) Oxford University. Adenoviral constructs were rendered replication-defective in mammalian cell lines by deletion of the E1 (essential for viral replication) and E3 loci (essential for counteracting *in vivo* eradication).

2.1.2 Modified vaccinia Ankara construct (MVA-NS)

The NS expression cassette was subcloned into the attenuated, non-replicating poxvirus MVA (modified vaccinia virus Ankara) shuttle vector pMVA-GFP-TD flanked by TKL (thymidine kinase gene left region) and TKR (thymidine kinase gene right region) generating the transfer vector pMVA-GFP-TD-NS. pMVA-GFP-TD-NS, drives the antigen expression using the vaccinia P7.5 early/late promoter, and expression

of Green Fluorescent Protein (GFP) using the fowlpox late promoter, FP4b. The production of the recombinant MVA-NS virus was based on *in vivo* recombination between the MVA-Red genome and homologous sequence (TKL and TKR) within the transfer vector pMVA-GFP-TD-NS. PCR was performed to check for the presence of NS transgene and absence of wt-MVA and MVA-Red virus. The MVA-NS is manufactured under Good Manufacturing Practice (GMP) conditions by the contract manufacturer IDT (Rosslau, Germany). Seed stocks of MVA-NS are now generated in the viral vector core, University of Oxford.

2.1.3 Immunogen

The immunogen for our virally vectored vaccines is the NS3-5B region (1985 amino acids; NS) of genotype 1b BK HCV strain (sequence accession number M58335; (**Folgori et al. 2006b; Colloca et al. 2012**)). The sequence is un-changed except for a point mutation (GlyAspAsp to AlaAlaGly) at positions 1711 to 1713 in the catalytic site of the NS5b which inactivates this RNA polymerase without reducing the expression of HCV proteins or processing of the polypeptide by the NS3 encoded protease (**Capone et al. 2006a**)**.**

2.2 Vaccine study designs and monitoring

2.2.1 Clinical trials

Descriptions of the trial arms, including number of participants, timing and dose of vaccinations received can be found in **Table 2-1**. The group sizes in this study are typical of those in a phase I study that needs to balance the requirement of meeting

the study end-points (safety and immunogenicity) with ethical and financial constraints.

A phase-I clinical trial of ChAd3-NS/Ad6-NS in healthy volunteers (**HCV001**) is registered in the ClinicalTrial.gov database (ID: NCT01070407; EudraCT N. 2007-004259-12). "A phase I study to assess the safety and immunogenicity of new Hepatitis C virus vaccine candidates ChAd3-NS and Ad6-NS."

A phase-I clinical trial of ChAd3-NS/Ad6-NS in HCV infected patients (**HCV002**) is registered in the ClinicalTrial.gov database (ID; EudraCT N. 2008-006127-32). "A Phase I study to assess the safety and immunogenicity of Ad6-NS and ChAd3-NS in patients with hepatitis C virus infection."

A phase-I clinical trial of ChAd3-NS/MVA-NS in healthy volunteers (**HCV003 Arm A**) and HCV infected patients (**HCV003 Arm B**) is registered in the ClinicalTrial.gov database (ID: NCT01296451; EudraCT Number: 2009-018260-10). "A Phase I study to assess the safety and immunogenicity of ChAd3-NS and MVA-NS in healthy volunteers and patients with hepatitis C virus infection"

Table 2-1 HCV vaccine trials described in this thesis

Table 2-1: Vaccine trials - Study arms, vaccinations given and dose, treatment given.

	Trial	Arm	n	Vaccines + Dose	Double prime	Treatment	Data Chapter
Healthy Volunteers	HCV003	A1	4	TW0:**MVA**	-	-	3
		A2	9	TW0:**ChAd3** TW8:**MVA**	-	-	3 /4
		A3	5	TW0:**ChAd3** TW8:**MVA** TW16:**ChAd3** TW24:**MVA**	-	-	5
		A4	4	Volunteers previously in Arm A2: TW0:**ChAd3** TW8:**MVA**	-	-	5
		A5	5	TW0:**ChAd3** TW8:**MVA** TW40:**MVA**	-	-	5
		A6	5	TW0:**ChAd3** TW8:**MVA** (2 x 10^7 pfu)	-	-	5
		A7	5	TW0:**ChAd3** TW8:**MVA** (2 x 10^6 pfu)	-	-	5
	HCV001^	A1	4	TW0:**Ad6** (5 x 10^8 vp) TW4:**Ad6** (5 x 10^8 vp) TW24:**ChAd3** (5 x 10^8 vp)	y	-	-
		A2	4	TW0:**Ad6** (5 x 10^9 vp) TW4:**Ad6** (5 x 10^9 vp) TW24:**ChAd3** (5 x 10^9 vp)	y	-	-
		A3	4	TW0:**Ad6** TW4:**Ad6** TW24:**ChAd3**	y	-	-
		A4	4	TW0:**Ad6** TW4:**Ad6** TW12:**ChAd3**	y	-	-
		B5	4	TW0:**ChAd3** (5 x 10^8 vp) TW4:**ChAd3** (5 x 10^8 vp) TW24: Ad6 (5 x 10^8 vp)	y	-	-
		B6	4	TW0:**ChAd3** (5 x 10^9 vp) TW4:**ChAd3** (5 x 10^9 vp) TW24: Ad6 (5 x 10^9 vp)	y	-	-
		B7	4	TW0:**ChAd3** TW4:**ChAd3** TW24:**Ad6**	y	-	-
		B8	4	TW0:**ChAd3** TW4:**ChAd3** TW12:**Ad6**	y	-	-
		C9	5	TW0:**Ad6** TW8:**ChAd3**	-	-	3
		C10	5	TW0:**ChAd3** TW8:**Ad6**	-	-	3
		C11	4	TW0:**ChAd3** (7.5 x 10^{10} vp) TW8:**Ad6** (7.5 x 10^{10} vp)	-	-	3

	Trial	Arm	n	Vaccines + Dose	Double prime	Treatment	Data Chapter
HCV+ Patients	HCV002	A1	2	TW14:**ChAd3** (5 x 10^8 vp) TW24:**Ad6** (5 x 10^8 vp)	-	peg-IFNa/Rib	6
		A2	2	TW14:**ChAd3** (5 x 10^9 vp) TW24:**Ad6** (5 x 10^9 vp)	-	peg-IFNa/Rib	6
		A3	6	TW14:**ChAd3** TW24:**Ad6**	-	peg-IFNa/Rib	6
		A4	6	TW2:**ChAd3** TW12:**Ad6**	-	peg-IFNa/Rib	6
		A5	4	TW14:**ChAd3** TW18:**ChAd3** TW28:**Ad6**	y	peg-IFNa/Rib	6
		A6	4	TW2:**ChAd3** TW6:**ChAd3** TW16:**Ad6**	y	peg-IFNa/Rib	6
		B1	2	TW0:**ChAd3** (5 x 10^8 vp) TW10:**Ad6** (5 x 10^8 vp)	-	-	6
		B2	2	TW0:**ChAd3** (5 x 10^9 vp) TW10:**Ad6** (5 x 10^9 vp)	-	-	6
		B3	4	TW0:**ChAd3** TW10:**Ad6**		-	6
	HCV003	B1	5	TW14:**ChAd3** TW22:**MVA**	-	peg-IFNa/Rib	6
		B2	5	TW2:**ChAd3** TW10:**MVA**	-	peg-IFNa/Rib	6
		C1	4	TW0:**ChAd3** TW8:**MVA**	-	-	6

Vaccine dose 2.5 x 10^{10} vp for Ads and 2 x 10^8 pfu for MVA unless otherwise stated. n = number of individuals

^ Used for comparisons with HCV003 only - Described in **Barnes *et al* 2012**

*Trial weeks for patients receiving peg-IFNa/Rib refer to weeks after start of treatment (duration of treatment 48 weeks)

All volunteers and patients gave written informed consent prior to enrolment and the studies were conducted according to the principles of the Declaration of Helsinki and in accordance with Good Clinical Practice (GCP). The clinical trials inclusion/exclusion criteria and discontinuation criteria can be found in **appendix 2-1**. Volunteers were recruited at the CCVTM (Centre for Clinical Vaccinology and Tropical Medicine), Churchill Hospital, Oxford. HCV+

Patients were recruited at the John Radcliffe Hospital, Oxford UK and at the Queen Elizabeth Hospital, Birmingham UK.

2.2.2 Vaccination route

All vaccines were administered intramuscularly (i.m.) in the deltoid region of the arm. The choice of the intramuscular route for Ads is based on the assumption that no co-infection of natural human adenovirus could occur at this site and there is a large body of data from clinical trials in humans using replication defective Ad5 and Ad6 based HIV-1 vaccines injected intramuscularly showing an excellent safety profile, no viral shedding, and high levels of immunogenicity (**Harro et al. 2009**). MVA-NS was given i.m. following data from A. Hill (**personal communication**) showing enhanced immunogenicity and less local reactivity (study Vac033) when MVA vectors are administered i.m. when compared to subcutaneous route.

2.2.3 Dose escalation

To determine the 'necessary and sufficient' dose capable of eliciting the desired T-cell response a dose escalation for ChAd3-NS and Ad6-NS was performed in healthy volunteers (**Barnes et al. 2012**) and in patients (**Kelly et al. 2015b**). The MVA dose was selected based on the use of MVA vectors in human studies (**Porter et al. 2011; Sheehy et al. 2012**). A dose de-escalation of MVA-NS performed in HCV003 arms A6 and A7 is described in **chapter 3**.

2.2.4 Safety

Volunteers systematically documented all symptoms and recorded a daily oral temperature. Solicited and unsolicited local and systemic adverse events were collected in diary cards and recorded in case report forms.

2.2.5 Viral load and full blood count (HCV002 and HCV003 Arm B)

Viral load and full blood count tests were performed by the John Radcliffe Hospital microbiology laboratory and biochemistry laboratories respectively. Viral kinetics were assessed using a quantitative DNA PCR (COBAS® AMPLICOR HCV Test, v2.0); lower limit of detection 15 IU/ml.

2.3 Blood processing

2.3.1 Plasma collection

6 ml of blood was collected in EDTA coated plasma tubes (K2EDTA vacutainer, BD 367839) or Sera tubes (SSTII advance vacutainers, BD 367958) and was centrifuged at 2000 g for 10 minutes at room temperature within 2 hours of collection. Supernatants (plasma or sera) were aspirated using and stored at -80 °C.

2.3.2 Peripheral blood mononuclear cell isolation, freezing, thawing

Peripheral blood mononuclear cells (PBMC) were isolated from whole blood (40-50mls collected per time point in Sodium heparin vacutainers, BD 368480) by layering blood diluted in RPMI on to Lymphoprep separation medium (Axis Shield

Diagnostics) and centrifuging at 2200 rpm (revolutions per minute) for 24 minutes at room temperature (with slow acceleration and braking). The layer of PBMC that forms is aspirated and washed in HBSS and centrifuged at 1700 rpm 7 minutes and then incubated for 5 minutes in ACK lysis buffer (Gibco #A10492-01) at room temperature before being washed in R10 at 1500 rpm 5 minutes and counted.

Cells were counted using a Guava Personal Cell Analysis system (Merck Millipore 0100-1430). The machine was calibrated daily using Guava check beads (4200-0070).

PBMC were cryopreserved in liquid nitrogen (-180 °C) in 1ml aliquots of 8-15x10^6 PBMC per vial in freezing medium (20% DMSO, 50% FCS and 30% RPMI) after freezing in “Mr frosties” at -80°C.

Vials of PBMC were warmed at 37 °C in a water bath until partially thawed and then were diluted gradually in 10mls of thawing medium (R10, 10% CTL wash CTL ltd ctlw-010, 30 U/ml DNAse Roche #10104159001), pelleted, and then washed in RPMI.

2.4 Peptides and Antigens

A set of 494 peptides, 15 amino-acids (aa) in length, overlapping by 11 aa (optimal for both CD4+ and CD8+ activation (**Kiecker et al. 2004**)) spanning the open-reading frame from NS3 to NS5B (1985 aa) of HCV genotype 1b strain BK (exactly matching the vaccine immunogen) were obtained from BEI resources (Full list of peptide sequences in **appendix 2-2**). Peptides were initially dissolved in dimethyl sulfoxide

(DMSO) and arranged into six pools labelled F to M and corresponding respectively to HCV viral proteins NS3p, NS3h, NS4, NS5A, NS5B I, NS5B II (**figure 2-1**; mean 82, range 73-112 peptides/pool). Each pool was split into 8-10 minipools (Fa, Fb, Fc etc) containing 9-12 individual 15mer peptides. For cross-reactivity experiments, similar peptide pools derived from HCV genotype 1a (H77 strain), genotype 3a (K3a; Genbank accession D28917), and genotype 4a (ED43; EMBL accession Y11604) HCV sequences were prepared identically. Optimal length peptides were purchased from Proimmune Ltd (Oxford, UK). Optimal peptides used to assess the cross-reactivity of HLA-B27 and HLA-B15 restricted protective epitopes were supplied by Christoph Neumann-Haefelin, University of Freiberg.

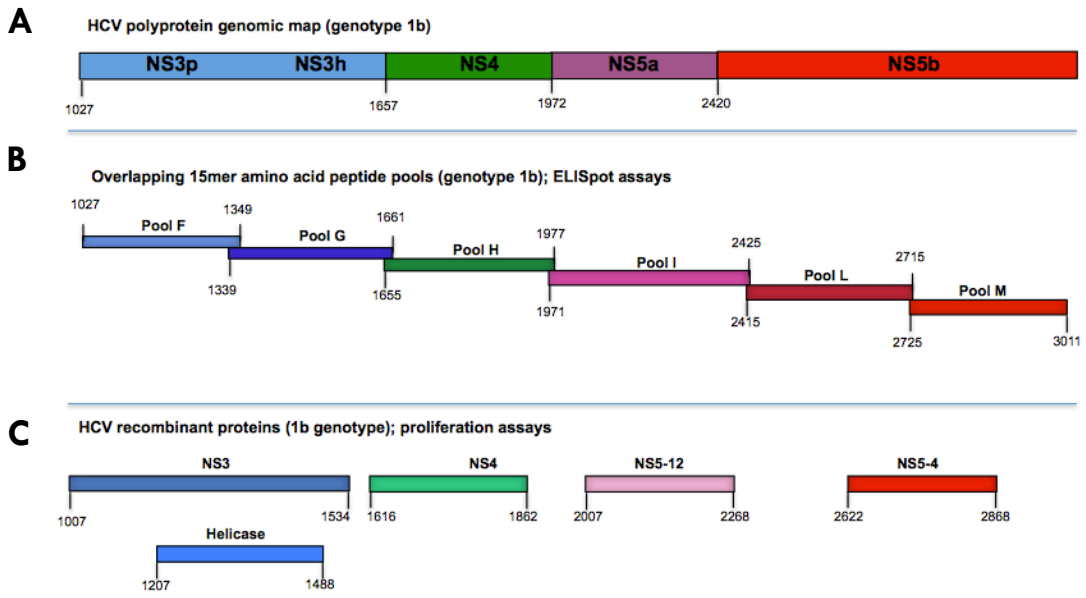


Figure 2-1 Peptide pools and recombinant proteins for immune assays: (**A**) Genomic map of HCV non-structural proteins (numbers denote amino-acid positions within the BK viral genome). (**B**) 15mer peptides overlapping by 11 amino-acids covering NS3-NS5b of BK viral genome were pooled into 6 overlapping pools (F-M) roughly corresponding to HCV protein products on protease cleavage of the HCV polyprotein. (**C**) Recombinant HCV proteins used in tritiated-thymidine incorporation assays are shown in relation to the HCV genome and peptide pools.

2.5 Enzyme-linked immunospot assay

2.5.1 ELISpot Assay

Ex vivo IFNγ ELISpot assays were performed as described previously on freshly isolated PBMC plated in triplicate at 1-2x10^5 PBMC per well (**Barnes et al. 2012**).

Millipore AIP plates (MSIP54510) were coated at 4 °C with 100 µl/well of anti-human IFNγ monoclonal antibody (5 µg/ml in PBS; MAbTech clone 1-D1K, cat. 3420-3) overnight or at 37 °C for 3 hours. Plates were then washed five times with PBS/0.05% tween and blocked by incubating with 200 µl/well of R10 for 2 hours at 37 °C.

Cells were incubated with either peptide pools (**figure 2-1)**, minipools, single 15mers, or optimal peptides (final concentration of 3 µg/ml per individual peptide) overnight (14-18 hours) at 37 °C. Internal controls for each sample were: DMSO (negative control, at the same volume as added with peptide), Concavalin A (1:200 dilution; positive control; Sigma C5275), FEC (3 µg/ml, mixed HLA class-I restricted peptides for Influenza virus, Epstein-Barr virus, and human CMV) and a CMV-lysate (virusys; 0.5 mg/ml diluted 1:100).

A commercially available pool of 15mer peptides (11 aa overlap) covering the hexon sequence from Ad5 were used to assess the induction of Ad-specific T-cells by ELISpot (Miltenyi 130-093-495).

The following day plates were washed 6 times with PBS/0.05%tween and the ELISpot plate was developed. Plates were incubated for 3 hours at room temperature with 100 µl/well of biotinylated mouse anti-human IFNγ monoclonal antibody (0.5 mg/ml; MAbTech clone 7-B6-1, cat. 3420-6) diluted in assay diluent (0.5% BSA/PBS). The plate was washed 5 times with PBS/0.05%tween and incubated with alkaline phosphatase-conjugated anti-biotin antibody diluted 1:750 in assay diluent (Vector Laboratories, cat. SP-3020) for 2 hours. The plate is then washed 4 times with PBS/0.05%tween and finally incubated at room temperature with 50 µl/well of filtered BCIP/NBT substrate solution (Pierce cat. 34042) for 7 minutes and washed with ddH_2O. Plates are air-dried overnight and read on an AID ELISpot plate reader.

2.5.2 Defining the positive cut-off for the ELISpot assay

Robust positive cut-offs for a single HCV-peptide pool (F-M) in healthy volunteers (48 SFC/10^6 PBMC) and patients (39 SFC/10^6 PBMC) were calculated by screening the peptide pools on 74 healthy HCV seronegative volunteers (**Barnes et al. 2012**) or using the DMSO (negative control wells) at screening of 58 HCV infected patients and taking the mean plus 3 standard deviations (**Kelly et al. 2015b**).

A positive response must exceed 3x background and a plate is failed if the DMSO negative control wells average > 11 spots per well (55 SFC/10^6 PBMC). Background wells (medium only, cells + DMSO) were typically 0-4 spots. Spot counts are converted to spots per million PBMC by multiplying by $\frac{1{,}000{,}000}{cells\ per\ well}$.

All results are quoted after background correction (the average response of the DMSO wells is subtracted from each positive pool). Total response to HCV NS was calculated by summing responses to positive pools after background correction.

In patients previously exposed to HCV or chronically infected, a vaccine-induced T-cell response was defined as either; i) a new positive pool response after vaccination that was not detected at baseline, or ii) an increase in T-cell response to a previously positive pool of >30% of baseline magnitude.

2.6 Fluorescence activated cell sorting (FACS)

2.6.1 MHC class I pentamer staining

PE (phycoerythrin) or allophycocyanin (APC)-labelled pentamers were obtained from ProImmune (**Table 2-2**). The specificity of pentamers against HCV epitopes was tested on HLA-matched pre-vaccination samples from healthy volunteers (**Barnes et al. 2012**). Control pentamers recognising CMV and FLU epitopes were also used (**Table 2-2**)

Pentamers were centrifuged at 4 °C (1400 g 10 minutes) and 1 µl was taken from the supernatant and used to stain 0.5-2 x 10^6 fresh or thawed PBMC in 50 µl PBS (dPBS Gibco 14190-094) in a 96-well plate. PBMC were then sequentially: stained with fixable NIR LIVE/DEAD dye (Life Technologies L10119) for 20 minutes, fixed for 20 minutes (1% paraformaldehyde), permeabilised for 30 minutes (for internal stains only; ebiosciences 10x perm buffer), and then stained with surface or internal

antibody cocktails separately for 30 minutes, all steps at room temperature. See **Table 2-3** (surface markers) and **Table 2-4** (Internal markers) for a list of markers in each panel.

Table 2-2 Antibody and fluorochrome/metal ion combinations used for staining PBMC

Antibody Target	CyTOF: Metal	CyTOF:Clone	FACS: Fluorochrome	FACS: Clone
Live/dead	Rh103	maleimide-DOTA	NIR (APC-Cy7)	Invitrogen
CD3 - Qdot	Cd112	S4.1 / Invitrogen	Pacific Orange	UCHT1 / Invitrogen
CD3 - Qdot	Sn114	S4.1 / Invitrogen	Pacific Orange	UCHT1 / Invitrogen
CD57	In115	HCD57 / Biolegend	-	-
Live/dead	La139	maleimide-DOTA	NIR	Invitrogen
Empty	Pr141	-	-	-
CD69	Nd142	FN50 / AbD Serotec	-	-
CD5	Nd143	UCHT2 / Biolegend	-	-
CD45RO	Nd144	UCLHL1 / Biolegend	-	-
CTLA4	Nd145	BNI3 / Beckton Dickinson	-	-
CD8	Nd146	SK1 / Biolegend	Pacific Blue	RPA-T8 / Beckton Dickinson
GMCSF	Sm147	BVD2-21C11 / Biolegend	-	-
CD45RA	Sm148	HI100 / eBioscience	FITC	HI100 / Beckton Dickinson
CD4	Sm149	SK3 / Biolegend	Qdot605	S3.5 / Invitrogen
MIP-1-β	Sm150	D21-1351 / Beckton Dickinson	PE	D21-1351 / Beckton Dickinson
Granzyme B	Eu151	GB11 / Abcam	AlexaFluor700	GB11 / Beckton Dickinson
TNFα	Sm152	Mab11 / eBiosciene	PeCy7	MAb11 / Beckton Dickinson
CD107α + CD107β	Eu153	H4A3 + H4B4 / Beckton Dickinson	-	-
CD27	Gd154	LG.7F9 / eBioscience	-	-
Tetramers	Gd155	Multiplexed	PE	-
CD13 + CD33	Dy156	WM15 / Biolegend; P67.6 / Santa Cruz	-	-
CD19	Gd157	HIB19 / Biolegend	-	-
CD16	Gd158	-	-	-
CD56	Tb159	NCAM16.2 / Beckton Dickinson	-	-
CD28	Dy160	CD28.2 / Beckton Dickinson	-	-
CD38	Dy161	HIT2 / Biolegend	PerCpCy5.5	HIT2 / Biolegend
γδ	Dy162	anti-FITC FIT-22 / Biolegend	-	-
Tetramers	Dy163	Multiplexed	PE	-
IL17	Dy164	BL168 / Biolegend	-	-
CD127	Ho165	A019D5 / Biolegend	APC	MB15-18C9 / Miltenyi
IL-2	Er166	MQ1-17H12 / eBioscience	APC	5344.111 / Beckton Dickinson
CD161	Er167	anti-APC APC003 / Biolegend	APC	191B8 / Miltenyi
CCR7	Er168	150503 / R&D	PeCy7	3D12 / Beckton Dickinson
Tetramers	Tm169	Multiplexed	PE	-
IFN-γ	Yb170	4S.B3 / eBioscience	AlexaFluor700	XMG1.2 / Beckton Dickinson
HLA-DR	Yb171	L243 / Biolegend	AlexaFluor700	G46-6 / Beckton Dickinson
CD40L	Tb172	24-31 / eBioscience	-	-
PD-1	Yb173	anti-PE PE001 / Biolegend	PeCy7	EH12.1 / Beckton Dickinson
CD62L	Yb174	DREG-56 / Biolegend	-	-
Tetramers	Lu175	Multiplexed	PE	-
Perforin	Yb176	B-D48 / Abcam	FITC	dG9 / Beckton Dickinson
CD25	-	-	Pe-Cy7	BC90 / Biolegend
FoxP3	-	-	Alexa700	PCH101 / ebiosciences
DNA	Ir191	dna intercalator	-	-
DNA	Ir193	dna intercalator	-	-
CCR4	-	-	PerCp-Cy5.5	TG6 / Biolegend
Tbet	-	-	BV605	4B10 / Biolegend
Eomes	-	-	eFluor660	WD1928 / eBiosciences
CD95	-	-	FITC / PE	DX2 / Miltenyi

Table 2-2 continued.

Virus + Peptide	Peptide Sequence	Metal Label Combination	FACS: Fluorochrome
HCV NS3 1406-1415	KLSGLGINAV	Gd155 + Dy163	PE or APC
HCV NS3 1073-1081	CVNGVCWTV	Gd155 + Tm169	PE
HCV NS3 1435-1443	ATDALMTGY	-	PE
CMV pp65 495-504	NLVPMVATV	Dy163 + Tm169	PE
FLU M1/MP 58-66	GILGFVFTL	Tm169 + Lu175	PE

For quantification of Treg subsets, frozen PBMC were thawed and stained with fixable NIR LIVE/DEAD stain, surface stained with CD3-PO, CD4-Qdot605, CD25-Pecy7, CD8-PB, CD127-APC antibodies, then fixed for an hour and stained with FoxP3-Alexa700 in permeabilisation buffer for 45-60 minutes according to ebiosciences One-step protocol for intracellular (nuclear) proteins using the Foxp3 / Transcription Factor Staining Buffer Set (00-5523-00). For intra-nuclear quantification of transcription factors T-bet and EOMES the same protocol was used. See **Table 2-5** Treg staining panel and **Table 2-6** for transcription factor panel**.**

2.6.2 FACS antibody titration

All FACS antibodies were titrated on the cell of interest at dilution factors between 1:5 and 1:400. A stain index for each antibody concentration was calculated (geoMFI positive gate – geoMFI negative gate / standard deviation of negative gate) and optimal concentration for a given staining protocol was chosen based on this.

2.6.3 Fluorescence minus one (FMO) and isotype controls

Where there was not a clear bimodal staining profile for an antibody to assist gating fluorescence minus one controls were performed – cells of interest were stained with the full FACS panel except one antibody and a comparison between stains with

and without a given Ab were used to define the gating strategy. For panels including MHC class I pentamers a CMV pentamer was used on a CMV+ healthy volunteers PBMC for FMOs. Isotype controls were used in rare cases where a difficulty in defining high and low expressing populations for a given marker was seen and to help pick optimal staining concentrations. Isotype controls and FC block were used in mouse experiments involving myeloid cells (**Maecker & Trotter 2006; Hulspas et al. 2009**).

Table 2-3 to Table 2-7 Antibody panels

Table 2-3: Pentamer staining surface panel

LSRII	Fluorochrome	Marker	Concentration
Blue	PE	Pentamer	1:50
	PeCy7	CCR7	1:50
	PerCp-Cy5.5	CD38	1:50
	FITC	CD45RA	1:50
Red	APC	CD127	1:50
	AlexaFluor700	HLA-DR	1:50
	APC-Cy7	L/D	1:1000
Violet	PB	CD8	1:200
	PO	CD3	1:50

Table 2-4: Pentamer staining internal panel

LSRII	Fluorochrome	Marker	Concentration
Blue	PE	Pentamer	1:50
	PeCy7	PD-1	1:50
	PerCp-Cy5.5	Granzyme A	1:100
	FITC	Perforin	1:50
Red	APC	CD161	1:100
	AlexaFluor700	Granzyme B	1:50
	APC-Cy7	L/D	1:1000
Violet	PB	CD8	1:200
	PO	CD3	1:50

Table 2-5: Treg staining Panel

LSRII	Fluorochrome	Marker	Concentration
Blue	FITC	CD45RA	1:50
	PeCy7	CD25	1:50
	PerCp-cy5.5	CCR4	1:25
Red	APC	CD127	1:50
	AlexaFluor700	FoxP3	1:12.5
	APC-Cy7	L/D	1:1000
Violet	Qdot605	CD4	1:200
	PB	CD8	1:200
	PO	CD3	1:50

Table 2-6:Transcription factor staining

LSRII	Fluorochrome	Marker	Concentration
Blue	PE	Pentamer	1:50
	PeCy7	CCR7	1:50
	Percp-Cy5.5	CD28	1:25
	FITC	CD95	1:50
Red	APC	EOMES	1:50
	AlexaFluor700	CD8	1:200
	APC-Cy7	L/D	1:1000
Violet	BV605	Tbet	1:25
	BV421	CD45RA	1:100
	PO	CD3	1:50

Table 2-7: Intracellular Cytokine staining panel

LSRII	Fluorochrome	Marker	Concentration
Blue	PE	Mip-1-β	1:100
	PeCy7	TNFα	1:25
	PeCy5	CD107α	1:20
Red	APC	IL-2	1:25
	AlexaFluor700	IFNγ	1:50
	APC-Cy7	L/D	1:1000
Violet	Qdot605	CD4	1:200
	PB	CD8	1:200
	PO	CD3	1:50

2.6.4 Intracellular cytokine staining (ICS)

ICS was performed as described previously (**Barnes et al. 2012**) on fresh PBMC or thawed PBMC after 3 hours resting at room temperature. Briefly, PBMC were stimulated using peptides in pool combinations (**figure 2-1**; F+G+H=NS3-4, I+L+M=NS5A-B, 1 μg/ml), or with individual pools, peptides (15mers and optimal 8mers, 1 μg/ml). The following controls were included for each sample: unstimulated negative control (DMSO), or PMA/Ionomycin positive control (50 and 500 ng/ml respectively). CD107α-PeCy5 was added at the time of stimulation. After overnight stimulation (Brefeldin A was added after 1 hour at 10 μg/ml), cells were stained with LIVE/DEAD Fixable Near-IR Dead dye, fixed (1% paraformaldehyde), permeabilised (ebiosciences 10x perm buffer) and stained with the following antibodies: CD3-PO, CD4-Qdot 605, CD8-PB, IFNγ-AlexaFluor700, IL-2-APC, TNFα-PE-Cy7, MIP-1β-PE. See **Table 2-5** ICS staining panel.

All ICS data are corrected for background by subtracting the cytokine production as a percentage of CD4+ or CD8+ T-cells in a matched unstimulated PBMC sample (DMSO negative control).

2.6.5 FACS Analysis

Photomultiplier tube (PMT) detector setup of FACS machines are shown in **Table 2-8**:

- BD LSRII (Peter Medawar building, Oxford, England)

- Mo-Flo (Peter Medawar building, Oxford, England)

- BD FACs Canto-II (CEINGE, Napoli, Italy)

Gating and analysis was performed in FlowJo (TreeStar). Cytokine co-expression and T-cell subset analysis (CD45RA vs CCR7 quadrants) was assessed using Boolean gating in Flowjo and graphs were produced using Pestle, and SPICE version 5.3, downloaded from http://exon.niaid.nih.gov (**Roederer et al. 2011**).

Table 2-8 Flow cytometer detector set up

Cytometer	LSRII					
Laser Name	**Wavelength**	**Detector**	**Channel**	**Mirror**	**Filter**	**Parameter**
Blue	488	A	7	755 LP	780/60 BP	PE-Cy7
		B	6	685 LP	695/40 BP	PerCP-Cy5-5
		C	5	655 LP	670/14 BP	PE-Cy5 / PerCp
		D	4	600 LP	610/20 BP	PE-Texas Red
		E	3	550 LP	575/26 BP	PE
		F	2	505 LP	530/30 BP	FITC /Alexa488
		G	1	-	488/10 BP	SSC
Violet	405	A	13	630 LP	655/8 BP	Qdot 655
		B	12	595 LP	605/12 BP	Qdot 605
		C	11	575 LP	585/15 BP	Qdot 585
		D	10	545 LP	560/20 BP	Qdot 565 / Pacific Orange
		E	9	475 LP	525/50 BP	AmCyan / Qdot625
						Qdot 525
		F	8	-	450/50 BP	Pacific Blue
Red	633	A	16	755 LP	780/60 BP	APC-Cy7 / APC- Alexa750
		B	15	710 LP	730/45 BP	Alexa Fluor 700
		C	14		670/14 BP	APC / Alexa647

Cytometer	Beckman Coulter MoFLo					
Laser Name	**Wavelength**	**Detector**	**Channel**	**Mirror**	**Filter**	**Parameter**
Blue	488	A	3	670LP	685/35 BP	PerCP-Cy5-5/PerCp
		B	2	505 LP	515/25 BP	FITC
		C	1	none	488/10	SSC
Green	532	A	8	740 LP	780/60	PE-Cy7
		B	7	685 LP	710/50	PE-Cy5.5
		C	6	635 LP	660/20	PE-Cy5
		D	5	600 LP	610/20	PE-Texas Red
		E	4	none	585/42	PE
Violet	405	A	11	600 LP	610/20	Qdot-605
		B	10	535 LP	560/40	Qdot565/Pacific Orange
		C	9	-	450/50	Pacific Blue
Red	642	A	14	740 LP	780/60 BP	APC-Cy7
		B	13	685 LP	710/50 BP	Alexa Fluor 700
		C	12	-	670/14 BP	APC

Cytometer	BD FACS Cantoll					
Laser Name	**Wavelength**	**Detector**	**Channel**	**Mirror**	**Filter**	**Parameter**
Blue	488	A	1	735 LP	780/60 BP	PE-Cy7
		B	2	655 LP	670 LP	PerCP / PerCp-Cy5.5
		C		610 LP		
		D	3	556 LP	585/42 BP	PE
		E	4	502 LP	530/30 BP	FITC / Alexa488
		F	5	-	488/10 BP	SSC
Red	633	A	6	735 LP	780/60 BP	APC-Cy7
		B		685 LP		
		C	7	-	660/20 BP	APC / Alexa647
Violet	405	A	9	502 LP	510/50 BP	AmCyan / Horizon 500
		B	8	-	450/50 BP	Pacific Blue / Horizon 450

2.7 *In vitro* T-cell lines

Short term CD8+ or CD4+ T-cell lines were generated by stimulating 2-4 x 10^6 PBMC in 1 ml of R10 in a 24 well plates with peptide (1 µg/ml) on day 0 and day 12. 50 U/ml of recombinant human IL-2 (Roche 11011456001) was added on day 4, 7, 12 and cells were harvested day 14-19.

2.8 Thymidine incorporation assay

Proliferation assays were performed on freshly isolated PBMC plated in triplicate at 2x10^5 PBMC per well (**Barnes et al. 2012**). Cells were stimulated with HCV proteins (**figure 2-1;** 1µg/ml; Mirkogen) for 5 days before addition of [methyl]-3H-thymidine (tritiated thymidine; Amersham Biosciences - TRA 120 specific activity 185 Gbq/mmol). The levels of incorporated tritiated thymidine, measured on a Packard bell Topcount NXT, in protein stimulated wells relative to unstimulated wells is used to calculate a SI (Stimulation Index; fold change above background). A positive response is defined as SI ≥3. Topcount NXT machine is calibrated weekly using a Perkin Elmer Cal/Norm Plate (7001044). Development of thymidine incorporation assays performed by Tony Brown.

2.9 Viral Sequence

2.9.1 HCV Viral Sequencing

Autologous viral sequencing was performed by Christabel Kelly (HCV002) and Johnny Halliday (HCV003) at baseline and viral relapse. Briefly, plasma was thawed and

concentrated (23,600 g at 4 °C for 60 minutes; 500 µl to 140 µl). Viral RNA was purified using QIAamp viral RNA mini kit (Qiagen 52904). Viral regions for sequencing were selected based on the location of previously mapped T-cell epitopes (vaccine-induced and pre-existing). RNA was reverse transcribed and 1st round PCR performed using Superscript III One-Step RT-PCR (Invitrogen) with specific primers and PCR cycling conditions (**appendix 2-3**). Second round PCR used High Fidelity *Taq* DNA polymerase (Roche). PCR products were gel or PCR purified (Qiagen). Products were sequenced bidirectionally using 2nd round internal primers and Prism Big Dye (Applied Biosystems) on an ABI 3100 automated sequencer. Cycling conditions were: 96 ˚C X 1 minute, followed by 30 cycles of 96 ˚C X 15 seconds, 50 ˚C X 10 seconds, 60 ˚C X 4 minutes. Sequences were analysed and aligned using Sequencher (v. 4.10.1) and Se-AI (v.2.0a11 http://tree.bio.ed.ac.uk/software/).

2.9.2 Sequence variability at T-cell epitopes at a population level

HCV sequences were downloaded from Los Alamos database (http://hcv.lanl.gov/content/index). Single variants with a prevalence of >5% were identified at each immunodominant epitope. Incomplete sequences and non-genotype 1a or 1b sequences were excluded. Sequence variability analysis performed by Christabel Kelly (**Chapter 6**) and Katrin Frohnmuller (**Chapter 3**).

2.9.3 IL28B genotyping

DNA was tested for polymorphism rs8099917 using ABI TaqMan allelic discrimination kit (Applied Biosystems) where G is the protective allele and T the risk allele as previously described. Performed by Rachel Townsend (**Bucci et al. 2013**).

2.10 Reagents

R10 – RPMI medium (GibcoBRL 11875-093) plus the following reagents: 10% by volume heat inactivated (1 hour 64 °C) fetal calf serum (FCS; Hyclone SH30070.03; a single defined batch was used for all experiments), 1% by volume 200 mM L-glutamine (GibcoBRL 25030-081) and 1% by volume 100x penicillin and streptomycin solution (GibcoBRL 15140-122).

RH10 – Prepared as above but using heat-inactivated (1 hour 64 °C) human serum (Sigma-Aldrich **H4522-100ML**) in place of FCS.

2.11 Adenoviral hexon neutralising antibody titers

Assessment of neutralizing antibody (nAb) titers against the adenoviral vaccine constructs was performed by staff at Okairos, Napoli Italy, on serum samples collected as above in Oxford. Briefly, $3.5x10^4$ HEK293 cells per well were seeded in a 96 well plate for 2 days. Each secreted alkaline phosphatase (SEAP)-expressing adenoviral vector was incubated for 1 hour at 37 °C alone or with serial dilutions of serum from trial volunteers, and was then added to the 95-100% confluent HEK293 cells, incubated for 1h and washed. SEAP expression was measured 24 hours later

using the chemiluminescent substrate (CSPD), from the Phospha-LightTM kit (Tropix Cat No T1016) without heat inactivation. Light emission (relative light units [RLU]) was monitored 45 minutes after the addition of the CSPD substrate using the Envision 2102 Multi-label reader (Perkin Elmer).

2.12 Statistical analysis

Data were analysed using GraphPad prism (version 6.0a). Nonparametric tests were used throughout (unless stated), paired for within-individual comparisons (Wilcoxon) and unpaired for group comparisons (Mann Whitney). Group averages are presented as medians unless otherwise stated. For correlations a nonparametric test was used (Spearman). For multiple comparisons a one-way ANOVA with Bonferroni correction was used. Two-tailed p values were used unless stated and a p value > 0.05 was considered statistically significant.

** = p ≤0.05; ** = p ≤0.01; *** = p ≤0.001; **** = p <0.0001*

3 Heterologous prime/boost vaccination strategies ChAd3-NS/MVA-NS vs. ChAd3-NS/Ad6-NS

3.1 Primary hypothesis

Heterologous prime-boost vaccination with ChAd3-NS followed by MVA-NS can safely induce high magnitude and functional HCV-specific CD4+ and CD8+ T-cell memory responses, overcoming the limitations of vaccination with ChAd3-NS/Ad6-NS.

3.2 Introduction

There is evidence to suggest HCV may be particularly susceptible to a T-cell based vaccine strategy and an effective vaccine against HCV is a highly desirable goal as it offers the most cost-effective and realistic means of drastically reducing the incidence of HCV infection globally. Viral vectors, in particular Ad and MVA based constructs, have emerged as some of the most potent vaccine strategies for priming and boosting antigen-specific T-cells.

In an attempt to overcome the issue of pre-existing anti-Ad immunity in humans, two low seroprevalence immunogenic adenoviruses, human Ad6 and chimpanzees ChAd3 encoding the HCV NS3-NS5B polyprotein, were assessed in a Phase I clinical trial in healthy volunteers (**Barnes et al. 2012**)(HCV001, **Table 2-1**). The magnitude and breadth of polyfunctional HCV-specific T-cells induced after a single priming vaccination with either vector was the most potent

described to date in human studies (**figure 1-4**) (**Barnes et al. 2012**). However, there were two limitations; firstly, heterologous Ad boosting failed to enhance T-cell responses above what is seen with priming. Subsequent analysis showed that this was most likely due to the induction of cross-reactive anti-Ad antibodies. This was unexpected since heterologous Ad/Ad vaccination using the same vectors in macaques had generated substantial responses after boosting (**Fattori et al. 2006**), suggesting that the vectors were serologically distinct. Secondly, CD8+ T-cells were the dominant subset induced by vaccination, whereas natural history, genetic and T-cell depletion studies show that both CD4+ and CD8+ T-cell subsets are critical for viral control (**Spada 2004; Lechner, Wong, et al. 2000; Lauer et al. 2004; Osburn et al. 2010; Urbani et al. 2006; Takaki et al. 2000; Gerlach et al. 1999)**.

I aimed to overcome these limitations by developing an HCV prophylactic T-cell vaccination strategy using the potent T-cell priming capabilities of ChAd3-NS but boosted with MVA-NS, so as to induce a more balanced CD4+ and CD8+ T-cell response, that is of higher magnitude both at the peak of response and in long term memory (**Mooij et al. 2008; Reyes-Sandoval et al. 2012**). As was described in depth in **Chapter 1,** effector and memory T-cells are highly heterogeneous in their function and phenotype. It is now clear that the overall quality, rather than any single parameter, such as magnitude, which determines the protective capacity of a T-cell response. I performed a comprehensive characterisation of vaccine-induced T-cell phenotype and functionality to assess the potential efficacy of this regimen as it moves to Phase II testing. Key parameter that can determine the protective efficacy of a T-cell response

(**Chapter 1**) were assayed longitudinally throughout the clinical trial for ChAd3-NS/MVA-NS regimen, with particular attention paid to the peak of the response (which may be most relevant to a therapeutic vaccination) and long-term after vaccination (of interest for a prophylactic vaccination). Where relevant, comparisons were made with T-cells induced by vaccination with a ChAd3-NS/Ad6-NS regimen and by natural infection with HCV and other viruses.

3.3 Key Questions

I address the following key questions:

1) Are ChAd3-NS and MVA-NS safe and well tolerated?
2) Does vaccination with MVA-NS effectively boost ChAd3-NS primed HCV-specific T-cell responses and is the magnitude of the surviving T-cell memory pool enhanced?
3) How broadly targeted is the T-cell response?
4) Are previously described 'protective epitopes' targeted?
5) Does the T-cell response show cross-recognition of non-vaccine HCV genotypes sequences?
6) Do the vaccine induced T-cells expand on re-exposure to antigen?
7) What capacity do these T-cells have for producing antiviral or immunomodulatory cytokines?
8) Do the induced CD8+ T-cells have the potential for cytolytic killing of target cells?
9) What is the phenotype of vaccine induced T-cells and is this influenced by the vaccine vector used to deliver the HCV NS genes?

Much of this work made up the manuscript: **Swadling** *et al*. A human vaccine strategy based on chimpanzee adenoviral and MVA vectors that primes, boosts, and sustains functional HCV-specific T cell memory. **Science Translational Medicine. 2014 Nov 5;6(261):261ra153.**

3.4 Chapter specific material & methods

3.4.1 Clinical trials

The volunteer group protocols discussed specifically in this chapter are described in **Table 3-1.** The clinical trials HCV003 and HCV001 are described in more detail in chapter 2. Briefly, healthy volunteers in arm A2 HCV003 were vaccinated i.m. with ChAd3-NS (2.5 x 10^{10} vp) and boosted 8 weeks later with MVA-NS (2 x 10^{8} pfu), both encoding NS (non-structural region of HCV genotype 1b BK strain, NS3-NS5B). Volunteers in Arm A1 HCV003 received a single MVA-NS vaccination (2 x 10^{8} pfu). Data from HCV003 was compared with historic data, or fresh analysis performed on frozen samples from the HCV001 trial, in which 9 volunteers received 2.5-7.5 x 10^{10} vp of ChAd3-NS followed by 2.5-7.5 x 10^{10} vp of Ad6-NS 8weeks later. The higher dose of 7.5 x 10^{10} vp of Adenoviral vector was used in 4/9 volunteers and showed no difference in immunogenicity to 2.5 x 10^{10} vp (**Barnes et al. 2012**).

Table 3-1: Vaccine trials described in chapter 3

	Trial	Arm	n	Vaccines + Dose
Healthy Volunteers	HCV003	A1	4	TW0: **MVA**
		A2	9	TW0: **ChAd3** TW8: **MVA**
		A3	5	TW0: **ChAd3** TW8: **MVA** TW16: **ChAd3** TW24: **MVA**
		A4	4	Volunteers previously in Arm A2: TW0: **ChAd3** TW8: **MVA**
		A5	5	TW0: **ChAd3** TW8: **MVA** TW40: **MVA**
		A6	5	TW0: **ChAd3** TW8: **MVA** (2×10^7 pfu)
		A7	5	TW0: **ChAd3** TW8: **MVA** (2×10^6 pfu)
	HCV001^	C10	5	TW0: **ChAd3** TW8: **Ad6**
		C11	4	TW0: **ChAd3** (7.5×10^{10} vp) TW8: **Ad6** (7.5×10^{10} vp)

Vaccine dose 2.5×10^{10} vp for Ads and 2×10^8 pfu for MVA unless otherwise stated.
^ Used for comparisons with HCV003 only - Described in **Barnes et al. 2012**

3.4.2 Immunoassays

Immunoassays are described in full in **Chapter 2** (Material and Methods). Briefly, PBMC stimulated with pools, minipools, or individual HCV peptides were tested in triplicate for their IFNγ production by ELISpot, or for the overnight induction of cytokines by ICS. Proteins covering the NS region encoded in the vaccine were used in 5-day proliferation assays, measured using the incorporation of tritiated-thymidine. HCV-specific class-I pentamer+ T-cell populations induced by vaccination were phenotyped directly *ex vivo* using multiparametric flow cytometry.

For the following chapter heterologous prime-boost vaccination with ChAd3-NS, followed 8 weeks later by Ad6-NS, will be referred to as ChAd3-NS/Ad6-NS, and prime-boost vaccination with ChAd3-NS, followed 8 weeks later by MVA-NS, will be referred to as ChAd3-NS/MVA-NS.

3.5 Results

3.5.1 Vaccination with ChAd3-NS and MVA-NS is safe and well tolerated

The majority of local and systemic adverse events (AEs) were mild or moderate (92%), they resolved within 48 hours, and no serious AEs were recorded. Systemic AEs were more common following MVA-NS (mean number/volunteer; 4.1 MVA-NS vs. 1.9 ChAd3-NS p=0.032). The proportion of volunteers experiencing one or more moderate/severe AE was not significantly different between the two vaccines (p = 0.689). Severe adverse events were observed in 5 volunteers post-MVA-NS and 2 volunteers post-ChAd3-NS (local pain/swelling, fatigue, migraine and feverishness) but these resolved within 24-48 hours. Overall, both ChAd3-NS and MVA-NS were very well tolerated with no serious adverse reactions (**figure 3-1**).

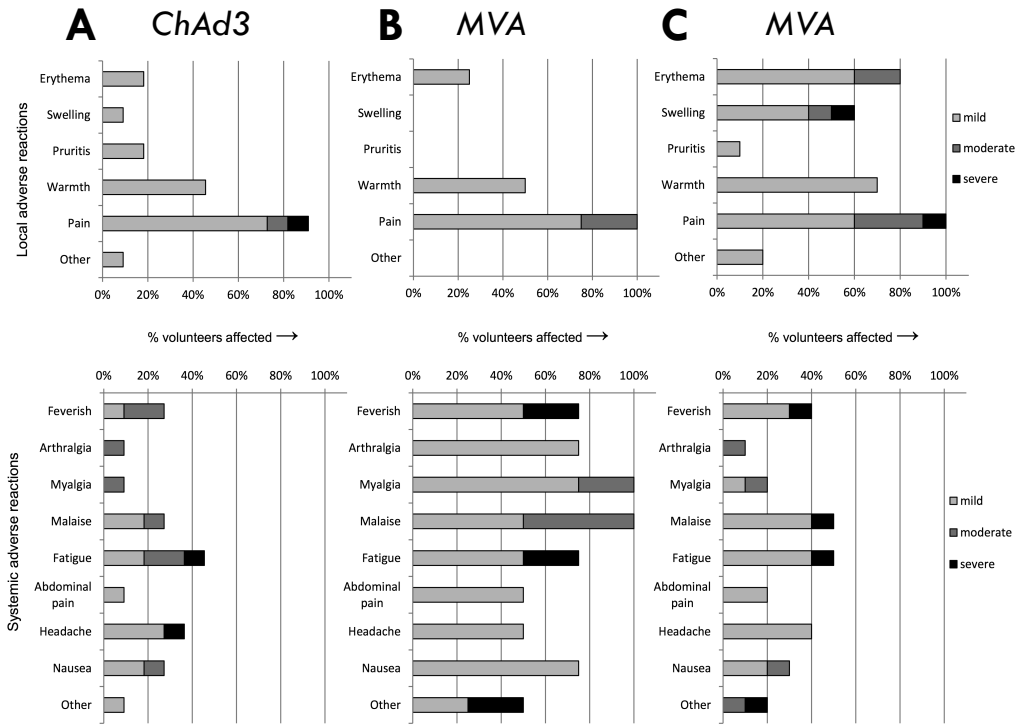


Figure 3-1 Safety data after vaccination: Safety data is shown following vaccination with ChAd3-NS (**A**) and MVA-NS as either prime (**B;** Arm A1, n=4) or boost (**C;** Arm A2, n=10). The percentage of volunteers with local (top panel) and systemic (bottom panel) adverse reactions are shown and shaded to indicate severity. Safety data were compiled by Richard Antrobus.

3.5.2 MVA-NS optimally boost HCV-specific T-cell responses primed by ChAd3-NS and induces a higher magnitude memory T-cell response

It has been previously shown that boosting with heterologous Ad6-NS does not enhance anti-HCV T-cell responses above the magnitude observed with ChAd3-NS prime vaccination in humans (**Barnes et al. 2012**). I evaluated the immunogenicity of a heterologous MVA-NS boost (2 x 10^8 pfu) 8 weeks post ChAd3-NS (2.5 x 10^{10} vp) prime in 9 healthy volunteers (Arm A2). All volunteers responded to ChAd3-NS prime, peaking 2-4 weeks after vaccination (median 1140, range 87-4427 spot forming cells [SFC]/10^6 PBMC; **figure 3-2A**). HCV

specific T-cell responses were significantly enhanced by MVA-NS boost in all volunteers, peaking 1-week post vaccination (median 2355, range 1490-6117, SFC/10^6 PBMC; peak post ChAd3-NS prime vs. peak post MVA-NS boost p=0.0039; **figure 3-2A-B**). In comparison to ChAd3-NS/Ad6-NS vaccination, ChAd3-NS/MVA-NS generated responses that were more sustained over time, and significantly greater in magnitude at the end of the study (EOS) 34-36 weeks after prime vaccination (**figure 3-2B-C;** median 443, range 138-1783 vs. median 98, range 10-1092 SFC/10^6 PBMC p=0.0109:). The peak response post MVA-NS was predictive of the size of the memory T-cell population (TW9 vs. TW34 [EOS]; Linear regression R^2=0.784, P=0.0034; **figure 3-2D**).

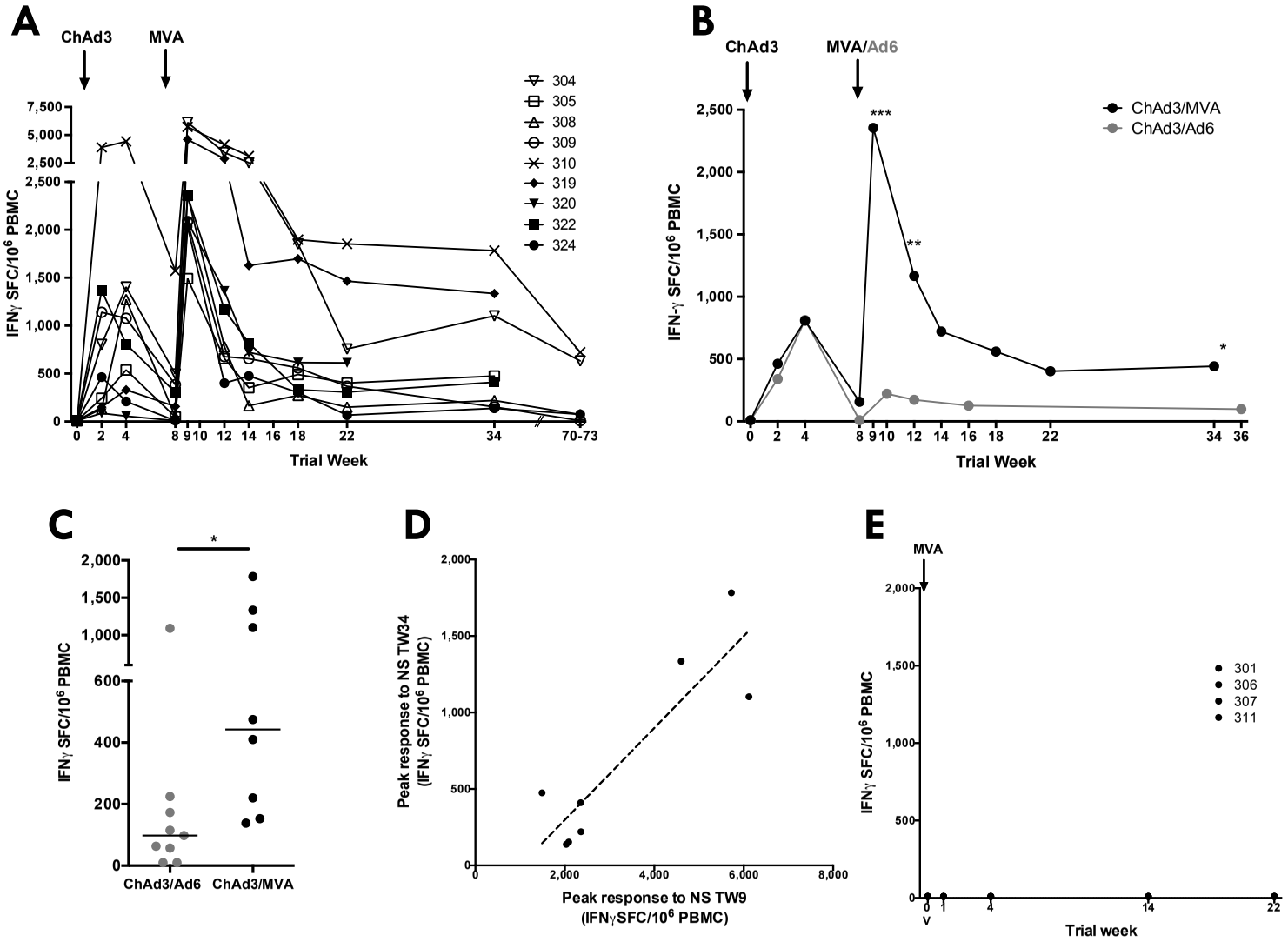

A
ChAd3
MVA
304
305
308
309
310
319
320
322
324
IFNγ SFC/10^6 PBMC
Trial Week
B
ChAd3
MVA/Ad6
ChAd3/MVA
ChAd3/Ad6
***
**
*
IFN-γ SFC/10^6 PBMC
Trial Week
C
*
IFNγ SFC/10^6 PBMC
ChAd3/Ad6
ChAd3/MVA
D
Peak response to NS TW34 (IFNγ SFC/10^6 PBMC)
Peak response to NS TW9 (IFNγSFC/10^6 PBMC)
E
MVA
301
306
307
311
IFNγ SFC/10^6 PBMC
V
Trial week

Figure 3-2 Magnitude of the T-cell response to HCV NS after ChAd3-NS/MVA-NS vs. after ChAd3-NS/Ad6-NS vaccine regimens: (A-E) The total *ex vivo* IFNγ ELISpot response to the NS region of HCV after vaccination (summed positive peptide pools responses corrected for background; see Materials and Methods 2.4). Arrows indicate vaccinations, and trial week indicates weeks since prime vaccination. (**A**) The kinetics of the response in volunteers who received ChAd3-NS/MVA-NS vaccination (n=9). Four volunteers were assessed at an extra time point a year and half after initial vaccination (TW70–73). (**B**) The median response to HCV NS for volunteers receiving ChAd3-NS/MVA-NS (black; n = 9) vs. ChAd3-NS/Ad6-NS (gray; n = 9). (**C**) A comparison of the total HCV NS response at TW34–36 in volunteers receiving ChAd3-NS/MVA (black) or ChAd3-NS/Ad6-NS (gray) vaccinations (P = 0.0109*). (**D**) Magnitude of response to HCV NS at the peak after MVA-NS vaccination (TW9) versus the end of the study (TW34) with linear regression (n=8; no TW34 data available for volunteer 320). (**E**) Magnitude of total response to HCV NS in four volunteers receiving MVA only as a prime vaccination.

The magnitude of the T-cell responses following MVA-NS boost vaccination, was significantly associated with magnitude at the time of boost (TW8 vs. TW9; R^2= 0.68 p=0.0429; not shown), which suggests that MVA is boosting pre-existing responses rather than priming new responses. HCV-specific T-cells remained detectable by IFNγ ELISpot in 4/5 patients tested at weeks 70-73 after their ChAd3-NS prime vaccination (median 302, range 10-732 SFC/10^6 PBMC; **figure 3-2A**).

MVA-NS was ineffective as a prime vaccination. No HCV specific T-cell response was detected in the four volunteers vaccinated with $2x10^8$ pfu MVA-NS prime alone (Arm A1; **figure 3-2E**).

To assess a possible non-specific 'bystander' expansion of non-HCV Ag-specific T-cells after vaccination, I monitored the T-cell response to HLA class I Influenza

(Flu), EBV and CMV epitopes, and to CMV lysate by IFNγ ELISpot; no change in the magnitude of the responses to these antigens was observed (**figure 3-3**).

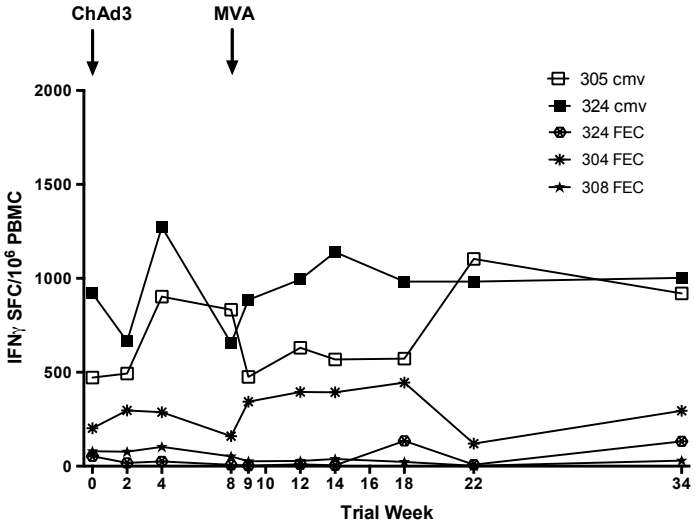


Figure 3-3 Magnitude of Flu, EBV and CMV-specific T-cell responses across the vaccine trial: PBMC from vaccinated volunteers were stimulated with a FEC peptide pool (see methods) and a CMV lysate and IFNγ producing cells were monitored by ELISpot at several time points throughout the vaccine trial.

3.5.3 Regulatory T-cells are not expanded after ChAd3-NS/MVA-NS vaccination

Due to the high magnitude T-cell response to our vaccines I assessed whether a transient or long-term expansion of Tregs occurred. Tregs persist due to homeostatic signalling by IL-2, but independently of IL-7 signalling; they therefore express CD25 (IL-2Rα) but relatively low levels of CD127 (IL-7Rα) compared to conventional CD4+ T-cells. A combination of staining with CD25, CD127 and FoxP3 has been used to define Tregs in the blood (**Mason et al. 2015; Liu et al. 2006; Seddiki et al. 2006; Miyara et al. 2009; Yu et al. 2012**).

Regulatory T-cells were quantified by FACS in 5 volunteers over the course of the

vaccine trial to assess whether expansion from baseline levels occurred at the peak of the HCV-specific T-cell response after prime or boost vaccination and whether the long-term Treg population was changed (**figure 3-4**). No significant change in the magnitude of Treg subsets was seen at any time point, and levels of Tregs in vaccinated volunteers were comparable to those seen in PBMC from 8 healthy unvaccinated volunteers (**figure 3-4**). HCV-specific T-cells are specifically induced by ChAd3-NS/MVA-NS vaccination without parallel induction of Tregs in the blood.

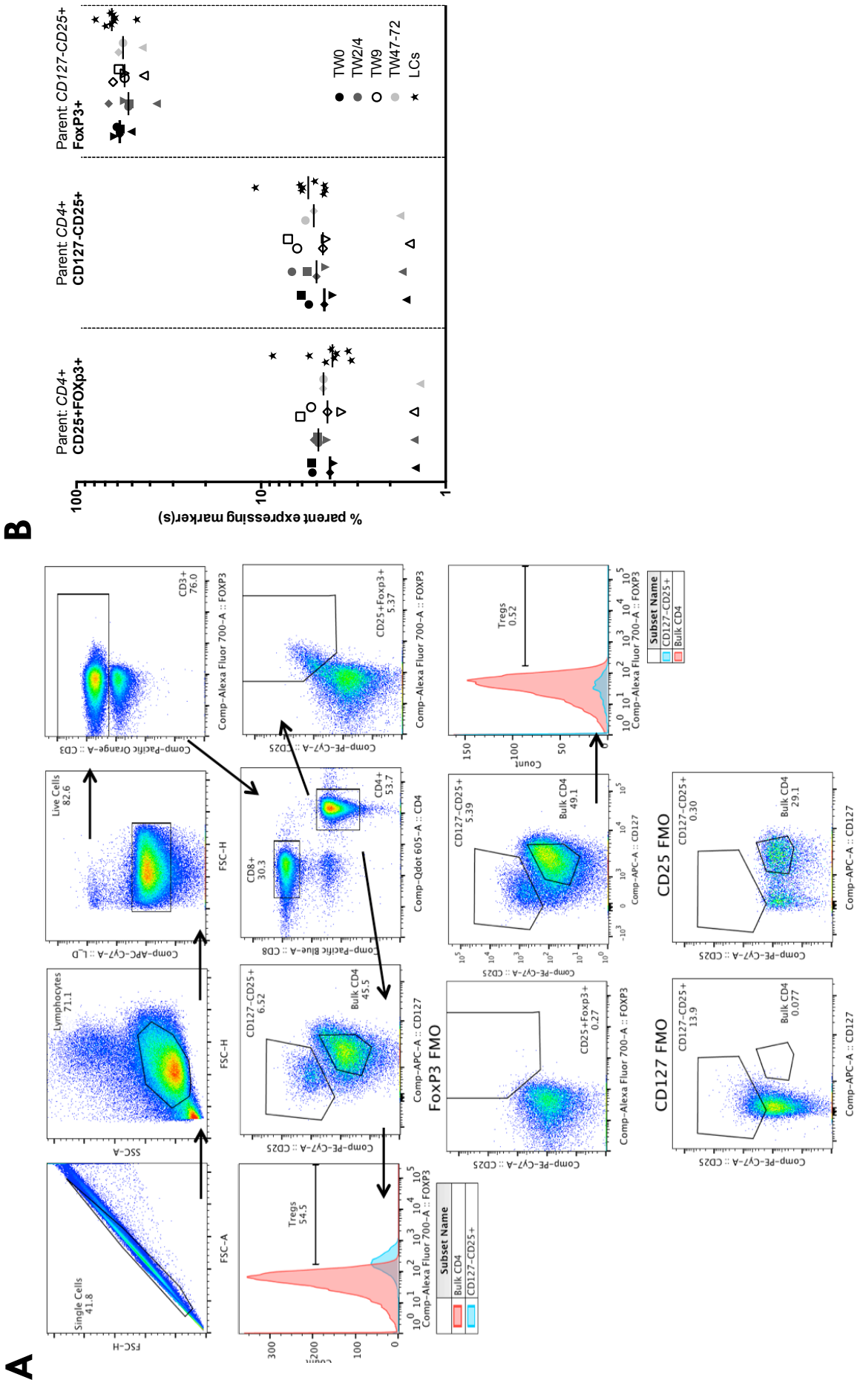

A
B
% parent expressing marker(s)
Parent: CD4+ CD25+FOXp3+
Parent: CD4+ CD127-CD25+
Parent: CD127-CD25+ FoxP3+
TW0
TW2/4
TW9
TW47-72
LCs
FoxP3 FMO
CD25 FMO
CD127 FMO
Subset Name
Bulk CD4
CD127-CD25+

Figure 3-4. CD4+ Tregs across the vaccine trial: (**A**) The gating strategy and FMO stains used to identify Tregs by FACS is shown (staining performed on volunteer 319 at TW9 except FMOs, which were performed on PBMCs from a healthy lymphocyte cone). (**B**) The percentage of CD4+ T-cells that were CD25+Foxp3+ or CD127-CD25+, and percentage of CD127-CD25+ that were Foxp3+ is shown for 5 vaccinated individuals pre-vaccination (TW0), at the peak of anti-HCV T-cell response after ChAd3-NS vaccination (TW2-4), at the peak anti-HCV T-cell response after MVA-NS boost vaccination (TW9) and at the end of the study (TW47-72; n=3). Individuals are identified by different symbols; bars show median values. The magnitude of Treg subsets is also shown for PBMCs from 8 healthy unvaccinated lymphocyte cones (LCs; stars).

3.5.4 MVA-NS boosts a broader HCV-specific T-cell response

The number of discrete antigenic targets induced in volunteers with diverse HLA allele combinations were measured to get an indication of the breadth of response to vaccination. The breadth of the response was defined as the number of pools, minipools, 15mer peptides, or individual epitopes targeted by the T-cells induced by vaccination (see section **2.4** for description of pools / minipools / 15mers / optimal peptides).

First I compared the breadth of T-cell responses induced by ChAd3-NS/MVA-NS to that induced by ChAd3-NS/Ad6-NS, using overlapping peptides covering the entire immunogen in 6 peptide pools. Boosting T-cell responses with MVA-NS enhances the breadth of the T-cell response, significantly increasing the peak number of peptide pools targeted (**figure 3-5A**; p = 0.0156*) and the magnitude of the response to each pool (not significant for pool I; **figure 3-5B**), when compared to ChAd3-NS prime in matched individuals. T-cell responses to HCV NS were significantly broader at the peak (p = 0.0010**) and long-term (p =

0.0355*) after MVA-NS boost compared to Ad6-NS boost and most individuals responded to all 6 peptide pools after boost vaccination (range 4-6; **figure 3-5A-C**). Although all peptide pools were targeted in patients from diverse HLA backgrounds (**figure 3-5C**), responses to NS3h dominated after both ChAd3-NS prime and MVA-NS boost (p = 0.0033; **figure 3-5B**). MVA-NS boost increased the magnitude, but did not affect the overall hierarchy of HCV antigen recognition (**figure 3-5B**).

Further dissection of responses at the minipool level (8-11 minipools per pool e.g. Fa-Fh) revealed that the mean number of minipools targeted after ChAd3-NS/MVA-NS was significantly higher after MVA-NS boost (ChAd3-NS/MVA-NS = 11 minipools targeted and ChAd3-NS/Ad6-NS = 2.3, p = 0.0011** tested 4 weeks post boost), with one volunteer targeting 31 of the 49 minipools covering HCV NS (310; **Table 3-2 and figure 3-5D*)***. Mini-pool analysis was performed at TW12, after some contraction of the T-cell response; therefore, the true number of epitopes targeted in each subject may be underestimated.

Where possible, minipools were mapped to individual 15mers, and optimal length peptides. Reactivity to a minipool in all cases corresponded to specificity for a single epitope in that minipool (**Table 3-2**). Responses to two immundominant epitopes located in NS3h restricted by HLA-A1 and HLA-A2 (marked bold in **Table 3-2**) were particularly prevalent and were selected for subsequent pentamer analysis (HCV $NS3_{1406-1415}$, KLSALGINAV; HCV $NS3_{1435-1443}$, ATDALMTGY).

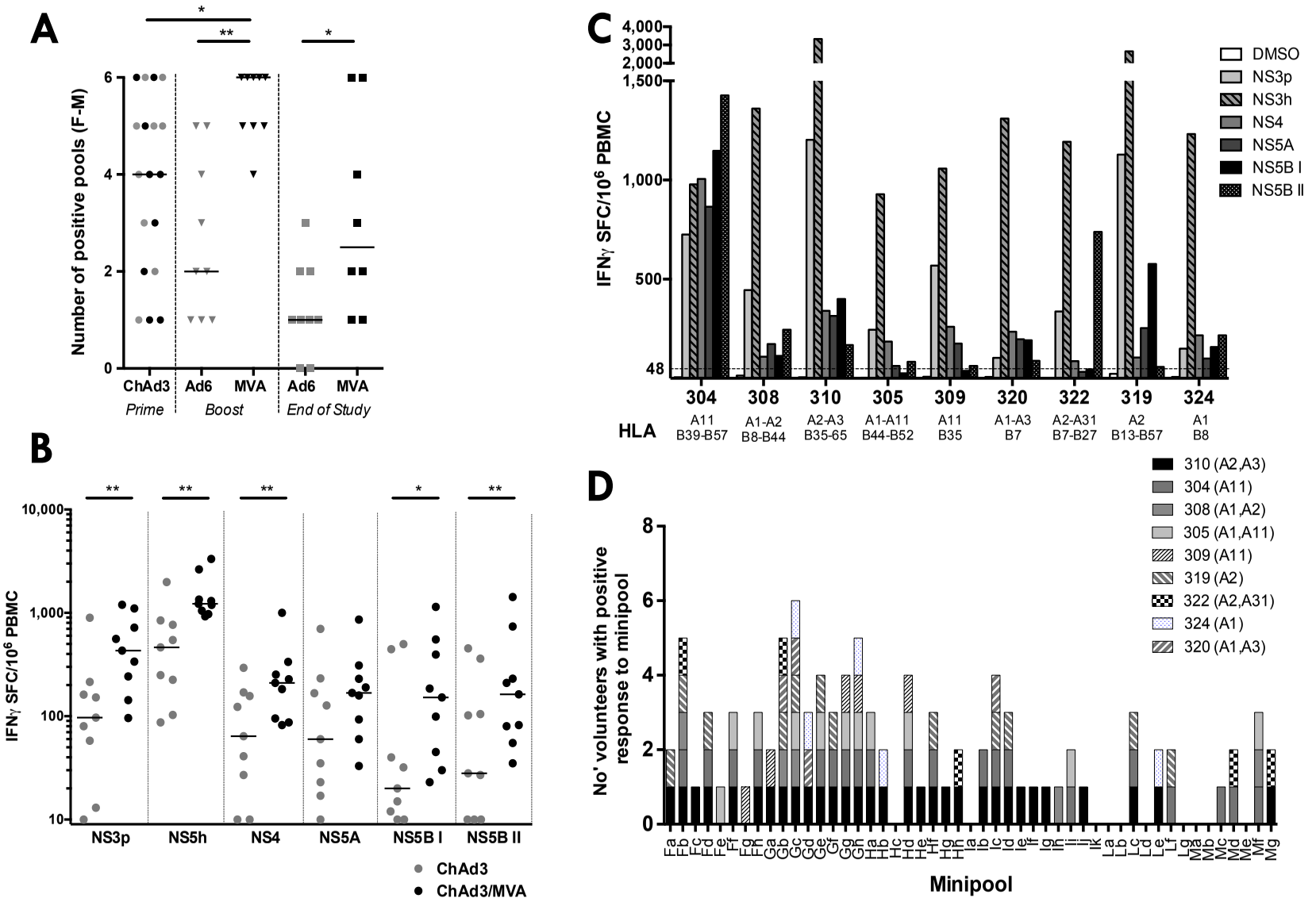

A
Number of positive pools (F-M)
ChAd3
Ad6
MVA
Ad6
MVA
Prime
Boost
End of Study
B
IFNγ SFC/10^6 PBMC
NS3p
NS5h
NS4
NS5A
NS5B I
NS5B II
ChAd3
ChAd3/MVA
C
IFNγ SFC/10^6 PBMC
DMSO
NS3p
NS3h
NS4
NS5A
NS5B I
NS5B II
HLA
304 A11 B39-B57
308 A1-A2 B8-B44
310 A2-A3 B35-65
305 A1-A11 B44-B52
309 A11 B35
320 A1-A3 B7
322 A2-A31 B7-B27
319 A2 B13-B57
324 A1 B8
D
No' volunteers with positive response to minipool
Minipool
310 (A2,A3)
304 (A11)
308 (A1,A2)
305 (A1,A11)
309 (A11)
319 (A2)
322 (A2,A31)
324 (A1)
320 (A1,A3)

Figure 3-5. Breadth of the T-cell responses to HCV NS after vaccination as measured by *ex vivo* IFNγ ELISpot: (**A**) The number of positive pools (F-M) assessed at the peak magnitude after; ChAd3-NS prime vaccination (TW2–4; black circles for those boosted with MVA-NS, grey circles if boosted with Ad6-NS), after Ad6-NS boost (TW10-12; gray triangles) or MVA-NS boost (TW9; black triangles) and at the end of the study post Ad6-NS (grey squares) or post MVA-NS (black squares). Bars, median (Ad6-NS boost versus MVA-NS boost, P = 0.0010**; EOS post-Ad6-NS versus EOS post-MVA-NS boost, P = 0.0355*). (**B**) The magnitude of the T-cell response to vaccination by pool (labelled with the HCV protein for that pool) after ChAd3-NS prime vaccination (TW2-4; open circles) and after MVA-NS boost vaccination (TW9; black triangles; IFNγ ELISpot, n=9). (**C**) The magnitude of the T-cell response to individual peptide pools 1 week after boost (TW9) for each volunteer after ChAd3-NS/MVA-NS vaccination. (**D**) The number of volunteers with a positive *ex vivo* ELISpot response to a minipool 4 weeks post MVA-NS boost vaccination. HLA-A alleles are given in brackets next to volunteer numbers.

Table 3-2. Specificity of T-cell response to HCV NS after vaccination

Volunteer	HLA A		HLA B		HLA C		Positive pools	Minipools	Peptide (minipool:peptide number-seqence)	Optimal (HLA Restriction)
304	11		39	57	12	6	F G H I L M	Fb, Fd, Ff, Fh Ge, Gf, Gg, Gh Ha, Hd, Hf Ib, Ic, Id, Ii Lc, Lf Mc, Md, Mf	Fb:11-QSFLATCVNGVCWTV/12-ATCVNGVCWTVYHGA Gh:153-VTLTHPITKYIMACM Ha:164-SVVIVGRIILSGRPA; Hf:207-ILAGYGAGVAGALVA Lf:400-LVNTWKSKKNPMGFS/401-WKSKKNPMGFSYDTR Mc: 444-RVYYLTRDPTTPLAR/445-LTRDPTTPLARAAWE	Fb: CVNGVCWTV (A2) Gh: TLTHPITK (A11) Lf: KSKKNPMG (B57) Mc: LTRDPTTPLAR
305	11	**1**	44	52	5	12	F **G** H I M	Fe, Ff, Fh **Gc**, Ge,Gg, Gh Ha, Hd Ii Mf	Ff: 56-QGYKVLVLNPSVAAT/57-VLVLNPSVAATLGFG **Gc: 103-VATDALMTGYTGDFD**; Gh: 149-HGPTPLLYRLGAVQN/150-PLLYRLGAVQNEVTL	Ff: VLVLNPSVAAT **Gc: ATDALMTGY (A1);** Gh: PLLYRLGAVQN
308	**2**	**1**	8	44	5	7	F **G** H I L M	Fb **Gb**, **Gc** Ih Mf	Fb:11-QSFLATCVNGVCWTV/12-ATCVNGVCWTVYHGA **Gb: 95-LAAKLSGLGINAVAY; Gc: 103-VATDALMTGYTGDFD**	Fb: CVNGVCWTV (A2) **Gb: KLSGLGINAV (A2); Gc: ATDALMTGY (A1)**
309	11		35		4		F G H I M	Fg Ga, Gg, Gh Hd	Ga: 83-VTVPHPNIEEVALSN/84-HPNIEEVALSNTGEI; Gh: 153-VTLTHPITKYIMACM	Ga: HPNIEEVAL (B35); Gh: TLTHPITKY (A11)
310	3	**2**	35	65	4	8	F **G** H I L M	Fa, Fb, Fc, Fd, Ff, Fh Ga, **Gb**, Gc, Gd, Ge, Gf, Gg, Gh, Ha, Hb, Hd, He, Hf, Hg, Hh Ib, Ic, Id, Ie, If, Ig, Ij, Lc, Le Mg	Fb:11-QSFLATCVNGVCWTV/12-ATCVNGVCWTVYHGA Ga: 83-VTVPHPNIEEVALSN/84-HPNIEEVALSNTGEI; **Gb: 95-LAAKLSGLGINAVAY** Hf:207-ILAGYGAGVAGALVA Le:391-RVCEKMALYDVVSTL	Fb: CVNGVCWTV (A2) **Gb: KLSGLGINAV (A2)**
319	**2**		13	57	6		F **G** H I L	Fa, Fb, Fd **Gb**, Gc, Ge, Gf Hf Ic, Id Lc, Lf	Fa:10-STATQSFLATCVNGV; Fb:11-QSFLATCVNGVCWTV/12-ATCVNGVCWTVYHGA **Gb: 95-LAAKLSGLGINAVAY;** Gf: 129-LRAYLNTPGLPVCQD Hf:207-ILAGYGAGVAGALVA Ic: 264-SRALWRVAAEEYVEV; Id: 274-PEFFTEVDGVRLHRY Lf:400-LVNTWKSKKNPMGFS/401-WKSKKNPMGFSYDTR	Fb: CVNGVCWTV (A2) Ga: HPNIEEVAL (B35); **Gb: KLSGLGINAV (A2)** Lf: KSKKNPMG (B57)
320	3	**1**	7		7		**G** H I L M	Gb, **Gc**, Gd Ic	Gb**:** 97-GINAVAYYRGLDVSV**;Gc: 103-VATDALMTGYTGDFD**; Gd: 118-RRGIYRFVTPGERPS	**Gc: ATDALMTGY (A1)**
322	**2**	31	27	7	7	2	F **G** H M	Fb **Gb** Hh Md, Mg	Fb:11-QSFLATCVNGVCWTV/12-ATCVNGVCWTVYHGA **Gb: 95-LAAKLSGLGINAVAY** Md: 454-WARMILMTHFFSILL; Mg: 489-IYHSLSRARPRWFML/490-LSRARPRWFMLCLLL	Fb: CVNGVCWTV (A2) **Gb: KLSGLGINAV (A2)**
324	**1**		8		7		F **G** H I L M	**Gc,** Gd, Gh Hb Le	**Gc: 103-VATDALMTGYTGDFD**; Gd: 109-TQTVDFSLDPTFTIE/110-DFSLDPTFTIETTTV; Gh: 153-VTLTHPITKYIMACM Hb: 167-RPAIVPDREFLYQEF Le:388-PARLIVFPDLGVRVC	**Gc: ATDALMTGY (A1);** Gh: TLTHPITKY (A11)

The peptide pools that were positive (see methods; >48 SFC/10^6 PBMC and 3X DMSO by ELISpot assay) at the peak of the T-cell response after ChAd3-NSmut/MVA-NSmut vaccination (TW9) are shown with each volunteer's HLA-type. Where possible T-cell responses were further mapped to minipool (at TW12), 15mer peptide or optimal peptide. The immunodominant responses to peptides 103 and 95 (Pool G; NS3) in HLA-A1 and HLA-A2 donors respectively are shown in bold and were tracked using MHC class I multimers

3.5.5 Vaccine-induced T-cells cross-recognise multiple HCV genotypes

As well as targeting multiple HCV epitopes, an effective global vaccine will need to cross-recognize variant sequences at the targeted epitopes from multiple viral genotypes.

I determined the capacity of the T-cells induced by ChAd3-NS/MVA-NS encoding the genotype-1b immunogen (BK strain) to target other globally prevalent HCV subtypes using overlapping peptides derived from genotypes 1a (H77), 3a (prevalent in Europe and America; K3a), and 4a (prevalent in the Middle East and Africa; ED43) sequences. Although subtypes 1a, 3a and 4a diverge significantly from genotype 1b at the amino-acid level (86%, 77%, and 78% sequence homology respectively)(**Simmonds et al. 1993**) responses to these subtypes were generated (**figure 3-6A**) with a comparable breadth and hierarchy (**figure 3-6B**) of the T-cell response, albeit at a lower magnitude. Responses to genotype 1a were approximately 60% and genotype 3a/4a 30% of those generated against genotype 1b (**figure 3-6**). I observed a direct correlation between the response to the genotype-1b immunogen and subtypes 1a, and 3a but not to 4a, albeit at a reduced magnitude (1b vs. 1a: R^2 =0.974, p=0.0018, 1b vs. 3a: R^2 =0.975, p=0.0017, 1b vs. 4a R^2 =0.045, p=0.734; **figure 3-6C**).

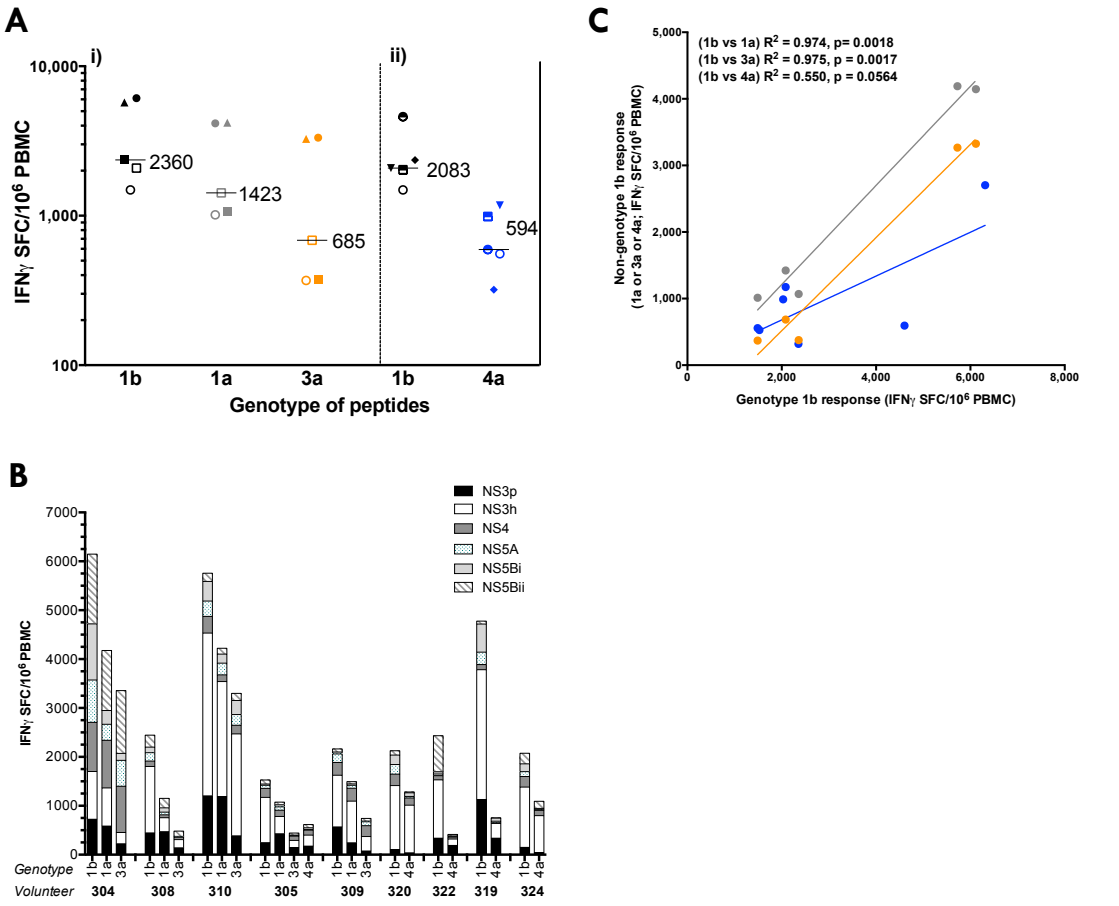


Figure 3-6. The cross-reactivity of ChAd3-NS/MVA-NS induced T-cells to peptides of genotype 1a, 2a and 4a HCV sequences: (**A-C**) *Ex vivo* IFNγ ELISpot (SFC/10^6 PBMC). (**A**) The total magnitude of T-cell responses to HCV NS genotype 1b sequence (vaccine strain) compared to (i) genotypes 1a, 3a or (ii) genotypes 4a sequences in volunteers at the peak of the response post ChAd3-NS/MVA-NS (TW9). Bars at median. (B) The magnitude of the T-cell response to peptide pools (labelled by corresponding HCV protein) at the peak post ChAd3-NS/MVA-NS (TW9) from genotype 1b (vaccine sequence) genotype 1a, 3a and 4a. (**C**) Linear regression and correlation of the total magnitude of HCV NS response against vaccine sequence versus against genotype 1a, 3a, and 4a HCV sequences.

Despite responses being lower in magnitude against non-vaccine sequence peptide pools, vaccine induced T-cells can recognise viral sequences from several major genotypes (1a, 3a and 4a) and, therefore, vaccination may offer cross-genotype protection.

3.5.6 T-cells targeting 'protective epitopes' are induced by vaccination

Certain HLA class I alleles are enriched in groups of individuals who spontaneously resolve HCV infection relative to those who fail to control the virus, and this is particularly evident in single source outbreaks (**Fitzmaurice et al. 2011; Kim et al. 2011; Neumann-Haefelin & Thimme 2007; Dazert et al. 2009**). These HLA alleles may mediate their effects on HCV via several mechanisms, the most common and easily determined being through their presentation of specific epitope targets that have a higher genetic barrier to escape – i.e. the epitopes they present require several complementary changes in the viral sequence to lose recognition by CD8+ T-cells (**Neumann-Haefelin. 2013**). The need for several complementary mutations delays the emergence of viral variants that have effectively escaped recognition, limiting viral spread and tipping the balance in favor of eradication by the immune system, rather than development of chronic HCV infection.

These protective T-cell responses represent highly desirable T-cell populations for an HCV vaccine due to their association with an increased rate of clearance of HCV. I assessed whether T-cells targeting a selection of these protective epitopes were induced by our vaccines, and where responses were detectable I investigated their *in vitro* recognition of common variant sequences. I hypothesized that T-cells targeting protective epitopes will show a broader recognition of viral variants than T-cells restricted by HLA alleles that have not been associated with spontaneous resolution (e.g. HLA-A2 restricted epitopes).

Frozen vials of PBMC from healthy HLA-B27+ or B15+ volunteers after ChAd3-NS prime and after MVA-NS or Ad6-NS boost vaccination were thawed and used for *ex vivo* pentamer and IFNγ ELISpot assays. PBMC were also cultured with vaccine sequence peptide, anti-CD28 and IL-2 before testing recognition of a panel of common viral variant sequence peptides by ICS. (Variant sequence peptides tested are listed in **Table 3-3** and the relative frequency of common variants at the protective epitopes is given in **Table 3-4**).

Ex vivo detectable T-cell responses against the HLA-B27 restricted epitope ($NS5B_{2841-2849}$ ARMILMTHF; vaccine sequence and genotype 1a and 1b consensus sequence; **Table 3-3**) were seen in 2/5 volunteers after ChAd3-NS prime, 4/5 volunteers after MVA-NS boost by IFNγ ELISpot (**figure 3-7A**) and 5/5 by MHC class I pentamer staining (**figure 3-7B**). Two of the most common viral variants observed in natural infection (V-------- and ---V-----; **Table 3-3**) were also recognized by T-cells but not in all individuals. Overall limited cross-recognition of viral variant sequences was seen *ex vivo*, however, responses were relatively weak and near the limit of detection for these assays (**figure 3-7A-B**).

Table 3-3. Protective epitopes – variants tested

	variant sequence	Peptide Number	Tetramer	Vaccine sequence + Cell line	Frequency
	$NS5B_{2841-2849}$				
HLA-B27	**ARMILMTHF**	R1	x	x	1a, 1b consensus
	V--V-L---	R4			
	-----LP--	R6			
	---V-----	R3			>5%
	V----LP--	R7			
	V--V-----	R2			
	V--V--S--	R5			
	V----L---	R8			>1%
	---V--P--	R21			
	-K-------	RR8			
	V--------	R15			>1%
	-----L---	R16			
	------P--	R22			
	------S--	R13			
	V---M-S--	RR17			>1%
HLA-B15	$NS5B_{2466-2474}$				
	GLRQKKVTF	EE23		x	
	CQ-------	EE1	x		1a consensus
	SQ-------	EE2			1b consensus
	SQ--R----	EE18			
	C--------	EE3			>5%
	S--------	EE4			>5%
	$NS5B_{2450-2458}$				
	LLRHHNMVY	EE6		x	1b consensus
	----R-L--	EE19			>5%
	----R----	EE20			
	---NR-L--	EE21			
	---Y--L--	EE12			
	---Y-----	EE13			
	------L--	EE5	x		1a consensus
	---N-----	EE22			

Amino acid substitutions from the vaccine sequence are indicated with the single letter amino acid code. The sequence used for *ex vivo* pentamer staining is highlighted with an x, and the peptide used for *in vitro* cell lines is the same as the vaccine insert. The genotype 1a and 1b consensus sequences are highlighted as are over variants representing >1 or >5% of sequences in the Los Alamos database (detailed analysis of variant frequencies in **Table 3-4**.

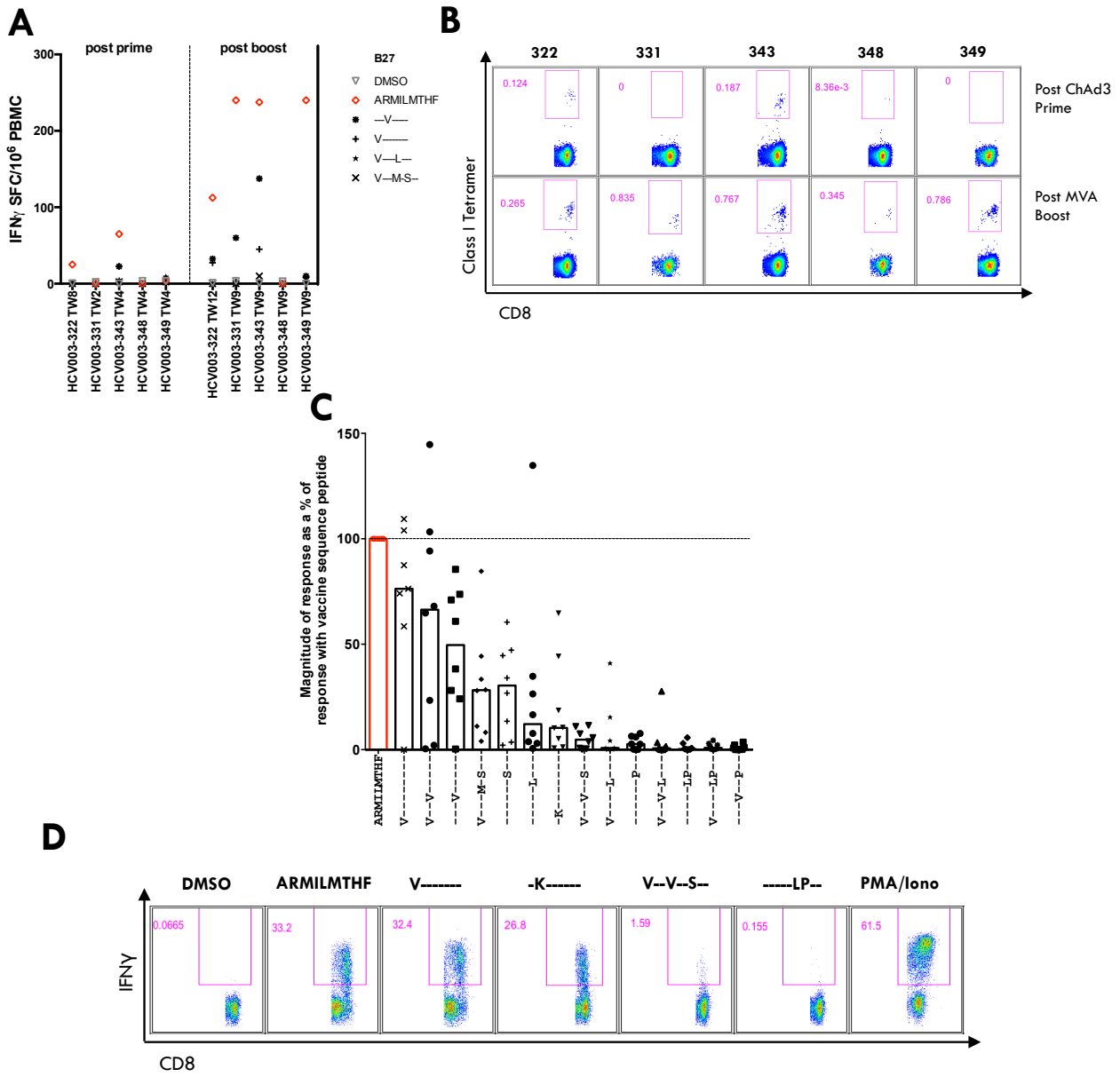


Figure 3-7. Induction of T-cells targeting an HLA-B27 restricted protective epitopes by vaccination: (**A**) *Ex vivo* IFNγ ELISpot response to $NS5B_{2841-2849}$ ARMILMTHF peptide and common viral variants and (**B**) FACS plots from *ex vivo* tetramer staining (Tetramer: $NS5B_{2841-2849}$ ARMILMTHF) from five vaccinees assessed post prime (2-4 weeks post ChAd3-NS) and post boost (1week post MVA-NS). (**C-D**) PBMC from five vaccinees post prime (2-4 weeks post ChAd3-NS) and post boost (1week post MVA-NS) were cultured with vaccine sequence optimal peptide (ARMILMTHF) for 14 days before being stimulated (5 hours) with vaccine sequence (red) and common viral variant sequence peptides (black). (**C**) Values are given as a percentage of total IFNγ+ response by CD8+ T-cells when stimulated by vaccine sequence peptide. Bars at median. (**D**) Example FACS plots of IFNγ production by ICS. Values are percentage of CD8+ T-cells making IFNγ.

Vaccine-induced T-cells targeting the HLA-B27-restricted HCV epitope $NS5B_{2841-2849}$ were expanded by culture with vaccine sequence peptide and their cross-recognition of all other genotype 1 viral variants listed in the Los Alamos database for this epitope was tested by ICS (**figure 3-7C;** example ICS plots in **figure 3-7D**). In one of the three individuals who had no *ex vivo* response to $NS5B_{2841-2849}$ after prime vaccination, responses could be cultured out, whereas response remained undetectable for two individuals. All 5 individuals had a detectable responses *ex vivo* after MVA-NS boost vaccination (**figure 3-8B**), suggesting that the responses seen in these two individuals post MVA-NS, which couldn't be cultured from PBMC taken post-ChAd3-NS vaccination, may have been primed by MVA-NS vaccination, which is in stark contrast to what is seen in individuals in group A1 who receive only MVA-NS vaccination (**figure 3-2E**). It is more likely that these responses are present after ChAd3-NS in all individuals but below the limit of detection but were ineffectively cultured in these cases.

ICS results post-culture suggest that certain mutations are tolerated by the antigen processing and presenting pathway better than others, with an A to V changes at position 1 and I to V at position 3 of $NS5B_{2841-2849}$ showing near complete cross-recognition by vaccine-induced T-cells (both substitutions with an alternative small hydrophobic amino acid; **figure 3-7C**). Alternatively, all variants containing an M to L substitution at position 6 were poorly recognised by vaccine primed T-cells (**figure 3-7C**). Overall the most common variants at this epitope are recognised and only rare variants are poorly recognised by T-cells primed with the genotype 1b consensus sequence (**Table 3-4**).

Table 3-4. Frequency of common genotype 1 variant sequences at protective epitopes

		HCV genotype		
		1a	1b	1c
HLA-B27 restricted epitope	ARMILMTHF	**85.45**	**87.01**	0
	VRM**V**LMTHF	0.61	0.43	**66.67**
	ARM**V**LMTHF	0.61	7.36	0
	VRM**V**L**L**THF	0	0.43	0
	VRM**V**LM**S**HF	0	0	0
	ARMIL**LP**HF	0	0	0
	VRMIL**LP**HF	0	0	0
	VRMIL**L**THF	2.42	0.43	0
	ARMILM**S**HF	0	0	0
	VRMILMTHF	1.21	2.16	0
	ARMIL**L**THF	0	0.43	0
	ARM**V**LM**P**HF	0	0.43	0
	ARMILM**P**HF	0	0	0
	A**K**MILMTHF	0	0	0
	VRMI**M**M**S**HF	0	0	0
	Total sequences:	**165**	**231**	**3**
	Other Variants	**V**RMI**M**MTHF (0,61) **V**RM**VM**MTHF (0,61) **V**RM**VMF**THF (0,61) ARMIL**I**THF (0,61) **V**RM**VLA**THF (0,61) **V**R**A**IL**L**THF (0,61)	ARMIL**L**THF (0,43) ARMIL**A**THF (0,43) **V**RMI**ML**THF (0,43) ARMI**M**MTHF (0,43)	**V**RM**V**LMTH**L** (33.3)

		HCV genotype		
		1a	1b	1c
HLA-B15 restricted epitopes	**C**QRQKKVTF (1a cons) SQRQKKVTF (1b cons) **CL**RQKKVTF S**L**RQKKVTF SQRQ**R**KVTF GLRQKKVTF	Sequencing data not available		
	Total sequences:			
	Other Variants			
		HCV genotype		
		1a	**1b**	**1c**
	LLRHHN**L**VY	**90.91**	5.19	**100**
	LLRHHNMVY	3.03	**87.45**	0
	LLR**Y**HN**L**VY	1.21	0.43	0
	LLR**Y**HNMVY	0.61	0.43	0
	LLRH**R**N**L**VY	0	0.43	0
	LLRH**R**NMVY	0	0	0
	LLR**NR**N**L**VY	0	0	0
	LLR**N**HNMVY	0	0.87	0
	Total sequences:	165	231	3
	Other Variants	L**I**RHHN**L**VY (0,61) LLRHHN**LI**Y (0,61) LLR**N**HN**L**VY (1,82) LLRHHNM**I**Y (1,21)	LLRHHNM**I**Y (1,73) LLRHH**S**MVY (0,87) **Q**LRHHNMVY (0,43) LLR**Y**HNM**I**Y (0,43) LLR**N**HN**L**VY (0,43) LLR**Y**HN**K**VY (0,43) LLR**NR**NM**I**Y (0,43) LLR**R**HNMVY (0,43)	

		HCV genotype		
		1a	1b	1c
HLA-A2 restricted epitopes	CINGVCWTV	**90.2**	41.59	33.33
	CVNGVCWTV	1.31	**45.57**	33.33
	CV**G**GVCWTV	0	5.5	0
	Total sequences:	**306**	**327**	**3**
	Other Variants	CING**A**CWTV (0.98) CINGVCW**SI** (0.98) CINGV**X**WTV (0.98) CIN**X**VCWTV (0.65) CI**S**GVCWTV (0.65) CING**X**CWTV (0.65) CINGVCW**S**V (0.33) CINGVCWT**X** (0.33) CING**X**CW**X**V (0.33) C**X**NGVCWTV (0.33) CVNG**A**CWTV (0.33) CINGV**F**WTV (0.33) CINGV**X**W**X**V (0.33) CINGVCW**X**V (0.33) CIN**X**VCW**X**V (0.33) CINGVCWT**A** (0.33) CI**X**GVCW**XX** (0.33)	CVNG**A**CWTV (2,75) CING**A**CWTV (1,53) CV**S**GVCWTV (0.61) C**L**NGVCWTV (0,61) C**I**NGVCW**S**V (0.31) C**I**NGV**W**WTV (0.31) C**T**NGVCWTV (0,31) CVNGV**F**WTV (0,31) CINGVCRTV (0,31) CVSGACWTV (0.31)	CING**A**CWTV (33,33)
		HCV genotype		
		1a	**1b**	**1c**
	KL**VA**LG**I**NAV	**43.46**	0	0
	KL**VA**LG**V**NAV	31.7	0.31	0
	KLSGLGLNAV	0.65	**42.81**	0
	KLS**S**LGLNAV	0	18.35	0
	KLS**A**LGLNAV	0	12.54	0
	KLSGLG**I**NAV	0	5.5	0
	Total sequences:	**306**	**327**	**3**
	Other Variants	35 others	29 others	KL**V**GLG**V**NAV (66,67) KL**V**G**P**G**V**NAV (33,33)

Table 3-4: Frequency of common genotype 1 variant sequences at protective epitopes – (data generated by Katrin Frohnmuller, University of Freiburg). The number of sequences used and the frequency of variants at protective epitopes were calculated using all sequences in the los alamos database or identified in (**Dazert et al. 2009; Ruhl et al. 2012**).

IFNγ ELISpot responses to the two B15 restricted epitopes ($NS5B_{2466\text{-}2474}$ vaccine sequence GLRQKKVTF, a rare variant; $NS5B_{2450\text{-}2458}$ vaccine sequence LLRHHNMVY and genotype 1b consensus) tested were weak or undetectable (not shown), however, small populations of T-cells binding an MHC class I pentamer loaded with a common variant peptide (------L--) were seen *ex vivo* for $NS5B_{2450\text{-}2458}$ (**figure 3-8A,C**). These pentamer+ populations targeting $NS5B_{2450\text{-}}$

$_{2458}$ could be grown to detectable levels from 3/4 individuals after prime vaccination and 4/4 after MVA-NS boost.

No detectable responses to NS5B$_{2466\text{-}2474}$ were seen by pentamer (variant sequence CQ--------) even after 14 days of culture with vaccine sequence peptide (**figure 3-8B-C**). The sequence of the variant peptide present within the pentamer, corresponding to the genotype 1a consensus, varies by two amino acids from the vaccine sequence, therefore, a lack of cross-recognition of this variant by epitopes primed and cultured with vaccine sequence peptide could explain a lack of pentamer staining. Unfortunately a pentamer containing the vaccine sequence peptide was not available at the time.

The breadth of recognition of common variants by B15 restricted vaccine-induced T-cells was tested by ICS after expansion of T-cells also (**figure 3-8D**). In one individual (105) where a response to NS5B$_{2466\text{-}2474}$ (GLRQKKVTF) could be cultured, cross-recognition was seen for all common viral variants. Poor cross-recognition of variants sequence peptides was seen at the epitope NS5B$_{2450\text{-}2458}$ (LLRHHNMVY), however, with complete loss of recognition seen for the genotype 1a consensus sequence (peptide EE5 ------L--) by ICS.

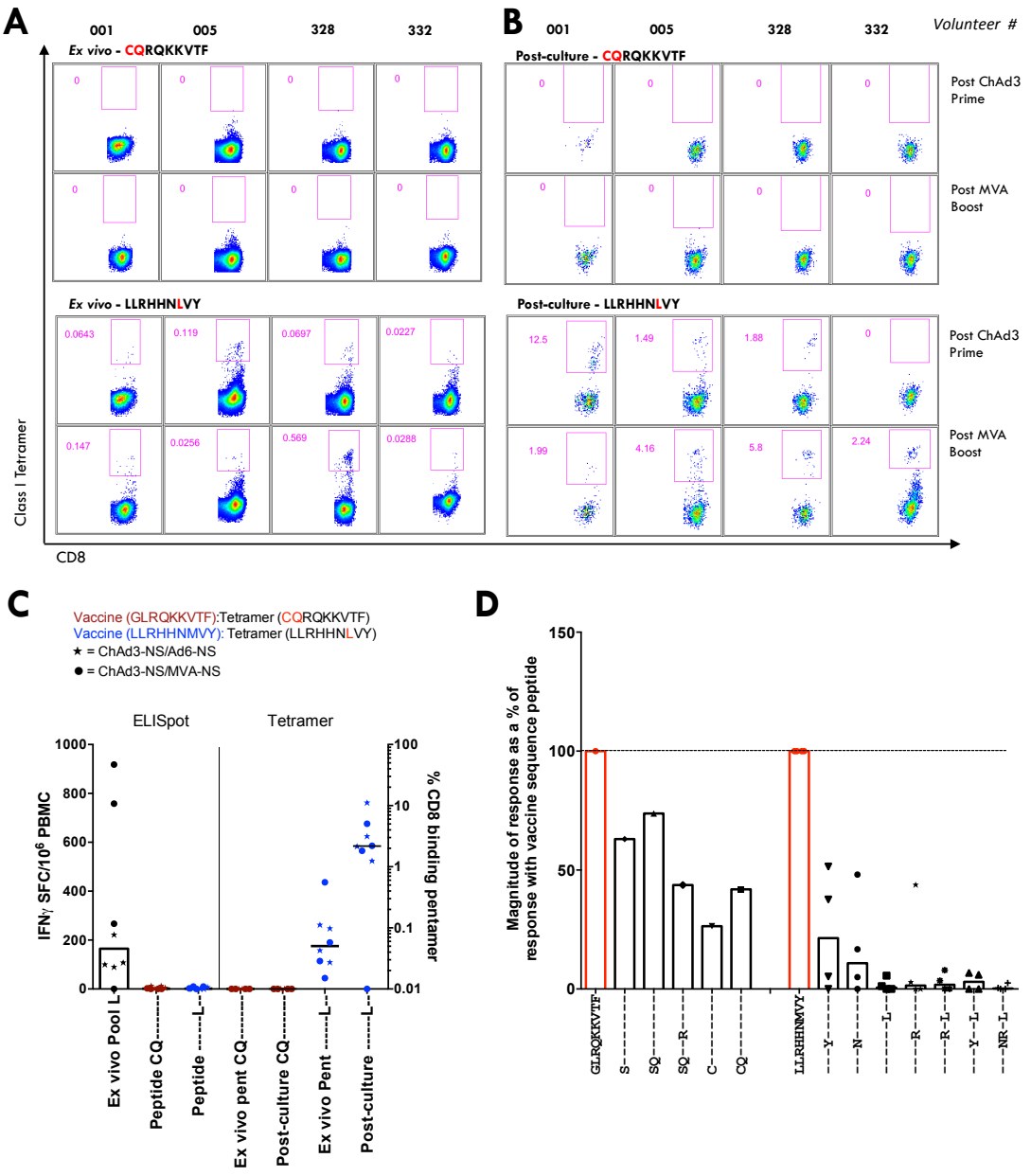


Figure 3-8. Induction of T-cells targeting HLA-B15 restricted protective epitopes by vaccination: FACS plots of *ex vivo* (**A**) and post culture (**B**) tetramer staining of PBMC (gated on CD8+) from four individuals assessed post prime (2-4 weeks post ChAd3-NS) and post boost (1-4 weeks post Ad6-NS 001 and 005, or post MVA-NS 328 and 332). Tetramers: CQRQKKVTF and LLRHHNLVY. (**C**) The IFNγ ELISpot response to pool L (containing both B15 restricted epitopes) and to single peptides matching the tetramer loaded sequence are shown with the % CD8+ binding pentamer *ex vivo* and post culture (14 days with peptide IL-2 and anti-CD28). (**D**) ICS was performed on PBMC post-culture using individual peptides (5 hour stimulation) matching the vaccine sequence (red) and peptides of common viral variant sequences (black). Values are given as a percentage of total IFNγ+ response by CD8+ T-cells when stimulated by vaccine sequence peptide. Bars at median.

Overall, T-cells targeting the B27 restricted epitope were induced in all individuals possessing the B27 allele and they showed recognition of many common viral variants. T-cells targeting the B15 restricted epitope $NS5B_{2466-2474}$ were induced in only one individual after vaccination, but these T-cells recognized all viral variants tested. T-cells targeting the B15 restricted epitope $NS5B_{2450-2458}$ were induced in all individuals, however, they did not recognize the majority of viral variants.

3.5.7 T-cell proliferative capacity is optimal long-term after MVA-NA boost vaccination

The ability of vaccine-induced HCV-specific T-cells to clonally expand on exposure to antigen is likely to be key to the effective control of HCV. The proliferative capacity of T-cells from vaccinated individuals was assessed in $^{[H]}$thymidine incorporation assays.

HCV recombinant protein antigens were used in this assay, which detects predominantly CD4+ T-cell proliferation. Strong proliferative responses to multiple HCV antigens (median number of proteins targeted at TW34/36: ChAd3-NS/MVA-NS vaccinated = 3.5; ChAd3-NS/Ad-NS vaccinated = 1) could be detected 6 weeks after MVA-NS boost, and these increased further when assessed 26 weeks after MVA-NS boost (Wilcoxon p=0.0391 NS3; **figure 3-9A**), consistent with the generation of a population of memory T-cells capable of rapid proliferation on re-exposure to antigen. Proliferative responses after MVA-

NS boost were significantly greater than those seen after heterologous Ad boost (**figure 3-9A**).

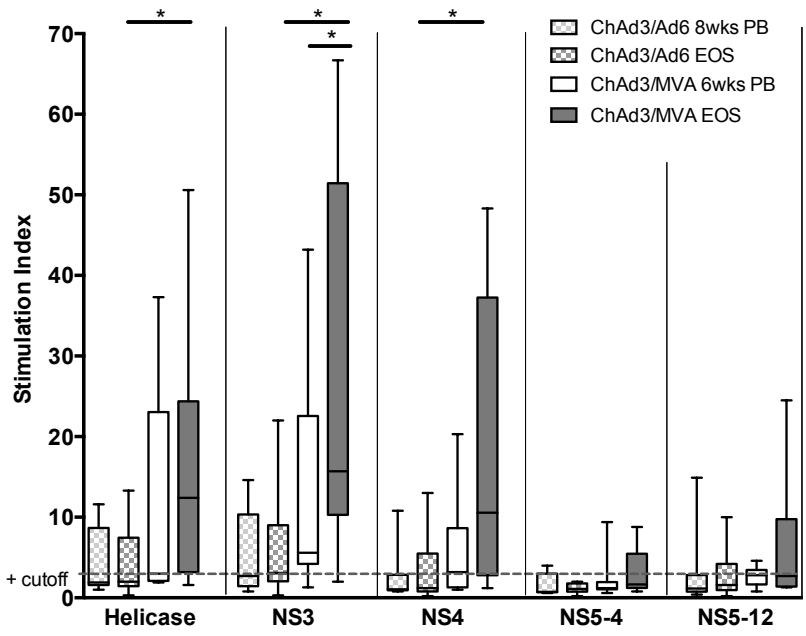
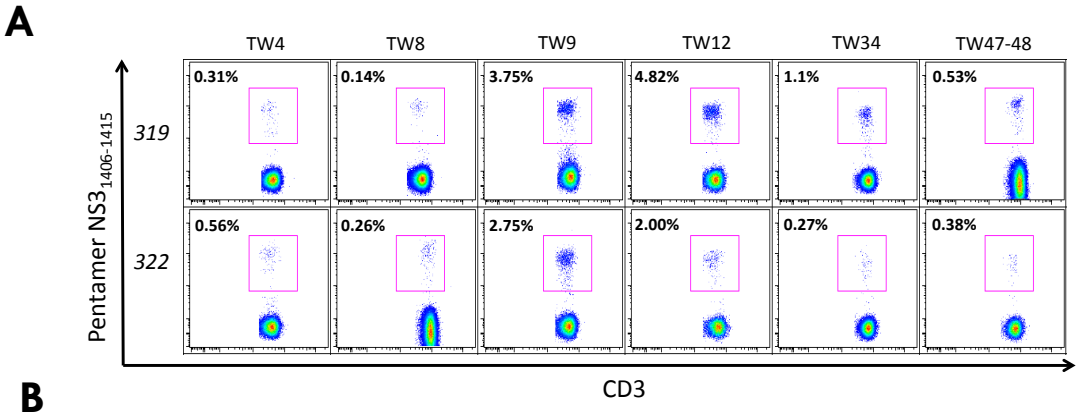
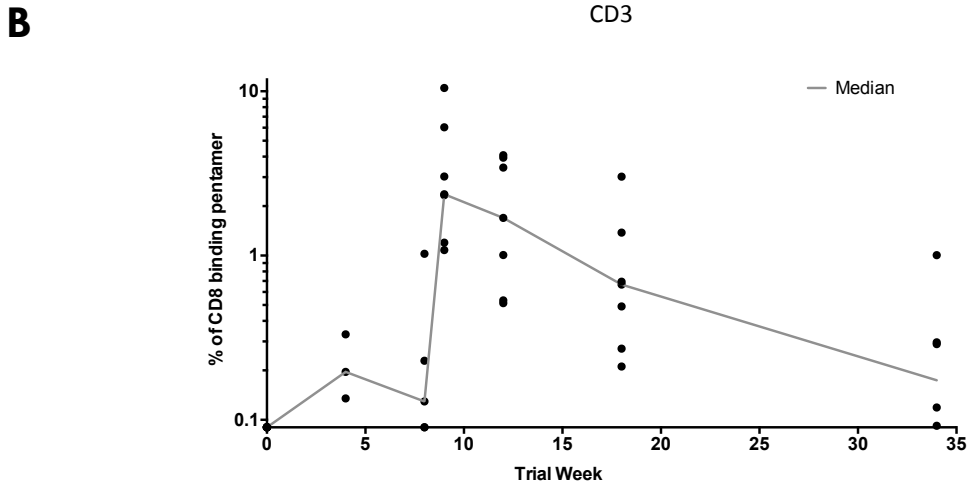
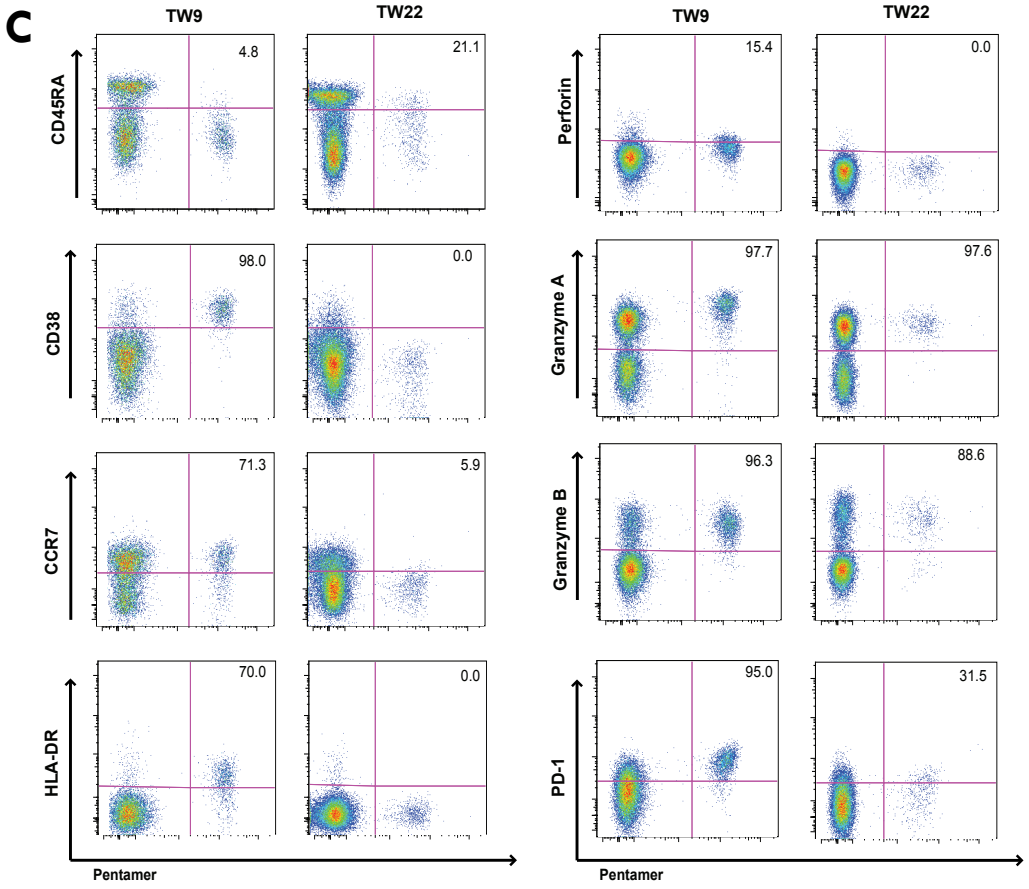


Figure 3-9. Proliferative capacity of vaccine-induced T-cells: The proliferative response of vaccine-induced T-cells (tritiated-thymidine incorporation) on stimulation with HCV proteins, plotted as box and whisker plots (max-min, IQR and median), is shown 6-8 weeks (TW14/16) and 26-28 weeks (TW34/36; End of study, EOS) after boost vaccination for ChAd3-NS/Ad6-NS (checkered bars; n=9) and ChAd3-NS/MVA-NS (solid bars; n=9) groups. Data are expressed as Stimulation index (SI). Positive cut off SI=3

To directly monitor the expansion of HCV-specific T-cells after vaccination PBMC were stained with MHC class I pentamers in HLA-A2 and HLA-A1 individuals (**figure 3-10**). *In vivo* expansion of HCV-specific T-cells was readily detectable after vaccination by ELISpot (**figure 3-2**) and by MHC class I pentamer staining also (**figure 3-10A-B**), with populations of up to 11% of CD8+ T-cells for a single HCV epitope seen 1 week after MVA-NS vaccination. HCV-specific T-cells also expanded readily *in vitro* when stimulated with peptide and IL-2 (**figure 3-7 & 3-8**) (**Barnes et al. 2012**).


A
TW4
TW8
TW9
TW12
TW34
TW47-48
Pentamer NS3 1406-1415
319
322
0.31%
0.14%
3.75%
4.82%
1.1%
0.53%
0.56%
0.26%
2.75%
2.00%
0.27%
0.38%
CD3


B
Median
% of CD8 binding pentamer
10
1
0.1
0
5
10
15
20
25
30
35
Trial Week


C
TW9
TW22
CD45RA
4.8
21.1
CD38
98.0
0.0
CCR7
71.3
5.9
HLA-DR
70.0
0.0
Pentamer
Perforin
15.4
0.0
Granzyme A
97.7
97.6
Granzyme B
96.3
88.6
PD-1
95.0
31.5
Pentamer

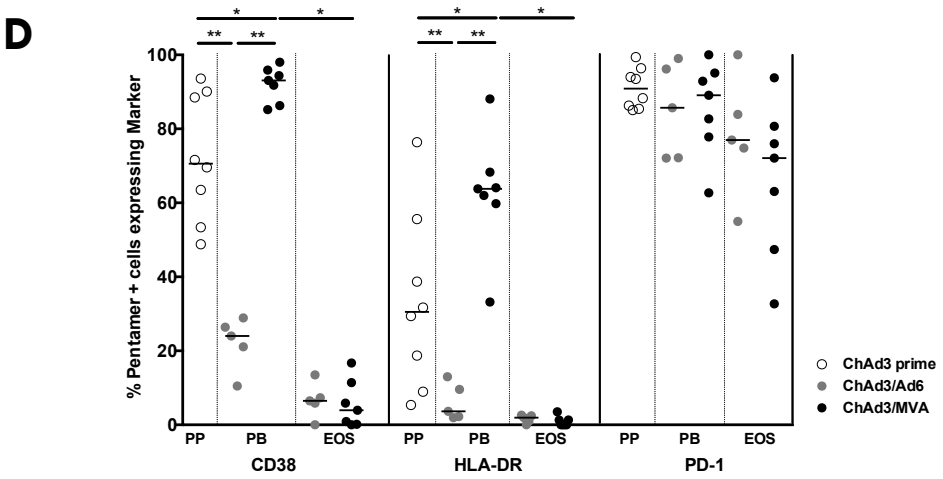


Figure 3-10. ***In vivo*** **expansion and** ***ex vivo*** **activation status of vaccine-induced T-cells by MHC class I pentamer staining:** (**A**) Example FACS plots of staining with tetramer ($NS3_{1406–1415}$) in volunteers 319 and 322 (vaccinated with ChAd3-NS/MVA-NS) over the study time course. Gated on live CD3+CD8+ cells. Values indicate percentage of CD8+ cells binding pentamer. (**B**) Magnitude of pentamer cloud: The percentage of CD8+ T-cells binding pentamer ($NS3_{1406–1415}$ or $NS3_{1435–1443}$) is shown for individual volunteers over the study time course. (**C**) Example FACS plots (volunteer 320, ChAd3-NS/MVA-NS) at the peak of the response (TW9, 1 week post MVA-NS boost) and at TW22 (14 weeks after MVA-NS boost) are shown for each phenotypic marker (Y axis) analysed against pentamer staining (x axis; $NS3_{1435-1443}$). The percentage of the pentamer+ population that expresses a given marker is shown (gated using Fluorescence minus one [FMO]; isotype control also used for PD-1). (**D**) Activation status: The percentage of the pentamer+ cells expressing phenotypic markers CD38, HLA-DR, and PD-1 4 weeks after ChAd3-NS prime (open circles; peak prime PP), after Ad6-NS boost (grey) at peak (post-boost PB; TW12) or end of study (EOS, TW36), or after MVA-NS boost (black) at peak (PB, TW9) or EOS (TW34). Comparisons are made between vaccine regimens and between time points within a single regimen. Only statistically significant differences are shown. All pentamer staining and phenotyping were performed *ex vivo* without culture.

The phenotype of HCV-specific T-cells induced by vaccination was assessed with FACS by costaining PBMC *ex vivo* with pentamers and a panel of antibodies against intracellular and surface markers (example plots in **figure 3-10C;** FACS panels described in **Tables 2-3 and 2-4**). After boosting with MVA-NS, HCV

specific T-cells were highly activated, as shown by the expression of CD38 in 80-100% pentamer+ cells, and with approximately 60% co-expressing HLA-DR (**figure 3-10D**). In contrast, after heterologous Ad6-NS boosting only 25% of HCV-specific CD8+ T-cells expressed CD38 with minimal HLA-DR co-expression. PD-1 expression (a molecule that has been associated with both T-cell activation and exhaustion) was also high post prime and boost vaccination, declining over the duration of the study (**figure 3-10D**).

HCV-specific T-cells primed by ChAd3-NS show good proliferative capacity *in vivo*, expanding rapidly when boosted with MVA-NS and *in vitro* when stimulated with peptide or protein. HCV-specific T-cells were maximally activated after MVA-NS boost, rather than Ad6-NS boost vaccination, and they differentiated into a population with a stronger re-call proliferation on protein stimulation long-term after vaccination.

3.5.8 MVA-NS boost vaccination enhances T-cell polyfunctionality

Intracellular cytokine staining (ICS) was used to assess the production of several cytokines relevant to viral control by vaccine-induced T-cells and to assess the balance of CD8+ and CD4+ T-cells induced by vaccination.

A feature of Adenoviral primed T-cell responses is a tendency to prime predominantly CD8+ T-cells (**Barnes et al. 2012**), however, a strong proliferative response to HCV proteins (**figure 3-9**) suggests a large population

of HCV-specific CD4+ T-cells may be induced by MVA-NS boost vaccination; this was confirmed by ICS.

HCV-specific cytokine producing CD4+ and CD8+ cells were readily detectable by ICS in all individuals after ChAd3-NS/MVA-NS vaccination (**figure 3-11**) and they persisted at detectable levels over a year after vaccination in those tested (example plots in **figure 3-11B**). MVA-NS induced significantly higher numbers of IFNγ, TNFα, and IL-2 producing CD4+ and CD8+ T-cells compared to those seen post ChAd3-NS prime, and heterologous Ad6-NS boost (**figure 3-11C;**
with the exception of TNFα producing CD8+ T-cells, and IL-2 producing CD4+ T-cells when compared with ChAd3-NS prime, although both showed increased median values).

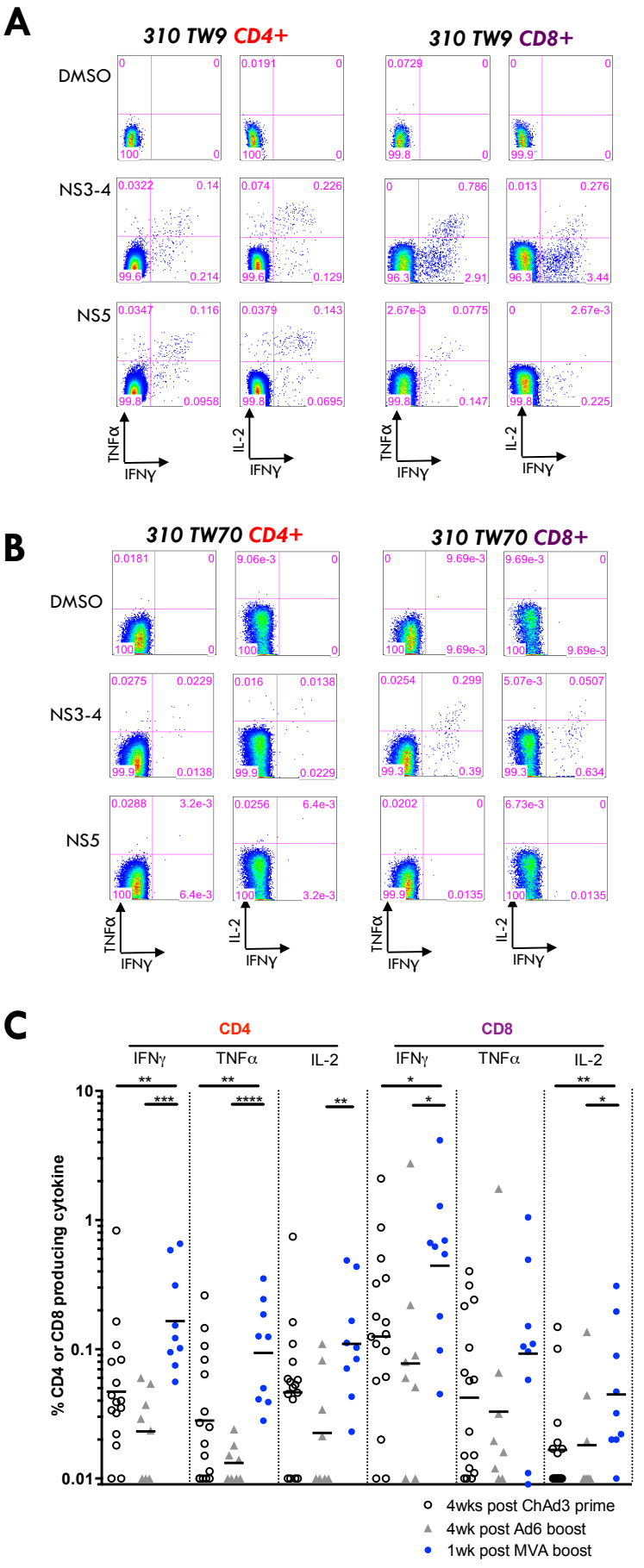

A
310 TW9 CD4+
310 TW9 CD8+
DMSO
NS3-4
NS5
TNFα
IFNγ
IL-2
B
310 TW70 CD4+
310 TW70 CD8+
C
CD4
CD8
IFNγ
TNFα
IL-2
% CD4 or CD8 producing cytokine
4wks post ChAd3 prime
4wk post Ad6 boost
1wk post MVA boost

Figure 3-11. Cytokine production by vaccine-induced T-cells: (A-B) Example FACS plots showing TNFα/IFNγ and IL-2/IFNγ by ICS for CD4+ and CD8+ T-cells stimulated with NS3–4, NS5, or DMSO in volunteer 310 (**A**) 1 week and (**B**) 62 weeks after MVA-NS boost vaccination (TW9 and TW70 respectively). (**C**) Comparison of cytokine production by T-cells after vaccination with ChAd3-NS, Ad6-NS, and MVA-NS. The percentage of total CD4+ or CD8+ T-cells producing IFNγ, TNFα, or IL-2 after stimulation with NS3–5 is shown at the peak after ChAd3-NS prime vaccination (open circles; TW4) and at the peak after boost vaccination with either heterologous Ad6-NS (gray triangles; TW12) or MVA-NS (blue circles; TW9). Summed response to NS after background subtraction (DMSO well). Values ≤0.01 were assigned 0.01. Bars, median.

Using Boolean gating and Spice analysis, I showed that the polyfunctionality of vaccine-induced CD4+ and CD8+ T-cells increased after MVA-NS vaccination, peaking at weeks 18 and 22 respectively (**figure 3-12A-B**). An equal proportion of CD4+ T-cells produced one (IL-2 or IFNγ), two (IFNγ plus IL-2 or TNFα) or three (IL-2, IFNγ and TNFα) cytokines, whilst CD8+ T-cells predominantly produced IFNγ early after vaccination (TW4/TW9) and produced IFNγ in conjunction with TNFα with or without IL-2 >10 weeks post boost (**figure 3-13**).

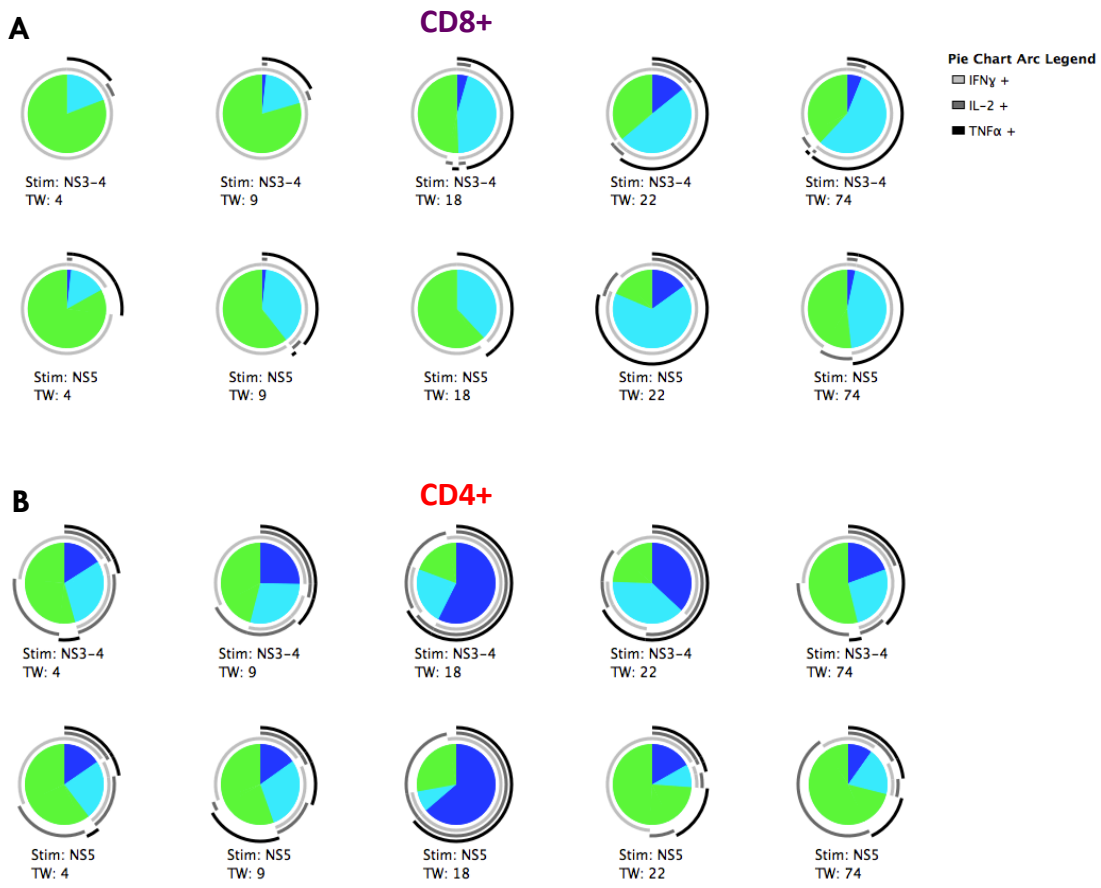


Figure 3-12. Polyfunctionality of HCV-specific CD4+ and CD8+ T-cells in volunteers receiving ChAd3-NS/MVA-NS vaccination: Cytokine combinations produced by HCV-specific CD8+ (**A**) and CD4+ (**B**) T-cells stimulated with peptide pools F+G+H (NS3-4 top row of pies) or I+L+M (NS5 bottom row of pies). Pie charts represent the proportion of cytokine-secreting T-cells that produce one (green), two (light blue) or all three (dark blue) cytokines measured (IL-2, IFNγ and TNFα). Pie arcs show the proportion of cytokine-producing cells that make a given cytokine. Pie base, median. Data is shown at the peak after ChAd3-NS priming (TW4 n=4-8), the peak after MVA-NS boost (TW9 n=4-9), at TW18 (n=1-3), at TW22 (n=2-4) and at TW74 (n=2-4; actual time points vary from TW70-74).

It has also been suggested that polyfunctionality can mean a larger per-cell production of cytokine relative to single cytokine producers (**Kannanganat et al. 2007; Bogdan et al. 1990; Darrah et al. 2007; Precopio et al. 2007**). I confirmed this with my ICS data, showing that the geometric mean fluorescence intensity (geoMFI), i.e. the amount of cytokine produced and stained in an individual cell, was significantly higher for triple cytokine producing (IFNγ+

TNFα+ IL-2+) T-cells for each individual cytokine, compared to dual and single cytokine producers for both CD4+ and CD8+ T-cells (with the exception of IL-2 production by CD8+ T-cells) for HCV-specific T-cells induced by vaccination (**figure 3-13;** also seen for adenoviral hexon, FEC, and CMV lysate stimulated T-cells; data not shown); the biggest differences were seen when comparing IFNγ production by polyfunctional and monofunctional T-cells (Median geoMFI of triple producing CD4+ and CD8+ 4131 and 10329 respectively, for single producing CD4+ and CD8+ 1322 and 1543 respectively; **figure 3-13**).

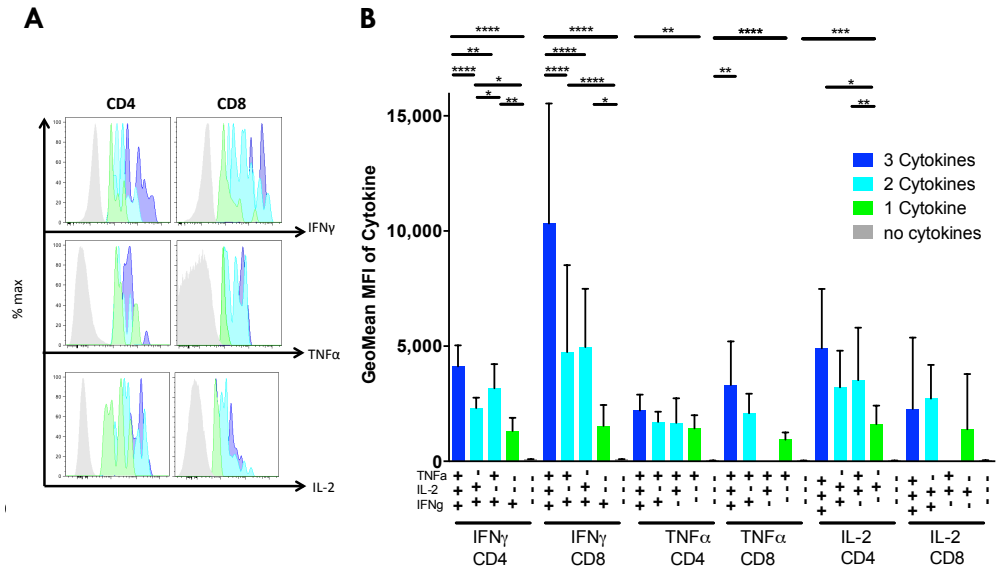


Figure 3-13. Polyfunctional cells make more cytokine per cell than mono-functional cells: **(A)** Example histograms of the fluorescence intensity for IFNγ, TNFα, and IL-2 for single, dual, or triple producing CD4+ and CD8+ T-cells (NS3-4 stimulated PBMC from 310 at TW18). (**B**) Grouped data for the geoMean MFI for each cytokine is shown for single, dual, and triple cytokine-producing T-cells. Data from all 9 ChAd3-NS/MVA-NS vaccinated volunteers at multiple time points (CD4+, n = 34; CD8+, n = 26; Median and upper quartile shown.

3.5.9 The cytolytic potential of MVA-NS induced HCV-specific T-cells

The potential for HCV-specific T-cells induced by vaccination to cytolytically kill infected T-cells was assessed by costaining HCV-specific T-cells with MHC class I pentamers and the pore-forming protein perforin, and granzymes A (GzA) and B (GzB). HCV specific T-cells post MVA-NS invariably expressed high levels of both GzA and GzB (**figure 3-14A**). Perforin expression on HCV-specific cells varied between individuals and appeared to be only transiently expressed on highly activated cells immediately after vaccination (**figure 3-14A**).

Rather than being constitutively expressed, it appears the rapid up-regulation of perforin is a key for cytolytic killing of infected cells (**Makedonas et al. 2010; Jo et al. 2012; Makedonas & Betts 2010**)**,** therefore, I assessed the up-regulation of perforin on vaccine-induced T-cells after stimulating and culturing PBMC with HCV-specific peptides. Pentamer+ T-cells expanded in all individuals at all time points, except from pre-vaccination PBMC, and expanded pentamer+ T-cells almost invariably up-regulated perforin (**figure 3-14B**; median 96.5% range 71.5-99.6% of pentamer+ expressing perforin post 7-day culture of PBMC taken at TW2-4, TW9 and TW47-72).

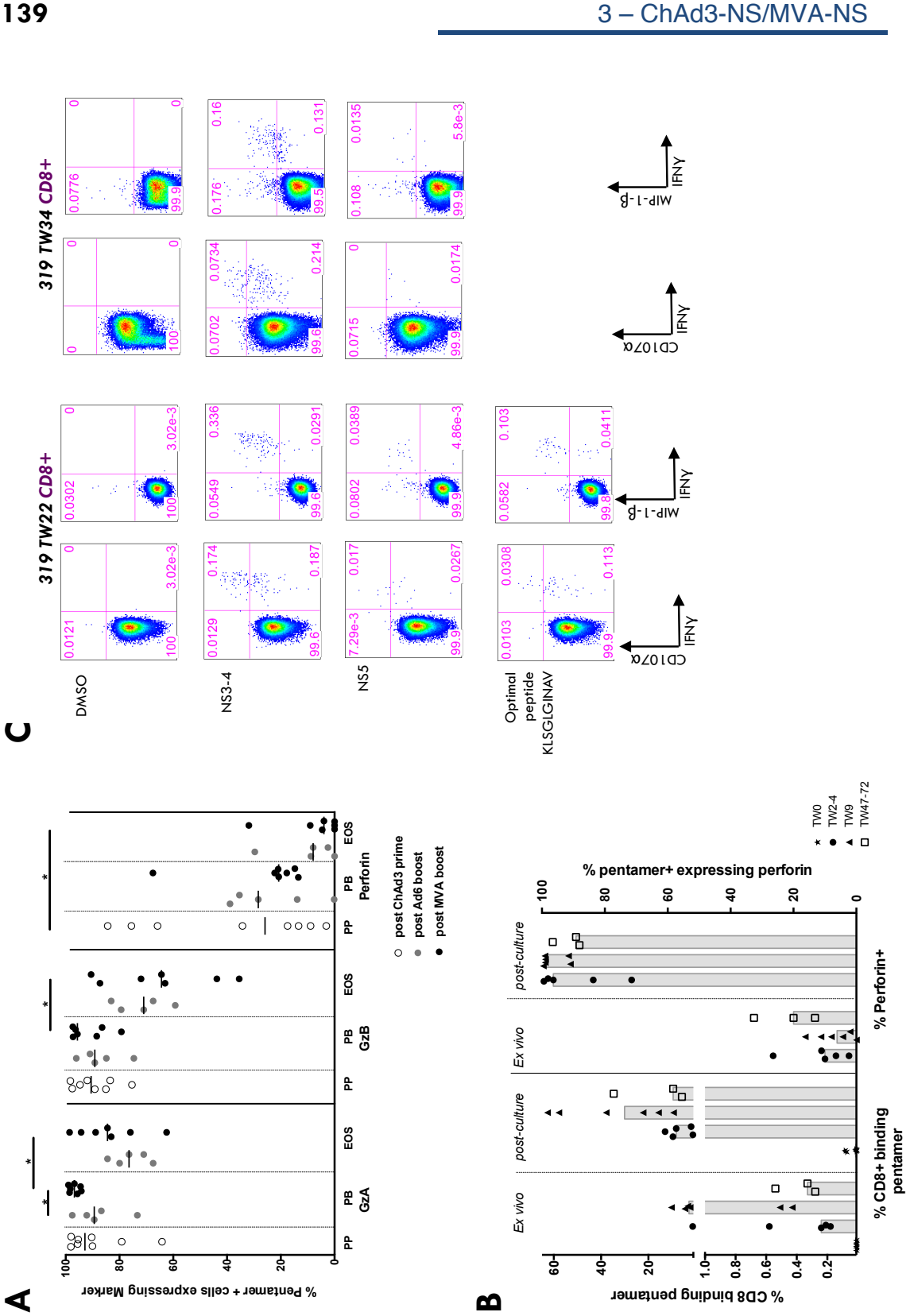

A
% Pentamer + cells expressing Marker
PP
PB
GzA
EOS
PP
PB
GzB
EOS
PP
PB
Perforin
EOS
post ChAd3 prime
post Ad6 boost
post MVA boost
B
% CD8 binding pentamer
Ex vivo
post-culture
Ex vivo
post-culture
% CD8+ binding pentamer
% pentamer+ expressing perforin
% Perforin+
TW0
TW2-4
TW9
TW47-72
C
319 TW22 CD8+
319 TW34 CD8+
DMSO
NS3-4
NS5
Optimal peptide KLSGLGINAV
CD107α
IFNγ
MIP-1-β
IFNγ

Figure 3-14. Cytotoxic potential of vaccine-induced T-cells: (A) The percentage of the pentamer+ (NS3 $_{1406–1415}$ or NS3$_{1435–1443}$) cells expressing granzyme A (GzA) granzyme B (GzB) and perforin is shown 4 weeks after ChAd3-NS prime (open circles; peak prime PP), after Ad6-NS boost (grey) at peak (post-boost PB; TW12) or end of study (EOS, TW36; gray), or after MVA-N (black) boost at peak (PB, TW9) or EOS (TW34). Example plots of phenotyping **figure 3-10C**. Comparisons are made between vaccine regimens and between time points within a single regimen. Only statistically significant differences are shown. (**B**) PBMC taken pre-vaccination (TW0; stars) at the peak after ChAd3-NS boost (TW2-4) at the peak after MVA-NS boost (TW9) or at the end of the vaccine study (TW47-72) were cultured with NS3 $_{1406–1415}$ (KLSGLGINAV) for 9 days before being stained with a pentamer loaded with the same peptide. The percentage of CD8+ T-cells binding the pentamer is shown ex vivo pre-culture and post-culture on the left y-axis. T-cells were costained with an anti-human perforin antibody pre-vaccination and post-culture and the percentage of pentamer+ T-cells expressing perforin is shown on the right y-axis. Bars at median. (**C**) Example FACS plots of *ex vivo* ICS 14 weeks (TW22) and 26 weeks (TW34) post MVA-NS boost in two ChAd3-NS/MVA-NS vaccinated individuals. PBMC were stimulated with NS3-4 (pools F, G, H), NS5 (pools I, L, M), a single peptide or DMSO (negative control). Staining for CD107α and MIP-1-β against IFNγ are shown gated on CD8+ T-cells.

The potential of antigen-specific cells to degranulate on peptide stimulation can also be assessed by ICS by measuring the surface mobilization of CD107α (lysosome-associated membrane protein ([LAMP]-1). CD107α expression was readily observed on vaccine induced CD8+ T-cells (example FACS plots shown in **figure 3-14C**).

Vaccine-induced CD8+ T-cells contained high levels of cytolytic effector molecules and they up-regulated perforin and degranulate on recognition of cognate antigen, suggesting that they have the capacity for cytolytic killing.

3.5.10 Viral vector combination has a profound effect on the T-cell memory subsets induced by vaccination

T-cell subsets have distinct functional patterns of gene expression (**Weng et al. 2012; Willinger et al. 2005; Roychoudhuri et al. 2014; Kaech, Wherry, et al. 2002**) and functionality. Certain subsets alone or in combination have been shown to mediate protection against different viral infections (**Hansen et al. 2009; Reyes-Sandoval et al. 2011; Northfield et al. 2007; Sridhar et al. 2013**).

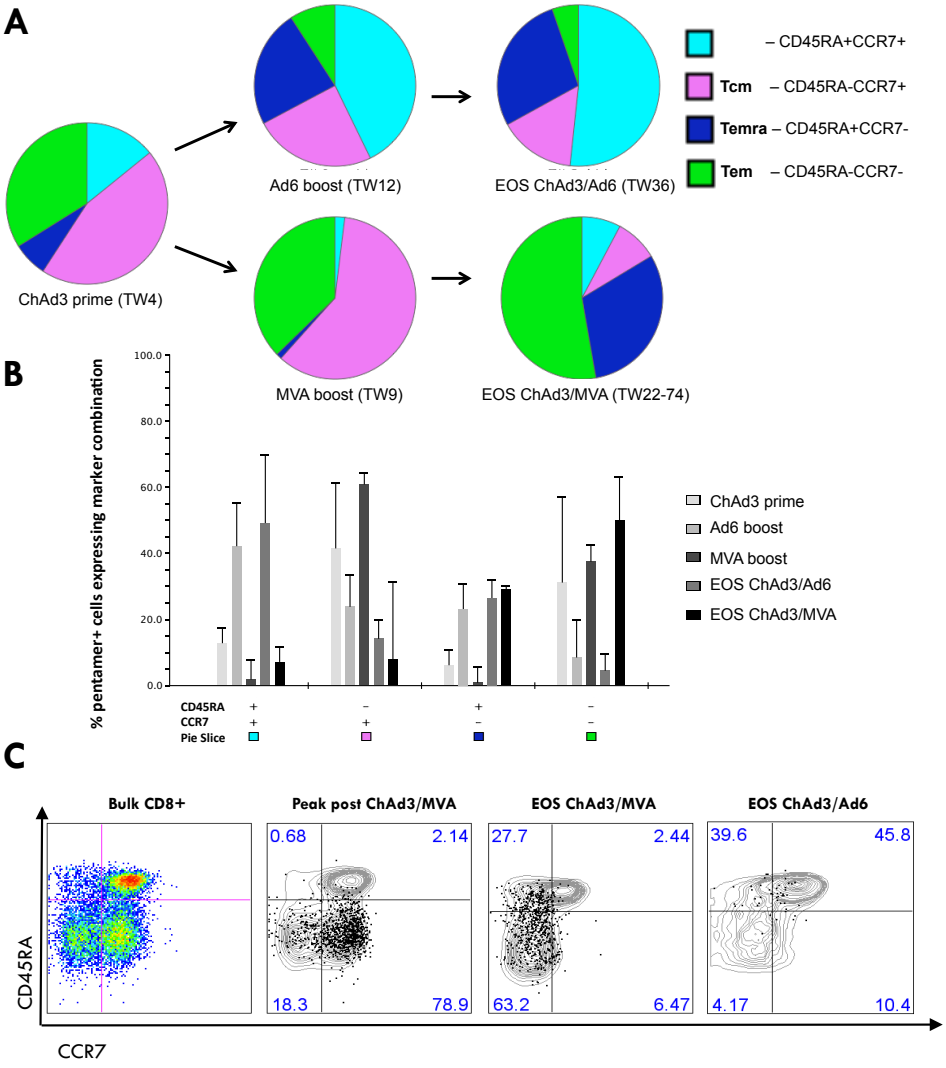


Figure 3-15. Memory phenotype of vaccine-induced CD8+ T-cells: (**A-C**) PBMC were costained with MHC class I pentamers (NS3 $_{1406–1415}$ or NS3$_{1435–1443}$) and with antibodies to human CD45RA and CCR7 *ex vivo*. Data are shown at the following time points: after ChAd3-NS prime (TW4, n = 8), peak after Ad6-NS boost (TW12, n = 5), at the end of the study after ChAd3-NS/Ad6-NS (TW36, n = 5; EOS ChAd3/Ad6), peak after MVA-NS boost (TW9, n = 7), and at the end of the study after ChAd3-NS/MVA-NS (TW22–74, n = 7; EOS ChAd3/MVA). (**A**) Pie charts show the proportion of the pentamer+ cells, which display the naïve, Tem, Temra, and Tcm phenotype at the time points listed above. Pie base, median. (**B**) Bar graph shows the percentage of pentamer+ cells displaying a particular phenotype. Median and upper quartile are shown. (**C**) Example FACS plots of CD45RA vs. CCR7 on bulk CD8+ T-cells (volunteer 320 tw9), and on pentamer+ T-cells (black dots) overlaid on bulk CD8+ T-cells (grey contours) from the same time point for the following: peak of response after ChAd3-NS/MVA-NS (volunteer 320 TW9); at the end of the study following ChAd3-NS/MVA-NS (volunteer 320 TW22) or following ChAd3-NS/Ad6-NS (volunteer 068 TW34).

After ChAd3-NS priming vaccination, a mixed pool of Tcm and Tem memory populations were detected (definitions of T-cell memory subsets described in **Chapter 1**; **figure 3-15**). In contrast, expanded HCV-specific T-cells after MVA-NS boost were predominantly CD45RA-. Importantly, the long-term memory population at the end of the study after heterologous Chad3-NS/Ad6-NS vaccination was predominantly lymph-node homing (CCR7+) T-cells that had re-expressed CD45RA (naïve-like CD45RA+CCR7+); in contrast after ChAd3-NS/MVA-NS regime the dominant population were peripheral organ-homing (CCR7-) Tem with low expression of CD45RA (**figure 3-15**). Vaccination with varying viral vector combinations can leave strikingly different populations of memory T-cells, with potentially disparate protective potential.

3.5.11 Optimising vaccine regimens – re-boosting strategies and MVA dose de-escalation

I next investigated whether re-boosting healthy volunteers with further ChAd3-NS and/or MVA-NS vaccinations can enhance the magnitude of the HCV-specific T-cell memory response.

Volunteers received the optimised prime-boost vaccine regimen of ChAd3-NS prime (TW0) and MVA-NS boost (TW8) and were then further vaccinated as follows: for arm A3 after a short interval of 8 weeks they received a second ChAd3-NS and a second MVA-NS 8 weeks later (all vaccines 8 weeks apart; short interval; **Table 3-1**); for arm A4 after a long interval of 39-86 post MVA-NS boost, they received a second ChAd3-NS and 8 weeks later a second MVA-NS (**Table 3-1**); for arm A5 volunteers received a second MVA-NS only (without a second ChAd3-NS) 32 weeks after their first MVA-NS boost.

When all four vaccines were given 8 weeks apart (**figure 3-16A**; arm A3) no expansion of the T-cell response to HCV NS was seen after the second ChAd3-NS and only a weak expansion was seen after the second MVA-NS. In 3/4 volunteers who received a second ChAd3-NS/MVA-NS long after the initial prime-boost vaccinations, T-cells expanded strongly to both the second ChAd3-NS and second MVA-NS (**figure 3-16B**). In volunteers who received a second MVA-NS 40 weeks after prime vaccination HCV NS-specific T-cells were also expanded (**figure 3-16C**). A measurable expansion of HCV-specific T-cells was only seen when a longer gap was allowed between the MVA-NS boost vaccination and re-vaccination with a second ChAd3-NS or MVA-NS (**figure 3-17A-B**). The

magnitude of the T-cell memory response at the end of the study (>8 weeks after the last vaccination) may be modestly enhanced by further vaccination (**figure 3-17B**).

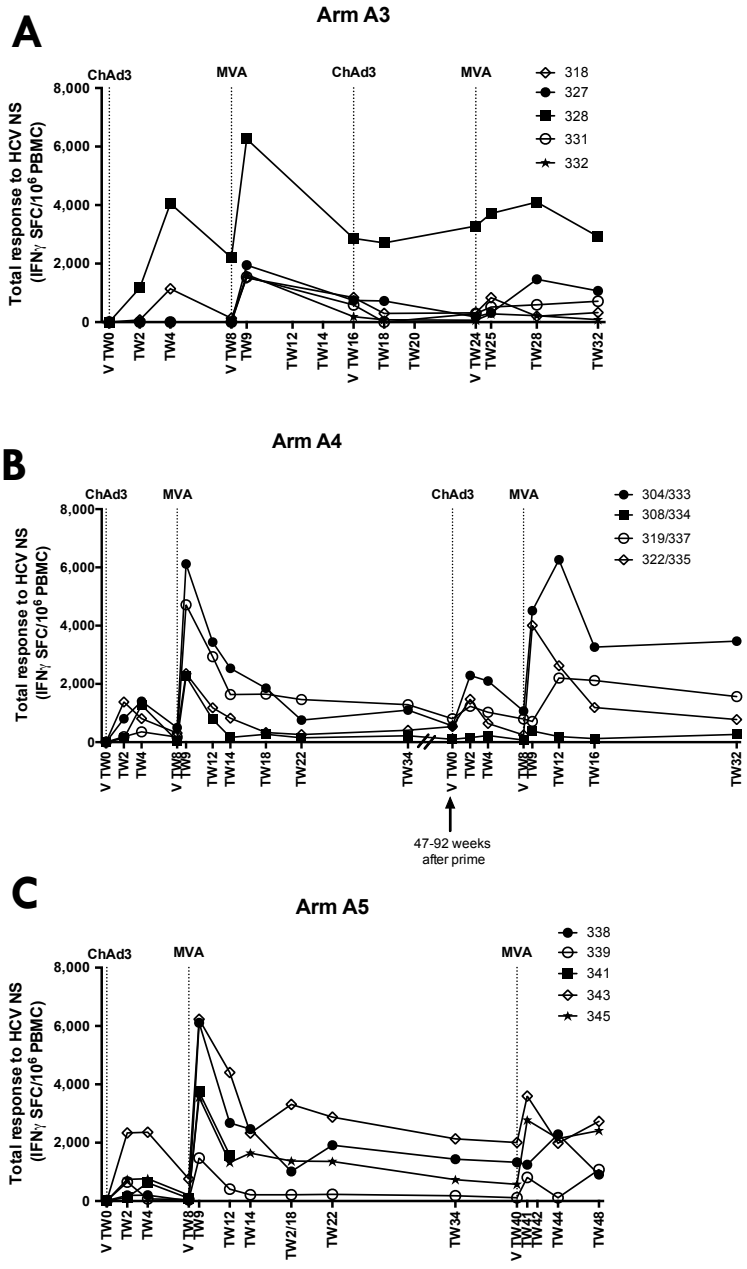


Figure 3-16A-C. Further boosting the magnitude of HCV-specific T-cells

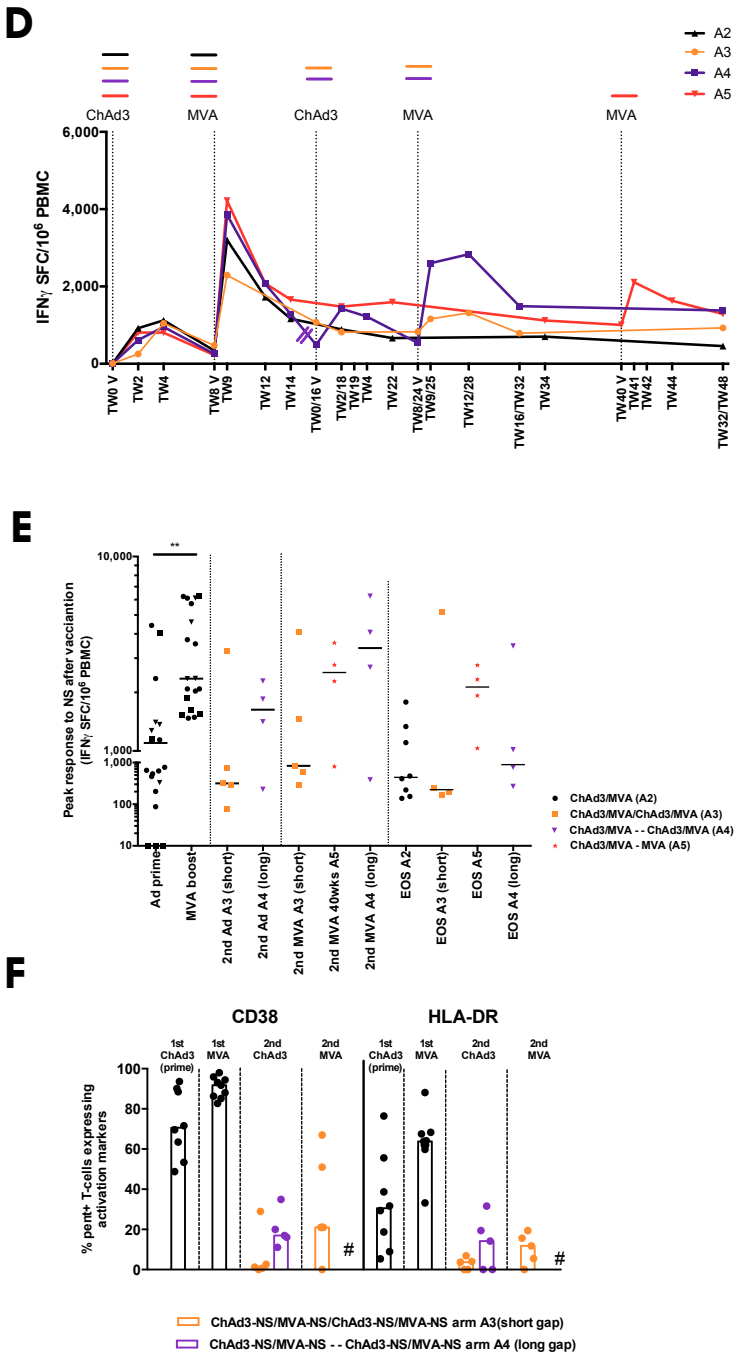


Figure 3-16. Further boosting the magnitude of HCV-specific T-cells: (A-F) Healthy volunteers were vaccinated with ChAd3-NS ($2.5x10^{10}$ vp, TW0) and MVA-NS ($2x10^{8}$ pfu, TW8) and were then further boosted with a second round of ChAd3-NS and MVA-NS (8 weeks apart) given either at trial week 16 [short gap; (**A**), arm A3; see **Table 3-1**] or at trial week 47-92 [long gap (**B**), arm A4] or a single MVA-NS at trial week 40 [(**C**), arm A5]. Immunogenicity was measured by *ex vivo* IFNγ ELISpot. The kinetics of individual volunteers HCV NS-specific T-cell response across the trial is shown (summed response to positive peptide pools). (**D**) Comparison of the kinetics of the T-cell response to vaccination in arms A3-5 (mean). Each group is coloured coded and vaccinations are indicated by a coloured dash above the

graph at the time of vaccination. (**E**) A comparison of the peak T-cell response to HCV NS after each vaccination by *ex vivo* IFNγ ELISpot. Bars at median. (**F**) Ex vivo MHC class I pentamer staining was performed on all HLA-A1 or A2 individuals ($NS3_{1435–1443}$ or $NS3_{1406–1415}$ respectively) from groups A2-A4 across the trial. Pentamer+ cells were co-stained with antibodies against the CD8+ T-cell activation markers CD38 and HLA-DR. The percentage of pentamer+ cells expressing these markers is shown, bars at median. # = not done.

HCV-specific T-cells were not strongly activated by a second round of ChAd3-NS and MVA-NS vaccination when given only 8 weeks (short interval) after the initial prime-boost, as shown by a lack of up-regulation of CD38, or HLA-DR (**figure 3-16C**). When a second ChAd3-NS was given at least 47 weeks after the ChAd3-NS prime vaccination, a small proportion of cells upregulated CD38 and HLA-DR.

At the peak of the T-cell response to ChAd3-NS prime and MVA-NS boost vaccinations HCV-specific T-cells were a mixed population of Tem and Tcm (CD45RA-) subpopulations (**figure 3-17**); the same mix of effector populations was seen when ChAd3-NS was administered 47-92 weeks (long interval) after the initial ChAd3-NS prime, but not when administered just 16 weeks after ChAd3-NS prime. The intensive vaccination regimen of ChAd3-NS/MVA-NS/ChAd3-NS/MVA-NS lead to population dominated by CD45RA re-expressing Temra and a smaller Tcm population than ChAd3-NS/MVA-NS alone (**figure 3-17**).

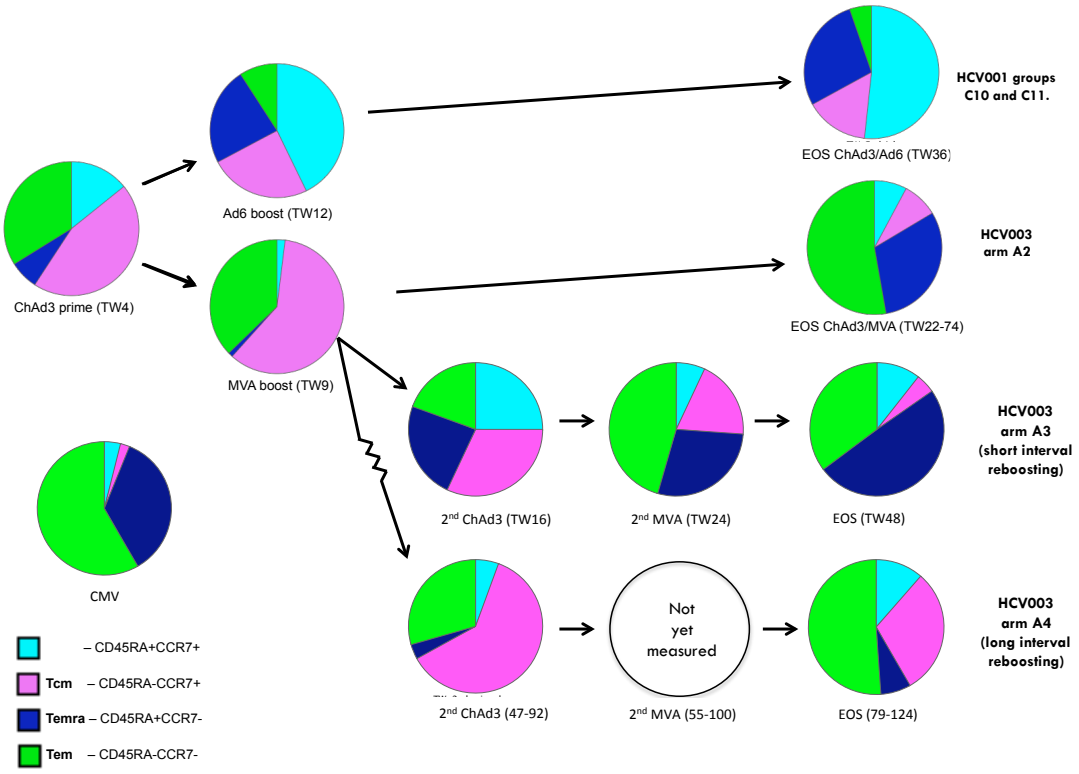


Figure 3-17. Memory phenotype of vaccine-induced CD8+ T-cells after re-boosting: PBMC were costained with pentamers to immunodominant epitopes in NS3 and with antibodies to human CD45RA and CCR7 *ex vivo* at the peak of the response following each vaccination. Pie charts show the proportion of the pentamer+ cells, which display the naïve, Tem, Temra, and Tcm phenotype at the time points listed above. Pie base, median. Also shown is the proportion of T-cell subsets for CMV-specific memory T-cells. The trial week is listed below each pie (weeks since ChAd3-NS prime vaccination). HCV001 groups C10 and C11, n = 10; CMV n= 10; HCV003 A2 n = 6, A3 n =4 and A4 n = 4. Example FACS plots in **figure 3-10C**).

A lower dose of MVA could be required due to difficulties in large scale manufacturing (**Cottingham & Carroll 2013**), but it will also reduce the cost of a vaccination and could reduce reactogenicity. The possibility of reducing the dose of MVA without affecting vaccine immunogenicity was also assessed (medium dose MVA-NS $2x10^7$ pfu arm A6; low dose MVA-NS $2x10^6$ pfu arm A7). No significant reduction in the T-cell response to MVA-NS boost is seen when

medium or low dose is used, although a trend for lower peak and memory responses is seen for the low MVA-NS dose (**figure 3-18**).

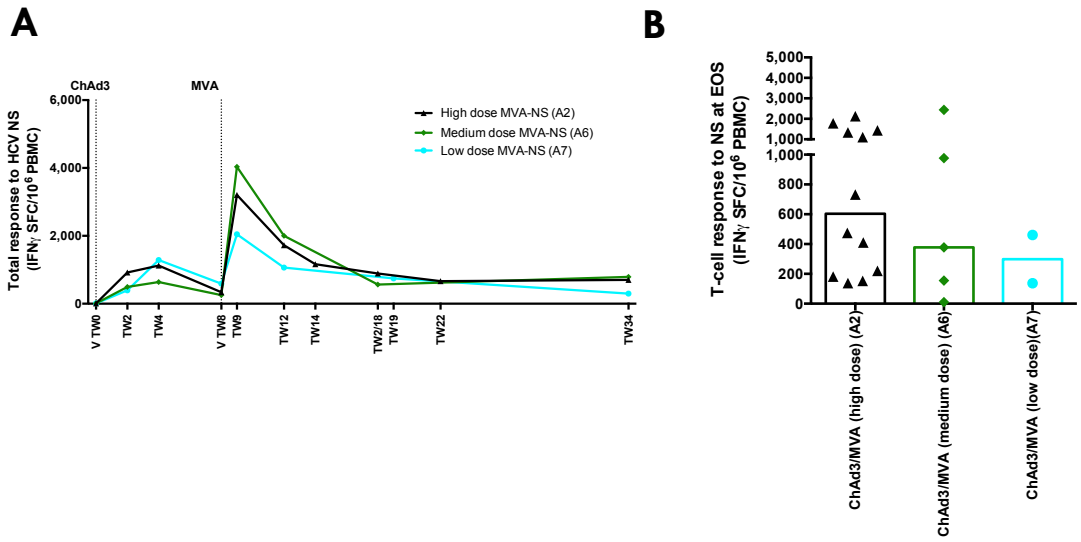


Figure 3-18. A dose de-escalation of MVA-NS: (**A-B**) Healthy volunteers were vaccinated with ChAd3-NS ($2.5x10^{10}$ vp) followed 8 weeks later by MVA-NS at high ($2x10^8$ pfu; black line; arm Arms A2, n = 9) medium ($2x10^7$ pfu; green line; arm A6) or low dose ($2x10^6$ pfu; turquoise line; arm A7; group mean is shown). (**A**) The kinetics of the T-cell response to HCV NS (sum of positive peptide pools, as measured by IFNγ ELISpot) after ChAd3-NS prime and MVA-NS boost (high, medium or low dose). (**B**) A comparison of the magnitude of the HCV-specific T-cell response at the end of the study (EOS). Bars at median.

3.6 Discussion

The primary hypothesis of the work described in this chapter was that vaccination of healthy humans with ChAd3-NS followed by MVA-NS could safely induce high-magnitude and high-quality HCV-specific CD4+ and CD8+ T-cells.

The experimental data presented here confirms this is the case. ChAd3-NS/MVA-NS vaccination generates very high numbers of both CD4+ and CD8+ T-cells, targeting multiple HCV antigens in all vaccinees, irrespective of host HLA

background. I show that vaccine-induced HCV-specific T-cells are polyfunctional, their functionality increased over time post-vaccination, and that heterologous prime/boost with ChAd3-NS and MVA-NS induced T-cells with phenotypic and functional profiles distinct from those elicited by heterologous ChAd3-NS/Ad6-NS vaccination.

Several key questions related to the quality of the T-cell response generated by vaccination were addressed in detail to help us better predict the potential efficacy of these candidate vaccines.

ChAd3-NS/MVA-NS vaccination was safe and well tolerated. No serious adverse events occurred after vaccination and no mild or moderate adverse event lasted longer than 48 hours, showing reactogenicity to be in line with several currently licensed vaccinations (http://www.cdc.gov/vaccinesafety/vaccines/flu-vaccine.html accessed on the 20-10-15; **Khromava et al. 2005; Cox et al. 2015**) and for analogous viral vectors (**Green et al. 2015; Casimiro et al. 2004; Parrino et al. 2007; Kreijtz et al. 2014; Overton et al. 2015; Ndiaye et al. 2015**).

Little is known about the ability of virally vectored vaccines to induce regulatory T-cells, which could influence vaccine efficacy and have a lasting effect on the vaccine recipient's immune system. The induction of Tregs has been associated with persistent HCV infection in humans (**Ward et al. 2007**), and with repeated low level HCV exposure in chimpanzees – with Treg induction in the latter causing increased rates of HCV persistence (**Park et al. 2013**). Treg expansion in

these studies may result from priming of T-cells in the tolerogenic liver environment however, as no induction of Tregs after vaccination with viral vectors encoding HCV antigens in the periphery was seen.

Although no defined cut-off for a protective response against HCV exists, responses in individuals who clear acute infection are typically in the region of a few hundred IFNγ producing cells per million PBMCs (Osburn et al. 2010; Urbani et al. 2006; Takaki et al. 2000; Gerlach et al. 1999). ChAd3-NS primed HCV-specific T-cell responses were boosted by MVA-NS vaccination to unprecedented magnitudes (median 2355 SFC/10^6 PBMC by IFNγ ELISpot) and these responses contracted proportionally to the peak response, so that a significantly higher 'set-point' of memory T-cells was seen after MVA-NS. Importantly for a prophylactic vaccine these responses remained detectable and functional over a year and a half after boost vaccination.

T-cell responses measured in the chronic phase of HCV infection are typically narrowly targeted to a limited number of epitopes, facilitating viral escape (**Lauer et al. 2004; Spada 2004; Urbani et al. 2006; Lechner, Wong, et al. 2000**). Because of the inherent mutability of HCV and the concomitant diversity of viral strains, even within a single genotype or subtype, such breadth improves the chances of peptide recognition of the incoming strain, as well as limiting further escape *in vivo*. T-cells induced by ChAd3-NS/MVA-NS recognized all 6 peptide pools in the majority of individuals and further mapping revealed as many as 31 epitope targets in a single individual; the breadth of the T-cell

response was significantly enhanced by MVA-NS boost relative to ChAd3-NS prime alone or in combination with Ad6-NS boost.

T-cell responses to certain key epitopes have been directly or indirectly (due to restriction by a particular HLA allele) associated with an increased rate of spontaneous resolution of HCV (so called 'protective epitopes') (**Fitzmaurice et al. 2011; Kim et al. 2011; Neumann-Haefelin & Thimme 2007; Dazert et al. 2009**) and these represent highly desirable targets for a T-cell mediated prophylactic HCV vaccine. It has been previously described that the high genetic barrier to T-cell escape - namely the requirement for several mutations within the epitope and surrounding compensatory mutations to avoid recognition by T-cells - and the cost to viral fitness of escape mutations, together limit HCV's ability to persist in natural infection **(Kim et al. 2011; Neumann-Haefelin & Thimme 2007; Dazert et al. 2009**). It is promising then that in healthy volunteers of the correct HLA type T-cells targeting protective epitopes were observed, and at relatively high magnitude *ex vivo* in the case of $NS5B_{2841-2849}$ (B27; ARMILMTHF). T-cells primed by our vaccine immunogen were highly cross-reactive to genotype 1 variants at two of the three epitopes tested, ($NS5B_{2841-2849}$ and $NS5B_{2466-2474}$). Memory T-cells, already primed in the periphery away for the tolerogenic environment of the liver, should be able to respond even more rapidly to HCV infection, further limiting the opportunity for HCV virus to escape and persist.

Since HCV exists as distinct genotypes that are broadly segregated geographically, I assessed the capacity of T-cells generated by MVA-NS boost

encoding a subtype-1b immunogen to target genotypes 1a, 3a and 4a viral sequences. In the context of a highly immunogenic vaccine, cross-reactive T-cell responses between heterologous viral genotypes are readily generated but at a reduced magnitude. Whether these responses are sufficient to provide protection will require efficacy studies in mixed genotype populations.

T-cells primed by ChAd3-NS clearly had the capacity for extensive proliferation on recognition of their cognate-antigen *in vivo*, as seen by the expansion on boosting with MVA-NS, and their proliferative potential was confirmed by *in vitro* culture with HCV peptides and proteins. The expansion of T-cells on boost vaccination was accompanied by phenotypic changes, and the strongest expression of markers of activation (HLA-DR, CD38 and PD-1) was seen on HCV-specific T-cells acutely after MVA-NS, suggesting the enhanced magnitude of response after MVA-NS is a result of stronger activation on a per cell basis.

CD4+ T-cell responses are known to play a central role in the generation and maintenance of effective CD8+ T-cell immunity (**Zajac et al. 1998**) and have been reproducibly associated with HCV viral control in both natural infection (**Gerlach et al. 1999; Thimme et al. 2001**) and in chimpanzee challenge studies (**Grakoui et al. 2003**). Whilst heterologous boosting with MVA-NS markedly increased the magnitude of the CD8+ T-cell responses compared to heterologous Ad vaccination, the increase in magnitude of polyfunctional CD4+ T-cell response was particularly striking. TNFα and IFNγ have been shown to act synergistically to offer enhanced killing of infected cells in some settings (**Bogdan et al. 1990; Liew et al. 1990; Chan et al. 1992**) and more polyfunctional T-cells may offer

better viral control (**Betts et al. 2006; Darrah et al. 2007; Kannanganat et al. 2007; Bogdan et al. 1990; Precopio et al. 2007**). It is, therefore, promising that ChAd3-NS/MVA-NS induced HCV-specific T-cells are highly polyfunctional, expressing a similar combination of cytokines as seen by HIV-specific T-cells in LTNPs and by CMV-specific T-cells (**Casazza et al. 2006**).

HCV-specific T-cells induced by ChAd3-NS/MVA-NS vaccination showed high expression of cytolytic markers and the capacity to up-regulate perforin and degranulate on activation suggesting they have good cytolytic capacity, though direct cytotoxicity against infected hepatocytes is yet to be demonstrated.

The innate signalling pathways stimulated and the persistence and quantity of antigen after vaccination can vary significantly between viral vectors which will have a profound effect of the T-cell response elicited (**Casimiro et al. 2003; Flatz et al. 2011; Hansen et al. 2009; Reyes-Sandoval et al. 2011**). Distinct combinations of T-cell memory phenotypes were seen during the peak and memory responses generated by ChAd3-NS and MVA-NS vaccinations. On seeing their cognate antigen CD45RA was strongly down regulated by vaccine-induced CD8+ T-cells, meaning the dominant populations after ChAd3-NS prime and MVA-NS boost are Tcm and Tem. There was little activation or expansion of CD8+ T-cells after Ad6-NS boost vaccination and the magnitude of the response and proportion of Tem:Tcm:Temra:Naïve T-cells did not change significantly from 4 weeks after boost to the end of the study; the response is dominated by T-cells with a 'naïve' like phenotype (CD45RA+CCR7+), despite the fact that these are functional antigen-experienced T-cells. These naïve-like cells may include a

population of Tscm (stem cell like memory T-cells). Tscm have recently been described as a CD45RA+CCR7+CD28+CD27+ naïve-like population in man, which also express CD95, IL2Rβ, CXCR3, and LFA-1 (**Gattinoni et al. 2011**);further phenotyping is needed to confirm this. Long-term after MVA-NS boost vaccination the T-cell memory response is dominated by Tem and Temra T-cells with 10-15% being Tcm. This evolution of CD8+ T-cell memory is striking, as a contraction towards a Tcm phenotype may have been expected. The overall functional significance of the balance of memory phenotypes induced by vaccination is not known, but a mixture of Tem, with immediate effector function, and the lymph node homing Tcm with good proliferative capacity is likely to be required (further investigation and discussion of the memory subtypes generated is presented in **Chapter 4**).

The possibility of further enhancing the peak and memory HCV-specific T-cell responses was investigated by vaccinating volunteers who had already received ChAd3-NS/MVA-NS with further rounds of ChAd3-NS and/or MVA-NS. The activation and expansion of HCV-specific T-cells is limited when further vaccinations are given shortly after the initial prime-boost, however, T-cells can respond strongly to re-exposure to antigen if enough time is given between vaccinations. The contraction of the T-cell response appeared markedly reduced after secondary ChAd3-NS or MVA-NS vaccinations when given long term after the initial prime-boost, and a higher memory set point was achieved in most individuals. By leaving a longer gap between vaccinations anti-vector immunity may be reduced, allowing better availability of antigen and better activation of HCV-specific T-cells. nAb and T-cells targeting the Ad vector have been shown to

limit transgene expression and T-cell induction after vaccination in mice and humans (**Steffensen et al. 2012; Sumida et al. 2004; Fitzgerald et al. 2003; Youil et al. 2002; Zak et al. 2012**). In our studies anti-ChAd3 neutralizing antibodies do not appear to contract measurably after boost and volunteers in arm A4, who received a second ChAd3-NS at least 42 weeks after their first ChAd3-NS, vaccination all had anti-ChAd3 nAb titers >600 at the time of their second ChAd3-NS vaccination but HCV-specific T-cells expanded in 3/4 of them. No correlation between the magnitude of the Ad hexon-specific T-cell response at the time of vaccination with ChAd3-NS and the HCV NS T-cell response to vaccination has been seen (**Barnes et al. 2012; Swadling et al. 2014**)(anti-vector immunity will be discussed in more detail in **Chapter 6**).

The HCV-specific T-cell response is still contracting at least 14 weeks after MVA-NS boost and T-cells continue to change phenotype and differentiate up until at least 26 weeks post MVA-NS, therefore, a longer gap between vaccinations may allow T-cell memory to evolve to a state where it can optimally responds to antigen re-exposure. In volunteers who received the most intensive vaccine regimen of ChAd3-NS/MVA-NS/ChAd3-NS/MVA-NS, all 8 weeks apart, T-cells assayed long term after the last vaccination showed a more terminally differentiated phenotype, whereas a larger population of Tcm persisted when a second round of ChAd3-NS/MVA-NS was given long term after the initial ChAd3-NS/MVA-NS prime-boost vaccinations. The T-cell subset that will offer best protection against HCV infection is not yet known and therefore it is difficult to predict the relative protective efficacy of each vaccination regimen.

Overall, ChAd3-NS/MVA-NS induced T-cells are remarkably similar to those induced by the highly efficacious yellow fever and smallpox (Dryvax) vaccines (i.e. Temra/Tem phenotype, polyfunctional, and PD-1+), which are associated with life long protection (**Ahmed & Akondy 2011; Akondy et al. 2009; Gaucher et al. 2008**). Furthermore, Tem and Temra cell subsets have been associated with protection against HIV-1 (**Northfield et al. 2007**) and flu (**Sridhar et al. 2013**) in natural history studies, and against simian immunodeficiency virus (SIV) (**Hansen et al. 2009; Hansen et al. 2011**) and malaria (**Reyes-Sandoval et al. 2011**) in vaccine studies - as could be the case with ChAd3-NS/MVA-NS induced Tem and Temra on HCV exposure.

3.7 Conclusion

Whilst the COP for HCV are not precisely defined, studies of T-cell immunity in natural infection suggest that a number of key parameters will be required. These include the targeting of multiple HCV antigens (**Lauer et al. 2004**), the generation of CD4+ and CD8+ T-cell subsets (**Lechner, Wong, et al. 2000; Grakoui et al. 2003; Shoukry et al. 2003; Urbani et al. 2006; Semmo et al. 2005; Gerlach et al. 1999; Thimme et al. 2001**), the maintenance of a memory pool over time with the capacity to proliferate (**Folgori et al. 2006a**), a population of circulating T-cells with immediate effector function (Urbani et al. 2006; Takaki et al. 2000), with no significant induction of Tregs (**Park et al. 2013**). A critical threshold for the magnitude of the T-cell response required has not been established though it is likely that in the context of a prophylactic

vaccine “more is better”. The T-cell vaccine regimen described here meets each of these criteria.

Whilst the diversity of the HCV genome represents a major challenge to vaccine development, a proportion of people infected with HCV are able to eradicate virus spontaneously and effective T-cell immunity appears to play a crucial role in this. Overall, we have generated a potent T-cell vaccine that may recapitulate and accelerate these events *in vivo* to prevent the development of chronic disease. I have extensively characterised the immune response to this vaccine regimen in humans, assessing many T-cell parameters which should be key to controlling HCV infection, which has lead the way to the first efficacy study of a T-cell vaccine for HCV. A phase–II study using this ChAd3-NS/MVA-NS regimen in intra-venous drug users is currently underway in Baltimore, USA, and provides proof of principle that this kind of study is now feasible (NCT01436357). This study will be the first double blinded, randomised, placebo-controlled trial of a vaccine to prevent HCV persistence and it will assess vaccine immunogenicity, efficacy, and safety in a larger cohort of volunteers with a broad range of HLA-types, exposed to different viral sub-types, and crucially whether this regimen can enhance the rate of spontaneous resolution of HCV infection.

The viral vector used has a profound effect on the quality of the immune response elicited. Ad and MVA constructs are currently being used to virally vector antigens from several pathogens (influenza A, respiratory syncytial virus, malaria, ebola, tuberculosis, and HBV in Oxford alone), therefore, data collected

here on the immune response to Ad and MVA can be applied to vaccine design for several diverse pathogens.

3.8 Summary of results

- Potent viral vector vaccines can be safely given to healthy volunteers, without induction of Tregs.
- MVA-NS vaccination boosts ChAd3-NS primed T-cell responses, enhancing the magnitude of the peak and memory HCV-specific T-cell response
- ChAd3-NS/MVA-NS induced HCV-specific T-cells target all 6 HCV polyprotein products in most healthy volunteers, regardless of their HLA, with one individual targeting as many as 31 different epitopes (median 11).
- T-cells targeting epitopes previously associated with protection against HCV infection were induced, and *in vitro* they recognised common viral variant sequences.
- MVA-NS boosted T-cells are highly functional – with improved proliferative capacity, antiviral and immunomodulatory cytokine production, and good cytotoxic potential.
- HCV-specific T-cells respond to further rounds of vaccination if given time to fully differentiate after initial prime-boost vaccination. The memory set point and phenotype of HCV-specific T-cells may be adjusted by further vaccination.
- A 10-fold drop in MVA-NS dose (2 x 10^7 pfu) does not limit immunogenicity as a boosting vector.

4 Mass cytometry – single cell analysis of the CD8+ vaccine-induced T-cell response

4.1 Primary hypothesis

Single cell analysis by mass cytometry and polychromatic fluorescence activated cell sorting will allow informative in-depth characterization of the T-cell response to vaccination and will show that ChAd3-NS/MVA-NS prime-boost vaccination induces CD8+ T-cells of high quality.

4.2 Introduction

T-cells play a key role in protective immune responses against HCV infection; however, the magnitude of the T-cell response has not been reproducibly associated with protection. The delineation of T-cells into distinct subsets according to their functionality and phenotype has shown that protection against diverse viral infection can be mediated by different subset of T-cells. No COP against HCV has been defined in NHP, or humans and this may reflect our inability to identify and measure the combination of T-cell subsets and effector functions that contribute to protection.

In a study comparing the T-cell response to three prime-boost combinations of vectored vaccines against HIV-1, *Flatz et al* showed that despite inducing a comparable magnitude of T-cells that were of a similar phenotype and effector function, gene expression profiling could clearly differentiate the T-cells induced by each regimen (**Flatz et al. 2011**); each vaccine regimen induced a unique

quality of T-cell, with potentially different protective capacity, but which would not have been discriminated had more in-depth characterization of the response not been employed.

The advent of sophisticated cytometric techniques, such as; multiparametric flow cytometry, mass cytometry (cytometry by time-of-flight; CyTOF), and single-cell gene expression profiling, mean we can now analyse multiple parameters simultaneously on a single T-cell, which will help us to better understand the heterogeneity within T-cells and enhance our ability to stratify them by function (**Newell et al. 2012; Flatz et al. 2011; Haining 2012a; Bendall et al. 2012**).

Through parallel advances in the software, hardware (high power solid-state lasers) and reagents (fluorochromes, quantum dots, tandem-dyes) fluorescence activated cell sorting (FACS) can now be used to resolve signals from up to 18 distinct fluorescent tags, however, limitations of cell autofluorescence and over-lapping excitation and emission spectra of fluorochromes mean FACS is reaching its practical limit of parameters that can be simultaneously assayed (**Bendall et al. 2012**).

Single-cell mass spectrometry does not suffer from the same limitation in the number of parameters detectable as it uses the ability of mass spectrometers to accurately distinguish up to 60 heavy metal isotopes simultaneously in clouds of ions (**Bendall et al. 2012**). By labelling antibodies specific for surface and intracellular proteins of interest with heavy metal isotopes CyTOF has been used

to assay up to 36 markers at a single cell level, with little cross talk (**Mason et al. 2015; Swadling et al. 2014; Newell et al. 2012**).

To produce a more in-depth picture of CD8+ T-cell diversity within vaccine-induced T-cells using CyTOF, I assembled a panel of 33 cell markers that are variably expressed on human CD8+ T-cells. I collected data on the DNA content, cell viability, and relative length of cells, as well as surveying for the induction of nine functional attributes, including six intracellular cytokines, CD107α/β, two cytotoxic granule components, and metal-labelled peptide-MHC tetramers for CMV, Influenza (Flu), and against two HCV epitopes.

The phenotype and functionality of vaccine-induced HCV-specific CD8+ T-cells were compared with T-cells induced by natural infection with CMV and Flu in parallel. A characteristic of the T-cell response to CMV is the induction of high magnitude effector memory populations that are maintained throughout life (**Gillespie et al. 2000; Munks et al. 2006**) – referred to here as 'persistent effector memory T-cells' or 'persistent Tem'. In contrast to other chronic viral infections, the archetypal murine virus being LCMV, CMV-specific T-cells do not show pronounced dysfunction, or T-cell exhaustion - they retain their proliferative capacity and immediate effector functions (**Snyder et al. 2008; Wherry & Ahmed 2004**); they, therefore, represent a highly desirable population of cells with several of the key characteristics required by a protective vaccine-induced memory response: they are high in magnitude, durable, highly functional, and they circulate systemically.

At the extremes of antigenic load *in vivo* T-cell responses are driven to exhaustion and even deletion (chronic or high level antigen exposure) or they contract to a small number of homeostatically cycling T-cells, maintained by cytokine signalling alone, or if antigen-addicted they can be deleted (cleared acute infection or antigenaemia) (**Wherry & Ahmed 2004**). It is hypothesised then that there is a sweet-spot of continuous but low level exposure to antigen that, when combined with appropriate inflammatory signals and effective antigen presentation, allows the maintenance of durable high frequency populations of effector memory CD8+ T-cells (**Tatsis et al. 2007; Snyder et al. 2008; Wherry & Ahmed 2004**). This low level exposure to antigen may be a characteristic shared by non-replicative adenoviruses and chronic controlled infection with CMV.

Persistent low levels of transcriptionally active adenovirus vector genomes have been detected by nested PCR in the liver, lymphatics and at the site of inoculation in mice up to two years after being vaccinated with replication-defective adenoviruses (**Tatsis et al. 2007**). Transgene-specific T-cells adoptively transferred 5 months after adenoviral vaccination expanded, suggesting the continued availability of antigen, and the T-cells induced retained the ability to produce anti-viral cytokines, to proliferate and retained an effector phenotype (**Tatsis et al. 2007**).

We have already seen that a large proportion of the T-cells that survive contraction of the response after ChAd3-NS/MVA-NS vaccination in humans also

retain their immediate effector function and possess markers of persistent Tem, and these cells are detectable over a year after vaccination (**figure 3-15**).

Using parallel in-depth analysis of CD8+ T-cells induced by vaccination or by natural infection with CMV I aimed to confirm that the shared phenotype of persistent effector memory T-cells in both settings, as seen by FACS, holds true when assessed using a larger subset of immunologically relevant markers by mass cytometry. I investigated the underlying transcriptional control of these phenotypes to determine whether they truly reflect T-cells with a conserved and shared transcriptional programme or just superficially similar populations.

4.3 Key Questions

I address the following key questions:

1) Can Mass cytometry be used to quantify the heterogeneity of CD8+ T-cells?
2) Do vaccine-induced antigen-specific T-cells produce a more restricted set of cytokine combinations than bulk CD8+ T-cells?
3) Which axes of difference (i.e. Naïve to Ag-experienced, highly proliferative to senescent, functional to exhausted etc.) are most important in defining phenotypic heterogeneity of CD8+ T-cells?
4) Do phenotypic similarities between ChAd3-NS/MVA-NS elicited T-cells remain when assaying a larger combinations of immunological relevant markers?

5) Is there a conserved gene expression profile of Tem between diverse priming events and between mice and men and how is this controlled at the transcriptional level?

Much of this work is described in the manuscripts:

Swadling *et al*. A human vaccine strategy based on chimpanzee adenoviral and MVA vectors that primes, boosts, and sustains functional HCV-specific T cell memory. **Science Translational Medicine. 2014 Nov 5;6(261):261ra153.**

Bolinger, Sims, Swadling *et al*. Adenoviral Vector Vaccination Induces a Conserved Program of CD8+ T Cell Memory Differentiation in Mouse and Man. **Cell Reports. 2015 Nov 11. pii: S2211-1247(15)01204-8**

4.4 Chapter specific material & methods

4.4.1 Heavy metal labelling of antibodies

Purified antibodies were labelled with heavy metal (lanthanide)-preloaded maleimide-coupled MAXPAR chelating polymers via the 'Pre-Load Method v1.1' according to the manufacturers recommendations and as previously described (**Newell et al. 2012**). Briefly, DN3 branched lyophilized polymers are mixed with 5 µl lanthanide and 100 µl L-buffer and incubated at 37 °C for 30-60 minutes. Polymers are then filtered in 3K filters (PALL P/N OD003C34) in eppendorfs and rinsed twice with 400µl L-buffer (spin 11000 g 15 minutes). 100 µl W-Buffer is added to the 3K filter and it is vortex briefly to resuspend loaded polymer.

Antibodies are partially reduced by filtering 100 µg in pre-wetted (R-buffer) 30K filters (Millipore UFC503096) in eppendorfs (11000 g for 10 minutes) with 300 µl R-buffer. Filters are washed with R-buffer and antibody is eluted in 100 µl TCEP solution (Pierce 77720) to give a final concentration of 4 mM TCEP before being incubated at 37 °C for 30 minutes.

Antibodies are washed twice with C-Buffer and once with W-buffer and are added to polymers in the 3K filters (spin 11000 g 20 minutes). The supernatant is then left at room temperature overnight. The next day 200 µl W-Buffer is added and the polymer-conjugated antibodies are filtered in 30K filters and washed 6 times and eluted in W-buffer (11000 g 5 minutes). 100 µl of antibody stabilizer is added and antibodies are stored long term at 4 °C. Nanodrop OD280 is taken and divided by 1.4 to give the concentration in mg/ml (polymers don't absorb at 280 nm).

Cells were also stained with three fluorochrome labelled flow antibodies (CD161-APC, gamma-delta-FITC [fluorescein isothiocyanate], and PD-1-PE) and then stained for anti-PE, anti-APC, and anti-FITC antibodies conjugated to metals. CD3 was stained using a Qdot antibody, which is composed of cadmium.

4.4.2 Tetramer loading and multiplexing

Tetramer generation was performed as previously described (**Toebes et al. 2006**), briefly: HLA-A*0201 MHC molecules folded with UV-cleavable peptides were biotinylated and purified. Peptides were exchanged by UV irradiation (365 nm) of MHC molecules (100 µg) on ice for 20 minutes with rotation, in presence of high

concentrations (20 µM) of CMV $pp65_{482-490}$ NLVPMVATV, FLU M1/MP_{58-66} GILGFVFTL, HCV $NS3_{1405-1415}$ KLSALGINAV and HCV NS3 $_{1073-1081}$ and were then incubated over night at 4 °C.

pMHC molecules were then tetramerised and labelled with heavy metal isotopes-coupled to streptavidin (1:4 molar ratio of streptavidin to loaded-MHC added stepwise at room temperature with 4 x 5 minute incubations). Tetramers were multiplexed by conjugating each tetramer to exclusive combinations of two heavy metals for each tetramer-peptide specificity (**Table 2-2**)(**Newell et al. 2013**). The specificity of tetramers was tested on PBMC from two HLA-matched unvaccinated individuals.

4.4.3 CyTOF sample preparation

Detailed methodology is described in (**Newell et al. 2012**). All CyTOF experiments were performed under the direction of Evan Newell (Stanford University) using previously optimized protocols (**Newell et al. 2012**) and previously conjugated and titrated antibodies – with the exception of anti-human CD161 and the HCV-specific tetramers, which were prepared with Joannah Fergusson (University of Oxford).

Cryopreserved cells were thawed and left overnight at 37°C. Dead cells were then removed by ficoll density separation. For stimulation, cells were cultured for 3 hours with 150 ng/ml PMA + 1 µM Ionomycin in the presence of brefeldin A (eBiosciences), monensin (eBiosciences), 2 mM anti-CD107α/β, 10 µM TNF protease inhibitor-2 (TAPI-2; VWR International; a metalloproteinase inhibitor that prevents stimulation-induced cleavage of CD62L) and dasatinib (a protein tyrosine kinase inhibitor which

prevents the internalisation and down regulation of TCR molecules). Cells were stained with a cocktail of fluorescently-labelled primary antibodies for 30 minutes on ice, washed with PBS, then stained with a cocktail of metal-conjugated surface antibodies and tetramers (including secondary antibodies against fluorescent tags) for 30 minutes on ice. Cells were washed and stained with a metal-labelled live/dead marker (20 µM maleimido-mono-amine-DOTA in PBS; B-272 macrocyclics.com) and incubated for 30 minutes on ice. Cells were washed several times in PBS before overnight fixation in 2% paraformaldehyde (Electron Microscopy Sciences) at 4 °C.

CyFACS buffer: 0.2 µm filtered, 0.1% BSA + 2 mM EDTA + 0.05% NaAzide in PBS (made with milliQ water and stored in glass wear that has not been washed with soap or contaminated with heavy metals).

Cells were washed in intracellular staining buffer (ebiosciences) and stained and permeabilised with metal-conjugated antibodies for intracellular markers in intracellular staining buffer on ice for 45 minutes. Cells were washed with PBS and stained labelled with 250 nM iridium DNA intercalators (iridium, DVS Sciences #201192A) for 20 minutes at room temperature and fixed again in 2% paraformaldehyde. Cells were finally washed twice in PBS and distilled water before dilution to achieve < 500 events/s on the mass cytometer.

Data were acquired and analysed on the CyTOF machine as previously described (**Newell et al. 2012**). Data was acquired and analysed on the fly using dual-count

mode with noise-reduction mode turned off. All other settings were either default or optimized with tuning solution as instructed by DVS sciences.

Heavy metal ions are not present at detectable levels in human cells meaning there is no equivalent to the autofluorescence seen in FACS experiments. The sensitivity of the detector is approximately equal across all ions, meaning this is not a factor in panel design, however, some attention has to be paid to the presence of impurities within the metal tags (usually of molecular mass + or – 1) and of oxygenated ions (appearing in the channel +16 molecular mass above what is expected for that heavy metal)(**Tricot et al. 2015**).

4.4.4 CyTOF analysis

Built-in cell-identifying software on the CyTOF creates an FCS file, enabling mass cytometry data to be analysed in a manner similar to standard flow cytometry data by FlowJo software (Treestar, Inc.; **figure 4-1B**).

Data was analysed using principal component analysis (PCA), a mathematical algorithm, which reduces the dimensionality of data whilst retaining information contained on the variation within the data set. PCA identifies directions, or principal components, in which the greatest variation is seen within the data. The principal components are orthogonal linear summary variables which can be expressed in terms of the original variables as a component loading, retaining the information of how much each original variable influences the summary principal component

(**Ringner 2008**) e.g. each cell is given a single value for each principal component which is calculated by summing the expression of a given variable multiplied by the variables component loading.

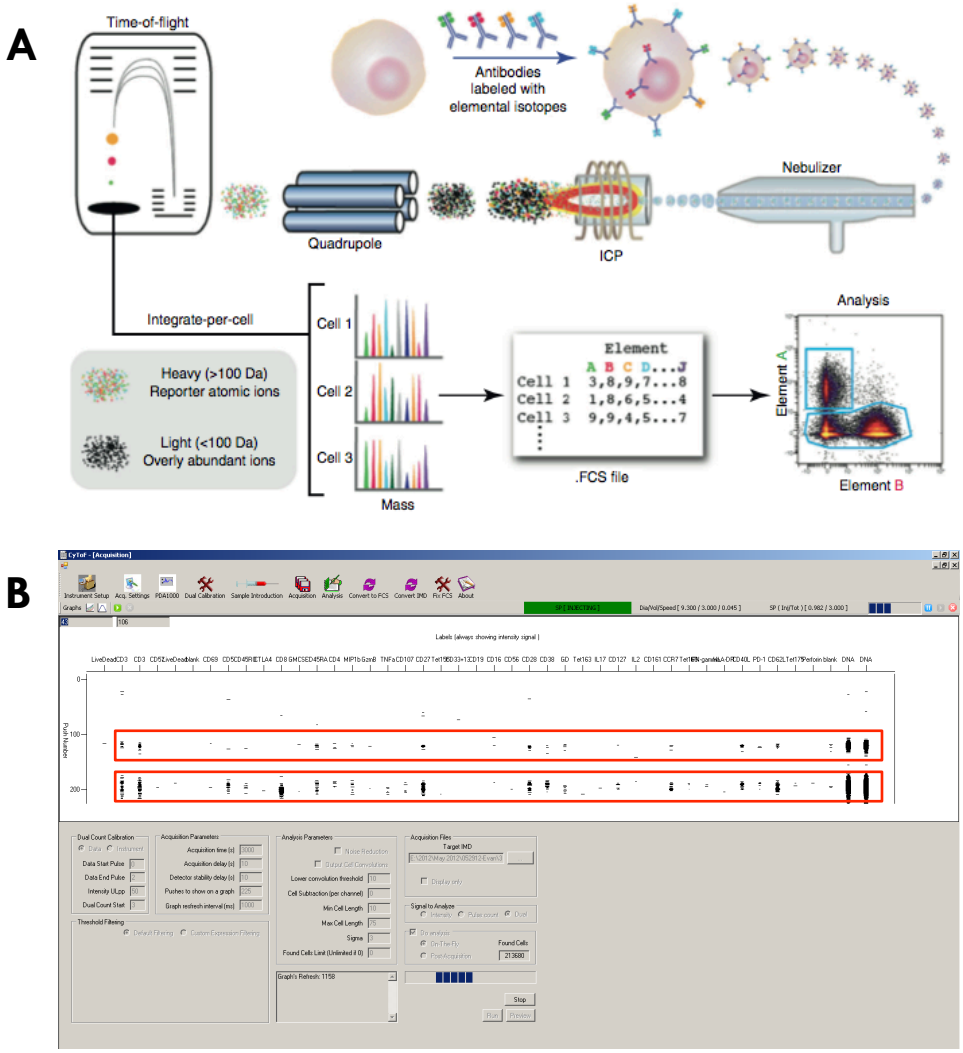


Figure 4-1. Cytometry by time-of-flight (CyTOF):

(**A**) **Cell progress through the mass cytometer.** Labelled cells are introduced as a stream of droplets containing single cells by the nebulizer. Cells are then vaporised, atomised and ionized in a vacuum by combining with a stream of Argon gas that has been heated by an inductively coupled loop to ~5500K. Overly abundant ions (O, C, N etc.) are filtered out by the quadrupoles and the elemental composition of the remaining heavy metal reporter ions is determined by time-of-flight mass spectrometry. Each cloud of atoms produced by a cell is repeatedly scanned by the TOF spectrometer over its ~300 μs lifespan and the simultaneous measurement of each heavy metal reporter ion (20-30 reads) is integrated for each gas

cloud. Clouds containing single cells are identified by the presence of DNA interchelators and the signal corresponding to each elemental tag is correlated with the presence of the respective marker and FCS files are created describing the expression levels of each marker displayed by each cell. (**B) Real time view CyTOF**. Each read of a given gas cloud is displayed as a push number on the Y-axis. The X-axis shows each metal ion labelled by the specificity of the antibody they are linked to. Two cells, identifiable by a signal in the DNA interchelator channel on the far right are shown. **(A)** Adapted from (**Bendall et al. 2011**).

For PCA, cells were gated on live CD3+CD8+ T-cells (principal component loaded using data from patient 319 at TW22 then applied to the other datasets) and the expression level (equivalent to MFI in FACS) for each metal-labelled antibody was exported to a tab-delimited text file with FlowJo v9.3.2 for further analysis with scripts written in Matlab. FCS files containing these additional parameters were created using a custom algorithm written in Java (text to FCS script generously provided by W. Moore). pdb files were also created using Matlab that could be read by PyMOL software (DeLano Scientific LLC). All Matlab scripts started with transformation of data into logicle biexponential scaling as described (**Newell et al. 2012**). Only informative markers (e.g. not CD3, CD8, CD13/CD33 etc.) and markers that stained well were included in the PCA analysis (21 of the 33 markers, listed in **figure 4-4A-C**).

4.5 Results

4.5.1 Mass cytometry: Introducing the technology

For analysis by CyTOF cells are prepared in a manor analogous to that used from FACS analysis (See **section 4.4**). Briefly, PBMC or cells of interest are sequential stained with MHC class I tetramers, live/dead differentiating dyes, and

antibodies against surface markers. They are then fixed and permeabilised and stained with antibodies against intracellular or intra-nuclear markers and DNA interchelators. Cells are extensively washed and then introduced into an inductively coupled plasma time-of-flight mass spectrometer (ICP-TOF-MS or CyTOF machine)(**Bandura et al. 2009**) in a stream of water droplets containing single cells. The progress of a cell through the CyTOF machine is described in **figure 4-1A**.

4.5.2 Validation of CyTOF data with FACS

T-cell phenotype and function was determined by CyTOF analysis in volunteers 319 and 322 at TW2/4 (peak T-cell response to ChAd3-NS prime vaccination), TW9 (peak T-cell response to MVA-NS boost vaccination), and at TW22 (memory, after contraction of the T-cell response; **figure 3-2B**), using frozen PBMC. CyTOF was also performed on PBMC from two healthy volunteers with CMV and/or FLU-specific CD8+ T-cell responses.

To confirm the staining conditions with our full panel and to test the specificity of our MHC class I tetramers a test panel was performed on two frozen PBMC samples from healthy donors (not shown). Only IL-8 was omitted from further experiments due to a lack of staining.

CyTOF data can be analysed as flow cytometry data using 2D plots of markers plotted one against another, and the expression of each marker/cytokine can be

recorded for gated cell populations. The gating strategy used to identify T-cells and tetramer+ cells is explained in **figure 4-2A.**

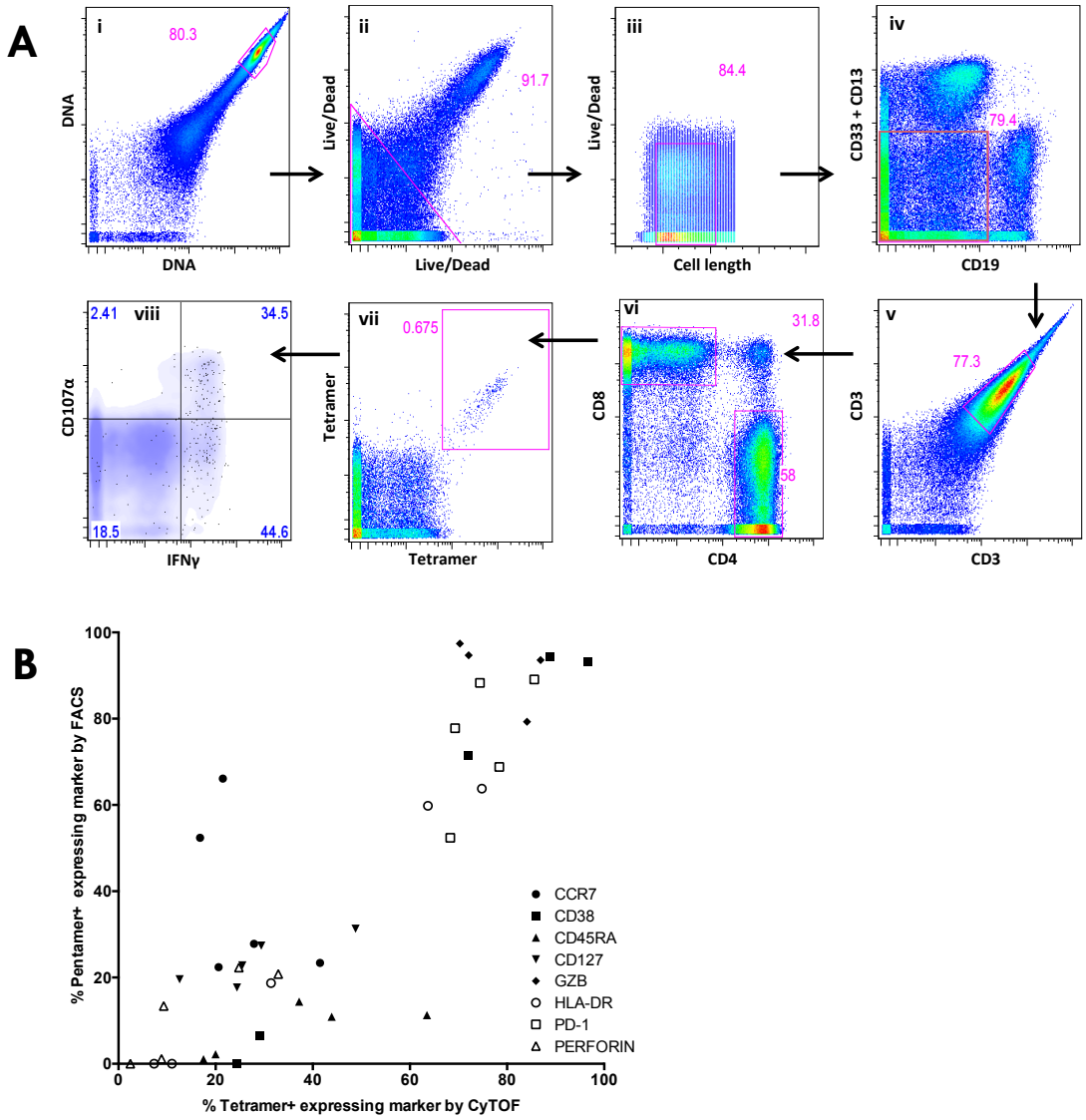


Figure 4-2. CyTOF validation:

(A) Gating strategy for mass cytometry: The gating strategy for CyTOF by mass cytometry is shown. (**i**) Without light scatter to identify individual cells DNA content is used (rhodium and iridium labelled DNA-intercalators). (**ii**) Maleimide-dota stains dead cells. Cell length (**iii**); calculated as the time it takes for the ion cloud to pass through the mass spectrophotometer) is used to identify single cells. (**iv**) CD13/CD33 and CD19 are used to gate out monocytes and B cells respectively. (**v**) and (**vi**) show gating of CD3+ and CD4+/CD8+ cells respectively. (**vii**) shows gating of $NS3_{1406-1415}$ tetramer+ cells and (**viii**) the CD107α and IFNγ co-staining (dots represent tetramer+ cells gated in (**vii**) and the underlying density plot is of total CD8+

after 3 hour PMA/Ionomycin stimulation). Plots from 319 TW22. Percentage of parent shown, except for (**viii**) which shows percentage of tetramer+ cells in each quadrant.

Figure 4-2 (B) A correlation between measurements of phenotypic markers on T-cells by FACS vs. by CyTOF. The percentage of pentamer+ (HCV $NS3_{1406-1415}$ KLSALGINAV) T-cells expressing a given phenotypic marker as measured by Fluorescent-associated cell sorting (Y-axis), or by Single-cell mass cytometry (CyTOF; x-axis) are plotted for volunteers 319 and 322 at TW9 and TW22 (1week and 14 weeks post MVA-NS vaccination respectively) and at TW4 (4 weeks post ChAd3-NS prime vaccination) for volunteer 319 (post-prime vaccination is not shown for volunteer 322 because the pentamer cloud by CyTOF was too small to accurately assess T-cell phenotype). The antibody clones are reported in supplementary table 2. Non-parametric spearman's rank correlation r = 0.8449 P<0.001 n=5.

Vaccine induced HCV-specific T-cells were readily observed by tetramer staining and frequencies of these matched those seen by flow cytometric pentamer staining (**Table 4-1**; r = 0.9910 p = 0.0001***, excluding 322 TW9 which stained weakly for the $NS3_{1406-1415}$ tetramer by CyTOF, highlighted red and 322 TW2 for which no FACS data is available).

Table 4-1. MHC class I multimer cloud size: FACS vs CyTOF (All to $NS3_{1406-1415}$, except* which is $NS3_{1073-1081}$)

Volunteer	Trial week	Pent cloud (%CD8)	
		CyTOF	FACS
319 TW4	TW4	0.20	0.20
319 TW9	TW9	1.48	1.50
319 TW22	TW22	0.64	0.76
322 TW2	TW2	0.23	-
322 TW9	TW9	0.41	2.23
322 TW22	TW22	0.11	0.19
355 TW9	TW9	0.07	0.25

The expression of surface and intracellular markers by CyTOF also closely matched those measured by flow cytometry (**figure 4-2b**; r = 0.8092 p <0.0001****).

4.5.3 Polyfunctionality of vaccine-induced HCV-specific T-cells

First I assessed the overall potential for cytokine production by HCV-specific CD8+ T-cells by stimulating cells with PMA/Ionomycin for 3 hours in the presence of dasatinib – to avoid the rapid down-regulation of TCR and subsequent lack of tetramer staining that accompanies peptide stimulation (**Lissina et al. 2009; Newell et al. 2012**). By identifying HCV-specific T-cells by MHC class I tetramers, rather than by their cytokine production when stimulated specifically with HCV peptides, I could identify HCV-specific T-cells that did not produce cytokine and I could compare the pattern of cytokine production with that of bulk CD8+ T-cells in the same PBMC sample. It has previously been shown that PMA/Ionomycin stimulation induced comparable cytokine production by T-cells to CD3/CD28 bead activation and that it allowed accurate tetramer staining (**Newell et al. 2012**).

I have shown that CD4+ and CD8+ T-cells induced by ChAd3-NS/MVA-NS peak in polyfunctionality 18-24 weeks post vaccination, as assessed by FACS ICS (**figure 3-12).** A progressive increase in polyfunctionality of HCV-specific CD8+ T-cells was again seen (a feature not seen in the bulk CD8+ population) by CyTOF ICS, with approximately 80% of cells having ≥ 3 functions of the 6 tested by trial week 22 (14 weeks post MVA-NS; **figure 4-3**). Evidence of a hierarchy of cytokine production by HCV-specific T-cells was observed, with the majority of single cytokine-producing CD8+ T-cells making Mip-1-β or IFNγ, dual cytokine-producing T-cells making Mip-1β and IFNγ or TNFα, whilst GM-CSF and IL-2

were only produced in combination with these three cytokines by the most polyfunctional T-cells (**figure 4-3**).

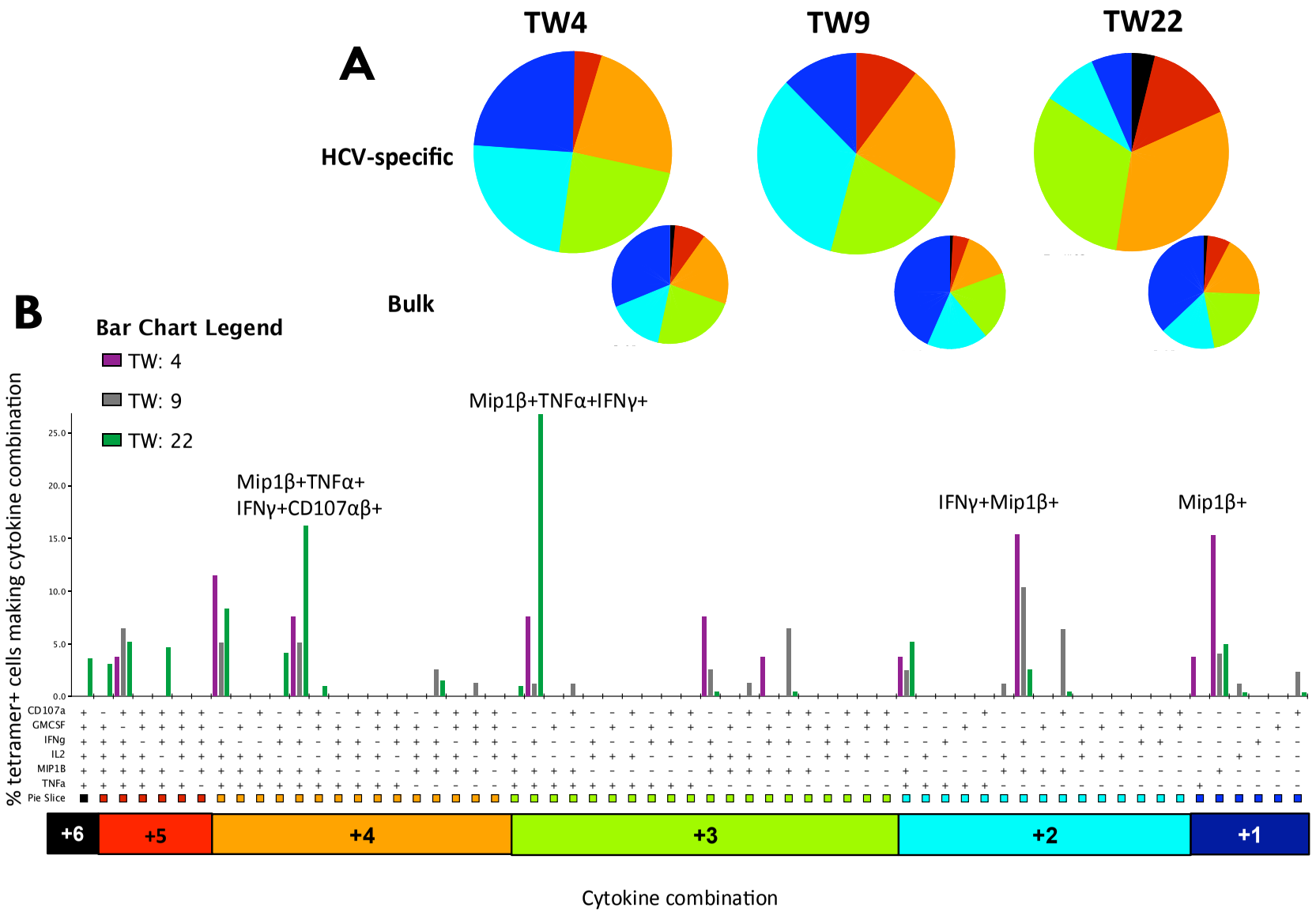

A
TW4
TW9
TW22
HCV-specific
Bulk
B
Bar Chart Legend
TW: 4
TW: 9
TW: 22
Mip1β+TNFα+IFNγ+
Mip1β+TNFα+
IFNγ+CD107αβ+
IFNγ+Mip1β+
Mip1β+
% tetramer+ cells making cytokine combination
25.0
20.0
15.0
10.0
5.0
0.0
CD107a
GMCSF
IFNg
IL2
MIP1B
TNFa
Pie Slice
+6
+5
+4
+3
+2
+1
Cytokine combination

Figure 4-3. Polyfunctionality of HCV-specific CD8+ T-cells analysed by CyTOF: Cytokine production is shown at the peak after ChAd3-NS priming (TW4), the peak after MVA-NS boost (TW9), and 14weeks after MVA-NS vaccination (TW22) for tetramer+ ($NS3_{1406-1415}$ HLA-A2) T-cells stimulated with PMA/Ionomycin for 3 hours. Data from volunteer 319. (**A**) Pie charts represent the proportion of tetramer positive (large pies) or bulk CD8+ (small pies) cytokine-secreting T-cells that produce one (dark blue), two (light blue), three (green), four (orange), five (red) or all 6 (black) cytokines (IL-2, IFNγ, TNFα, GMCSF, MIP-1-β, CD107α/β). Pie base, median. (**B**) Bar graph shows the percentage of tetramer+ cells, which produced a certain combination of cytokines at each time point (TW4, purple / TW9, brown / TW22, green). Bars, Median. The combinations of cytokines that are most common are labelled with text. Analysed using SPICE software.

The ability to produce TNFα appeared to emerge later on after contraction of the T-cell response, which may account for the peak in polyfunctionality around TW22 (**figure 3-12 and figure 4-2**). A small number of the possible combinations of cytokines are represented by populations of T-cells in the bulk CD8+ or in tetramer+ populations suggesting tight transcriptional control of the combination of cytokines secreted by a cell.

4.5.4 A picture of T-cell complexity – 3D-PCA

One of the challenges of using this technology is to incorporate the data from 33 antibodies in an informative way. The magnitude of this problem is seen when comparing the possible combinations of markers in a 9-color analysis (~500) and a 33 colour one (~8,500,000,000; according to the formula 2^N-1).

By reducing the dimensionality of the data most of the information contained within the variation in expression of markers on CD8+ T-cells can be retained but it can be visualized and interrogated more readily. I used principal

component analysis [PCA; reviewed in (**Genser et al. 2007; Ringner 2008**)] to produce a small number of summary variables, or principal components, which summaries the total variation in expression of markers between individual CD8+ T-cells. PCA identifies the principal directions, or axes, in which data varies. Here I used PCA as a way to distil the information from 21 parameters measured on PMA/Ionomycin stimulated T-cells.

The PCA was loaded with expression data from patient 319 at TW22, as this patient had the largest populations of 'memory' CD8+ T-cells and a relatively large HCV-specific pentamer cloud (observed by FACS). The contribution of each marker (component loading) for the first three principal components (PC1-3) are shown in **figure 4-4A-C**.

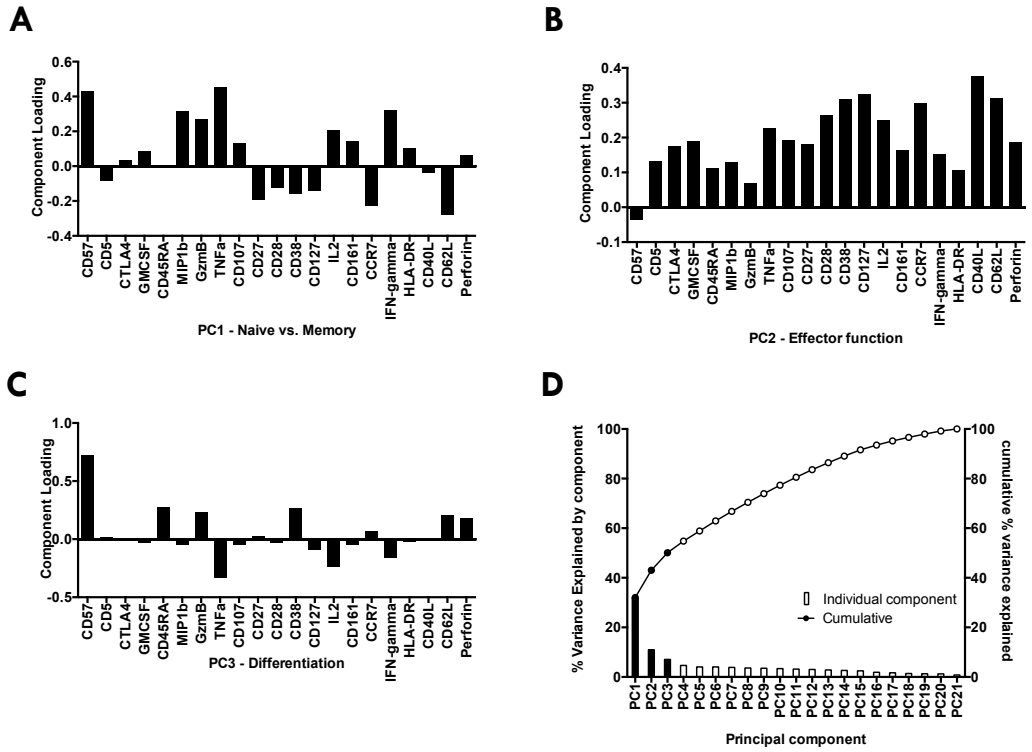


Figure 4-4. Principal component analysis (PCA) of T-cell immunity in human vaccinees: The PCA was loaded with the relative expression of the markers listed on the x-axis of the bar graphs above (**A-C**) for all CD8+ T-cells from volunteer 319 at TW22. PCA produces

summary variables/principal components that summaries as much variation in the expression of these markers across CD8+ T-cells as possible. The three components (PC1, PC2, PC3, **A-C**) summarising the most variation are shown with the weighting coefficients/component loading for each marker. (**D**) The percentage of the overall variation in the markers assayed on CD8+ T-cells explained by each principal component is plotted individually (bars) and cumulatively (line).

The relative amount of variation explained by each component can be calculated (expressed as the percentage of total variance) and this can be used to quantify the effectiveness of this analysis (**figure 4-4D**). The first principal component explains the largest amount of variation in marker expression, with each subsequent component explaining the next largest amount of variation, such that information can be gathered not only about which markers combine to form an axis of heterogeneity (e.g. from naïve to memory experienced, from weak to strong cytokine production) but also which axis has the biggest influence on CD8+ T-cell phenotypic heterogeneity – and potential therefore the immunological importance of that axis of variation. In this analysis, the first three principle components account for 50% of the total variation in expression of the markers assayed within CD8+ T-cells (**figure 4-4D**). Additional variance can be explained by further principle components, however, their contribution was small (**figure 4-4D**); therefore, I restricted the analysis to the first three components.

To visualize the phenotypic complexity of the CD8+ T-cell compartment I plotted PC1-3 for each individual CD8+ T-cell from each sample tested in the protein structure program PyMol to produce a 3D-PCA image. (**figure 4-5**). CD8+ T-cells clustered in defined but overlapping niches resulting in an "L-shaped" plot along

the PC 1-3 axis (**figure 4-5**). This pattern was observed in all 5 individuals at all time points and was almost identical to that seen by Newell *et al* previously (**Newell et al. 2012**).

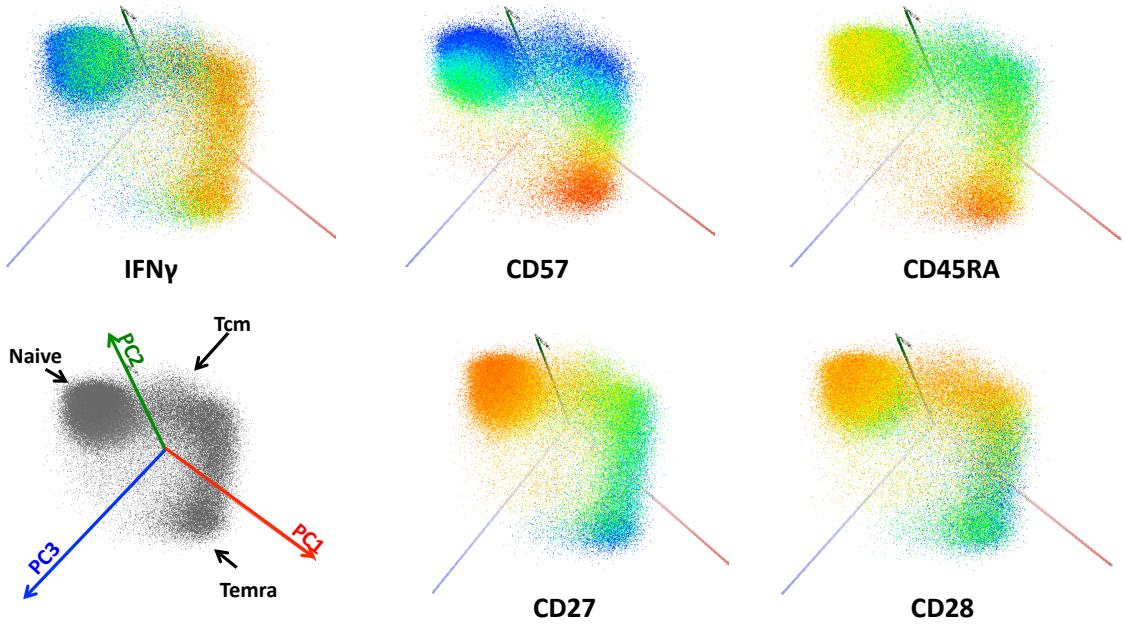


Figure 4-5. 3D Principle Component Analysis of CD8+ T-cells: The first three principal components were plotted using the protein-imaging program PyMOL (PC1 axis in red, PC2 axis in green and PC3 axis in blue). A) Bulk CD8+ T-cells. Each dot represents a single CD8+ T-cell and in the images above the cells are coloured (blue = low, red = high) according to their relative expression within the CD8+ population of IFNγ, CD57, CD45RA, CD28, and CD27. A plot showing all CD8+ T-cells as grey dots shows the shape of the CD8+ T-cells in space according to the first 3 PCs with the relative locations of naïve, Tcm and Temra populations highlighted by arrows. Data from volunteers 319 and 322.

Although PCA is unsupervised, the apparent meaning of each component can be deduced based on our knowledge of previously-defined CD8+ T-cell subsets by looking at the markers that most influence the PC (PC1: naïve vs. memory, PC2: effector function, PC3: T-cell differentiation status; **figure 4-6A-C**). For instance the markers that have the largest (positive or negative) component loading for a

given PCA will have a stronger effect on the value a cell will be assigned for a PCA or where an individual T-cell will fall on that PC axis. A cell that expresses combinations of CD57, Mip-1-β, granzyme B, TNFα, IL-2 IFNγ or perforin will have a high PC1 value (antigen-experienced CD8+ T-cell), and cells expressing a combination of CD27, CD28, CD127, CD62L, CCR7 will sit at the opposite end of PC1 with a large negative value (Naïve CD8+ T-cell).

Another way of extracting meaning from the PCA is to colour each cell on a 3D-PCA plot by the intensity of expression of a single marker relative to all other CD8+ T-cells (low = blue, red = high; **figure 4-5**). In this manner I could assess whether cells expressing a marker cluster together on the 3D-PCA or whether they are scattered throughout. I could identify where previously defined T-cell subsets sit and if a niche did not fit a classic definition of a T-cell subset I could identify which markers are defining it as a unique cluster of cells. Naïve CD8+ T-cells were easily identified as a large cluster of cells expressing CD27, CD28, CD45RA, and low levels of IFNγ and CD57. Antigen-experienced CD8+ T-cells formed an 'L-shaped' arm extending from the naïve cells; moving along this arm there is a progressive loss of CD27 and CD28 and it is where the majority of the IFNγ cells sit. CD57 and high (re)expression of CD45RA was seen at the end of this arm, furthest from the naïve cells.

I then gated on CD8+ T-cell subsets defined using their CD45RA and CCR7 expression and overlaid them on a 2D-PCA plots as shown in **figure 4-6A**. I also did the reverse, gating on areas of the 2D-PCA and looking at the expression of CD45RA and CCR7 of cells falling in a specific area of the 2D-PCA (**figure 4-6B**).

Both analyses show that the cluster of cells low in PC1 are indeed Naïve T-cells and that Tcm occupy a niche closet to the naïve, with Tem, and Temra cells occupying distinct but overlapping areas of the PCA as you move progressively further from the naïve CD8+ T-cells.

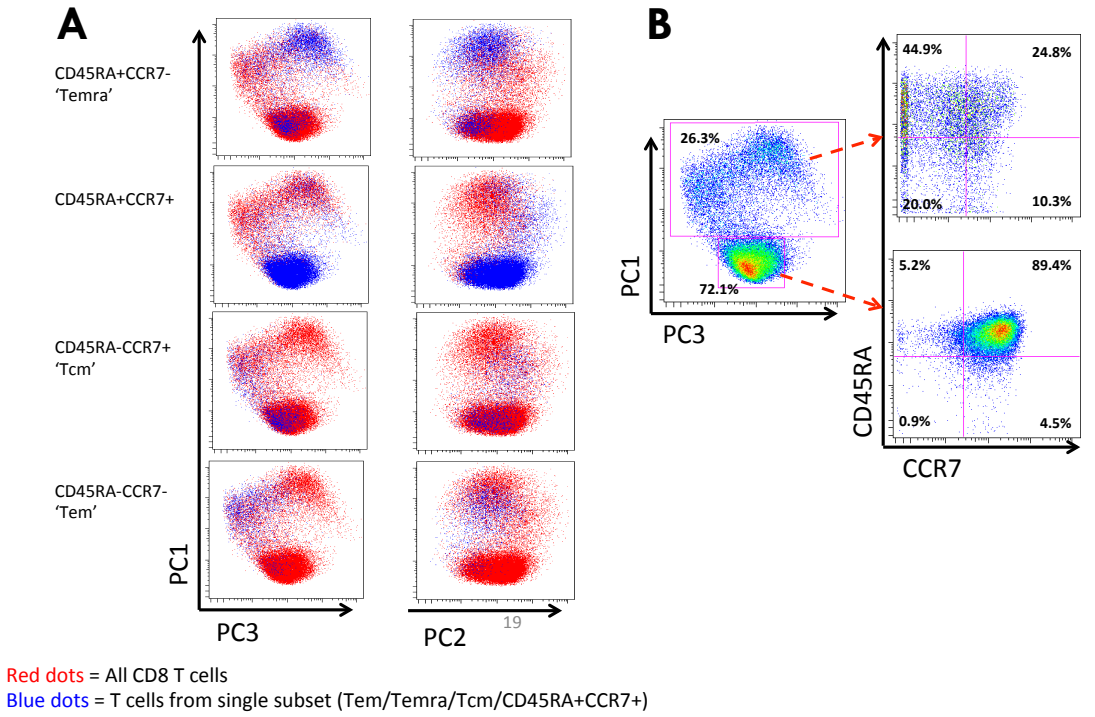


Figure 4-6. Plotting T-cell memory subsets against principal components: (**A**) Bulk CD8+ T-cells were split into four subsets using CD45RA and CCR7 expression and each of these four subsets (blue) were overlaid on bulk CD8+ T-cells (red) and plotted using their values for PC1 vs. PC3 or PC1 vs. PC2. Example plots from volunteer 319 (TW4) are shown. (**B**) PC1 was plotted against PC3 for bulk CD8+ T-cells and the putative 'naïve' population (low in PC1 and mid for PC3), and 'non-naïve populations' (mid-high in PC1) were gated on and their CD45RA vs. CCR7 expression is shown. Example plots from volunteer 319 (TW4).

CD8+ T-cell subsets are not only defined by the surface markers they express but also by the effector functions they possess, in particular the cytokines they produce. I next gated on the CD8+ T-cells that produced a single cytokine to see if the production of that cytokine was restricted to cells that occupied a specific niche within the PCA (**figure 4-7**).

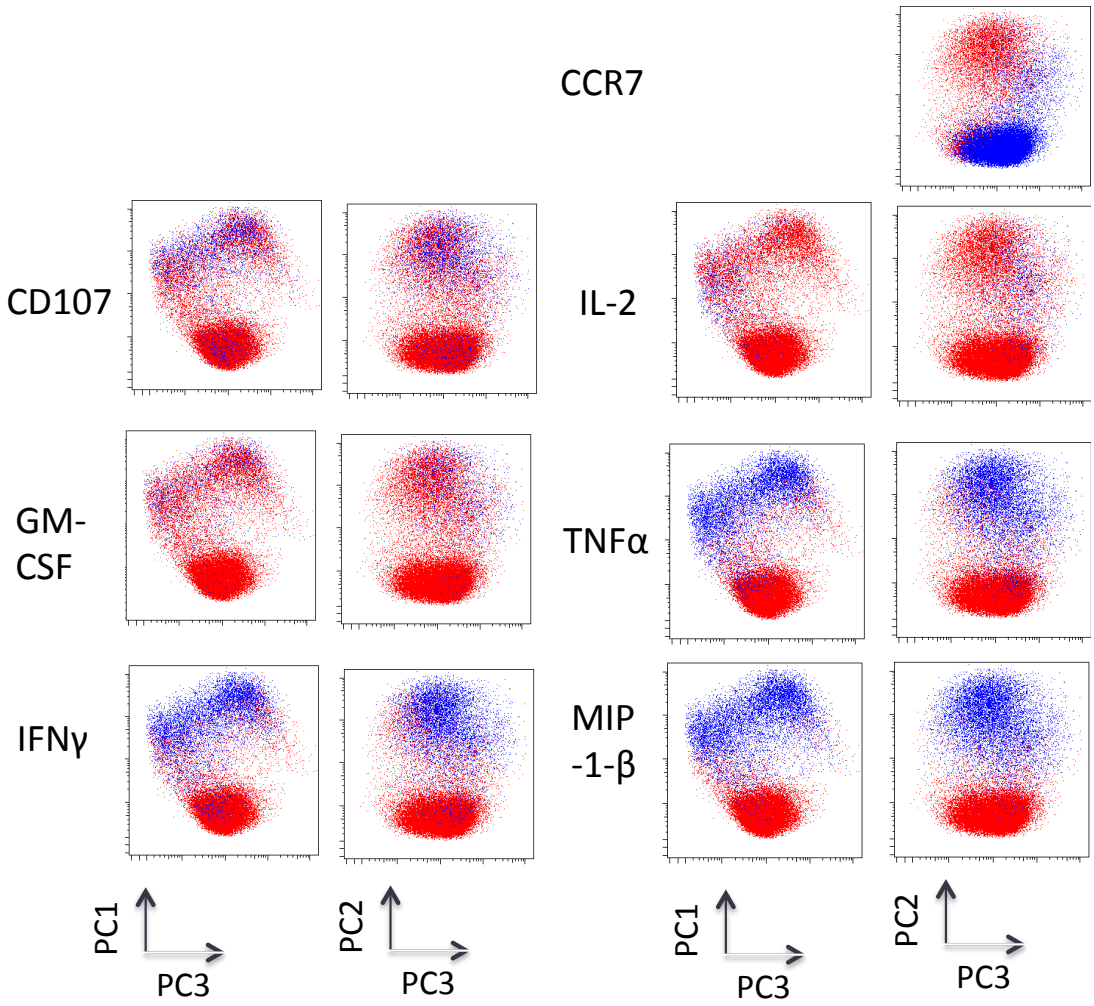


Figure 4-7. Cytokine producing CD8+ T-cells: Example plots of CD8+ T-cells (volunteer 319 TW4) stimulated with PMA/Ionomycin showing cells producing a given cytokine (blue) or CCR7 overlaid on total CD8+ T-cells (red) plotting PC1 vs. PC3 or PC2.

IFNγ, MIP-1-β and TNFα were produced by cells covering the vast majority of the memory population, scattered throughout the 'L-shaped' arm, but with a weaker expression by cells close to the Naïve cluster, in particular where Tcm cells sit, and with the highest expression co-localising with Temra cells. IL-2 production correlated well with CCR7 production and Tcm. The most polyfunctional cells, possessing 8 effector functions all occupied a position furthest from naïve T-cells, overlapping with Temra. (**figure 4-8**).

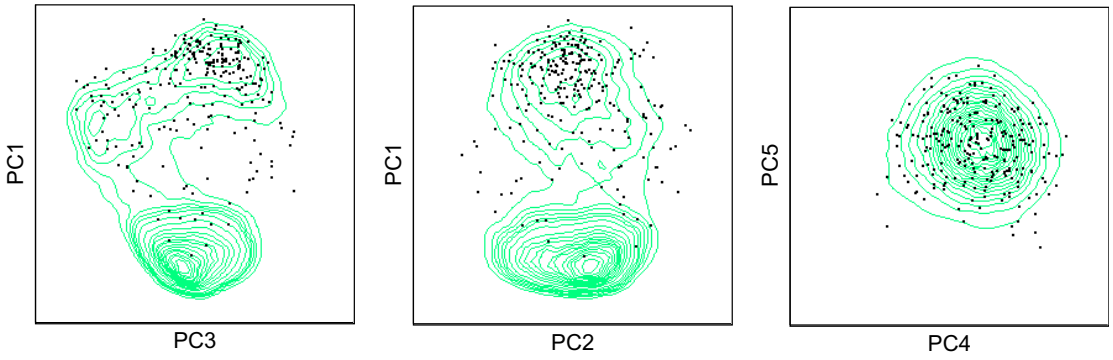


Figure 4-8. CD8+ T-cells possessing 8 functions: Example plots of CD8+ T-cells (volunteer 319 TW4) stimulated with PMA/Ionomycin showing cells producing IFNγ, MIP-1-β, TNFα, IL-2, CD107αβ, GM-CSF, granzyme B and perforin (black) overlaid on contours showing total CD8+ T-cells (green).

4.5.5 Vaccine-induced T-cells on the continuum

Next I plotted the HCV, Flu, and CMV-specific tetramer+ T-cells on the 3D-PCA showing they also occupy restricted niches, but which overlap with bulk populations (**figure 4-9**). After ChAd3-NS prime vaccination HCV-specific T-cells appear to occupy a niche close to the naïve population, in the area occupied by Tcm (CD45RA-CCR7+) and FLU-specific T-cells (**figure 4-9**), agreeing with a mixed Tcm/Tem phenotype seen by FACS (**figure 3-15**). After MVA-NS boosting the cells occupy a broader area across the antigen-experienced regions of the continuum (**figure 4-9**). At the latest time point studied, TW22, the majority of HCV-specific T-cells sit in a niche at the end of the 'L-shaped arm', in a similar location to CMV-specific and Tem/Temra cells (high in PC3; **figure 4-9**).

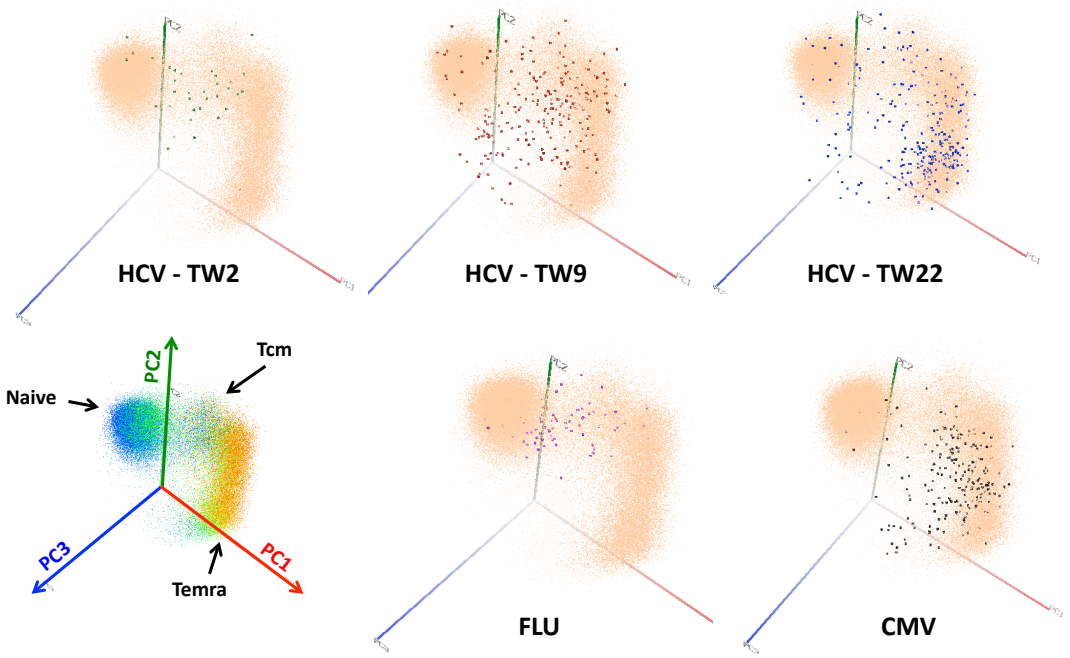


Figure 4-9. 3D Principal Component Analysis of vaccine-induced CD8+ T-cells: 3D-PCA of vaccine-induced HCV-specific T-cells: Each pink dot represents a single CD8+ T-cell (bulk CD8+ T-cells from 319 and 322) and plotted on the same axis are the tetramer+ (NS3 $_{1406\text{-}1415}$ HLA-A2) T-cells at TW2 (peak after ChAd3-NS prime, green) at TW9 (peak after MVA-NS boost, red) and at TW22 (blue). The location of CMV (black) and FLU (purple) specific T-cells, stained using tetramers on PBMC from healthy unvaccinated volunteers (LC037 and LC046), are also shown. The bulk CD8+ T-cells are shown in the bottom left image, coloured for their relative expression of IFNγ with the locations of Naïve, Tcm and Temra populations highlighted by arrows for reference.

Although PC4 and PC5 were uninformative when looking at bulk CD8+ T-cells, immediately after vaccination highly activated cells (expressing CD38 and HLA-DR) could be uniquely identified separately from the bulk CD8+ T-cells due to their high PC4 and low PC5 values (**figure 4-10**). By TW22 the acute expression of activation markers was lost by vaccine-induced cells (**figure 4-10**, **figure 3-10D**). The peak in magnitude of the T-cell response after ChAd3-NS prime vaccination varies between individuals, falling 2 or 4 weeks after vaccination (**figure 3-2A**), and the peak in magnitude correlates well with a spike in

activation status of the vaccine-induced T-cells (**figure 3-10D)**; by plotting PC4/PC5 for each time point it is clear that by TW4 T-cells induced in volunteer 319 have lost their activation markers and that the true 'peak' response to prime vaccination may have preceded this time point. PC4 and PC5 clearly showed that in the acute phase of T-cell activation and expansion after a controlled antigen exposure, such as vaccination, T-cells show a distinct combination of phenotypic markers, which represents one of the most defining axis of variation in CD8+ T-cells.

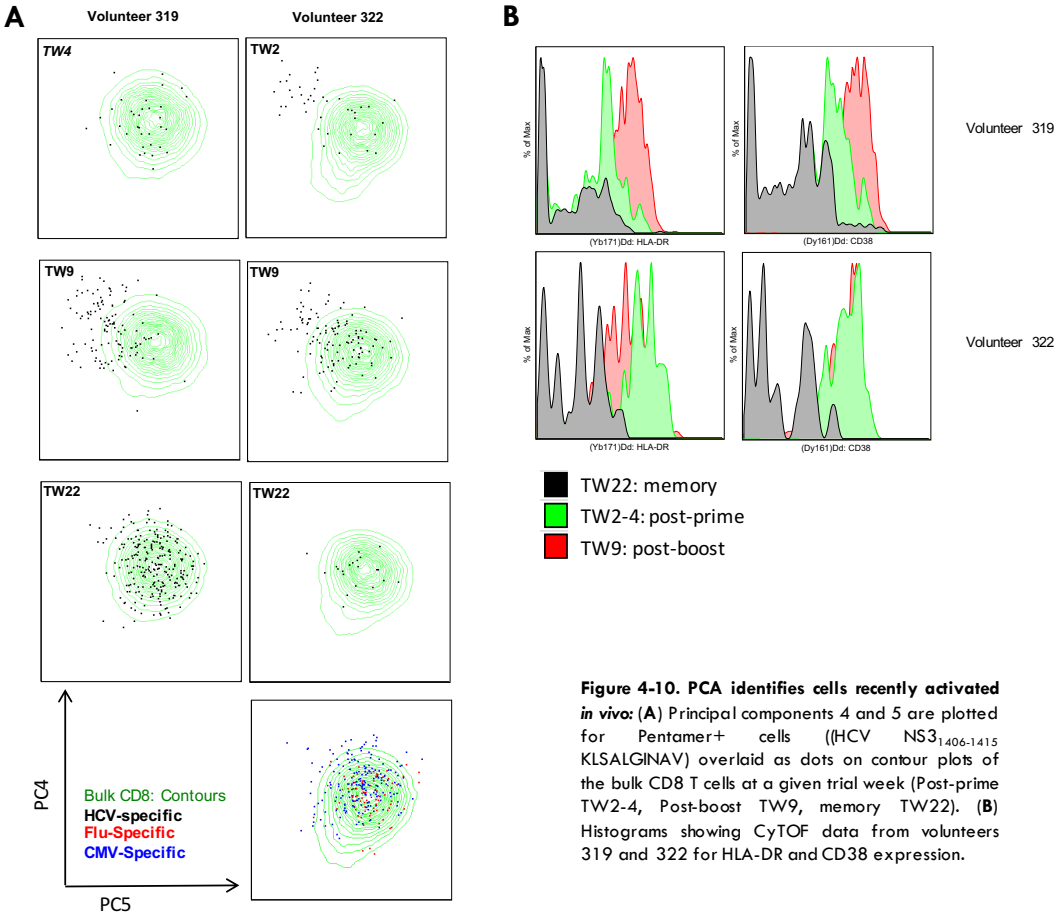


Figure 4-10. PCA identifies cells recently activated *in vivo:* (**A**) Principal components 4 and 5 are plotted for Pentamer+ cells ((HCV $NS3_{1406-1415}$ KLSALGINAV) overlaid as dots on contour plots of the bulk CD8 T cells at a given trial week (Post-prime TW2-4, Post-boost TW9, memory TW22). (**B**) Histograms showing CyTOF data from volunteers 319 and 322 for HLA-DR and CD38 expression.

Figure 4-10. PCA identifies cells recently activated *in vivo:* (**A**) Principal components 4 and 5 are plotted for Pentamer+ cells ((HCV $NS3_{1406-1415}$ KLSALGINAV) overlaid as dots on contour plots of the bulk CD8+ T-cells at a given trial week (Post-prime TW2-4, Post-boost TW9, memory TW22). (**B**) Histograms showing CyTOF data from volunteers 319 and 322 for HLA-DR and CD38 expression.

The HCV-specific T-cells induced after ChAd3-NS prime and MVA-NS boost vaccination are phenotypically distinct and the contraction from the peak response to the resting CD8+ memory T-cells is accompanied by a clear and strong change in phenotype.

4.5.6 A shared T-cell phenotype between ChAd/MVA and CMV induced T-cells.

A large proportion of the T-cells that survive contraction of the response after ChAd3-NS/MVA-NS vaccination retain their immediate effector function and these cells are detectable over a year after vaccination (**figure 3-2A**). I used the CyTOF dataset and FACS staining to confirmed the distribution of effector-memory associated phenotypic markers on CMV and vaccine-induced memory T-cell responses in parallel.

The majority of CMV-specific T-cells and a subset of memory T-cells long-term after ChAd3-NS/MVA-NS vaccination possessed many of the functions that define persistent Tem: production of antiviral and pro-inflammatory cytokines (IFNγ, MIP-1-β, TNFα) and degranulation on peptide stimulation, high expression of granzyme B and low expression of CD127, CCR7 and CD62L (**figure 4-11A**). The proportion T-cells induced by ChAd3-NS/Ad6-NS, ChAd3-NS/MVA-NS or CMV infection was assessed by co-staining PBMC with MHC class I pentamers and antibodies targeting CD45RA and CCR7 (**figure 4-11B**).

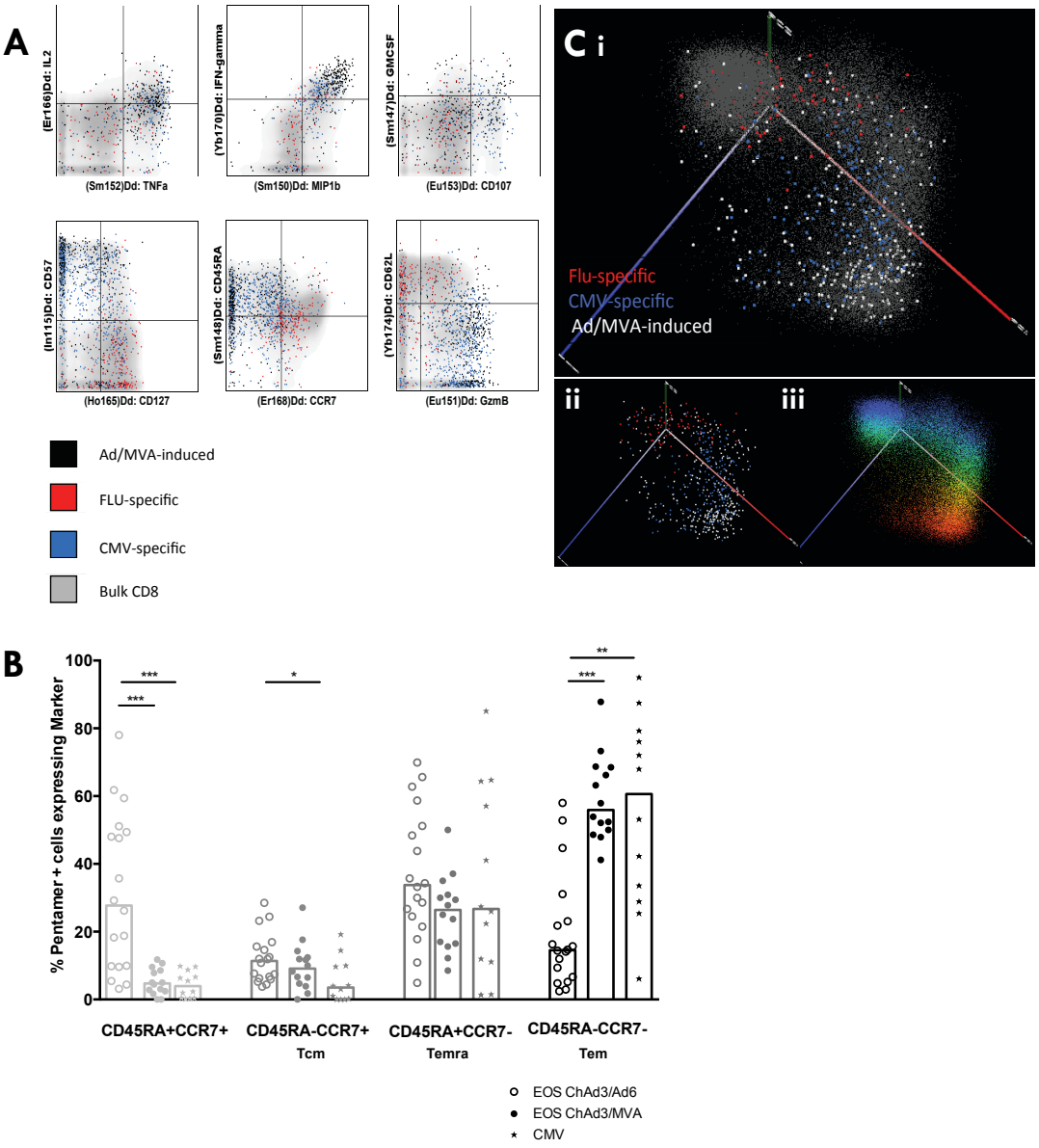


Figure 4-11. Mass cytometry and FACS reveal a shared phenotype of T-cells induced by virally vectored vaccines and CMV: (**A**) Example plots of intracellular cytokine staining on stimulated cells, or surface and internal markers on un-stimulated cells. Bulk CD8+ T-cells are shown as a density plots in grey and Ag-specific cells (319 and 322 TW22) are overlaid as black, red (Flu-specific) or blue dots (CMV-specific). (**B**) FACS analysis of memory subsets of pentamer+ cells co-stained with CD45RA and CCR7. Bars at median. (Ci-iii) 3D-PCA of vaccine-induced CD8+ T-cells. The first three principal components were plotted in PyMOL (PC1 axis in red, PC2 axis in green, and PC3 axis in blue). (**Ci**) Each grey dot represents a single Bulk CD8+ T-cell, and Ag-specific cells (n=2) are overlaid as white (319 and 322 TW22), red (Flu-specific) or blue dots (CMV-specific). (**Cii**) only Ag-specific cells are show. (**Ciii**) Bulk CD8+ cells are coloured according to their relative expression of the marker CD57, with red cells showing the highest expression and blue the lowest.

As was previously shown (**figure 3-15**) the vaccine vector combination has a strong influence on the proportion of memory T-cells subsets induced. Both ChAd3-NS/MVA-NS-induced and CMV-specific CD8+ T-cells were predominantly Tem, with a small subset of Temra re-expressing CD45RA. Extending the analysis to include 21 markers assayed by CyTOF and analysed by hypothesis-free 3D-PCA CMV-specific and vaccine-induced CD8+ T-cell responses clearly demonstrated a shared phenotype, and one distinct from T-cell responses to the non-persistent pathogen influenza (**figure 4-11C**). This was most clearly demonstrated by expression of CD57, a molecule highly associated with CMV-specific populations (**Kern et al., 1999**). Overlapping populations of CD57+CD127- CD8+ T-cells can be seen in both CMV-specific and vaccine-induced responses in man (**figure 4-11A,C**).

4.5.7 A conserved transcriptional programme of persistent Tem in mice and man is controlled by a subset of key transcription factors

To assess whether the shared phenotype of CMV-induced and ChAd3/MVA-induced T-cell memory was driven by a conserved transcriptional programme the transcriptome of the memory T-cell responses to Adenoviral constructs and (H)CMV/MCMV in mice and man were compared. The gene expression profiling of T-cells induced by Ad vaccination and MCVM infection, described below, was performed by **Bea Bolinger, Stuart Sims and Emanuele Marchi**; this work informed the choice of transcription factors I analysed in **section 4.5.8.**

Transgene-specific (β-Gal) CD8+ T-cells from adenoviral vaccinated mice and MCMV-specific T-cells were sorted from PBMC at the time of peak magnitude of response and from the resting memory pool (**Bolinger et al. 2015**). RNA was extracted from these cells and used in a microarray to assess the gene expression signature of persistent Tem after Ad vaccination or MCMV infection in mice relative to that of Naïve T-cells from the same animals. MCMV-induced and Ad vaccination induced memory T-cells shared 663 up-regulated and 290 down-regulated genes (compared to naïve CD8+ T-cells; **figure 4-12A**) and using gene set enrichment analysis (GSEA) a strong and highly significant enrichment of genes were up or down-regulated in expression in persistent Tem cells in the two settings (**figure 4-12B-C**).

A list of differential expressed genes (DEGs) associated with persistent Tem in mice was then compared with the list of regulated genes in (H)CMV-specific T-cells relative to naïve CD8+ T-cells in humans (**Hertoghs et al. 2010**). Again there was a strong and highly significant enrichment of the same genes in persistent Tem after Ad vaccination and MCMV infection with human CMV infection (**figure 4-12C-D**). This indicates a conserved pattern of response seen in both species to diverse antigen-exposures. No enrichment was seen when comparing DEGs in human CMV-specific T-cells with DEG in exhausted T-cells after LCMV infection (**Hertoghs et al. 2010**).

Remarkably, the most significantly up-regulated gene as T-cells differentiate from Naïve T-cells to persistent memory in all three settings was the T-box transcription factor (TF) Tbx21 (Tbet). Many other TFs previously associated

with T-cell differentiation state were regulated, therefore, GSEA was repeated with a much reduced gene list, including only transcription factors and the same strong highly significant enrichment of DEGs was observed (**figure 4-13A-B**)

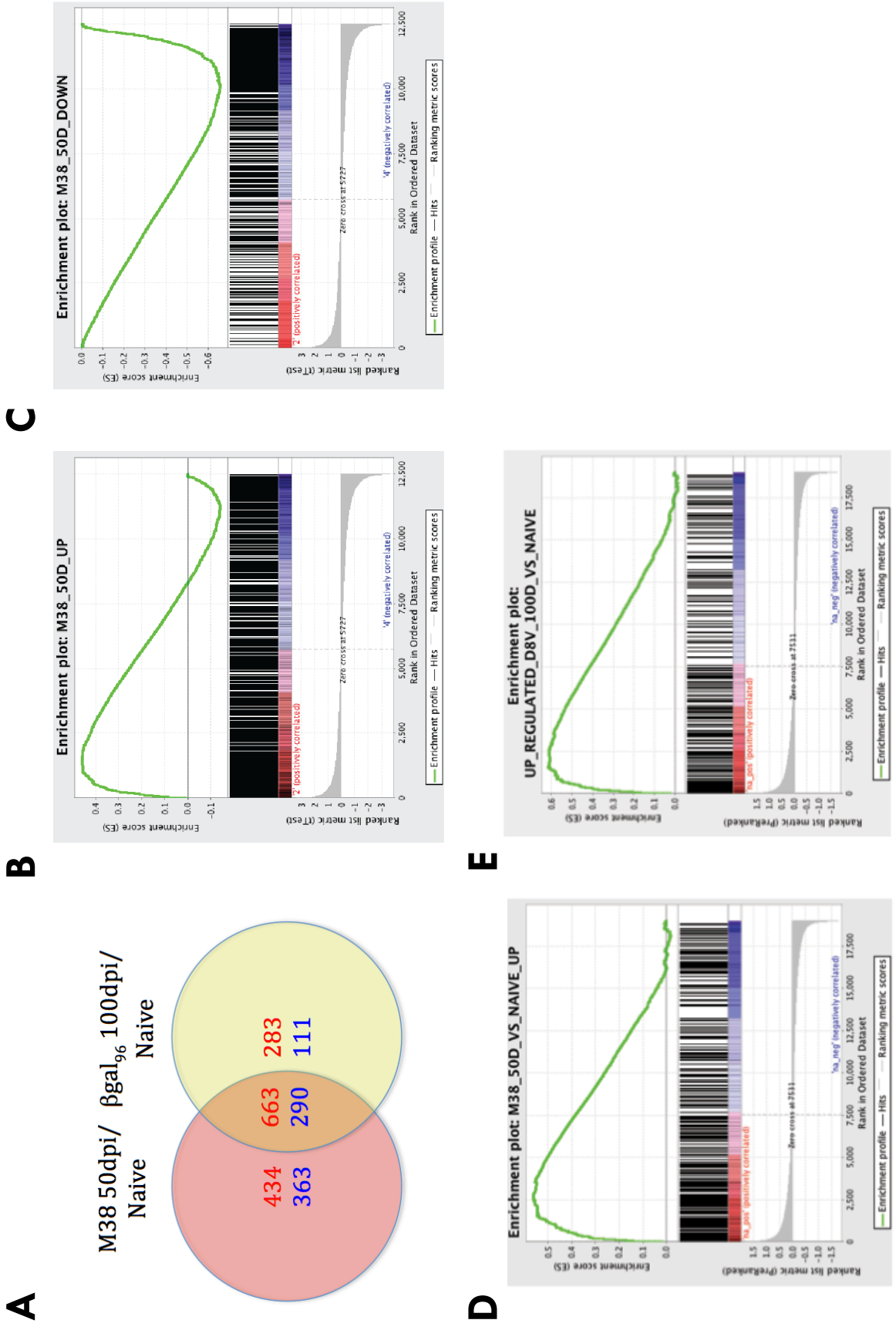

A
M38 50dpi/ Naive
βgal96 100dpi/ Naive
434
663
283
363
290
111
B
Enrichment plot: M38_50D_UP
C
Enrichment plot: M38_50D_DOWN
D
Enrichment plot: M38_50D_VS_NAIVE_UP
E
Enrichment plot: UP_REGULATED_D8V_100D_VS_NAIVE

Figure 4-12. MCMV- and βgal-specific persistent CD8+ Tem cells share a conserved transcriptional programme: (**A**) Venn diagram showing the number of differentially expressed genes (relative to naïve CD8+ T-cells) between M38- (red; day 50) and bgal96(yellow; day 100) specific CD8+ T-cells. Filter criteria of at least 2-fold change $P<0.05$ compared to naïve CD8+ T-cells. Up-regulated genes are indicated in red and down-regulated genes in blue. CD8+ T-cells specific for the epitopes M38 and βgal96 were tetramer stained and sorted from C57BL/6 mice immunised intravenously with 1 x 10^9 vp Ad-LacZ or 1x10^6 pfu MCMV. (**B-E**) Gene set enrichment analysis (GSEA) of differential expressed genes up (**B**) or down (**C**) regulated in M38-specific (relative to Naïve T-cells) vs. ranked list of genes in bgal96-specific $CD8^+$ Tem cells. (**D**) GSEA of genes up-regulated in M38-specific vs. ranked list of genes in human CMV-specific persistent $CD8^+$ Tem cells (**Hertoghs et al., 2010**). (**E**) GSEA of genes up-regulated in $bgal_{96}$-specific T-cells vs. rank list of genes in human CMV-specific $CD8^+$ Tem cells.

PCA was performed both with expression data on all measurable genes and using TFs alone. Again persistent memory T-cells in mice and man cluster together (**figure 4-13C)**. Remarkably, an almost identical clustering of persistent Tem populations could be observed when TFs alone were used for the PCA (**figure 4-13D**), indicating that the changes in expression which define persistent Tem are tightly controlled by a small subset of transcriptional regulators and that the gene expression profile of T-cells in these distinct settings have a conserved differentiation state.

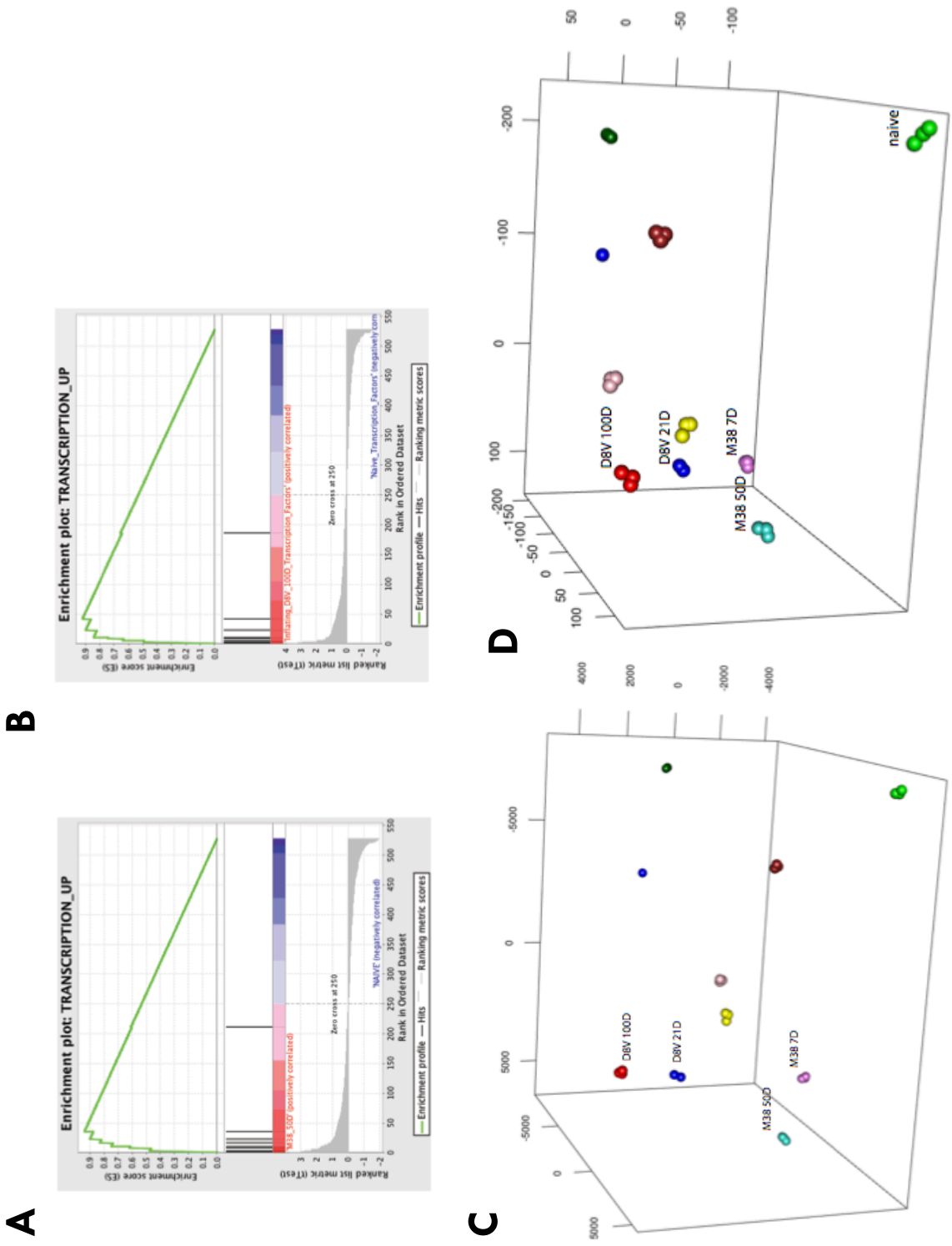

A
B
C
D
Enrichment plot: TRANSCRIPTION_UP
Enrichment score (ES)
Ranked list metric (TTest)
Rank in Ordered Dataset
Enrichment profile
Hits
Ranking metric scores
Zero cross at 250
M38_50D (positively correlated)
NAIVE (negatively correlated)
Naive_Transcription_Factors (negatively correlated)
naive
D8V 100D
D8V 21D
M38 7D
M38 50D

Figure 4-13. Tem show a distinct conserved gene expression profile that can be recapitulated with analysis of transcription factors alone: (**A-B**) GSEA of differential expressed transcription factors up-regulated in M38-specific (**A**) and bgal96-specific (**B**) CD8+ Tem cells (relative to naïve T-cells) vs. ranked list of genes in human CMV-specific persistent CD8+ Tem cells (**Hertoghs et al. 2010**). (**C**) 3D-PCA of the entire set of probe intensities (following removal only of controls and weakly detected probes, 17062 total probes). The transcription profiles plotted are: naïve (green), $bgal_{96}$-specific Tem d21 (blue), $bgal_{96}$-specific Tem d100 (red), $bgal_{497}$-specific Tcm d21 (yellow), $bgal_{497}$-specific $_{Tcm}$ d100 (dark green), M38-specific Tem d7 (violet), M38-specific Tem d50 (turquoise), M45-specific Tcm d7 (pink) and M45-specific Tcm CD8+ T-cells d50 (brown). (**D**) As above but PCA performed using only transcription factors (Hertoghs et al. 2010). P≤0.05 compared to naïve CD8+ T-cells.

4.5.8 T-box transcription factor expression in vaccine and CMV-induced CD8+ T-cells in man

Two T-box TFs, known to be involved in the control of differentiation, homeostasis, and effector function of T-cells, were highlighted by gene expression analysis of Tem in mice and men. Tbet, originally identified as the TF responsible for commitment of CD4+ T-cells to the T-helper type I lineage (**Szabo et al. 2000**), appears to also drive a programme of gene expression that confers cytolytic potential and production of antiviral cytokines (in particular IFNγ) in CD8+ T-cells (**Smith et al. 2012; Rao et al. 2010; Doering et al. 2012; Kao et al. 2011; Hersperger et al. 2011**). Another TF with a somewhat overlapping role in controlling effector functions of T-cells, Eomesodermin (Eomes) appears to be required for efficient memory development (**Banerjee et al. 2010**) but has also been associated with T-cell exhaustion (**Wherry 2011; Doering et al. 2012; Paley et al. 2012**).

Tbet+Eomes- T-cells have an intrinsically low homeostatic turnover and have been shown to give rise to Tbet+Eomes+ cells when exposed to cognate antigen (**Paley et al. 2012**). Both subsets were shown to be essential for control of chronic LCMV and repeated exposure to high levels of antigen can deplete the Tbet+Eomes- precursor population, leading to an accumulation of the terminally differentiated Tbet+Eomes+ cells. In the setting of chronic HBV, HCV, or HIV-1 infection a depletion of Tbet+ cells and subsequent loss of effector functions has been noted (**Kao et al. 2011; Hersperger et al. 2011; Ribeiro-dos-Santos et al. 2012**) and subsequent clearance of both HBV and HCV was associated with a higher percentage of Tbet+ antigen-specific T-cells in the acute phase of infection (**Kurktschiev et al. 2014; Paley et al. 2012**).

The intra-nuclear expression of Tbet and Eomes was assessed in CMV and vaccine-induced T-cells to see if they share a conserved subset specific pattern of expression of these TFs and to assess whether a desirable population of Tbet+Eomes- T-cells persists after vaccination. In bulk CD8+ T-cells the single expression (**figure 4-14A**) or co-expression (**figure 4-14B**) of these TFs showed a clear associations with memory subset. Eomes is expressed by a small number of Tcm but the majority of Tem and Temra. Tbet is expressed by a subset of Tem and the majority of Temra.

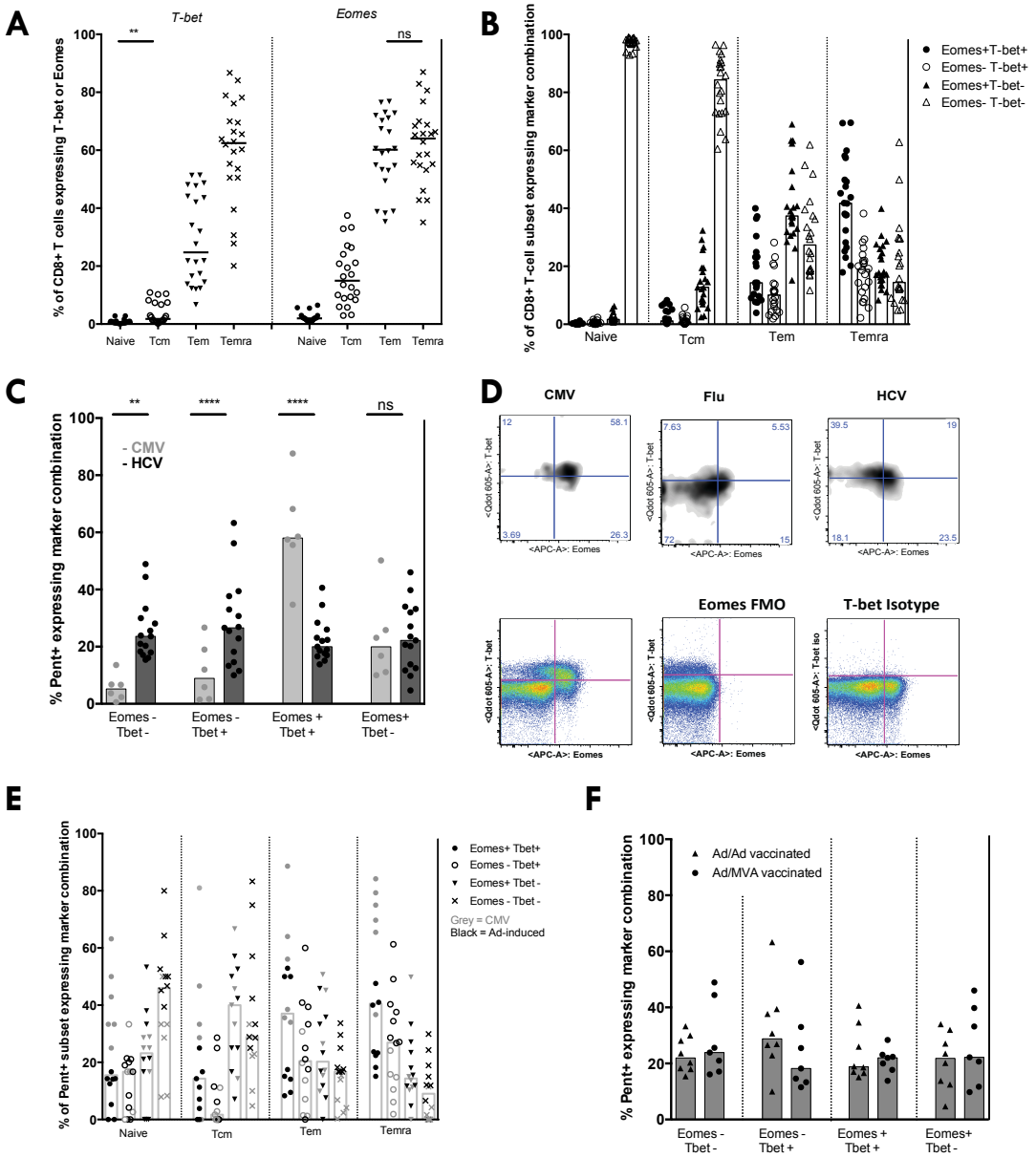


Figure 4-14. Eomes and Tbet expression on bulk and antigen-specific T-cells: (**A**) Eomes and T-bet single expression and (**B**) co-expression on CD8+ T-cell subsets (naïve: CD45RA+CCR7+; Tcm: CD45RA-CCR7+; Tem: CD45RA-CCR7-; Temra: CD45RA+CCR7-; n=22). Bars at median. All comparisons of T-bet and Eomes expression between any two T-cell subsets were highly significant (P<0.0001****) unless stated for (**A**). (**C**) HCV-specific memory CD8+ T-cells induced by virally vectored vaccine regimes (black; 8- 26weeks post boost vaccination) or by natural infection with CMV (grey) were identified by pentamer staining and their expression of T-bet and Eomes was assessed (CMV n=8; ChAd3-NS/Ad6-NS vaccination n=8, ChAd3-NS/MVA-NS n=6). Bars at median. (**D**) Example FACS plots showing T-bet vs. Eomes co-staining and gating controls. (**E**) Co-expression of Tbet and Eomes on HCV-specific

memory T-cells induced by virally vectored vaccine regimes (black; 8-26weeks post boost vaccination) or by natural infection with CMV (grey) split by T-cell memory subsets (as was done for bulk CD8+ T-cells in (**B**). (**F**) A comparison of the co-expression of T-bet and Eomes on vaccine induced T-cells in individuals who received either ChAd3-NS/Ad6-NS or ChAd3-NS/MVA-NS heterologous prime-boost vaccination regimes. Bars at median.

CMV-specific and vaccine-induced T-cells identified by pentamers showed similar co-staining patterns for Eomes and Tbet to bulk CD8+ T-cells, however, the vaccine-induced T-cells were somewhat enriched for the Tbet+Eomes- precursor population (**figure 4-14C-D**). Flu-specific T-cells were assessed in a single individual (**figure 4-14D**) and expressed little Tbet or Eomes, consistent with their Tcm/Naïve-like phenotype. A subset specific co-expression was seen for antigen-specific T-cells also, when split by CD45RA/CCR7 expression (**figure 4-14E**). No difference was seen in the expression of Tbet and Eomes when comparing T-cells induced by ChAd3-NS/Ad6-NS vs. ChAd3-NS/MVA-NS vaccine regimens (**figure 4-14F**).

Overall these data confirmed that ChAd3-NS/MVA-NS induced HCV-specific T-cells in humans are dominated by effector-memory populations that are enriched for Tbet+Eomes- T-cells; they share a conserved transcriptional programme with CMV-specific responses from the same individuals, which is underpinned by a subset of key TFs. This programme of differentiation is conserved in mice and man.

4.6 Discussion

To increase the resolution of the functional and phenotypic assessment of vaccine induced CD8+ T-cells I developed a mass spectrometry (CyTOF) assay to assess multiple parameters simultaneously at a single cell resolution. Despite using very different techniques to assay the binding of antibodies to proteins of immunological interest, highly correlated results were seen when using CyTOF or FACS, validating the phenotyping performed.

As has been previously described (**Seder et al. 2008; La Gruta et al. 2004; Viola & Lanzavecchia 1996; Newell et al. 2012**), a clear hierarchy of cytokine production (MIP-1-β>IFNγ>IL-2) was seen by bulk and antigen-specific T-cells, even when extending this analysis to a larger number of simultaneously assayed functions.

The duration, intensity, and context of antigen exposure at the time of priming has been shown to influence the cytokine production of T-cells, with an optimal antigen exposure and co-stimulation leading to an increase in functions expressed (**Seder et al. 2008; La Gruta et al. 2004; Viola & Lanzavecchia 1996; Newell et al. 2012**). MIP-1-β and IFNγ are most readily released by CD8+ T-cells, after limited stimulation, and IL-2 production is only triggered when a T-cell has been exposed to optimal levels of antigen and co-stimulation (**Viola & Lanzavecchia 1996**). Overstimulation or chronic activation appears to lead to a reversal of this state, with subsequent loss of functions following a similar hierarchy (**Wherry 2011**). I showed that T-cells induced by ChAd3-NS/MVA-NS

vaccination are highly functional, with polyfunctionality peaking around 12 weeks post after MVA-NS boost vaccination. The per cell production of cytokine and the combinations of cytokines produced by vaccine-induced T-cells was comparable to that seen by CMV-specific T-cells assessed in parallel, and surpassed that of Flu-specific T-cells.

Next I assessed the overall quality of T-cells, incorporating both functional and phenotypic markers. PCA was used to reduce the dimensionality of the CyTOF dataset to a more readily interrogated form, to investigate the heterogeneity of CD8+ T-cell phenotypes, and to assess which axis of variation are the most important when subdividing CD8+ T-cells.

By performing PCA I was able to visualise the complexity in the bulk CD8+ T-cell population in 3D plots, showing that the naïve T-cells are distinct in their expression pattern and the niche in which they occupy. Theoretically T-cells can occupy any area within this 3D plot; however, they concentrated in discrete niches, suggesting a tightly coordinated control of the expression of functional and phenotypic markers assayed. The majority of antigen experienced T-cells are positioned within an 'L-Shaped arm' that extends from the naïve population emphasizing the continuous nature of CD8+ T-cell differentiation. This pattern was observed in all five individuals at all time points. Despite almost a third (6/21: CD5, CD161, CTLA-4, CD127, CD40L, CD38) of the markers used to load the PCA being different in our analysis to that performed by Newell *et al*, it is remarkable that the same 'shape' is seen by 3D-PCA of CD8+ T-cells (**Newell et al. 2012**).

There is a progressive loss of markers associated with naïve or early differentiated T-cells (CD28/CD27/CCR7/CD62L) and gain in expression of markers associated with senescence (CD57, re-expression CD45RA, granzyme B) as you move from the naïve population around to the end of the 'L-shaped arm' of memory T-cells, passing through the Tcm, Tem and then Temra niches. Tcm occupy a niche closest to the naïve, as has been noted before and is suggested by a closer gene expression profile (**Kaech, Hemby, et al. 2002; Roychoudhuri et al. 2014**).

PC1 explains the largest amount of variation in phenotypic markers and in this instance clearly showed that the axis of variation that separates out CD8+ T-cells the most is their differentiation state, from naïve to terminal differentiation. The next most important axes of variation were in the effector functions and markers of terminal differentiation or senescence, e.g. the combination and amount of cytokines produced, the expression of cytolytic markers and markers associated with proliferative senescence and terminal differentiation.

The PCA analysis described here and in **Newell et al. (2012)** validate the use of CD45RA/CCR7 co-expression to broadly separate out T-cell subsets as it shows that they describe functionally and phenotypically distinct subsets of CD8+ T-cells even when expression data on a larger subset of markers are used. However, there was perhaps a larger overlap between subsets than was expected, which may explain why subsets defined using the same phenotypic markers do not consistently show such separate functionality in all settings.

Although this analysis lacks a temporal aspect needed to identify the sequence of differentiation of CD8+ T-cells and the fluidity of expression of the markers assayed, the relationships between subset phenotypes correlates well with the relationships identified by comparing gene expression profiles; for instance with Naïve and Tcm being closely related and Tem and Temra being progressively less naïve-like (**Haining et al. 2008**). It also confirmed the difference in T-cell phenotype of the memory T-cell response seen after acute influenza infection and to persistent CMV-infection and allowed a more in-depth comparison of ChAd3-NS/MVA-NS induced T-cells with previously assayed antigen-specific populations. No unique clusters of cells or new axis of variation amongst CD8+ T-cells were identified from assaying the protein levels of the markers used here; we may be getting close to defining a minimal set of functionally distinct T-cell subsets, or more likely we have not yet uncovered all of the key proteins controlling T-cell functionality *in vivo*.

The phenotype and functionality of vaccine induced HCV-specific T-cells evolves over time and with re-exposure to antigen by boost vaccination, consistent with changes in the phenotype of T-cells across the vaccine trials seen by flow cytometry (**Chapter 3**). The phenotype of effector T-cells (Teff) at the peak of the T-cell response was distinct from bulk CD8+ T-cells and they were easily separated by principal components PC4 and PC5 - which were heavily influenced by markers of activation, shown to be transiently expressed on vaccine-induced T-cells in **chapter 3** (**figure 3-10D**). The effect MVA-NS vaccination is easily seen as the boosted CD8+ T-cells appear to become more heterogeneous but co-

localising with a Tcm and Tem like phenotype. By TW22, 14 weeks post MVA-NS vaccination T-cells had cluster more tightly, in an area defined by T-cells with the strongest immediate effector functions. Despite the 'set-point' for the magnitude of the remaining memory T-cell response being established somewhere between 6 and 16 weeks after MVA-NS vaccination (**figure 3-2A**) the phenotype and cytokine profile of T-cells continues to evolve; the protective capacity and the capacity to respond to repeated vaccination or challenge will also evolve with implications for the design of vaccine regimens.

I further investigated the similarities between our vaccine-induced CD8+ T-cells and T-cells induced by CMV infection. A three way-comparison of the gene expression profiles of persistent Tem induced by MCVM and Ad in mice and by CMV in man showed that a conserved pattern of gene expression is seen in persistent Tem in these diverse settings, which is distinct from that of Tcm, naïve T-cells, or exhausted T-cells. The similarity in gene expression pattern could be recapitulated using TFs alone, showing it is tightly controlled at the level of transcription by a relatively small network of transcription regulators. ChAd3-NS/MVA-NS vaccination induced persistent Tem T-cells analogous to CMV-specific responses studied in parallel, and which expressed high levels of Tbet. Of particular note was an enrichment for T-cells with a T-bet^{hi}/Eomes^{lo} phenotype long-term after vaccination, which is the pattern of TFs displayed by intrahepatic T-cells preceding spontaneous resolution, rather than chronic infection (**Kurktschiev et al. 2014; Paley et al. 2012**). Although the frequency of vaccine-induced T-cells in humans does not reach those seen for inflationary persistent Tem responses to MCMV and Ad in mice, a shared phenotype and

underlying transcriptional control is seen and frequencies are comparable with those seen after intramuscular inoculation in mice (**Bolinger et al. 2013**).

These studies were not aimed at defining the underlying antigen presentation or cytokine signalling driving fate choice in T-cells, but to investigate if a conserved programme of differentiation drives persistent Tem development in these diverse settings. The controlled expression of a small group of TFs drives the differentiation and concomitant functionality of persistent Tem, with Tbet and Eomes being key players, but with context dependent roles (**Kao et al. 2011; Doering et al. 2012**).

Tbet and Eomes expression are modulated in accordance with both TCR signalling (hence the importance of antigen levels and duration) and through cytokine signalling. Tbet is reduced on clearance of acute infections or on removal of antigen, but in the presence of repeated low level antigen exposure it is expressed. Tbet maintains CD8+ T-cell effector function, allows cells to persist, whilst tempering the expression of PD-1 and associated exhaustion of T-cells (**Kao et al. 2011**). Cytokines are critical mediators of differentiation and homeostasis and T-bet expression appears to be responsive to inflammatory cytokine signalling, in particular IL-12, a signature of intracellular infection (**Intlekofer et al. 2008**). A key difference between chronic MCMV and LCMV infection in mice is the level of IL-2 and IL-12 produced by DCs and macrophages (**Dalod et al. 2002**), which may determine T-cell exhaustion or persistent effector function via control of Tbet expression (**Takemoto et al. 2006**).

Joshi et al. (**2007**) showed a graded expression of Tbet is seen with increasing concentration of inflammatory cytokines. High expression of Tbet, KLRG-1 and dependence on IL-15 signalling for survival when there is much inflammation leads to persistence of Tem, however, antigen above a certain threshold dives exhaustion and deletion, potentially by straining the regenerative capacity of Tbet+Eomes- and driving the accumulation of Tbet+Eomes+.

The durability and functionality of the T-cells induced by ChAd3-NS/MVA-NS vaccination is likely a result of these viral vectors hitting the 'sweet-spot' of T-cell activation and inflammation due to their natural ability to induce an anti-viral innate responses and inflammation and their ability to persist long-term after vaccination (**Tatsis et al. 2007**). Although MVA-NS appears to be rapidly cleared (**Ramírez et al. 2000**), it induces strong acute activation of T-cells, expanding the HCV-specific T-cell pool, however, the persistence of antigen or transcriptionally active ChAd3-NS from priming provides the context in which T-cells, in particular Tem/Temra can persist without becoming exhausted.

4.7 Conclusion

In this chapter I set out to assess the possibility of using a new single cell technique to assay multiple phenotypic markers on single cells induced by our virally vectored vaccines. After validating this technique I used the data to better characterise the T-cell response to vaccination, in immunologically meaningful phenotypic and functional analysis. I used PCA to reduce the dimensionality of the data produced so that I could investigate the overall phenotypic

heterogeneity of CD8+ T-cells and then investigate where vaccine induced T-cells sit in relation to all CD8+ T-cells and other antigen specific T-cells. I expanded the comparison with CMV-specific T-cells to confirm a shared-phenotype and functionality and conserved pattern of gene expression that is tightly controlled by a small subset of TFs

Due to a lack of correlates of protection and well-characterised animal models phase II efficacy studies represent the only way to truly test the effectiveness of candidate prophylactic vaccines. Vaccines must be pre-ranked and assessed prior to phase II testing and one way in which we can pick candidate vaccines is on their immunogenicity (and of course safety) in small phase I studies. T-cell magnitude is only a single parameter of importance when assessing the overall potential protective efficacy of a T-cell response and here I have characterized the immune response to ChAd3-NS/Ad6-NS and ChAd3-NS/MVA-NS vaccine regimens to unparalleled depths and put the response in the context of other antigen-specific T-cell responses. Different T-cell subsets mediate protection in different settings and the overall 'quality' of the T-cell response is therefore a characteristic of relevance when assessing candidate vaccines. A mixed population of HCV-specific T-cell memory subsets resulted from ChAd3-NS/MVA-NS vaccination, and these T-cells survived long-term, which is relevant to a prophylactic vaccine. Both LN homing Tcm and circulating Tem/Temra cells were elicited, but of particular interest, a large proportion of the memory response are persistent Tem.

We were able to overcome the limitations of using fluorescent labelling of antibodies by using heavy metal tags detected by mass cytometry. Parallel developments of hardware, software, and reagents, as has been seen with FACS, should see improvement in data quality and make this technology more widely applicable.

T-cells have the capacity to perform diverse roles within the immune system and multiple signals are incorporated during maturation, priming, but also during the life-time of a T-cell to ensure correct magnitude of T-cells with relevant functions are present where they are needed. For antiviral CD8+ T-cells the availability of cognate antigen as well as the inflammatory milieu appears to control T-cell differentiation at least in part at the level of the transcriptome. We do not yet have the ability to predict the protective capacity of a population of T-cells through phenotypic or functional analysis and are unable to effectively manipulate signals to drive T-cells towards a particular type of T-cell. As more markers are used to interrogate cells and the possible combinations of their expression increase, it is likely that more heterogeneity within the CD8+ T-cell compartment will be uncovered. We may reach the theoretical limit of finding that every cell is phenotypically and/or functionally distinct from all others, however, some of these differences are likely to be subtle, and the challenge will be to determine whether meaningful biological differences exist between cells that occupy different CD8+ T-cell niches and to deconvolute the signalling pathways that drive these niches so that they may be manipulated in the direction of clear T-cell correlates of protection.

4.8 Summary of findings

- CyTOF can be used to effectively assay >30 markers and parameters of interest on resting or stimulated single CD8+ T-cells.
- Vaccine-induced HCV-specific CD8+ T-cell phenotypes and patterns of cytokine production were consistent between FACS and CyTOF analysis.
- A clear and tightly controlled hierarchy of cytokine co-production was seen by vaccine-induced T-cells.
- The complexity of CD8+ T-cell phenotypes was visualised and T-cell memory subsets were shown to occupy discrete but overlapping niches.
- Much of the variation in CD8+ T-cell phenotype is explained by the transition from naïve-memory, and different expression of markers by previously described memory subsets.
- CD8+ T-cells that have recently been exposed to antigen show a discrete phenotype.
- Persistent effector memory T-cells induced by ChAd3-NS/MVA-NS vaccination and natural infection with CMV shared a highly conserved phenotype and functionality, which is also seen in T-cells induced by MCMV and Ad vaccination in mice.
- The differentiation in to effector memory CD8+ T-cells in these diverse settings is at least in part controlled at the level of transcription by the combined expression of a small subset of transcription factors.

5 The MHC class II invariant chain as a genetic enhancer of CD8+ T-cell responses

5.1 Primary Hypothesis

Linking antigen to MHC class II invariant chain (Ii) within T-cell vaccines can enhance the magnitude, kinetics, and breadth of the CD8+ T-cell response without affecting T-cell phenotype or function. Tethering to Ii stabilises antigen or allows antigen to persist within APCs, allowing prolonged presentation and enhanced T-cell activation.

5.2 Introduction

Several genetic enhancers – sequences that are encoded within a DNA or virally vectored vaccine as adjuvants to enhance their immunogenicity - have been investigated, one of the most promising of which is the MHC class II invariant chain (Ii or CD74). When a transgene within a viral vector or DNA plasmid is tethered directly to Ii the transgene-specific T-cell response is enhanced (**Holst et al. 2008; Capone et al. 2014**), however, the mechanism driving this effect is not yet understood. I investigated which domains of Ii are involved in this adjuvant effect and how the inclusion of Ii affects a transduced APC - "transduced" is used here to mean the natural *in vitro* infection of cells with Ad vectors by mixing the two in cell culture, without additional stimulus.

Ii is a non-polymorphic type II trans-membrane protein, first identified as the chaperone for MHC (major histocompatibility) class II molecules (MHC-II; **figure**

5-1A; reviewed in (**Blum et al. 2013; Roche & Furuta 2015**)). The main function of Ii is to stabilise the interaction of the α and β chains as they are formed in the endoplasmic reticulum (ER) and to occupy the peptide-binding groove of the MHC class II molecules. Ii inhibits peptide loading within the ER and targets MHC-II to the endosomal network via its endolysosomal targeting sequence signal peptide (ESS)(**Sandoval & Bakke 1994**). Ii is sequentially cleaved in the late endosome by cathepsins to class II-associated invariant chain peptide (CLIP) - CLIP sits within the peptide-binding groove of MHC-II molecules – which is then displaced by exogenous peptides for presentation to CD4+ T-cells (**figure 5-1A**).

Ii was originally included as a genetic adjuvant in an attempt to target antigen to the MHC class II presentation pathway by bringing antigen in close proximity to MHC-II molecules when Ii is replaced with peptide in the endolysosome. Potentially through this mechanism, the inclusion of the Ii sequence enhances the CD4+ T-cell response to DNA and viral vectored vaccines (**Table 5-1**), and the inclusion of KEY motif alone, or the replacement of CLIP within the Ii sequence with epitopes can also enhance CD4+ T-cell responses (**Voutsas et al. 2007; Malcherek et al. 1998**).

Along with the modest improvement in CD4+ T-cell responses a much more significant enhancement of the CD8+ T-cell response was noted (**Holst et al. 2008**). Although enhancement of CD4+ T-cell responses is highly relevant to virally vectored T-cell vaccines for HCV antigens, it is the more robust and

stronger enhancement of CD8+ T-cell responses that is investigated in this chapter.

Table 5-1. Evidence of Ii-mediated adjuvanticity

Described in:	Vector	Antigen	Invariant chain	Enhanced antigen-specific response	
				CD4+ T-cells	CD8+ T-cells
Murine models					
Malachek et al. 1998	DNA	tetanus toxin	mIi	Y	nd
Sponaas et al. 1999	DNA	hen egg lysozyme	mIi	Y	nd
Diepold et al. 2001	DNA, Ad5	OVA	mIi	Y	Y
Rowe et al. 2006	lentivirus	OVA	mIi	Y	Y
Holst et al. 2008	Ad5	LCMV: GP or NP	mIi	Y	Y
Grujic et al. 2009	DNA (gene gun), Ad5	LCMV glycoprotein	mIi	Y	Y
Mikklesen et al. 2011	Ad5	HCV NS3	mIi	nd	Y
Steffensen et al. 2013	Ad5 Ad35	LCMV glycoprotein	mIi	nd	Y
Jensen et al. 2013	Ad5	*L.monocytogenes*: LLO or p60	mIi		
Capone et al. 2014	ChAd3, MVA	HCV NS3-5b	mIi and hIi	Y	Y
NHP					
Spencer et al. 2014	ChAd63, MVA	ME.TRAP	mIi and hIi	Y	Y
Capone et al. 2014	ChAd3, MVA	HCV NS3-5b	mIi and hIi	Y	Y

MHC class II invariant chain (P35); LLO = listeriolysin O; *L.monocytogenes* = *listeria monocytogenes*; mIi = murine MHC class II invariant chain (CD74); MVA = modified vaccinia Ankara; NP = nucleoprotein

The classical pathway for presenting short peptides to CD8+ T-cells in the context of MHC class I molecules (MHC-1; **figure 5-1B**) involves the cytosolic digestion of proteins to optimal length (8-10 amino acids) or N-terminal extended proteins by the proteasome (and in some rare cases involving other cytosolic peptidase; (**Donoso et al. 2005; Tsvetkov et al. 2009**))**.** The main substrates for the proteasome are cytosolic endogenous proteins and viral proteins for the classical MHC class I pathway, and exogenous proteins, retro-translocated from phagosomes or endosomes to the cytosol, for cross-presentation (reviewed in**:** (**Raghavan et al. 2008; Blum et al. 2013**)). The

peptides are transported into the ER by TAP (transporter associated with antigen processing), and where needed N-terminal cleaved to optimal length peptides by endoplasmic reticulum aminopeptidase 1 (ERAP1; ERAAP in mice) and ERAP2. These peptides associate with the protein-loading complex (PLC), which differs slightly between HLA allotypes, but commonly involves: tapasin, endoplasmic reticulum protein 57 (ERp57), calnexin (CAL), calreticulin (CRT) and the MHC-I heterodimer.

A

MHC class II

Figure 5-1A was adapted from figure 4 in **Blum et al 2013.**

B

MHC class I

Figure 5-1B was adapted from figure 3 in **Blum et al 2013.**

Figure 5-1. Antigen presentation on MHC class I and MHC class II molecules: (A) MHC class II pathway: MHC-II α and β chains are translated by ER-associated ribosomes and are brought together and stabilised into MHC-II heterodimers by the MHC class II invariant chain (Ii; highlighted in blue). Ii forms a trimer and stabilises three heterodimers simultaneously to form a nonamer. Ii provides the endolysosomal sorting sequence, which leads the MHC-II-Ii complexes via the trans-golgi network to mature endosomes. MHC-II-Ii can also reach the cell surface and be transported back into endosomes. In the acidic environment of the late endosome, MHC class II compartment (MIIC) and phagolysosomes cathepsins cleave Ii sequentially, leaving the CLIP peptide in the peptide-binding groove of MHC-II molecules. HLA-DM associates with MHC-II-CLIP, causing a conformational change that releases CLIP and allows cathepsin cleaved peptides to bind to MHC-II. Protein substrates for cathepsins and other endosome resident proteases are delivered to the late endosomes by phagocytosis, endocytosis, and autophagy, allowing both exogenous and endogenous proteins to be presented on MHC-II. Binding of high affinity peptides releases HLA-DM and frees MHC-II-peptide molecules to traffic to the cell surface for presentation to CD4+ T-cells. (**B**) **MHC class I pathway:** MHC-I molecules present short peptides which are derived from native proteins, defective ribosomal products (DRiPs), viral proteins and retro-translocated exogenous proteins (for cross-presentation). The main source of peptides for MHC-I loading are the degradation products of the proteasome, which cleaves proteins in the cytosol to peptides that are transported via TAP to the ER. When in the ER peptides can be trimmed by ERAP-1 and ERAP-2 or they can bind directly to MHC-I heterodimers in protein loading complexes (PLCs). Initially MHC-I heterodimers in the ER are stabilised by interactions with calnexin (CXN), which allows the binding of β2microglobulin, and then association with calreticulin (CRT), tapasin, and ERp57. Tapasin stabilises MHC-I heterodimers in the PLC in close proximity with TAP, which supplies cytosolic peptides. Only on binding of high affinity peptides are tapasin and the PLC released from MHC-I-peptide molecules, which are then allowed to traffic to the cell surface for presentation of peptides to CD8+ T-cells. **Figure 5-1A** is figure 4 in **Blum et al. 2013 and Figure 5-1B is figure 3 in Blum et al. 2013.**

The loading of high affinity peptides stabilise the MHC-I molecule and release the PLC, allowing MHC-I:peptide complexes to traffic through the golgi to the cell surface for presentation to CD8+ T-cells (**figure 5-1B**).

The classical MHC class I pathway does not involve Ii, however, recent evidence suggests a role of Ii in TAP-independent (vacuolar) cross-presentation, whereby

Ii binds to and stabilises MHC-I molecules and mediates their trafficking to the endolysosome – in much the same way as it dose for MHC-II molecules - where exogenous peptides can be loaded (**Basha et al. 2012**). Cross-presentation may also involve retro-translocation of exogenous proteins from endosomes to the cytosol (TAP-dependent), before being processed in the same manner as endogenous cytosolic proteins independent of Ii (**Raghavan et al. 2008**).

Ii does not only enhance CD8+ T-cell responses when tethered to antigen within Ad vectors but has been shown to enhance responses when included in DNA plasmids, lentiviral vectors, and MVA (**Table 5-1**). The adjuvant effect is seen with both murine and human Ii sequences (**Spencer et al. 2014; Capone et al. 2014**) and with a wide selection of model and complex antigens including the NS region of HCV (**Table 5-1**). This effect is observed in inbred and outbred mice and cynomolgus macaques (**Spencer et al. 2014; Capone et al. 2014**). The T-cells induced by Ii containing vectors have been shown to mediate enhanced protection against challenge with LCMV (**Holst et al. 2008; Grujic et al. 2009**), vaccinia (**Mikkelsen et al. 2011**), *l.monocytogenes* (**Jensen et al. 2013**) and to limit tumour growth (**Sorensen et al. 2009; Sorensen et al. 2010**) in mouse models, but the mechanism by which linking antigen to Ii improves T-cell responses is not understood.

Ii is a complex protein with many functional domains and roles within the cell, not all of which are involved in antigen processing (**figure 5-2**). In much the same way as it controls trafficking of MHC-II molecules, Ii acts as a chaperone for CD1d (**Kang & Cresswell 2002**) and for the neonatal Fcγ receptor molecules (**Ye**

et al. 2008), both of which are structurally related to MHC-II. Ii has been shown to associate with CD70 (a CD27 ligand) and mediate its delivery to the immunological synapse (**Zwart et al. 2010**), and it binds to myosin-II, limiting cell migration in DCs (**Faure-André et al. 2008**). Ii also functions as a surface receptor for macrophage migration inhibitory factor (MIF; reviewed in (**Matza et al. 2003; Leng et al. 2003**). The cytosolic domain of Ii is released on binding MIF and it acts as a essential transcription factor in B-cell maturation and survival, signalling through NfκB and upregulating anti-apoptotic markers such as BCL-Xl and BCL-2 (**Starlets et al. 2006**).

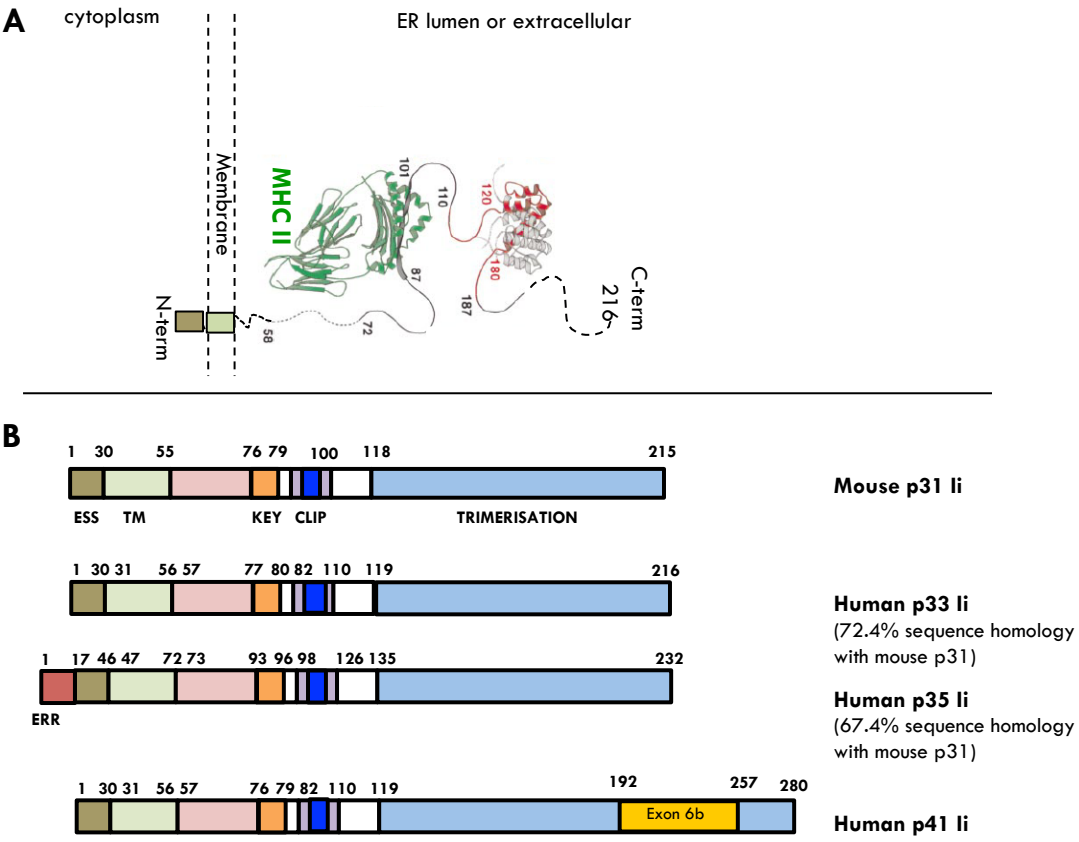


Figure 5-2. The known functional domains of Ii: (**A**) Ii is represented interacting with MHC class II (green) and with another Ii chain via its trimerisation domain (red). (**B**) Aligned representation of murine Ii and the main human isoforms of Ii. The key domains are labelled and numbered according to their amino acid position along the murine Ii sequence. The 30 amino acid cytosolic tail at the N-terminal of the Ii encodes the endolysosomal sorting sequence (ESS; a di-leucine based signal). Attached to this are a type-II transmembrane region (amino acids 30-55) and a large luminal domain, which contains the KEY motif and CLIP (class II-associated invariant chain peptide) - the residues that interact with MHC Class II molecules - and a trimerisation domain. CLIP is the section of Ii that sits directly within the binding groove of MHC class II molecules and KEY binds to MHC-II causing a conformational change that makes the MHC-II peptide-binding groove receptive to peptides. Human p35 and p41 isoforms of Ii (numbered according to their molecular weight) have an additional 17 amino acids at the beginning of Ii, which encodes an ER retention sequence (ERR). Human p41 isoform contains an additional exon.

Some potential ways in which linking antigen to Ii can improve the T-cell response are: increased antigen stability - leading to prolonged antigen availability; replacement of (potentially) down-regulated Ii; enhanced targeting of Ii to existing or novel antigen processing pathways, including cross-presentation; enhanced co-stimulation by APCs transduced with Ii (e.g. through trafficking of CD70).

It is important to understand the underlying mechanisms of Ii-linked adjuvanticity as this may allow us to further manipulate and optimise genetic vaccines, it may give us new insight into the immunology of T-cell activation and antigen presentation, and it could allow us to design new genetic adjuvants not based on endogenous proteins, reducing the opportunity for off target effects. I investigated whether Ad encoded Ii can traffic to the surface of transduced cells because a greatly increased surface expression of Ii could lead to a break in tolerance.

The mechanism by which Ii-encoding Ads show enhanced CD8+ T-cell induction could be mediated by any combination of known or unknown roles of Ii, therefore, to narrow down the possible mechanism of action I used truncated and variant versions of Ii with additions or deletions to identify the essential domains of Ii for this adjuvant effect. I investigated changes in intracellular processing of antigen in cells transduced with Ii encoding Ads and I investigated changes in the surface expression of Ii.

5.3 Key Questions

I address the following key questions:

1) Which functional domains or residues are essential for Ii's role as a genetic enhancer of CD8+ T-cell responses when linked to antigen?
2) What is the minimal sequence that can mediate the adjuvant effect of Ii?
3) Can the effect of Ii be recapitulated *in vitro*?
4) What is the intracellular mechanism of enhanced CD8+ T-cell responses to Ii-linked antigen? Does tethering of Ii to antigen lead to increased antigen stability and/or enhanced presentation of antigen on transduced APCs?
5) Does Ii-linked antigen elicit the same quality of T-cells?
6) Does Ad encoded Ii traffic to the transduced cell's surface?

5.4 Chapter specific material & methods

5.4.1 Reagents and consumables

FACS buffer – PBS + 1% FCS

Thawing media – 1 ml of 10X CTL wash (Cellular technologies ltd. CTLW-010), 2 µl benzonase (Merck 70746-4), 9 ml R20 for JAWSII cells, R10 for all other cell types.

All other reagents as described in **chapter 2** or where relevant below.

5.4.2 - 6.4.7 Murine *in vivo* experiments

5.4.2 Invariant chain containing Adenoviral constructs

Adenoviral constructs were designed and made in house by Okairos, Italy, or were kindly provided by Peter Holst (University of Copenhagen, Denmark). Murine Ii p31 (mIi) insert (accession number NM_1042605.1) was obtained from plasmid Murine Ii opt. PJH#66, kindly provided by Peter Holst, and the human Ii (p35, NCBI reference sequence: NM_004355.2) insert was synthesized by GeneArt (Life Technologies, Paisley, UK).

mIi p31 sequence:

MDDQRDLISNHEQLPILGNRPREPERCSRGALYTGVSVLVALLLAGQATTAYFLYQQQGRLDKL
TITSQNLQLESLRMKLPKSAKPVSQMRMATPLLMRPMSMDNMLLGPVKNVTKYGNMTQDH
VMHLLTRSGPLEYPQLKGTFPENLKHLKNSMDGVNWKIFESWMKQWLLFEMSKNSLEEKKPT
EAPPKEPLDMEDLSSGLGVTRQELGQVTL

All full and truncated Ii sequences were cloned at the N-terminus of the transgene

under HCMV and BGHpA control and then transferred into the Ad vector by homologous recombination in BJ5183 cells. Recombinant viruses were purified as described previously (**Colloca et al. 2012**). All Ad constructs were E1E3 deleted and therefore non-replicative except in E1 supplemented cell lines. Ad constructs that I used personally for *in vivo* and *in vitro* experiments are listed in **Table 5-2.** Where data from experiments performed by others are presented within the thesis the Ad constructs used are not listed in **Table 5-2**.

Table 5-2. Non-replicative Ad vectors used in murine *in vitro* and *in vivo* experiments.

Ad construct	Viral particles per ml	Ad used in	IFU:vp ratio
Ad5-OVA	$1.64x10^{12}$	*in vivo*, BMDC, JAWSII	36
	$1.47x10^{12}$	B3Z	33
	$1.63x10^{11}$	*in vivo*	-
Ad5-mli(1-50)-OVA	$2.29x10^{12}$	*in vivo*, BMDC, JAWSII, B3Z	36
Ad5-mli(1-70)-OVA	$3.09x10^{11}$	*in vivo*, BMDC	28
Ad5-mli(1-75)-OVA	$4.22x10^{11}$	*in vivo,* BMDC, JAWSII, B3Z	32
Ad5-mli(1-80)-OVA	$4.57x10^{11}$	*in vivo,* BMDC, JAWSII	32
Ad5-mli(1-105)-OVA	$8.70x10^{11}$	*in vivo*	-
Ad5-mli(50-215)-OVA	$1.20x10^{12}$	*in vivo*, BMDC	33
Ad5-mli-OVA	$1.26x10^{12}$	*in vivo*, JAWSII, B3Z	45
	$4.29x10^{11}$	B3Z, BMDC	45

Ad construct	Viral particles per ml	Ad used in	IFU:vp ratio
ChAd3-NS	$1.00x10^{11}$	BMDC	51
ChAd3-mli-NS	$2.60x10^{9}$	BMDC	-
ChAd3-hli(P33)-NS	$5.80x10^{12}$	BMDC	114
ChAd3-hli(1-97)-NS	$3.69x10^{11}$	BMDC	93
ChAd63-hli	$3.39x10^{11}$	BMDC	75
Ad5-eGFP	$3.27x10^{11}$	*in vivo*, BMDC, HeLa	-
Ad5-mli-eGFP	$1.40x10^{12}$	*in vivo*, BMDC, HeLa	-
ChAd3-eGFP	$1.91x10^{9}$	*in vivo*, THP-1	-

Ad = Adenovirus; BMDC = bone marrow derived dendritic cells; OVA = ovalbumin; IFU = infectious units; eGFP = enhanced green fluorescent protein

5.4.3 Animals and *in vivo* vaccinations

All *in vivo* murine experiments were performed at Okairos laboratories using the mouse house at CEINGE, Napoli Italy. All experimental procedures were approved by the local animal ethics council and were performed in accordance with national and international laws and policies (EEC Council Directive 86/609; Italian Legislative Decree 116/92). The ethical committee of the Italian Ministry of Health approved this research. Animal handling procedures were performed under anaesthesia, and

all efforts were made to reduce animal numbers and minimise suffering. Six-week-old female C57BL/6, BALB/c, or F1 (C57BL/6 x BALB/c cross) mice were purchased from Charles River (Como, Italy). All day-to-day care of the mice was performed by trained mouse house staff at CEINGE.

Vaccines were injected intramuscularly (unless otherwise stated) into the two quadriceps of the hind legs of 6-8 week old female C57BL/6 mice (for OVA containing Ad vectors) or BALB/c (GFP containing Ad vectors) 50µl per quadricep at various doses (3×10^5 – 1×10^7 vp). Ad constructs were diluted in A195 buffer for vaccinations: 10 mM Tris HCl, 75 mM NaCl, 1 mM $MgCl_2$, 0.02% PS80 (synonym of Tween 80), 5% Sucrose w/v, 0.1 mM EDTA, 10 mM L-Histidine, 0.5% ethanol v/v.

All animal handling was done under the supervision and with the assistance of Morena D'Alise, Maria Luisa Esposito and Mariarosaria Naddeo (Okairos, Italy).

5.4.4 Isolation of mouse splenocytes

Isolation of mouse splenocytes was performed according to the Okairos SOP IU-001 (**appendix 6-1**).

5.4.5 *Ex vivo* murine IFNγ ELISpot

Murine IFNγ ELISpots were performed according to the Okairos SOP IU-002 (**appendix 5-2**; U-CyTech CT665). ELISpots were performed *ex vivo* in quadruplicate on murine splenocytes and all values are given as spot forming cells per million PBMC or splenocytes. For OVA containing vaccinations the read out for

immunogenicity by ELISpot was SFC/10^6 cells after overnight stimulation with $OVA_{257-264}$ (SIINFEKL) peptide on splenocytes from C57BL/6 mice collected two weeks after vaccination. For GFP containing vaccinations in BALB/c mice the peptide $GFP_{200-208}$ HYLSTQSAL was used. The addition of DMSO (Sigma D2650) at the same concentration as added with peptide in quadruplicate, and duplicate wells stimulated with concanavalin A (conA; 1:200 Sigma C5275), were used as a negative and positive controls respectively for each individual mouse.

An ELISpot response was considered positive when all of the following conditions were met: a response of at least 50 SFC/10^6 PBMC or splenocytes to at least one peptide or peptide pool; the number of spots seen in positive wells was at least three times the number detected in the mock control wells (DMSO).

5.4.6 *Ex vivo* CD74 expression on leukocyte subsets

The surface expression of CD74 (Ii) was measured *ex vivo* on B-cells, DCs, and T-cells in blood and splenocytes from 6 week-old female BALB/c mice and from thawed healthy human PBMC.

Murine PBMC are isolated from blood as follows. 0.5 ml of blood is extracted from anaesthetised mice by retro-orbital bleed. Blood tubes are briefly centrifuged and 0.5ml ACK (ACK red blood cell lysing buffer; Gibco A10492-01) is added to the blood before transferring to a 15 ml falcon containing a further 2.0 ml of ACK. Blood is

incubated with ACK for 15 minutes at room temperature (RT), then washed in PBS (GIBCO 14190-094; 150 g 5 minutes) and resuspended in 3.0 ml ACK and incubated for a further 15 minutes. The remaining cells are washed in PBS and filtered (steriflip filters 0.22 µm Millipore SCGP00525) and transfer to a 96 well plate.

Splenocytes were isolated as above (**5.4.4**; **appendix 5-1**) and Human PBMC were thawed as described in **chapter 2**.

Murine antibodies were titrated on murine splenocytes (CD19/CD74/CD11c/CD3; **Table 5.3**). Human antibodies were supplied by the CEINGE human antibody core. Murine CD74 and human CD74 antibodies was used for assessing endogenous CD74 expression on murine and human cells respectively and the staining cross-reactivity of each antibody was also assessed in combination or alone in the opposite species.

Table 5-3. FACS reagents used in Chapter 5 (all anti-mouse unless stated)

Mouse Antibodies	Fluorochrome	Dilution	Staining Conc (µg/ml)	Titrated on	Manufacturer
CD3	APC	1:33	6ug/ml	-	BD 553066
CD3e	PeCy7	1:100	2ug/ml	Splenocytes	BD 552774
CD11c	PeCY7	1:33	6ug/ml	-	BD 558079
CD19	BV510	1:200	1ug/ml	Splenocytes	BD 562956
CD19	APC/Cy7	1:100	2ug/ml	-	BD 115530
KLRG-1	BV421	1:100	1ug/ml	Splenocytes	Biolegend 138413
CD127	eFluor660	1:100	2ug/ml	Splenocytes	eBiosciences 50-1271-82
CD127	PerCp-eFluor710	1:100	2ug/ml	Splenocytes	eBiosciences 46-1273-82
CD62L	Alexa488	1:50	10ug/ml	Splenocytes	Biolegend 104420
H-2KB-SIINFEKL	PE	1:100	2ug/ml	-	Biolegend 141604
CD8a	BV510	1:200	0.5ug/ml	Splenocytes	Biolegend 100751
CD27	PerCp-Cy5.5	1:100	2ug/ml	Splenocytes	Biolegend 124214
anti mouse CD16/CD32 Fc block	-	1:25	20ug/ml	-	BD 553142
anti mouse CD74 clone LN1	FITC	1:100	5ug/ml	Splenocytes	BD 555318
anti human CD74 clone LN2	PE	1:50	-	THP-1 cells	Biolegend 326808
isotype (mouse CD74)	Rat IgG2b FITC	1:100	5ug/ml	-	BD 553988
isotype (human CD74)	Mouse IgG1 PE	1:50	-	-	BD 400113

Pentamers
OVA – H2Kb-SIINFEKL
RSV – H2Kd SYIGSINNI

$1x10^6$ murine cells were stained in 96 well round bottomed plates with FC block (FcγRIII/FcγRII; BD Purified Rat Anti-Mouse CD16/CD32 553142) 1:25 in 50 µl PBS for 20 minutes on ice. Human or Murine cells are then washed in 150 µl PBS (all washes performed by addition of PBS up to 200 µl per well and then centrifugation at 125g 5 minutes) and stained with fixable Live Dead (L/D) dye (1:1000, in 50 µl PBS) for 20 minutes at RT. Cells are then washed with PBS (150 µl), and stained for 30 minutes at RT with surface antibody mix (**Table 5.4** for murine cells and **Table 5.5** for human cells). Cells were washed in PBS twice (200 µl) and were acquired on a FACS Canto flow cytometer and analysed using Flowjo.

Table 5-4. Murine CD74 surface panel

Laser	Fluorochrome	Marker	Concentration
Blue	PE	+/- CD74 (human)	1:50
	PeCy7	CD11c	1:33
	FITC	+/- CD74 (murine)	1:100
Red	APC	CD3	1:33
	APC-Cy7	L/D	1:1000
Violet	BV510	CD19	1:200

Table 5-5. Human CD74 surface panel

Laser	Fluorochrome	Marker	Concentration
Blue	PE	+/- CD74 (human)	1:50
	PerCp-Cy5.5	CD19	1:5
	FITC	+/- CD74 (murine)	1:100
Red	APC	CD3	1:5
	APC-Cy7	-	-
Violet	PB	L/D	1:1000

5.4.7 MHC class I pentamer staining

6 week old female C57BL/6 mice were vaccinated at $5x10^6$ or $1x10^7$ vp with Ad5 vectors encoding OVA N-terminally tethered to full length or truncated versions of mIi. Blood was taken for pentamer staining at weeks 2, 4, 10 and 18 after vaccination.

Murine PBMC are isolated from blood as above (**5.4.6**). Pentamers are centrifuged at 10,000 rpm for 10 minutes at 4 °c to pellet aggregates before use. Cells are resuspended in 40 µl PBS and 10 µl of supernatant is added from centrifuged

pentamers. Cells are stained with pentamers for 20 minutes at RT. Cells are washed in PBS and stained with fixable near infrared (NIR) L/D dye (1:20 dilution in sterile water, 1 µl per 50 µl in each well e.g. 1:1000 dilution from DMSO stock) for 20 minutes at RT. Cells are washed and resuspend in 50 µl of surface staining/memory panel (**Table 5.6**) for 30 minutes at RT. Cells are washed in FACS buffer then fixed with ebiosciences FACS fix/perm (005123-43) diluted from concentrate 1:4 in diluent for 20 minutes at RT. Cells are finally washed once in FACS buffer and once in PBS before being resusended in 200 µl PBS and analysed on FACS Canto-II.

A titration of MHC class I pentamer (1, 10, 20, 30 µl per tube) was performed in 96 well round-bottomed plates and FACS tubes to optimized staining conditions (not shown). 10 µl per well in plates was optimal. FMOs for pentamer staining panel were performed on splenocytes from an unvaccinated BALB/c mouse and a mouse vaccinated with PanAd3-RSV (0.5ml per mouse taken by retro-orbital bleed from anaesthetized mice) two weeks previously (pentamer H-2Kd- SYIGSINNI).

Table 5-6. Mouse Pentamer staining panel

Laser	Fluorochrome	Marker	Concentration
Blue	PE	Pentamer	1:5
	PeCy7	CD3	1:100
	PerCp-Cy5.5	CD27	1:100
	Alexa488	CD62L	1:50
Red	eFluor660	CD127	1:100
	APC-Cy7	L/D + CD19	1:1000
Violet	BV510	CD8	1:200
	BV421	KLRG-1	1:100

5.4.8 – 5.4.15 Murine *in vitro* experiments

For *in vitro* experiments all viral particle doses for cell transduction are calculated as infectious units, taking in to account the infectivity of each batch of vaccine, not just the number of viral particles.

5.4.8 Cell count and viability

All cell counts were performed using a Merck Millipore Muse cell analyser using the muse count & viability kit (Merck Millipore MCH100102). To confirm cell viability when cell count or viability was low trypan blue (0.4% Sigma T8154) staining was used (Cell:trypan blue:PBS 1:2:7 dilution).

5.4.9 Bone marrow derived dendritic cell (BMDC) culture

The protocol for generation and purification of bone marrow dendritic cells (BMDC) was adapted from (**Muccioli et al. 2011**). Briefly, to isolate bone marrow leukocytes, a 6-10 week old female F1 mouse is sacrificed and dissected to remove the tibias and femurs of the hind legs. The ends of the bones are cut off and the inside of the bones infused with RPMI using a sterile syringe inside a petri dish. Bone marrow leukocytes clumps are broken up and the cell suspension washed twice in RPMI (1200 rpm for 5 minutes) after collection in a 15 ml falcon. Red blood cells are lysed using ACK lysis buffer (5 minutes RT) and washed with RPMI and counted (approximately 25 x 10^6 cells per femur). 2-3 x10^6 cells are cultured in 10 ml R10 in a T75 flask (BD 353136) with 10 ng/ml of recombinant murine granulocyte-macrophage colony-stimulating factor (rGM-CSF; Invitrogen PMC2015). Cells were cultured at 37 °C with 5% CO_2. On

day 3 cultures are supplemented with 10 mls of R10 with 20 ng/ml rGM-CSF. On day 6 of culture the media is harvested, cells are pelleted (1200 rpm for 5 minutes) and resuspended in 20 ml of fresh R10 supplemented with 10 ng/ml rGM-CSF. On day 10 the cultured BMDC are stripped from the plate using pre-warmed trypsin (0.25% Sigma T3924) and cell dissociation solution (Sigma, C5789-100ml) 1:1 mix (incubated 7 minutes in a CO_2 incubator at 37 °C and 5% CO_2). Cultured cells are counted and a small sample is stained for viability and anti-murine CD11c and is analysed on the FACS canto-II to ensure enrichment for CD11c+ BMDCs.

5.4.10 BMDC – Transduction & CD74 surface expression

BMDC are harvested using 1:1 mix of cell dissociation solution and trypsin and counted. BMDC were plated at 150,000 cells per well in a 48-well plate in 200 µl R2 with virus at a multiplicity of infection (MOI) 0.8 to 100. After 1 hour incubation the volume was raised to 500 µl total with final concentration of 10 ng/ml rGM-CSF (recombinant granulocyte macrophage colony-stimulating factor) and incubated for the remaining 23 hours.

Cells are harvested again with 1:1 mix of cell dissociation solution and trypsin and transferred to a 96-well plate for staining. Cells are washed in PBS (200 µl) then stained with fixable NIR L/D stain in PBS at RT for 20 minutes. Cells are washed in PBS and stained with CD11c-Pe-Cy7 (1:100) in FACS buffer (PBS + 1%FCS) for eGFP containing adenoviral constructs. For mIi or hIi containing adenoviral constructs mIi (CD74-FITC 1:100) and/or hIi (CD74-PE 1:50) are also added. Uninfected cells were

also stained and cells infected at all MOI used are stained in parallel with isotype antibodies for CD74, matched for: the manufacturer, fluorochrome, and antibody isotype. BMDC are stained for 30 minutes at RT. Cells are then washed once in FACS buffer and once in PBS before being resuspended in PBS for analysis on the FACS CantoII.

5.4.11 BMDC – Antigen presentation assay

Cultured BMDC are isolated as above. BMDC are centrifuged and resuspended in R2 (RPMI + 2% FCS; 200,000 BMDC per well 150 µl total volume), plated in 48 well plates and transduced with Ad vectors at MOI 100. BMDC are incubated with virus at 37 °C with 5% CO_2 for 1 hour before adding 350 µl of R10 + rGM-CSF (final concentration of 10 ng/ml) and incubating for the remainder of the infection (total of 12-96 hours).

After transduction BMDC are harvested as above, washed in RPMI twice, and resuspended in PBS. Cells are transferred to a 96-well plate for staining. BMDC are pelleted and FC block is added (1:25 50 µl final volume) and cells are incubated for 20 minutes on ice. Cells are washed in PBS and stained with fixable violet live/dead dye (Thermo fisher L34955; 1:100) in PBS for 20 minutes at RT, washed in RPMI and stained with anti-murine CD11c-PeCy7 and anti-H2-Kb-SIINFEKL-PE (1:100; **Table 5-3**) for 30 minutes at RT. Cells were washed twice in PBS and immediately analysed on the FACS canto-II.

Uninfected BMDC were peptide pulsed with 2 μg/ml OVA peptide for 3 hours at 37 °C with 5% CO_2 before being washed twice in PBS, FC blocked on ice for 20 minutes, and then surface stained with fixable violet live/dead dye (1:1000), CD11c-PeCy7 (1:33) and anti-H2-K^b-SIINFEKL-PE antibody (1:100). BMDC infected with Ad5-mIi(50-215)-OVA were used for anti-H2-K^b-SIINFEKL-PE and CD11c-PeCy7 FMOs. Voltages and gating were checked with BMDC infected with Ads containing full length mIi and unstained and uninfected cells, but were left unchanged from the peptide experiment. Photomulitplier tube (PMT) voltages were kept constant between time points from the same BMDC infection.

5.4.12 JAWSII – Culture and Antigen presentation

JAWSII is an immortalized immature myeloid DC cell line derived from the bone marrow of p53-/- C57BL/6 mice. I obtained JAWSII cells from ATCC (CRL-11904 lot 58943585). JAWSII cells were cultured in R20 (prepared as R10 but with 20% FCS) supplemented with 5 ng/ml rGM-CSF at 37 °C and 5% CO_2. Cells were passaged by taking off the culture media washing cells in RPMI (1200 rpm for 5 minutes) and re-suspend in 2X volume of freshly supplemented medium and plating in two separate T75 flasks once or twice a week. JAWSII were transduced, stained, and analysed by FACS as described for BMDC (**5.4.11**). See **Table 5-7** for subculture conditions. JAWSII cells were thawed in a water bath at 37 °C by agitating until a small amount of ice was visible. Cells were then transferred to a 15 ml centrifuge tube containing 9 ml of pre-warmed R10. Cells were pelleted (125 g 5 minutes) and resuspended in 5 ml R20

(R10 containing 20% FCS) and placed in a T25 flask overnight. Viability and cell count was performed and cells are seeded at 0.5-0.7 x 10^6 cells/ml for passage 1.

5.4.13 THP-1 - Culture, maturation, and transduction

THP-1 cells are a human monocyte-like cell line derived from human leukaemia patient (ATCC#TIB-202). THP-1 were supplied in culture medium by James Ussher (University of Oxford) at passage 5 (Previously purchased from ATCC TIB-202).

Cells were grown in R10 in a CO_2 incubator at 37 °C and 5% CO_2. THP-1 were passaged 2-3 times a week, seeding at approximately 1-2 x 10^5 cells/ml, to ensure cells remained in exponential growth phase and concentrations did not exceed 1 x 10^6 cells/ml. See **Table 5-7** for subculture conditions.

Differentiation to macrophages-like cells was induced by stimulation with 200 nM PMA (phorbol 12-myristate 12-acetate; Sigma P8139) for 24-72 hours (**Daigneault et al. 2010**). 1x10^6 THP-1 were plated in 6-well plates in 3ml of R10 and 200 nM PMA was added for 24 hours.

Table 5-7. Subculturing conditions for human and murine cell lines

	Surface Area (mm^2)	Trypsin volume (ml of 0.05%)	Growth Medium (ml)	HeLa cells		JAWS II		THP-1	
				Seeding density (x 10^6)	Cells at Confluency (x 10^6)	Seeding density (x 10^6)	Cells at Confluency (x 10^6)	Seeding density (x 10^6)	Max Cell suspension Conc (x 10^6)
6-well plate	962	2	3.0-5.0	0.30	1.20	0.30	1.20	0.20	1.00
12-well plate	401	1	1.0-2.0	0.10	0.40	0.10	0.40	0.10	1.00
24-well plate	200	0.5	0.5-1.0	0.05	0.20	0.05	0.20	0.10	1.00
T25 flask	2500	5	5.0-12.5	0.70	2.80	0.70	2.80	0.10	1.00
T75 flask	7500	10	10-37.5	2.10	8.40	2.10	8.40	0.20	1.00

5.4.14 HeLa - Culture, maturation, and transduction

HeLa is an adherent immortalized human epithelial cell line. Cells were grown in a CO_2 incubator at 37 °C and 5% CO_2. See **Table 5-7** for subculture conditions. HeLa cells are not treated or activated before infection, but are readily transducible.

For transduction, 200,000 HeLa cells per well in a 24 well plate were left overnight to become confluent and on day 2 the 400,000 HeLa cells per well were transduced at MOI 50 with Ad vectors for 6, 24, or 48 hours. Cells were harvested by collecting the culture medium and incubating at 37 °C and 5% CO_2 with 300 µl per well of pre-heated trypsin. Inhibitors were added 4 hours after transduction with Ad vectors. Radicicol (500 µM, 1000X), 17-AAG (1000X), Chloroquine (90 mM, 1000X), and MG132 (10 mM, 1000X) were supplied by Mariano Stornaiuolo (Università degli Studi di Napoli Federico II, Napoli Italy). Lactacystin – Sigma L6785 (20 mM, used at 10 µM).

5.4.15 B3Z T-cell activation assay

B3Z is a murine T-cell hybridoma that has specific reactivity against the ovalbumin peptide $OVA_{257–264}$ (SIINFEKL)(**Karttunen & Shastri 1991**). B3Z express the *Escherichia coli* β-galactosidase (*lacZ*) gene, under control of the IL-2 enhancer region or the 'nuclear factor of activated T-cells (NFAT) element' and it is therefore, specifically induced on activation of the B3Z T-cells through TCR signalling. Activation of transduced T-cells results in synthesis of both IL-2 and β-galactosidase, which remains sequestered within the activated cells and this can be assayed for by

measuring the breakdown of the β-galactosidase substrate CPRG [Chlorophenol Red-β-D-galactopyranoside; Sigma 59767) to the coloured substrate Chlorophenol red.

B3Z cells were thawed in a water bath at 37 °C by agitating until a small amount of ice was visible. 5 x 10^6 B3Z were resuspended in 30 ml pre-warmed R10 and split between two T25 flasks. B3Z are split 1:2 every two days by pelleting and resuspending at 150,000-200,000 cells per ml in R10.

50,000 BMDC (isolated and cultured as above) per well (96 well round-bottomed plate) were transduced with Ad5-OVA constructs at MOI 0.5 for 24 hours before being mixed with B3Z cells (cultured as above) at a ratio of 1:2 or 1:4 (BMDC:B3Z) and cultured at in a CO_2 incubator at 37°C with 5% CO_2 for 12 hours. CPRG containing B3Z substrate (0.125% tergitol [NP-40; sigma NP40S-100ml], 9 mM $MgCL_2$, 0.15 mM CPRG [Chlorophenol Red-β-D-galactopyranoside; Sigma 59767), 100 mM β-merceptoethanol in PBS) was then added to each well and the plate was left at 4 °C overnight before being developed for 5 hours at 37 °C. Absorbance of Chlorophenol Red was measured at OD 570-620 nm. 0.15 mM EDTA plus 300 mM glycine in ddH_2O was added to inactivate β-galactosidase at the end of the reaction.

5.5 Results

5.5.1 The Shortened constructs – Narrowing down to key domains

The mechanisms by which the genetic adjuvant Ii enhances CD8+ T-cell responses when linked to a virally vectored transgene were initially investigated

by assessing which domains within the Ii sequence were essential for the adjuvant effect.

I also wanted to define a minimal sequence that could retain the full adjuvant effect, but that shared little sequence homology with the full length endogenous Ii sequence, so as to minimise the chances of breaking tolerance or of having off target effects within transduced cells. Autoantibodies recognising Ii have been observed in patients with axial spondyloarthiritis, and although no causal link to disease has been elucidated these studies highlight a possible risk of using endogenously expressed protein within vector constructs (**Baraliakos et al. 2013; Baerlecken et al. 2013**).

The adjuvant effect is only apparent *in vivo* when Ii is physically attached to the N-terminus of the transgene, as Ii expression by the same Ad but from a different transgene (**Sorensen et al. 2009**) or Ii C-terminally linked to transgene do not enhance CD8+ T-cell responses in vivo (**D'Alise personal communication**). This suggests an intracellular mechanism of Ii on the cell in which the adenoviral vector genome is present and shows the importance of the positioning of Ii and the transgene at the time of translation by ribosomes, rather than an effect of increased local concentration of Ii.

E1E3 deleted Ad5 constructs containing the model antigen OVA linked to variant Ii sequences (truncated versions of Ii and variants including specific additions or deletions) were used to vaccinate i.m. C57BL/6 mice and the immunogenicity of each construct was assessed by IFNγ ELISpot two weeks post vaccination. The Ii variants tested are described in **figure 5-3**.

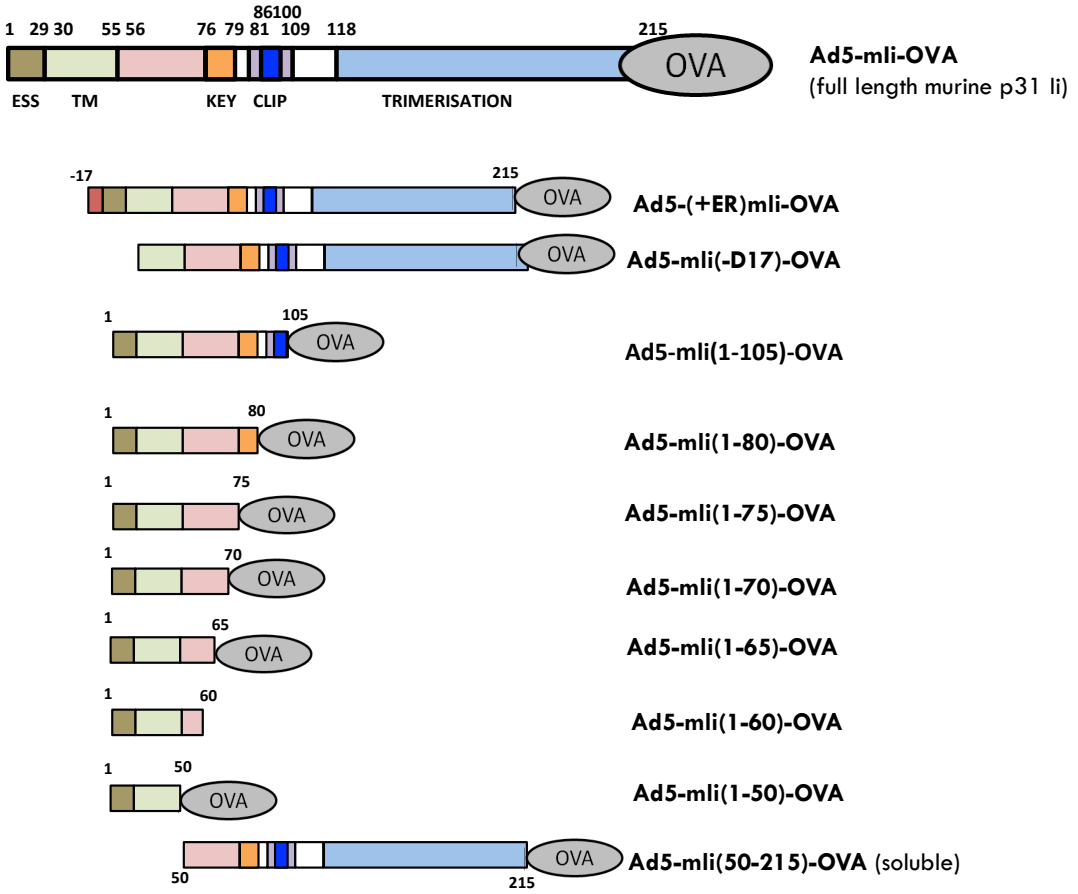


Figure 5-3. mli variants: Diagram of Ad5 vectors encoding full-length murine p31 Invariant chain (mli) and trimmed or mutated variants of mli fused to ovalbumin antigen (OVA). Numbers indicate amino acid position along mli. Variants are colour coded throughout this chapter. ESS = endolysosomal sorting sequence; TM = transmembrane region; CLIP = class II-associated invariant chain peptide; (ER) = indicates addition of endoplasmic reticulum retention sequence; (D17) = indicates removal of ESS.

First the trimerisation region, which is important for is role as a MHC class II chaperone and MIF signalling receptor, was removed (Ad5-mIi(1-105)-OVA) and

another construct containing just the transmembrane region and ESS were tested (Ad5-mIi(1-50)-OVA; **figure 5-3**). Vaccination with Ad5-mIi(1-50)-OVA induced the same CD8+ T-cell response to the immundominant peptide $OVA_{257-264}$ (SIINFEKL) as unlinked OVA, therefore, inclusion of the transmembrane region and ESS alone cannot enhance T-cell responses (**figure 5-4A**).

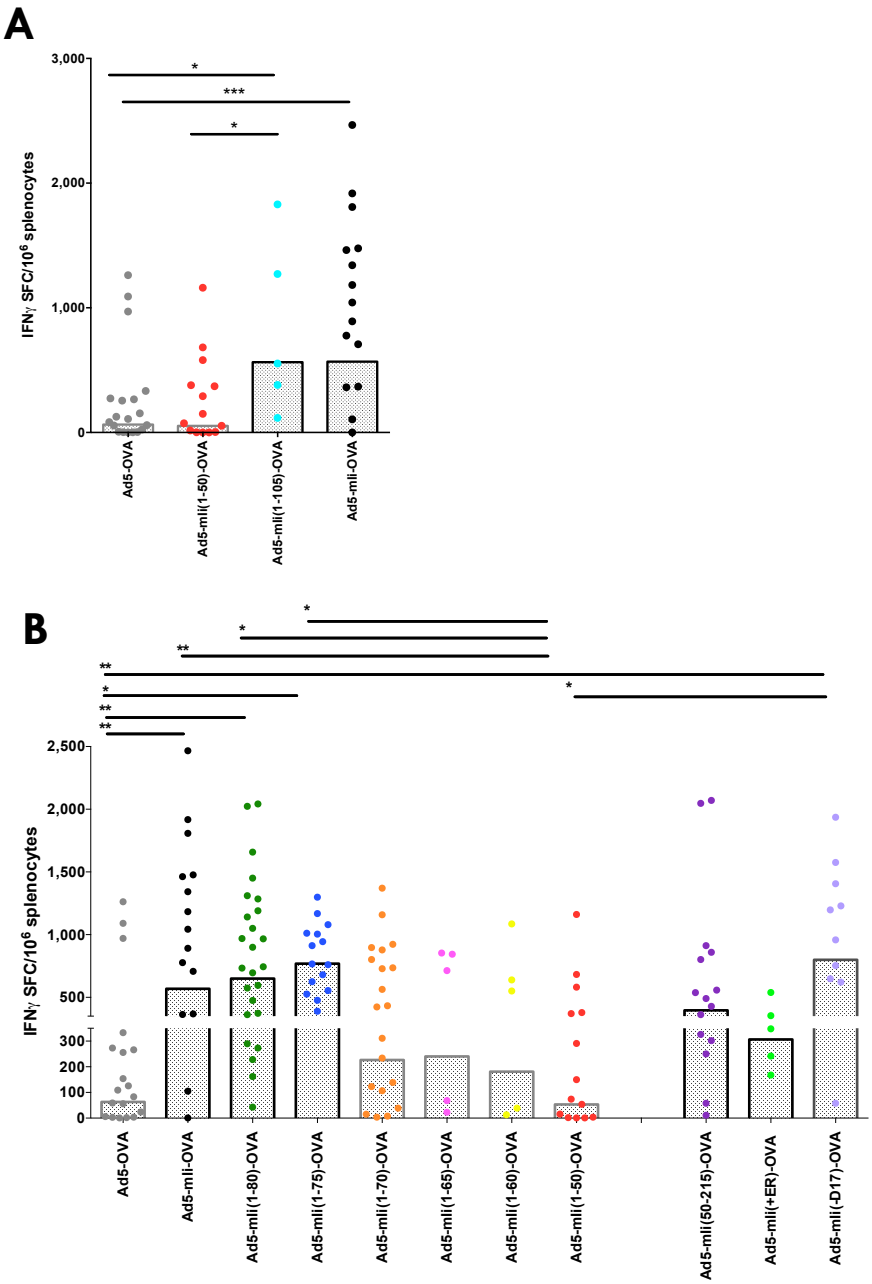


Figure 5-4. T-cell responses in mice immunized with Ad5-OVA +/- mli variants: (**A-B**) The immunogenicity of Ad5 vectors containing OVA alone, or linked to mli or mli variants were tested *in vivo* by vaccinating C57BL/6 mice intramuscularly ($3x10^6$ vp) and assessing the T-cell response to $OVA_{257-264}$ by IFNγ ELISpot on splenocytes two weeks later. Data shown as the mean (quadruplicate wells) number of spots per million cells for peptide stimulated wells after subtraction of background (mean of quadruplicate DMSO wells). Bars at geometric mean. (**A**) A comparison of the immunogenicity of Ad5-OVA with Ad5-mli-OVA, Ad5-mli(1-50)-OVA and Ad5-mli(1-105)-OVA. Results combined from 5 experiments. (**B**) A comparison of the immunogenicity of Ad5-OVA with Ad5 constructs containing OVA N-terminally tethered to the following mli variants: mli(1-80), mli(1-75), mli(1-70), mli(1-65), mli(1-60), mli(1-50), mli(50-215), mli(+ER), mli(-D17). Results combined from 5 experiments. Kruskal-wallis ANOVA with Dunn's correction comparing all means.

Deletion of the trimerisation region - over half of the p31 Ii sequence (amino acids 106-215) was tolerated and inclusion of mIi(1-105) retained the full adjuvant effect seen with full length mIi. Ii was further truncated to residues 1-80 (Ad5-mIi(1-80)-OVA), removing the CLIP region, which occupies the peptide-binding groove when bound to MHC-II molecules, without losing its ability to enhance CD8+ T-cell responses (**figure 5-4B**).

Sequential deletion of 5 amino acids at a time from 1-80 to 1-50 was then performed to see if certain residues are essential for the affect of Ii. A dose escalation was performed for Ad5-OVA and Ad5-mIi-OVA constructs (**D'Alise personal communication**) and a dose near the breakpoint (the dose at which you lose immunogenicity; **Colloca et al. 2012**) for these construct was chosen, so as to optimise the enhancement seen when full length Ii was encoded by the Ad construct. Despite using inbred mice at this limiting dose of Ad there is still heterogeneity seen in T-cell responses to the immunodominant epitope $OVA_{257-264}$, with some mice receiving Ad5-OVA showing very strong responses and some

receiving Ad5-mIi-OVA with weak or absent responses; nevertheless, there does not seem to be a binary response to Ii variants, with a loss of adjuvant effect when essential residues are removed. There is a gradual loss in the proportion of strong responders to vaccination as you delete more amino acids beyond 1-75 (**figure 5-4B**).

As previously discussed, Ii has been shown to directly interact with MHC class I molecules and to aid in their localisation to endolysosomal compartments, so that they can be loaded with exogenously sourced peptides for cross-presentation (**Basha et al. 2012**). An attractive and relatively simple model of the adjuvant effect of Ii may, therefore, involve enhanced cross-presentation of transgene derived peptides in endosomes of cells transduced with Ii containing Ads. Our data suggests that this is not the case as the deletion of the ESS (Ad5-mIi(D17)-OVA) did not lead to a loss of the adjuvant effect (**figure 5-4B**).

Human Ii isoform p35 contains an additional 17 amino acids at its N-terminal, which encodes an ER retention sequence (ERR) that is absent in human p31 and p33 and murine Ii (**figure 5-2**). To assess whether these residues may enhance the effect of linkage of mIi to transgene and whether ER retention is important in the mechanism for enhance T-cell responses I tested a constract containing mIi where the human ER retention sequence was added to the N-terminus of mIi and tested the immunogenicity in an Ad5 OVA containing construct (Ad5-mIi(ER)-OVA). Although only 5 mice were tested there is an indication that the T-cell response is not further enhanced by addition of ER retention sequence to mIi (**figure 5-4B**).

When OVA was linked to a N-terminally truncated Ii sequence, omitting the transmembrane domain (Ad5-mIi(50-215)-OVA) the adjuvant effect of Ii was retained. This construct lacks the transmembrane region, therefore, it should be translated and processed exclusively within the cytoplasm, without trafficking through the ER.

Next I wanted to assess at a more limiting dose of Ad vectors whether mIi variants 1-80 or 50-215 could perform as well as full-length mIi. At 3 x 10^5 vp only OVA linked to full-length mIi and mIi with the addition of human ER retention sequence [mII(+ER)] induced a T-cell response at week 2 post-vaccination at detectable levels (**figure 5-5**). At 1x10^6 vp again full length mIi with or without the ER retention sequence out performed Ads encoding mIi(1-80) or mIi(50-215).

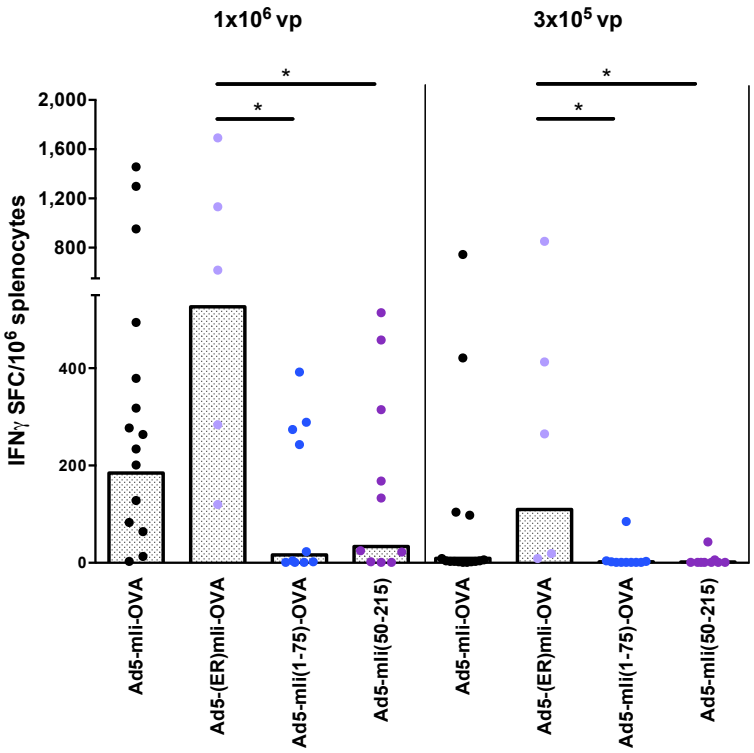
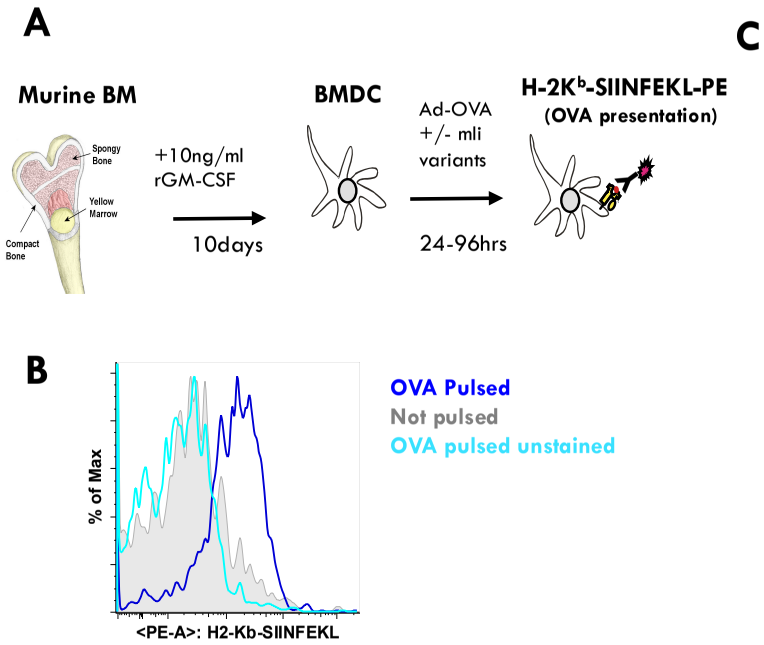


Figure 5-5. Immunogenicity of Ii containing Ad vectors at limiting doses: The immunogenicity of Ad5 vectors containing OVA linked to mIi or the mIi variants which enhanced responses at high vaccine doses [mIi(1-75) and mIi(50-215)] were tested *in vivo* by vaccinating C57BL/6 mice intramuscularly with $1x10^6$ or $3x10^5$ vp. Immunogenicity was assessed by measuring the T-cell response to $OVA_{257-264}$ by IFNγ ELISpot on splenocytes two weeks after vaccination. Data shown as the mean (quadruplicate wells) number of spots per million cells for peptide stimulated wells after subtraction of background (mean of quadruplicate DMSO wells). Bars at geometric mean

Much of the Ii sequence can be removed without loss of the adjuvant effect, in particular the domains that are key for their interactions with MHC class I and II (KEY, CLIP, and ESS). It appears that amino-acids between residues 50 and 75 in mIi are important for the adjuvant effect of Ii on T-cell responses, however, at limiting doses of vaccine no shortened variant of Ii can equal the performance of full length Ii, suggesting a potential role of several domains in the mechanism of action.

5.5.2 The mechanism – Improved Ag presentation

Covalent linkage of transgene to Ii not only enhances the magnitude of the peak and memory antigen-specific T-cell response to viral vectors, it also appears to accelerates the kinetics of the response and it affects both dominant and subdominant epitopes (**Holst et al. 2008; Capone et al. 2014**). One explanation for how linkage of antigen to Ii could have such a wide ranging effect on the T-cell response could be that it perturbs the normal antigen presentation pathway, causing increased MHC-I presentation, which in turn could lead to a stronger clonal expansion of primary and secondary responses (**Mehlhop-Williams & Bevan 2014; Curtsinger & Mescher 2010**). We are fortunate that there is a well characterized antibody which recognizes the immunodominant epitope $OVA_{257-264}$ (SIINFEKL) when it is associated with its MHC class I molecule H-$2K^b$; by fluorescently labelling this antibody we can directly measure the number of MHC-I presenting this peptide on a given APC and assess whether there is more presentation of epitopes within a transgene when linked to Ii (**figure 5-6A**). An initial study by a collaborator showed this to be the case when using full length Ii (**Holst et al. 2011**). I extend this analysis to see if the level of antigen presentation correlates directly with the *in vivo* immunogenicity of OVA tethered to Ii variants, and to assess whether the kinetics of presentation are changed.



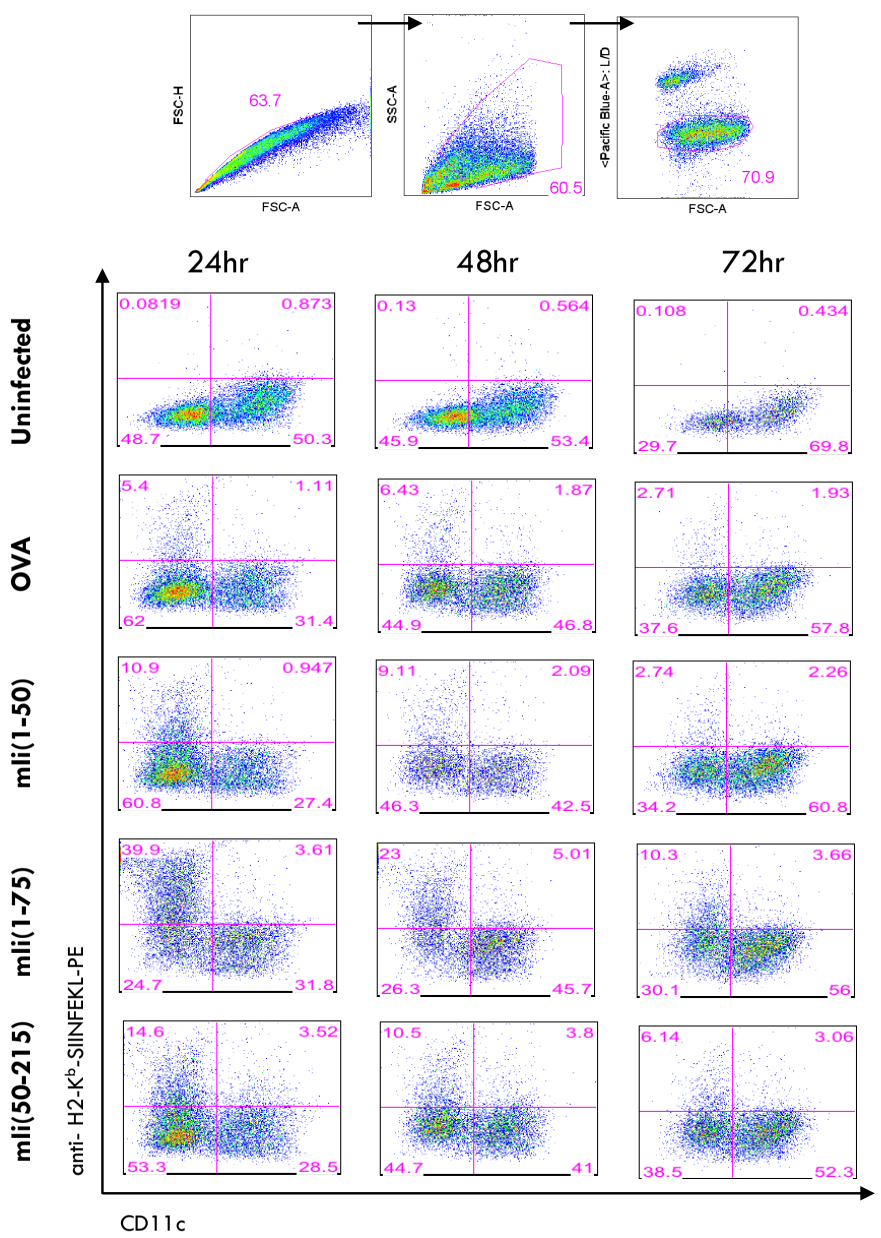


Figure 5-6. Assessing presentation of an immunodominant OVA peptide on murine DC in vitro: (**A**) Schematic of experimental set up for bone marrow derived dendritic cell (BMDC) culture, transduction, and measurement of surface presentation of the immunodominant OVA epitope ($OVA_{257-264}$) on MHC class I. Murine bone marrow cells are harvested from the tibia and femur of F1 mice (C57BL/6 X BALB/c) and enriched for BMDC by culturing for 10 days with rGM-CSF. BMDC are infected with Ad vectors containing OVA linked to mli and variants. 24h post infection, cells were stained with a monoclonal antibody recognizing the ovalbumin-derived peptide SIINFEKL bound to H-2Kb. (**B**) The specificity of H-2K^b-SIINFEKL-PE was confirmed by staining BMDC after pulsing with OVA peptide for 3 hours. (**C**) Example plots of H-2K^b-SIINFEKL-PE vs CD11c on live uninfected BMDC or live BMDC infected with Ad5-OVA +/- mli variants 24, 48 or 72 hours previously.

I first optimised our bone marrow derived dendritic cells (BMDC) harvesting method and FACS panel to ensure that H2-K^b was not stripped from the cells when removing adherent cells for culture flasks and to ensure there is clear staining of H2-K^b-SIINFEKL-PE. H2-K^b-SIINFEKL was readily detectable on BMDC that were pulsed with 2 μg/ml OVA peptide for 3 hours but did not stain un-pulsed BMDC (**figure 5-6B**).

I next infected BMDC *in vitro* with Ad5-OVA encoding several mIi variants and used FACS analysis to directly measure the MHC-I surface presentation of OVA peptide 24-72 hours post infection. Although BMDC cultures are enriched for CD11c+ DCs after 10 days culture with rGM-CSF, both CD11c+ and CD11c- populations were detected and both populations presented SIINFEKL (**figure 5-6C**). I analysed presentation on total live BMDC and CD11c+ cells looking at both the percentage of cells that present SIINFEKL and the amount of expression on a per cell basis (geoMFI [geometric mean fluorescent intensity]). Initially, looking at presentation 24 hours after infection of BMDC, there is clearly an enhanced presentation of SIINFEKL on MHC-I above that seen with Ad5-OVA for constructs containing OVA linked to mIi(1-75), mIi(50-215), or full length mIi, both when looking at all live cells and specifically at CD11c+ cells, for geoMFI (**figure 5-7A**) and the percentage of cells presenting OVA (**figure 5-7B**). Tethering OVA to mIi (1-50) or mIi(1-70) did not show enhanced presentation. Surprisingly, the inclusion of mIi(1-80) also did not enhance the presentation of OVA on infected cells significantly, and residues mIi(1-75) [which is essentially the same as mIi(1-80) but omitting the 5 amino acids encoding the KEY motif] consistently outperformed the full length mIi; this was especially apparent when looking at

live cells, suggesting there may be a CD11c- population in which linkage of OVA to mIi(1-75) selectively enhances OVA presentation, more so than full length mIi. SIINFEKL presentation was assessed on BMDC infected at both MOI 20 (not shown) and 200 and the same pattern of enhanced presentation for constructs containing mIi(1-75), mII(50-215) and full mIi was seen.

The enhancement of antigen presentation when including the minimal residues mIi(1-75), or the soluble trans-membrane domain lacking mIi(50-215), or full length mIi recapitulates the results seen when assessing T-cell responses *in vivo* by IFNγ ELISpot, with the exception of constructs containing mIi(1-80) which appeared to underperform by antigen presentation relative to T-cell induction (**figure 5-4B**). Several vials of Ad5-mIi(1-80)-OVA were tested from the same batch that showed enhanced immunogenicity by ELISpot (**figure 5-4B**) but none showed significant enhancement of OVA presentation.

I next assessed the kinetics of the presentation on infected BMDC by assessing presentation at 24, 48, and 72 hours with Ad-OVA containing mIi variants to see if the adjuvant effect may be mediated by a short period of enhanced antigen presentation immediately after transduction of a cell by Ii containing Ads. Although the relative difference in antigen presentation above that for unlinked Ad5-OVA decreases over time, at 48 and 72 hours enhanced presentation is still seen for Ad constructs containing mIi(1-75), mIi(50-215) and full length mIi on both CD11c+ (**figure 5-7C**) and total live BMDC (**figure 5-7D**). The enhanced presentation of SIINFEKL when OVA is linked to mIi(1-75) and full length mIi relative to mIi(1-50) was confirmed in JAWSII cells (immortalized immature

myeloid DC cell line derived from the bone marrow of p53-/- C57BL/6 mice; not shown).

Linking Ad5 encoded OVA to mIi variants mIi (1-75), mIi(50-215) and full-length mIi leads to a larger number of class I molecules presenting OVA peptide SIINFEKL per cell (higher geoMFI) and a larger number of cells presenting OVA on infected BMDC (all live cells, and CD11c+ subsets) relative to infection with Ad5-OVA. mIi(1-75) outperforms even full-length mIi and 1-80 for enhancing antigen presentation, and it appears to maintain this improved presentation longer than full length and soluble mIi versions. There is a direct association between the Ad constructs that show enhanced OVA presentation and those that induce the largest OVA-specific CD8+ T-cell response in mice.

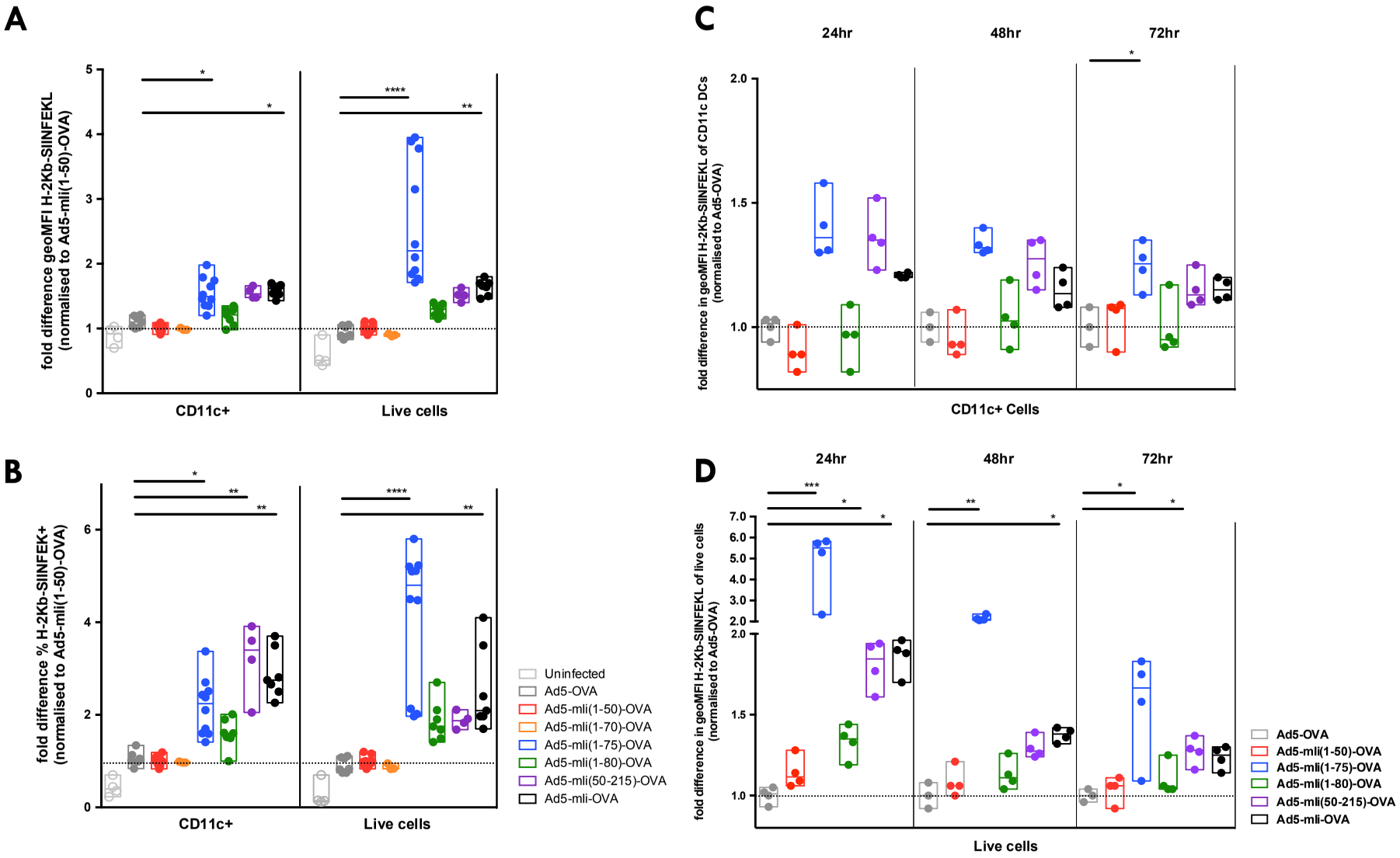

A
fold difference geoMFI H-2Kb-SIINFEKL (normalised to Ad5-mli(1-50)-OVA)
CD11c+
Live cells
B
fold difference % H-2Kb-SIINFEK+ (normalised to Ad5-mli(1-50)-OVA)
CD11c+
Live cells
Uninfected
Ad5-OVA
Ad5-mli(1-50)-OVA
Ad5-mli(1-70)-OVA
Ad5-mli(1-75)-OVA
Ad5-mli(1-80)-OVA
Ad5-mli(50-215)-OVA
Ad5-mli-OVA
C
24hr
48hr
72hr
fold difference in geoMFI H-2Kb-SIINFEKL of CD11c DCs (normalised to Ad5-OVA)
CD11c+ Cells
D
24hr
48hr
72hr
fold difference in geoMFI H-2Kb-SIINFEKL of live cells (normalised to Ad5-OVA)
Live cells
Ad5-OVA
Ad5-mli(1-50)-OVA
Ad5-mli(1-75)-OVA
Ad5-mli(1-80)-OVA
Ad5-mli(50-215)-OVA
Ad5-mli-OVA

Figure 5-7. The effect of tethering OVA to mIi and its variants on *in vitro* surface antigen presentation by murine DCs: (A-B) The fold difference in geoMFI for H-2k^{b}-SIINFEKL-PE antibody on CD11c+ or total live BMDC (**A**) and the fold difference in the percentage of total live or CD11c+ BMDC presenting SIINFEKL (positive gate defined using uninfected BMDC). (**B**) 24 hours after transduction (MOI 100) relative to values for Ad5-mIi(1-50)-OVA within the same experiment. Combined results from 5 experiments using 3 batches of culture BMDC. Line at 1 (no difference with values for Ad5-mIi(1-50)-OVA). (**C-D**) The fold difference in geoMFI for H-2k^{b}-SIINFEKL-PE antibody on CD11c+ (**C**) or total live BMDCs (**D**) relative to Ad5-OVA) 24,48, or 72 hours after transduction (MOI 100). Line at 1 (no difference with values for Ad5-OVA). (**A-D**) Bars at max and minimum, line at median. Kruskal-Wallis ANOVA with Dunn's correction for all statistics comparing Ad5-OVA vs. Ad5-OVA linked to mIi variants.

5.5.3 Correlating improved presentation with T-cell activation and proliferation

T-cell activation occurs when the integrated value of signals delivered through the TCR (signal 1), various co-stimulatory molecules (signal 2) and inflammatory cytokines (signal 3) exceeds a certain threshold (**Curtsinger & Mescher 2010**). It is likely then that an increased level of presentation of a specific peptide by APCs would lead to a higher number of activate antigen-specific T-cells and greater T-cell proliferation after vaccination with Ads encoding Ii.

To confirm that an enhanced level and duration of antigen presentation on APCs can lead to a larger number of activated T-cells I took a murine T-cell hybridoma that has specific reactivity against the ovalbumin peptide $OVA_{257–264}$ (B3Z) and presented antigen to it by infecting BMDC with Ad5-OVA or Ad5 with OVA linked to variants of mIi. B3Z cells have been engineered to express beta-galactosidase

on triggering of their TCR (**Karttunen & Shastri 1991**), therefore, the activity of this enzyme (as measured by the breakdown of chlorophenol red β-D galactopyranoside [CPRG] to a coloured precipitate [chlorophenol red]) corresponds directly to the number of active B3Z cells; I can, therefore, measure the number of active B3Z that results when antigen is presented to B3Z by BMDC transduced with different mIi containing constructs (**figure 5-8A**).

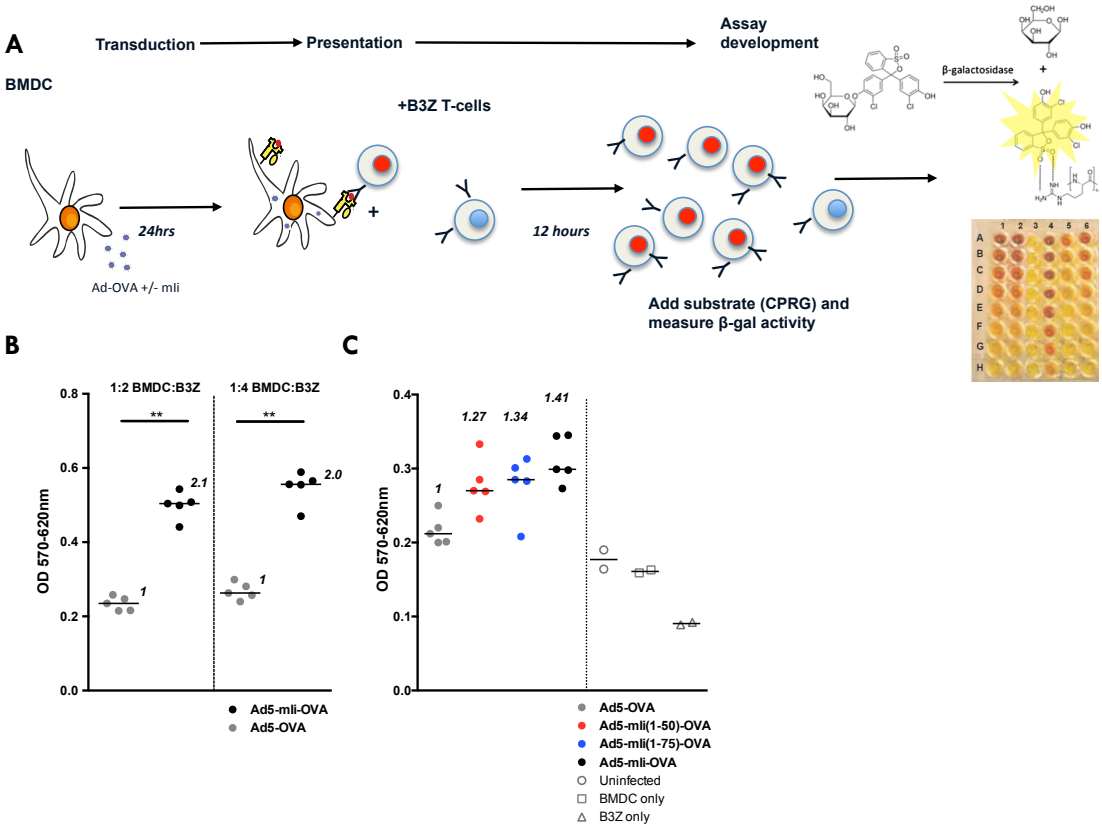


Figure 5-8. Increased presentation correlates with increased proliferation of antigen specific T-cells *in vitro*: (**A**) Schematic of experimental set up. BMDC were transduced for 24 hours with Ad-OVA +/- mIi variants (MOI 0.5), then mixed with B3Z at various target:effector ratios. 12 hours later B3Z activation and proliferation was assessed indirectly by monitoring the relative activity of β-galactosidase (breakdown of CPRG substrate). B3Z T-cells, a CD8+ T-cell clone with specificity for the OVA epitope SIINFEKL, contain a lacZ reporter gene linked to the nuclear factor of activated T-cells (NFAT) expression, therefore, expression of β-galactosidase is restricted to T-cells activated through their TCR. Relative concentration of chlorophenol red (chromogenic substrate of β-galactosidase digested CPRG) is expressed as

OD 570-620nm. (**B**) Relative number of activated of B3Z T-cell clones after culture with BMDC infected with Ad5-mIi-OVA vs. Ad5-OVA at effector:target ratios 1:2 or 1:4. (**C**) Relative number of active B3Z T-cells after culture with BMDC infected with Ad5-OVA+/_ mIi variants. Italicized numbers represent the fold increase in OD over Ad5-OVA infected BMDC. CRPG and digestion product molecular images taken from (**Sicard et al. 2014**).

After optimizing the MOI (0.5) and the co-culture time (12 hours; data not shown) two effector to target ratios of BMDC:B3Z were assessed (1:2 or 1:4; **figure 5-8B**). Both assay conditions showed a two fold increase in the number of activated T-cells when OVA was linked to Ii relative to unlinked OVA. The assay was extended to test Ads encoding OVA linked to mIi(1-75) and mIi(1-50) (**figure 5-8C**). Although a smaller fold difference in T-cell activation was seen, the same trend for enhanced T-cell activation and proliferation is seen when OVA is tethered to mIi (1-75) or full-length mIi.

It is unclear whether a larger number of MHC class I-TCR interactions between an APC and T-cell would lead to a stronger clonal expansion of activated T-cells or to a larger number of productive APC:T-cell interactions that effectively activate T-cells, however, by either mechanism or a combination of the two, increasing antigen presentation on an Ad-transduced APCs encoding mIi leads to a larger number of activated and proliferating CD8+ T-cells.

5.5.4 Holst *et al* – Blocking the class I and class II presentation pathways

The intracellular mechanism by which N-terminal linkage of Ii to an antigen when encoded in a plasmid or viral vector leads to enhanced MHC class I

presentation on the transduced cell's surface was investigated by Holst *et al*. Ii contains multiple functional domains and it interacts with machinery of both the class I (**Basha et al. 2012**) and class II presentation pathways (**Blum et al. 2013**); there are, therefore, multiple mechanisms by which tethering antigen to Ii can lead to more efficient class I presentation.

Several molecules involved in antigen processing and loading or trafficking of MHC-I and MHC-II molecules were blocked using specific inhibitors by Holst *et al* (**unpublished, personal communication**) to assess whether antigen linked to Ii progresses through the classical MHC class I antigen presentation pathway or through a novel pathway. For each inhibitor BMDC were infected with Ad5-mIi-OVA and the H2-K^b-SIINFEKL staining was assessed by FACS, and in parallel BMDC were infected with Ad5-eGFP to ensure inhibitors did not affect cell transduction.

First, to show the classical MHC class II antigen presentation pathway is not involved chloroquine and Bafilomycin A1 (endosomal acidification inhibitors), Leupeptin and Pepstatin A + E64d (lysosomal protease inhibitors) were added to BMDC cell culture 6 hours before assessing presentation. No effect on Ad5-eGFP transduction or SIINFEKL presentation was seen with these inhibitors. This is not surprising as the full Ii adjuvant effect is seen *in vitro* and *in vivo* when ESS, KEY motif and CLIP are removed (**figure 5-4B)** and in MHC class II knock-out mice (**Holst et al. 2011**), showing the class II presentation pathway does not play a role in mIi-linked enhancement of CD8+ T-cell responses. *Pseudomonas aeruginosa* exotoxin A (Sec61 inhibitor) has been shown to inhibit translocation

of the exogenous peptide into the cytosol for cross-presentation in DCs (**Rock 2006**) and addition of this to cultures had no effect on SIINFEKL presentation.

No T-cell response is induced in TAP knock-out mice when infected with Ad5-mIi-OVA, showing that the classical Class I pathway is needed and that mIi does not allow loading of antigen on to MHC-I molecules via a TAP-independent pathway (**Holst *et al* unpublished**). Brefeldin A (an inhibitor of protein export from the ER to the golgi apparatus via blocking of COPI-mediated transport vesicles) inhibited all surface presentation of SIINFEKL in transduced BMDC, however, intracellular accumulation of SIINFEKL loaded on H2-K^b was observed. Enhanced presentation of Ii-linked antigen is dependent on the direct class I presentation pathway and not the class II pathway, cross-presentation, or a novel antigen processing pathway.

5.5.5 Tethering antigen to Ii leads to rapid degradation by the proteasome

What is not clear is whether tethering of Ii to Ad vectored antigen changes the kinetics of antigen accumulation or degradation within the cell, which could have an impact on the availability of peptides from the tethered antigen for loading on to MHC-I. To assess this I infected HeLa cells with Ad5-eGFP or Ad5-mIi-eGFP and monitored the eGFP accumulation within cells by FACS. Ad5-eGFP infected cells rapidly accumulated eGFP and almost all cells were eGFP positive 24 hours after infection (MOI 50; example plots and histogram **figure 5-9A-B**). When eGFP was tethered to mIi, eGFP could be detected above background but at a

much lower concentration than with Ad5-eGFP, with only 20-25% of cells being eGFP+ 24 hours after infection (**figure 5-9C**). This was unexpected, as I had predicted that an enhanced stability of antigen, or the sequestering of Ii-antigen to a protected compartment within the cell would have resulted in the prolonged availability of Ad encoded antigen when linked to Ii, and that this would have resulted in enhanced T-cell responses.

One of the earliest stages of antigen processing for loading on to MHC-I molecules is the proteasomal degradation of proteins in the cytosol (**Rock et al. 1994**). Only a small fraction of cellular proteins are efficiently processed to peptides of sufficient length and form for presentation on MHC class I molecules, but the majority of peptides presented on MHC-I are processed through the proteasome (**Rock et al. 1994**).

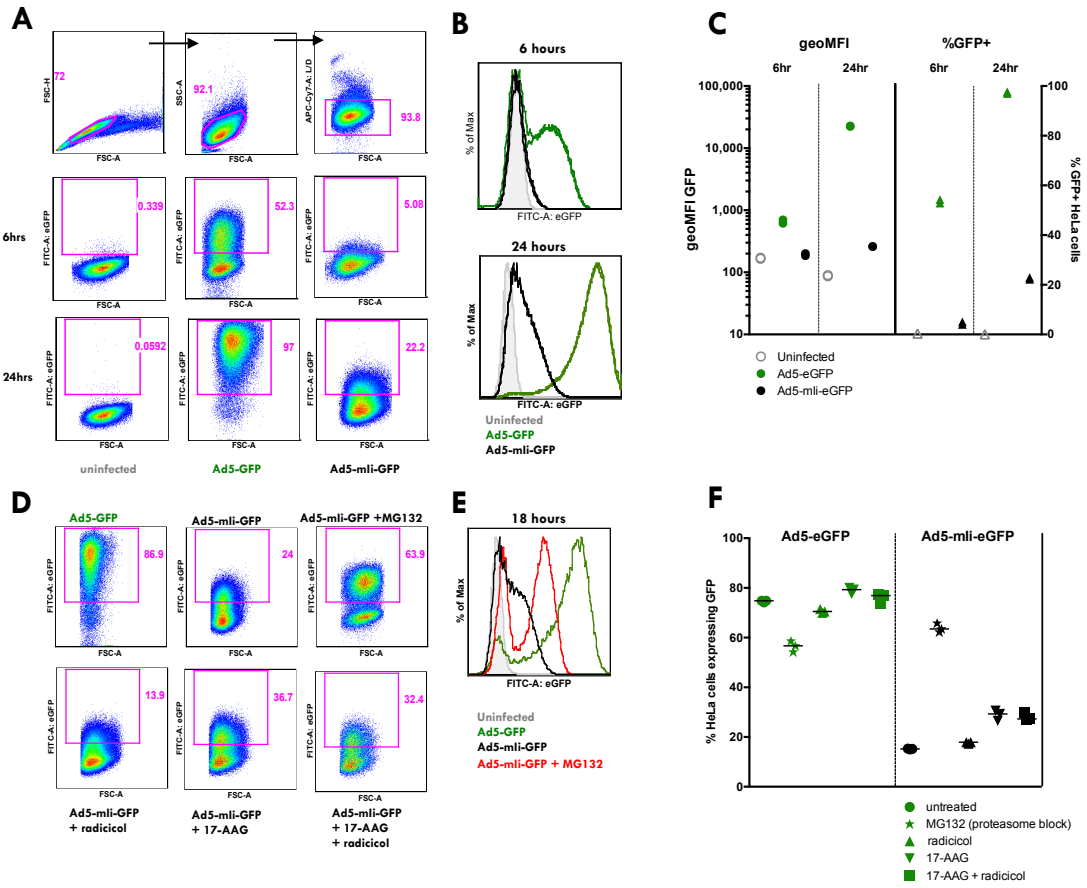


Figure 5-9. eGFP N-terminal linked to mli within an adenoviral vector is rapidly degraded and this degradation is blocked by inhibiting the proteasome: (**A-C**) eGFP transgene expression in HeLa cells transduced 6 or 24 hours earlier with Ad5-eGFP or Ad5-mli-eGFP (MOI 50), assayed by FACS. Gating strategy and example plots (**A**), histograms (**B**) and geoMFI or percentage eGFP positive HeLA cells (**C**). (**D-F**) eGFP transgene expression of HeLa cells transduced 18 hours earlier with Ad5-eGFP or Ad5-mli-eGFP after treatment with MG132 (proteasome inhibitor), radicicol and 17-AAG (heat shock protein 70 and heat shock protein 90 inhibitors). Gating strategy and example plots (**D**), histograms (**E**) and geoMFI or percentage eGFP positive HeLA cells (**F**).

To test whether the accelerated degradation of antigen when linked to Ii is proteasome dependent, I infected HeLa cells with Ad5-eGFP or Ad5-mIi-eGFP in the presence of MG132 (a potent proteasome inhibitor) and two heat shock protein 70 and 90 inhibitors (17-AAG/tanespimycin and radicicol; example plots and histograms **figure 5-9D-E**). HSP70 binds to misfolded proteins and

mediates the interaction with ubiquitin E3 ligases, therefore its inhibition would reduce the efficiency of ubiquitination of the misfolded proteins it interacts with (**Pratt et al. 2010**). HSP90 binds to HSP70 and regulates its interaction with E3 ligases (**Pratt et al. 2010**). These inhibitors had little effect on the accumulation of eGFP by Ad5-eGFP infected HeLa cells, however, there is much redundancy in the role of chaperones and E3 ligases within a cell, meaning ubiquitination of Ii-antigen may not have been prevented by inhibiting HSP70, or enhanced by inhibiting HSP90. The lack of accumulation of eGFP when linked to mIi could be reversed, however, by blocking the proteasome with MG132 (**figure 5-9F**). This shows that eGFP is still produced and in a fluorescent conformation when linked to Ii but that it is rapidly broken down by the proteasome.

Rapid and specific targeting of antigen to the proteasome appears to be enough to enrich cells with optimal peptides for loading on to MHC -I molecules in the ER, which in turn leads to enhanced activation of T-cells.

5.5.6 Linkage of antigen to Ii within Ad vectors does not change the phenotype of antigen-specific T-cells induced

N-terminal tethering of Ii to a transgene within Ad, DNA, or MVA can enhance the CD8+ T-cell response and this is most likely due to enhanced presentation of linked antigens on MHC-I. It is clear that the antigenic history or strength and number of antigen exposures has a profound effect on the phenotype and function of T-cells (**Masopust et al. 2006**)(**Chapter3**). I next assessed whether linkage of Ii to antigen changes the T-cell phenotype of Ad-induced T-cells *in vivo*.

I vaccinated C57BL/6 mice with low or medium dose ($1x10^6$ or $1x10^7$ vp) of Ad5-mIi(1-50)-OVA (no adjuvant effect) or Ad5-mIi(1-105)-OVA (full effect of Ii linkage) and measured the H-2K^b-SIINFEKL tetramer response in the blood at several time points after vaccination (gating strategy and specificity of pentamer staining shown in **figure 5-10A**). As with the TW2 ELISpot data, some variation in the magnitude of response is seen between mice, however, a trend for higher T-cell responses to SIINFEKL at all time points assessed (TW2-18), and a prolonged peak response is seen when OVA is linked to mIi(1-105) compared with when tethered to mIi1-50 (**figure 5-10B**). The difference in magnitude seen in the blood at day 10 was mirrored in the spleen at TW11 (**figure 5-10C-D**).

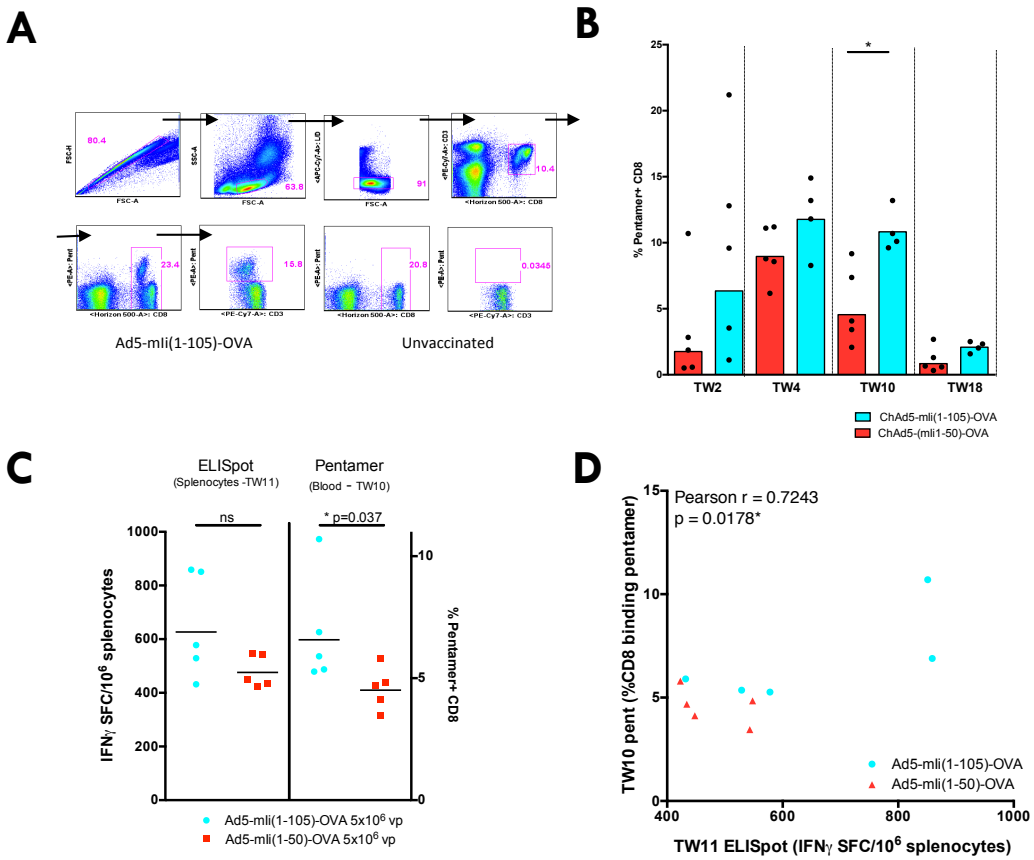


Figure 5-10. MHC class I pentamer staining of OVA-specific T-cell populations after transduction with Ad5-mli(1-105)-OVA or Ad5-mli(1-50)-OVA: (A-D) C57BL/6 mice were vaccinated with $1x10^7$ vp of Ad5-mli(1-105)-OVA or Ad5-mli(1-50)-OVA. PBMC were stained with MHC class I pentamer (H-$2K^b$-SIINFEKL) longitudinally after vaccination. (**A**) Gating strategy for MHC class I pentamers and testing of pentamer specificity in an unvaccinated C57BL/6 mouse. (**B**) Kinetics of the OVA-specific T-cell response followed in the blood by OVA pentamer of vaccinated mice. Bars at median. (**C-D**) The magnitude of SIINFEKL-specific T-cell response to Ad5-mli(1-105)-OVA or Ad5-mli(1-50)-OVA measured *ex vivo* in the blood 11 weeks (trial week 11; TW11) after vaccination by IFNγ ELISpot or 10 weeks (TW10) after vaccination by MHC class I pentamer staining (**C**). (**D**) Linear regression or ELISpot TW11 and percentage of CD8+ T-cell binding pentamer at TW10.

The phenotype of the T-cells induced is almost identical at all time points, however, when taking the average of each group (**figure 5-11**). At the peak of the response (TW4) the OVA-specific T-cells are predominantly SLECs (KLRG-1+CD127-) in all mice (**figure 5-11C**). As the T-cell response contracts the percentage of T-cells expressing CD27 and CD127 increases (due to re-expression or selective persistence of T-cells expressing these markers) but KLRG-1 expression is maintained. At TW18 the memory T-cell response is predominantly made up of Tem as is expected after Ad vaccination (**chapter 4; figure 5-11D**). There is no gross change in the phenotype of T-cells induced by Ad constructs where the transgene is tethered to mIi.

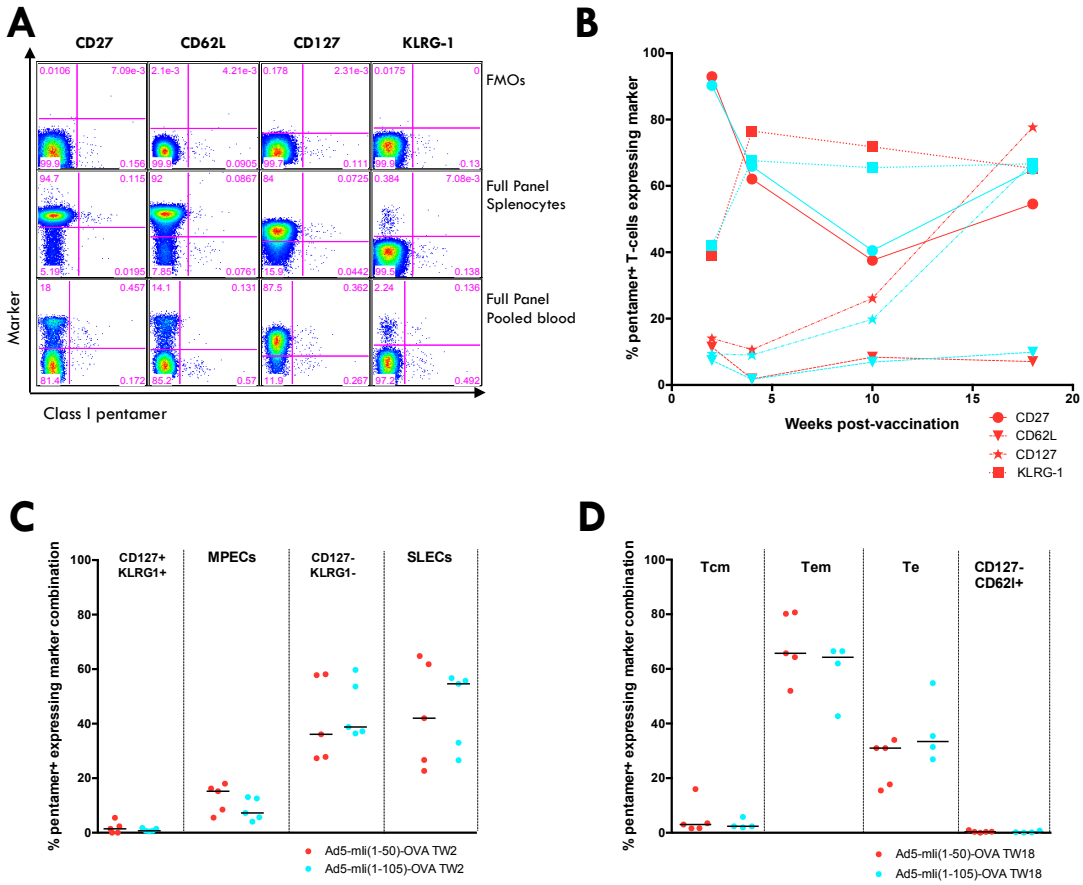


Figure 5-11. Phenotyping of OVA-specific T-cells: C57BL/6 mice were vaccinated with $1x10^7$ vp of Ad5-mli(1-105)-OVA or Ad5-mli(1-50)-OVA. PBMC were costained with MHC class I pentamer (H-2K^b-SIINFEKL) and antibodies for murine CD27, CD62L, CD127 and KLGR1. (**A**) Example FACS plots and FMOs. (**B**) Longitudinal analysis of markers on OVA-specific T-cells after vaccination. Mean expression by pentamer+ T-cells (n = 5 Ad5-mli(1-50)-OVA red line; n = 4 Ad5-mli(1-105)-OVA turquoise line) (**C**) Co-expression of KLRG1 and CD127 during the acute phase of the response was used to assess the proportion of effector T-cell subsets 2 weeks after vaccination (namely: short lived effector cells [SLEC} and memory precursor effector cells [MPEC]). (**D**) Co-expression of CD127 and CD62L was used to assess the T-cell memory subsets 18 weeks post-vaccination. (**C-D**). Bars at median.

5.5.7 Surface expression of CD74 on APCs

To assess the cell intrinsic effect of transduction with an Ad encoding Ii colleagues at Okairos infected JAWSII cells with Ad5-OVA or Ad5-mIi-OVA and the gene expression profile of these cells was assessed 24 hours later by

microarray (**D'Alise personal communication**). No genes were significantly up- or down-regulated by Ii-encoding Ad transduction relative to Ad transduction, which suggests that any increased antigen presentation is achieved by re-targeting of antigen, rather then major changes in the physiology of transduced cells, which may be favourable from a safety point of view.

Because Ii is a self-antigen, expressed throughout the immune system on MHC class II presenting cells (such as B-cells, DCs, monocytes and macrophages) and active T-cells it should be widely tolerated; however, one of the potential problems of using a self-antigen, such as Ii, is the possibility of breaking tolerance and of inducing an immune response to the self-antigen.

It is possible that the delivery of Ii to cells via an Ad could lead to increased surface expression of Ii, increasing the possibility of breaking tolerance. I set out to assess whether infection of cells *in vitro* – in a human monocytic cell line (THP-1), murine myeloid DC cell line (JAWSII) and murine BMDCs - can lead to increased surface expression. I assessed the surface expression of CD74 on several murine and human cell populations and assessed whether any changes in expression resulted from transduction with Ads that did or did not encode murine or human Ii.

Initially I assessed *in vivo* the endogenous surface expression of Ii on blood lymphocyte populations in mice and man. CD74 is expressed on the surface of the majority of DCs (CD11c+; 69.6% in BALB/c mice) and B-cells (CD19+; 76.2%

in BALB/c mice and 90% in human PBMC) but not CD3+ T-cells (**figure 5-12A-B).**

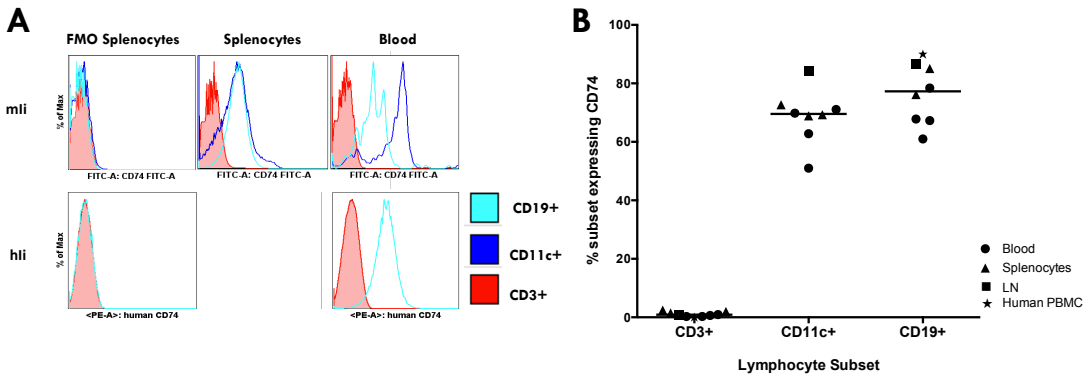


Figure 5-12. Surface expression of Ii (CD74) on murine and human PBMC subsets: (**A-B**) Murine PBMC, murine splenocytes and human PBMC were stained with subset specific markers and anti-CD74 antibodies to assess the surface expression of CD74. (**A**) Histograms showing expression levels on leukocyte subsets and FMO controls. (**B**) Percentage of CD3+ (T-cells) CD19+ (B-cells) and CD11c+ (Dendritic cells; mouse PBMC and splenocytes only) expressing CD74. Bars at median.

I next confirmed the specificity or cross-reactivity of murine and human CD74 antibody by staining Human PBMC (**figure 5-13**) and murine PBMC (**figure 5-14**) with antibodies to both human and murine CD74. Few human PBMC stained with the murine CD74 antibody (<1% for all subsets) alone or co-stained for both murine and human CD74. There is possibility of infecting human cells with an Ad encoding mIi and assessing endogenous and Ad encoded Ii separately using these antibodies. Some cross-recognition (shown by co-staining) and non-specific binding of murine CD74 was seen on human CD11c+ DCs (29.4%) and B-cells (9.7%), suggesting these antibodies may not be useful for uniquely identifying endogenous hIi and Ad encoded mIi on transduced human cell lines.

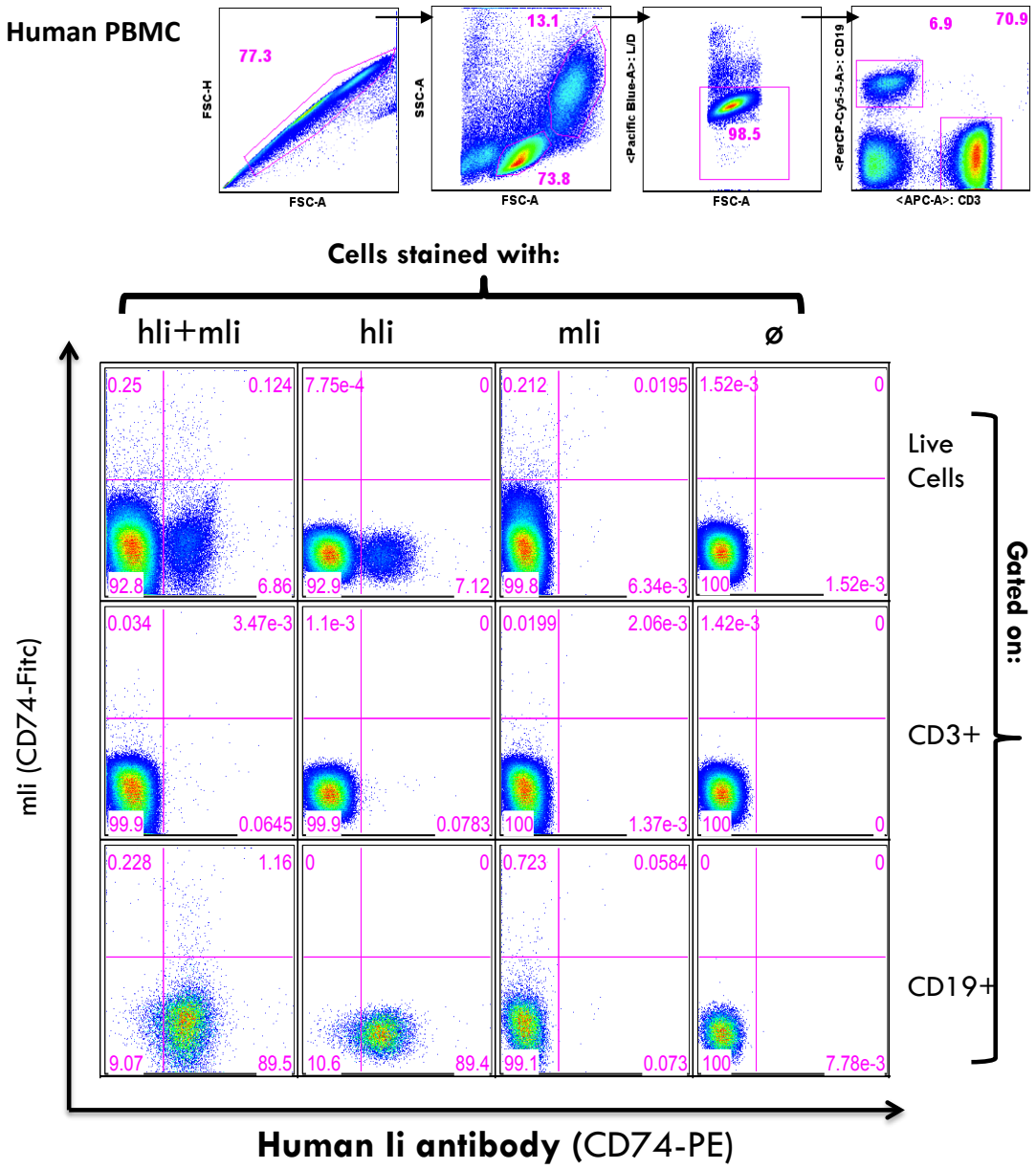


Figure 5-13. Assessing the specificity of human and murine CD74 antibodies on human PBMC: The gating strategy for isolating CD3+, CD19+ cells are shown in the top right. Human PBMC were stained ex vivo with a murine and a human anti-CD74 FACS antibody singly or in combination to assess cross-recognition and non-specific binding on T-cells, B-cells and total live PBMC.

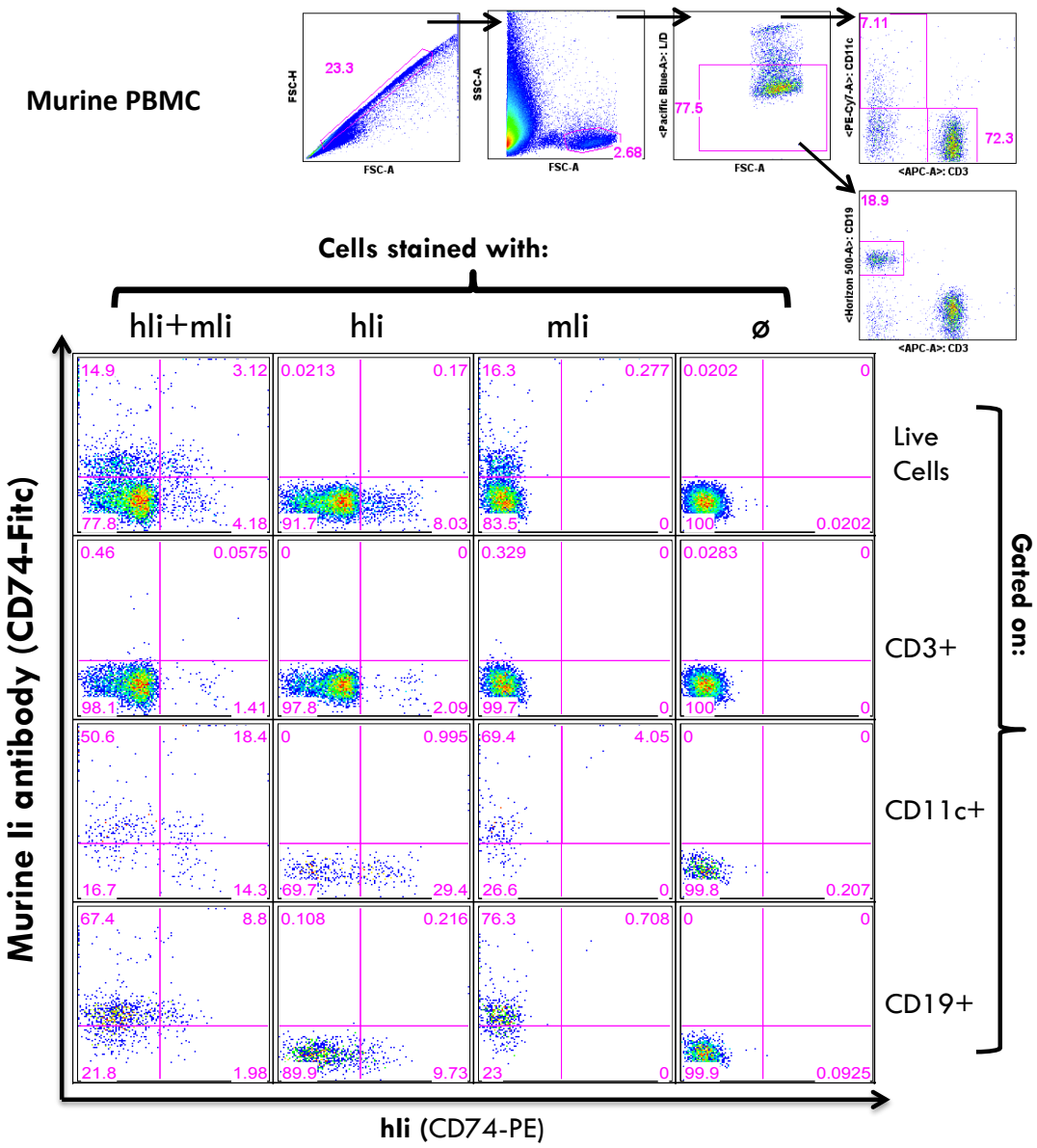


Figure 5-14. Assessing the specificity of human and murine CD74 antibodies on murine PBMC: The gating strategy for isolating CD3+, CD19+, and CD11c+ leukocytes is shown in the top right. Murine PBMC isolated from blood were stained *ex vivo* with a murine and a human anti-CD74 FACS antibody singularly or in combination to assess cross-recognition and non-specific binding on T-cells, B-cells, dendritic cells and total live PBMC.

5.5.8 Assessing CD74 surface expression after transduction: Human model – THP-1

To assess the surface expression of CD74 on a human APC after transduction with an Ii containing Ad I used the human monocytic cell line THP-1. THP-1 were

not readily infected with Ad5-eGFP as monocytes, however, when matured to macrophages THP-1 were readily transduced (1.1% of THP-1 monocytes vs. 59.9% of THP-1 macrophages at MOI 20; **figure 5-15A-B**). Maturation of THP-1 cells was induced by stimulation with 200 nM PMA for 24 hours. CD74 surface expression was seen to increase on maturation in one study (**Mittar et al. 2011**).

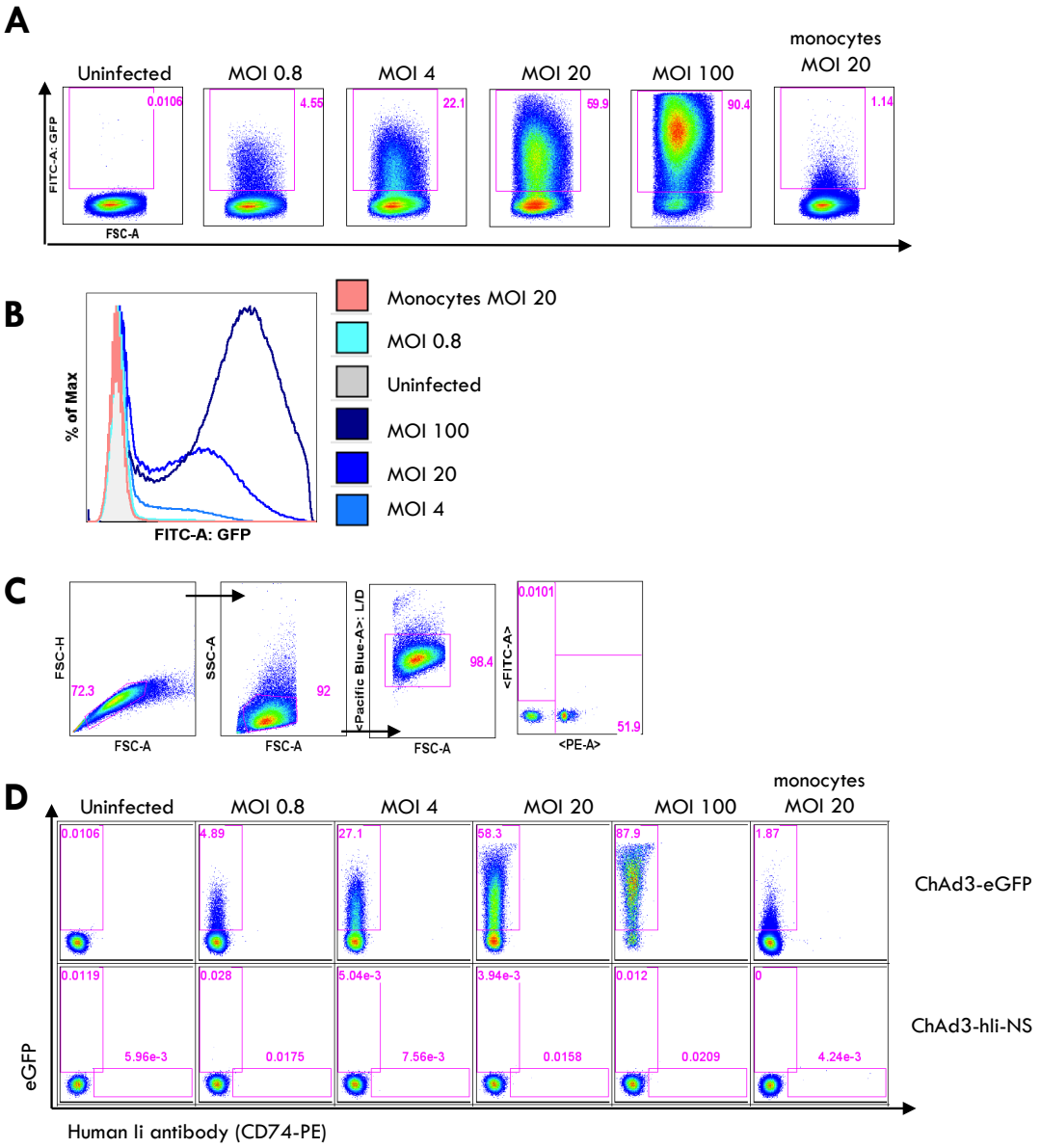


Figure 5-15. Transduction and surface CD74 staining of human THP-1 cell line: (A-B) Matured THP-1 macrophages (uninfected, MOI 0.8/4/20/100) or immature monocyte THP-1

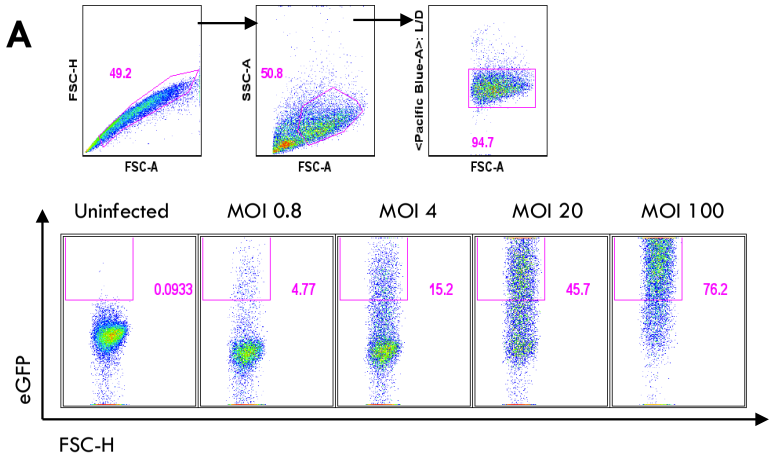
(MOI 20) were cultured with Ad5-eGFP for 24 hours to assess transduction efficiency and transgene expression. (**A**) Example plots and (**B**) histograms showing eGFP expression by FACS. (**C-D**) THP-1 macrophages were cultured with ChAd3-eGFP (top row) or ChAd3-hIi(p35)-NS (bottom row) for 24 hours at various MOI and were stained with anti-human CD74 antibody and assayed by FACS for eGFP and surface CD74 expression. THP-1 monocytes were also transduced with ChAd3-eGFP and ChAd3-NS (MOI 20). Gating strategy (**C**) and FACS plots (**D**) are shown.

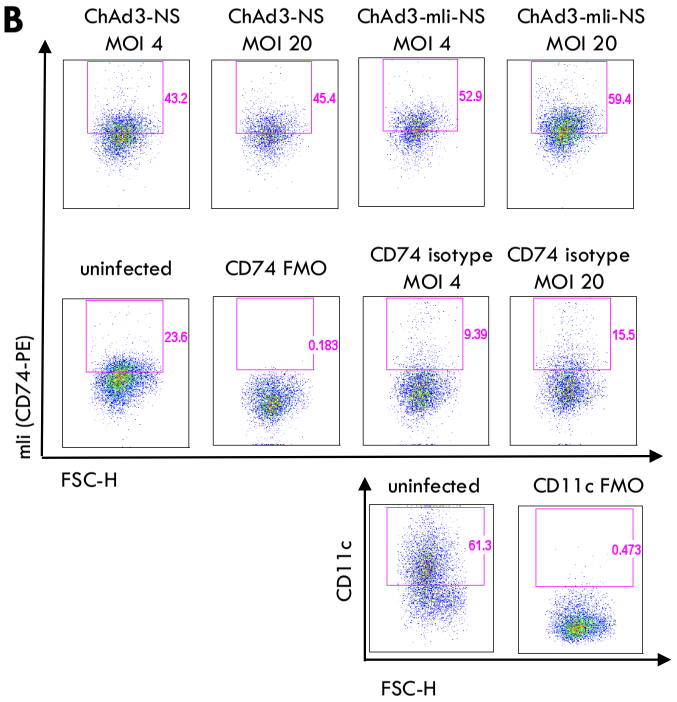
THP-1 macrophages were harvested and infected in parallel with ChAd3-hIi(P35)-NS (non-structural region of HCV genotype 1b BK strain) or ChAd3-eGFP (infection control) at MOI ranging from 0.8 to 100 (gating strategy, **figure 5-15C**). As with Ad5-eGFP, THP-1 macrophages were readily infected with ChAd3-eGFP, however, no endogenous hIi staining was seen in stimulated or unstimulated cells, and in THP-1 infected with ChAd3 constructs, whether they contained hIi or not, no surface CD74 expression was observed (**figure 5-15D**). Anti-guinea pig IgG beads were stained with hIi (CD74-PE) to confirm its fluorescence (**figure 5-15C**), but no CD74 staining was seen on THP-1 cells even when titrating the CD74-PE antibody from dilution factor 1:200 to 1:10 (not shown). Although readily infected with Ads and capable of producing transgene, THP-1 macrophages do not express CD74 and no CD74 expression can be induced by ChAd3-hIi-NS transduction.

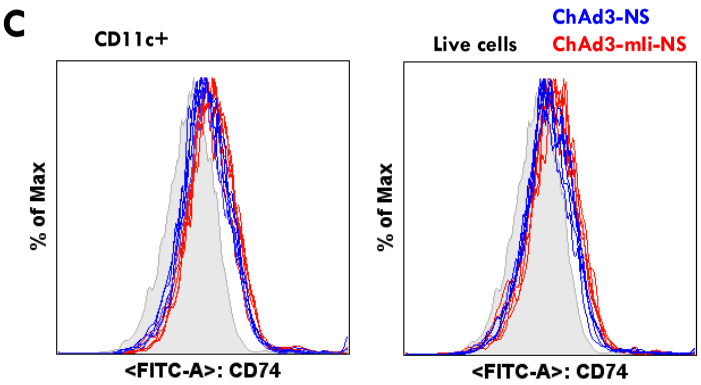
5.5.9 Assessing CD74 surface expression after transduction: Murine model – BMDC

Next I assessed surface CD74 expression in a murine infection model using BMDC. BMDC were readily transduced with Ad5-eGFP in a dose-dependent manner (**figure 5-16A**). Uninfected BMDC showed a low expression of CD74,

with approximately 25% of CD11c+ BMDC expressing surface CD74; however, on transduction CD74 was upregulated on BMDC regardless of whether the Ad construct contained Ii (**figure 5-16B**); however, a significant difference in the expression of surface CD74 on CD11c+ BMDC is seen when BMDC were transduced with ChAd3-mIi-NS at MOI 4 or 20 compared to ChAd3-NS (**figure 5-16C-D**). A trend for a higher expression of CD74 on total live cells when infected with ChAd3-mIi-NS relative to ChAd3-NS is also seen, however, the difference is not significant (not shown).


A
FSC-H
FSC-A
49.2
SSC-A
50.8
<Pacific Blue-A>: L/D
94.7
Uninfected
MOI 0.8
MOI 4
MOI 20
MOI 100
0.0933
4.77
15.2
45.7
76.2
eGFP
FSC-H


B
ChAd3-NS MOI 4
ChAd3-NS MOI 20
ChAd3-mli-NS MOI 4
ChAd3-mli-NS MOI 20
43.2
45.4
52.9
59.4
uninfected
CD74 FMO
CD74 isotype MOI 4
CD74 isotype MOI 20
23.6
0.183
9.39
15.5
mli (CD74-PE)
FSC-H
uninfected
CD11c FMO
61.3
0.473
CD11c
FSC-H


C
CD11c+
Live cells
ChAd3-NS
ChAd3-mli-NS
% of Max
% of Max
<FITC-A>: CD74
<FITC-A>: CD74

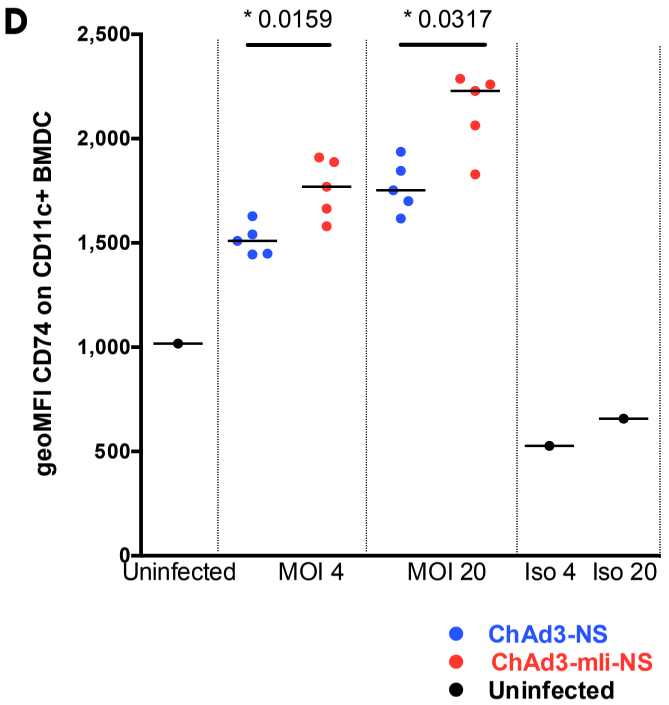

D
* 0.0159
* 0.0317
geoMFI CD74 on CD11c+ BMDC
2,500
2,000
1,500
1,000
500
0
Uninfected
MOI 4
MOI 20
Iso 4
Iso 20
ChAd3-NS
ChAd3-mli-NS
Uninfected

Figure 5-16. Surface CD74 staining of murine BMDC transduced with Ad encoding mIi: (A) BMDC were cultured with Ad5-eGFP for 24 hours at various MOI and analysed by FACS for eGFP expression to assess transduction efficiency and transgene expression. (**B-D**) BMDC were transduced with ChAd3-NS or ChAd3-mIi-NS (MOI 4 and 20) for 24 hours and then stained with anti-murine CD74 and CD11c antibodies and assessed by FACS. The following controls were assessed by FACS in parallel: Uninfected BMDC, and ChAd3-mIi-NS infected BMDC stained with an isotype control, or stained as FMOs for CD11c and CD74 antibodies. (**C**) Histograms showing surface CD74 expression on CD11c+ or total live BMDC replicates (n = 5). (**D**) geoMFI of CD74 on transduced CD11c+ BMDC, uninfected BMDC or transduced isotype stained BMDC. Lines at median.

I next assessed the impact of infecting BMDC with Ad constructs containing hIi, which also enhances CD8+ T-cell responses *in vivo* in vaccinated mice (**Capone et al. 2014; Spencer et al. 2014**). Surface CD74 was assessed using both murine CD74 (endogenous Ii) and human CD74 (Ad encoded hIi) on cells transduced with ChAd3-hIi(P31)-NS, ChAd3-mIi(1-97)-NS [the human version of mIi(1-80) but with the additional 17 amino acid human ER retention sequence], ChAd63-hIi (without linked transgene) and ChAd3-NS (not encoding mIi or hIi; controls used for gating shown in **figure 5-17A**). All transduced BMDC cells (total live cells or CD11c+) showed an increased surface expression of endogenous murine CD74 relative to uninfected BMDC, but the level of CD74 induction by Ad transduction was the same regardless of whether the Ad contained hIi (**figure 5-17B-C**).

A slightly higher expression of surface hIi was seen in all transduced BMDC but it did not differ significantly between Ads that did or did not encode hIi (**figure 5-17B-C**). It is likely that an increased expression of murine CD74 on transduction of cells leads to more non-specific binding or cross-recognition with human

CD74 antibody. Ad encoded Ii does not appear to specifically traffic to the surface of transduced cells.

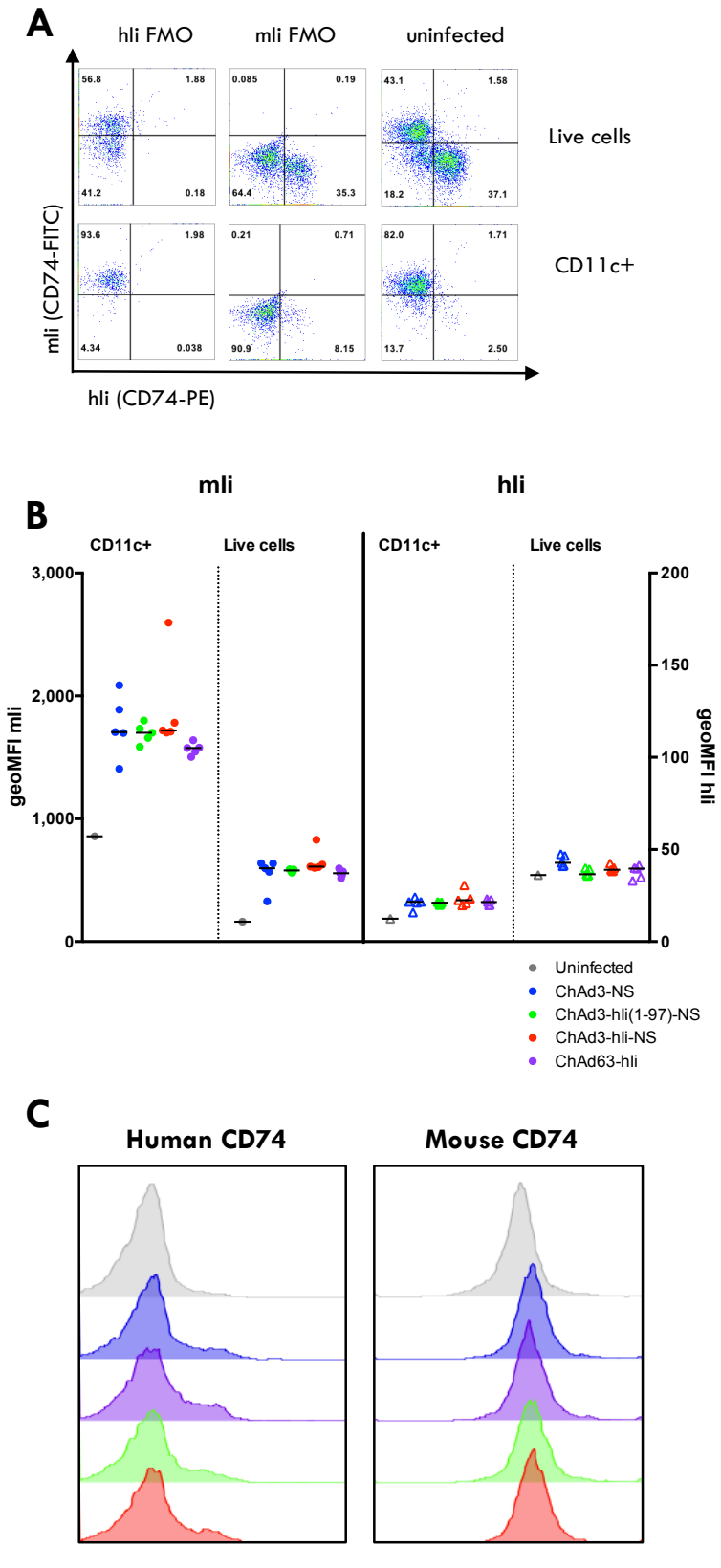


Figure 5-17. Surface CD74 staining of murine BMDC transduced with Ad encoding hIi: BMDC were transduced with ChAd3-NS, ChAd3-hIi(p35)-NS, ChAd3-hIi(1-97)-NS, or ChAd63-hIi (MOI 20) for 24 hours and then stained with anti-murine CD74, anti-human CD74 and CD11c antibodies and assessed by FACS. (**A**) Gating strategy and FMOs showing co-staining for anti-human and anti-murine CD74 on BMDCs. (**B**) geoMFI of anti-murine (left) or anti-human CD74 antibodies assessed by FACS on CD11c+ or total live BMDC after transduction. Bars at median, n=5 (except uninfected n=1). (**C**) Aligned histograms showing fluorescence intensity for anti-human or anti-mouse CD74 after transduction.

In summary, many MHC class II expressing human and murine cells express surface CD74 (CD11c+ DCs and CD19+ B-cells). A subset of BMDC express surface CD74, however, human THP-1 do not; both are readily transduced by Ads. No induction of endogenous CD74 or trafficking of Ad encoded CD74 makes it to the surface of THP-1, but when transduced, BMDC show an increase in surface CD74. Interestingly a greater upregulation of surface CD74 is seen when BMDC are infected with mIi encoding, but not hIi encoding Ads. There is the possibility of Ad encoded Ii getting to the surface of transduced cells, however, the increased expression due to activation and infection of cells is a much larger shift than that seen between Ads encoding Ii or not.

5.6 Discussion

When linking an antigen to Ii within a genetic vaccine (Adenovirus, MVA, lentivirus, DNA plasmid) the CD8+ T-cell response is consistently enhanced in magnitude (**Holst et al. 2008; Capone et al. 2014; Mikkelsen et al. 2011; Holst et al. 2011**), however, the mechanism by which this occurs is not well understood.

I set out to identify which functional domains of Ii are essential for its role as a genetic enhancer of CD8+ T-cell responses and have identified mIi(1-75) as a minimal sequence that performs as well, if not better, than full-length mIi as a genetic adjuvant. Over half of the Ii sequence is not needed for its role as a genetic adjuvant, including the trimerisation region and the regions associated with MHC class II presentation (including KEY, CLIP, ESS). The overall aim of linking Ii to antigen is to improve the CD8+ T-cell response, therefore, despite differences in performance in *in vitro* assays, the *in vivo* immunogenicity of Ii constructs remains the key assay for ranking the efficiency of Ii variants. No variant of Ii consistently outperformed full length mIi as a genetic enhancer of the CD8+ T-cell response to Ad vaccination, however, a minimal sequence of residues mIi(1-75), and a construct lacking the transmembrane region [mIi(50-215)] could match the adjuvant effect of full length mIi at all but the most limiting dose. The effect of combining the N-terminal and C-terminal truncations by including just mIi(50-75) is yet to be tested.

Next I investigated whether increased class I presentation of epitopes within the transgene when linked to Ii could explain the enhanced T-cell response. The same pattern of Ii variants that could enhance T-cell responses *in vivo* was seen when assessing the level of antigen presentation after *in vitro* infection of BMDC in almost all cases. mIi(1-75) when linked to OVA consistently led to the most antigen presentation on MHC-I after Ad transduction. Interestingly Ad5-mIi(1-75)-OVA showed a particular ability to enhance presentation in CD11c- BMDC. Of note, CD11c+ DCs isolated from Ad5-OVA vaccinated mice could induce

proliferation in OVA-specific T-cell lines, whereas CD11c- DCs could not (**Lindsay et al. 2010**), and transgene-specific CD8+ T-cells are not induced by Ad5 vaccination in BATF3-deficient mice, which lack CD11c+ cross-presenting CD8α+ and langerin+ DCs (**Quinn et al. 2015**); therefore, CD11c+ DCs are required for optimal CD8+ T-cell priming by Ads *in vivo,* and a role for non-hematopoietic cells in the maintenance of CD8+ T-cells has also been observed (**Bassett et al. 2011**). Whether there are cell type specific effects of Ii and Ii variants on antigen presentation and whether these are relevant *in vivo* or merely artefacts of the *in vitro* system should be further investigated.

It is unlikely that the machinery of the classical MHC class II presentation pathway is involved in the enhanced CD8+ T-cell responses to Ii-linked antigen as Ii retains this effect in several settings lacking this pathway, such as: in MHC class II knock-out mice (**Holst et al. 2011**); when the ESS, CLIP and KEY motif are removed from Ii; when the class II pathway is blocked by neutralisation of endosomes or inhibitors of lysosomal proteases. It is also unlikely that the vacuolar (TAP-independent) cross-presentation pathway is involved as there is no requirement for Ii to localise to endolysosomes and the blocking of Sec61 (**Peter Holst personal communication**) and the neutralisation of endosomal pH does not abrogate the Ii adjuvant effect. Antigen presentation does not persist when the classical class I presentation pathway is perturbed, for instance in TAP knock out mice or when the proteasome or transport of proteins to the cell surface through the golgi are inhibited.

I have shown that the mechanism of action of Ii is at least in part through enhanced antigen presentation on MHC-I molecules and this is independent of the MHC class II presentation pathway, cross-presentation, and does not involve a novel pathway of antigen processing. It is the result of specific re-targeting of antigen to the proteasome. Gene expression profiling of JAWSII cells infected with an Ad encoding Ii did not show any differentially expressed genes relative to transduction with unlinked Ad, therefore, no physiological change in the cell other than that which comes with Ad infection is needed. To rule out the possibility of mechanisms other than a specific increased in surface presentation of Ii-linked antigen I would like to test whether a DC transduced with Ad-mIi and pulsed with a peptide can enhance activation of a cell lines specific for that peptide.

Next I showed that linkage of Ii leads to rapid breakdown of the otherwise stable eGFP and that inhibitors of the proteasome could block this. Ubiquitin-dependent targeting of proteins to the proteasome (ubiquitin-proteasome pathway; UPP) has been shown to be crucial for effective MHC class I presentation and is the main source of optimal peptides for loading on to MHC-I (**Rock et al. 1994; Gaczynska et al. 1993**). Selective inhibitors of the proteasome block the bulk of protein degradation and limit the appearance of MHC molecules on the surface of cells, and mutations that block ubiquitination sites can prevent generation of antigenic peptides (**Gaczynska et al. 1993**). Despite approximately 70% of proteasome products being too small to bind MHC-I molecules the remaining optimal length or N-terminal extended peptides represent the mains source of class I presented peptides (**Tortorella et al.**

2000; Rock et al. 2004). These are transported via TAP to the ER where the endoplasmic aminopeptidase (ERAP) trims peptides for loading and stabilisation of class I heterodimers (**Shastri et al. 2003; Saric et al. 2002**). It is expected then that specific targeting of transgene products to the proteasome would lead to enhanced antigen presentation on MHC-I molecules.

One questions which remains to be answered is whether antigen tethered to Ii effectively enters the ER membrane and is retro-translocated to the cytosol by the endoplasmic-reticulum-associated protein degradation (ERAD) pathway - and if so if this is relevant to the enhanced targeting to the proteasome - or whether the whole process occurs in the cytosol. Cytosolic proteins can bypass ubiquitination and degradation by the 26s proteasome subunit by targeting directly to the 20s subunit, but misfolded and senescent cytosolic or ER-targeted proteins are subject to more prolonged quality control and show a greater requirement for targeting to the UPP (**Huang et al. 2011**). Some effect of ERAD inhibition with Kifunensine has been seen on Ii-linked adjuvanticity (**Holst, personal communication**) but human p31 was not affected, suggesting some Ii constructs may cycle through the ER but that this may not be essential for increased degradation. Ii constructs lacking the transmembrane domain can enhance T-cell responses, but they have less of an effect than full length Ii at low doses. Cell fractionation, whereby centrifugation is used to lyse cells and separate all membrane compartments, including the ER, from cytosol, suggests Ii does not enter the membrane and immunohistochemistry showed Ii-eGFP associates with the cytosolic side of the ER but whether Ii-antigen integrates within the ER was unclear (**performed in collaboration with Mariano**

Stornaiuolo, Università degli Studi di Napoli Federico II, Napoli Italy; data not shown).

Several approaches for enhancing the targeting of antigen to the proteasome have been assessed, in particular the direct linkage of antigen to ubiquitin within genetic vaccines, with mixed results **(Andersson & Barry 2004; Tobery & Siliciano 1997; Barry et al. 1995; Vidalin et al. 1999; Weinberger et al. 2013; Grant et al. 1995).** Vidalin *et al* linked HCV core protein to Ub in several conformations, with stabilizing and non-stabilising N-terminal residues, but saw no improvement in the T-cell responses induced (**Vidalin et al. 1999**). Agreeing with the idea that increased antigen presentation can lead to enhanced T-cell responses, gene-based vaccination of mice induced a higher magnitude T-cell response to GFP when linked to ubiquitin only in constructs where enhanced proteasomal degradation was seen (**Andersson & Barry 2004**). Moreover, they showed that when the same strategy was used with influenza NP only T-cell responses to the subdominant epitopes were enhanced, suggesting degradation and presentation of the dominant epitopes were already optimal and could not be improved (**Andersson & Barry 2004**)**.** Delogu *et al* showed that the most destabilizing ubiquitin construct, with the most rapid intracellular degradation, when linked to TB antigens could not only enhanced the magnitude of responses but shifted T-cell responses towards TH1-type responses and showed the best protection against a mouse model of pulmonary TB (**Delogu et al. 2000**)

Why then is antigen linked to Ii rapidly degraded within a cell? Ii interacts within the ER with calnexin, a chaperone protein involved in refolding of

transmembrane proteins and targeting for endoplasmic reticulum associated degradation (ERAD). Increased Ii degradation is seen when calnexin binding residues are mutated and for truncated variants of Ii lacking calnexin binding domains (**Romagnoli & Germain 1995**); by linking antigen to the c-terminal of Ii chain its interaction with calnexin may be sterically hindered, or in the case of our shortened variant Ii constructs calnexin binding residues may be lacking, leading to rapid ER translocation and subsequent degradation. Several misfolded and mutated Ii constructs have been shown to bind irreversibly to MHC class II ,blocking effective presentation. Ii folding is tightly regulated within cells and misfolded or non-trimerised Ii is rapidly recognised and targeted by ERAD machinery for translocation to the cytosol for degradation (**Sevilla et al. 2004**). The removal of a single glycosylation site on human p41 Ii led to rapid degradation via the UPP (**Sevilla et al. 2004**). The folding of Ii is, therefore, naturally regulated by the UPP.

Interestingly, truncated Ii (1-108 residues only) can still efficiently trimerise (**Ashman & Miller 1999**) and the transmembrane region of Ii is of type-II, which is particularly prone to misfolding due to the requirement for translation to halt after the initial fold of the protein allowing it to fold back on itself through the ER and for continuation of translation. We may be indirectly enhancing ubiquitination and proteasomal degradation, not by including Ub, but by tethering Ii, a highly regulated and readily ubiquitinated protein, to our transgenes; this focussed degradation of transgene can in turn enhance antigen processing, presentation, and concomitant antigen-specific CD8+ T-cell responses.

Ii enhances the magnitude of T-cell response to a single vaccination and it can do so in a setting where T-cell help is lacking (**Holst et al. 2007**). The T-cells induced by Ii containing constructs have been shown to be more polyfunctional, more cytolytic (**Mikkelsen et al. 2011**) and more able to mediate protection in several settings (**Mikkelsen et al. 2011; Sorensen et al. 2010; Grujic et al. 2009; Holst et al. 2008**), therefore, they appear more functional on a per cell basis as well as being higher in magnitude. I saw no difference in the differentiation status and phenotype of the T-cells induced at the peak and in the memory response to Ad vectors when Ii was linked to the transgene. The dose of virus can have a profound effect on the T-cells induced and the relatively high doses given to mice may not be representative of what will be seen in man, where differences in the T-cell quality are more readily observed when changing dose, administration route, or type of vaccine vectors.

One of the potential problems of using a self-antigen, such as Ii, is the possibility of breaking tolerance and of inducing an immune response to the self-antigen. Anti-CLIP antibodies have been observed in axial spondyloarthiritis patients (**Baerlecken et al. 2013; Baraliakos et al. 2013**), and despite no direct link between autoantibodies and pathogenesis of the disease being elucidated yet, these studies highlight the possibility of inducing anti-Ii immunity and the associated safety concerns. No evidence of an induction of T-cells or antibody responses to Ii in mice or NHP when encoded in genetic vaccines has been seen to date, with the exception of a weak T-cell response to murine or human invariant chain in macaques (**Spencer et al. 2014; Capone et al. 2014**). These

T-cells were mapped to regions that differed between the endogenous macaque Ii and the Ad encoded murine or human Ii but did not cross-recognise macaque Ii, suggesting self-tolerance to endogenous Ii was not broken (**Spencer et al. 2014**).

I assessed the surface expression of Ii/CD74 on transduced cells to see if Ad-encoded Ii traffics to the surface. Although not naturally expressed on the surface of THP-1 cells, no surface expression could be induced by transduction with Ads encoding Ii. Ad transduction of BMDC itself led to an increased surface CD74 expression, regardless of whether Ad encoded Ii or not. The inclusion of hIi within Ad5 did not lead to a higher induction of surface CD74 above Ad alone; however, mIi-encoding Ads induced significantly higher CD74 surface expression than Ads that did not encode mIi, but this difference was relatively small when compared to the overall change caused by Ad infection itself. The increased surface CD74 can not be directly attributed Ad encoded Ii or to endogenous Ii in this model.

Although investigation of the mechanism underlying enhanced CD4+ T-cell responses when antigen is tethered to full length Ii was not assessed here (**Malcherek et al. 1998; Sponaas et al. 1999; Capone et al. 2014**), the mechanism is likely to be quite different to that described for enhanced CD8+ T-cell responses. Enhanced presentation on MHC-II molecules of antigen when linked to Ii could result in increased activation and expansion of CD4+ T-cells, however, the intracellular mechanism for enhanced presentation is unlikely to involve the proteasome, as peptides are cleaved and loaded in the late endosome/MHC class II compartment. A similar approach could be taken to

investigate the key domains of Ii for enhanced CD4+ T-cell induction, such as the sequential truncation of Ii. It may prove more difficult to enhance CD4+ and CD8+ T-cell responses to viral vectors together without including much of the Ii sequence.

To further clarify the mechanism of Ii-linked adjuvanticity it will be important to confirm the ubiquitination of Ii-antigen by western blot and to mutate key lysine residues within Ii to see if this inhibits the breakdown of Ii-antigen. Lysines could also be introduced to the Ii sequence to aid degradation, potentially improving immunogenicity. If the ER retention is key, several alternative ER retention sequences and type-II transmembrane regions could be assessed to see if targeting to the proteasome can be further enhanced. HLA allotypes have different requirements for the protein loading complex (**Raghavan et al. 2008**) and different strengths of association with Ii, which should be further investigated as this may elucidate key interactions for the Ii effect and will indicate how broadly applicable this technology may be in humans.

The first assessment of Ad and MVA vectors encoding the full length human Ii have been approved and will be performed in Oxford in collaboration with Okairos (now owned by GSK) as part of the PEACHI trial (EU FP7; EudraCT Number: 2014-000730-30) in early 2016.

5.7 Conclusion

When physically tethered to the N-terminal of a transgene within genetic vaccines Ii can increase the magnitude of T-cell responses to that specific transgene, broadening the response and enhancing T-cell responses to subdominant epitopes, whilst retaining the phenotype and functionality of Ad-induced T-cells. The effect of tethering antigen to Ii is particularly robust as it is retained in several species (NHP, inbred and outbred mice), when using several methods of introducing genetic material (Plasmid, lentivirus, Ad, MVA), for almost all antigens tested (including model antigens eGFP, OVA, structural genes of HCV, Ebola glycoproteins, tumour antigens) and for subdominant and immunodominant epitopes within the transgene. The effect of Ii is not just limited to primary responses but can also improve expansion of memory T-cells (**Steffensen et al. 2013; Capone et al. 2014**), which may be more sensitive to the level of antigen presentation than naïve T-cells due to a lower expression of TCR and increased expression of tyrosine phosphatases (**Mehlhop-Williams & Bevan 2014**).

This technology is broadly applicable and understanding its mechanism should tell us something fundamental about the processing of antigens for class I presentation and the effect of improved presentation on the elicited T-cell responses. For instance, it appears that the availability of optimal length peptides can often be a limiting step in antigen presentation on class I. Ii enhances the magnitude of T-cell responses for a single antigen exposure and it can do so in a setting where T-cell help is lacking. The inclusion of Ii may

abrogate the need for boosting vaccinations or may make T-cell induction in a CD4+ deficient setting, such as HIV infection, possible. Of particular importance to HCV Ii encoding Ads showed not only enhanced CD4+ and CD8+ T-cell magnitude but also enhanced the breadth of response, and showed better recognition of heterologous HCV genotype (**Capone et al. 2014**). In the context of LCMV challenge the enhanced breadth of response afforded by Ii-linkage of antigen prevented T-cell escape and loss of viral control (**Holst et al. 2008**).

It is important that we further dissect the intracellular pathways leading to proteasomal degradation of Ii-tethered antigen, as this may allow a minimal Ii construct to mediate the same adjuvant effect or it may aid in the design of genetic adjuvants distinct from Ii which cause the same focused transgene degradation but with less opportunity for off target effects within a transduced cell.

5.8 Summary of findings

- A minimal sequence of mIi(1-75) could match the *in vivo* immunogenicity and *in vitro* enhanced antigen presentation seen with full-length mIi.
- The effect of Ii linkage could be recapitulated *in vitro*, suggesting that Ii affects the transduced antigen presenting cell and its interaction with T-cells directly.
- The effect of Ii linkage is independent of the MHC class II presentation pathway (retained when endosomal peptidases are inhibited, when key/CLIP and ESS residues are removed) but is lost when class I presentation is disturbed.
- Increased and prolonged antigen presentation on MHC-I was identified as the main mechanism underlying enhanced CD8+ T-cell expansion on vaccination with Ii encoding Ads.
- Ii-linked antigen is more rapidly degraded by the proteasome, which may highlight this as a limiting step in antigen presentation on MHC-I for many epitopes.
- It is not clear if Ii-antigen complexes cycle through the ER and if so if this is required for enhanced targeting of antigen to the proteasome.
- There is no clear impact on T-cell quality when Ii is included in Ad vectors in mice.
- Surface expression of Ii is upregulated when a cell is transduced with an Ad vector but any further increase caused by Ad encoded Ii trafficking to the surface of the cell is minimal (for mIi) or not seen (for hIi).

6 A therapeutic T-cell vaccine for HCV

6.1 Primary hypothesis

Virally vectored vaccines can safely induce functional HCV-specific T-cells in patients with chronic HCV infection.

6.2 Introduction

Despite great advances in the treatment options for HCV there remains a compelling argument for the continued development of not only prophylactic but also therapeutic candidate vaccines for HCV (**Walker & Grakoui 2015**). It is likely that globally a significant proportion of HCV+ patients will not have access to treatment and surveillance programs, as has been the case for antiretroviral therapy for HIV (**Dutta et al. 2015**). Reinfection with HCV is also a real problem in some high-risk cohorts (**Grady et al. 2013; Aspinall et al. 2013**). An effective stand-alone therapeutic vaccine, or more likely, a vaccine to be used as an adjunct to IFN-free DAA therapy, to increase clearance rates, shorten treatment length, or to block persistence on reinfection, remains a desirable global health target.

The impact of HCV infection on the HCV-specific T-cell response is most clearly demonstrated when the extremes of viral load are assessed. Functional HCV-specific CD4+ and CD8+ T-cells can persist for decades after spontaneously resolved HCV infection (**Takaki et al. 2000**), and the presence of T-cell memory

significantly reduces the risk of persistence on reinfection (**Shoukry et al. 2003; Osburn et al. 2010; Sacks-Davis et al. 2015; Bassett et al. 2001**). In contrast, in the setting of chronic infection where viral loads are high, HCV-specific T-cells are often undetectable in the blood, and when present are of poor quality (**Zhang et al. 2009; Urbani et al. 2006; Wedemeyer et al. 2002; Diepolder et al. 1995; Gerlach et al. 1999**)**.** The reasons why T-cells are low in magnitude and dysfunctional during chronic infection (discussed in more detail in **chapter 1**) include: T-cell exhaustion, T-cell priming in the tolerogenic environment of the liver, inhibition by Tregs, and T-cell escape. Whether a T-cell vaccine can overcome these obstacles, by enhancing existing weak responses or by generating *de novo* T-cell responses is a fundamental important question that will be addressed by the studies described in this chapter.

The role of T-cells in control of HCV during PEG-IFNα/rib therapy is currently debated, but is relevant where therapeutic vaccination is planned in adjunct to IFN-based therapy. With PEG-IFNα/rib therapy a consistent finding is that HCV viral load declines in two phases on treatment, rapid initial decline, followed by a slow rate of further decline over several weeks. Mathematical modelling suggests the rapid initial decline is as a direct result of the anti-viral properties of IFNγ, and the further slow decline is T-cell mediated (**Neumann et al. 1998**).

The effect of IFNα on vaccination is currently not known. Interferon may enhance response to vaccination by induction of co-stimulatory molecules on DCs, however it also induces lymphopaenia and has anti-proliferative effects on T-cells, which may limit T-cell induction (**Crouse et al. 2015**). Vaccination with Ad itself induces IFNα,

but this does not affect the gene expression of Ad vectors *in vivo* (**Huarte et al. 2006**). HCV-specific T-cells have been shown to both increase (**Kamal et al. 2002; Cramp et al. 2000**) and decrease during PEG-IFNα/rib therapy (**Barnes et al. 2002; Burton et al. 2008**).

In a mouse model of persistent viral infection, T-cell induction by vaccination was limited by the presence of high viral loads (**Wherry et al. 2005**); therefore, I assessed vaccine immunogenicity in patients with high (untreated) to low viral loads (2 or 14weeks lead-in of PEG-IFNα/rib before vaccination) to assess the impact of therapy and viral load at the time of vaccination on T-cell induction.

6.3 Key questions

I address the following key questions:

1) Can ChAd3-NS and Ad6-NS be given safely to HCV+ patients alone or in combination with IFN-based therapy?
2) Does ChAd3-NS/Ad6-NS prime-boost vaccination induce HCV-specific T-cells in patients?

If an HCV-specific T-cell response is induced by vaccination:

3) Do T-cells so generated impact on HCV RNA?
4) What do the induced T-cells target and are they able to cross-recognise variant HCV sequences?
5) Are they expanded memory responses or newly primed responses?

6) What are the phenotype and functionality of HCV-specific T-cells pre-vaccination and post-vaccination?

7) Does MVA-NS boost vaccination induce a higher magnitude CD4+ and CD8+ T-cell response in HCV+ patients, as it does in healthy volunteers?

Much of this work was published in the manuscript:

Kelly, Swadling *et al*. Chronic HCV infection subverts vaccine induced T cell immunity in humans. **Hepatology. 2015 Oct 16.**

6.4 Chapter specific material & methods

6.4.1 Clinical trial patient enrolment

A full list of the inclusion/exclusion criteria and discontinuation criteria can be found in **appendix 2-1**. Patients were HCV genotype 1 and aged between 18-65. Patients with: HIV, HBV, immunosuppressive illness, Ad6 or ChAd3 neutralising-Ab (nAbs) titer >200), or evidence of cirrhosis (clinical, biochemical or histological) were excluded. Patients were recruited at Oxford University NHS Trust and Queen Elizabeth Hospital Birmingham, UK. All volunteers gave written informed consent, and the studies were conducted in accordance with Good Clinical Practice.

6.4.2 HCV002 study design

Study Groups and vaccination regimes are detailed (**Table 6-1**). A phase-I clinical trial of ChAd3-NS/AD6-NS vaccination in HCV+ Patients (HCV002; EudraCT: 2008-006127-

32) was approved by Medicines and Healthcare products Regulatory Agency (MHRA), registered in the ClinicalTrial.gov database (ID: NCT01094873) and ethically approved (GTAC reference: GTAC162).

Arm A (n=27) received concurrent PEG-IFNα/rib therapy (48 weeks), and Arm B (n=8) received vaccine alone. Patients in A1-A3 received 5×10^{8}, 5×10^{9}, or 2.5×10^{10} vp ChAd3-NS and Ad6-NS 10 weeks apart, 14 weeks after starting PEG-IFNα/rib. All patients in A1-3 had a >2log drop in viral load before vaccination. Arm A4 received 2.5×10^{10} vp 2 weeks after starting PEG-IFNα/rib. Arm A5 received two priming vaccinations with ChAd3-NS given 4 weeks apart before Ad6-NS boost vaccination 10 weeks after the second priming vaccine, with the first vaccine given 14 weeks after the start of PEG-IFNα/rib. Arm A6 received the same vaccination schedule as Arm A5 but with the first vaccination given 2 weeks after the start of PEG-IFNα/rib. Arm B groups received respectively 5×10^{8}, 5×10^{9}, or 2.5×10^{10} vp, with ChAd3-NS prime/Ad6-NS boost given 10 weeks apart without concomitant PEG-IFNα/rib. Vaccines were administered intramuscularly.

Two volunteers withdrew from Arm A2 prior to vaccination after starting IFNα, and two patients received prime vaccine only (021; rash post-prime, and 031; difficulties in venesection). Overall 23 patients in Arm A received both vaccines. All volunteers in Arm B received both vaccines. 5 patients stopped PEG-IFNα/rib early; 3 with IFNα related side effects (16-30 weeks), one after virological breakthrough (24 weeks) and one withdrew from the study for personal reasons unrelated to the study (12 weeks). Volunteers documented all symptoms and recorded temperature daily, Solicited and

unsolicited adverse events were recorded. All volunteers that received any vaccine were included in the analysis.

6.4.3 HCV003 Arms B and C study design

Study Groups and vaccination regimes are detailed (**Table 6-1**). A phase-I clinical trial of ChAd3-NS/MVA-NS vaccination in healthy volunteers (**HCV003 Arm A; Table 6-1**) and HCV infected patients (**HCV003 Arm B**) is registered in the ClinicalTrial.gov database (ID: NCT01296451; EudraCT Number: 2009-018260-10).

Arm A (n=10) received concurrent PEG-IFNα/rib therapy (48 weeks), and Arm B (n=4) received vaccine alone. Patients in arm B1 and B2 received 14 or 2 weeks of therapy respectively before being vaccinated. All patients in arms B and C received ChAd3-NS prime (2.5 x 10^{10} vp) followed 8 weeks later by MVA-NS (2 X 10^{8} pfu).

Table 6-1. Therapeutic vaccine trials

Table 6-1: Therapeutic vaccine trials - Study arms, vaccinations given and dose, treatment given.

	Trial	Arm	n	Vaccines + Dose	Double prime	Treatment	Data Chapter
HCV+ Patients	HCV002	A1	2	TW14: **ChAd3** (5 x 10^{8} vp) TW24: **Ad6** (5 x 10^{8} vp)	-	peg-IFNα/Rib	6
		A2	2	TW14: **ChAd3** (5 x 10^{9} vp) TW24: **Ad6** (5 x 10^{9} vp)	-	peg-IFNα/Rib	6
		A3	6	TW14: **ChAd3** TW24: **Ad6**	-	peg-IFNα/Rib	6
		A4	6	TW2: **ChAd3** TW12: **Ad6**	-	peg-IFNα/Rib	6
		A5	4	TW14: **ChAd3** TW18: **ChAd3** TW28: **Ad6**	y	peg-IFNα/Rib	6
		A6	4	TW2: **ChAd3** TW6: **ChAd3** TW16: **Ad6**	y	peg-IFNα/Rib	6
		B1	2	TW0: **ChAd3** (5 x 10^{8} vp) TW10: **Ad6** (5 x 10^{8} vp)	-	-	6
		B2	2	TW0: **ChAd3** (5 x 10^{9} vp) TW10: **Ad6** (5 x 10^{9} vp)	-	-	6
		B3	4	TW0: **ChAd3** TW10: **Ad6**		-	6
	HCV003	B1	4	TW14: **ChAd3** TW22: **MVA**	-	peg-IFNα/Rib	6
		B2	4	TW2: **ChAd3** TW10: **MVA**	-	peg-IFNα/Rib	6
		C1	4	TW0: **ChAd3** TW8: **MVA**	-	-	6

Vaccine dose 2.5 x 10^{10} vp for Ads and 2 x 10^{8} pfu for MVA unless otherwise stated. n = number of individuals
^ Used for comparisons with HCV003 only - Described in **Barnes *et al* 2012**
*Trial weeks for patients receiving peg-IFNα/Rib refer to weeks after start of treatment (treatment duration 48 weeks)

6.4.4 Immunoassays

Immunoassays are described in full in **chapter 2**. Briefly, PBMC stimulated with pools, minipools, or individual HCV peptides were tested in triplicate for their IFNγ production by ELISpot, or for the overnight induction of cytokines by ICS. Proteins covering the NS region encoded in the vaccine were used in 5-day proliferation assays, measured using the incorporation of tritiated-thymidine. HCV-specific class-I pentamer+ T-cell populations were phenotyped directly *ex vivo* using multiparametric flow cytometry.

6.4.5 CD8+ T-cell depletion ELISpots

All CD8+ T-cell depletion assays were performed by Christabel Kelly or Anthony Brown. To determine whether T-cells recognizing specific HCV peptides are CD8+ or CD4+, depletion ELISpots were performed. Anti-CD8 beads (50 µL per $5x10^6$ PBMC; Miltenyi 130-045-201) are washed three times with PBS/2%FCS to remove sodium azide. PBMC are pelleted and resuspended in chilled (4 °C) PBS/2%FCS with CD8+ beads and incubated for 20 minutes at 4 °C. The PBMC bead mix is then placed on a Dynal magnet until the supernatant is clear and the liquid is removed. This procedure is repeated twice. CD8+ depleted cells are then used in an ELISpot as described in **chapter 2**.

6.5 Results

6.5.1 HCV002 trial (ChAd3-NS/Ad6-NS) patient characteristics and virological outcome

Patients had a median age of 43 (range 24-65) years, mean baseline ALT 54 (range 16-151) IU/mL, median baseline HCV RNA 1.13 $x10^6$ (range 3868-11.65 $x10^6$) IU/mL. Fourteen (56.5%) of the patients treated with PEG-IFNα/rib achieved SVR, 10 non-SVR and 1 was lost to follow up. IL28B genotyping showed TT n= 22, GT n= 9, GG n= 1 (**Table 6-2**).

6.5.2 Vaccination with Ad6-NS and ChAd3-NS is well tolerated

The primary endpoints of the Phase I study HCV002 were safety and immunogenicity. When administered to healthy volunteers ChAd3-NS and Ad6-NS have a good safety record (**Barnes et al. 2012**), but had not previously been given to HCV infected patients, who possess a different mixture of comorbidities.

Table 6-2. HCV002 trial patient demographics and treatment outcome

Table 6-2: HCV002 trial - Patient demographics and treatment outcome

Patient	Group	Sex	Age	HCV subtype	Fibrosis Score: (Ishak or *Kpa)	Baseline ALT (IU/L)	Treatment (IFN/RBV) Duration (weeks)	Baseline HCV RNA (IU/ml)	SVR	IL28B (SNP rs8099917)
21 (prime only)	A1	F	65	1a	3	28	48	$1.98x10^6$	Y	nd
20	A1	M	54	1	3	40	48	$1.54x10^6$	Y	TT
30	A1	M	56	1a	4	28	48	15995	Y	TT
31 (prime only)	A2	M	36	1a	2	56	48	$6.3 x10^6$	N	TT
24	A2	M	42	1b	3	69	48	$11.3x10^6$	Y	TT
28	A3	M	58	1a	2	144	48	$4.14x10^6$	N	TT
48	A3	M	53	1a	4	84	48	$2.93x10^6$	N	TT
50	A3	M	50	1a	1	42	48	761224	N	GT
100	A3	M	24	1b	7.5*	54	48	$1.31x10^6$	Lost to FU	GG
27	A3	F	33	1	2	18	48	22228	Y	GT
36	A3	F	32	1b	nd	16	30	9199	Y	TT
101	A4	M	43	1a	6*	71	24	$1.89x10^6$	N	GT
106	A4	M	44	1a	5.4*	26	48	$3.08x10^6$	N	TT
54	A4	M	44	1a	0	44	48	824830	N	GT
45	A4	F	35	1a	2	74	16	343163	N	TT
39	A4	M	31	1b	1	72	48	$11.5x10^6$	Y	GT
102	A4	M	30	1b	1	151	48	584666	Y	GT
37	A5	M	35	1b	3	113	48	$10.2x10^6$	Y	TT
38	A5	M	28	1b	2*	69	48	631606	Y	TT
55	A5	M	35	1a	1	76	24	398842	Y	TT
56	A5	F	61	1b	4	36	24	31025	Y	TT
40	A6	M	39	1b	2	26	48	$2.45x10^6$	N	TT
25	A6	M	43	1a	2	56	48	$8.40x10^6$	N	TT
43	A6	M	54	1a	2	77	48	$11.65x10^6$	Y	TT
103	A6	M	36	1b	7.3*	59	48	36678	Y	TT
34	B1	M	55	1a	1	41	NA	$9.03x10^6$	NA	TT
29	B1	F	49	1a	1	47	NA	392438	NA	TT
35	B2	F	55	1a	1	35	NA	831657	NA	GT
44	B2	F	33	1b	1	51	NA	$1.69x10^6$	NA	TT
46	B3	M	53	1a	1	101	NA	$2.79X10^6$	NA	GT
51	B3	F	43	1a	1	76	NA	$1.65x10^6$	NA	TT
52	B3	M	59	1a	3	46	NA	$2.55x10^6$	NA	GT
53	B3	M	49	1a	2	31	NA	3868	NA	TT

Duration of IFNα/Ribavirin therapy and outcome of therapy in all vaccinated patients is shown. Fibrosis scores were determined by pre-treatment liver biopsies or by fibroscan*. SVR = undetectable viral load by PCR 6 months following end of therapy. IL28B status was determined at SNP rs80990917. (NA= not applicable, nd=Not done, FU=follow up).

Mild local and systemic side-effects were reported, consistent with previous trials of Adenoviral vectors in healthy volunteers. Overall vaccination was well tolerated with no vaccine-related serious adverse events, however, some expected treatment related side effects were seen (data not shown) (**Fried et al. 2002**). Alanine aminotransferase (ALT) levels were measured as a surrogate for liver inflammation. No increase in ALT levels >30% above pre-vaccine were seen in arm B. A transient increase in liver transaminases was observed in two patients in arm A peaking at 103 IU/L and 339 IU/L respectively (**Figure 6-1A**); A liver biopsy was performed in patient 038 that showed mild non-specific inflammation only, in keeping with HCV infection.

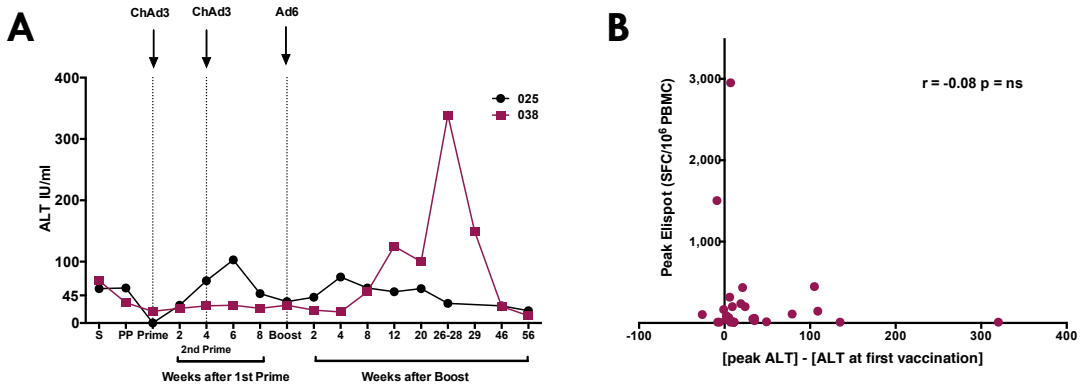


Figure 6-1. Liver enzymes in relation to vaccination: (**A**) Kinetics of Alanine aminotransferase (ALT) in relation to vaccination is shown in two patients with transient elevations in ALT. Patient 024 (Arm A2) received medium dose vaccination (5 x 10^9 vp) and 038 (Arm A5) received high dose vaccination (2.5 x 10^{10} vp). Liver biopsy of 038 showed non-specific inflammation. (**B**) Correlation between peak IFNγ ELISpot response at any time point and maximum change in ALT after vaccination (Peak ALT after vaccination – ALT at time of vaccination) for all patients in HCV002.

6.5.3 Heterologous ChAd3-NS prime/Ad6-NS boost induces HCV specific T-cell responses

Initially, a vaccine dose escalation was performed in patients who had received 14 weeks lead-in of PEG-IFNα/rib from 5 x 10^8 vp of ChAd3-NS prime and Ad6-NS boost up to the optimal dose used in healthy volunteers, 2.5 x 10^{10} vp (**Table 6-1**). No T-cell responses were detected at low and medium vaccine doses by IFNγ ELISpot (data not shown; Arms A1 and A2). At the highest dose (Arms A3 and A4) HCV-specific T-cells were detected in 8/12 individuals receiving a single prime/boost (median 107 SFC/10^6 PBMC; range 10-2953) peaking 2-4 weeks following boost vaccination (**figure 6-1A**). Double prime/boost vaccination (4 weeks apart, Arms A5 and A6) induced a response in 4/8 vaccinees (median 36.5 SFC/10^6 PBMCs; range 10-317) (**figure 6-1B**) and did not significantly enhance

the response (**figure 6-1C**). When data from all patients were combined there was a significant increase in HCV T-cell responses after boost, but not after priming vaccination (**figure 6-1D**).

Previously, a transient depletion of T-cells specific for CMV, influenza, and EBV during PEG-IFNα/rib therapy has been described (**Humphreys et al. 2012**), however, a clear effect of treatment on anti-viral T-cell responses was not observed here (**figure 6-3**).

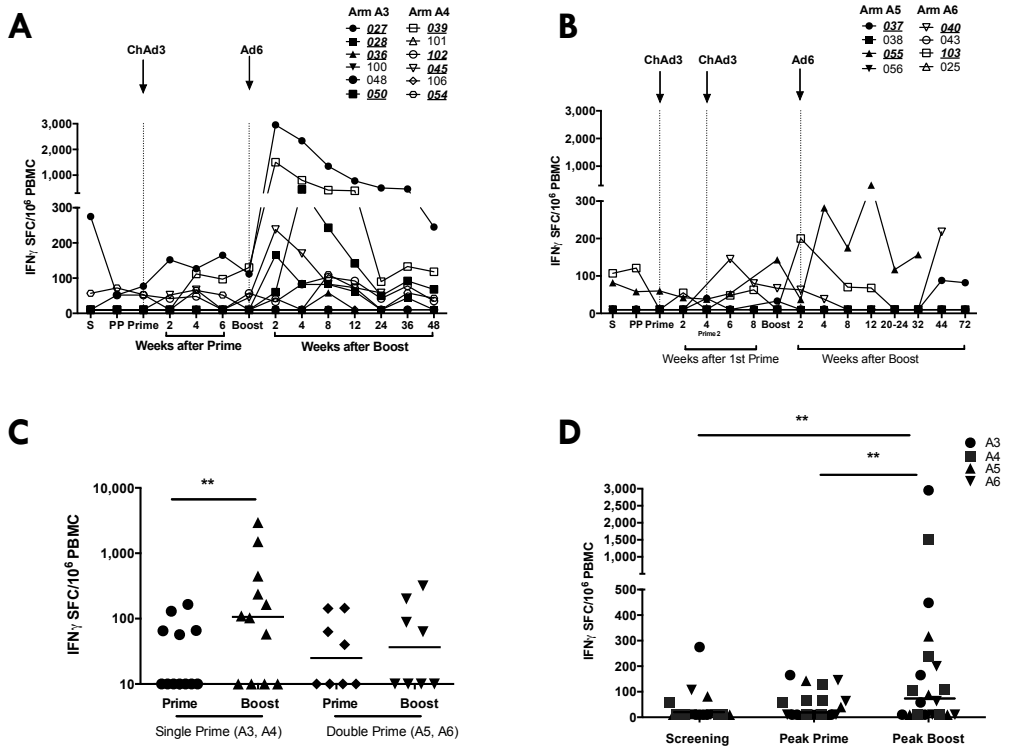


Figure 6-2. Patients on treatment - Magnitude of HCV specific T-cell responses after ChAd3-NS (prime) and Ad6-NS (boost) vaccination: (**A-D**) The total *ex vivo* IFNγ ELISpot response across NS peptide pools are shown (sum of positive pools). (**A**) The kinetics of the response in individual patients receiving single prime, (**B**) or double prime vaccination (dose; 2.5 X 10^{10} vp) with PEG-IFNα/rib (S = screening. PP= pre-priming). (**C**) A comparative analysis of the magnitude of HCV-specific T-cells following single prime or double prime vaccination, and (**D**) at baseline in comparison to peak post-prime and peak post-boost

vaccination is shown. (**E**) The kinetics of the HCV specific T-cell response (solid lines) and HCV RNA. Patients with a positive response to vaccination are underlined (**A-B**).

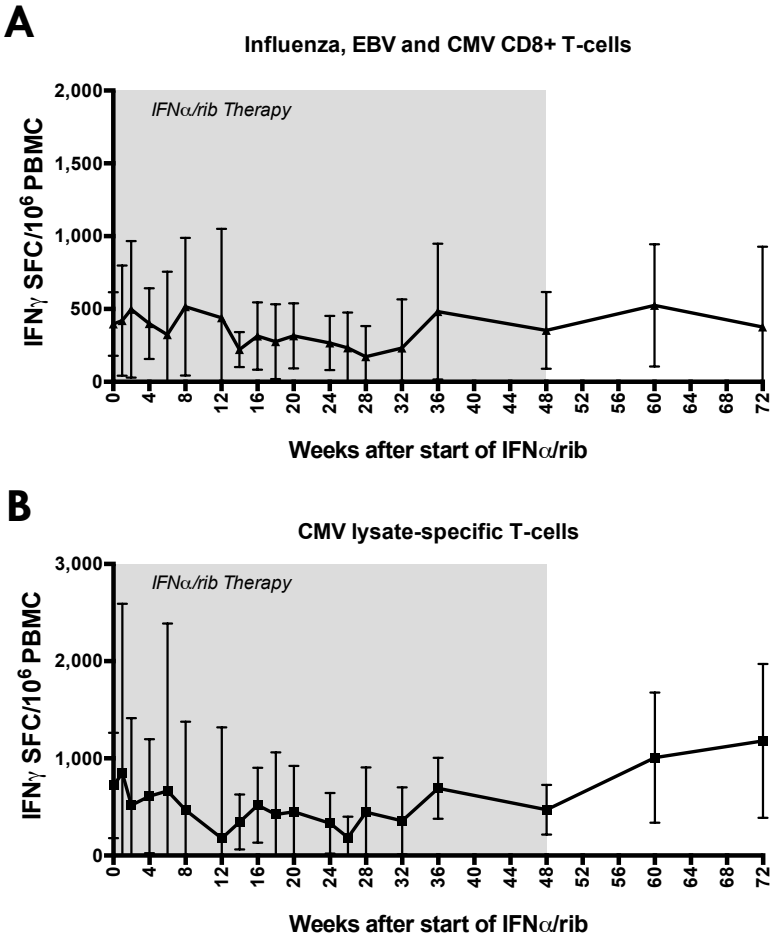


Figure 6-3. The magnitude of non-HCV antiviral T-cells during the study: *Ex vivo* IFNγ ELISpot response to (**A**) a pool of influenza, EBV, and CMV (FEC) CD8+ T-cell epitopes or (**B**) CMV lysate in patients that showed a positive response to these peptides at any point during the trial (CMV n=8; FEC n=11). Bars represent the mean +/- SEM for patients in arms A3 - A6 receiving concurrent PEG-IFNα/rib therapy (period of therapy shaded in grey).

6.5.4 Vaccination at high or low HCV viral load

I next assessed the effect of vaccination in untreated HCV+ patients receiving prime/boost vaccination alone (HCV002 Arm B; **Table 6-1**) in a dose escalation

strategy (5×10^8, 5×10^9, 2.5×10^{10} vp). At the low and medium dose 2/4 patients responded to vaccination. At the higher dose, T-cells were induced in 3/4 patients (median post-prime 78 SFC/10^6 PBMC; range 10-478, median post-boost 121 SFC/10^6 PBMC; range 10-390). There was no effect of vaccination on HCV viral load (**figure 6-4A**).

Mouse models of LCMV have shown that therapeutic vaccination may be more efficacious after viral suppression (**Wherry et al. 2005**), therefore, I compared vaccination 14 weeks after PEG-IFNα/rib therapy, when HCV RNA was undetectable in 9/10 volunteers (Arms A3, A5), vaccination 2 weeks after therapy (Arms A4, A6) when HCV viral loads were significantly higher (median 0 vs. 11, 441 IU/mL, p=0.0002***), and untreated patients (Arm B), with high viral loads (median 2,300,000 IU/mL). There was no difference in vaccine responses between the three groups, (**figure 6-4B**) and overall no correlation between the viral load at time of priming vaccination and the peak T-cell response thereafter (**figure 6-4C**).

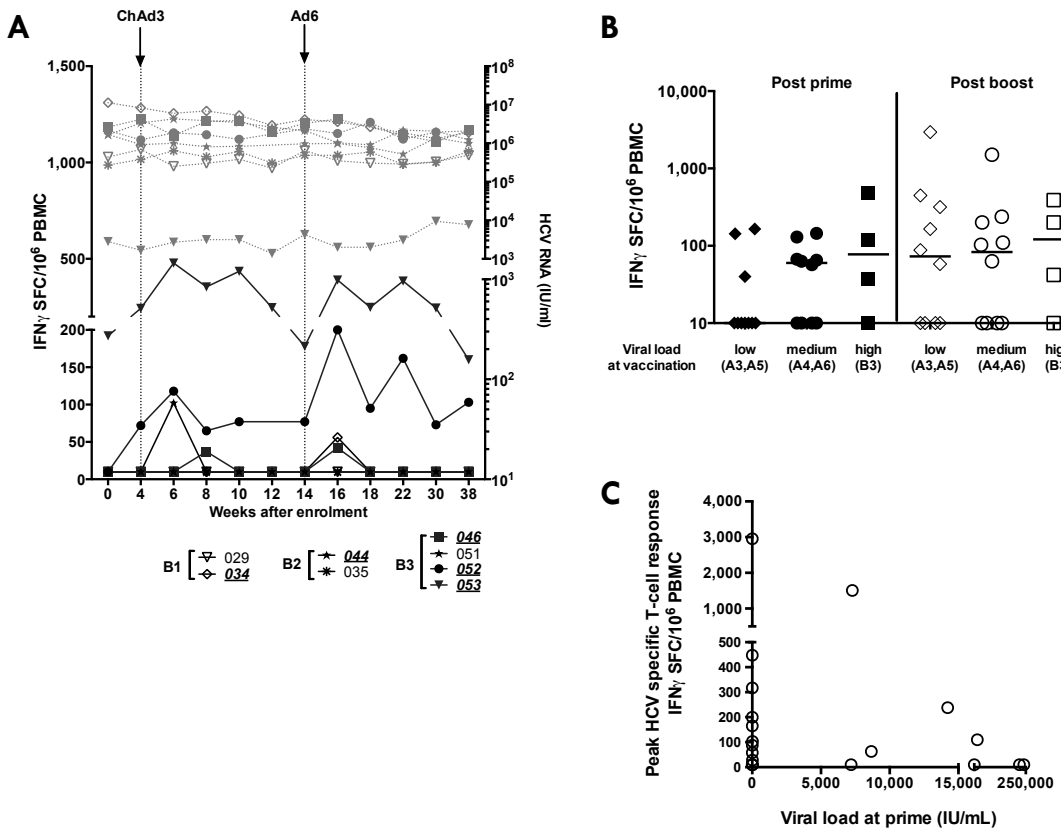


Figure 6-4. Untreated patients - Magnitude of HCV specific T-cell responses after ChAd3-NS (prime) and Ad6-NS (boost) vaccination: (**A**) The kinetics of the HCV specific T-cell response (solid lines) and HCV RNA (grey dotted lines) in individual patients receiving heterologous prime/boost vaccination at low, medium, and high dose (groups B1, B2, B3 respectively; Table 6-1) without PEG-IFNα/rib. Patients with a positive response are underlined. (**B**) The magnitude of the T-cell response in low (A3 and A5), medium (A4 and A6), and high (B3) viral load patient groups 14 or 2 weeks into, or without, PEG-IFNα/rib (all high dose vaccination; 2.5 X 10^{10} vp). Dotted line at positive cut-off. (**C**) HCV RNA (IU/mL) at time of prime vaccination vs. peak HCV specific T-cell response for groups A3-6.

6.5.5 HCV specific T-cell responses in chronic HCV infection, compared to healthy volunteers

The magnitude of the response was significantly lower in HCV infected patients compared with healthy volunteers vaccinated with an identical regimen as part

of a previous study (**Barnes et al. 2012**); mean +/- SD HCV vs. healthy volunteers; post-prime 49.25 +/- 54.15 vs. 1476 +/- 978.8 p<0.0001****, post-boost 317.3 +/- 704.7 vs. 2183+/- 4633 p = 0.0052** respectively; **figure 6-5A**). The kinetics of the response also differed between these groups; the high magnitude response that was observed after priming vaccination in healthy volunteers was markedly attenuated in HCV infected patients (**figure 6-5B**).

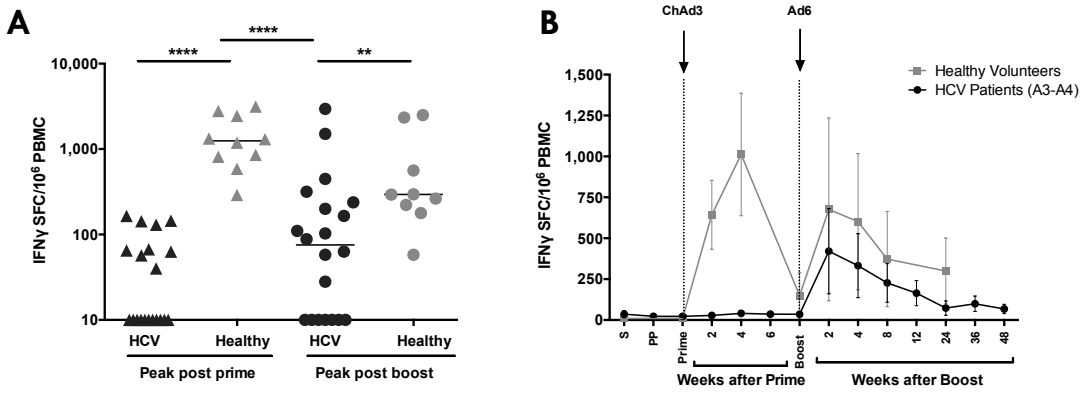


Figure 6-5. Magnitude of HCV specific T-cell responses in healthy volunteers compared to HCV infected patients: (**A**) A comparison of the magnitude of the T-cell responses to HCV NS after high dose vaccination with ChAd3-NS prime (single or double) and Ad6-NS boost (2.5 X 10^{10} vp) in healthy volunteers (grey n = 10. Groups 7 and 10; **Barnes et al. 2012**) and HCV patients (black, n=20, groups A3-6). Responses shown are the total positive *ex vivo* IFNγ ELISpot response across all NS peptide pools at peak magnitude post prime and peak post boost. Bars at median. (**B**) Kinetics of the total *ex vivo* IFNγ ELISpot response across all NS peptide pools in HCV infected patients (A3-4) and healthy volunteers (group 10; **Barnes et al. 2012**) receiving single prime and boost vaccination. Bars at Mean and SEM.

6.5.6 Anti-vector immunity in response to vaccination

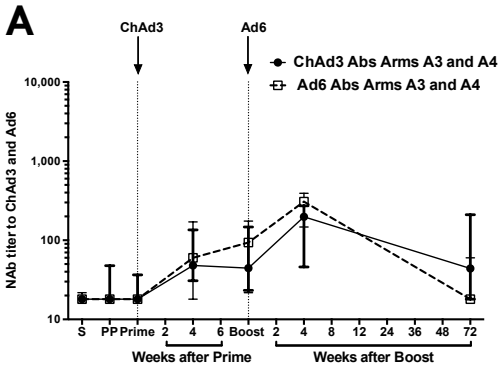
One potential mechanism limiting the immunogenicity of Ad vectors in HCV+ patients is the existence of anti-vector neutralising antibodies, which can lead to

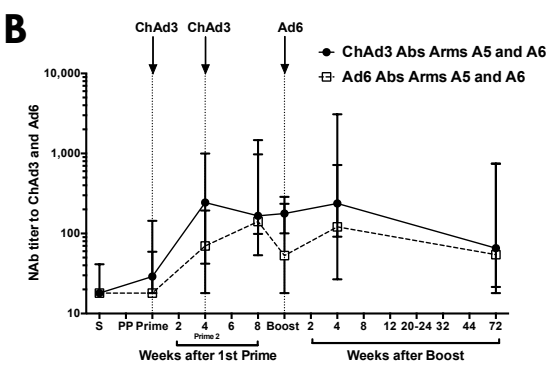
the clearance of the Ad vector before transgene proteins can be produced (**Steffensen et al. 2012; Zak et al. 2012; Quinn et al. 2013**).

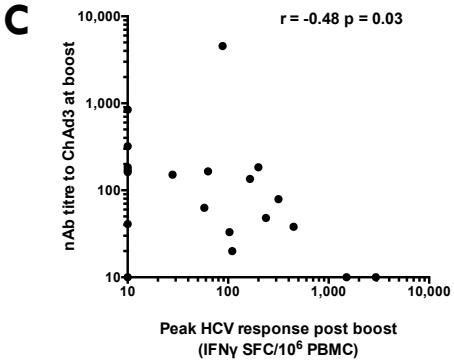
Following priming vaccination, ChAd3 nAbs that were cross-reactive with Ad6 were readily detectable and maintained to the time of heterologous boost in both single prime and double prime study groups (**figure 6-6A-B**). I found a negative correlation between anti-ChAd3 ($r = -0.48$, $p = 0.03$*; **figure 6-6C**) or Ad6 (Kelly et al 2015) nAbs at the time of boost vaccination with peak IFNγ ELISpot thereafter.

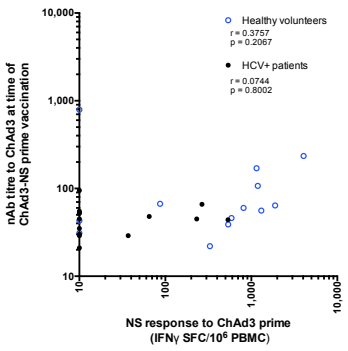
ChAd3 was selected as the vector for our vaccines due to its low seroprevalence, and the majority of both patients and healthy volunteers tested had undetectable titers of nAb against ChAd3 pre-vaccination (15/28 healthy volunteers [HCV003 arm A2,A3,A5] and 23/37 HCV+ patients [HCV002 A3-A6 B1-B3, HCV003 B1-2 and C] arms). The peak T-cell response to HCV NS after ChAd3 prime vaccination did not correlate with the ChAd3 nAb titer at the time of prime vaccination in those that had a detectable nAb response (**figure 6-6D**). The one healthy volunteer that had a ChAd3 nAb titer >200 (331, screen ChAd3 nAb titer of 791) at screening did not have a detectable HCV NS specific T-cell response post prime vaccination, but did nonetheless respond well to MVA-NS boost vaccination (peak T-cell response to HCV NS of 1543 SFC/10^6 PBMC 1 week after MVA-NS boost vaccination). Robust anti-vector T-cell responses were observed following both priming and heterologous boosting vaccination, showing that T-cell responses are not generally defective in patients with HCV infection or during PEG-IFNα/rib therapy (**figure 6-6E-G**). Overall nAb titers were lower in patients

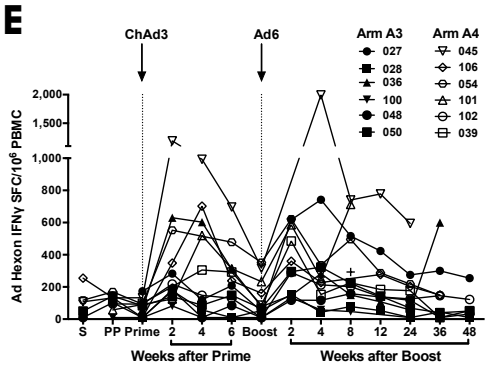
than healthy volunteers after ChAd3-NS prime and Ad6-NS boost (**figure 6-6H**), which may explain why HCV-specific T-cells are more effectively boosted by heterologous Ad/Ad in patients and why the hexon response peaks post boost in patients but post prime in healthy volunteers (**figure 6-6G**). The majority of healthy volunteers had a nAb titers over 200 (median 270 range 49-4608) at the time of Ad6-NS boost but no such correlation between the magnitude of the T-cell response post-Ad6-NS boost and nAb titer at the time of boost was observed (**Barnes et al. 2012**).

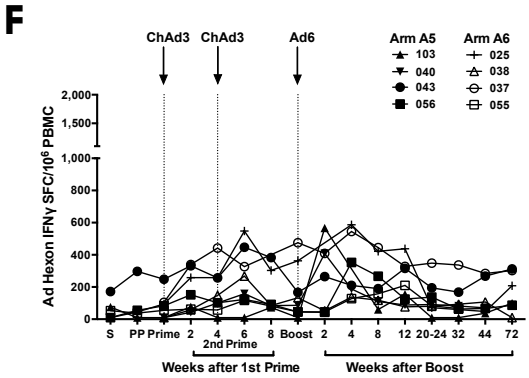

A
ChAd3
Ad6
ChAd3 Abs Arms A3 and A4
Ad6 Abs Arms A3 and A4
NAb titer to ChAd3 and Ad6
10,000
1,000
100
10
S PP Prime 2 4 6 Boost 2 4 8 12 24 36 48 72
Weeks after Prime
Weeks after Boost

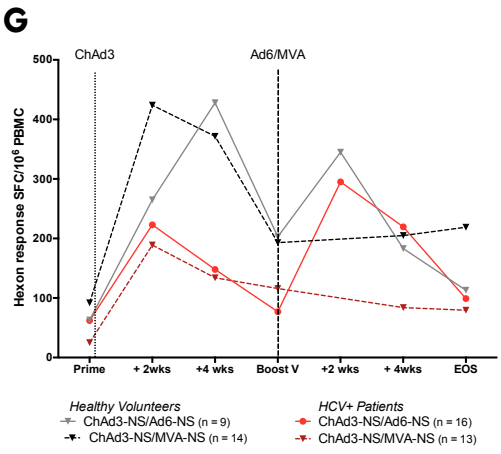

B
ChAd3 ChAd3
Ad6
ChAd3 Abs Arms A5 and A6
Ad6 Abs Arms A5 and A6
NAb titer to ChAd3 and Ad6
10,000
1,000
100
10
S PP Prime 2 4 6 8 Boost 2 4 8 12 20-24 32 44 72
Prime 2
Weeks after 1st Prime
Weeks after Boost


C
r = -0.48 p = 0.03
nAb titre to ChAd3 at boost
10,000
1,000
100
10
10 100 1,000 10,000
Peak HCV response post boost
(IFNγ SFC/10⁶ PBMC)


D
Healthy volunteers
r = 0.3757
p = 0.2067
HCV+ patients
r = 0.0744
p = 0.8002
nAb titre to ChAd3 at time of
ChAd3-NS prime vaccination
10,000
1,000
100
10
NS response to ChAd3 prime
(IFNγ SFC/10⁶ PBMC)


E
ChAd3
Ad6
Arm A3
027
028
036
100
048
050
Arm A4
045
106
054
101
102
039
Ad Hexon IFNγ SFC/10⁶ PBMC
2,000
1,500
1,000
800
600
400
200
0
S PP Prime 2 4 6 Boost 2 4 8 12 24 36 48
Weeks after Prime
Weeks after Boost


F
ChAd3 ChAd3
Ad6
Arm A5
103
040
043
056
Arm A6
025
038
037
055
Ad Hexon IFNγ SFC/10⁶ PBMC
2,000
1,500
1,000
800
600
400
200
0
S PP Prime 2 4 6 8 Boost 2 4 8 12 20-24 32 44 72
2nd Prime
Weeks after 1st Prime
Weeks after Boost


G
ChAd3
Ad6/MVA
Hexon response SFC/10⁶ PBMC
500
400
300
200
100
0
Prime + 2wks +4 wks Boost V +2 wks + 4wks EOS
Healthy Volunteers
ChAd3-NS/Ad6-NS (n = 9)
ChAd3-NS/MVA-NS (n = 14)
HCV+ Patients
ChAd3-NS/Ad6-NS (n = 16)
ChAd3-NS/MVA-NS (n = 13)

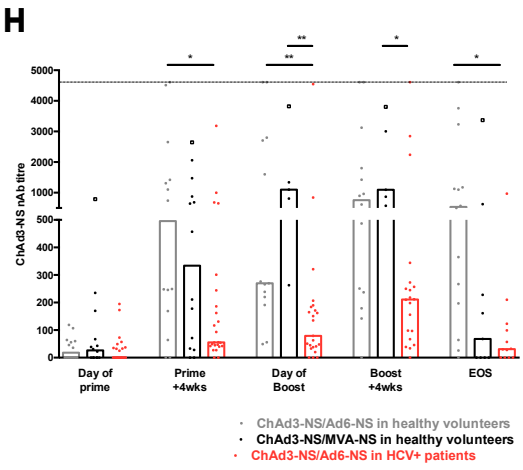

H
ChAd3-NS nAb titre
5000
4000
3000
2000
1000
500
400
300
200
100
0
Day of prime
Prime +4wks
Day of Boost
Boost +4wks
EOS
ChAd3-NS/Ad6-NS in healthy volunteers
ChAd3-NS/MVA-NS in healthy volunteers
ChAd3-NS/Ad6-NS in HCV+ patients

Figure 6-6. Anti-vector immunity – neutralising antibodies and anti-hexon T-cell response: **(A-B)** Neutralising Abs (nAbs) to hexon of priming ChAd3 vector and the heterologous boosting vector (Ad6) are shown for (A) single prime and (B) double prime vaccinees as group data (dose 2.5 X 10^{10} vp; Arms A3-A6.) (**C**) The nAb titer to ChAd3 vs. the peak magnitude of the HCV specific T-cell response (*ex vivo* IFNγ ELISpot response across all NS peptide pools, 2-4 weeks after boosting vaccination) is shown. (**D**) The nAb titer to ChAd3 at the time of ChAd3-NS prime vaccination in patients (black) of healthy volunteers (blue) vs. the peak magnitude of the HCV specific T-cell response to prime vaccination (*ex vivo* IFNγ ELISpot response across all NS peptide pools, 2-4 weeks after prime vaccination) is shown. (**E-F**) The magnitude of anti-adenovirus (Ad5 hexon proteins) T-cell responses (by *ex vivo* IFNγ ELISpot), in patients receiving (**E**) single prime or (**F**) double prime vaccination is shown. (**G-H**) The median magnitude of anti-adenovirus (Ad5 hexon proteins) T-cell responses (by *ex vivo* IFNγ ELISpot) (**G**) and the titer of anti-ChAd3 nAb (**H**) are shown for healthy volunteers and patients (on and off treatment) who were vaccinated with ChAd3-NS/Ad6-NS (single prime only) or ChAd3-NS/MVA-NS. Bars at median. Healthy volunteer 331 (high nAb titer pre-screen) is highlighted as an open circle.

6.5.7 The relationship between the sequence of the circulating virus and the vaccine immunogen

T-cell responses were mapped to individual peptides using IFNγ ELISpot. Fifteen antigenic targets were identified spanning the vaccine immunogen (**Table 6-3** and **figure 6-7**). Of these, 13 were CD8+ T-cell epitopes previously described in natural infection and two were novel CD8+ epitopes mapped to optimal length; $NS5B_{2804\text{-}2814}$ LTRDPTTPLAR and $NS4B_{1891\text{-}1899}$ ALVVGVVCA (**Kelly** et **al. 2015b**). The most commonly identified epitope was $NS3_{1406}$ (KLSGLGINAV) a well described HLA-A2 epitope, targeted in 6/17 HLA-$A2^{+}$ patients (all HLA-A2+ volunteers showed a strong response to this epitope **Table 3-2**). Depletion ELISpots and ICS confirmed that mapped responses were CD8+. No mapped responses were made by CD4+ T-cells.

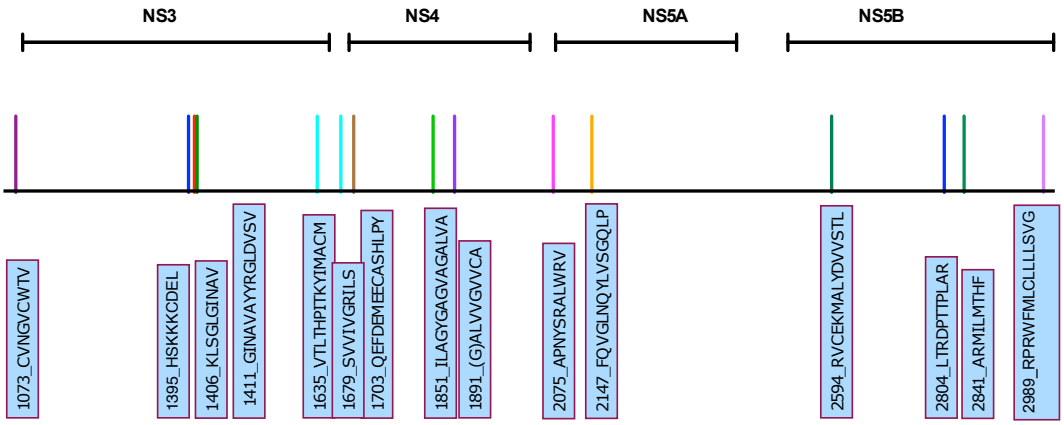


Figure 6-7. Epitopes mapped to HCV genomic regions: Epitopes targeted by vaccine induced T-cells are represented by different coloured vertical lines at the corresponding position along the HCV genome and the start position and amino acid sequence at each epitope are indicated below.

The endogenous viral sequence at the 15 CD8+ T-cell epitopes was determined at baseline and time of viral relapse in all patients (**Table 6-4).** At 14/15 epitopes, viral and vaccine immunogen sequence differed by 1-4 amino acids in patients targeting those epitopes (**Table 6-5**).

Table 6-3. T-cell responses mapped to individual peptides/pools in HCV+ patients

Group (vaccines)	Patient	HLA-A		HLA-B		HLA-C		pre-vaccination +ve pools (IFNγ SFC/10^6PBMC)	post vaccination +ve pools (IFNγ SFC/10^6 PBMC, week of peak response)	Mapped to peptide (parent pool)
A3 (Wks 14,24)	**27**	30	2	44		7	5	F (40), G (45), H (170), L (120)	F (213, Wk26), G (748, Wk26), H (922, Wk26), L (918, Wk26), M (152, Wk26)	CVNGVCWTV (F) KLSGLGINAV (G) LTTGSVVIVGRIILS/ SVVIVGRIILSGRPA (H) QEFDEMEECASHLPY (H) ILAGYGAGVAGALVA (H) RVCEKMALYDVVSTL (L) RPRWFMLCLLLLSVG (M)
	28	11	2	44	37	6	5	-	G (88, Wk26) H (43, Wk26), M (35, Wk26)	KLSGLGINAV (G)
	36	3	2	44	51	16	14	-	G (59, Wk32)	-
	100	24	2	13	60	6	10	-	-	-
	48	1	3	8	35	4	7	-	-	-
	50	2	30	8	49	7		-	F (50, Wk38), G (388, Wk28)	KLSGLGINAV (G)
A4 (Wks 2, 12)	**39**	24	30	13	7	6	7	-	G (80, Wk14), H (85, Wk14), I (794, Wk14), M (510, Wk14)	TPSPAPNYSRALWRV/ APNYSRALWRVAAEE (I) FQVGLNQYLVGSQLP (I) LSRARPRWFMLCLLL/ RPRWFMLCLLLLSVG (M)
	101	24	3	81	35	18	4	-	-	-
	102	68	3	27	39	1	7	M (52)	M (104, Wk20)	-
	45	11	1	8	7	7		-	G (238, Wk14)	HSKKKCDEL (G) VTLTHPITKYIMACM (G)
	106	3	29	35		4	8	-	-	-
	54	23	2	27	7	1	7	M (72)	M (110, Wk20)	ARMILMTHF (M)
A5 (Wks 14,18,28)	**37**	1	2	49	44	5	7	-	L (40, Wk18)	-
	38	66	2	41	18	7	17	-	-	-
	55	2	2	13	39	6	12	M (81)	F (88 Wk36), G (112, Wk36), M (143, Wk36)	CVNGVCWTV (F) KLSGLGINAV (G) LTRDPTTPLAR (M)
	56	2	30	18	8	6	5	-	-	
A6 (Wks 2,6, 16)	**40**	24	2	60	7	7	10	-	G (145, Wk8),	KLSGLGINAV (G)
	43	2	1	62	7	7	10	-	-	-
	103	2	2	44		5	16	F (120)	F (67, Wk10), G (164, Wk18)	CVNGVCWTV (F) KLSGLGINAV (G)
	25	2	68	18	65	7	8	-	-	-
B3 (Wks 4, 14)	**46**	1	2	8	44	4	7	-	G (42, Wk16)	-
	51	11	32	18	51	2	5	-	-	-
	52	1	2	7	65	7	8	-	G (200, Wk16)	GINAVAYYRGLDVSV (G)
	53	2	26	64		8		F (52), H(165), I (43)	F (92, Wk8), G (50, Wk6), H (270, Wk6), I (81, Wk6)	CVNGVCWTV (F) Fh (minpool only) ALVVGVVCA (G) Hf (minipool only)

Responses post-vaccination are shown. 'New' responses, only detectable after vaccination, are highlighted in red. The magnitude of the response and the study week of the response are given in parenthesis. Responses mapped to the epitope or peptide level are shown.

Table 6-4. Circulating HCV sequence at immunogenic T-cell epitopes

Table 6-4: Circulating HCV sequence at immunogenic T-cell epitopes

A) HLA-A1 epitope **B**) HLA-B8 epitope **C**) HLA-B27 epitope **D**) HLA-A2 epitopes **E**) epitopes of unknown HLA restriction.

(A)

	Pt No.	T	L	T	H	P	I	T	K
	45	**I**	-	-	-	-	-	-	-
HLA-A11	45B	I/L	-	-	-	-	-	-	-
+ve	28	-	-	-	-	-	-	-	-
pts	28B	-	-	-	-	-	-	-	-
	51	-	-	-	-	-	V	-	-
	43	-	-	-	-	-	V	-	-
	55	-	-	-	-	-	V	-	-
	103	-	-	-	-	-	-	-	-
	52	-	-	-	-	-	-	-	-
	106	-	-	-	-	-	V	-	-
	54	-	-	-	-	-	-	-	-
	27	-	-	-	-	-	V	-	-
HLA-A11	38	V	-	-	-	-	-	-	-
neg pts	53	?	?	-	-	-	-	-	-
	101	-	-	-	-	-	-	-	-
	102	-	-	-	-	-	V	-	-
	40	-	-	-	-	-	V	-	-
	40B	-	-	-	-	-	V	-	-
	48	nd							
	39	nd							
	50	nd							
	46	nd							
	36	nd							
	37	nd							
	56	nd							
	100	nd							

(B)

	Pt No.	H	S	K	K	K	C	D	E	L
	45	-	-	-	**R**	-	-	-	-	-
HLA-B8	45B	-	-	-	R	-	-	-	-	-
+ve	44	-	-	-	-	-	-	-	-	-
pts	50	-	-	-	-	-	-	-	-	-
	48	-	-	-	-	-	-	-	-	-
	46	-	-	-	-	-	-	-	-	-
	53	-	-	R	-	-	-	-	-	-
	40	-	-	-	-	-	-	-	-	-
	40B	-	-	-	-	-	-	-	-	-
	25	-	-	-	-	-	-	-	-	-
	51	-	-	-	-	-	-	-	-	-
	52	-	-	-	-	-	-	-	-	-
HLA-B8	39	-	-	-	-	-	-	-	-	-
neg pts	103	-	-	-	-	-	-	-	-	-
	27	-	-	-	-	-	-	-	-	-
	28	-	-	-	-	-	-	-	-	-
	28B	-	-	-	-	-	-	-	-	-
	38	-	-	-	-	-	-	-	-	-
	43	-	-	-	-	-	-	-	-	-
	55	-	-	-	-	-	-	-	-	-
	54	-	-	-	-	-	-	-	-	-
	37	-	-	-	R	-	-	-	-	-
	100	-	-	-	-	-	-	-	-	-
	102	-	-	-	-	-	-	-	-	-
	56	n	d							
	101	n	d							
	36	n	d							

(C)

	Pt No.	A	R	M	I	L	M	T	H	F
HLA-B27	54	**V**	-	-	-	-	**L**	-	-	-
+ve pts	102	-	-	-	V	-	-	-	-	-
	28	-	-	-	-	-	-	-	-	-
	28B	-	-	-	-	-	-	-	-	-
	48	-	-	-	-	-	-	-	-	-
	50	-	-	-	-	-	-	-	-	-
	39	-	-	?	-	-	-	-	-	-
	101	V	-	-	-	-	L	-	-	-
	45	-	-	-	-	-	-	-	-	-
	37	-	-	-	-	-	-	-	-	-
	38	-	-	-	-	-	-	-	-	-
	55	-	-	-	-	-	-	-	?	-
HLA-B27	40	-	-	-	-	-	-	-	-	-
neg pts	43	-	-	-	-	-	-	-	-	-
	103	-	-	-	V	-	-	-	-	-
	46	-	-	-	-	-	-	-	-	-
	52	-	-	-	-	-	-	-	-	-
	53	-	-	-	-	-	-	-	-	-
	51	-	-	-	-	-	?	-	-	-
	27	n	d							
	25	n	d							
	36	n	d							
	100	n	d							
	106	n	d							
	56	n	d							

(D)

	Pt No.	C	V	N	G	V	C	W	T	V	K	L	S	G	L	G	I	N	A	V	A	L	Y	D	V	V	S	T	L	I	L	A	G	Y	G	A	G	V
	27	-	**I**	-	-	-	-	-	-	-	-	-	**V**	**S**	-	-	**L**	-	-	-	-	-	-	-	-	-	-	**K**	-	-	-	-	-	-	-	-	-	-
HLA-A2	28	-	I	-	-	-	-	-	-	-	-	-	**V**	**A**	-	-	-	-	-	-	-	-	-	-	-	-	-	K	-	-	-	-	-	-	-	-	-	-
+ve	28B	-	I	-	-	-	-	-	-	-	-	-	**V**	**A**	-	-	**V**	-	-	-	-	-	-	-	-	-	-	K	-	-	-	-	-	-	-	-	-	-
pts	40	-	**I**	-	-	-	-	-	-	-	-	-	**V**	**A**	**M**	-	**V**	-	-	-	-	-	-	-	-	-	-	K	-	n	d							
	40B	-	I	-	-	-	-	-	-	-	-	-	V	A	M	-	V	-	-	-	-	-	-	-	-	-	-	K	-	n	d							
	103	-	**I**	-	-	-	-	-	-	-	-	-	**V**	**A**	-	-	-	-	-	-	-	-	-	-	-	-	-	-	-	-	-	-	-	-	-	-	-	-
	50	-	I	-	-	-	-	-	-	-	-	-	**V**	**A**	-	-	**V**	-	-	-	-	-	-	-	-	-	-	K	-	-	-	-	-	-	-	-	-	-
	50B	n	d									n	d																	n	d								
	52	-	I	-	-	-	-	-	-	-	-	-	V	A	-	-	V	-	-	-	-	-	-	-	-	-	-	K	-	-	-	-	-	-	-	-	-	-
	44	-	I	S	G	A	-	-	-	-	-	-	V	A	-	-	V	-	-	-	-	-	-	-	-	-	-	-	-	n	d							
	46	-	I	-	-	-	-	-	-	-	-	-	V	A	-	-	-	-	-	-	-	-	-	-	-	-	-	K	-	-	-	-	-	-	-	-	-	-
	38	-	I	-	-	-	-	-	-	-	-	Q	-	-	-	-	L	-	-	-	-	-	-	-	-	-	-	-	-	-	-	-	-	-	-	-	-	-
	36	-	I	-	-	-	-	-	-	-	-	n	d									-	-	-	-	-	-	-	-	-	-	-	-	-	-	-	-	-
	43	-	I	-	-	-	-	-	-	-	-	-	-	V	A	-	-	V	-	-	-	-	-	-	-	-	-	-	K	-	-	-	-	-	-	-	-	?
	25	-	I/-	-	-	-	-	-	-	-	-	-	-	V	V	-	-	-	-	-	-	-	-	-	-	-	-	-	R	-	-	-	-	-	-	-	-	-
	55	-	**I**	-	-	-	-	-	-	-	-	-	-	**V**	**A**	-	-	**V**	-	-	-	-	-	-	E	-	-	-	K	-	n	d							
	37	-	I	-	-	-	?	?	-	-	-	-	-	-	-	-	L	-	-	-	-	-	-	-	D	-	-	-	-	-	-	-	-	-	-	-	-	-
	53	-	**I**	-	-	-	-	-	-	-	-	-	-	V	T	-	-	V	-	-	-	-	-	-	-	-	-	-	-	-	n	d							
	100	-	-	-	-	-	-	-	-	-	-	-	-	-	-	-	L	-	-	-	-	-	-	-	-	-	-	-	-	-	-	-	-	-	-	-	-	-
	54	-	I	-	-	-	-	-	-	-	-	-	-	V	A	M	-	V	-	-	-	-	-	-	-	-	-	-	K	-	n	d							
	56	n	d									n	d									n	d							-	-	-	-	-	-	-	-	-	-
	48	-	I	-	-	-	-	-	-	-	-	-	-	V	A	-	-	V	-	-	-	-	-	-	-	-	-	-	K	-	n	d							
HLA-A2	39	-	I	-	-	-	-	-	-	-	-	-	-	V	A	-	-	-	-	-	-	-	-	-	-	-	-	-	K	-	-	-	-	-	-	-	-	-	-
-ve	45	-	I	-	-	-	-	-	-	-	-	-	-	V	A	-	-	-	-	-	-	-	-	-	-	-	-	-	K	-	-	-	-	-	-	-	-	-	-
pts	45B	-	I	-	-	-	-	-	-	-	-	-	-	V	A	-	-	-/V	-	-	-	-	-	-	-	-	-	-	K	-	n	d							
	51	-	I	-	-	-	-	-	-	-	-	-	-	V	A	-	-	V	-	-	-	-	-	-	-	-	-	-	K	-	n	d							
	101	-	I	-	-	-	-	-	-	-	-	n	d									n	d							-	-	-	-	-	-	-	-	-	-
	102	-	-	-	-	-	-	-	-	-	-	-	-	-	-	-	L	-	-	-	-	n	d							-	-	-	-	-	-	-	-	-	-

(E)

Pt No.	G	I	N	A	V	A	Y	Y	R	G	L	D	V	S	V	S	V	V	I	V	G	R	I	I	L	Q	E	F	D	E	M	E	E	C	A	S	H	L	P	Y
43	-	V	-	-	-	-	-	-	-	-	-	-	-	-	-	C	-	-	-	-	-	-	V	V	-	R	-	-	-	-	-	-	-	-	S	Q	-	-	-	-
55	-	V	-	-	-	-	-	-	-	-	-	-	-	-	-	C	-	-	-	-	-	-	-	V	-	R	-	-	-	-	-	-	-	-	S	Q	-	-	-	-
103	-	-	-	-	-	-	-	-	-	-	-	-	-	-	-	C	-	-	-	-	-	-	V	V	-	-	-	-	-	-	-	-	-	-	S	Q	-	-	-	-
28	-	-	-	-	-	-	-	-	-	-	-	-	-	-	-	C	-	-	-	-	-	-	V	V	-	R	-	-	-	-	-	-	-	-	S	Q	-	-	-	-
28B	-	V	-	-	-	-	-	-	-	-	-	-	-	-	-	C	-	-	-	-	-	-	V	V	-	R	-	-	-	-	-	-	-	-	S	Q	-	-	-	-
52	-	**V**	-	-	-	-	-	-	-	-	-	-	-	-	-	C	-	-	-	-	-	-	V	V	-	-	-	-	-	-	-	-	-	-	S	Q	-	-	-	-
106	-	V	-	-	-	-	-	-	-	-	-	-	-	-	-	C	-	-	-	-	-	-	-	V	-	R	-	-	-	-	-	-	-	-	S	Q	-	-	-	-
25	-	-	-	-	-	-	-	-	-	-	-	-	-	-	-	C	-	-	-	-	-	-	V	V	-	R	-	-	-	-	-	-	-	-	S	Q	-	-	-	-
45	-	I	-	-	-	-	-	-	-	-	-	-	-	-	-	C	-	-	-	-	-	-	-	V	-	R	-	-	-	-	-	-	-	-	S	Q	-	-	-	-
045B	-	I/V	-	-	-	-	-	-	-	-	-	-	-	-	-	C	-	-	?	-	-	-	-	V	-	R	-	-	-	-	-	-	-	-	S	Q	-	-	-	?
51	-	V	-	-	-	-	-	-	-	-	-	-	-	-	-	C	-	-	-	I	-	-	V	V	-	-	-	-	-	-	-	-	-	K	-	S	Q	-	-	-	-
54	-	V	-	-	-	-	-	-	-	-	-	-	-	-	-	C	-	-	-	-	?	-	-	V	-	R	-	-	-	-	-	-	-	-	S	Q	-	-	-	-
27	-	L	-	-	-	-	-	-	-	-	-	-	-	-	-	**C**	-	-	-	-	-	-	**V**	**V**	-	**R**	-	-	-	-	-	-	-	-	**S**	**Q**	-	-	-	-
38	-	L	-	-	-	-	-	-	-	-	-	-	-	-	-	C	-	-	-	-	-	-	V	V	-	-	-	-	-	-	-	-	-	M	-	del	-	-	-	-
53	n	d														C	-	-	-	-	-	?	V	V	-	R	-	-	-	-	-	-	-	-	S	Q	-	-	-	-
101	n	d														C	-	-	-	-	-	-	-	-	-	R	-	-	-	-	-	-	-	-	S	Q	-	-	-	-
102	n	d														C	-	-	-	-	-	-	-	V	-	R	-	-	-	-	-	-	-	-	S	Q	-			
40	-	V	-	-	-	-	-	-	-	-	-	-	-	-	-	C	-	-	-	-	-	-	-	V	-	R	-	-	-	-	-	-	-	-	S	Q	-	-	-	-
040B	-	V	-	-	-	-	-	-	-	-	-	-	-	-	-	C	-	-	-	-	-	-	-	V	-	R	-	-	-	-	-	-	-	-	S	Q	-	-	-	-
48	-	V	-	-	-	-	-	-	-	-	-	-	-	-	-	n	d									n	d													
39	-	-	-	-	-	-	-	-	-	-	-	-	-	-	-	n	d									n	d													
50	-	V	-	-	-	-	-	-	-	-	-	-	-	-	-	n	d									n	d													
46	-	-	-	-	-	-	-	-	-	-	-	-	-	-		n	d									n	d													
36	n	d														n	d									n	d													
37	n	d														n	d									n	d													
56	n	d														n	d									n	d													
100	n	d														n	d									n	d													

Pt No.	A	P	N	Y	S	R	A	L	W	R	V	A	A	E	E	L	T	R	D	P	T	T	P	L	A	R	F	Q	V	G	L	N	Q	Y	L	V	G	S	Q	L	P	A	L	V	V	G	V	V	C	A
28	-	-	-/Y	-	K	F	-	-	-	-	-	S	-	-	-	-	-	-	-	-	-	-	-	-	-	-	-	R	-	-	H	E	-	P	-	-	-	-	-	-	-	-	-	-	-	-	-	-	-
028B	S	-	-	-	K	F	-	-	-	-	-	S	-	-	-	-	-	-	-	-	-	-	-	-	-	-	-	R	-	-	H	E	-	P	-	-	-	-	-	-	-	-	-	-	-	-	-	-	-
45	-	-	-	-	K	F	-	-	-	-	-	S	-	-	-	-	-	-	-	-	-	-	-	-	-	-	-	R	-	-	H	E	-	P	-	-	-	-	-	-	-	-	-	-	-	-	-	-	-
045B	n	d														-	-	-	-	-	-	-	-	-	-	-	n	d															n	d							
103	-	-	-	-	-	-	-	-	-	-	-	-	-	-	-	-	-	-	-	-	-	-	-	-	-	-	-	-	-	-	-	-	V	-	-	-	-	-	-	-	-	-	-	-	-	-	-	-	-
46	-	-	-	-	T	F	-	-	-	-	-	S	-	-	-	-	-	-	-	-	-	-	-	-	-	-	-	R	-	-	H	-	Y	P	-	-	-	-	-	-	-	-	-	-	-	-	-	-	-
39	-	-	-	-	**T**	**F**	-	-	-	-	-	**S**	-	-	-	-	-	-	-	-	-	-	-	-	-	-	-	**R**	-	-	**H**	**D**	-	**P**	-	-	-	-	-	-	-	-	-	-	-	-	-	-	-
38	-	-	-	-	T	F	-	-	-	-	-	-	-	-	-	-	-	-	-	-	-	-	-	-	-	-	-	L	-	-	-	-	-	-	-	-	-	-	-	-	-	-	-	-	-	-	-	-	-
55	-	-	-	-	T	F	-	-	-	-	-	S	-	-	-	-	-	-	-	-	**I**	-	-	-	-	-	-	R	-	-	H	D	-	P	-	-	-	-	-	-	-	-	n	d					
56	n	d														-	-	-	-	-	-	-	-	-	-	-	n	d															-	-	-	-	-	-	-	-	-
43	-	-	-	-	T	F	-	-	-	-	-	S	-	-	-	-	-	-	-	-	-	-	-	-	-	-	-	S	-	-	H	D	-	P	-	-	-	-	-	-	-	-	-	-	-	-	-	-	-
51	-	-	-	-	T	F	-	-	-	-	-	S	-	-	-	-	-	-	-	-	-	-	-	-	-	-	-	R	-	-	H	-	Y	P	-	-	-	-	-	-	-	-	n	d					
48	-	-	-	-	T	F	-	-	-	-	-	S	-	-	-	-	-	-	-	-	-	-	-	-	-	-	-	R	-	-	H	D	-	-	-	-	-	-	-	-	-	-	n	d					
52	n	d														-	-	-	-	-	-	-	-	-	-	-	n	d															-	-	-	-	-	-	-	-	-
53	-	-	-	-	K	F	-	-	-	-	-	S	-	-	-	-	-	-	-	-	-	-	-	-	-	-	-	R	-	-	H	E	-	O	-	-	-	-	-	-	-	-	**n**	**d**					
54	-	-	-	-	T	F	-	-	-	-	-	S	-	-	-	-	-	-	-	-	-	-	-	-	-	-	-	R	-	-	H	D	-	P	-	-	-	-	-	-	-	-	n	d					
25	-	-	-	-	T	F	-	-	-	-	-	S	-	-	-	-	-	-	-	-	-	-	-	-	-	-	-	R	-	-	H	D	-	P	-	-	-	-	-	-	-	-	-	-	-	-	-	-	-
106	-	-	-	-	T	F	-	-	-	-	-	S	-	-	-	nd											-	R	-	-	H	D	-	P	-	-	-	-	-	-	-	-	-	-	-	-	-	-	-
102	n	d														-	-	-	-	-	-	-	-	-	-	-	n	d															-	-	-	-	-	-	-	-	-
101	n	d														-	-	-	-	-	-	-	-	-	-	-	n	d															-	-	-	-	-	-	-	-	-
36	n	d														nd											n	d															-	-	-	-	G/R	-	-	-	-
100	n	d														nd											n	d															-	-	-	-	-	-	-	-	-
37	n	d														-	-	-	-	-	-	-	-	-	-	-	n	d															-	-	-	-	-	-	-	-	-
40	n	d														-	-	-	-	-	-	-	-	-	-	-	n	d															n	d							
040B	n	d														-	-	-	-	-	-	-	-	-	-	-	n	d															n	d							
27	n	d														-	-	-	-	-	-	-	-	-	-	-	n	d															n	d							
50	n	d														-	-	-	-	-	-	-	-	-	-	-	n	d															n	d							

Viral sequence was determined at baseline and at any point of viral relapse (designated by B after patient ID). The HCV vaccine immunogen sequence is given in the top line of each table. A dashed line below indicates that an amino acid is identical to that in the vaccine immunogen. The epitopes to which individual patients have made a T-cell response (as measured by ex vivo IFNγ-ELISpot assay) are shown in bold red font. nd= not determined ? = Amino-acid not called.

Table 6-5. HCV Viral sequence at mapped T-cell epitopes in patients who responded to vaccination with ChAd3-NS/Ad6-NS

Pt No.	Epitope/15mer identified	Viral sequence at epitope
27	CVNGVCWTV KLSGLGINAV LTTGSVVIVGRIILS / SVVIVGRIILSGRPA QEFDEMEECASHLPY ILAGYGAGVAGALVA RVCEKMALYDVVSTL RPRWFMLCLLLLSVG	C**I**NGVCWTV KL**VS**LG**L**NAV **C**VVIVGR**VV**L **R**EFDEMEEC**SQ**HLPY ILAGYGAGVAGALVA RVCEKMALYDVVS**K**L RPRWF**WF**CLLLL**AA**G
28	KLSGLGINAV	KL**VA**LGI/**V**NAV
28B	no detectable response	KL**VA**LG**V**NAV
50	KLSGLGINAV	KL**VA**LG**V**NAV
50B	no detectable response	KL**VA**LG**V**NAV
39	TPSPAPNYSRALWRV / APNYSRALWRVAAEE FQVGLNQYLVGSQLP LSRARPRWFMLCLLL / RPRWFMLCLLLLSVG	APNY**TF**ALWRV**SA**EEY F**R**VGL**HD**Y**P**VGSQLP nd*
45	HSKKKCDEL VTLTHPITKYIMACM	HSK**R**KCDEL **II**LTHPITKYIMACM
45B	no detectable response no detectable response	HSK**R**KCDEL **II**L/VTHPITKYIMACM
54	ARMILMTHF	**V**RMI**LL**THF
55	CVNGVCWTV KLSGLGINAV LTRDPTTPLAR	C**I**NGVCWTV KL**VA**LG**V**NAV LTRDP**I**TPLAR
103	KLSGLGINAV	KL**VA**LGINAV
40	KLSGLGINAV	KL**VAM**G**V**NAV
40B	No response to KLSGLGINAV CVNGVCWTV	KL**VAM**G**V**NAV C**I**NGVCWTV
53	CVNGVCWTV ALVVGVVCA	C**I**NGVCWTV nd*
52	GINAVAYYRGLDVSV	G**V**NAVAYYRGLDVSV

The amino acid sequence of the epitopes targeted in each patient is shown alongside the endogenous viral sequence in the patient. Non-homologous amino acids are highlighted in **red.** nd*=not determined. B = assessed after viral relapse

6.5.8 Cross-recognition of variants by vaccine-induced T-cells

I next assessed whether vaccine induced T-cells could recognise endogenous viral peptide-variants using IFNγ ELISpot and HLA class-I pentamers. Vaccine induced T-cells targeting the vaccine immunogen at $NS3_{1406}$ KLSGLGINAV, $NS3_{1395}$ HSKKKCDEL and $NS5B_{2804}$ LTRDPTTPLA failed to recognise circulating autologous variants at these epitopes (**figure 6-8A-C**). In addition, T-cells

targeting the dominant $NS3_{1406}$ epitope, failed to recognise an additional two variant peptides (KLVALGINAV and KLVSLGLNAV) in the patient cohort. HLA-class-I pentamers (epitopes $NS3_{1406}$ and $NS3_{1073}$) matching either vaccine immunogen or endogenous variants confirmed the loss of cross-reactivity to the $NS3_{1406}$ KLSGLGINAV endogenous variants (**figure 6-9**). Partially cross-reactive T-cell responses between vaccine immunogen and endogenous viral sequences were observed at epitopes $NS3_{1073}$ CVNGVCWTV and $NS3_{1411-1425}$ GINAVAYYRGLDVSV (**figure 6-8D-E**).

Sequence analysis at epitopes where HLA restriction was defined showed that genetic mismatch between immunogen and circulating virus was significantly associated with response to vaccination (p = 0.0063**; **figure 6-8F**). For example, at the HLA-B8 $NS3_{1395}$HSKKKCDEL epitope, circulating virus matched the immunogen in 4/6 HLA-B8 patients, however, the only patient responding to this epitope (patient 045) had the well described escape variant $NS3_{1395}$ HSK**R**KCDEL (**Timm et al. 2004**) at baseline. Similarly, at epitope LTRDPTTPLAR, 25 viral sequences matched the immunogen but only the patient with a variant epitope (LTRDP**I**TPLAR) responded to vaccination (**Table 6-4** and patient 055 **Table 6-5**). Nevertheless, genetic mismatch did not guarantee a response to vaccination, and no specific viral sequence at any epitope was predictive of a response to vaccination. For example, at epitope HLA-A2 $NS5_{2594}$ ALYDDVSTL identical endogenous epitope variants (ALYDVVS**K**L) were found in 8/17 HLA-A2 patients, only one of whom (027) made a T-cell response to this epitope after vaccination. Similarly at epitope HLA-A2 $NS3_{1406}$ KLSGLGINAV 3/4 variant epitopes identified in vaccine responders were also found in HLA-A2 non-responders (**Table 6-4**).

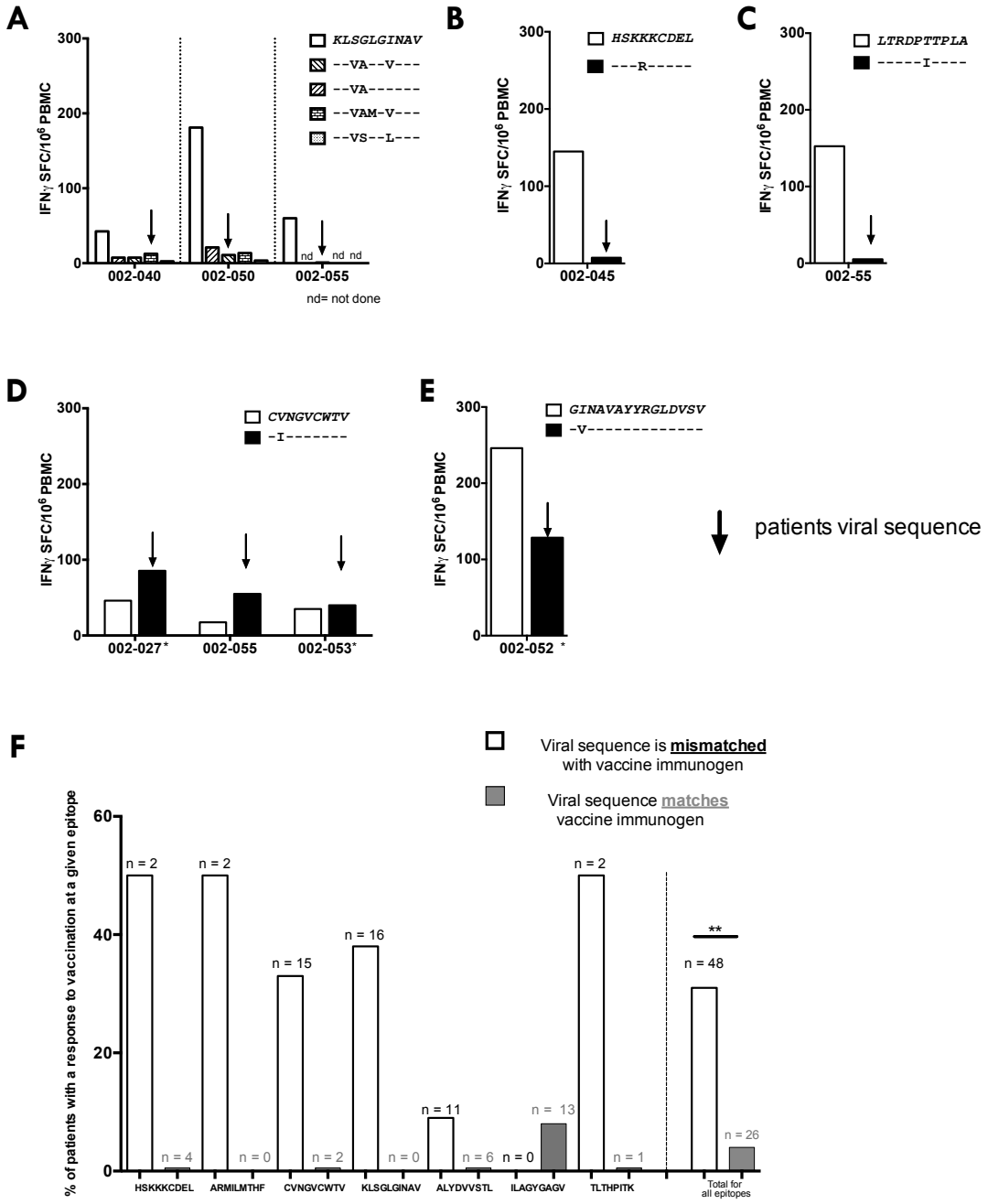


Figure 6-8. The cross-reactivity of vaccine induced T-cells to circulating viral antigen and the frequency of responders to vaccination when viral sequence is matched or mismatched with vaccine immunogen: (**A-E**) T-cell responses (IFNγ ELISpot) to peptide variants homologous to vaccine immunogen and circulating autologous virus at epitopes (**A**) KLSGLGINAV (patients 040, 050 and 055), (**B**) HSKKKCDEL (patient 045), (**C**) LTRDPTTPLA (patient 055), (**D**) CVNGVCWTV (patient 027, 055 and 053), and (**E**) GINAVAYYRGLDVSV (patient 052). Vaccine sequence in italics, with endogenous variants below. Arrow=Patient's viral sequence. (**F**) The percentage of HCV patients (with endogenous viral sequence that is completely homologous (matched) or mismatched with vaccine immunogen) who have a

detectable T-cell response (IFNγ ELISpot) at any time after vaccination to a given epitope target with known HLA restriction.

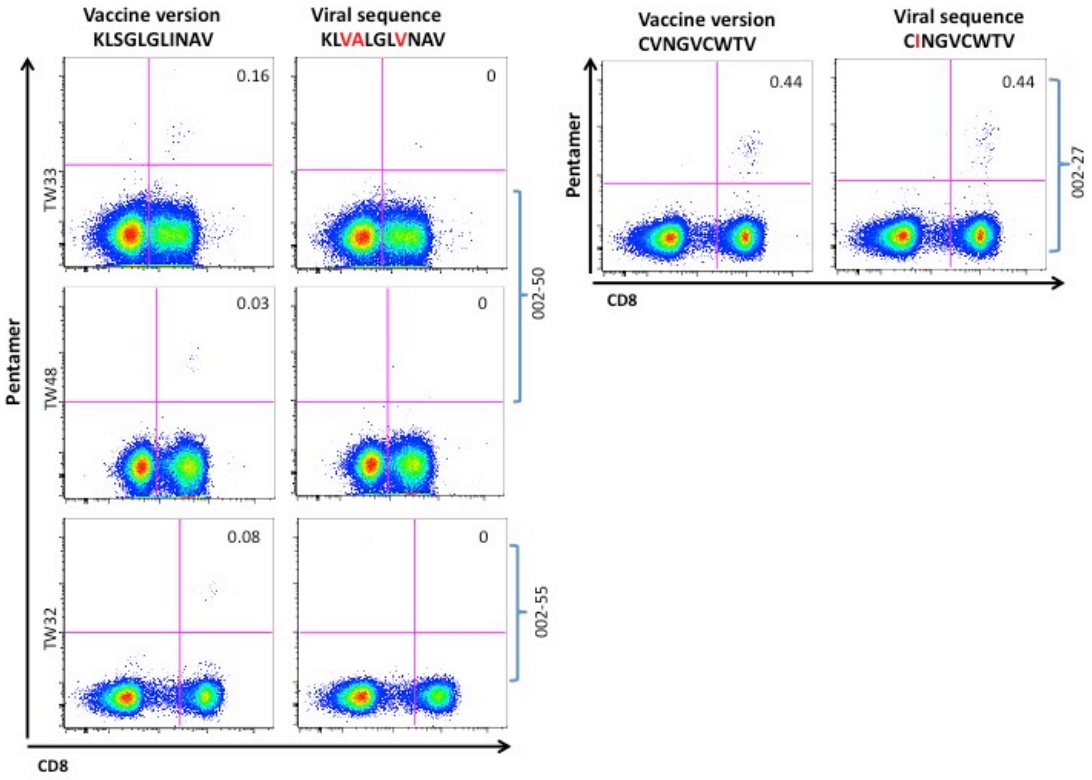


Figure 6-9. Cross-reactivity of T-cells targeting HLA-A2 restricted epitopes by MHC class I pentamer staining: CD8+ T-cells induced by the vaccine immunogen at epitopes KLSGLGLINAV ($NS3_{1406}$; left panels) and CVNGVCWTV ($NS3_{1073}$; right panels) stained with MHC class I pentamers loaded with peptides matching the vaccine sequence of a common variant sequence (amino acids that vary from vaccine immunogen are highlighted in red. % pentamer+ $CD8^+$ T-cells is represented in the top right of each plot. Cells are gated on live $CD3^+$ cells. Patient numbers are shown to the right of plots.

6.5.9 Sequence variation at the population level

Using genotype-1a/1b sequences from the los Alamos database I evaluated the variability of the 15 vaccine induced T-cell epitopes at the population level by Shanon Entropy Score (SES; median 2149 sequences, range 1131-3896 /epitope). T-cell epitopes were generally variable at a population level (**figure 6-10A**). The

most dominant $NS3_{1406}$ KLSGLGINAV was the most variable, with no single variant present in > 30% of sequences at population level (**figure 6-10B**). A minority of epitopes were found to be highly conserved (e.g. $NS4B_{1851}$ ILAGYGAGV in 97.3% of genotype-1 sequences and homologous to vaccine immunogen; SES 0.35; **figure 6-10C**). However, at one conserved epitope $NS5B_{2804}$ LTRDPTTPLAR (SES 0.28) where 89% of population genotype-1 sequences were identical with the vaccine immunogen (**figure 6-10D**) the viral sequence in the only vaccinee responding to this epitope was a non cross-reactive variant.

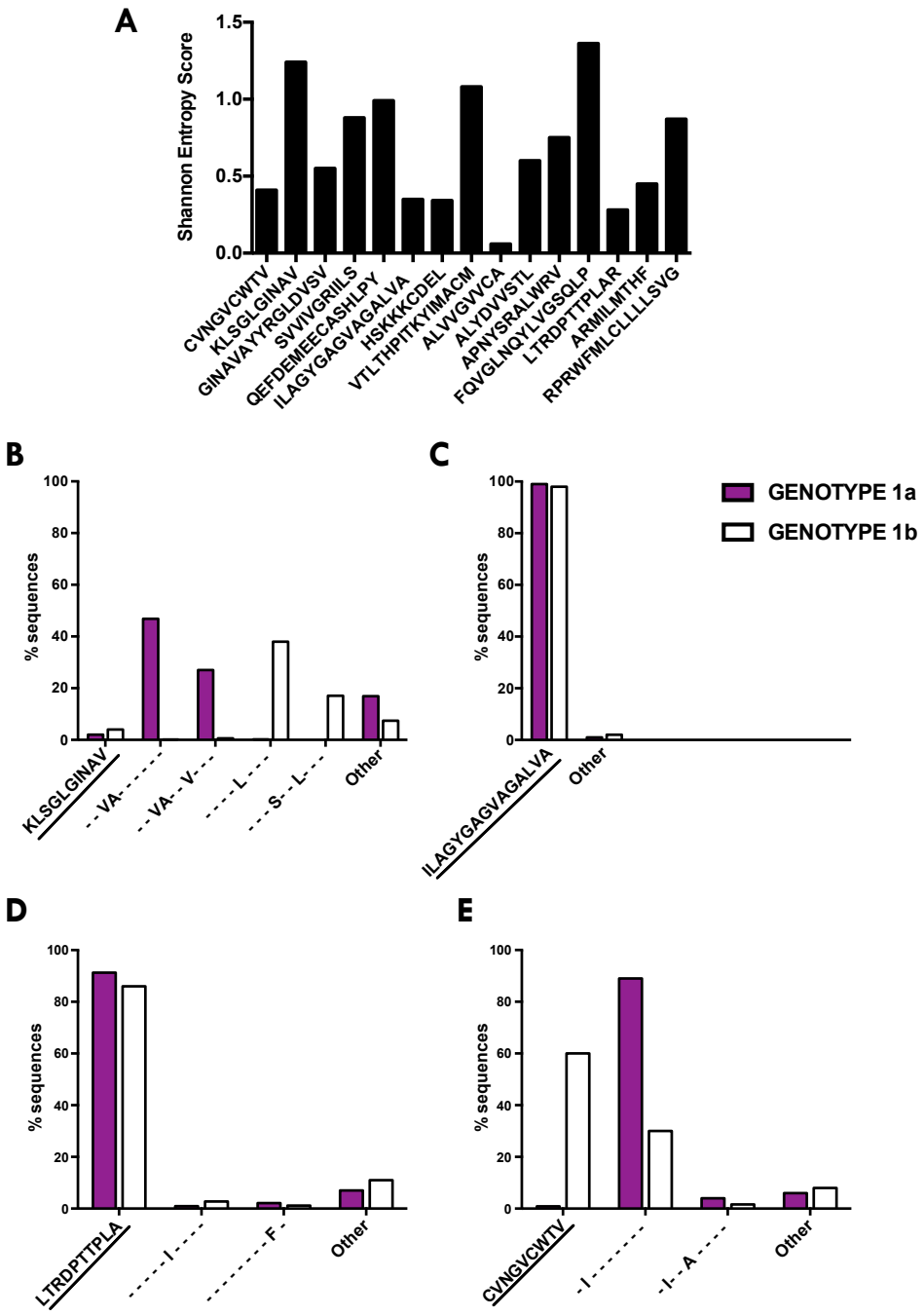


Figure 6-10. Viral variability at a population level of HCV T-cell epitopes: (**A**) The degree of variability in genotype 1 HCV sequences at identified epitopes in patients vaccinated with ChAd3-NS/Ad6-NS is defined using Shannon Entropy in a median of 2149 sequences (range 1131-3896) for each epitope derived from the Los Alamos database. A low Shannon entropy score indicates a conserved epitope. (**B-E**) The population level frequency of HCV sequence variants at 4 epitopes grouped by subtype 1a or 1b is given. The variant that corresponds to the vaccine immunogen version is underlined (x axis).

6.5.10 Vaccine-induced T-cell function in patients with Chronic HCV

I next used HLA class-I pentamers to examine the magnitude and phenotype of vaccine-induced CD8+ T-cells pre-vaccination, post-boost, and at the end of the study, and compared these with previously published data using an identical vaccine regime in healthy volunteers (**Barnes et al. 2012**)(**figure 6-11**). This analysis confirmed that the magnitude of the responses were significantly lower in HCV infected patients than healthy volunteers at the epitope level (**figure 6-11A**). A subset of patients had small but detectable CD8+ T-cell responses pre-vaccination and changes in the phenotype of these T-cell responses after vaccination was assessed and compared with healthy volunteers (**figure 6-11B-C**). The proportion of pentamer+ HCV-specific T-cells was high in patients for the effector memory subset (CCR7-/CD45RA) at baseline, and remained significantly enriched after vaccination compared to healthy volunteers. There was no difference in bulk CD8+ memory subsets in patients compared to healthy volunteers (**figure 6-11D**). In patients, pentamer+ T-cells were generally low in markers of cytotoxicity and activation (granzyme B, granzyme A, perforin, and CD38 and HLA-DR; data not shown for HLA-DR and granzyme A) at baseline. Although expression of these markers increased in response to vaccination they remained significantly lower than that observed in healthy volunteers at peak response post-boost (**figure 6-11C**). For Granzyme B this difference was maintained to the end of the study. PD-1 expression was high at baseline and remained high after vaccination in patients and healthy volunteers (**figure 6-11C**), although interpretation of this observation is complicated by the fact that PD-1 expression is both a marker of exhaustion and activation.

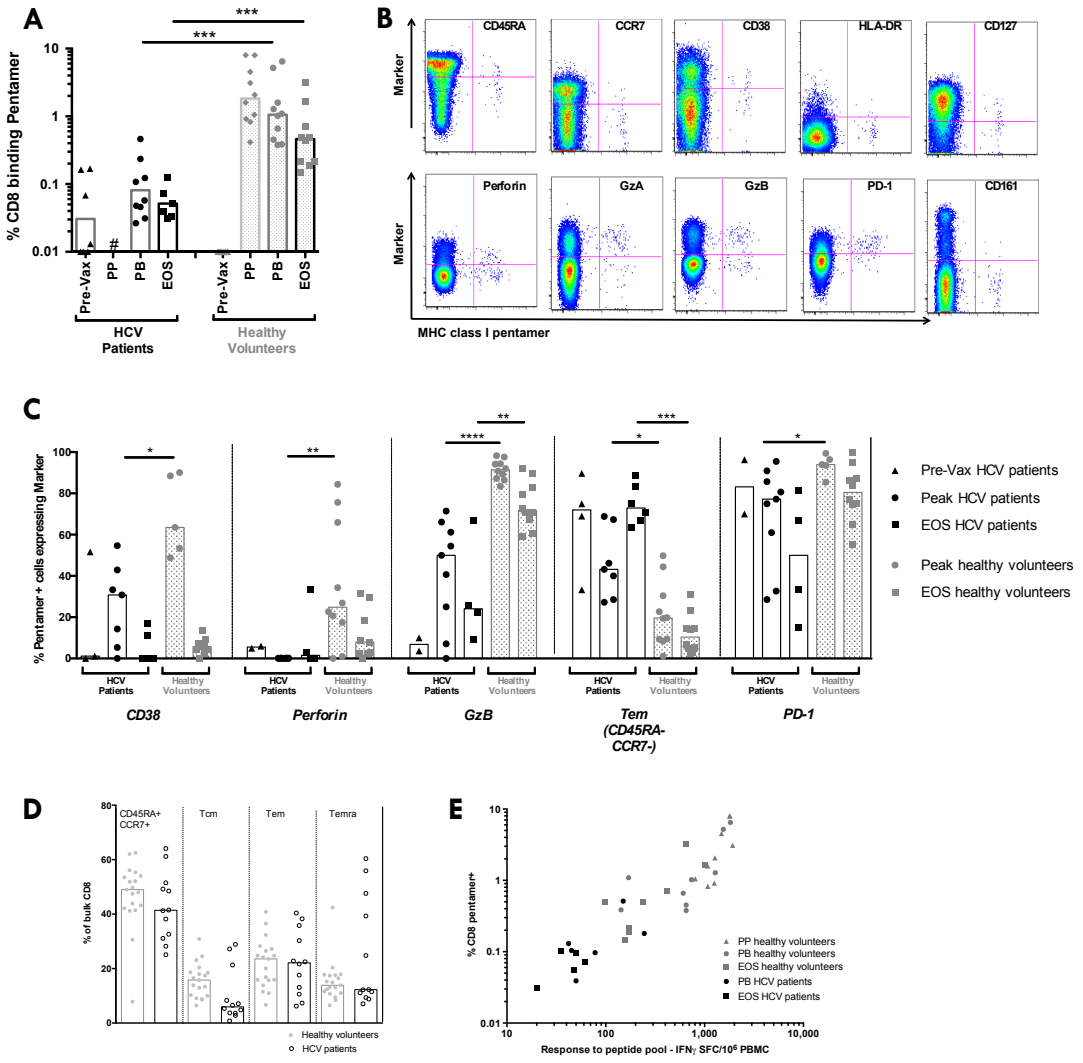


Figure 6-11. Comparison of Phenotype and function of vaccine induced HCV-specific T-cells in patients vs. healthy volunteers: (**A**) Magnitude of HCV-specific CD8+ T-cell responses *ex vivo* detected by MHC class I pentamers ($NS3_{1436}$ ATDALMTY, $NS3_{1406}$ KLSGLGINAV, $NS3_{1073}$ CVNGVCWTV) in healthy volunteers (grey) vs. HCV-infected patients (black) pre-vaccination (pre-vax), post-prime (PP); 2-4 weeks after ChAd3-NS, post Ad6-NS boost vaccination (PB); 2-8 weeks, and at the end of the study (EOS); 22-50 weeks post-boost. Bars at median. Mann-whitney t-test. (**B**) Representative FACS plots are shown for MHC class I pentamer and marker staining. ($NS3_{1406}$ KLSGLGINAV, GzA = granzyme A; GzB = granzyme B). (**C**) % of pentamer+ cells expressing a given marker in patients pre-vaccination (triangles), at the peak of the response (dots, 2-4weeks post Ad6-NS boost) or at the end of the study (EOS; squares, 22-50 weeks post Ad6-NS boost). For comparison the % of pentamer+ cells expressing a given marker in healthy volunteers (grey) receiving the same vaccinations are shown at the peak of the response (dots, 2-4weeks post ChAd3-NS prime) or at the end of the study (EOS; squares, 22-50 weeks post Ad6-NS boost). Bars at median. Mann-whitney t-test (patient screen vs patient EOS, healthy peak vs. Patient peak, healthy EOS vs Patient EOS). (**D**)

A comparison of the bulk CD8+ T-cell memory subsets in healthy volunteers vs. patients: Naïve-like (CD45RA+CCR7+), central memory (Tcm: CD45RA-CCR7+), terminal effector memory (Temra: CD45RA+CCR7-). (**E**) The magnitude of the HCV-specific T-cell response to vaccination correlating ELISpot vs. pentamer staining. Spearmans rank: healthy volunteers r = 0.8207 P<0.0001; patients r = 0.7443 p=0.0108.

A strong positive correlation between the magnitude of response as measured by ELISpot and pentamer staining suggested a population of pentamer+ cells that do not make IFNγ is not present in patients or volunteers (**figure 6-11E**).

Using intra-cellular cytokine staining CD4+ T-cell responses to HCV NS were detectable, but at a low level only (**figure 6-12**). CD8+ T-cell responses were weaker than those in healthy volunteers after ChAd3-NS prime vaccination and peaked after Ad6-NS boost vaccination in patients, as has been showed by ELISpot and pentamer staining. CD8+ T-cells produced IFNγ with some coexpression of IL-2, but with a distinct lack of TNFα production, in patients (**figure 6-12**).

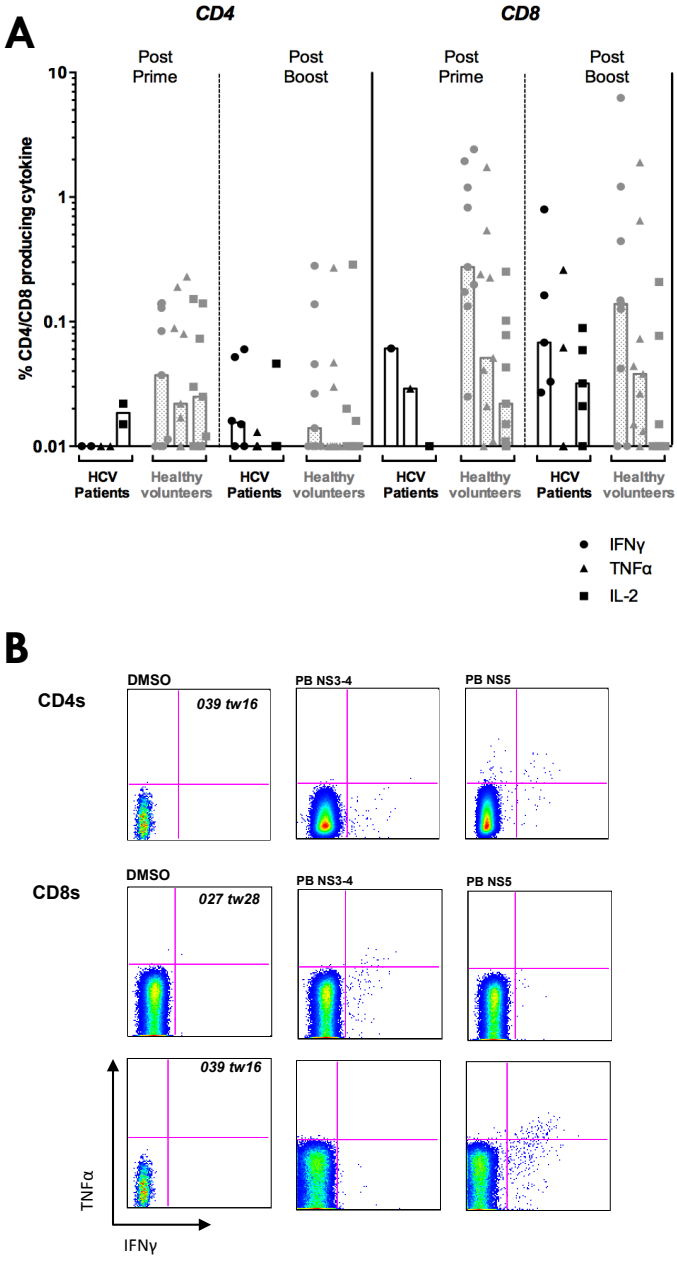


Figure 6-12. Cytokine production by vaccine-induced cells in HCV+ patients: (**A**) PBMC were stimulated with peptide pools F + G + H (NS3–4) or I + L + M (NS5). The percentage of total CD4+/CD8+ IFNγ, TNFα, or IL-2 producing T-cells at the peak post prime vaccination (2-8 weeks post ChAd3-NS) or post boost (2-4 weeks post Ad6-NS) in patients (Black) and healthy volunteers (grey). ICS was performed on all patients with an IFNγ, ELISpot response >150 SFC/10^6 PBMC. All values are after background subtraction (DMSO wells). Bars at median. (**B**) Example FACS plots showing staining of TNFα/IFNγ for CD4+ and CD8+ T-cells Patient number and treatment week are shown.

The breadth of a T-cell response is particularly important for limiting immune escape by HCV. In contrast to the broad responses detected in healthy volunteers, responses were significantly narrower when considering the number of peptide pools targeted in patients (healthy volunteers, median 5 positive pools, range 2-6 vs. HCV+ patients median 1 positive pool, range 0-5 $p < 0.0001$**** (**figure 6-13A**). A defect in *in vitro* expansion on activation with cognate antigen has been reproducibly recognised for HCV-specific T-cells (**Folgori et al. 2006a; Semmo et al. 2005; Lauer et al. 2004**). On stimulation with recombinant HCV proteins vaccine-induced HCV-specific T-cells in patients showed little or no expansion (median SI 3.5; range 3-14.6), in stark contrast to data in healthy volunteers (**figure 6-13B**). The defect in proliferative capacity appears to be specific for HCV antigens as a robust proliferative response by CMV-specific antiviral T-cells in HCV infected patients was seen (median SI 173.6; range 30.2-1104.0). Overall these data suggest that T-cells induced by vaccination in HCV infected patients remain at least partially functionally attenuated.

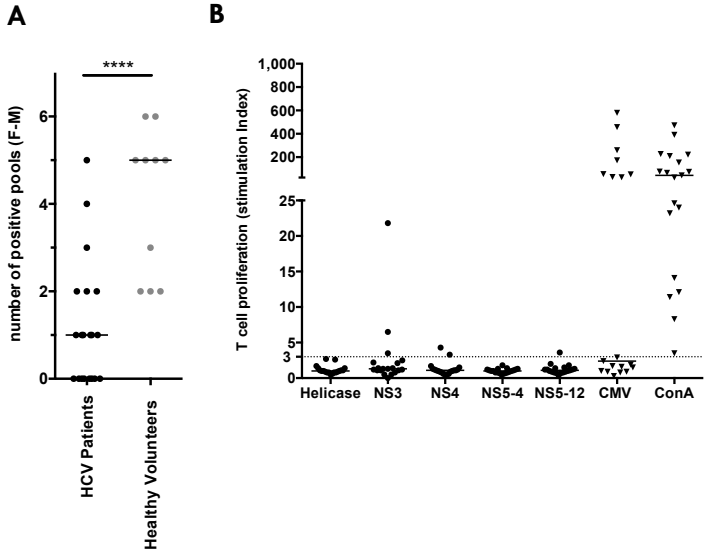


Figure 6-13. Breath and proliferative capacity of vaccine-induced T-cells in HCV+ patients: (**A**) Breadth of responses *ex vivo*. IFNγ ELISpot data for HCV infected patients (black) vs.

healthy volunteers (grey). The responses shown are the number of positive pools (see chapter 2) measured at peak magnitude during the study. (**B**) The proliferative response to recombinant HCV proteins in patients 4 weeks post Ad6-NS boost, plotted as Stimulation Index (SI). SI ≥ 3 was defined as positive. Responses to positive control antigens (concanavilin A and CMV lysate) are shown. Bars at median.

6.5.11 The magnitude and kinetics of the T-cell response in patients receiving MVA-NS boost vaccination

ChAd3-NS primed HCV-specific T-cell responses are optimally boosted by MVA-NS, rather than Ad6-NS, in healthy volunteers. Next I assessed whether the ChAd3-NS/MVA-NS vaccine regimen can induce a more balanced CD4+ and CD8+ T-cell response, of enhanced breadth, magnitude, and functionality compared to ChAd3-NS/Ad6-NS vaccine regimen in HCV infected patients, as it does in healthy volunteers.

Patients infected with genotype 1 HCV were vaccinated with ChAd3-NS after 2 (arm B2; **Table 6-1; figure 6-14A-D**) or 14 (arm B1; **figure 6-14E-H**) weeks lead-in of IFNα/rib treatment or without treatment (arm C; **figure 6-15A-D**) and all were boosted with MVA-NS 8 weeks after prime vaccination.

4/8 treated (**figure 6-14)** and 4/4 untreated (**figure 6-15**) HCV+ patients had a positive response to vaccination (defined in **Chapter 2**; a new positive pool or >30% increase in the baseline response to a single peptide pool), with the peak of the response for most individuals coming after MVA-NS boost.

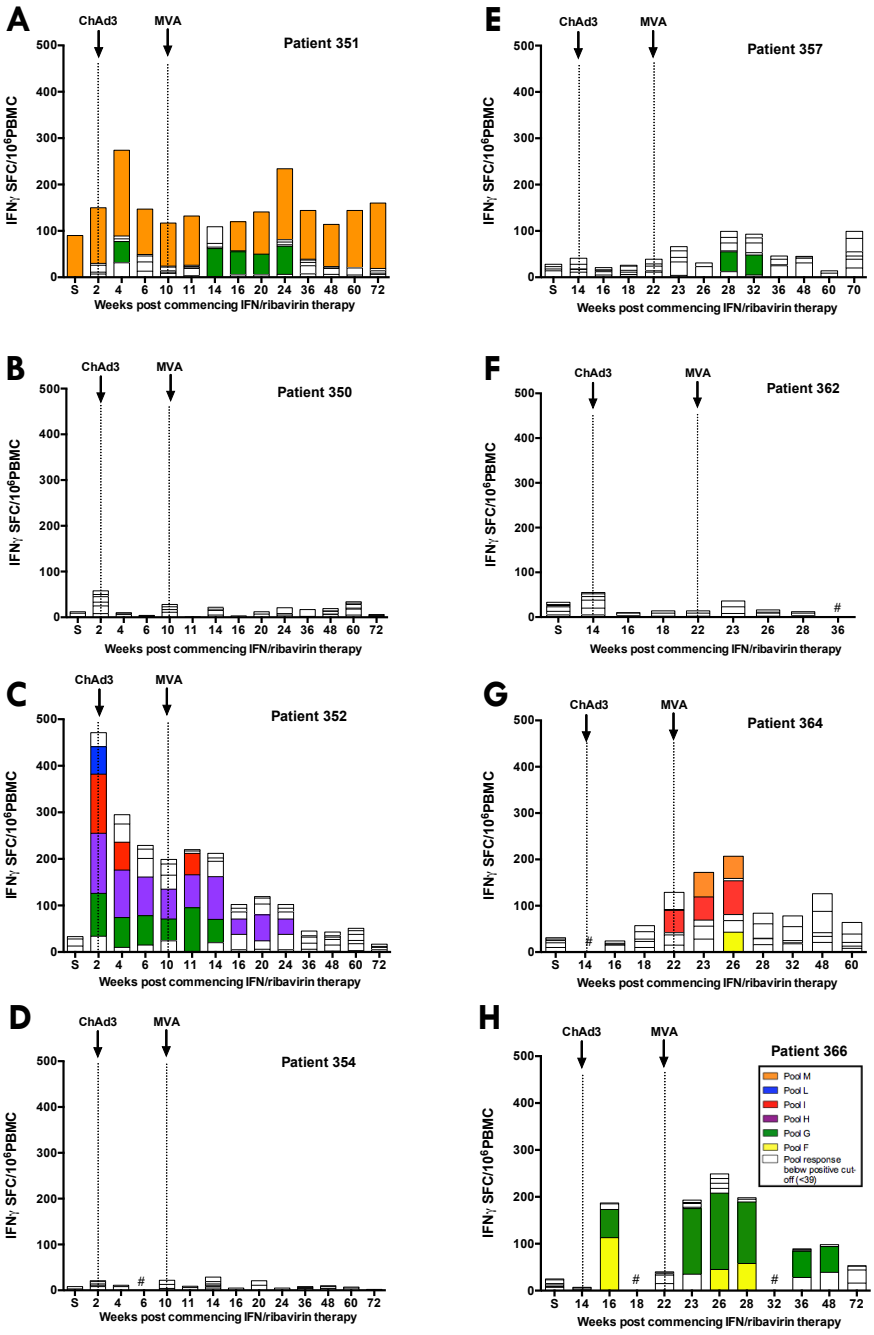


Figure 6-14. Magnitude of HCV specific T-cell responses by peptide pool in IFNα/ribavirin treated HCV+ patients receiving ChAd3-NS/MVA-NS: (**A-H**): The total *ex vivo* IFNγ ELISpot response across NS peptide pools are shown across the clinical trial for a single patient. Positive responses (>41 SFC/10^6 PBMC) to a pool are coloured. S = Screen. (**A-D**) received 2 weeks of IFNα/ribavirin treatment (48 weeks total) before vaccination, and (**E-H**) received 14 weeks of IFNα/ribavirin treatment before vaccination. Vaccinations are indicated by dashed lines.

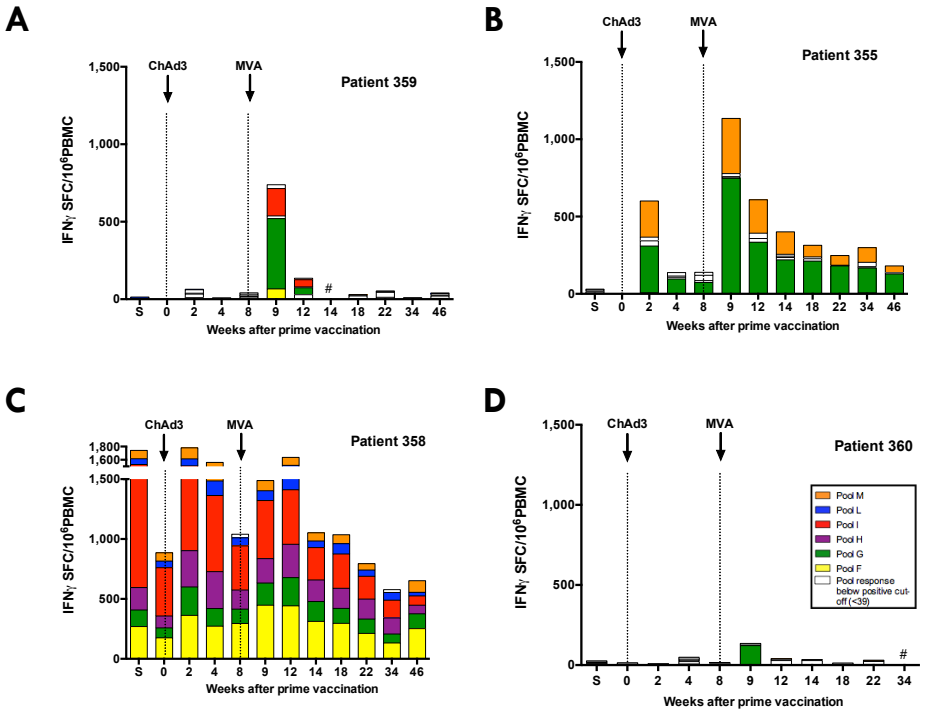


Figure 6-15. Magnitude of HCV specific T-cell responses by peptide pool in untreated HCV+ patients receiving ChAd3-NS/MVA-NS: (**A-D**): The total *ex vivo* IFNγ ELISpot response across NS peptide pools are shown across the clinical trial for a single patient. Positive responses (>41 SFC/10^6 PBMC) to a pool are coloured. S = Screen. Vaccinations are indicated by dashed lines.

When all HCV+ patients are considered together there is no significant induction of HCV-specific T-cells by prime ($p = 0.2187$) or boost vaccination ($p = 0.2031$), and T-cell responses are significantly lower in magnitude than those seen in healthy volunteers receiving the same vaccines (**figure 6-16A**). There is no clear pattern to the kinetics of the T-cell response to ChAd3-NS/MVA-NS vaccination in HCV+ patients, with some patients showing T-cell expansion after: both prime and boost vaccination (patients 351, 366, 358 and 355); after MVA-NS boost only (patients 357, 360 and 364); showing no novel detectable T-cell response to either vaccine (patients 350, 354, 352, 362; **figure 6-16B-C**). Although the peak magnitude of the T-cell response is seen after MVA-NS boost in most patients it

varied from 1 week to 6 weeks post vaccination, unlike in healthy volunteers where a peak 1 week post-MVA-NS is consistently seen (**figure 3-2**). Vaccination and induction of T-cells had no effect on HCV RNA in untreated patients (**figure 6-16C**). There is a trend for a higher T-cell response to vaccination in untreated patients, with high viral loads, relative to those receiving 2 weeks lead in of IFNα/rib (with medium viral load) and those who had undetectable or low viral load (14 weeks lead in of IFNα/rib pre-vaccination; **figure 6-16D**).

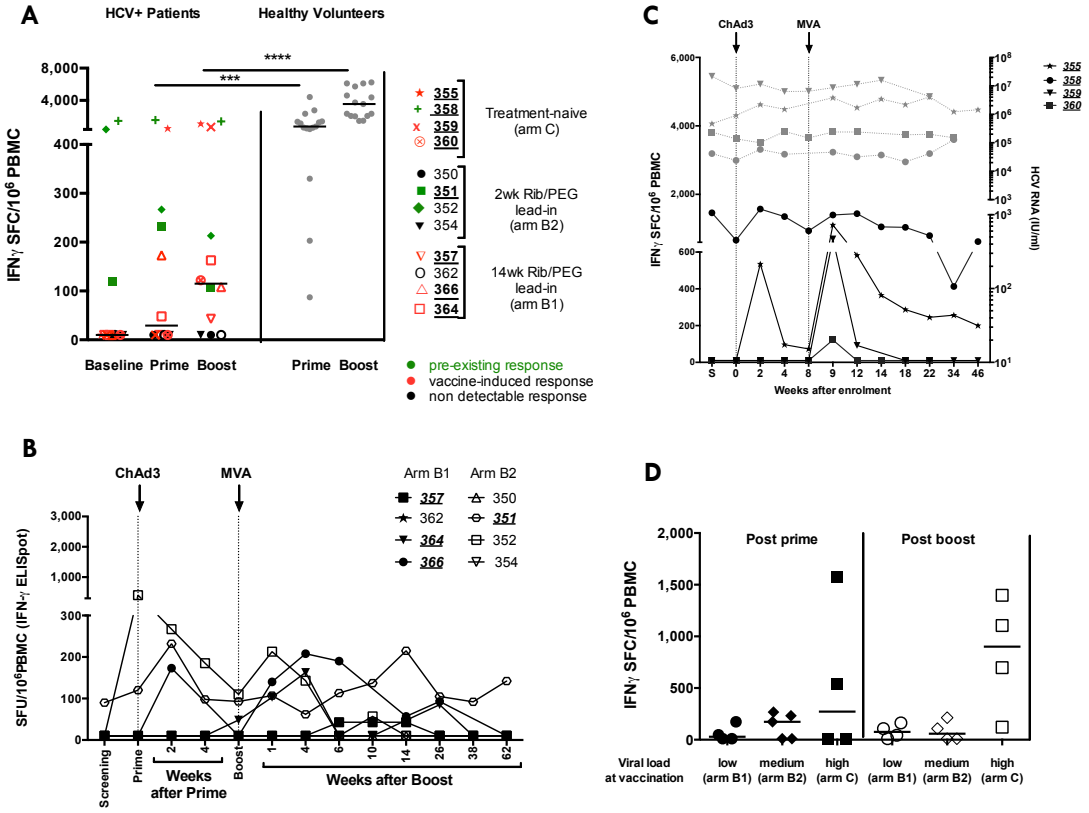


Figure 6-16. Magnitude of HCV specific T-cell responses after ChAd3-NS (prime) and MVA-NS (boost) vaccination in HCV+ patients: (**A-D**): The total *ex vivo* IFNγ ELISpot response to HCV NS is shown (sum of positive pools). Patients with a positive response are underlined. (**A**) A comparison of the total HCV-specific T-cell response in HCV+ patients at baseline and at the peak of the response post-ChAd3-NS prime or MVA-NS boost. Patients dots are coloured according to whether they had a pre-existing response to HCV NS (green),

whether they developed a detectable response post-vaccination (red) or whether no detectable response was seen across the trial (black). Also shown is the peak T-cell response to HCV NS after ChAd3-NS and MVA-NS in healthy volunteers (grey). Bar at median. Mann-Whitney t-test. (**B-C**) The kinetics of the response in individual HCV+ patients receiving ChAd4-NS/MVA-NS with 2 (arm B2) or 14 (arm B1) weeks lead-in of PEG-IFNα/rib pre-vaccination (**B**) or untreated vaccinated patients (C; arm C). (**C**) HCV RNA (IU/ml; grey dotted lines). S = screening. (**D**) A comparison of the peak response after ChAd3-NS prime and after MVA-NS boost vaccination in HCV+ patients that had low (arm B1), medium (arm B2) or high (arm C) viral loads at the time of vaccination. Bar at median. ($p>0.05$ Kruskal-Wallis multiple comparisons ANOVA for prime, and for boost).

There was no significant difference in magnitude of the peak or memory (measured 26 weeks after boost vaccination) HCV NS-specific T-cell response in treated or untreated HCV+ patients who received Ad6-NS vs. MVA-NS boost vaccination, despite MVA-NS being significantly more immunogenic in healthy volunteers (**figure 6-17A**).

Only T-cell responses targeting regions of HCV contained within the vaccine immunogen (non-structural region NS3-NS5b) were expanded during the trial in HCV+ patients; the T-cell response targeting the structural regions (Core, E1, E2, p7 and NS2; see **figure 1-1**) was unchanged throughout the trial in all patients (**figure 6-17B**).

In healthy volunteers boost vaccination with MVA-NS significantly enhanced the number of peptide pools targeted by the vaccine-induced HCV-specific T-cells, relative to Ad6-NS boost (**figure 3-5**). The number of positive peptide pools at the peak of the T-cell response during the trial was significantly reduced in patients relative to healthy controls, and patients who received MVA-NS did not

have a broader response than those who received Ad6-NS boost vaccination (p = 0.182; **figure 6-17C**)

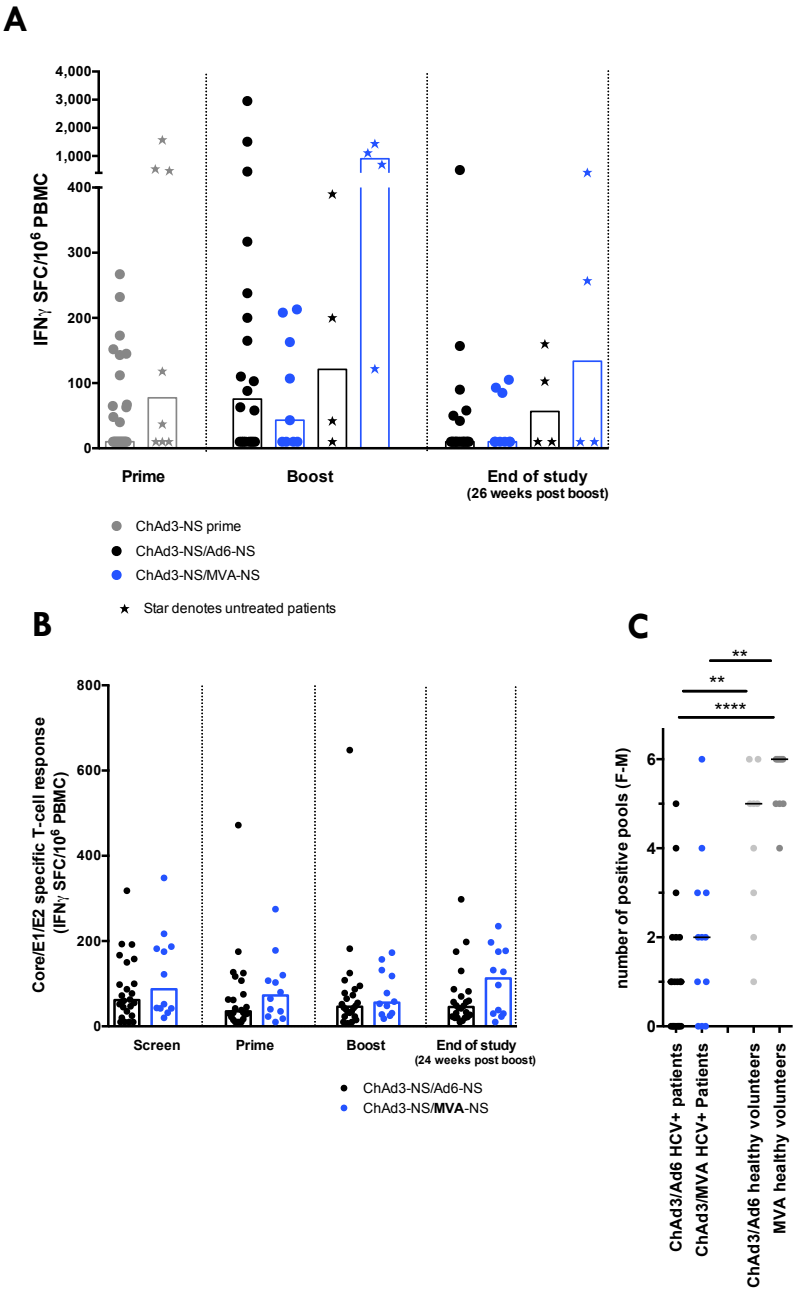


Figure 6-17. Comparison of the HCV-specific T-cell induction by ChAd3-NS/MVA-NS vs. ChAd3-NS/Ad6-NS vaccine regimens in HCV+ patients: (**A**) A comparison of the peak *ex vivo* IFNγ ELISpot response to HCV NS (sum of positive pools) in IFNα/rib treated or untreated HCV+ patients after ChAd3-NS prime vaccination, and after Ad6-NS or MVA-NS boost vaccination, and 26 weeks after Ad6-NS or MVA-NS boost vaccination (end of study). (**B**) The T-cell response to peptide pools covering the regions of HCV not included in the vaccine immunogen (Core, E1, E2, p7 and NS2; genotype 1b J4 sequence), tested in parallel (Kruskal-

Wallis multiple comparisons ANOVA, $p > 0.05$). (**C**) A comparison of the peak breadth of the T-cell response in patients and healthy volunteers receiving ChAd3-NS/MVA-NS or ChAd3-NS/Ad6-NS - defined as the maximum number of positive pools (out of 6 pools tested; labelled F-M; see **section 2.4**) at any time during the vaccine trial. Bar at median. Mann-Whitney t-test.

6.5.12 MVA-NS boosted T-cells target sequences that are mismatched between vaccine and circulating virus

The autologous virus was sequenced at three antigenic targets at baseline in all HCV+ patients vaccinated with ChAd3-NS/MVA-NS (HCV003 arms B1, B2, C; **Table 6-1**) and after boost vaccination for untreated patients (HCV003 arm C; sequencing performed by John Halliday). In all instances where a T-cell response was detected after vaccination the patient's autologous virus had 1-3 amino acids different within the epitope from the vaccine immunogen sequence (**Table 6-6**). The viral sequence in the only patient to make a T-cell response to the HLA-B8 restricted $NS3_{1395}$ epitope was a rare variant (2.1% of sequences in the los Alamos database) HSK**R**KCDEL; all other patients viral sequences were identical to the vaccine immunogen (87% of sequences in los Alamos database), including two HLA-B8+ patients. This variant sequence was poorly recognised by ChAd3-NS/Ad6-NS induced T-cells (**figure 6-8**). No change in viral sequence was seen after vaccination at the three epitope targets sequenced.

Table 6-6. Circulating HCV sequence at immunogenic epitopes (HCV003 trial)

A) HLA-B8 epitope **B**) HLA-A2 epitope C) epitops of unknown HLA restriction.

(A)

	Pt No.	H	S	K	K	K	C	D	E	L
HLA-B8 +ve pts	359	-	-	-	R	-	-	-	-	-
	354	-	-	-	-	-	-	-	-	-
	362	-	-	-	-	-	-	-	-	-
HLA-B8 neg pts	357	-	-	-	-	-	-	-	-	-
	350	-	-	-	-	-	-	-	-	-
	351	-	-	-	-	-	-	-	-	-
	352	-	-	-	-	-	-	-	-	-
	356	-	-	-	-	-	-	-	-	-
	355	-	-	-	-	-	-	-	-	-
	358	-	-	-	-	-	-	-	-	-
	360	-	-	-	-	-	-	-	-	-

(B)

	Pt No.	K	L	S	G	L	G	I	N	A	V
HLA-A2 +ve pts	357	-	-	V	A	-	-	V	-	-	-
	351	-	-	-	A	-	-	L	-	-	-
	354	-	-	T	A	M	-	-	-	-	-
	355	-	-	V	A	-	-	V	-	-	-
	360	-	-	V	A	-	-	-	-	-	-
	362	-	-	V	A	-	-	-	-	-	-
	350	-	-	V	A	-	-	-	-	-	-
	352	-	-	V	A	-	-	V	-	-	-
	356	-	-	-	-	-	-	L	-	-	-
	358	-	-	V	A	-	-	V	-	-	-
	359	-	-	V	A	-	-	V	-	-	-

(C)

Pt No.	S	R	A	R	P	R	W	F	M
357	-	-	-	-	-	-	-	-	W
351	-	-	-	-	-	-	-	-	-
355	-	-	-	-	-	-	-	-	W
360	-	-	-	-	-	-	-	-	W
362	-	-	-	-	-	-	-	L	W
350	-	-	-	-	-	-	-	-	W
352	-	-	-	-	-	-	-	-	W
356	-	-	-	-	-	-	-	I	-
358	-	-	-	-	-	-	-	-	W
359	-	-	-	-	-	-	-	-	W
365	P	-	-	-	-	-	-	P	-
361	-	-	-	-	-	-	-	-	W

Viral sequence was determined at baseline. The HCV vaccine immunogen sequence is given in the top line of each table. A dashed line below indicates that an amino acid is identical to that in the vaccine immunogen. The epitopes to which individual patients have made a T-cell response (as measured by *ex vivo* IFNγ-ELISpot assay) are shown in bold red font.

6.5.13 Functionality of the T-cell response in patients receiving MVA-NS boost vaccination

I next compared the capacity of vaccine-induced T-cells to produce antiviral and immunomodulatory cytokines in patients who received ChAd3-NS/Ad6-NS vs. ChAd3-NS/MVA-NS vaccines (**figure 6-18A**). Cytokine producing HCV-specific T-cell populations were again low in magnitude and MVA-NS failed to boost a stronger CD4+ or CD8+ T-cell response relative to Ad6-NS boost, in stark contrast to what was seen in healthy volunteers (**figures 6-12 and 3-11**). HCV-specific T-cells boosted by MVA-NS in HCV+ patients failed to proliferate on stimulation with recombinant HCV proteins (**figure 6-18B**; data shown for stimulation of PBMC 6 weeks post MVA-NS boost; PBMC taken 24-26 weeks post (n = 3) and 40-62 weeks post (n = 7) MVA-NS also showed a stimulation index <7 for all proteins in all patients).

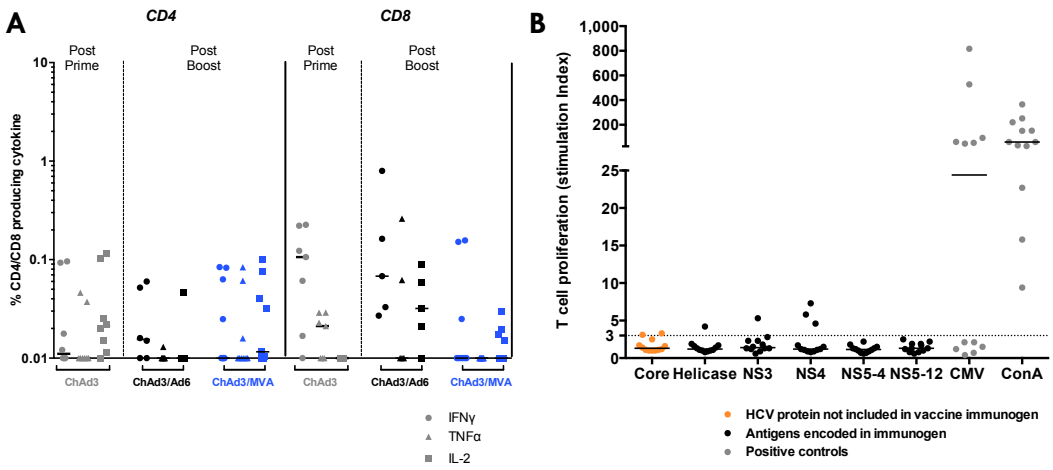


Figure 6-18. Functional analysis of MVA-NS boosted HCV-specific T-cells in HCV+ patients: (**A**) Cytokine production: PBMC were stimulated with peptide pools F + G + H (NS3–4) or I + L + M (NS5). The percentage of total CD4+/CD8+ IFNγ, TNFα, or IL-2 producing T-cells at the peak post-prime vaccination (2-8 weeks post-ChAd3-NS; grey), post-Ad6-NS boost (2-4 weeks post-Ad6-NS; black) or post-MVA-NS boost vaccination in HCV+ patients (Blue). ICS was performed on patients with an IFNγ ELISpot response >150 SFC/10^6 PBMC where PBMC were available (ChAd3-NS/Ad6-NS vaccinees: 024 and 027, 039, 103 post boost only; ChAd3-NS/MVA-NS vaccinees: 355, 358, 351, and 352, 360 post boost only). All values are after background subtraction (DMSO wells). Bars at median. Example FACS plots shown in **figure 6-12**. (**B**) **Proliferative capacity**: The proliferative response to recombinant HCV proteins in patients 6 weeks post MVA-NS boost, plotted as Stimulation Index (SI). SI ≥ 3 was defined as positive. Responses to positive control antigens (concanavilin A and CMV lysate) are shown (grey). Bars at median.

The phenotype of HCV NS-specific T-cells at the peak of the response post MVA-NS boost was assessed in patients 355, 360 (TW9) and 357 (TW28) (**figure 6-19**). A subset of inhibitory coreceptors characteristic of exhausted T-cells (PD-1, Tim-3, CTLA-4 and 2B4; (**Bengsch et al. 2010**) were also assessed on vaccine-induced T-cells. HCV NS-specific T-cells expressed high levels of CD38, perforin (**figure 6-19A**), and HLA-DR (not shown) immediately after MVA-NS vaccination, similar to that seen in healthy volunteers; in all patients fewer pentamer+ cells

expressed granzyme B and PD-1 after MVA-NS boost in HCV+ patients than in healthy controls. Pentamer+ T-cells in HCV+ patients did not express higher levels of inhibitory receptors than vaccine-induced T-cells long-term after vaccination in healthy volunteers, with the exception of Tim-3 (although not significantly different), which was also expressed on a subset of CMV-specific T-cells (**figure 6-19B**).

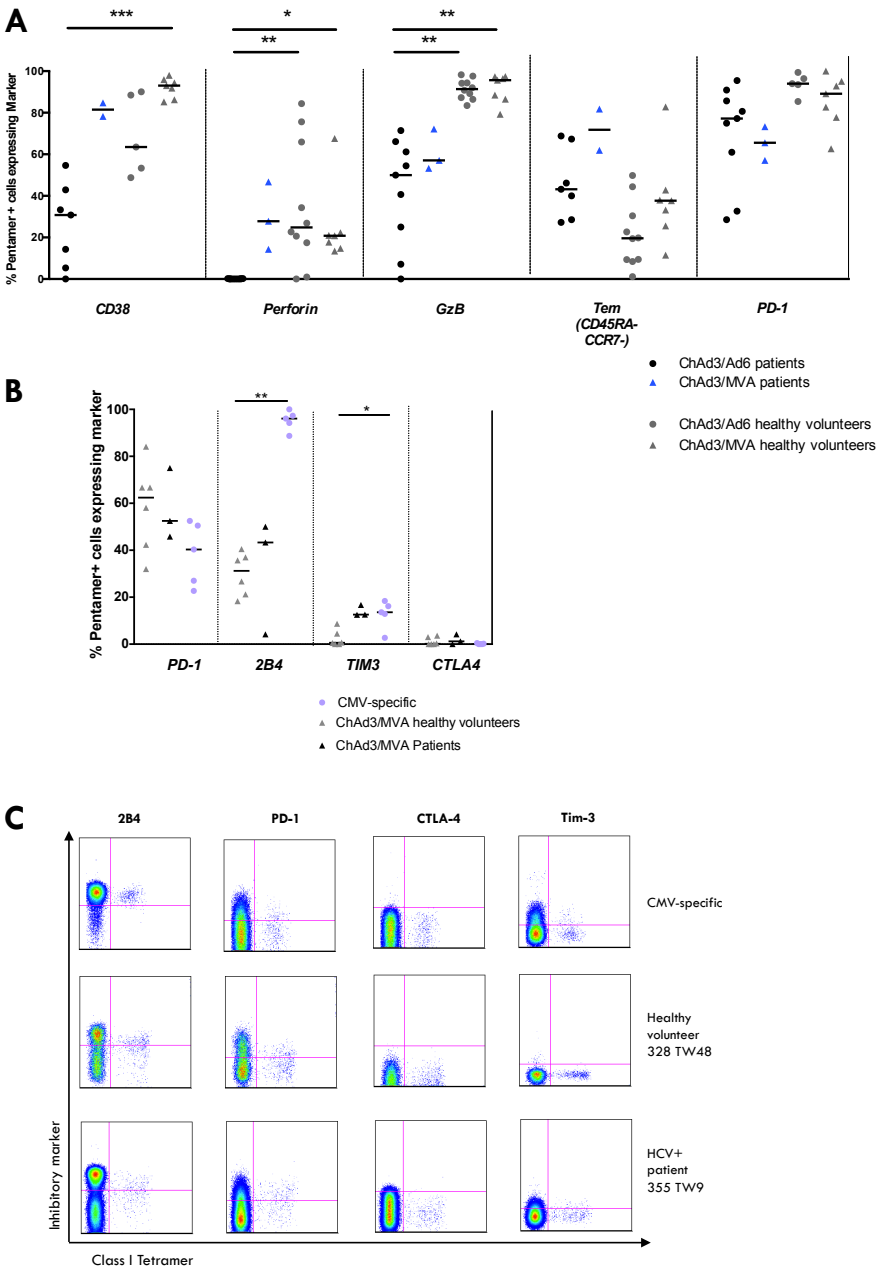


Figure 6-19. A comparison of Phenotype of vaccine induced HCV-specific T-cells in patients vs. healthy volunteers after Ad6-NS or MVA-NS boost vaccination: (**A**) The percentage of pentamer+ cells ($NS3_{1436}$ ATDALMTY, $NS3_{1406}$ KLSGLGINAV, $NS3_{1073}$ CVNGVCWTV) expressing a given marker in HCV+ patients (355, 357, 360; ChAD3-NS/MVA-NS), healthy volunteers (hcv003 arm A2, ChAD3-NS/MVA-NS; HCV001 groups 9, Ad6-NS/ChAd3-NS and groups 10-11 ChAd3-NS/Ad6-NS). CD8+ CMV-specific T-cells ($pp65_{495-504}$) in healthy volunteers were also assessed. Bars at median. (Kruskal-wallis multiple comparison ANOVA with Dunn's correction, significant differences are illustrated). (**A**) Pentamer+ cells were stained *ex vivo* at the time of peak magnitude of the T-cell response during the trial (as measured by IFNγ ELISpot; 2-4 weeks post ChAd3-NS or Ad6-NS; 1-6 weeks post MVA-NS) in HCV+ patients and healthy volunteers. Example FACS plots in **figure 6-11**. (**B**) Inhibitory receptor staining of pentamer+ cells was performed at the time of peak magnitude of the T-cell response during the trial (as above) in patients, at the end of the trial (48-74 weeks post ChAd3-NS prime; 2 healthy volunteers from HCV003 arm A3, ChAd3-NS/MVA-NS/ChAd3-NS/MVA-NS and 3 from arm A2, ChAd3-NS/MVA-NS) in healthy volunteers. (**C**) Example FACS plots of T-cell surface inhibitory marker expression gated on total CD8+ T-cells.

6.5.14 HLA-A2 allele does not have a dominant impact on overall response

In healthy volunteers there is an immunodominance of pool G (**figure 3-5**) and in all HLA-A2 individuals a significant proportion of the T-cell response is targeted at a single epitope in NS3 ($NS3_{1406}$ KLSGLGINAV). This epitope was the most commonly targeted in patients (**Table 6-3**) but all patients circulating virus had variant sequences at this epitope (**figure 6-8F**). Despite the immunodominance of this HLA-A2-restricted epitope there is no difference in the induction of T-cells by vaccination overall in patients that have the HLA-A2 allele compared to those that do not (**figure 6-18**).

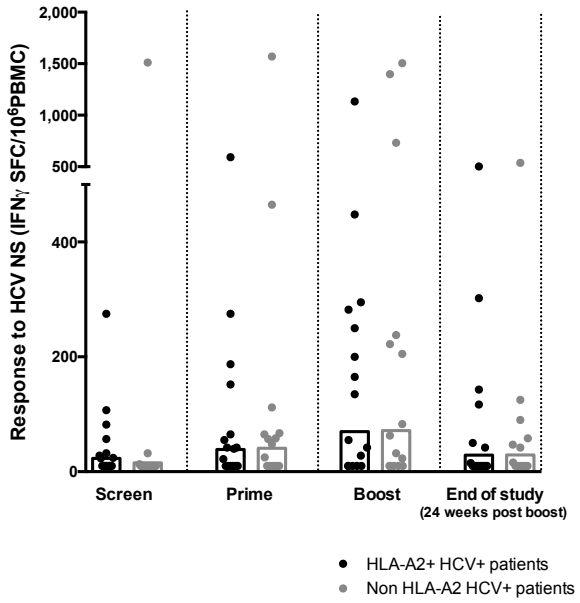


Figure 6-20. A comparison of the total T-cell response to HCV NS in HCV+ patients with and without the HLA-A2 allele: A comparison of the *ex vivo* IFNγ ELISpot response to HCV NS (sum of positive pools) in HCV+ patients who do (black) or do not (grey) possess the HLA-A2 allele. Data shown at screen and for the peak T-cell response after ChAd3-NS prime, and after Ad6-NS or MVA-NS boost vaccinations. Bars at median. (Mann-Whitney t-test $p > 0.05$ at each time point).

6.5.15 Culturing pre-vaccination HCV-specific T-cells

One possible reason why vaccine-induced T-cells are not expanded to the same degree as in healthy volunteers and why they are phenotypically different could be that HCV NS-specific T-cells are already primed during HCV infection in patients and that vaccination is boosting pre-existing and pre-exhausted T-cells rather than priming *de novo* responses. I identified 6 HLA-A2+ patients who developed a detectable T-cell response after vaccination to $NS3_{1406}$ (but who showed no detectable response pre-vaccination by ICS, pentamer or IFNγ ELISpot) and attempted to expand T-cells to detectable levels from frozen pre-vaccination PBMC. 2 of the 6 HCV+ patients developed pentamer clouds to this

epitope by day 19 of culture (all were negative at day 0, day 12 and at all time points when cultured with DMSO; **figure 6-21**). PBMC from 3 healthy HLA-A2+ volunteers who showed strong responses to this epitope after-vaccination were also cultured; as expected these volunteers did not develop a pentamer clouds at day 19, showing our cell culture method does not prime *de novo* responses.

In some cases the IFNγ ELISpot is insensitive to the detection of HCV specific T-cell responses that are present pre-vaccine in HCV-infected patients, therefore, vaccination may be boosting pre-existing T-cells rather than inducing *de novo* responses. The absence of cultured responses in all individuals who respond to vaccination could suggest some responses are primed by vaccination, however, it is also likely that our culture method is not sensitive enough to expand all pre-primed responses.

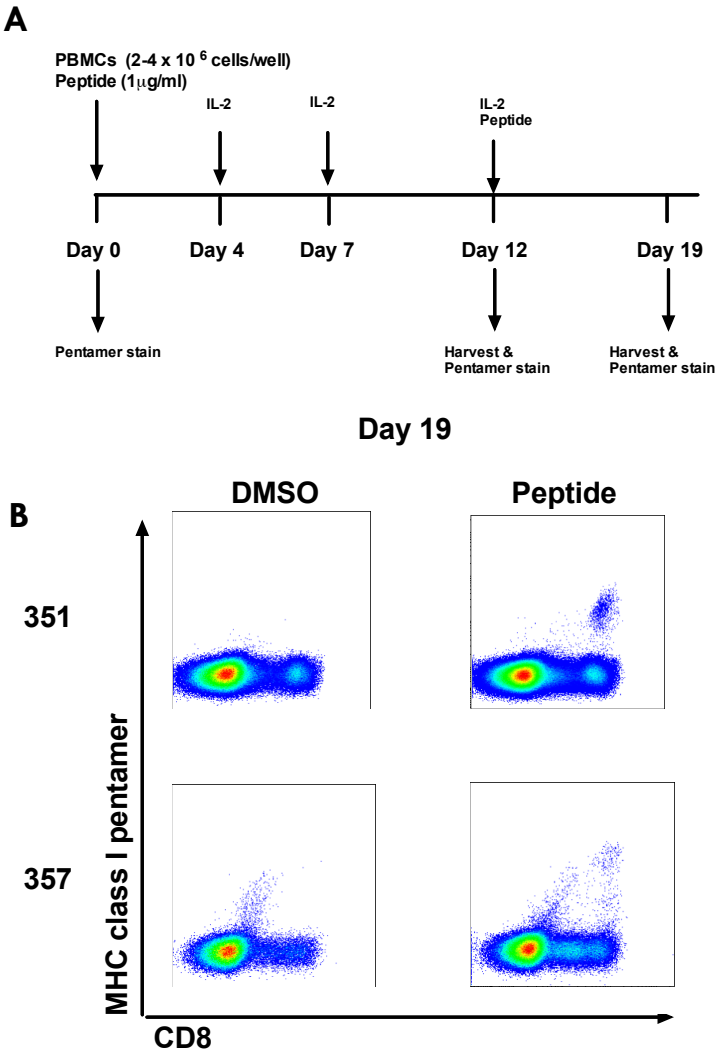


Figure 6-21. CD8+ T-cell responses exist below the limit of detection in HCV+ patients pre-vaccination: (**A**) Frozen PBMC taken pre-vaccination from HLA-A2+ patients who developed a detectable response to $NS3_{1406}$ after vaccination were cultured with the 15mer (LAAKLSGLGINAVAY; optimal epitope highlighted in bold) peptide and recombinant human IL-2 for 19 days. PBMC were stained with MHC class I pentamer ($NS3_{1406}$ KLSGLGINAV) at day 0, 12 and 19 of the culture. (**B**) Example plots for the two patients for which $NS3_{1406}$ specific T-cells could be grown from pre-vaccine PBMC.

6.6 Discussion

The clinical trials described here are the first to assess the capacity of potent HCV T-cell vaccines to restore anti-viral T-cell responses in patients with chronic HCV infection and to assess in detail the complex interplay between HCV-specific T-cell induction and circulating viral variants in the context of T-cell immunotherapy.

We had previously shown that HCV T-cell vaccines ChAd3-NS and Ad6-NS could induce high-magnitude, polyfunctional CD4+ and CD8+ T-cells targeting multiple HCV antigens after a single injection (**Barnes et al. 2012**). When the same vaccines were given to patients with chronic HCV, T-cell responses were rarely detected after priming vaccination. Only after heterologous adenoviral boosting vaccination are CD8+ T-cells generated but these are at a lower magnitude, target fewer antigens than was observed in healthy volunteers, and HCV-specific CD4+ T-cells were largely absent. Although HCV-specific T-cells are generated in some patients, these do not typically target circulating virus because of an absence of sequence homology between circulating viral variants and the vaccine immunogen at T-cell epitopes. Furthermore, when T-cells are induced they appear to be functionally attenuated.

Vaccination was well tolerated with no clear evidence of liver immunopathology. This was expected since HCV infects only the minority of hepatocytes (<20%) and in the context of acute HCV infection, when T-cells are maximally generated, severe hepatic inflammation is rare. Whilst transient elevation in liver

transaminases was observed in two patients, this was not clearly temporally related to vaccination and neither patient had a vaccine induced T-cell response. Although murine models of LCMV infection and other human models of persistent viruses support the hypothesis that T-cells may be maximally induced in the context of viral suppression (**Klenerman & Hill 2005; Wherry et al. 2005**), I found no correlation between HCV viral load and the T-cell response after vaccination.

One confounder to consider is that both PEG-IFNα and ribavirin have been shown to attenuate cellular immune responses (**Barnes et al. 2004; Barnes et al. 2009; Rizza et al. 2011**); however, influenza, EBV and CMV specific T-cell responses were unaffected by PEG-IFNα/rib therapy and T-cells targeting the hexon of the Ad vectors were readily expanded on vaccination in patients, suggesting that therapy did not induce a global impairment of T-cell durability or expansion. Although a trend for higher T-cell responses in untreated patients was seen the group median was not significantly different from that of treated patients. The recent licensing of IFN-free DAA regimens mean that the immunomodulatory effects of PEG-IFNα/rib will not be an issue when testing therapeutic vaccines as an adjunct to DAA therapy.

It is well established that in chronic HCV disease, T-cells are found at a low magnitude and are functionally attenuated with reduced proliferative capacity. The reasons for this may include persistent high-level antigen exposure, inhibition by regulatory T-cells, and dysfunctional T-cell priming in the tolerogenic liver environment (reviewed in (**Protzer et al. 2012; Knolle &**

Thimme 2014; Bowen et al. 2005). I sought to assess whether a potent T-cell vaccine, could overcome these factors, either by enhancing existing weak responses or by generating new HCV-specific T-cell responses. An important comparison with vaccination in healthy volunteers should be made: HCV-specific T-cell induction by vaccination occurs in some, but not all HCV+ patients, whereas all healthy volunteers prime novel HCV-specific T-cell responses after vaccination. Both the magnitude and the breadth of the HCV-specific T-cell response after vaccination are significantly lower in HCV+ patients than healthy volunteers.

In order to better understand why some patients responded to vaccination and others did not, the sequence of endogenous virus in patients was evaluated (performed by Christabel Kelly and Johnny Halliday). In vaccine responders there was sequence divergence between circulating viral sequence and vaccine immunogen at T-cell targets, with a loss of cross-reactivity between these variants. No variant sequence at a given epitope was predictive of a response to vaccine however, with both responders and non-responders often sharing the same variant sequence at an epitope. HCV T-cell vaccines may induce T-cell responses in chronic infection, but primarily in the absence of homologous antigen stimulation. The corollary of this is that these T-cells will be unable to target endogenous virus or inhibit viral replication. The finding that vaccination had no effect on HCV viral load is in keeping with these data.

In contrast, T-cells were generally not induced when there was sequence homology between the vaccine immunogen and endogenous virus at known T-

cell epitopes; in this context vaccination was unable to restore functional immunity. In a recent study a chimpanzee, chronically infected with HCV for 7 years and cured using unlicensed NS5a and NS5b inhibitors, maintained a relatively stable intrahepatic T-cell response to at least 4 immunodominant HCV epitopes at detectable levels 2 years after cure (**Callendret et al. 2014**); when the chimpanzee was re-infected with the same J4/91 genotype 1b strain of HCV mutational escape of two of the four epitopes was temporally correlated with rebound of HCV after initial control. Interestingly, two of the epitopes targeted by a detectable intrahepatic T-cell response remained intact, however, the T-cells targeting these epitope appeared exhausted and dysfunctional and failed to expand on rechallenge. Despite two years of convalescence after DAA cure of HCV, T-cells were narrowly targeted and failed to expand on rechallenge.

Another chimpanzee study where DAA treatment was combined with therapeutic vaccination (Ad6/ChAd63/DNA or Ad6/MVA/MVA/ChAd63, all containing the same NS region used in our vaccines) showed the same result: only CD8+ T-cell responses were expanded by vaccination and despite initial control, DAA-resistant HCV variants emerged but were not controlled by the HCV-specific T-cells. Most vaccine-induced T-cells targeted epitopes that were not conserved in the circulating virus, and where epitopes were matched and remained intact, intrahepatic T-cells were exhausted and failed to control virus (**Callendret et al. 2015**). Even where a sustained multifunctional T-cell response against an intact epitope was observed in the blood, localised exhaustion of T-cells targeting this epitope was seen in the liver (**Callendret et al. 2015**).

Therefore, even in the face of an inescapable T-cell response rapid exhaustion of T-cells by relatively low level HCV replication and the tolerogenic liver environment can lead to the development of chronic HCV infection (**Callendret et al. 2015**). This study and the work described here emphasises the need for a particularly broad and cross-reactive T-cell response for the effective control of HCV. These observations are also relevant for vaccine development against other variable pathogens such as HIV and for cancer immunotherapy, where mismatch between vaccine immunogen and endogenous antigens will commonly arise.

Failure to respond to vaccine in the context of an epitope that is matched between virus and vaccine may be a result of T-cell exhaustion. Detection of T-cell responses where mismatch occurred may therefore either be the result of *de novo* priming, or represent expanded memory responses; the latter potentially demonstrating the phenomenon of "original antigen sin" (enhanced memory responses to cross-reactive epitopes)(**Klenerman & Zinkernagel 1998**). Modifying the antigen to broaden the cross-reactivity, may recruit further T-cell pools (**Kelly et al. 2015b**), but it will be challenging to overcome the limitations for therapeutic vaccination posed by T-cell exhaustion and escape.

The importance of anti-vector immunity in determining the magnitude of response to vaccination is unclear for both healthy volunteers and HCV+ patients. A negative correlation between the anti-Ad hexon nAb titer at the time of boost vaccination and the response to boost vaccination with Ad6-NS was seen in patients, however, an equivalent correlation was not seen in healthy volunteers or for nAb titers and response to Ad prime vaccination. Indeed, healthy

volunteers with anti-Ad nAb titers above 1000 (volunteers 038, 062, 037, 026, and 072) at the time of Ad6-NS boost vaccination showed strong HCV-specific T-cell induction. It is also not uncommon for patients and healthy volunteers with no detectable T-cell response post-ChAd3-NS prime to have a strong T-cell induction after MVA-NS boost (patients 359 and 360, healthy volunteers 327, 331, 332, 348). One way to limit anti-Ad nAb induction is to pre-transduce autologous DCs with viral vectors before vaccination; a recent study using this technique also found a weak T-cell induction in patients which had no impact on viral load (**Zabaleta et al. 2015**).

T-cells generated by vaccination were functionally impaired in HCV infected patients compared to healthy volunteers; they were low in proliferative capacity, and lacked markers of cytotoxicity, T-cell activation and TNF-α production, a phenotype that is characteristic of chronic viral exposure **(Penna et al. 2007; Wherry 2011**). The marked lack of T-cell proliferation may reflect the fact that the proliferation assay uses recombinant HCV proteins that preferentially detects CD4+ T-cell responses. It has also been shown that there is a hierarchical loss of function during T-cell exhaustion (**Wherry et al. 2003b**), such that proliferative capacity may be lost relatively early after prolonged antigen exposure in comparison to IFNγ production.

Due to its constant exposure to foreign antigens from the portal vein, immune stimulation in the liver is tightly regulated (**Protzer et al. 2012**). The liver is enriched for Tregs, natural killer (NK), and natural killer T-cells (NKT) and specialised liver-resident DCs, macrophages (kupffer cells), and liver sinusoidal

endothelial cells (LSEC)(**Protzer et al. 2012**). Liver-resident DCs, LSEC, kupffer cells, and even hepatocytes have been shown to present antigen and prime T-cells *in vitro*, however, the T-cells they prime are often quiescent, in particular when primed in the presence of high levels of inhibitory and inflammatory cytokines IL-10, TGF-β, TNFα, and expression of PDL-1, which are constitutively expressed by several of the liver-resident cells named above (**Gehring et al. 2007; Knolle & Thimme 2014; Protzer et al. 2012; Bowen et al. 2005**). Ineffective priming or functioning of HCV-specific T-cells in the liver, or regulation of HCV-specific T-cells primed elsewhere that home to the liver may be limiting vaccine immunogenicity or the impact of expanded T-cells on HCV RNA in patients.

A further explanation for partial dysfunction of vaccine-induced T-cells is that HCV infection per-se inhibits the priming of naïve T-cells to produce functional T-cell memory. HCV infection has been associated with a loss of other viral (CMV) specific mature effector memory CD8+ T-cells (**Lucas et al. 2004**), however, in the absence of liver cirrhosis, there is little evidence that HCV infected patients respond abnormally to routine clinical vaccines (**Buxton & Kim 2008**), and here patients generated robust anti-vector T-cell responses following vaccination. An alternative explanation is that vaccination is not priming truly naïve T-cells, but is stimulating memory responses that were generated early in infection but that were rendered partially dysfunctional following viral exposure. Historic infection with a virus that matched the vaccine immunogen or the transient emergence of viral variants within the swarm of quasispecies within a host that match the vaccine immunogen could have lead to priming of T-cells

that no longer recognise circulating virus but that respond to vaccination. The degree of dysfunction could depend on the duration of antigen exposure at the epitope level - with more functional responses associated with viral escape early in infection. In support of this I found pre-existing T-cell responses below the limit of detection that expanded on vaccination but failed to recognise autologous viral sequences.

A lack of expansion of CD4+ T-cells by vaccination even where there was sequence mismatch between the immunogen and circulating virus, could indicate that rather than viral escape, other mechanisms of immune evasion are used by HCV to avoid CD4+ T-cell recognition. In one study 75% of CD8+ but only 18% of CD4+ T-cell epitopes showed amino acid changes during the development of persistent HCV infection (**Fuller et al. 2010**). However, viral escape of the dominant CD4+ T-cell responses to DNA/rVV vaccination in chimpanzees resulted in persistence of HCV after challenge (**Puig et al. 2006**).

MVA-NS was shown to optimally boost ChAd3-NS primed T-cells in healthy volunteers, however, there was no difference in T-cell induction by Ad6-NS or MVA-NS containing regimens in patients. MVA-NS failed to broaden the response or expand CD4+ T-cell responses, as it does in healthy volunteers. In one untreated patient (355) a T-cell response of comparable magnitude and kinetics with that seen in healthy volunteers was observed, however, the response was narrowly targeted, dominated by monofunctional IFNγ CD8+ T-cells and had no effect on HCV RNA.

The potency of a T-cell vaccine in healthy volunteers alone can not predict its efficacy as a therapeutic vaccine in HCV+ patients, but the importance of the immunogen and the concomitant breadth and depth of the T-cell response to vaccination is again highlighted as a key parameter when tackling highly divergent viruses.

6.7 Conclusion

The generation of robust CD4+ T-cell responses is thought to be a key determinant of viral clearance as evidenced both experimentally in natural history studies (**Schulze zur Wiesch et al. 2012; Grakoui et al. 2003; Gerlach et al. 1999; Semmo et al. 2005**) and through large host genome wide association studies that identify HLA class-II alleles as critical genes associated with spontaneous resolution (**Duggal et al. 2013**). Virally vectored vaccination of HCV+ patients induced predominately CD8+ T-cells, which is likely to have a major impact on their efficacy.

The utility of an immunotherapeutic approach for HCV can be debated. Recently licensed DAA therapies will transform our capacity to treat patients, with recent phase-IIb/III studies showing viral clearance rates of more than 90% (**Afdhal et al. 2014**). However, impacting on the HCV epidemic may require the treatment of IVDUs who frequently live in chaotic social settings (**Martin et al. 2013**) – therefore, vaccines administered as adjuvant immunotherapy that markedly shorten therapy duration would be beneficial. In addition, the development of a prophylactic HCV vaccine remains an important goal and the assessment of T-

cell induction in the presence of circulating viral variants may be readily assessed through therapeutic vaccine strategies, and so inform rational vaccine design. The capacity of a T-cell vaccine to induce a functional T-memory, and so protect individuals from reinfection after drug induced viral clearance, will depend on the recovery of T-cell function after therapy. Recent data suggests that both NK and T-cell function may recover after all oral DAA therapy, in contrast to IFN-based treatments (**Martin et al. 2014; Serti et al. 2015**), therefore the assessment of T-cell vaccines in DAA cured patients will be of particular interest.

This work highlights the formidable challenges in developing an effective immunotherapeutic vaccine for HCV with implications for immunotherapy against variable pathogens in general and cancer. It is still not clear why T-cells that do not recognise the circulating virus, and therefore should not be driven to exhaustion by antigen exposure, are still partially exhausted when boosted or primed by our virally vectored vaccines. Nor is it clear why pre-existing responses, the majority of which also do not target circulating virus, are not boosted by vaccination or why T-cells in all patients with virus that is mismatched to the vaccine at a given epitope do not expand on vaccination.

Additional strategies, such as the use of check-point modulation may be a useful adjunct (**Gardiner et al. 2013**), although the safety profile of these are unlikely to be clinically acceptable for the treatment of HCV where DAA represent an alternative curative treatment strategy. In 2/3 HCV chronically infected chimpanzees PD-1 blockade had no effect on viral load or T-cell responses

(**Fuller et al. 2013**). One chimpanzee, who had a broader T-cell response during initial infection, did respond to PD-1 blockade, with expansion and broadening of both CD4+ and CD8+ T-cell responses coinciding with a significant drop in viral load; which rebounded on withdrawal of blockade. Checkpoint-modulation alone therefore can have an effect on viral load in some cases and may benefit from combination with a therapeutic vaccination to broaden responses.

In conclusion I have shown that a highly potent T-cell vaccine regimen is not able to restore T-cell function during chronic HCV disease and that without determining circulating viral sequence for variable pathogens, the true value of T-cell induction cannot be accurately assessed.

6.8 Summary of findings

- Potent viral vector vaccines can be safely given to HCV+ patients
- HCV-specific T-cells can be induced in patients and the peak of the T-cell response to vaccination is seen after boost vaccination with Ad6-NS or MVA-NS
- The kinetics, magnitude, breadth and functionality of the T-cell response induced in patients differs markedly from that seen in healthy volunteers.
- Vaccination had no effect on HCV RNA levels.
- When the vaccine immunogen and a patients autologous virus share the same sequence at a T-cell epitope no T-cell induction is seen after vaccination.
- T-cells that are induced in HCV+ patients fail to recognise autologous viral sequences at T-cell epitopes and are partially dysfunctional.

7 Discussion

7.1 A prophylactic vaccine for HCV

The idea that prevention is better than cure holds true for HCV infection. An effective prophylactic vaccine remains the most cost-effective and realistic means to significantly reduce the worldwide mortality and morbidity associated with persistent HCV infection (**Krahn et al. 2005; Hahn et al. 2009; Pronker et al. 2013**). Even a vaccine with modest efficacy could provide significant reduction in prevalence beyond treatment alone (**Scott et al. 2015**). The prospects for a HCV vaccine have improved greatly in the last decade and there is now strong evidence from studies of natural infection in patients and from vaccine studies in animal models that HCV would be highly amenable to a prophylactic T-cell vaccine (**Osburn et al. 2010; Dahari et al. 2010; Mehta et al. 2002; Folgori et al. 2006b; Callendret et al. 2015**). A vaccine that can accelerate HCV-specific immunity on exposure to HCV by inducing T-cells that respond with greater vigour on re-encountering their cognate antigen should favor clearance over persistence of HCV (**Ahmed & Gray 1996**).

I have shown here that a vaccine regimen using a low seroprevalence chimpanzee-derived adenovirus as a priming vaccine (ChAd3-NS), boosted with a modified vaccinia Ankara (MVA-NS) encoding the non-structural region of HCV (NS3-NS5b genotype 1b) can overcome the limitations of previous heterologous Ad/Ad regimens (**Barnes et al. 2012**) and can induce a high magnitude durable HCV-specific T-cell response in healthy volunteers (**Swadling et al. 2014**). Boosting with MVA-NS enhanced the magnitude and functionality of the peak

and lasting memory T-cells response to HCV and it induced a more broadly targeted and more balanced CD4+ and CD8+ T-cell response.

7.2 Single cell analysis of vaccine-induced T-cells

It is essential that candidate T-cell vaccines are assessed and ranked not only on the level of T-cell induction but the quality of the T-cells they induce. Both pools of effector and memory T-cells are highly heterogeneous in terms of their phenotype, functionality, and longevity, and many factors influence the effectiveness of a T-cell response (**Newell et al. 2012; Kaech, Hemby, et al. 2002; Kaech & Wherry 2007; Haining 2012b; Appay, van Lier, et al. 2008**). Researchers are beginning to define T-cell subsets possessing different effector functions and at different stages of maturation and have been able to link these phenotypes not only to functionality, but importantly to protective efficacy (**Hansen et al. 2009; Rollier et al. 2011; Northfield et al. 2007; Sridhar et al. 2013**).

Here I have used single cell analysis to better define the immune response to ChAd3-NS and MVA-NS. CyTOF was used to compare the variation in expression of immunologically relevant proteins on bulk CD8+ T-cells, virus-specific T-cells (CMV and flu), on HCV-specific T-cells induced by vaccination. Although no novel T-cell subsets were identified by this analysis it validated the use of classic definitions of T-cell subsets using markers of LN-homing capacity (CCR7, CD62L), antigen experience (CD45RA/RO, CD27, CD28, CD57), cytolytic capacity, and cytokine production to broadly define distinct T-cell subsets, but with the caveat

that there is much overlap in functionality and phenotype (**Swadling et al. 2014; Newell et al. 2012**). The evolution of the vaccine-induced T-cell response over time was observed and ICS and phenotyping confirmed that ChAd3-NS/MVA-NS induced HCV-specific T-cells were of good quality: they expanded rapidly on exposure to cognate antigen *in vivo* and *in vitro*, coexpressed several key antiviral and immunomodulatory cytokines, degranulated and expressed markers of cytolytic potential, expressed few inhibitory receptors, and were phenotypically similar to T-cells induced by CMV infection or vaccination with yellow fever or smallpox vaccines **(Bolinger et al. 2015; Hertoghs et al. 2010; Ahmed & Akondy 2011; Akondy et al. 2009; Gaucher et al. 2008**).

The exact correlates of immune protection against persistent HCV infection have not been clearly defined, and indeed may never be achieved given the heterogeneity contained within small study populations of patients with primary infection and the real limitations of animal models of HCV infection. All arms of the immune response play a role in HCV clearance and deconvolution of the relative contributions and the essential requirements of an effective HCV-specific immune response is a huge challenge.

Nevertheless, an effective T-cell memory response will require a number of key characteristics if it is to enhance control of HCV. These include the targeting of multiple HCV antigens (**Lauer et al. 2004**), the generation of both $CD4^+$ and $CD8^+$ T-cell subsets (**Lechner, Wong, et al. 2000; Grakoui et al. 2003; Osburn et al. 2010; Urbani et al. 2006; Gerlach et al. 1999**), the maintenance of a

memory pool over time with the capacity to proliferate (**Folgori et al. 2006a**), and a population of circulating T-cells with immediate effector function (**Urbani et al. 2006; Takaki et al. 2000**). Overall I have shown that vaccination with the prime/boost regimen of ChAd3-NS/MVA-NS induces T-cells that meet these criteria. This regimen will now be tested in a phase II efficacy study to assess whether the T-cells induced are of appropriate quality to protect on exposure to HCV.

Mass cytometry represents an exciting new tool for the analysis of immune cells and parallel advances in the reagents, hardware, and data analysis tools will broaden the scope of single cell analysis previously limited by the number of parameters that could be simultaneously measured by FACS. CyTOF will still rely on well-characterised antibodies to proteins of known function however, it is relatively costly, labour intensive, and does not allow the recovery of assayed cells, therefore, for many experiments FACS analysis will likely remains the first choice assay for visualising protein expression on a single cell basis.

7.3 Why are Adenoviruses such good vectors?

I have shown that the combination of vectors used and the timing of vaccinations had a profound effect on the T-cell subsets induced. Why MVA cannot prime a T-cell response and why Ad vectors induce a much more CD8+ biased T-cell response than MVA are not well understood. A much better understanding of the types of cells transduced and presenting virally vectored antigens *in vivo*

ultimately should allow us to manipulate the homing and differentiation status of vaccine-induced antigen-specific T-cells to match COP.

MVA is more cytopathic *in vitro* and is rapidly cleared *in vivo* (**Ramirez et al. 2003**), and it downregulates both co-stimulatory molecules (CD40, CD80 and CD86) and MHC class I and II on infected and non-infected DCs (**Guzman et al. 2012**). *In vivo* transgene expression and antigen presentation after vaccination with MVA appears to occur in a context that is effective for boosting but not priming T-cells (**Swadling et al. 2014**). Both Ad and MVA vectors have been genetically manipulated so that they do not replicate in mammalian cells or cause disease and so that they are more efficient transgene delivery systems, however, not all immunomodulatory genes have been identified and removed and continued optimisation of the vectors is needed. The expression of distinct immunomodulatory genes and of divergent innate immune response elicited by Ad and MVA vectors could explain some of the differences in the T-cell response to these vectors.

Replication-defective Ad vectors persist long term and provide continuous low-level antigen (**Tatsis et al. 2007; Snyder et al. 2008**). Post-Ad vaccination a population of persistent Tem that possess immediate effector function, and that circulate systemically are maintained. T-cell activation is controlled by the integrated signalling from TCR-triggering, costimulatory or inhibitory ligand binding, and inflammatory cytokine signalling (**Curtsinger & Mescher 2010**). Ad vectors can provide the correct strength of signal in the right context for the induction of a highly functional Tem population, resisting anergy, tolerance and

exhaustion. CMV-derived vectors also induce predominantly Tem CD8+ T-cells and promising efficacy studies in NHP of rhesus-derived CMV vectors encoding HIV-1 antigens may have prompted a paradigm shift to a preference for the induction of persistent Tem rather than Tcm (**Makedonas & Betts 2010; Picker 2014; Hansen et al. 2011; Zinkernagel & Hengartner 2006**) for T-cell vaccines. A balanced induction of Tcm and Tscm, with a strong reconstitution and proliferative capacity, as well as frontline circulating Tem and Temra with immediate effector function is likely to be most efficacious for an antiviral T-cell vaccine.

7.4 Ii as a genetic adjuvant

A better understanding of the intracellular processing of antigen is required to optimise the T-cell response to vectored vaccines. As I have shown here, one way to manipulate the processing of antigen is to tether the transgene to MHC class II invariant chain (Ii). The use of Ii as a genetic enhancer has been broadly applicable, enhancing CD8+ T-cell responses to several antigens, with various vaccine vectors (MVA, ChAd, Ad, lentivirus, DNA), in mice and macaques (**Capone et al. 2014; Spencer et al. 2014; Jensen et al. 2013**) and this technology will now be tested for the first time in humans (PEACHI: EudraCT Number: 2014-000730-30).

By tethering antigen to Ii within a vaccine construct the antigen is specifically targeted for proteasomal degradation, which enhances its presentation on MHC-I and in turn enhances the magnitude of the antigen-specific T-cell response.

There is not a clear relationship between the abundance a peptide presented on MHC-I and the abundance of the protein from which it is derived within a cell (**Mackay et al. 2009**) and the vast majority of proteins are degraded without supplying peptide to the ER for loading on MHC-I (**Rock et al. 2004; Tortorella et al. 2000**); improving the efficiency of antigen processing for many epitopes could then improve presentation and T-cell induction.

How tethering Ii to an antigen targets it to the proteasome and whether ubiquitination is required needs further investigation. A simple way to assess this would be to use targeted removal or addition of lysines, on which ubiquitin is attached, within the Ii sequence to see if the adjuvant effect is retained. Other type-II transmembrane regions or sequence that disrupt protein folding should be assessed to see if alternative sequences can also improve the processing of antigen when encoded in viral vectors.

The relative importance of the peptide-translocation and peptide-editing of TAP and ERAPs respectively should also be investigated as possible limiting steps in antigen processing for presentation on MHC-I. The antigen presentation capabilities of liver resident APCs and hepatocytes should be examined as this will impact on the peptides presented by HCV infected cells.

The mechanism by which Ii-linkage can enhance CD4+ T-cell responses should also be investigated as an enhanced CD4+ T-cell response would be beneficial to many, if not all, T-cell vaccines.

7.5 Subversion of the T-cell response by HCV

Therapeutic vaccination with Ad and MVA vectors was able to induce HCV-specific T-cells in some patients, showing that there is not a complete impairment of antigen processing, presentation, and T-cell expansion; however, responses are low in magnitude and narrowly targeted. Despite administering vaccines intramuscularly, the availability of antigen outside of the liver does not appear to significantly enhance T-cell expansion or priming. The magnitude of the T-cell response to ChAd3-NS/Ad6-NS or ChAd3-NS/MVA-NS was higher than for other candidate HCV vaccines (reviewed in **Halliday et al. 2011; Swadling et al. 2013**), and in some cases higher than that seen in patients that spontaneous resolve infection, however, no effect on HCV RNA was seen.

One of the key findings from the assessment of vaccines in HCV+ patients is that analysis of the T-cell response to vaccination or natural infection with variable pathogens must include analysis of circulating viral sequence (**Kelly et al. 2015b; Bengsch et al. 2007**). HCV uses two key mechanism to avoid recognition by T-cells: Viral escape (**Soderholm et al. 2006; Dazert et al. 2009; Neumann-Haefelin & Thimme 2007**), whereby changes in the viral sequence render the virus no longer recognizable by specific T-cells, and T-cell exhaustion, where T-cells targeting intact epitopes are rendered dysfunctional due to persistent exposure to antigen and inhibitory signals (**Schulze zur Wiesch et al. 2012; Day et al. 2006; Gabriele Missale et al. 2012; Penna et al. 2007; Wherry 2011**). The phenotype of exhausted or escaped T-cells are markedly different

(**Bengsch et al. 2007**) as are the mechanisms by which T-cell responses may be rejuvenated in the two settings.

Both the acquisition and the loss of effector functions by antiviral T-cells appears to occur on a continuum (**Wherry 2011; Viola & Lanzavecchia 1996**), which may not be linear. Directly measuring the proliferative capacity, polyfunctionality, and cytolytic potential of T-cells remains the best way to identify exhausted cells, as putative markers of exhaustion or terminal differentiation, such as PD-1 (**Kasprowicz et al. 2008; Duraiswamy et al. 2011; Bowen et al. 2008; Odorizzi et al. 2015**) CD45RA+ reexpression (**Akondy et al. 2009; Northfield et al. 2007**) and CD57 (**Bolinger et al. 2015**) can equally be expressed on functional cells, as was seen for HCV-specific T-cells after vaccination of healthy volunteers.

7.6 Vaccination after cure and T-cell recovery

It remains to be seen how T-cells recover following pharmacological eradication of HCV, in particular for IFN-free DAA treatment. Patients who respond most rapidly to IFNα/ribavirin treatment showed the weakest T-cell recovery in one study (**Pembroke et al. 2012**) and a better restoration of HCV-specific T-cell recovery was seen when patients were treated during the acute phase of infection relative to those treated after a period of chronic infection (**Missale et al. 2012**). The pleiotropic effects of IFNα on the immune system (**Odorizzi & Wherry 2013**) make it difficult to discern whether IFNα/ribavirin treatment is limiting T-cell recovery or whether clearance of antigen has little effect on HCV-

specific T-cell responses (**Park et al. 2012; G Missale et al. 2012; Barnes et al. 2009; Abdel-Hakeem et al. 2010**). Recently, HCV-specific CD8+ T-cells in IFN-free DAA cured chimpanzees were shown to recover *in vitro* proliferative capacity but no expansion or change in phenotype of intrahepatic HCV-specific T-cells was seen long-term after DAA cure (**Callendret et al. 2014**) and DAA treatment combined with virally vectored vaccines did not protect from reinfection in chimpanzee studies (**Callendret et al. 2015**).

The ChAd3-NS/MVA-NS vaccine regimen characterised here will be given to IFN-free DAA cured patients to assess T-cell recovery after removal of HCV (PEACHI EudraCT Number: 2014-000730-30). It will be important to have full length sequence of the patients HCV before treatment, so that we can assess whether T-cells that target matched sequences between the immunogen and the pre-existing virus can be expanded in this setting, where they cannot in recently cured or chronically infected patient's (**Kelly et al. 2015**). One of the limitations of the work performed here was the need for targeted viral sequencing. Full length sequencing of major and minor variants is now possible using next generation sequencing technology and this will allow a more complete analysis of the interaction between vaccine induced T-cells and viral sequence.

Another therapeutic option that could be applied post-cure is the blockade of inhibitory signalling to aid in T-cell recovery as an adjunct to vaccination. The continued assessment of inhibitory receptor blockade is needed as it was shown to be ineffective for severely exhausted T-cells in the liver in one study (**Nakamoto et al. 2008**) and may require concurrent depletion of Tregs to allow

anti-viral T-cell expansion rather than selective expansion of Tregs (**Penaloza-MacMaster et al. 2015**).

A major limitation for natural history and vaccine studies in humans is the inability to monitor immune responses in the liver directly. HCV-specific T-cell responses in the blood are valid biomarkers of intrahepatic T-cell activity in chimpanzee studies (**Callendret et al. 2014; Shin et al. 2008**). Phase II efficacy testing of ChAd-NS/MVA-NS vaccines should give an indication of whether the HCV-specific T-cell response in blood is a good biomarker of a protective T-cell response (NCT01436357).

Overall this work highlights the formidable challenges in restoring T-cell immunity after HCV infection, with implications for immunotherapy against variable pathogens in general and cancer.

7.7 Next generation of immunogen design

The major challenge in generating an effective prophylactic T-cell vaccine for HCV is the generation of a broad and cross-reactive T-cell response, which can recognise diverse HCV strains, and that can resist viral escape. Immunogen design is therefore crucial.

The assessment of multiple HCV immunogens was not possible here, however, the paucity of T-cell induction at epitopes where the vaccine immunogen and circulating viral sequences matched highlights the difficulty in recovering T-cell responses in patients previously infected with HCV, and suggests the priming of

T-cells targeting novel epitopes may be required (**Kelly et al. 2015**). Several approaches to immunogen design that have been applied to HIV and HCV T-cell vaccines could be applied to virally vectored HCV vaccines.

In many countries multiple viral genotypes circulate, for example in the United Kingdom approximately 50% of people are infected with genotypes 1a or 1b and 50% with genotype-3 (**Messina et al. 2014**). Cross-genotypic protection can be achieved through administering more than one genotype-specific vaccine at a population level, or through the design of immunogens within a single vaccine that target multiple genotypes.

Due to the capacity to HCV to escape T-cell responses by muttion, detailed analysis of individual epitopes within an immunogen will be required to optimise vaccine immunogen design (**Bull et al. 2015; Kelly et al. 2015b; von Delft et al. 2015**). Using an *in vitro* priming assay several peptide sequences were ranked according to the cross-recognition of the T-cells they primed for one immunodominant epitope within our vaccine immunogen (**Kelly et al. 2015b**). Promisingly, of the sequences tested, the vaccine variant at $NS3_{1406}$ induced T-cells with the best cross-recognition of variants at this epitope. Unfortunately, to perform this analysis for all epitope targeted on diverse HLA-backgrounds by an immunogen such as the whole NS region of HCV will be labor intensive and will not necessarily translate perfectly when tested *in vivo*.

The removal of variable or immunodominant epitopes may remove competition and enhance responses to subdominant T-cell epitopes **(Im et al. 2011; Holst et**

al. 2015). However, there may be reasons other than competition limiting these subdominant responses, such as low magnitude naïve precursor T-cells or inefficient antigen processing (**Wölfl et al. 2008**).

We now have access to a wealth of sequencing data for HCV, which has allowed the design of immunogens containing only the most highly conserved regions of HCV, which are most likely to offer pan-genotypic coverage (**Borthwick et al. 2014**). Immunogens designed *in silico* from the most highly conserved stretches of the HCV sequence for genotype 1, genotypes 1-4, or all published HCV sequences are currently undergoing pre-clinical testing in Oxford (**Barnes, personal communication**). Alternatively multivalent mosaic immunogens, that encode antigens derived from multiple genotypes could be used (**Fischer et al. 2007**) and temporal or spatial separation of vaccines containing distinct immunogens can broaden T-cell responses (**Rosario et al. 2010**). The use of natural stretches of sequence may be preferable as it ensures T-cells target naturally processed antigens.

Manipulating antigen processing and presentation may lead to greater T-cell induction but ultimately it is essential that T-cells target epitopes that are intact and presented by infected cells.

7.8 The future of Oxford's HCV vaccine programme

Several clinical trials using the vectors described here are on-going:

The ChAd3-NS/MVA-NS HCV vaccine regime has progressed to a phase II efficacy study, which will take place in an intra-venous drug using community in the US (NCT01436357). This study will be the first double blinded, randomized, placebo-controlled trial of a vaccine to prevent HCV persistence. The trial will enrol approximately 350 subjects and is set up to assess the immunogenicity, efficacy and safety of this vaccine regimen in a cohort of patients with a broad range of HLA types, exposed to different viral subtypes. This study will test the novel hypotheses that a vaccine designed to elicit cellular immunity can prevent a serious human viral infection and that a reduction in the rate of viral persistence, rather than sterilizing immunity, is a viable endpoint for a vaccine trial.

The ChAd3-NS/MVA-NS vaccine regimen characterised here will be given to DAA cured patients to assess vaccine immunogenicity after IFN-free pharmacological clearance of HCV (PEACHI EudraCT Number: 2014-000730-30). This trial will help us to understand if HCV leaves a lasting mark on HCV-specific immunity and if targeted vaccination to prevent persistence on reinfection with HCV could be effective.

Co-infection of HCV and HIV-1 is common and HCV-mediated liver disease is one of the leading causes of death for patients on HAART (**Chen et al. 2014**), therefore, HIV-1 infected or HIV-1/HCV co-infected patients represent unique immunological settings in which an effective vaccine for HCV is required. The immunogenicity and safety of our ChAd3-NS/MVA-NS vaccine regimen and the effect of coadministration of candidate virally vectored HCV and HIV-1 vaccines are currently being tested in healthy volunteers and HIV-1+ patients on HAART

therapy (PEACHI EudraCT Number: 2014-000730-30).

Clearance of HCV can occur without the induction of a measurable antibody response, however, vaccine induced neutralising antibodies, when targeting circulating virus, also show effective control of HCV (**Houghton 2011; Verstrepen et al. 2011**). Ideally a potent T-cell vaccine would be combined with an antigen capable of generating broadly cross-reactive neutralising antibodies against HCV envelope. Combined vaccination with HCV-specific antibody and T-cell inducing vaccines are currently being tested in pre-clincial models (**Chmielewska et al. 2014**).

Over the next few years we will get a better understanding of whether our T-cell vaccines can be effective in HIV-1+ patients, whether we can coadminister HIV-1 and HCV vaccines without loss of immunogenicity, whether next generation vectors encoding Ii are more immunogenic in humans, and whether IFN-free DAA-mediated cure can restore T-cell immunity, facilitating effective vaccination in patients previously exposed to HCV. For me, the most exciting results will come from efficacy testing of ChAd3-NS/MVA-NS in at risk populations, which should give us some indication of the power of pre-priming HCV-specific T-cells before exposure to HCV.

We may already have an effective prophylactic vaccine for HCV, however the continued development of candidate prophylactic and therapeutic HCV vaccines will inform our understanding of immunity to persistence viral infections, vaccine-induced immunity, and the complex interactions between host and virus.

8 Appendix 2-1 - Informed Consent

All patients will sign and date the informed consent form before any study specific procedures are performed. The information sheet will be made available to the patient at least 24 hours prior to the screening visit. At the screening visit, the patient will be fully informed of all aspects of the trial, the potential risks and their obligations. The following general principles will be emphasised:

- Participation in the study is entirely voluntary
- Refusal to participate involves no penalty or loss of medical benefits
- The patient may withdraw from the study at any time
- The patient is free to ask questions at any time to allow him or her to understand the purpose of the study and the procedures involved
- The study involves research of an investigational vaccine
- There is no direct benefit for participating

Inclusion and Exclusion Criteria

For the purpose of the inclusion and exclusion criteria non-response to previous treatment is defined as a viral decline of < 2 logs 12 weeks into therapy with IFN monotherapy or IFN/ribavirin combination therapy, or persistent viremia 24 weeks into treatment. Relapse is defined as HCV RNA undetectable at the end of treatment but detectable within 6 months of stopping treatment.

Inclusion Criteria

The **healthy volunteers** must satisfy all the following inclusion criteria to be eligible for the study:

- Healthy adults aged 18 to 55 years (inclusive)
- Resident in or near the trial sites for the duration of the vaccination study
- Able and willing (in the Investigator's opinion) to comply with all study requirements
- For women of child bearing potential, willingness to practice continuous effective contraception during the study and a negative pregnancy test on the day(s) of vaccination
- Men, including those with pregnant partners, should use barrier contraception until 3 months after the last vaccination
- Written informed consent

The **patients** with HCV must satisfy all the following inclusion criteria to be eligible for the study:

- HCV infected with genotype-1 infection (any viral load)
- Patients must not be currently receiving any treatment for HCV infection.
- Adults aged 18 to 65 years (inclusive)
- Resident in or near the trial sites for the duration of the vaccination study
- Able and willing (in the Investigator's opinion) to comply with all study requirements
- Liver transaminases may be within normal limits or elevated.

- For men in Arm B, including those with pregnant partners, a willingness to use barrier contraception until six months after completing treatment with IFN/ribavirin
- For women in Arm B, of child bearing potential, a willingness to practice continuous effective contraception during the study and a negative pregnancy test on the day(s) of vaccination.
- For men in arm C, including those with pregnant partners, a willingness to use barrier contraception until three months after the last vaccination
- Written informed consent
- Patients with HCV in must be treatment naïve to previous IFN and ribavirin combination therapy. They may be included if they have been previously treated with interferon monotherapy but relapsed after treatment.
- Patients with HCV in the untreated vaccine groups may be treatment naïve, or have been previously treated with interferon monotherapy or interferon and ribavirin therapy and relapsed after treatment

Exclusion Criteria

The subjects (both healthy individuals or **patients**) may not enter the study if any of the following exclusion criteria apply:

- Participation in another research study involving an investigational product in the 30 days preceding enrolment, or planned use during the study period
- Prior receipt of a recombinant simian or human adenoviral vaccine
- Clinical, biochemical (abnormal liver synthetic dysfunction defined by an elevated blood prothrombin time or a low blood albumin level), ultrasonographic, or liver biopsy (histology) evidence of cirrhosis or portal hypertension
- Any confirmed or suspected immunosuppressive or immunodeficient state, including HIV infection; asplenia; recurrent, severe infections and chronic (more than 14 days) immunosuppressant medication within the past 6 months (inhaled and topical steroids are allowed)
- History of allergic disease or reactions likely to be exacerbated by any component of the vaccine, e.g., Kathon
- History of clinically significant contact dermatitis
- Any history of anaphylaxis in reaction to vaccination
- Pregnancy, lactation or willingness/intention to become pregnant during the study
- History of cancer (except basal cell carcinoma of the skin and cervical carcinoma in situ)
- Suspected or known current alcohol abuse as defined by an alcohol intake of greater than 42 units every week
- Current suspected or known injecting drug abuse
- Seropositive for hepatitis B surface antigen (HBsAg)
- Seropositive for HIV (antibodies to HIV) at screening
- Any other significant disease, disorder or finding, which, in the opinion of the Investigator, may either put the patient at risk because of

participation in the study, or may influence the result of the study, or the patient's ability to participate in the study
- Any other finding which in the opinion of the investigators would significantly increase the risk of having an adverse outcome from participating in the protocol
- Individuals who have had a temperature >38°C in the 3 days preceding vaccination.
- Patients likely to have been infected with HCV within the last 12 months

In addition to the above listed exclusion criteria:

Patients with HCV may not enter arms B1 and B2 of the study if any of the following exclusion criteria applies:
- Patients are non-responders to previous IFN-α monotherapy
- Patients who received IFN-α and ribavirin or PEG-IFN and ribavirin in the past and who were non-responders or who relapsed during or after therapy
- Patients with a known allergy to ribavirin or interferon-α
- Haemoglobin less than 10g/dl
- Severe neutropenia or thrombocytopenia
- Patients who have had a heart attack or who have suffered from any other severe heart disease in the last 6 months
- Patients with haemoglobinopathies
- Autoimmune hepatitis
- Autoimmune disease
- History of organ transplantation
- Uncontrolled seizures
- Uncontrolled severe psychiatric conditions

Patients with HCV may not enter arm C if they were previous non-responders to interferon monotherapy, or interferon and ribavirin combination therapy,

Vaccination exclusion criteria

Patients who enter arm B1 will only be vaccinated if they have a >2 log decline in viral load at week 12 of IFN-α and ribavirin therapy. Vaccination will then occur at week 14 into IFN-α and ribavirin therapy. Patients in arm B1 who do not have a >2 log decline in viral load at week 12 of IFN-α and ribavirin therapy will stop all treatment and be withdrawn from the study.

The following adverse events constitute contraindications to administration of vaccine at that point in time; if any one of these adverse events occurs at the time scheduled for vaccination, the subject may be vaccinated at a later date, or withdrawn at the discretion of the investigator. The subject must be followed until resolution of the event as with any adverse event.

- Acute disease at the time of vaccination. (Acute disease is defined as the presence of a moderate or severe illness with or without fever.) All vaccines can be administered to persons with a minor illness such as

diarrhoea, mild upper respiratory infection with or without low-grade febrile illness, *i.e.*, temperature of <37.5°C/99.5°F).

- Temperature of ≥37.5°C (99.5°F) at the time of vaccination.
- Elevation in ALT >3x ULN and a bilirubin>2x ULN at the time of vaccination

Re-vaccination exclusion criteria

Patients who have undetectable viremia at week 12 but who have subsequent virological breakthrough with virological relapse to high levels of viremia before the end of treatment will stop PEG-IFN and ribavirin at that point and will not receive further vaccinations. However these patients may continue to attend for immunological assessment for the duration of the study.

The following adverse events associated with vaccine immunisation constitute absolute contraindications to further administration of vaccine. If any of these events occur during the study, the subjects must be withdrawn and followed until resolution of the event, as with any adverse event.

- Anaphylactic reaction following administration of vaccine
- Pregnancy
- Elevation in ALT >20x upper limit of normal at any time during the study

Withdrawal of Subjects

Subjects may withdraw or be withdrawn for any of the reasons given below. The reason for withdrawal will be recorded in the Case Report Form (CRF). If withdrawal is due to an adverse event, appropriate follow-up visits or medical care will be arranged until the adverse event has resolved or stabilised. Any subject who is withdrawn from the study may be replaced, if that is possible within the specified time frame. The Local Safety Committee (LSC) may recommend withdrawal of subjects.

Discontinuation Criteria

In accordance with the current revision of the Declaration of Helsinki (amended October 2000, with additional footnotes added 2002 and 2004) and any other applicable regulations, a subject has the right to withdraw from the study at any time and for any reason and is not obliged to give his or her reasons for doing so. The Investigator may withdraw the subject at any time in the interests of the subject's health and well-being.

In addition the subject may withdraw/be withdrawn for any of the following reasons:

- Administrative decision by the Investigator
- Ineligibility (either arising during the study or retrospective, having been overlooked at screening)
- Significant protocol deviation
- Patient non-compliance with treatment regime or study requirements
- An adverse event which requires discontinuation of the vaccination regimen or results in inability to continue to comply with study procedures (see below)

9 Appendix 2-2 – Peptides covering vaccine immunogen

Appendix 2-2: Vaccine immunogen peptide set, NS3-NS5b HCV genotype 1b BK strain

POOL F		POOL G		POOL H	
Peptide	Sequence	Peptide	Sequence	Peptide	Sequence
1	APITAYSQQTRGLLG	79	AGARLVVLATATPPG	157	ADLEVVTSTWVLVGG
2	AYSQQTRGLLGCIIT	80	LVVLATATPPGSVTV	158	VVTSTWVLVGGVLAA
3	QTRGLLGCIITSLTG	81	ATATPPGSVTVPHPN	159	TWVLVGGVLAALAAY
4	LLGCIITSLTGRDKN	82	PPGSVTVPHPNIEEV	160	VGGVLAALAAYCLTT
5	IITSLTGRDKNQVEG	83	VTVPHPNIEEVALSN	161	LAALAAYCLTTGSVV
6	LTGRDKNQVEGEVQV	84	HPNIEEVALSNTGEI	162	AAYCLTTGSVVIVGR
7	DKNQVEGEVQVVSTA	85	EEVALSNTGEIPFYG	163	LTTGSVVIVGRIILS
8	VEGEVQVVSTATQSF	86	LSNTGEIPFYGKAIP	164	SVVIVGRIILSGRPA
9	VQVVSTATQSFLATC	87	GEIPFYGKAIPIEAI	165	VGRIILSGRPAIVPD
10	STATQSFLATCVNGV	88	FYGKAIPIEAIRGGR	166	ILSGRPAIVPDREFL
11	QSFLATCVNGVCWTV	89	AIPIEAIRGGRHLIF	167	RPAIVPDREFLYQEF
12	ATCVNGVCWTVYHGA	90	EAIRGGRHLIFCHSK	168	VPDREFLYQEFDEME
13	NGVCWTVYHGAGSKT	91	GGRHLIFCHSKKKCD	169	EFLYQEFDEMEECAS
14	WTVYHGAGSKTLAGP	92	LIFCHSKKKCDELAA	170	QEFDEMEECASHLPY
15	HGAGSKTLAGPKGPI	93	HSKKKCDELAAKLSG	171	EMEECASHLPYIEQG
16	SKTLAGPKGPITQMY	94	KCDELAAKLSGLGIN	172	CASHLPYIEQGMQLA
17	AGPKGPITQMYTNVD	95	LAAKLSGLGINAVAY	173	LPYIEQGMQLAEQFK
18	GPITQMYTNVDQDLV	96	LSGLGINAVAYYRGL	174	EQGMQLAEQFKQKAL
19	QMYTNVDQDLVGWQA	97	GINAVAYYRGLDVSV	175	QLAEQFKQKALGLLQ
20	NVDQDLVGWQAPPGA	98	VAYYRGLDVSVIPTI	176	QFKQKALGLLQTATK
21	DLVGWQAPPGARSLT	99	RGLDVSVIPTIGDVV	177	KALGLLQTATKQAEA
22	WQAPPGARSLTPCTC	100	VSVIPTIGDVVVVAT	178	LLQTATKQAEAAAPV
23	PGARSLTPCTCGSSD	101	PTIGDVVVVATDALM	179	ATKQAEAAAPVVESK
24	SLTPCTCGSSDLYLV	102	DVVVVATDALMTGYT	180	AEAAAPVVESKWRAL
25	CTCGSSDLYLVTRHA	103	VATDALMTGYTGDFD	181	APVVESKWRALETFW
26	SSDLYLVTRHADVIP	104	ALMTGYTGDFDSVID	182	ESKWRALETFWAKHM
27	YLVTRHADVIPVRRR	105	GYTGDFDSVIDCNTC	183	RALETFWAKHMWNFI
28	RHADVIPVRRRGDSR	106	DFDSVIDCNTCVTQT	184	TFWAKHMWNFISGIQ
29	VIPVRRRGDSRGSLL	107	VIDCNTCVTQTVDFS	185	KHMWNFISGIQYLAG
30	RRRGDSRGSLLSPRP	108	NTCVTQTVDFSLDPT	186	NFISGIQYLAGLSTL
31	DSRGSLLSPRPVSYL	109	TQTVDFSLDPTFTIE	187	GIQYLAGLSTLPGNP
32	SLLSPRPVSYLKGSS	110	DFSLDPTFTIETTTV	188	LAGLSTLPGNPAIAS
33	PRPVSYLKGSSGGPL	111	DPTFTIETTTVPQDA	189	STLPGNPAIASLMAF
34	SYLKGSSGGPLLCPS	112	TIETTTVPQDAVSRS	190	GNPAIASLMAFTASI
35	GSSGGPLLCPSGHAV	113	TTVPQDAVSRSQRRG	191	IASLMAFTASITSPL
36	GPLLCPSGHAVGIFR	114	QDAVSRSQRRGRTGR	192	MAFTASITSPLTTQS
37	CPSGHAVGIFRAAVC	115	SRSQRRGRTGRGRRG	193	ASITSPLTTQSTLLF
38	HAVGIFRAAVCTRGV	116	RRGRTGRGRRGIYRF	194	SPLTTQSTLLFNILG
39	IFRAAVCTRGVAKAV	117	TGRGRRGIYRFVTPG	195	TQSTLLFNILGGWVA
40	AVCTRGVAKAVDFVP	118	RRGIYRFVTPGERPS	196	LLFNILGGWVAAQLA
41	RGVAKAVDFVPVESM	119	YRFVTPGERPSGMFD	197	ILGGWVAAQLAPPSA
42	KAVDFVPVESMETTM	120	TPGERPSGMFDSSVL	198	WVAAQLAPPSAASAF
43	FVPVESMETTMRSPV	121	RPSGMFDSSVLCECY	199	QLAPPSAASAFVGAG
44	ESMETTMRSPVFTDN	122	MFDSSVLCECYDAGC	200	PSAASAFVGAGIAGA
45	TTMRSPVFTDNSSPP	123	SVLCECYDAGCAWYE	201	SAFVGAGIAGAAVGS
46	SPVFTDNSSPPAVPQ	124	ECYDAGCAWYELTPA	202	GAGIAGAAVGSIGLG
47	TDNSSPPAVPQSFQV	125	AGCAWYELTPAETSV	203	AGAAVGSIGLGKVLV
48	SPPAVPQSFQVAHLH	126	WYELTPAETSVRLRA	204	VGSIGLGKVLVDILA
49	VPQSFQVAHLHAPTG	127	TPAETSVRLRAYLNT	205	GLGKVLVDILAGYGA
50	FQVAHLHAPTGSGKS	128	TSVRLRAYLNTPGLP	206	VLVDILAGYGAGVAG
51	HLHAPTGSGKSTKVP	129	LRAYLNTPGLPVCQD	207	ILAGYGAGVAGALVA
52	PTGSGKSTKVPAAYA	130	LNTPGLPVCQDHLEF	208	YGAGVAGALVAFKVM
53	GKSTKVPAAYAAQGY	131	GLPVCQDHLEFWESV	209	VAGALVAFKVMSGEM
54	KVPAAYAAQGYKVLV	132	CQDHLEFWESVFTGL	210	LVAFKVMSGEMPSTE
55	AYAAQGYKVLVLNPS	133	LEFWESVFTGLTHID	211	KVMSGEMPSTEDLVN
56	QGYKVLVLNPSVAAT	134	ESVFTGLTHIDAHFL	212	GEMPSTEDLVNLLPA
57	VLVLNPSVAATLGFG	135	TGLTHIDAHFLSQTK	213	STEDLVNLLPAILSP
58	NPSVAATLGFGAYMS	136	HIDAHFLSQTKQAGD	214	LVNLLPAILSPGALV
59	AATLGFGAYMSKAHG	137	HFLSQTKQAGDNFPY	215	LPAILSPGALVVGVV
60	GFGAYMSKAHGIDPN	138	QTKQAGDNFPYLVAY	216	LSPGALVVGVVCAAI
61	YMSKAHGIDPNIRTG	139	AGDNFPYLVAYQATV	217	ALVVGVVCAAILRRH
62	AHGIDPNIRTGVRTI	140	FPYLVAYQATVCARA	218	GVVCAAILRRHVGPG
63	DPNIRTGVRTITTGA	141	VAYQATVCARAQAPP	219	AAILRRHVGPGEGAV
64	RTGVRTITTGAPVTY	142	ATVCARAQAPPPSWD	220	RRHVGPGEGAVQWMN
65	RTITTGAPVTYSTYG	143	ARAQAPPPSWDQMWK	221	GPGEGAVQWMNRLIA
66	TGAPVTYSTYGKFLA	144	APPPSWDQMWKCLIR	222	GAVQWMNRLIAFASR
67	VTYSTYGKFLADGGC	145	SWDQMWKCLIRLKPT	223	WMNRLIAFASRGNHV
68	TYGKFLADGGCSGGA	146	MWKCLIRLKPTLHGP	224	LIAFASRGNHVSPTH
69	FLADGGCSGGAYDII	147	LIRLKPTLHGPTPLL	225	ASRGNHVSPTHYVPE
70	GGCSGGAYDIIICDE	148	KPTLHGPTPLLYRLG	226	NHVSPTHYVPESDAA
71	GGAYDIIICDECHST	149	HGPTPLLYRLGAVQN	227	PTHYVPESDAAARVT
72	DIIICDECHSTDSTT	150	PLLYRLGAVQNEVTL	228	VPESDAAARVTQILS
73	CDECHSTDSTTILGI	151	RLGAVQNEVTLTHPI	229	DAAARVTQILSSLTI
74	HSTDSTTILGIGTVL	152	VQNEVTLTHPITKYI	230	RVTQILSSLTITQLL
75	STTILGIGTVLDQAE	153	VTLTHPITKYIMACM	231	ILSSLTITQLLKRLH
76	LGIGTVLDQAETAGA	154	HPITKYIMACMSADL	232	LTITQLLKRLHQWIN
77	TVLDQAETAGARLVV	155	KYIMACMSADLEVVT	233	QLLKRLHQWINEDCS
78	QAETAGARLVVLATA	156	ACMSADLEVVTSTWV	234	RLHQWINEDCSTPCS
				235	WINEDCSTPCSGSWL

Appendix 2-2: Vaccine immunogen peptide set, NS3-NS5b HCV genotype 1b BK strain

POOL I	
Peptide	Sequence
236	DCSTPCSGSWLRDVW
237	PCSGSWLRDVWDWIC
238	SWLRDVWDWICTVLT
239	DVWDWICTVLTDFKT
240	WICTVLTDFKTWLQS
241	VLTDFKTWLQSKLLP
242	FKTWLQSKLLPQLPG
243	LQSKLLPQLPGVPFF
244	LLPQLPGVPFFSCQR
245	LPGVPFFSCQRGYKG
246	PFFSCQRGYKGVWRG
247	CQRGYKGVWRGDGIM
248	YKGVWRGDGIMQTTC
249	WRGDGIMQTTCPCGA
250	GIMQTTCPCGAQITG
251	TTCPCGAQITGHVKN
252	CGAQITGHVKNGSMR
253	ITGHVKNGSMRIVGP
254	VKNGSMRIVGPKTCS
255	SMRIVGPKTCSNTWH
256	VGPKTCSNTWHGTFP
257	TCSNTWHGTFPINAY
258	TWHGTFPINAYTTGP
259	TFPINAYTTGPCTPS
260	NAYTTGPCTPSPAPN
261	TGPCTPSPAPNYSRA
262	TPSPAPNYSRALWRV
263	APNYSRALWRVAAEE
264	SRALWRVAAEEYVEV
265	WRVAAEEYVEVTRVG
266	AEEYVEVTRVGDFHY
267	VEVTRVGDFHYVTGM
268	RVGDFHYVTGMTTDN
269	FHYVTGMTTDNVKCP
270	TGMTTDNVKCPCQVP
271	TDNVKCPCQVPAPEF
272	KCPCQVPAPEFFTEV
273	QVPAPEFFTEVDGVR
274	PEFFTEVDGVRLHRY
275	TEVDGVRLHRYAPAC
276	GVRLHRYAPACRPLL
277	HRYAPACRPLLREEV
278	PACRPLLREEVTFQV
279	PLLREEVTFQVGLNQ
280	EEVTFQVGLNQYLVG
281	FQVGLNQYLVGSQLP
282	LNQYLVGSQLPCEPE
283	LVGSQLPCEPEPDVA
284	QLPCEPEPDVAVLTS
285	EPEPDVAVLTSMLTD
286	DVAVLTSMLTDPSHI
287	LTSMLTDPSHITAET
288	LTDPSHITAETAKRR
289	SHITAETAKRRLARG
290	AETAKRRLARGSPPS
291	KRRLARGSPPSLASS
292	ARGSPPSLASSSASQ
293	PPSLASSSASQLSAP
294	ASSSASQLSAPSLKA
295	ASQLSAPSLKATCTT
296	SAPSLKATCTTHHVS
297	LKATCTTHHVSPDAD
298	CTTHHVSPDADLIEA
299	HVSPDADLIEANLLW
300	DADLIEANLLWRQEM
301	IEANLLWRQEMGGNI
302	LLWRQEMGGNITRVE
303	QEMGGNITRVESENK
304	GNITRVESENKVVVL
305	RVESENKVVVLDSFD
306	ENKVVVLDSFDPLRA
307	VVLDSFDPLRAEEDE
308	SFDPLRAEEDEREVS

POOL I	
Peptide	Sequence
309	LRAEEDEREVSVPAE
310	EDEREVSVPAEILRK
311	EVSVPAEILRKSKKF
312	PAEILRKSKKFPAAM
313	LRKSKKFPAAMPIWA
314	KKFPAAMPIWARPDY
315	AAMPIWARPDYNPPL
316	IWARPDYNPPLLESW
317	PDYNPPLLESWKDPD
318	PPLLESWKDPDYVPP
319	ESWKDPDYVPPVVHG
320	DPDYVPPVVHGCPLP
321	VPPVVHGCPLPPIKA
322	VHGCPLPPIKAPPIP
323	PLPPIKAPPIPPPRR
324	IKAPPIPPPRRKRTV
325	PIPPPRRKRTVVLTE
326	PRRKRTVVLTESSVS
327	RTVVLTESSVSSALA
328	LTESSVSSALAELAT
329	SVSSALAELATKTFG
330	ALAELATKTFGSSES
331	LATKTFGSSESSAVD
332	TFGSSESSAVDSGTA
333	SESSAVDSGTATALP
334	AVDSGTATALPDQAS
335	GTATALPDQASDDGD
336	ALPDQASDDGDKGSD
337	QASDDGDKGSDVESY
338	DGDKGSDVESYSSMP
339	GSDVESYSSMPPLEG
340	ESYSSMPPLEGEPGD
341	SMPPLEGEPGDPDLS
342	LEGEPGDPDLSDGSW
343	PGDPDLSDGSWSTVS
344	DLSDGSWSTVSEEAS
345	GSWSTVSEEASEDVV
346	TVSEEASEDVVCCSM
347	EASEDVVCCSMSYTW

POOL L	
Peptide	Sequence
348	DVVCCSMSYTWTGAL
349	CSMSYTWTGALITPC
350	YTWTGALITPCAAEE
351	GALITPCAAEESKLP
352	TPCAAEESKLPINAL
353	AEESKLPINALSNSL
354	KLPINALSNSLLRHH
355	NALSNSLLRHHNMVY
356	NSLLRHHNMVYATTS
357	RHHNMVYATTSRSAG
358	MVYATTSRSAGLRQK
359	TTSRSAGLRQKKVTF
360	SAGLRQKKVTFDRLQ
361	RQKKVTFDRLQVLDD
362	VTFDRLQVLDDHYRD
363	RLQVLDDHYRDVLKE
364	LDDHYRDVLKEMKAK
365	YRDVLKEMKAKASTV
366	LKEMKAKASTVKAKL
367	KAKASTVKAKLLSVE
368	STVKAKLLSVEEACK
369	AKLLSVEEACKLTPP
370	SVEEACKLTPPHSAK
371	ACKLTPPHSAKSKFG
372	TPPHSAKSKFGYGAK
373	SAKSKFGYGAKDVRN
374	KFGYGAKDVRNLSSK
375	GAKDVRNLSSKAVNH
376	VRNLSSKAVNHIHSV
377	SSKAVNHIHSVWKDL
378	VNHIHSVWKDLLEDT
379	HSVWKDLLEDTVTPI
380	KDLLEDTVTPIDTTI
381	EDTVTPIDTTIMAKN
382	TPIDTTIMAKNEVFC
383	TTIMAKNEVFCVQPE
384	AKNEVFCVQPEKGGR
385	VFCVQPEKGGRKPAR
386	QPEKGGRKPARLIVF
387	GGRKPARLIVFPDLG
388	PARLIVFPDLGVRVC
389	IVFPDLGVRVCEKMA
390	DLGVRVCEKMALYDV
391	RVCEKMALYDVVSTL
392	KMALYDVVSTLPQVV
393	YDVVSTLPQVVMGSS
394	STLPQVVMGSSYGFQ
395	QVVMGSSYGFQYSPG
396	GSSYGFQYSPGQRVE
397	GFQYSPGQRVEFLVN
398	SPGQRVEFLVNTWKS
399	RVEFLVNTWKSKKNP
400	LVNTWKSKKNPMGFS
401	WKSKKNPMGFSYDTR
402	KNPMGFSYDTRCFDS
403	GFSYDTRCFDSTVTE
404	DTRCFDSTVTENDIR
405	FDSTVTENDIRVEES
406	VTENDIRVEESIYQC
407	DIRVEESIYQCCDLA
408	EESIYQCCDLAPEAR
409	YQCCDLAPEARQAIK
410	DLAPEARQAIKSLTE
411	EARQAIKSLTERLYI
412	AIKSLTERLYIGGPL
413	LTERLYIGGPLTNSK
414	LYIGGPLTNSKGQNC
415	GPLTNSKGQNCGYRR
416	NSKGQNCGYRRCRAS
417	QNCGYRRCRASGVLT
418	YRRCRASGVLTTSCG
419	RASGVLTTSCGNTLT
420	VLTTSCGNTLTCYLK

POOL M	
Peptide	Sequence
421	SCGNTLTCYLKASAA
422	TLTCYLKASAACRAA
423	YLKASAACRAAKLQD
424	SAACRAAKLQDCTML
425	RAAKLQDCTMLVNAA
426	LQDCTMLVNAAGLVV
427	TMLVNAAGLVVICES
428	NAAGLVVICESAGTQ
429	LVVICESAGTQEDAA
430	CESAGTQEDAASLRV
431	GTQEDAASLRVFTEA
432	DAASLRVFTEAMTRY
433	LRVFTEAMTRYSAPP
434	TEAMTRYSAPPGDPP
435	TRYSAPPGDPPQPEY
436	APPGDPPQPEYDLEL
437	DPPQPEYDLELITSC
438	PEYDLELITSCSSNV
439	LELITSCSSNVSVAH
440	TSCSSNVSVAHDASG
441	SNVSVAHDASGKRVY
442	VAHDASGKRVYYLTR
443	ASGKRVYYLTRDPTT
444	RVYYLTRDPTTPLAR
445	LTRDPTTPLARAAWE
446	PTTPLARAAWETARH
447	LARAAWETARHTPVN
448	AWETARHTPVNSWLG
449	ARHTPVNSWLGNIIM
450	PVNSWLGNIIMYAPT
451	WLGNIIMYAPTLWAR
452	IIMYAPTLWARMILM
453	APTLWARMILMTHFF
454	WARMILMTHFFSILL
455	ILMTHFFSILLAQEQ
456	HFFSILLAQEQLEKA
457	ILLAQEQLEKALDCQ
458	QEQLEKALDCQIYGA
459	EKALDCQIYGACYSI
460	DCQIYGACYSIEPLD
461	YGACYSIEPLDLPQI
462	YSIEPLDLPQIIERL
463	PLDLPQIIERLHGLS
464	PQIIERLHGLSAFSL
465	ERLHGLSAFSLHSYS
466	GLSAFSLHSYSPGEI
467	FSLHSYSPGEINRVA
468	SYSPGEINRVASCLR
469	GEINRVASCLRKLGV
470	RVASCLRKLGVPPLR
471	CLRKLGVPPLRVWRH
472	LGVPPLRVWRHRARS
473	PLRVWRHRARSVRAR
474	WRHRARSVRARLLSQ
475	ARSVRARLLSQGGRA
476	RARLLSQGGRAATCG
477	LSQGGRAATCGKYLF
478	GRAATCGKYLFNWAV
479	TCGKYLFNWAVKTKL
480	YLFNWAVKTKLKLTP
481	WAVKTKLKLTPIPAA
482	TKLKLTPIPAASQLD
483	LTPIPAASQLDLSGW
484	PAASQLDLSGWFVAG
485	QLDLSGWFVAGYSGG
486	SGWFVAGYSGGDIYH
487	VAGYSGGDIYHSLSR
488	SGGDIYHSLSRARPR
489	IYHSLSRARPRWFML
490	LSRARPRWFMLCLLL
491	RPRWFMLCLLLLSVG
492	FMLCLLLLSVGVGIY
493	LLLLSVGVGIYLLPN
494	LLLSVGVGIYLLPNR

10 Appendix 2-3 PCR conditions for viral sequencing

(sequencing performed and optimised by Christabel Kelly and Johnny Halliday)

Primers 5'-3'	1stR PCR cycle	2ndR PCR cycle	Length	Epitope
Ext: ATCACGGCGTACGCCCAGCAGA ATCGGCGTGCCTCGTGACCA Int: AGCCTAACTGGCCGGGACAA TCCGAGGAGCCGCAAGTGCA	50°C X 30mins, 94°C X 2mins, 39 cycles of 94°C X15secs, 52°C X 30secs, 68°C X 30secs, final elongation at 68°C X 5mins	94°C X 2mins then 39 cycles of 94°C X 15secs, 55°C X30secs, 72°C X30secs then final elongation at 72°C X 2mins	250bp	CVNGVCWTV
Ext: GACAAAAACCAAGTGGAGGG GAGGACCTTCCCCAGTCC Int: CCTACGGCAAGTTCCTTGC AGCGTGRTTGTCTCAATGG	50°C X 45mins, 94°C X 2mins, 39 cycles of 94°C X 30secs, 52°C X 30secs, 68°C X 2mins, final elongation at 68°C X 10mins	94°C X 2mins then 39 cycles of 94°C X 30secs, 52°C X30secs, 72°C X30secs then final elongation at 72°C X 5mins	528bp	KLSGLGINAV, HSKKKCDEL, ATDALMTGY, TLTHPVTK
Ext: as above Int: TGTGTCACYCAGACAGTCG GGGCCCTTCTGCTTGAACTGC	As above	94°C X 2mins then 39 cycles of 94°C X 30secs, 57°C X30secs, 72°C X 1min then final elongation at 72°C X 5mins	747bp	SVVIVGRIIL QEFDEMEECASHLPY
Ext: GCTCGCYGAGCAGTTCAAGC TYGACCATGACCCGTCGC Int: GCTCGYGAGCAGTTCAAGC GGCTATYAGCCCGGTTCATCC	50°C X45mins, 94°C X 2mins, 39 cycles of 94°C X30secs, 54°C X 30secs, 68°C X 2mins, final elongation at 68°C X 10mins	94°C X 2mins then 39 cycles of 94°C X 30secs, 55°C X30secs, 72°C X 1min then final elongation at 72°C X 5mins	575bp	Geno1a: ILAGYGAGV ALVVGVVCAA
Ext: as above Int: AGGAACATGTGGAGTGGG GTTYTCTGACTCAACCCTGG	As above	94°C X 2mins then 39 cycles of 94°C X 30secs, 53°C X30secs, 72°C X 45secs then final elongation at 72°C X 5mins	570bp	Geno1a APNYSRAL FQVGLNQYLVGSQLP
Ext: GTGGAAGTGTCTCAYACG ATGTTYCCGCCCATCTCCTGCCG Int: CGARCAGGGAATGCAGCTCGC AGCCGGTTCATCCACTGC	50°C X45mins, 94°C X 2mins, 39 cycles of 94°C X30secs, 54°C X 30secs, 68°C X 2mins, final elongation at 68°C X 10mins	94°C X 2mins then 39 cycles of 94°C X 30secs, 55°C X30secs, 72°C X 45secs then final elongation at 72°C X 5mins	550bp	Geno1b ILAGYGAGV ALVVGVVCAA
Ext: as above Int: CACCTGCCCATGTGGAGC AGGGGTCGGTRAGCATG	As above	As above	430bp	Geno1b APNYSRAL FQVGLNQYLVGSQLP
Ext: CCACATCAACTCCGTGTGG TTCATCGGTTGGGGAGGAGG Int: CCACATCAACTCCGTGTGG CCACACACGAGCATGGTGC	50°C X45mins, 94°C X 2mins, 39 cycles of 94°C X30secs, 53°C X 30secs, 68°C X 2mins, final elongation at 68°C X 10mins	94°C X 2mins then 39 cycles of 94°C X 30secs, 53°C X30secs, 72°C X 45secs then final elongation at 72°C X 7mins	580bp	AYDVVSTL
Ext: GGCGACGACTTAGTCGTTATCTGTG TTCAAGCTGGTCCCTGGCTATAAGG Int: GTTATCTGTGAAAGTGCGGGGTCC GGCTATAAGGACGCTAAAGAAATGG	50°C X30mins, 94°C X 2mins, 39 cycles of 94°C X15secs, 55°C X 30secs, 68°C X 30secs, final elongation at 68°C X 5mins	94°C X 2mins then 39 cycles of 94°C X 15secs, 57°C X30secs, 72°C X 30secs then final elongation at 72°C X 2mins	288bp	LTRTDPTTPL
Ext: CCACATCAACTCCGTGTGG TTCATCGGTTGGGGAGGAGG Int: GCCTGCTACTCCATAGAACC TTCATCGGTTGGGGAGGAG	50°C X45mins, 94°C X 2mins, 39 cycles of 94°C X30secs, 53° X 30secs, 68°C X 90secs, final elongation at 68°C X 10mins	94°C X 2mins then 39 cycles of 94°C X 30secs, 55°C X30secs, 72°C X 40secs then final elongation at 72°C X 4mins	390bp	Geno 1a RPRWFMCLLLLSVG
Ext: CGCTGYTTTGACTCAACG ATTGGCCTGGAGTGTTTA Int: CYCACTTCTTCTCCATCC ATTGGCCTGGAGTGTTTA	As above	94°C X 2mins then 39 cycles of 94°C X 30secs, 51°C X30secs, 72°C X 40secs then final elongation at 72°C X 4mins	487bp	Geno 1b RPRWFMCLLLLSVG

11 Appendix 5-1 Isolating mouse splenocytes

SOP Ref No	**SOP-IU001**
SOP title	**Standard operating procedure for isolation of mouse splenocytes**
Category	**Laboratory**
Date version 1 issued	**21th June 2007**
Version	**1.0**

STANDARD OPERATING PROCEDURE FOR ISOLATION OF MOUSE SPLENOCYTES

INTRODUCTION

The procedure described below is used to isolate splenocytes from immunized mice. The spleen is aseptically removed from the mouse right after sacrifice and splenocytes are prepared by mechanical disruption of the organ through a stainless steel mesh. Red blood cells are removed by lysis and splenocytes are resuspended in complete culture medium, counted and used to test specific cell-mediated immune responses.

MATERIALS

Equipment (those listed or equivalent)

1. Sterile disposable serological pipets
2. Pipet-Aid Filler/Dispenser (Falcon 7591)
3. Pipetman (Gilson P200- Gilson P20)
4. Petri dish (Falcon 1007) 3cm (15*30mm)
5. Stainless steel meshes
6. Sterilized forceps and scissors
7. Sterile 50 ml polypropylene centrifuge tube (falcon)
8. Sterile 15 ml polypropylene centrifuge tube (falcon)
9. Sterile tips for pipetman (Molecular Bio Products 2069 and 2079E)
10. Biological safety cabinet
11. 70μm Nylon cell strainer (Falcon 2350)

Reagents (those listed or equivalent)

1. R10 medium:

- RPMI medium 1640 (GibcoBRL 11875-093)
- 10% heat inactivated FBS
- 55mM 2-mercaptoethanol (GibcoBRL 21985-023), diluted 1:1000
- 1M HEPES buffer (GibcoBRL 15630-080), diluted 1:100
- 200mM L-glutamine (GibcoBRL 25030-081), diluted 1:100
- 100X penicillin-streptomicin solution (GibcoBRL 15140-122), diluted 1:100

2. Sterile PBS
3. ACK lysing buffer (GibcoBRL 79-0422 DG)

PROCEDURE

1. For each test mouse label one sterile 15 ml conical tube with mouse code number and add 3ml of R10. Have ready three pairs of sterilized scissors/forceps.

2. Sacrifice mice, disinfect fur with alcohol and open the skin with first pair of scissor/forceps. With animals lying on their right flank, open peritoneum in correspondence of the spleen with the second pair of scissor/forceps. Aseptically remove spleen using the third sterile scissors and forceps and place it in a 15ml tube containing 3ml of R10.

3. Once under biological hood, place freshly removed spleen in a 30*15mm Petri dishes containing a sterile stainless steel mesh. With forceps snatch and press the organ against the mesh until mostly fibrous tissue remains. Discard fibrous tissue.

4. Further disperse clumps in the splenocytes suspension by pipetting up and down with a 5ml serological pipette in the Petri dish through the mesh several times.

5. Carefully transfer cell suspension into a 50ml conical tube previously labeled with each animal code number.

6. Wash the mesh and dish bottom with further 3ml of R10 medium with a new 5ml serological pipette and add wash to the tube containing cell suspension.

7. Spin tubes at 1200 rpm for 10' at room temperature (RT).

8. Red Blood Cell (RBC) osmhotic lysis: with a 5ml serological pipette resuspend cell pellets in 3ml of ACK lysing buffer and pipette up and down vigorously three times.

9. Incubate 5’ at room temperature by gently shaking.

10. Stop lysis by adding up to 30ml of sterile PBS and spin at 1200 rpm for 10' at RT

11. Gently brake pellets by tapping the tube, and wash cells by re-suspending in 20ml of R10 with a 25ml serological pipette, spin at 1200 rpm for 10' at RT

12. Gently brake pellets by tapping the tube, finally re-suspend cell pellet in 20ml of R10 medium with a 25ml serological pipette, and filter cells through a 70μm Nylon cell strainer to remove RBC lysis-derived membranes into a new 50ml conical tube labeled with animal code number.

13. Count viable cells by diluting 1:20 in Guava ViaCount reagent.

14. If cells must be tested in ELIspot, spin at 1200 rpm for 10' at RT and finally resuspend cells at $8x10^6$/ml in R10.

15. If splenocytes must be shipped, resuspend them in 50ml of R10 in step 12, and close firmly the tube. Shipment must be at 4 ^oC.

12 Appendix 5-2 Murine ELISpot protocol

SOP Ref No	**SOP IU-002**
SOP title	**Standard operating procedure for evaluation of Interferon-gamma-producing T-cells by ELISpot assay following HCV-specific stimulation in the mouse**
Category	**Laboratory**
Date version 1 issued	**21 June 2007**
Version	**4.0**
Author(s)	**Stefania Capone / Mariarosaria Naddeo**
Modification history	

STANDARD OPERATING PROCEDURE FOR EVALUATION OF INTERFERON-GAMMA-PRODUCING T CELLS BY ELISPOT ASSAY FOLLOWING HCV-SPECIFIC STIMULATION IN THE MOUSE

Author: Stefania Capone
Date: June 12, 2007
Approval: Dr. Antonella Folgori

INTRODUCTION

An ELIspot assay capable of detecting IFN-gamma-producing precursor T cells in a sample of splenocytes can be utilized to estimate the frequency of antigen-specific T-lymphocytes induced by vaccination. The splenocytes are serially diluted and placed in microplate wells coated with anti-mouse IFN-γ antibody. They are cultured for 20 hours with antigen, in the form of overlapping 15mer peptide pools covering the vaccine a.a. sequence, resulting in the restimulation of the precursor cells and secretion of IFN-γ. The cells are washed away, leaving the secreted IFN bound to the antibody-coated wells in concentrated areas where the cells were sitting. The captured IFN-γ is detected with biotinylated anti-mouse IFN antibody followed by alkaline phosphatase-conjugated streptavidin. The addition of insoluble alkaline phosphatase substrate results in dark spots in the wells at the sites where the cells were located, leaving one spot for each T cell that secreted IFN-gamma. The number of spots per well is directly related to the precursor frequency of antigen-specific T cells.

MATERIALS

1. Sterile PBS
2. R10 medium:
   - RPMI medium 1640 (GibcoBRL 11875-093)
   - 10% heat inactivated FBS (56 °C 30 min.)
   - 1M HEPES buffer (GibcoBRL 15630-080), diluted 1:100
   - 200mM L-glutamine (GibcoBRL 25030-081), diluted 1:100
   - 100X penicillin-streptomicin solution (GibcoBRL 15140-122), diluted 1:100
   - 55mM 2-mercaptoethanol (GibcoBRL 21985-023), diluted 1:1000
3. Coating mAb:
   anti-mouse IFN-γ antibody (U-Cytech CT665-C, 0.5mg/vial); dissolve the powder in 250μl add sterile H_2O (final concentration is 2mg/ml) and store at 4 °C or at –20 °C for prolonged period

4. Detecting mAb:
   biotinylated anti-mouse IFN-γ antibody (U-Cytech CT665-D, 50μg/vial); dissolve the powder in 500μl add sterile H_2O and wait until that the powder is dissolved completely. Store at 4 °C or at –20 °C for prolonged period.
5. Concanavalin A (Sigma C5275) stock at 2mg/ml in PBS
6. Dimethyl sulfoxide, DMSO (Sigma D2650)
7. ACK lysing buffer (GIBCO 79-0422 DG)
8. HCV 15mer peptides, stock solution at 40mg/ml in 100% DMSO (stored in small aliquots at -80°C). Single peptides are mixed in equal amounts into 6 peptide pools, and concentration of each pool is adjusted to reach 0.4mg/ml of each single peptide in the mixture by adding DMSO.
9. Wash buffer: PBS-0.05%Tween-20
10. Assay buffer: PBS-5%FBS-0.005%Tween-20
11. Streptavidin-Alkaline Phosphatase conjugate (PharMingen 13043E)
12. NBT/BCIP 1-Step solution (PIERCE 34042)
13. 96 well plates with PVDF membrane (Millipore Multiscreen HTS MSIP4510)

PROCEDURE

Day 1

Coating of MSIP plates: dilute anti-mouse IFN-γ coating antibody 1:200 in sterile PBS (final conc. 20μg/ml), dispense 100μl per well, leave over night (O/N) at 4 °C. Plates may be stored with coating solution in the refrigerator for up to 3 days

Note. Optional: coating of MSIP plates 2h at 37°C

Day 2

Wash plates 3 times with sterile PBS, 200μl per well. Discard PBS, carefully tap the plate on a paper towel to remove the excess of liquid

Blocking: dispense 200μl per well of R10 medium, leave in CO_2 incubator at 37 °C at least for 2 hours.

Note. Alternatively blocked plates (2h at 37°C) can be stored O/N at +4°C and used the day after.

5. Antigen dilutions:

- Dilute single peptides at 1μg/ml **(final conc)** in R10 50 μl will be plated/well (50ng/well)
- Dilute peptide pools at 2μg/ml in R10 for each single peptide. 50 μl will be plated/well (100ng/well of each single peptide contained in the pool)
- As positive control, dilute ConA at 10μg/ml in R10 (dilute 1:200 a 2mg/ml stock solution), 50 μl will be plated/well
- As negative control, dilute DMSO in R10 at the same concentration of the peptide solutions, 50 μl will be plated/well

6. Plating:
   Discard blocking buffer, plate in each well:

a. 50μl of single peptide, peptide pool, ConA or DMSO solution
b. 50μl of mouse splenocytes at $8X10^6$/ml ($4x10^5$ splenocytes/well) in duplicate, and 25μl of cell suspension+25μl of R10 ($2x10^5$ splenocytes/well) in duplicate

Leave plates O/N (18-20hours) in CO_2 incubator at 37 °C

Day 3

7. Wash plates 7 times with 200µl/well of wash buffer (see in the above Materials section for buffer composition)
8. Prepare biotinylated antibody solution by diluting 1:100 the mAb stock in assay buffer (see in the above Materials section for buffer composition) and filter through 22µm filter to remove precipitates, immediately before adding to plates.
9. Discard washing buffer, carefully tap the plate on a paper towel to remove the excess of liquid, dispense 50µl/well of detecting Ab solution. Leave plate 3-4 hours at room temperature
10. Wash plates 4x with 200µl/well of wash buffer (see in the above Materials section for buffer composition)
11. Prepare SA-AP solution by diluting 1:2500 the SA-AP stock in assay buffer (see in the above Materials section for buffer composition). Discard washing buffer, carefully tap the plate on a paper towel to remove the excess of liquid, dispense 50µl/well of SA-AP solution, leave at RT for 2 hours
12. Wash plates 4x with 200µl/well of wash buffer (see in the above Materials section for buffer composition)
13. NBT/BCIP ready to use solution, equilibrated at room temperature, must be filtered through 22µm filter to remove precipitates, immediately before adding to plates
14. Development: discard washing buffer, carefully tap the plate on a paper towel to remove the excess of liquid, dispense 50µl/well of filtered NBT/BCIP, and leave plates at room temperature while monitoring spots development (5-10min). Stop the reaction by washing wells on both sides of the nylon membrane with dd water
15. Air-dry plates, count spots using an automated ELIspot reader

13 References

Abdel-Hakeem, M. S., Bédard, N., Badr, G., Ostrowski, M., Sékaly, R. P., Bruneau, J., Willems, B., Heathcote, E. J. and Shoukry, N. H. (2010). Comparison of immune restoration in early versus late alpha interferon therapy against hepatitis C virus. *J. Virol.* **84**, 10429–35.

Abdelwahab, S. F., Zakaria, Z., Sobhy, M., Rewisha, E., Mahmoud, M. A., Amer, M. A., Del Sorbo, M., Capone, S., Nicosia, A., Folgori, A., Hashem, M. and El-Kamary, S. S. (2012). Hepatitis C Virus-Multispecific T-Cell Responses without Viremia or Seroconversion among Egyptian Health Care Workers at High Risk of Infection. *Clin. Vaccine Immunol.* **19**, 780–786.

Afdhal, N., Zeuzem, S., Kwo, P., Chojkier, M., Gitlin, N., Puoti, M., Romero-Gómez, M., Zarski, J. P., Agarwal, K., Buggisch, P., Foster, G. R., Braeu, N., Buti, M., Jacobson, I. M., Subramanian, G. M., Ding, X., Mo, H., Yang, J. C., Pang, P. S., Symonds, W. T., McHutchison, J. G., Muir, A. J., Mangia, A., Marcellin, P. and Investigators, I.-1 (2014). Ledipasvir and Sofosbuvir for Untreated HCV Genotype 1 Infection. *N. Engl. J. Med.* **370**, 1889–1898.

Ahlen, G., Nyström, J., Pult, I., Frelin, L., Hultgren, C. and Sallberg, M. (2005). In vivo clearance of hepatitis C virus nonstructural 3/4A–expressing hepatocytes by DNA vaccine–primed cytotoxic T lymphocytes. *J. Infect. Dis.* **192**, 2112–2116.

Ahmed, R. and Akondy, R. S. (2011). Insights into human CD8+ T-cell memory using the yellow fever and smallpox vaccines. *Immunol. Cell Biol.* **89**, 340–345.

Ahmed, R. and Gray, D. (1996). Immunological memory and protective immunity: understanding their relation. *Science* **272**, 54–60.

Akazawa, D., Moriyama, M., Yokokawa, H., Omi, N., Watanabe, N., Date, T., Morikawa, K., Aizaki, H., Ishii, K., Kato, T., Mochizuki, H., Nakamura, N. and Wakita, T. (2013). Neutralizing antibodies induced by cell culture-derived hepatitis C virus protect against infection in mice. *Gastroenterology* **145**, 447–455.e4.

Akondy, R. S., Monson, N. D., Miller, J. D., Edupuganti, S., Teuwen, D., Wu, H., Quyyumi, F., Garg, S., Altman, J. D., Del Rio, C., Keyserling, H. L., Ploss, A., Rice, C. M., Orenstein, W. A., Mulligan, M. J. and Ahmed, R. (2009). The Yellow Fever Virus Vaccine Induces a Broad and Polyfunctional Human Memory CD8+ T Cell Response. *J. Immunol.* **183**, 7919–7930.

Alter, M. J., Kruszon-Moran, D., Nainan, O. V, McQuillan, G. M., Gao, F., Moyer, L. A., Kaslow, R. A. and Margolis, H. S. (1999). The prevalence of hepatitis C virus infection in the United States, 1988 through 1994. *N. Engl. J. Med.*

341, 556–562.

Alvarez-Lajonchere, L., Shoukry, N. H., Gra, B., Amador-Cañizares, Y., Helle, F., Bédard, N., Guerra, I., Drouin, C., Dubuisson, J., González-Horta, E. E., Martínez, G., Marante, J., Cinza, Z., Castellanos, M. and Dueñas-Carrera, S. (2009). Immunogenicity of CIGB-230, a therapeutic DNA vaccine preparation, in HCV-chronically infected individuals in a Phase I clinical trial. *J. Viral Hepat.* **16**, 156–167.

Andersson, H. A. and Barry, M. A. (2004). Maximizing antigen targeting to the proteasome for gene-based vaccines. *Mol. Ther.* **10**, 432–446.

Angelosanto, J. M., Blackburn, S. D., Crawford, A. and Wherry, E. J. (2012). Progressive Loss of Memory T Cell Potential and Commitment to Exhaustion during Chronic Viral Infection. *J. Virol.* **86**, 8161–8170.

Appay, V. and Rowland-Jones, S. L. (2004). Lessons from the study of T-cell differentiation in persistent human virus infection. *Semin. Immunol.* **16**, 205–212.

Appay, V., Douek, D. C. and Price, D. A. (2008a). CD8(+) T cell efficacy in vaccination and disease. *Nat. Med.* **14**, 623–628.

Appay, V., van Lier, R. A. W., Sallusto, F. and Roederer, M. (2008b). Phenotype and function of human T lymphocyte subsets: Consensus and issues. *Cytom. Part A* **73A**, 975–983.

Ashman, J. B. and Miller, J. (1999). A Role for the Transmembrane Domain in the Trimerization of the MHC Class II-Associated Invariant Chain. *J. Immunol.* **163**, 2704–2712.

Aspinall, E. J., Corson, S., Doyle, J. S., Grebely, J., Hutchinson, S. J., Dore, G. J., Goldberg, D. J. and Hellard, M. E. (2013). Treatment of hepatitis C virus infection among people who are actively injecting drugs: a systematic review and meta-analysis. *Clin. Infect. Dis.* **57 Suppl 2**, S80–9.

Badovinac, V. P., Porter, B. B. and Harty, J. T. (2002). Programmed contraction of CD8(+) T cells after infection. *Nat. Immunol.* **3**, 619–626.

Badovinac, V. P., Messingham, K. A. N., Jabbari, A., Haring, J. S. and Harty, J. T. (2005). Accelerated CD8+ T-cell memory and prime-boost response after dendritic-cell vaccination. *Nat. Med.* **11**, 748–756.

Baerlecken, N. T., Nothdorft, S., Stummvoll, G. H., Sieper, J., Rudwaleit, M., Reuter, S., Matthias, T., Schmidt, R. E. and Witte, T. (2013). Autoantibodies against CD74 in spondyloarthritis. *Ann. Rheum. Dis.* **73**, 1211–1214.

Bandura, D. R., Baranov, V. I., Ornatsky, O. I., Antonov, A., Kinach, R., Lou, X.,

Pavlov, S., Vorobiev, S., Dick, J. E. and Tanner, S. D. (2009). Mass Cytometry: Technique for Real Time Single Cell Multitarget Immunoassay Based on Inductively Coupled Plasma Time-of-Flight Mass Spectrometry. *Anal. Chem.* **81**, 6813–6822.

Banerjee, A., Gordon, S. M., Intlekofer, A. M., Paley, M. A., Mooney, E. C., Lindsten, T., Wherry, E. J. and Reiner, S. L. (2010). Cutting edge: The transcription factor eomesodermin enables CD8+ T cells to compete for the memory cell niche. *J. Immunol.* **185**, 4988–4992.

Baraliakos, X., Baerlecken, N., Witte, T., Heldmann, F. and Braun, J. (2013). High prevalence of anti-CD74 antibodies specific for the HLA class II-associated invariant chain peptide (CLIP) in patients with axial spondyloarthritis. *Ann. Rheum. Dis.*

Barber, D. L., Wherry, E. J., Masopust, D., Zhu, B., Allison, J. P., Sharpe, A. H., Freeman, G. J. and Ahmed, R. (2006). Restoring function in exhausted CD8 T cells during chronic viral infection. *Nature* **439**, 682–687.

Barnes, E., Harcourt, G., Brown, D., Lucas, M., Phillips, R., Dusheiko, G. and Klenerman, P. (2002). The dynamics of T-lymphocyte responses during combination therapy for chronic hepatitis C virus infection. *Hepatology* **36**, 743–754.

Barnes, E., Ward, S. M., Kasprowicz, V. O., Dusheiko, G., Klenerman, P. and Lucas, M. (2004). Ultra-sensitive class I tetramer analysis reveals previously undetectable populations of antiviral CD8+ T cells. *Eur. J. Immunol.* **34**, 1570–7.

Barnes, E., Gelderblom, H. C., Humphreys, I., Semmo, N., Reesink, H. W., Beld, M. G. H. M., van Lier, R. A. W. and Klenerman, P. (2009). Cellular Immune Responses during High-Dose Interferon-α Induction Therapy for Hepatitis C Virus Infection. *J. Infect. Dis.* **199**, 819–828.

Barnes, E., Folgori, a., Capone, S., Swadling, L., Aston, S., Kurioka, a., Meyer, J., Huddart, R., Smith, K., Townsend, R., Brown, a., Antrobus, R., Ammendola, V., Naddeo, M., O'Hara, G., Willberg, C., Harrison, a., Grazioli, F., Esposito, M. L., Siani, L., Traboni, C., Oo, Y., Adams, D., Hill, a., Colloca, S., Nicosia, a., Cortese, R. and Klenerman, P. (2012). Novel Adenovirus-Based Vaccines Induce Broad and Sustained T Cell Responses to HCV in Man. *Sci. Transl. Med.* **4**, 115ra1–115ra1.

Barouch, D. H., Liu, J., Li, H., Maxfield, L. F., Abbink, P., Lynch, D. M., Iampietro, M. J., SanMiguel, A., Seaman, M. S., Ferrari, G., Forthal, D. N., Ourmanov, I., Hirsch, V. M., Carville, A., Mansfield, K. G., Stablein, D., Pau, M. G., Schuitemaker, H., Sadoff, J. C., Billings, E. A., Rao, M., Robb, M. L., Kim, J. H., Marovich, M. A., Goudsmit, J. and Michael, N. L. (2012). Vaccine protection against acquisition of neutralization-resistant SIV challenges in rhesus monkeys. *Nature* **482**, 89–93.

Barry, M. A., Lai W. C. and Johnston, S. A. (1995). Protection Against Mycoplasma-Infection Using Expression-Library Immunization. *Nature* **377**, 632–635.

Bartosch, B., Dubuisson, J. and Cosset, F.-L. (2003). Infectious hepatitis C virus pseudo-particles containing functional E1-E2 envelope protein complexes. *J. Exp. Med.* **197**, 633–642.

Basha, G., Omilusik, K., Chavez-Steenbock, A., Reinicke, A. T., Lack, N., Choi, K. B. and Jefferies, W. A. (2012). A CD74-dependent MHC class I endolysosomal cross-presentation pathway. *Nat. Immunol.* **13**, 237–245.

Bassett, S. E., Guerra, B., Brasky, K., Miskovsky, E., Houghton, M., Klimpel, G. R. and Lanford, R. E. (2001). Protective immune response to hepatitis C virus in chimpanzees rechallenged following clearance of primary infection. *Hepatology* **33**, 1479–1487.

Bassett, J. D., Yang, T. C., Bernard, D., Millar, J. B., Swift, S. L., McGray, A. J. R., VanSeggelen, H., Boudreau, J. E., Finn, J. D., Parsons, R., Evelegh, C., Damjanovic, D., Grinshtein, N., Divangahi, M., Zhang, L., Xing, Z., Wan, Y. and Bramson, J. L. (2011). CD8+ T-cell expansion and maintenance after recombinant adenovirus immunization rely upon cooperation between hematopoietic and nonhematopoietic antigen-presenting cells. *Blood* **117**, 1146–1155.

Bendall, S. C., Simonds, E. F., Qiu, P., Amir, E. D., Krutzik, P. O., Finck, R., Bruggner, R. V, Melamed, R., Trejo, A., Ornatsky, O. I., Balderas, R. S., Plevritis, S. K., Sachs, K., Pe'er, D., Tanner, S. D. and Nolan, G. P. (2011). Single-cell mass cytometry of differential immune and drug responses across a human hematopoietic continuum. *Science (80-.).* **332**, 687–696.

Bendall, S. C., Nolan, G. P., Roederer, M. and Chattopadhyay, P. K. (2012). A deep profiler's guide to cytometry. *Trends Immunol.* **33**, 323–332.

Bengsch, B., Spangenberg, H. C., Kersting, N., Neumann-Haefelin, C., Panther, E., von Weizsacker, F., Blum, H. E., Pircher, H. and Thimme, R. (2007). Analysis of CD127 and KLRG1 expression on hepatitis C virus-specific CD8+ T cells reveals the existence of different memory T-cell subsets in the peripheral blood and liver. *J. Virol.* **81**, 945–953.

Bengsch, B., Seigel, B., Ruhl, M., Timm, J., Kuntz, M., Blum, H. E., Pircher, H. and Thimme, R. (2010). Coexpression of PD-1, 2B4, CD160 and KLRG1 on exhausted HCV-specific CD8+ T cells is linked to antigen recognition and T cell differentiation. *PLoS Pathog.* **6**, e1000947.

Bengsch, B., Martin, B. and Thimme, R. (2014). Restoration of HBV-specific CD8+T cell function by PD-1 blockade in inactive carrier patients is linked to T cell differentiation. *J. Hepatol.* **61**, 1212–1219.

Bennett, H., McEwan, P., Sugrue, D., Kalsekar, A. and Yuan, Y. (2015). Assessing the Long-Term Impact of Treating Hepatitis C Virus (HCV)-Infected People Who Inject Drugs in the UK and the Relationship between Treatment Uptake and Efficacy on Future Infections. *PLoS One* **10**, e0125846.

Benova, L., Awad, S. F., Miller, F. D. and Abu-Raddad, L. J. (2015). Estimation of hepatitis C virus infections resulting from vertical transmission in Egypt. *Hepatology* **61**, 834–842.

Betts, M. R., Brenchley, J. M., Price, D. A., De Rosa, S. C., Douek, D. C., Roederer, M. and Koup, R. A. (2003). Sensitive and viable identification of antigen-specific CD8+ T cells by a flow cytometric assay for degranulation. *J. Immunol. Methods* **281**, 65–78.

Betts, M. R., Nason, M. C., West, S. M., De Rosa, S. C., Migueles, S. A., Abraham, J., Lederman, M. M., Benito, J. M., Goepfert, P. A., Connors, M., Roederer, M. and Koup, R. A. (2006). HIV nonprogressors preferentially maintain highly functional HIV-specific CD8+ T cells. … **107**, 4781–4789.

Blum, J. S., Wearsch, P. A. and Cresswell, P. (2013). Pathways of Antigen Processing. *Annu. Rev. Immunol.* **31**, 443–473.

Boettler, T., Spangenberg, H. C., Neumann-Haefelin, C., Panther, E., Urbani, S., Ferrari, C., Blum, H. E., von Weizsäcker, F. and Thimme, R. (2005). T cells with a CD4+CD25+ regulatory phenotype suppress in vitro proliferation of virus-specific CD8+ T cells during chronic hepatitis C virus infection. *J. Virol.* **79**, 7860–7867.

Bogdan, C., Moll, H., Solbach, W. and Rollinghoff, M. (1990). Tumor Necrosis Factor-Alpha in Combination with Interferon-Gamma, but Not with Interleukin-4 Activates Murine Macrophages for Elimination of Leishmania-Major Amastigotes. *Eur. J. Immunol.* **20**, 1131–1135.

Bogdan, C., Moll, H., Solbach, W. and Röllinghoff, M. (1990). Tumor necrosis factor-α in combination with interferon-γ, but not with interleukin 4 activates murine macrophages for elimination ofLeishmania major amastigotes. *Eur. J. Immunol.* **20**, 1131–1135.

Bolinger, B., Sims, S., O'Hara, G., de Lara, C., Tchilian, E., Firner, S., Engeler, D., Ludewig, B. and Klenerman, P. (2013). A new model for CD8+ T cell memory inflation based upon a recombinant adenoviral vector. *J. Immunol.* **190**, 4162–4174.

Bolinger, B., Sims, S., Swadling, L., O'Hara, G., de Lara, C., Baban, D., Saghal, N., Lee, L. N., Marchi, E., Davis, M., Newell, E., Capone, S., Folgori, A., Barnes, E. and Klenerman, P. (2015). Adenoviral Vector Vaccination Induces a Conserved Program of CD8(+) T Cell Memory Differentiation in Mouse and Man. *Cell Rep.*

Borthwick, N., Ahmed, T., Ondondo, B., Hayes, P., Rose, A., Ebrahimsa, U., Hayton, E.-J., Black, A., Bridgeman, A., Rosario, M., Hill, A. V. S., Berrie, E., Moyle, S., Frahm, N., Cox, J., Colloca, S., Nicosia, A., Gilmour, J., McMichael, A. J., Dorrell, L. and Hanke, T. (2014). Vaccine-elicited Human T Cells Recognizing Conserved Protein Regions Inhibit HIV-1. *Mol. Ther.* **22**, 464–475.

Bots, M. and Medema, J. P. (2006). Granzymes at a glance. *J. Cell Sci.* **119**, 5011–5014.

Bowen, D. G. and Walker, C. M. (2005). Mutational escape from CD8+ T cell immunity: HCV evolution, from chimpanzees to man. *J. Exp. Med.* **201**, 1709–1714.

Bowen, D., McCaughan, G. and Bertolino, P. (2005). Intrahepatic immunity: a tale of two sites? *Trends Immunol.* **26**, 512–517.

Bowen, D. G., Shoukry, N. H., Grakoui, A., Fuller, M. J., Cawthon, A. G., Dong, C., Hasselschwert, D. L., Brasky, K. M., Freeman, G. J., Seth, N. P., Wucherpfennig, K. W., Houghton, M. and Walker, C. M. (2008). Variable patterns of programmed death-1 expression on fully functional memory T cells after spontaneous resolution of hepatitis C virus infection. *J. Virol.* **82**, 5109–14.

Brahmer, J. R., Drake, C. G., Wollner, I., Powderly, J. D., Picus, J., Sharfman, W. H., Stankevich, E., Pons, A., Salay, T. M., McMiller, T. L., Gilson, M. M., Wang, C., Selby, M., Taube, J. M., Anders, R., Chen, L., Korman, A. J., Pardoll, D. M., Lowy, I. and Topalian, S. L. (2010). Phase I Study of Single-Agent Anti–Programmed Death-1 (MDX-1106) in Refractory Solid Tumors: Safety, Clinical Activity, Pharmacodynamics, and Immunologic Correlates. *J. Clin. Oncol.* **28**, 3167–3175.

Bråve, A., Ljungberg, K., Wahren, B. and Liu, M. a (2007). Vaccine delivery methods using viral vectors. *Mol. Pharm.* **4**, 18–32.

Brimacombe, C. L., Grove, J., Meredith, L. W., Hu, K., Syder, A. J., Flores, M. V., Timpe, J. M., Krieger, S. E., Baumert, T. F., Tellinghuisen, T. L., Wong-Staal, F., Balfe, P. and McKeating, J. A. (2011). Neutralizing antibody-resistant hepatitis C virus cell-to-cell transmission. *J. Virol.* **85**, 596–605.

Brinster, C., Chen, M., Boucreux, D., Paranhos-Baccala, G., Liljeström, P., Lemmonier, F. and Inchauspé, G. (2002). Hepatitis C virus non-structural protein 3-specific cellular immune responses following single or combined immunization with DNA or recombinant Semliki Forest virus particles. *J. Gen. Virol.* **83**, 369–381.

Bucci, C., von Delft, A., Christian, A., Flemming, V. M., Harrison, A., Halliday, J., Collier, J., Manganis, C., Klenerman, P., Irving, W. and Barnes, E.

(2013). “Favourable” IL28B polymorphisms are associated with a marked increase in baseline viral load in hepatitis C virus subtype 3a infection and do not predict a sustained virological response after 24 weeks of therapy. *J. Gen. Virol.* **94**, 1259–1265.

Bukczynski, J., Wen, T., Ellefsen, K., Gauldie, J. and Watts, T. H. (2004). Costimulatory ligand 4-1BBL (CD137L) as an efficient adjuvant for human antiviral cytotoxic T cell responses. *Proc. Natl. Acad. Sci.* **101**, 1291–1296.

Bukh, J., Miller, R. H. and Purcell, R. H. (1995). Genetic heterogeneity of hepatitis C virus: quasispecies and genotypes. - Abstract - UK PubMed Central. *Semin. Liver Dis.* **15**, 41–63.

Bull, R. A., Leung, P., Gaudieri, S., Deshpande, P., Cameron, B., Walker, M., Chopra, A., LLOYD, A. R., Luciani, F. and Investigators, H.-P. (2015). Transmitted/Founder Viruses Rapidly Escape from CD8(+) T Cell Responses in Acute Hepatitis C Virus Infection. *J. Virol.* **89**, 5478–5490.

Burton, D. R. (2002). Antibodies, viruses and vaccines. *Nat. Rev. Immunol.* **2**, 706–713.

Burton, J. R., Klarquist, J., Im, K., Smyk-Pearson, S., Golden-Mason, L., Castelblanco, N., Terrault, N., Rosen, H. R. and Group, V.-C. S. (2008). Prospective analysis of effector and regulatory CD4+ T cells in chronic HCV patients undergoing combination antiviral therapy. *J. Hepatol.* **49**, 329–338.

Buxton, J. a and Kim, J. H. (2008). Hepatitis A and hepatitis B vaccination responses in persons with chronic hepatitis C infections: A review of the evidence and current recommendations. *Can. J. Infect. Dis. Med. Microbiol.* **19**, 197–202.

Cabrera, R., Tu, Z. K., Xu, Y. L., Firpi, R. J., Rosen, H. R., Liu, C. and Nelson, D. R. (2004). An immunomodulatory role for CD4(+)CD25(+) regulatory T lymphocytes in hepatitis C virus infection. *Hepatology* **40**, 1062–1071.

Callendret, B., Eccleston, H. B., Hall, S., Satterfield, W., Capone, S., Folgori, A., Cortese, R., Nicosia, A. and Walker, C. M. (2014). T-Cell Immunity and Hepatitis C Virus Reinfection After Cure of Chronic Hepatitis C With an Interferon-Free Antiviral Regimen in a Chimpanzee. *Hepatology* **60**, 1531–1540.

Callendret, B., Eccleston, H. B., Hall, S., Satterfield, W., Capone, S., Folgori, A., Cortese, R., Nicosia, A. and Walker, C. M. (2015). Persistent HCV replication despite priming of functional CD8+ T cells by combined therapy with a vaccine and direct acting antiviral. *Hepatology* . Oct 29. doi: 10.1002/hep.28309. [Epub ahead of print]

Capone, S., Meola, A., Ercole, B. B., Vitelli, A., Pezzanera, M., Ruggeri, L.,

Davies, M. E., Tafi, R., Santini, C., Luzzago, A., Fu, T.-M., Bett, A., Colloca, S., Cortese, R., Nicosia, A. and Folgori, A. (2006a). A novel adenovirus type 6 (Ad6)-based hepatitis C virus vector that overcomes preexisting anti-ad5 immunity and induces potent and broad cellular immune responses in rhesus macaques. *J. Virol.* **80**, 1688–1699.

Capone, S., Zampaglione, I., Vitelli, A., Pezzanera, M., Kierstead, L., Burns, J., Ruggeri, L., Arcuri, M., Cappelletti, M., Meola, A., Ercole, B. B., Tafi, R., Santini, C., Luzzago, A., Fu, T.-M., Colloca, S., Ciliberto, G., Cortese, R., Nicosia, A., Fattori, E. and Folgori, A. (2006b). Modulation of the immune response induced by gene electrotransfer of a hepatitis C virus DNA vaccine in nonhuman primates. *J. Immunol.* **177**, 7462–7471.

Capone, S., Reyes-Sandoval, A., Naddeo, M., Siani, L., Ammendola, V., Rollier, C. S., Nicosia, A., Colloca, S., Cortese, R., Folgori, A. and Hill, A. V. S. (2010). Immune responses against a liver-stage malaria antigen induced by simian adenoviral vector AdCh63 and MVA primeâ€“boost immunisation in non-human primates. *Vaccine* **29**, 256–265.

Capone, S., D'Alise, A. M., Ammendola, V., Colloca, S., Cortese, R., Nicosia, A. and Folgori, A. (2013). Development of chimpanzee adenoviruses as vaccine vectors: challenges and successes emerging from clinical trials. *Expert Rev. Vaccines* **12**, 379–393.

Capone, S., Naddeo, M., D'Alise, A. M., Abbate, A., Grazioli, F., Del Gaudio, A., Del Sorbo, M., Esposito, M. L., Ammendola, V., Perretta, G., Taglioni, A., Colloca, S., Nicosia, A., Cortese, R. and Folgori, A. (2014). Fusion of HCV Nonstructural Antigen to MHC Class II-associated Invariant Chain Enhances T-cell Responses Induced by Vectored Vaccines in Nonhuman Primates. *Mol. Ther.*

Casazza, J. P., Betts, M. R., Price, D. a, Precopio, M. L., Ruff, L. E., Brenchley, J. M., Hill, B. J., Roederer, M., Douek, D. C. and Koup, R. a (2006). Acquisition of direct antiviral effector functions by CMV-specific CD4+ T lymphocytes with cellular maturation. *J. Exp. Med.* **203**, 2865–2877.

Casimiro, D. R., Chen, L., Fu, T.-M., Evans, R. K., Caulfield, M. J., Davies, M. E., Tang, A., Chen, M., Huang, L., Harris, V., Freed, D. C., Wilson, K. A., Dubey, S., Zhu, D.-M., Nawrocki, D., Mach, H., Troutman, R., Isopi, L., Williams, D., Hurni, W., Xu, Z., Smith, J. G., Wang, S., Liu, X., Guan, L., Long, R., Trigona, W., Heidecker, G. J., Perry, H. C., Persaud, N., Toner, T. J., Su, Q., Liang, X., Youil, R., Chastain, M., Bett, A. J., Volkin, D. B., Emini, E. A. and Shiver, J. W. (2003). Comparative immunogenicity in rhesus monkeys of DNA plasmid, recombinant vaccinia virus, and replication-defective adenovirus vectors expressing a human immunodeficiency virus type 1 gag gene. *J. Virol.* **77**, 6305–6313.

Casimiro, D. R., Bett, A. J., Fu, T.-M., Davies, M. E., Tang, A., Wilson, K. A., Chen, M., Long, R., McKelvey, T., Chastain, M., Gurunathan, S., Tartaglia, J.,

Emini, E. A. and Shiver, J. (2004). Heterologous human immunodeficiency virus type 1 priming-boosting immunization strategies involving replication-defective adenovirus and poxvirus vaccine vectors. *J. Virol.* **78**, 11434–11438.

Catanese, M. T. and Dorner, M. (2015). Advances in experimental systems to study hepatitis C virus in vitro and in vivo. *Virology* **479-480**, 221–233.

Chan, J., Xing, Y., Magliozzo, R. S. and Bloom, B. R. (1992). Killing of virulent Mycobacterium tuberculosis by reactive nitrogen intermediates produced by activated murine macrophages. *J. Exp. Med.* **175**, 1111–1122.

Cheent, K. and Khakoo, S. I. (2011). Natural killer cells and hepatitis C: action and reaction. *Gut* **60**, 268–278.

Chen, S. L. and Morgan, T. R. (2006). The natural history of hepatitis C virus (HCV) infection. *Int. J. Med. Sci.* **3**, 47–52.

Chen, P. J., Wang, J. T., Hwang, L. H., Yang, Y. H., Hsieh, C. L., Kao, J. H., Sheu, J. C., Lai, M. Y., Wang, T. H. and Chen, D. S. (1992). Transient immunoglobulin M antibody response to hepatitis C virus capsid antigen in posttransfusion hepatitis C: putative serological marker for acute viral infection. *Proc. Natl. Acad. Sci.* **89**, 5971–5975.

Chen, H., Xiang, Z. Q., Li, Y., Kurupati, R. K., Jia, B., Bian, A., Zhou, D. M., Hutnick, N., Yuan, S., Gray, C., Serwanga, J., Auma, B., Kaleebu, P., Zhou, X., Betts, M. R. and Ertl, H. C. J. (2010). Adenovirus-Based Vaccines: Comparison of Vectors from Three Species of Adenoviridae. *J. Virol.* **84**, 10522–10532.

Chen, J. Y., Feeney, E. R. and Chung, R. T. (2014a). HCV and HIV co-infection: mechanisms and management. *Nat. Rev. Gastroenterol. Hepatol.* **11**, 371.

Chen, J., Zhao, Y., Zhang, C., Chen, H., Feng, J., Chi, X., Pan, Y., Du, J., Guo, M., Cao, H., Chen, H., Wang, Z., Pei, R., Wang, Q., Pan, L., Niu, J., Chen, X. and Tang, H. (2014b). Persistent hepatitis C virus infections and hepatopathological manifestations in immune-competent humanized mice. *Cell Res.* **24**, 1050–1066.

Chmielewska, A. M., Naddeo, M., Capone, S., Ammendola, V., Hu, K., Meredith, L., Verhoye, L., Rychlowska, M., Rappuoli, R., Ulmer, J. B., Colloca, S., Nicosia, A., Cortese, R., Leroux-Roels, G., Balfe, P., Bienkowska-Szewczyk, K., Meuleman, P., McKeating, J. A. and Folgori, A. (2014). Combined Adenovirus Vector and Hepatitis C Virus Envelope Protein Prime-Boost Regimen Elicits T Cell and Neutralizing Antibody Immune Responses. *J. Virol.* **88**, 5502–5510.

Choo, Q. L., Kuo, G., Weiner, A. J., Overby, L. R., Bradley, D. W. and Houghton,

M. (1989). Isolation of a cDNA clone derived from a blood-borne non-A, non-B viral hepatitis genome. *Science (80-.).* **244**, 359–362.

Choo, Q. L., Kuo, G., Ralston, R., Weiner, A., Chien, D., Van Nest, G., Han, J., Berger, K., Thudium, K. and Kuo, C. (1994). Vaccination of chimpanzees against infection by the hepatitis C virus. *Proc. Natl. Acad. Sci.* **91**, 1294–1298.

Chung, R. T., Gordon, F. D., Curry, M. P., Schiano, T. D., Emre, S., Corey, K., Markmann, J. F., Hertl, M., Pomposelli, J. J., Pomfret, E. A., Florman, S., Schilsky, M., Broering, T. J., Finberg, R. W., Szabo, G., Zamore, P. D., Khettry, U., Babcock, G. J., Ambrosino, D. M., Leav, B., Leney, M., Smith, H. L. and Molrine, D. C. (2013). Human Monoclonal Antibody MBL-HCV1 Delays HCV Viral Rebound Following Liver Transplantation: A Randomized Controlled Study. *Am. J. Transplant.* **13**, 1047–1054.

Colloca, S., Barnes, E., Folgori, A., Ammendola, V., Capone, S., Cirillo, A., Siani, L., Naddeo, M., Grazioli, F., Esposito, M. L., Ambrosio, M., Sparacino, A., Bartiromo, M., Meola, A., Smith, K., Kurioka, A., O'Hara, G. A., Ewer, K. J., Anagnostou, N., Bliss, C., Hill, A. V. S., Traboni, C., Klenerman, P., Cortese, R. and Nicosia, A. (2012). Vaccine Vectors Derived from a Large Collection of Simian Adenoviruses Induce Potent Cellular Immunity Across Multiple Species. *Sci. Transl. Med.* **4**, 115ra2–115ra2.

Conway, J. M. and Perelson, A. S. (2015). Post-treatment control of HIV infection. *Proc. Natl. Acad. Sci.* **112**, 5467–5472.

Cooper, S., Erickson, A. L., Adams, E. J., Kansopon, J., Weiner, A. J., Chien, D. Y., Houghton, M., Parham, P. and Walker, C. M. (1999). Analysis of a successful immune response against hepatitis C virus. *Immunity* **10**, 439–449.

Cottingham, M. G. and Carroll, M. W. (2013). Recombinant MVA vaccines: Dispelling the myths. *Vaccine*.

Cox, A. L., Mosbruger, T., Lauer, G. M., Pardoll, D., Thomas, D. L. and Ray, S. C. (2005). Comprehensive analyses of CD8+ T cell responses during longitudinal study of acute human hepatitis C. *Hepatology* **42**, 104–112.

Cox, M. M. J., Izikson, R., Post, P. and Dunkle, L. (2015). Safety, efficacy, and immunogenicity of Flublok in the prevention of seasonal influenza in adults. *Ther. Adv. vaccines* **3**, 97–108.

Cramp, M. E., Rossol, S., Chokshi, S., Carucci, P., Williams, R. and Naoumov, N. V (2000). Hepatitis C virus-specific T-cell reactivity during interferon and ribavirin treatment in chronic hepatitis C. *Gastroenterology* **118**, 346–355.

Crouse, J., Kalinke, U. and Oxenius, A. (2015). Regulation of antiviral T cell responses by type I interferons. *Nat. Rev. Immunol.* **15**, 231–242.

Curtsinger, J. M. and Mescher, M. F. (2010). Inflammatory cytokines as a third signal for T cell activation. *Curr. Opin. Immunol.* **22**, 333–340.

D'Ambrosio, R., Aghemo, A., Rumi, M. G., Ronchi, G., Donato, M. F., Paradis, V., Colombo, M. and Bedossa, P. (2012). A morphometric and immunohistochemical study to assess the benefit of a sustained virological response in hepatitis C virus patients with cirrhosis. *Hepatology* **56**, 532–543.

Dahari, H., Feinstone, S. M. and Major, M. E. (2010). Meta-analysis of hepatitis C virus vaccine efficacy in chimpanzees indicates an importance for structural proteins. *Gastroenterology* **139**, 965–974.

Daigneault, M., Preston, J. A., Marriott, H. M., Whyte, M. K. B. and Dockrell, D. H. (2010). The Identification of Markers of Macrophage Differentiation in PMA-Stimulated THP-1 Cells and Monocyte-Derived Macrophages. *PLoS One* **5**, e8668.

Dalod, M., Salazar-Mather, T. P., Malmgaard, L., Lewis, C., Asselin-Paturel, C., Brière, F., Trinchieri, G. and Biron, C. a (2002). Interferon alpha/beta and interleukin 12 responses to viral infections: pathways regulating dendritic cell cytokine expression in vivo. *J. Exp. Med.* **195**, 517–528.

Darrah, P. A., Patel, D. T., De Luca, P. M., Lindsay, R. W. B., Davey, D. F., Flynn, B. J., Hoff, S. T., Andersen, P., Reed, S. G., Morris, S. L., Roederer, M. and Seder, R. A. (2007). Multifunctional TH1 cells define a correlate of vaccine-mediated protection against Leishmania major. *Nat. Med.* **13**, 843–850.

Davis, G. L., Nelson, D. R., Terrault, N., Pruett, T. L., Schiano, T. D., Fletcher, C. V, Sapan, C. V, Riser, L. N., Li, Y. F., Whitley, R. J., Gnann, J. W. and Grp, C. A. S. (2005). A randomized, open-label study to evaluate the safety and pharmacokinetics of human hepatitis C immune globulin (Civacir) in liver transplant recipients. *Liver Transpl.* **11**, 941–949.

Day, C. L., Kaufmann, D. E., Kiepiela, P., Brown, J. A., Moodley, E. S., Reddy, S., Mackey, E. W., Miller, J. D., Leslie, A. J., DePierres, C., Mncube, Z., Duraiswamy, J., Zhu, B., Eichbaum, Q., Altfeld, M., Wherry, E. J., Coovadia, H. M., Goulder, P. J. R., Klenerman, P., Ahmed, R., Freeman, G. J. and Walker, B. D. (2006). PD-1 expression on HIV-specific T cells is associated with T-cell exhaustion and disease progression. *Nature* **443**, 350–354.

Dazert, E., Neumann-Haefelin, C., Bressanelli, S., Fitzmaurice, K., Kort, J., Timm, J., McKiernan, S., Kelleher, D., Gruener, N., Tavis, J. E., Rosen, H. R., Shaw, J., Bowness, P., Blum, H. E., Klenerman, P., Bartenschlager, R. and Thimme, R. (2009). Loss of viral fitness and cross-recognition by CD8+ T cells limit HCV escape from a protective HLA-B27-restricted human immune response. *J. Clin. Invest.* **119**, 376–386.

de Jong, Y. P., Dorner, M., Mommersteeg, M. C., Xiao, J. W., Balazs, A. B., Robbins, J. B., Winer, B. Y., Gerges, S., Vega, K., Labitt, R. N., Donovan, B. M., Giang, E., Krishnan, A., Chiriboga, L., Charlton, M. R., Burton, D. R., Baltimore, D., Law, M., Rice, C. M. and Ploss, A. (2014). Broadly neutralizing antibodies abrogate established hepatitis C virus infection. *Sci. Transl. Med.* **6**, 254ra129.

Delogu, G., Howard, A., Collins, F. M. and Morris, S. L. (2000). DNA vaccination against tuberculosis: expression of a ubiquitin-conjugated tuberculosis protein enhances antimycobacterial immunity. *Infect. Immun.* **68**, 3097–3102.

Di Bisceglie, A. M., Janczweska-Kazek, E., Habersetzer, F., Mazur, W., Stanciu, C., Carreno, V., Tanasescu, C., Flisiak, R., Romero-Gómez, M., Fich, A., Bataille, V., Toh, M. L., Hennequi, M., Zerr, P., Honnet, G., Inchauspe, G., Agathon, D., Limacher, J. M. and Wedemeyer, H. (2014). Efficacy of Immunotherapy With TG4040, Peg-Interferon, and Ribavirin in a Phase 2 Study of Patients With Chronic HCV Infection. *YGAST* **147**, 119–U220.

Diepolder, H. M., Zachoval, R., Hoffmann, R. M., Wierenga, E. A., Santantonio, T., Jung, M. C., Eichenlaub, D. and Pape, G. R. (1995). Possible mechanism involving T-lymphocyte response to non-structural protein 3 in viral clearance in acute hepatitis C virus infection. *Lancet* **346**, 1006–1007.

Doering, T. A., Crawford, A., Angelosanto, J. M., Paley, M. A., Ziegler, C. G. and Wherry, E. J. (2012). Network Analysis Reveals Centrally Connected Genes and Pathways Involved in CD8(+) T Cell Exhaustion versus Memory. *Immunity* **37**, 1130–1144.

Donoso, G., Herzog, V. and Schmitz, A. (2005). Misfolded BiP is degraded by a proteasome-independent endoplasmic-reticulum-associated degradation pathway. *Biochem. J.* **387**, 897–903.

Dorner, M., Horwitz, J. A., Robbins, J. B., Barry, W. T., Feng, Q., Mu, K., Jones, C. T., Schoggins, J. W., Catanese, M. T., Burton, D. R., Law, M., Rice, C. M. and Ploss, A. (2011). A genetically humanized mouse model for hepatitis C virus infection. *Nature* **474**, 208–11.

Drane, D., Maraskovsky, E., Gibson, R., Mitchell, S., Barnden, M., Moskwa, A., Shaw, D., Gervase, B., Coates, S., Houghton, M. and Basser, R. (2009). Priming of CD4+ and CD8+ T cell responses using a HCV core ISCOMATRIX vaccine: a phase I study in healthy volunteers. *Hum. Vaccin.* **5**, 151–157.

Duggal, P., Thio, C. L., Wojcik, G. L., Goedert, J. J., Mangia, A., Latanich, R., Kim, A. Y., Lauer, G. M., Chung, R. T., Peters, M. G., Kirk, G. D., Mehta, S. H., Cox, A. L., Khakoo, S. I., Alric, L., Cramp, M. E., Donfield, S. M., Edlin, B. R., Tobler, L. H., Busch, M. P., Alexander, G., Rosen, H. R., Gao, X., Abdel-Hamid, M., Apps, R., Carrington, M. and Thomas, D. L. (2013). Genome-

wide association study of spontaneous resolution of hepatitis C virus infection: data from multiple cohorts. *Ann. Intern. Med.* **158**, 235–245.

Duraiswamy, J., Ibegbu, C. C., Masopust, D., Miller, J. D., Araki, K., Doho, G. H., Tata, P., Gupta, S., Zilliox, M. J., Nakaya, H. I., Pulendran, B., Haining, W. N., Freeman, G. J. and Ahmed, R. (2011). Phenotype, Function, and Gene Expression Profiles of Programmed Death-1hi CD8 T Cells in Healthy Human Adults. *J. Immunol.* **186**, 4200–4212.

Dutta, A., Barker, C. and Kallarakal, A. (2015). The HIV Treatment Gap: Estimates of the Financial Resources Needed versus Available for Scale-Up of Antiretroviral Therapy in 97 Countries from 2015 to 2020. *Plos Med.* **12**, e1001907.

Elmowalid, G. A., Qiao, M., Jeong, S.-H., Borg, B. B., Baumert, T. F., Sapp, R. K., Hu, Z., Murthy, K. and Liang, T. J. (2007). Immunization with hepatitis C virus-like particles results in control of hepatitis C virus infection in chimpanzees. *Proc. Natl. Acad. Sci.* **104**, 8427–8432.

Erickson, A. L., Kimura, Y., Igarashi, S., Eichelberger, J., Houghton, M., Sidney, J., McKinney, D., Sette, A., Hughes, A. L. and Walker, C. M. (2001). The outcome of hepatitis C virus infection is predicted by escape mutations in epitopes targeted by cytotoxic T lymphocytes. *Immunity* **15**, 883–895.

Ewer, K. J., O'Hara, G. A., Duncan, C. J. A., Collins, K. A., Sheehy, S. H., Reyes-Sandoval, A., Goodman, A. L., Edwards, N. J., Elias, S. C., Halstead, F. D., Longley, R. J., Rowland, R., Poulton, I. D., Draper, S. J., Blagborough, A. M., Berrie, E., Moyle, S., Williams, N., Siani, L., Folgori, A., Colloca, S., Sinden, R. E., Lawrie, A. M., Cortese, R., Gilbert, S. C., Nicosia, A. and Hill, A. V. S. (2013). Protective CD8+ T-cell immunity to human malaria induced by chimpanzee adenovirus-MVA immunisation. *Nat. Commun.* **4**, 2836.

Farci, P., Alter, H. J., Wong, D. C., Miller, R. H., Govindarajan, S., Engle, R., Shapiro, M. and Purcell, R. H. (1994). Prevention of hepatitis C virus infection in chimpanzees after antibody-mediated in vitro neutralization. *Proc. Natl. Acad. Sci.* **91**, 7792–7796.

Farci, P., Shimoda, A., Wong, D., Cabezon, T., DeGioannis, D., Strazzera, A., Shimizu, Y., Shapiro, M., Alter, H. J. and Purcell, R. H. (1996). Prevention of hepatitis C virus infection in chimpanzees by hyperimmune serum against the hypervariable region 1 of the envelope 2 protein. *Proc. Natl. Acad. Sci.* **93**, 15394–15399.

Farci, P., Shimoda, A., Coiana, A., Diaz, G., Peddis, G., Melpolder, J. C., Strazzera, A., Chien, D. Y., Munoz, S. J., Balestrieri, A., Purcell, R. H. and Alter, H. J. (2000). The outcome of acute hepatitis C predicted by the evolution of the viral quasispecies. *Science (80-.).* **288**, 339–344.

Fattori, E., Zampaglione, I., Arcuri, M., Meola, A., Ercole, B. B., Cirillo, A., Folgori, A., Bett, A., Cappelletti, M. and Sporeno, E. (2006). Efficient immunization of rhesus macaques with an HCV candidate vaccine by heterologous priming–boosting with novel adenoviral vectors based on different serotypes. *Gene Ther.* **13**, 1088–1096.

Faure-André, G., Vargas, P., Yuseff, M.-I., Heuzé, M., Diaz, J., Lankar, D., Steri, V., Manry, J., Hugues, S., Vascotto, F., Boulanger, J., Raposo, G., Bono, M.-R., Rosemblatt, M., Piel, M. and Lennon-Duménil, A.-M. (2008). Regulation of Dendritic Cell Migration by CD74, the MHC Class II-Associated Invariant Chain. *Science (80-.).* **322**, 1705–1710.

Fauvelle, C., Felmlee, D. J., Crouchet, E., Lee, J., Heydmann, L., Lefèvre, M., Magri, A., Hiet, M.-S., Fofana, I., Habersetzer, F., Foung, S. K. H., Milne, R., Patel, A. H., Vercauteren, K., Meuleman, P., Zeisel, M. B., Bartenschlager, R., Schuster, C. and Baumert, T. F. (2015). Apolipoprotein E Mediates Evasion From Hepatitis C Virus Neutralizing Antibodies. *Gastroenterology*.

Feld, J. J., Kowdley, K. V, Coakley, E., Sigal, S., Nelson, D. R., Crawford, D., Weiland, O., Aguilar, H., Xiong, J., Pilot-Matias, T., DaSilva-Tillmann, B., Larsen, L., Podsadecki, T. and Bernstein, B. (2014). Treatment of HCV with ABT-450/r-Ombitasvir and Dasabuvir with Ribavirin. *N. Engl. J. Med.* **370**, 1594–1603.

Feray, C., Gigou, M., Samuel, D., Ducot, B., Maisonneuve, P., Reynes, M., Bismuth, A. and Bismuth, H. (1998). Incidence of hepatitis C in patients receiving different preparations of hepatitis B immunoglobulins after liver transplantation. *Ann. Intern. Med.* **128**, 810–+.

Firbas, C., Jilma, B., Tauber, E., Buerger, V., Jelovcan, S., Lingnau, K., Buschle, M., Frisch, J. and Klade, C. S. (2006). Immunogenicity and safety of a novel therapeutic hepatitis C virus (HCV) peptide vaccine: a randomized, placebo controlled trial for dose optimization in 128 healthy subjects. *Vaccine* **24**, 4343–4353.

Fischer, W., Perkins, S., Theiler, J., Bhattacharya, T., Yusim, K., Funkhouser, R., Kuiken, C., Haynes, B., Letvin, N. L., Walker, B. D., Hahn, B. H. and Korber, B. T. (2007). Polyvalent vaccines for optimal coverage of potential T-cell epitopes in global HIV-1 variants. *Nat. Med.* **13**, 100–106.

Fitzgerald, J. C., Gao, G.-P., Reyes-Sandoval, A., Pavlakis, G. N., Xiang, Z. Q., Wlazlo, A. P., Giles-Davis, W., Wilson, J. M. and Ertl, H. C. J. (2003). A simian replication-defective adenoviral recombinant vaccine to HIV-1 gag. *J. Immunol.* **170**, 1416–1422.

Fitzmaurice, K., Petrovic, D., Ramamurthy, N., Simmons, R., Merani, S., Gaudieri, S., Sims, S., Dempsey, E., Freitas, E., Lea, S., McKiernan, S., Norris, S., Long, A., Kelleher, D. and Klenerman, P. (2011). Molecular footprints reveal the impact of the protective HLA-A*03 allele in hepatitis C

virus infection. *Gut* **60**, 1563–1571.

Flatz, L., Roychoudhuri, R., Honda, M., Filali-Mouhim, A., Goulet, J.-P., Kettaf, N., Lin, M., Roederer, M., Haddad, E. K., Sékaly, R. P. and Nabel, G. J. (2011). Single-cell gene-expression profiling reveals qualitatively distinct CD8 T cells elicited by different gene-based vaccines. *Proc. Natl. Acad. Sci. U. S. A.* **108**, 5724–5729.

Fleming, V. M., Harcourt, G., Barnes, E. and Klenerman, P. (2010). Virological footprint of CD4+ T-cell responses during chronic hepatitis C virus infection. *J. Gen. Virol.* **91**, 1396–1406.

Florholmen, J., Kristiansen, M. G., Steigen, S. E., Sørbye, S. W., Paulssen, E. J., Kvamme, J. M., Konopski, Z., Gutteberg, T. and Goll, R. (2011). A rapid chemokine response of macrophage inflammatory protein (MIP)-1α, MIP-1β and the regulated on activation, normal T expressed and secreted chemokine is associated with a sustained virological response in the treatment of chronic hepatitis C. *Clin. Microbiol. Infect.* **17**, 204–209.

Folgori, A., Spada, E., Pezzanera, M., Ruggeri, L., Mele, a, Garbuglia, a R., Perrone, M. P., Del Porto, P., Piccolella, E., Cortese, R., Nicosia, a and Vitelli, a (2006a). Early impairment of hepatitis C virus specific T cell proliferation during acute infection leads to failure of viral clearance. *Gut* **55**, 1012–1019.

Folgori, A., Capone, S., Ruggeri, L., Meola, A., Sporeno, E., Ercole, B. B., Pezzanera, M., Tafi, R., Arcuri, M., Fattori, E., Lahm, A., Luzzago, A., Vitelli, A., Colloca, S., Cortese, R. and Nicosia, A. (2006b). A T-cell HCV vaccine eliciting effective immunity against heterologous virus challenge in chimpanzees. *Nat. Med.* **12**, 190–197.

Freeman, A. J., Marinos, G., Ffrench, R. A. and Lloyd, A. R. (2001). Immunopathogenesis of hepatitis C virus infection. *Immunol. Cell Biol.* **79**, 515–536.

Frese, M., Schwärzle, V., Barth, K., Krieger, N., Lohmann, V., Mihm, S., Haller, O. and Bartenschlager, R. (2002). Interferon-γ inhibits replication of subgenomic and genomic hepatitis C virus RNAs - Frese - 2003 - Hepatology - Wiley Online Library. *Hepatology* **35**, 694–703.

Frey, S. E., Houghton, M., Coates, S., Abrignani, S., Chien, D., Rosa, D., Pileri, P., Ray, R., Di Bisceglie, A. M., Rinella, P., Hill, H., Wolff, M. C., Schultze, V., Han, J. H., Scharschmidt, B. and Belshe, R. B. (2010). Safety and immunogenicity of HCV E1E2 vaccine adjuvanted with MF59 administered to healthy adults. *Vaccine* **28**, 6367–6373.

Fried, M. W., Shiffman, M. L., Reddy, K. R., Smith, C., Marinos, G., Gonçales, F. L., Häussinger, D., Diago, M., Carosi, G., Dhumeaux, D., Craxì, A., Lin, A., Hoffman, J. and Yu, J. (2002). Peginterferon alfa-2a plus ribavirin for

chronic hepatitis C virus infection. *N. Engl. J. Med.* **347**, 975–982.

Fuller, M. J., Shoukry, N. H., Gushima, T., Bowen, D. G., Callendret, B., Campbell, K. J., Hasselschwert, D. L., Hughes, A. L. and Walker, C. M. (2010). Selection-driven immune escape is not a significant factor in the failure of CD4 T cell responses in persistent hepatitis C virus infection. *Hepatology* **51**, 378–387.

Fuller, M. J., Callendret, B., Zhu, B., Freeman, G. J., Hasselschwert, D. L., Satterfield, W., Sharpe, A. H., Dustin, L. B., Rice, C. M., Grakoui, A., Ahmed, R. and Walker, C. M. (2013). Immunotherapy of chronic hepatitis C virus infection with antibodies against programmed cell death-1 (PD-1). *Proc. Natl. Acad. Sci. U. S. A.*

Gaczynska, M., Rock, K. L. and Goldberg, A. L. (1993). Role of proteasomes in antigen presentation. *Enzyme Protein* **47**, 354–69.

Gale, M. and Foy, E. M. (2005). Evasion of intracellular host defence by hepatitis C virus. *Nature* **436**, 939–945.

Gardiner, D., Lalezari, J., Lawitz, E., DiMicco, M., Ghalib, R., Reddy, K. R., Chang, K. M., Sulkowski, M., Marro, S. O., Anderson, J., He, B., Kansra, V., McPhee, F., Wind-Rotolo, M., Grasela, D., Selby, M., Korman, A. J. and Lowy, I. (2013). A randomized, double-blind, placebo-controlled assessment of BMS-936558, a fully human monoclonal antibody to programmed death-1 (PD-1), in patients with chronic hepatitis C virus infection. *PLoS One* **8**, e63818.

Gattinoni, L., Lugli, E., Ji, Y., Pos, Z., Paulos, C. M., Quigley, M. aacute ire F., Almeida, J. R., Gostick, E., Yu, Z., Carpenito, C., Wang, E., Douek, D. C., Price, D. A., June, C. H., Marincola, F. M., Roederer, M. and Restifo, N. P. (2011). A human memory T cell subset with stem cell-like properties. *Nat. Med.* **17**, 1290–1297.

Gaucher, D., Therrien, R., Kettaf, N., Angermann, B. R., Boucher, G., Filali-Mouhim, A., Moser, J. M., Mehta, R. S., Drake, D. R., Castro, E., Akondy, R., Rinfret, A., Yassine-Diab, B., Said, E. A., Chouikh, Y., Cameron, M. J., Clum, R., Kelvin, D., Somogyi, R., Greller, L. D., Balderas, R. S., Wilkinson, P., Pantaleo, G., Tartaglia, J., Haddad, E. K. and Sékaly, R.-P. (2008). Yellow fever vaccine induces integrated multilineage and polyfunctional immune responses. *J. Exp. Med.* **205**, 3119–3131.

Gehring, A. J., Sun, D., Kennedy, P. T. F., Nolte-'t Hoen, E., Lim, S. G., Wasser, S., Selden, C., Maini, M. K., Davis, D. M., Nassal, M. and Bertoletti, A. (2007). The level of viral antigen presented by hepatocytes influences CD8 T-cell function. *J. Virol.* **81**, 2940–9.

Genser, B., Cooper, P. J., Yazdanbakhsh, M., Barreto, M. L. and Rodrigues, L. C. (2007). A guide to modern statistical analysis of immunological data. *BMC*

Immunol. **8**, 27.

Gerlach, J. T., Diepolder, H. M., Jung, M.-C., Gruener, N. H., Schraut, W. W., Zachoval, R., Hoffmann, R., Schirren, C. A., Santantonio, T. and Pape, G. R. (1999). Recurrence of hepatitis C virus after loss of virus-specific CD4+ T-cell response in acute hepatitis C. *Gastroenterology* **117**, 933–941.

Gerlach, J. T., Diepolder, H. M., Zachoval, R., Gruener, N. H., Jung, M.-C., Ulsenheimer, A., Schraut, W. W., Schirren, C. A., Waechtler, M., Backmund, M. and Pape, G. R. (2003). Acute hepatitis C: high rate of both spontaneous and treatment-induced viral clearance. *YGAST* **125**, 80–88.

Gillespie, G. M., Wills, M. R., Appay, V., O'Callaghan, C., Murphy, M., Smith, N., Sissons, P., Rowland-Jones, S., Bell, J. I. and Moss, P. A. (2000). Functional heterogeneity and high frequencies of cytomegalovirus-specific CD8(+) T lymphocytes in healthy seropositive donors. *J. Virol.* **74**, 8140–8150.

Gilligan, M. G., Knox, P., Weedon, S., Barton, R., Kerr, D. J., Searle, P. and Young, L. S. (1998). Adenoviral delivery of B7-1 (CD80) increases the immunogenicity of human ovarian and cervical carcinoma cells. *Gene Ther.* **5**, 965–974.

Golden-Mason, L., Klarquist, J., Wahed, A. S. and Rosen, H. R. (2008). Cutting Edge: Programmed Death-1 Expression Is Increased on Immunocytes in Chronic Hepatitis C Virus and Predicts Failure of Response to Antiviral Therapy: Race-Dependent Differences. *J. Immunol.* **180**, 3637–3641.

Goulder, P. J. R. and Walker, B. D. (2012). HIV and HLA Class I: An Evolving Relationship. *Immunity* **37**, 426–440.

Gowans, E. J., Roberts, S., Jones, K., Dinatale, I., Latour, P. A., Chua, B., Eriksson, E. M. Y., Chin, R., Li, S., Wall, D. M., Sparrow, R. L., Moloney, J., Loudovaris, M., Ffrench, R., Prince, H. M., Hart, D., Zeng, W., Torresi, J., Brown, L. E. and Jackson, D. C. (2010). A phase I clinical trial of dendritic cell immunotherapy in HCV-infected individuals. *J. Hepatol.* **53**, 599–607.

Grady, B. P., Schinkel, J., Thomas, X. V and Dalgard, O. (2013). Hepatitis C virus reinfection following treatment among people who use drugs. *Clin. Infect. Dis.* **57 Suppl 2**, S105–10.

Grakoui, A., WYCHOWSKI, C., LIN, C., Feinstone, S. M. and Rice, C. M. (1993). Expression and Identification of Hepatitis C Virus Polyprotein Cleavage Products. *J. Virol.* **67**, 1385–1395.

Grakoui, A., Shoukry, N. H., Woollard, D. J., Han, J.-H., Hanson, H. L., Ghrayeb, J., Murthy, K. K., Rice, C. M. and Walker, C. M. (2003). HCV persistence and immune evasion in the absence of memory T cell help. *Science (80-.).* **302**, 659–662.

Grant, E. P., Michalek, M. T., Goldberg, A. L. and Rock, K. L. (1995). Rate of antigen degradation by the ubiquitin-proteasome pathway influences MHC class I presentation. *J. Immunol.* **155**, 3750–3758.

Green, C. A., Scarselli, E., Sande, C. J., Thompson, A. J., de Lara, C. M., Taylor, K. S., Haworth, K., Del Sorbo, M., Angus, B., Siani, L., Di Marco, S., Traboni, C., Folgori, A., Colloca, S., Capone, S., Vitelli, A., Cortese, R., Klenerman, P., Nicosia, A. and Pollard, A. J. (2015). Chimpanzee adenovirus- and MVA-vectored respiratory syncytial virus vaccine is safe and immunogenic in adults. *Sci. Transl. Med.* **7**, 300ra126–300ra126.

Grujic, M., Holst, P. J., Christensen, J. P. and Thomsen, A. R. (2009). Fusion of a viral antigen to invariant chain leads to augmented T-cell immunity and improved protection in gene-gun DNA-vaccinated mice. *J. Gen. Virol.* **90**, 414–422.

Guzman, E., Cubillos-Zapata, C., Cottingham, M. G., Gilbert, S. C., Prentice, H., Charleston, B. and Hope, J. C. (2012). Modified vaccinia virus Ankara-based vaccine vectors induce apoptosis in dendritic cells draining from the skin via both the extrinsic and intrinsic caspase pathways, preventing efficient antigen presentation. *J. Virol.* **86**, 5452–5466.

Habersetzer, F., Baumert, T. F. and Stoll-Keller, F. (2009). GI-5005, a yeast vector vaccine expressing an NS3-core fusion protein for chronic HCV infection. *Curr. Opin. Mol. Ther.* **11**, 456–462.

Habersetzer, F., Honnet, G., Bain, C., Maynard Muet, M., Leroy, V., Zarski, J. P., Feray, C., Baumert, T. F., Bronowicki, J. P., Doffoël, M., Trépo, C., Agathon, D., Toh, M. L., Baudin, M., Bonnefoy, J. Y., Limacher, J. M. and Inchauspe, G. (2011). A Poxvirus Vaccine Is Safe, Induces T-Cell Responses, and Decreases Viral Load in Patients With Chronic Hepatitis C. *YGAST* **141**, 890–899.e4.

Hahn, J. A., Wylie, D., Dill, J., Sanchez, M. S., Lloyd-Smith, J. O., Page-Shafer, K. and Getz, W. M. (2009). Potential impact of vaccination on the hepatitis C virus epidemic in injection drug users. *Epidemics* **1**, 47–57.

Haining, W. N. (2012a). The numerology of T cell functional diversity. *Immunity* **36**, 10–12.

Haining, W. N. (2012b). Travels in time: assessing the functional complexity of T cells. *Proc. Natl. Acad. Sci. U. S. A.* **109**, 1359–1360.

Haining, W. N., Ebert, B. L., Subrmanian, A., Wherry, E. J., Eichbaum, Q., Evans, J. W., Mak, R., Rivoli, S., Pretz, J., Angelosanto, J., Smutko, J. S., Walker, B. D., Kaech, S. M., Ahmed, R., Nadler, L. M. and Golub, T. R. (2008). Identification of an evolutionarily conserved transcriptional signature of CD8 memory differentiation that is shared by T and B cells. *J. Immunol.* **181**, 1859–1868.

Halliday, J., Klenerman, P. and Barnes, E. (2011). Vaccination for hepatitis C virus: closing in on an evasive target. *Expert Rev. Vaccines* **10**, 659–672.

Hansen, S. G., Vieville, C., Whizin, N., Coyne-Johnson, L., Siess, D. C., Drummond, D. D., Legasse, A. W., Axthelm, M. K., Oswald, K., Trubey, C. M., Piatak, M., Lifson, J. D., Nelson, J. A., Jarvis, M. A. and Picker, L. J. (2009). Effector memory T cell responses are associated with protection of rhesus monkeys from mucosal simian immunodeficiency virus challenge. *Nat. Med.* **15**, 293–299.

Hansen, S. G., Ford, J. C., Lewis, M. S., Ventura, A. B., Hughes, C. M., Coyne-Johnson, L., Whizin, N., Oswald, K., Shoemaker, R., Swanson, T., Legasse, A. W., Chiuchiolo, M. J., Parks, C. L., Axthelm, M. K., Nelson, J. A., Jarvis, M. A., Piatak, M., Lifson, J. D. and Picker, L. J. (2011). Profound early control of highly pathogenic SIV by an effector memory T-cell vaccine. *Nature* **473**, 523–527.

Harro, C., Sun, X., Stek, J. E., Leavitt, R. Y., Mehrotra, D. V, Wang, F., Bett, A. J., Casimiro, D. R., Shiver, J. W., DiNubile, M. J., Quirk, E. and Grp, M. V.-001 S. (2009). Safety and Immunogenicity of the Merck Adenovirus Serotype 5 (MRKAd5) and MRKAd6 Human Immunodeficiency Virus Type 1 Trigene Vaccines Alone and in Combination in Healthy Adults. *Clin. Vaccine Immunol.* **16**, 1285–1292.

Heller, T., Werner, J. M., Rahman, F., Mizukoshi, E., Sobao, Y., Gordon, A. M., Sheets, A., Sherker, A. H., Kessler, E., Bean, K. S., Herrine, S. K., Stevens, M., Schmitt, J. and Rehermann, B. (2013). Occupational exposure to hepatitis C virus: early T-cell responses in the absence of seroconversion in a longitudinal cohort study. *J. Infect. Dis.* **208**, 1020–1025.

Henderson, D. K. (2003). Managing occupational risks for hepatitis C transmission in the health care setting. *Clin. Microbiol. Rev.* **16**, 546–+.

Hersperger, A. R., Martin, J. N., Shin, L. Y., Sheth, P. M., Kovacs, C. M., Cosma, G. L., Makedonas, G., Pereyra, F., Walker, B. D., Kaul, R., Deeks, S. G. and Betts, M. R. (2011). Increased HIV-specific CD8+ T-cell cytotoxic potential in HIV elite controllers is associated with T-bet expression. *Blood* **117**, 3799–3808.

Hertoghs, K. M. L., Moerland, P. D., van Stijn, A., Remmerswaal, E. B. M., Yong, S. L., van de Berg, P. J. E. J., van Ham, S. M., Baas, F., Ten Berge, I. J. M. and van Lier, R. A. W. (2010). Molecular profiling of cytomegalovirus-induced human CD8+ T cell differentiation. *J. Clin. Invest.* **120**, 4077–4090.

Hézode, C., Fontaine, H., Dorival, C., Zoulim, F., Larrey, D., Canva, V., De Ledinghen, V., Poynard, T., Samuel, D., Bourlière, M., Alric, L., Raabe, J.-J., Zarski, J. P., Marcellin, P., Riachi, G., Bernard, P.-H., Loustaud-Ratti, V., Chazouilleres, O., Abergel, A., Guyader, D., Metivier, S., Tran, A., Di

Martino, V., Causse, X., Dao, T., Lucidarme, D., Portal, I., Cacoub, P., Gournay, J., Grando-Lemaire, V., Hillon, P., Attali, P., Fontanges, T., Rosa, I., Petrov-Sanchez, V., Barthe, Y., Pawlotsky, J.-M., Pol, S., Carrat, F., Bronowicki, J. P. and Group, C. S. (2014). Effectiveness of telaprevir or boceprevir in treatment-experienced patients with HCV genotype 1 infection and cirrhosis. *Gastroenterology* **147**, 132–142.e4.

Holst, P. J., Bartholdy, C., Stryhn, A., Thomsen, A. R. and Christensen, J. P. (2007). Rapid and sustained CD4(+) T-cell-independent immunity from adenovirus-encoded vaccine antigens. *J. Gen. Virol.* **88**, 1708–1716.

Holst, P. J., Sorensen, M. R., Mandrup Jensen, C. M., Orskov, C., Thomsen, A. R. and Christensen, J. P. (2008). MHC class II-associated invariant chain linkage of antigen dramatically improves cell-mediated immunity induced by adenovirus vaccines. *J. Immunol.* **180**, 3339–3346.

Holst, P. J., Orskov, C., Thomsen, A. R. and Christensen, J. P. (2010). Quality of the Transgene-Specific CD8+ T Cell Response Induced by Adenoviral Vector Immunization Is Critically Influenced by Virus Dose and Route of Vaccination. *J. Immunol.* **184**, 4431–4439.

Holst, P. J., Christensen, J. P. and Thomsen, A. R. (2011). Vaccination against lymphocytic choriomeningitis virus infection in MHC class II-deficient mice. *J. Immunol.* **186**, 3997–4007.

Holst, P. J., Jensen, B. A. H., Ragonnaud, E., Thomsen, A. R. and Christensen, J. P. (2015). Targeting of Non-Dominant Antigens as a Vaccine Strategy to Broaden T-Cell Responses during Chronic Viral Infection. *PLoS One* **10**, e0117242.

Horner, S. M. (2014). Activation and Evasion of Antiviral Innate Immunity by Hepatitis C Virus. *J. Mol. Biol.* **426**, 1198–1209.

Houghton, M. (2011). Prospects for prophylactic and therapeutic vaccines against the hepatitis C viruses. *Immunol. Rev.* **239**, 99–108.

Houghton, M. and Abrignani, S. (2005). Prospects for a vaccine against the hepatitis C virus. *Nature* **436**, 961–966.

Houghton, M., Law, J. L. and Tyrrell, D. L. (2013). An inactivated hepatitis C virus vaccine on the horizon? *Gastroenterology* **145**, 285–288.

Huang, L., Marvin, J. M., Tatsis, N. and Eisenlohr, L. C. (2011). Cutting Edge: Selective role of ubiquitin in MHC class I antigen presentation. *J. Immunol.* **186**, 1904–1908.

Huarte, E., Larrea, E., Hernandez-Alcoceba, R., Alfaro, C., Murillo, O., Arina, A., Tirapu, I., Azpilicueta, A., Hervas-Stubbs, S., Bortolanza, S., Perez-Gracia, J. L., Civeira, M. P., Prieto, J., Riezu-Boj, J. I. and Melero, I. (2006).

Recombinant adenoviral vectors turn on the type I interferon system without inhibition of transgene expression and viral replication. *Mol. Ther.* **14**, 129–138.

Hulspas, R., O'Gorman, M. R. G., Wood, B. L., Gratama, J. W. and Sutherland, D. R. (2009). Considerations for the control of background fluorescence in clinical flow cytometry. *Cytom. Part B Clin. Cytom.* **76B**, 355–364.

Humphreys, I. S., von Delft, A., Brown, A., Hibbert, L., Collier, J. D., Foster, G. R., Rahman, M., Christian, A., Klenerman, P. and Barnes, E. (2012). HCV genotype-3a T cell immunity: specificity, function and impact of therapy. *Gut* **61**, 1589–1599.

Im, E.-J., Hong, J. P., Roshorm, Y., Bridgeman, A., Létourneau, S., Liljeström, P., Potash, M. J., Volsky, D. J., McMichael, A. J. and Hanke, T. (2011). Protective efficacy of serially up-ranked subdominant CD8+ T cell epitopes against virus challenges. *PLoS Pathog.* **7**, e1002041.

Intlekofer, A. M., Takemoto, N., Wherry, E. J., Longworth, S. A., Northrup, J. T., Palanivel, V. R., Mullen, A. C., Gasink, C. R., Kaech, S. M., Miller, J. D., Gapin, L., Ryan, K., Russ, A. P., Lindsten, T., Orange, J. S., Goldrath, A. W., Ahmed, R. and Reiner, S. L. (2005). Effector and memory CD8+ T cell fate coupled by T-bet and eomesodermin. *Nat. Immunol.* **6**, 1236–1244.

Intlekofer, A. M., Banerjee, A., Takemoto, N., Gordon, S. M., Dejong, C. S., Shin, H., Hunter, C. a, Wherry, E. J., Lindsten, T. and Reiner, S. L. (2008). Anomalous type 17 response to viral infection by CD8+ T cells lacking T-bet and eomesodermin. *Science* **321**, 408–411.

Ishii, S. and Koziel, M. J. (2008). Immune responses during acute and chronic infection with hepatitis C virus. *Clin. Immunol.* **128**, 133–147.

Jensen, S., Steffensen, M. A., Jensen, B. A. H., Schlüter, D., Christensen, J. P. and Thomsen, A. R. (2013). Adenovirus-Based Vaccine against Listeria monocytogenes: Extending the Concept of Invariant Chain Linkage. *J. Immunol.* **191**, 4152–4164.

Jo, J., Aichele, U., Kersting, N., Klein, R., Aichele, P., Bisse, E., Sewell, A. K., Blum, H. E., Bartenschlager, R., Lohmann, V. and Thimme, R. (2009). Analysis of CD8+ T-cell-mediated inhibition of hepatitis C virus replication using a novel immunological model. *Gastroenterology* **136**, 1391–1401.

Jo, J., Bengsch, B., Seigel, B., Rau, S. J., Schmidt, J., Bisse, E., Aichele, P., Aichele, U., Joeckel, L., Royer, C., Sá Ferreira, K., Borner, C., Baumert, T. F., Blum, H. E., Lohmann, V., Fischer, R. and Thimme, R. (2012). Low perforin expression of early differentiated HCV-specific CD8+ T cells limits their hepatotoxic potential. *J. Hepatol.* **57**, 9–16.

Kaech, S. M. and Wherry, E. J. (2007). Heterogeneity and cell-fate decisions in

effector and memory CD8+ T cell differentiation during viral infection. *Immunity* **27**, 393–405.

Kaech, S. M., Wherry, E. J. and Ahmed, R. R. (2002a). Effector and memory T-cell differentiation: implications for vaccine development. *Nat. Rev. Immunol.* **2**, 251–262.

Kaech, S. M., Hemby, S., Kersh, E. and Ahmed, R. (2002b). Molecular and functional profiling of memory CD8 T cell differentiation. *Cell* **111**, 837–851.

Kaech, S. M., Tan, J. T., Wherry, E. J., Konieczny, B. T., Surh, C. D. and Ahmed, R. (2003). Selective expression of the interleukin 7 receptor identifies effector CD8 T cells that give rise to long-lived memory cells. *Nat. Immunol.* **4**, 1191–1198.

Kamal, S. M., Fehr, J., Roesler, B., Peters, T. and Rasenack, J. W. (2002). Peginterferon alone or with ribavirin enhances HCV-specific CD4 T-helper 1 responses in patients with chronic hepatitis C. *YGAST* **123**, 1070–1083.

Kanagavelu, S., Termini, J. M., Gupta, S., Raffa, F. N., Fuller, K. A., Rivas, Y., Philip, S., Kornbluth, R. S. and Stone, G. W. (2014). HIV-1 adenoviral vector vaccines expressing multi-trimeric BAFF and 4-1BBL enhance T cell mediated anti-viral immunity. *PLoS One* **9**, e90100.

Kang, S. J. and Cresswell, P. (2002). Regulation of intracellular trafficking of human CD1d by association with MHC class II molecules. *EMBO J.* **21**, 1650–1660.

Kannanganat, S., Ibegbu, C., Chennareddi, L., Robinson, H. L. and Amara, R. R. (2007). Multiple-cytokine-producing antiviral CD4 T cells are functionally superior to single-cytokine-producing cells. *J. Virol.* **81**, 8468–8476.

Kao, C., Oestreich, K. J., Paley, M. A., Crawford, A., Angelosanto, J. M., Ali, M.-A. A., Intlekofer, A. M., Boss, J. M., Reiner, S. L., Weinmann, A. S. and Wherry, E. J. (2011). Transcription factor T-bet represses expression of the inhibitory receptor PD-1 and sustains virus-specific CD8+ T cell responses during chronic infection. *Nat. Immunol.* **12**, 663–671.

Kaplan, D. E., Sugimoto, K., Newton, K., Valiga, M. E., Ikeda, F., Aytaman, A., Nunes, F. A., Lucey, M. R., Vance, B. A., Vonderheide, R. H., Reddy, K. R., McKeating, J. A. and Chang, K. M. (2007). Discordant Role of CD4 T-Cell Response Relative to Neutralizing Antibody and CD8 T-Cell Responses in Acute Hepatitis C. *Gastroenterology* **132**, 654–666.

Karttunen, J. and Shastri, N. (1991). Measurement of ligand-induced activation in single viable T cells using the lacZ reporter gene. *Proc. Natl. Acad. Sci.* **88**, 3972–3976.

Kasprowicz, V., Schulze zur Wiesch, J., Kuntzen, T., Nolan, B. E., Longworth,

S., Berical, A., Blum, J., McMahon, C., Reyor, L. L., Elias, N., Kwok, W. W., McGovern, B. G., Freeman, G., Chung, R. T., Klenerman, P., Lewis-Ximenez, L., Walker, B. D., Allen, T. M., Kim, A. Y. and Lauer, G. M. (2008). High Level of PD-1 Expression on Hepatitis C Virus (HCV)-Specific CD8+ and CD4+ T Cells during Acute HCV Infection, Irrespective of Clinical Outcome. *J. Virol.* **82**, 3154–3160.

Kelly, C., Klenerman, P. and Barnes, E. (2011). Interferon lambdas: the next cytokine storm. *Gut* **60**, 1284–1293.

Kelly, C., Swadling, L., Brown, A., Capone, S., Folgori, A., Salio, M., Klenerman, P. and Barnes, E. (2015a). Cross-reactivity of hepatitis C virus specific vaccine-induced T cells at immunodominant epitopes. *Eur. J. Immunol.* **45**, 309–316.

Kelly, C., Swadling, L., Capone, S., Brown, A., Richardson, R., Halliday, J., von Delft, A., Oo, Y., Mutimer, D., Kurioka, A., Hartnell, F., Collier, J., Ammendola, V., Del Sorbo, M., Grazioli, F., Luisa Esposito, M., Di Marco, S., Siani, L., Traboni, C., Hill, A. V. S., Colloca, S., Nicosia, A., Cortese, R., Folgori, A., Klenerman, P. and Barnes, E. (2015b). Chronic Hepatitis C Virus infection subverts vaccine induced T-cell immunity in humans. *Hepatology*.

Khakoo, S. I., Thio, C. L., Martin, M. P., Brooks, C. R., Gao, X., Astemborski, J., Cheng, J., Goedert, J. J., Vlahov, D., Hilgartner, M., Cox, S., Little, A.-M., Alexander, G. J., Cramp, M. E., O'Brien, S. J., Rosenberg, W. M. C., Thomas, D. L. and Carrington, M. (2004). HLA and NK cell inhibitory receptor genes in resolving hepatitis C virus infection. *Science (80-.).* **305**, 872–874.

Khromava, A. Y., Eidex, R. B., Weld, L. H., Kohl, K. S., Bradshaw, R. D., Chen, R. T., Cetron, M. S. and Group, Y. F. V. S. W. (2005). Yellow fever vaccine: an updated assessment of advanced age as a risk factor for serious adverse events. *Vaccine* **23**, 3256–3263.

Kiecker, F., Streitz, M., Ay, B., Cherepnev, G., Volk, H. D., Volkmer-Engert, R. and Kern, F. (2004). Analysis of antigen-specific T-Cell responses with synthetic peptides - What kind of peptide for which purpose? *Hum. Immunol.* **65**, 523–536.

Kim, A. Y., Kuntzen, T., Timm, J., Nolan, B. E., Baca, M. A., Reyor, L. L., Berical, A. C., Feller, A. J., Johnson, K. L., Schulze zur Wiesch, J., Robbins, G. K., Chung, R. T., Walker, B. D., Carrington, M., Allen, T. M. and Lauer, G. M. (2011). Spontaneous control of HCV is associated with expression of HLA-B 57 and preservation of targeted epitopes. *Gastroenterology* **140**, 686–696.e1.

Kim, Y., Vaughan, K., Greenbaum, J., Peters, B., Law, M. and Sette, A. (2012). A meta-analysis of the existing knowledge of immunoreactivity against hepatitis C virus (HCV). *PLoS One* **7**, e38028.

Kim, W. R., Smith, J. M., Skeans, M. A., Schladt, D. P., Schnitzler, M. A., Edwards, E. B., Harper, A. M., Wainright, J. L., Snyder, J. J., Israni, A. K. and Kasiske, B. L. (2014). OPTN/SRTR 2012 Annual Data Report: liver. *Am. J. Transplant* **14 Suppl 1**, 69–96.

Klade, C. S., Wedemeyer, H., Berg, T., Hinrichsen, H., Cholewinska, G., Zeuzem, S., Blum, H., Buschle, M., Jelovcan, S., Buerger, V., Tauber, E., Frisch, J. and Manns, M. P. (2008). Therapeutic vaccination of chronic hepatitis C nonresponder patients with the peptide vaccine IC41. *Gastroenterology* **134**, 1385–1395.

Klade, C. S., Schuller, E., Boehm, T., von Gabain, A. and Manns, M. P. (2012). Sustained viral load reduction in treatment-naive HCV genotype 1 infected patients after therapeutic peptide vaccination. *Vaccine* **30**, 2943–2950.

Klenerman, P. (2000). Viral Escape and the Failure of Cellular Immune Responses. *Science (80-.).* **289**, 2003a–2003.

Klenerman, P. and Hill, A. (2005). T cells and viral persistence: lessons from diverse infections. *Nat. Immunol.* **6**, 873–879.

Klenerman, P. and Thimme, R. (2012). T cell responses in hepatitis C: the good, the bad and the unconventional. *Gut* **61**, 1226–1234.

Klenerman, P. and Zinkernagel, R. M. (1998). Original antigenic sin impairs cytotoxic T lymphocyte responses to viruses bearing variant epitopes. *Nature* **394**, 482–485.

Knolle, P. A. and Thimme, R. (2014). Hepatic Immune Regulation and Its Involvement in Viral Hepatitis Infection. *YGAST* **146**, 1193–1207.

Kohli, A., Osinusi, A., Sims, Z., Nelson, A., Meissner, E. G., Barrett, L. L., Bon, D., Marti, M. M., Silk, R., Kotb, C., Gross, C., Jolley, T. A., Sidharthan, S., Petersen, T., Townsend, K., Egerson, D., Kapoor, R., Spurlin, E., Sneller, M., Proschan, M., Herrmann, E., Kwan, R., Teferi, G., Talwani, R., Diaz, G., Kleiner, D. E., Wood, B. J., Chavez, J., Abbott, S., Symonds, W. T., Subramanian, G. M., Pang, P. S., McHutchison, J., Polis, M. A., Fauci, A. S., Masur, H. and Kottilil, S. (2015). Virological response after 6 week triple-drug regimens for hepatitis C: a proof-of-concept phase 2A cohort study. *Lancet* **385**, 1107–1113.

Krahn, M. D., John-Baptiste, A., Yi, Q., Doria, A., Remis, R. S., Ritvo, P. and Friedman, S. (2005). Potential cost-effectiveness of a preventive hepatitis C vaccine in high risk and average risk populations in Canada. *Vaccine* **23**, 1549–1558.

Krawczynski, K., Alter, M. J., Tankersley, D. L., Beach, M., Robertson, B. H., Lambert, S., Kuo, G., Spelbring, J. E., Meeks, E., Sinha, S. and Carson, D. A. (1996). Effect of immune globulin on the prevention of experimental hepatitis C virus infection. *J. Infect. Dis.* **173**, 822–828.

Kreijtz, J. H. C. M., Goeijenbier, M., Moesker, F. M., van den Dries, L., Goeijenbier, S., De Gruyter, H. L. M., Lehmann, M. H., Mutsert, G. de, van de Vijver, D. A. M. C., Volz, A., Fouchier, R. A. M., van Gorp, E. C. M., Rimmelzwaan, G. F., Sutter, G. and Osterhaus, A. D. M. E. (2014). Safety and immunogenicity of a modified-vaccinia-virus-Ankara-based influenza A H5N1 vaccine: a randomised, double-blind phase 1/2a clinical trial. *Lancet Infect. Dis.* **14**, 1196–1207.

Kuiken, C., Yusim, K., Boykin, L. and Richardson, R. (2005). The Los Alamos hepatitis C sequence database. *Bioinformatics* **21**, 379–384.

Kurktschiev, P. D., Raziorrouh, B., Schraut, W., Backmund, M., Wächtler, M., Wendtner, C.-M., Bengsch, B., Thimme, R., Denk, G., Zachoval, R., Dick, A., Spannagl, M., Haas, J., Diepolder, H. M., Jung, M.-C. and Gruener, N. H. (2014). Dysfunctional CD8+ T cells in hepatitis B and C are characterized by a lack of antigen-specific T-bet induction. *J. Exp. Med.* **211**, 2047–2059.

Kwak, K., Yemelyanova, A. and Roden, R. B. S. (2011). Prevention of cancer by prophylactic human papillomavirus vaccines. *Curr. Opin. Immunol.* **23**, 244–251.

La Gruta, N. L., Turner, S. J. and Doherty, P. C. (2004). Hierarchies in cytokine expression profiles for acute and resolving influenza virus-specific CD8+ T cell responses: correlation of cytokine profile and TCR avidity. *J. Immunol.* **172**, 5553–5560.

Lam, B. P., Jeffers, T., Younoszai, Z., Fazel, Y. and Younossi, Z. M. (2015). The changing landscape of hepatitis C virus therapy: focus on interferon-free treatment. *Therap. Adv. Gastroenterol.* **8**, 298–312.

Lauer, G. M. and Walker, B. D. (2001). Hepatitis C virus infection. *N. Engl. J. Med.* **345**, 41–52.

Lauer, G. M., Barnes, E., Lucas, M., Timm, J., Ouchi, K., Kim, A. Y., Day, C. L., Robbins, G. K., Casson, D. R., Reiser, M., Dusheiko, G., Allen, T. M., Chung, R. T., Walker, B. D. and Klenerman, P. (2004). High resolution analysis of cellular immune responses in resolved and persistent hepatitis C virus infection. *YGAST* **127**, 924–936.

Lavanchy, D. (2011). Evolving epidemiology of hepatitis C virus. *Clin. Microbiol. Infect.* **17**, 107–115.

Lavillette, D., Morice, Y., Germanidis, G., Donot, P., Soulier, A., Pagkalos, E., Sakellariou, G., Intrator, L., Bartosch, B., Pawlotsky, J. M. and Cosset, F. L. (2005). Human serum facilitates hepatitis C virus infection, and neutralizing responses inversely correlate with viral replication kinetics at the acute phase of hepatitis C virus infection. *J. Virol.* **79**, 6023–6034.

Law, M., Maruyama, T., Lewis, J., Giang, E., Tarr, A. W., Stamataki, Z., Gastaminza, P., Chisari, F. V, Jones, I. M., Fox, R. I., Ball, J. K., McKeating, J. A., Kneteman, N. M. and Burton, D. R. (2008). Broadly neutralizing antibodies protect against hepatitis C virus quasispecies challenge. *Nat. Med.* **14**, 25–27.

Lechner, F., Wong, D. K., Dunbar, P. R., Chapman, R., Chung, R. T., Dohrenwend, P., Robbins, G., Phillips, R., Klenerman, P. and Walker, B. D. (2000a). Analysis of successful immune responses in persons infected with hepatitis C virus. *J. Exp. Med.* **191**, 1499–1512.

Lechner, F., Sullivan, J., Spiegel, H., Nixon, D. F., Ferrari, B., Davis, A., Borkowsky, B., Pollack, H., Barnes, E., Dusheiko, G. and Klenerman, P. (2000b). Why do cytotoxic T lymphocytes fail to eliminate hepatitis C virus? Lessons from studies using major histocompatibility complex class I peptide tetramers. *Philos. Trans. R. Soc. B Biol. Sci.* **355**, 1085–1092.

Leng, L., Metz, C. N., Fang, Y., Xu, J., Donnelly, S., Baugh, J., Delohery, T., Chen, Y., Mitchell, R. A. and Bucala, R. (2003). MIF signal transduction initiated by binding to CD74. *J. Exp. Med.* **197**, 1467–1476.

Leroux-Roels, G., Depla, E., Hulstaert, F., Tobback, L., Dincq, S., Desmet, J., Desombere, I. and Maertens, G. (2004). A candidate vaccine based on the hepatitis C E1 protein: tolerability and immunogenicity in healthy volunteers. *Vaccine* **22**, 3080–3086.

Li, K. and Lemon, S. M. (2012). Innate immune responses in hepatitis C virus infection. *Semin. Immunopathol.*

Li, Y., Wang, X., Douglas, S. D., Metzger, D. S., Woody, G., Zhang, T., Song, L. and Ho, W.-Z. (2005). CD8+ T cell depletion amplifies hepatitis C virus replication in peripheral blood mononuclear cells. *J. Infect. Dis.* **192**, 1093–1101.

Liew F. Y., Li, Y. and Milott, S. (1990). Tumor-Necrosis-Factor-Alpha Synergizes with Ifn-Gamma in Mediating Killing of Leishmania-Major Through the Induction of Nitric-Oxide. *J. Immunol.* **145**, 4306–4310.

Lin, Y., Kwon, T., Polo, J., Zhu, Y. F., Coates, S., Crawford, K., Dong, C., Wininger, M., Hall, J., Selby, M., Coit, D., Medina-Selby, A., McCoin, C., Ng, P., Drane, D., Chien, D., Han, J., Vajdy, M. and Houghton, M. (2008). Induction of Broad CD4+ and CD8+ T-Cell Responses and Cross-Neutralizing Antibodies against Hepatitis C Virus by Vaccination with Th1-Adjuvanted Polypeptides Followed by Defective Alphaviral Particles Expressing Envelope Glycoproteins gpE1 and gpE2 and N. *J. Virol.* **82**, 7492–7503.

Lindenbach, B. D. and Rice, C. M. (2005). Unravelling hepatitis C virus replication from genome to function. *Nature* **436**, 933–938.

Lindenbach, B. D. and Rice, C. M. (2013). The ins and outs of hepatitis C virus entry and assembly. *Nat. Rev. Microbiol.* **11**, 688–700.

Lindsay, R. W. B., Darrah, P. A., Quinn, K. M., Wille-Reece, U., Mattei, L. M., Iwasaki, A., Kasturi, S. P., Pulendran, B., Gall, J. G. D., Spies, A. G. and Seder, R. A. (2010). CD8+ T cell responses following replication-defective adenovirus serotype 5 immunization are dependent on CD11c+ dendritic cells but show redundancy in their requirement of TLR and nucleotide-binding oligomerization domain-like receptor signaling. *J. Immunol.* **185**, 1513–1521.

Lissina, A., Ladell, K., Skowera, A., Clement, M., Edwards, E., Seggewiss, R., van den Berg, H. A., Gostick, E., Gallagher, K., Jones, E., Melenhorst, J. J., Godkin, A. J., Peakman, M., Price, D. A., Sewell, A. K. and Wooldridge, L. (2009). Protein kinase inhibitors substantially improve the physical detection of T-cells with peptide-MHC tetramers. *J. Immunol. Methods* **340**, 11–24.

Liu, W., Putnam, A. L., Xu-Yu, Z., Szot, G. L., Lee, M. R., Zhu, S., Gottlieb, P. A., Kapranov, P., Gingeras, T. R., Fazekas de St Groth, B., Clayberger, C., Soper, D. M., Ziegler, S. F. and Bluestone, J. A. (2006). CD127 expression inversely correlates with FoxP3 and suppressive function of human CD4+ T reg cells. *J. Exp. Med.* **203**, 1701–1711.

Locksley, R. M., Killeen, N. and Lenardo, M. J. (2001). The TNF and TNF receptor superfamilies: integrating mammalian biology. *Cell* **104**, 487–501.

Logvinoff, C., Major, M. E., Oldach, D., Heyward, S., Talal, A., Balfe, P., Feinstone, S. M., Alter, H., Rice, C. M. and McKeating, J. A. (2004). Neutralizing antibody response during acute and chronic hepatitis C virus infection. *Proc. Natl. Acad. Sci.* **101**, 10149–10154.

Lohmann, V., Körner, F., Koch, J., Herian, U., Theilmann, L. and Bartenschlager, R. (1999). Replication of subgenomic hepatitis C virus RNAs in a hepatoma cell line. *Science* **285**, 110–113.

Losikoff, P. T., Mishra, S., Terry, F., Gutierrez, A., Ardito, M. T., Fast, L., Nevola, M., Martin, W. D., Bailey-Kellogg, C., De Groot, A. S. and Gregory, S. H. (2014). HCV Epitope, Homologous to Multiple Human Protein Sequences, Induces a Regulatory T Cell Response in Infected Patients. *J. Hepatol.*

Lucas, M., Vargas-Cuero, A. L., Lauer, G. M., Barnes, E., Willberg, C. B., Semmo, N., Walker, B. D., Phillips, R. and Klenerman, P. (2004). Pervasive influence of hepatitis C virus on the phenotype of antiviral CD8+ T cells. *J. Immunol.* **172**, 1744–1753.

Lugli, E., Dominguez, M. H., Gattinoni, L., Chattopadhyay, P. K., Bolton, D. L.,

Song, K., Klatt, N. R., Brenchley, J. M., Vaccari, M., Gostick, E., Price, D. A., Waldmann, T. A., Restifo, N. P., Franchini, G. and Roederer, M. (2013). Superior T memory stem cell persistence supports long-lived T cell memory. *J. Clin. Invest.* **123**, 594–599.

Mackay, L. K., Long, H. M., Brooks, J. M., Taylor, G. S., Leung, C. S., Chen, A., Wang, F. and Rickinson, A. B. (2009). T Cell Detection of a B-Cell Tropic Virus Infection: Newly-Synthesised versus Mature Viral Proteins as Antigen Sources for CD4 and CD8 Epitope Display. *PLoS Pathog.* **5**, e1000699.

Maecker, H. T. and Trotter, J. (2006). Flow cytometry controls, instrument setup, and the determination of positivity. *Cytometry. A* **69A**, 1037–1042.

Makedonas, G. and Betts, M. R. (2010). Living in a house of cards: re-evaluating CD8+ T-cell immune correlates against HIV. *Immunol. Rev.* **239**, 109–124.

Makedonas, G., Banerjee, P. P., Pandey, R., Hersperger, A. R., Sanborn, K. B., Hardy, G. A. D., Orange, J. S. and Betts, M. R. (2009). Rapid up-regulation and granule-independent transport of perforin to the immunological synapse define a novel mechanism of antigen-specific CD8+ T cell cytotoxic activity. *J. Immunol.* **182**, 5560–5569.

Makedonas, G., Hutnick, N., Haney, D., Amick, A. C., Gardner, J., Cosma, G., Hersperger, A. R., Dolfi, D., Wherry, E. J., Ferrari, G. and Betts, M. R. (2010). Perforin and IL-2 Upregulation Define Qualitative Differences among Highly Functional Virus-Specific Human CD8+ T Cells. *PLoS Pathog.* **6**, e1000798.

Malcherek, G., Wirblich, C., Willcox, N., Rammensee, H. G., Trowsdale, J. and Melms, a (1998). MHC class II-associated invariant chain peptide replacement by T cell epitopes: engineered invariant chain as a vehicle for directed and enhanced MHC class II antigen processing and presentation. *Eur. J. Immunol.* **28**, 1524–33.

Malek, T. R. (2008). The biology of interleukin-2. *Annu. Rev. Immunol.* **26**, 453–479.

Martin, N. K., Hickman, M., Hutchinson, S. J., Goldberg, D. J. and Vickerman, P. (2013). Combination interventions to prevent HCV transmission among people who inject drugs: modeling the impact of antiviral treatment, needle and syringe programs, and opiate substitution therapy. *Clin. Infect. Dis.* **57 Suppl 2**, S39–45.

Martin, B., Hennecke, N., Lohmann, V., Kayser, A., Neumann-Haefelin, C., Kukolj, G., Böcher, W.-O. and Thimme, R. (2014). Restoration of HCV-specific CD8+ T cell function by interferon-free therapy. *J. Hepatol.* **61**, 538–543.

Martin, N. K., Foster, G. R., Vilar, J., Ryder, S., E Cramp, M., Gordon, F., Dillon, J. F., Craine, N., Busse, H., Clements, A., Hutchinson, S. J., Ustianowski, A.,

Ramsay, M., Goldberg, D. J., Irving, W., Hope, V., De Angelis, D., Lyons, M., Vickerman, P. and Hickman, M. (2015). HCV treatment rates and sustained viral response among people who inject drugs in seven UK sites: real world results and modelling of treatment impact. *J. Viral Hepat.* **22**, 399–408.

Mason, G. M., Lowe, K., Melchiotti, R., Ellis, R., de Rinaldis, E., Peakman, M., Heck, S., Lombardi, G. and Tree, T. I. M. (2015). Phenotypic Complexity of the Human Regulatory T Cell Compartment Revealed by Mass Cytometry. *J. Immunol.* **195**, 2030–2037.

Masopust, D., Ha, S.-J., Vezys, V. and Ahmed, R. (2006). Stimulation history dictates memory CD8 T cell phenotype: implications for prime-boost vaccination. *J. Immunol.* **177**, 831–839.

Matloubian, M., Concepcion, R. J. and Ahmed, R. (1994). CD4+ T cells are required to sustain CD8+ cytotoxic T-cell responses during chronic viral infection. *J. Virol.* **68**, 8056–8063.

Matza, D., Kerem, A. and Shachar, I. (2003). Invariant chain, a chain of command. *Trends Immunol.* **24**, 264–268.

McKinney, E. F., Lee, J. C., Jayne, D. R. W., Lyons, P. A. and Smith, K. G. C. (2015). T-cell exhaustion, co-stimulation and clinical outcome in autoimmunity and infection. *Nature* **523**, 612–616.

Mehlhop-Williams, E. R. and Bevan, M. J. (2014). Memory CD8+ T cells exhibit increased antigen threshold requirements for recall proliferation. *J. Exp. Med.* **211**, 345–356.

Mehta, S. H., Cox, A., Hoover, D. R., Wang, X.-H., Mao, Q., Ray, S., Strathdee, S. A., Vlahov, D. and Thomas, D. L. (2002). Protection against persistence of hepatitis C. *Lancet* **359**, 1478–1483.

Merani, S., Petrovic, D., James, I., Chopra, A., Cooper, D., Freitas, E., Rauch, A., di Iulio, J., John, M., Lucas, M., Fitzmaurice, K., McKiernan, S., Norris, S., Kelleher, D., Klenerman, P. and Gaudieri, S. (2011). Effect of immune pressure on hepatitis C virus evolution: insights from a single-source outbreak. *Hepatology* **53**, 396–405.

Merkenschlager, M., Terry, L., Edwards, R. and Beverley, P. C. L. (1988). Limiting dilution analysis of proliferative responses in human lymphocyte populations defined by the monoclonal antibody UCHL1: implications for differential CD45 expression in T cell memory formation. *Eur. J. Immunol.* **18**, 1653–1662.

Messina, J. P., Humphreys, I., Flaxman, A., Brown, A., Cooke, G. S., Pybus, O. G. and Barnes, E. (2014). Global distribution and prevalence of hepatitis C virus genotypes. *Hepatology*.

Meunier, J.-C., Russell, R. S., Goossens, V., Priem, S., Walter, H., Depla, E., Union, A., Faulk, K. N., Bukh, J., Emerson, S. U. and Purcell, R. H. (2008). Isolation and characterization of broadly neutralizing human monoclonal antibodies to the e1 glycoprotein of hepatitis C virus. *J. Virol.* **82**, 966–973.

Mikkelsen, M., Holst, P. J., Bukh, J., Thomsen, A. R. and Christensen, J. P. (2011). Enhanced and Sustained CD8+ T Cell Responses with an Adenoviral Vector-Based Hepatitis C Virus Vaccine Encoding NS3 Linked to the MHC Class II Chaperone Protein Invariant Chain. *J. Immunol.* **186**, 2355–2364.

Missale, G., Pilli, M., Zerbini, A., Penna, A., Ravanetti, L., Barili, V., Orlandini, A., Molinari, A., Fasano, M., Santantonio, T. and Ferrari, C. (2012a). Lack of full CD8 functional restoration after antiviral treatment for acute and chronic hepatitis C virus infection. *Gut* **61**, 1076–1084.

Missale, G., Pilli, M., Zerbini, A., Penna, A., Ravanetti, L., Barili, V., Orlandini, A., Molinari, A., Fasano, M., Santantonio, T. and Ferrari, C. (2012b). Lack of full CD8 functional restoration after antiviral treatment for acute and chronic hepatitis C virus infection. *Gut* **61**, 1076–1084.

Mittar, D., Paramban, R. and McIntyre, C. (2011). Flow Cytometry and High-Content Imaging to Identify Markers of Monocyte-Macrophage Differentiation.

Miyara, M., Yoshioka, Y., Kitoh, A., Shima, T., Wing, K., Niwa, A., Parizot, C., Taflin, C., Heike, T., Valeyre, D., Mathian, A., Nakahata, T., Yamaguchi, T., Nomura, T., Ono, M., Amoura, Z., Gorochov, G. and Sakaguchi, S. (2009). Functional Delineation and Differentiation Dynamics of Human CD4(+) T Cells Expressing the FoxP3 Transcription Factor. *Immunity* **30**, 899–911.

Mooij, P., Alla-Jhagjhoorsingh, S. S., Koopman, G., Beenhakker, N., van Haaften, P., Baak, I., Nieuwenhuis, I. G., Kondova, I., Wagner, R., Wolf, H., Gomez, C. E., Najera, J. L., Jiménez, V., Esteban, M. and Heeney, J. L. (2008). Differential CD4(+) versus CD8(+) T-cell responses elicited by different poxvirus-based human immunodeficiency virus type I vaccine candidates provide comparable efficacies in primates. *J. Virol.* **82**, 2975–2988.

Moore, A. C., Kong, W.-P., Chakrabarti, B. K. and Nabel, G. J. (2002). Effects of antigen and genetic adjuvants on immune responses to human immunodeficiency virus DNA vaccines in mice. *J. Virol.* **76**, 243–250.

Morin, T. J., Broering, T. J., Leav, B. A., Blair, B. M., Rowley, K. J., Boucher, E. N., Wang, Y., Cheslock, P. S., Knauber, M., Olsen, D. B., Ludmerer, S. W., Szabo, G., Finberg, R. W., Purcell, R. H., Lanford, R. E., Ambrosino, D. M., Molrine, D. C. and Babcock, G. J. (2012). Human Monoclonal Antibody HCV1 Effectively Prevents and Treats HCV Infection in Chimpanzees. *PLoS Pathog.* **8**,.

Muccioli, M., Pate, M., Omosebi, O. and Benencia, F. (2011). Generation and Labeling of Murine Bone Marrow-derived Dendritic Cells with Qdot Nanocrystals for Tracking Studies. *Jove-Journal Vis. Exp.* e2785.

Munks, M. W., Cho, K. S., Pinto, A. K., Sierro, S., Klenerman, P. and Hill, A. B. (2006). Four distinct patterns of memory CD8 T cell responses to chronic murine cytomegalovirus infection. *J. Immunol.* **177**, 450–458.

Naggie, S., Osinusi, A., Katsounas, A., Lempicki, R., Herrmann, E., Thompson, A. J., Clark, P. J., Patel, K., Muir, A. J., McHutchison, J. G., Schlaak, J. F., Trippler, M., Shivakumar, B., Masur, H., Polis, M. A. and Kottilil, S. (2012). Dysregulation of innate immunity in hepatitis C virus genotype 1 IL28B-unfavorable genotype patients: Impaired viral kinetics and therapeutic response. *Hepatology* **56**, 444–454.

Nakamoto, N., Kaplan, D. E., Coleclough, J., Li, Y., Valiga, M. E., Kaminski, M., Shaked, A., Olthoff, K., Gostick, E., Price, D. A., Freeman, G. J., Wherry, E. J. and Chang, K. M. (2008). Functional Restoration of HCV-Specific CD8 T Cells by PD-1 Blockade Is Defined by PD-1 Expression and Compartmentalization. *Gastroenterology* **134**, 1927–1937.e2.

Nakamoto, N., Cho, H., Shaked, A., Olthoff, K., Valiga, M. E., Kaminski, M., Gostick, E., Price, D. A., Freeman, G. J., Wherry, E. J. and Chang, K. M. (2009). Synergistic reversal of intrahepatic HCV-specific CD8 T cell exhaustion by combined PD-1/CTLA-4 blockade. *PLoS Pathog.* **5**, e1000313.

Ndiaye, B. P., Thienemann, F., Ota, M., Landry, B. S., Camara, M., Dièye, S., Dieye, T. N., Esmail, H., Goliath, R., Huygen, K., January, V., Ndiaye, I., Oni, T., Raine, M., Romano, M., Satti, I., Sutton, S., Thiam, A., Wilkinson, K. A., Mboup, S., Wilkinson, R. J., McShane, H. and investigators, M. 030 trial (2015). Safety, immunogenicity, and efficacy of the candidate tuberculosis vaccine MVA85A in healthy adults infected with HIV-1: a randomised, placebo-controlled, phase 2 trial. *Lancet. Respir. Med.* **3**, 190–200.

Negro, F., Forton, D., Craxì, A., Sulkowski, M. S., Feld, J. J. and Manns, M. P. (2015). Extrahepatic Morbidity and Mortality of Chronic Hepatitis C. *Gastroenterology*.

Netski, D. M., Mosbruger, T., Depla, E., Maertens, G., Ray, S. C., Hamilton, R. G., Roundtree, S., Thomas, D. L., McKeating, J. and Cox, A. (2005). Humoral immune response in acute hepatitis C virus infection. *Clin. Infect. Dis.* **41**, 667–675.

Neumann, A. U., Lam, N. P., Dahari, H., Gretch, D. R., Wiley, T. E., Layden, T. J. and Perelson, A. S. (1998). Hepatitis C viral dynamics in vivo and the antiviral efficacy of interferon-alpha therapy. *Science (80-.).* **282**, 103–107.

Neumann-Haefelin, C. (2013). HLA-B27-mediated protection in HIV and

hepatitis C virus infection and pathogenesis in spondyloarthritis: two sides of the same coin? *Curr. Opin. Rheumatol.* **25**, 426–433.

Neumann-Haefelin, C. and Thimme, R. (2007). Impact of the genetic restriction of virus-specific T-cell responses in hepatitis C virus infection. *Genes Immun.* **8**, 181–192.

Newell, E. W., Sigal, N., Bendall, S. C., Nolan, G. P. and Davis, M. M. (2012). Cytometry by Time-of-Flight Shows Combinatorial Cytokine Expression and Virus-Specific Cell Niches within a Continuum of CD8+ T Cell Phenotypes. *Immunity* **36**, 142–152.

Newell, E. W., Sigal, N., Nair, N., Kidd, B. A., Greenberg, H. B. and Davis, M. M. (2013). Combinatorial tetramer staining and mass cytometry analysis facilitate T-cell epitope mapping and characterization. *Nat. Biotechnol.* **31**, 623–629.

Ng, V. and Saab, S. (2011). Effects of a Sustained Virologic Response on Outcomes of Patients With Chronic Hepatitis C. *Clin. Gastroenterol. Hepatol.* **9**, 923–930.

Northfield, J. W., Loo, C. P., Barbour, J. D., Spotts, G., Hecht, F. M., Klenerman, P., Nixon, D. F. and Michaëlsson, J. (2007). Human Immunodeficiency Virus Type 1 (HIV-1)-Specific CD8+ TEMRA Cells in Early Infection Are Linked to Control of HIV-1 Viremia and Predict the Subsequent Viral Load Set Point. *J. Virol.* **81** (11), 5759-5765.

Odorizzi, P. M. and Wherry, E. J. (2013). An Interferon Paradox. *Science* **340** (6129), 155-156.

Odorizzi, P. M., Pauken, K. E., Paley, M. a, Sharpe, A. and Wherry, E. J. (2015). Genetic absence of PD-1 promotes accumulation of terminally differentiated exhausted CD8+ T cells. *J. Exp. Med.* **212**, 1125–1137.

Ohs, I., Windmann, S., Wildner, O., Dittmer, U. and Bayer, W. (2013). Interleukin-encoding adenoviral vectors as genetic adjuvant for vaccination against retroviral infection. *PLoS One* **8**, e82528.

Osburn, W. O., Fisher, B. E., Dowd, K. A., Urban, G., Liu, L., Ray, S. C., Thomas, D. L. and Cox, A. L. (2010). Spontaneous Control of Primary Hepatitis C Virus Infection and Immunity Against Persistent Reinfection. *YGAST* **138**, 315–324.

Overton, E. T., Stapleton, J., Frank, I., Hassler, S., Goepfert, P. A., Barker, D., Wagner, E., von Krempelhuber, A., Virgin, G., Meyer, T. P., Müller, J., Bädeker, N., Grünert, R., Young, P., Rösch, S., Maclennan, J., Arndtz-Wiedemann, N. and Chaplin, P. (2015). Safety and Immunogenicity of Modified Vaccinia Ankara-Bavarian Nordic Smallpox Vaccine in Vaccinia-Naive and Experienced Human Immunodeficiency Virus-Infected

Individuals: An Open-Label, Controlled Clinical Phase II Trial. *Open forum Infect. Dis.* **2**, ofv040.

Ozer Etik, D., Ocal, S. and Boyacioglu, A. S. (2015). Hepatitis C infection in hemodialysis patients: A review. *World J. Hepatol.* **7**, 885–895.

Paley, M. A., Kroy, D. C., Odorizzi, P. M., Johnnidis, J. B., Dolfi, D. V, Barnett, B. E., Bikoff, E. K., Robertson, E. J., Lauer, G. M., Reiner, S. L. and Wherry, E. J. (2012). Progenitor and terminal subsets of CD8+ T cells cooperate to contain chronic viral infection. *Science (80-.).* **338**, 1220–1225.

Pancholi, P., Perkus, M., Tricoche, N., Liu, Q. and Prince, A. M. (2003). DNA immunization with hepatitis C virus (HCV) polycistronic genes or immunization by HCV DNA priming-recombinant canarypox virus boosting induces immune responses and protection from recombinant HCV-vaccinia virus infection in HLA-A2.1-transgenic mice. *J. Virol.* **77**, 382–390.

Park, S. H., Shin, E. C., Capone, S., Caggiari, L., De Re, V., Nicosia, A., Folgori, A. and Rehermann, B. (2012). Successful Vaccination Induces Multifunctional Memory T-Cell Precursors Associated With Early Control of Hepatitis C Virus. *YGAST* 1–17.

Park, S.-H., Veerapu, N. S., Shin, E.-C., Biancotto, A., McCoy, J. P., Capone, S., Folgori, A. and Rehermann, B. (2013). Subinfectious hepatitis C virus exposures suppress T cell responses against subsequent acute infection. *Nat. Publ. Gr.* **19**, 1638–1642.

Parrino, J., McCurdy, L. H., Larkin, B. D., Gordon, I. J., Rucker, S. E., Enama, M. E., Koup, R. A., Roederer, M., Bailer, R. T., Moodie, Z., Gu, L., Yan, L. and Graham, B. S. (2007). Safety, immunogenicity and efficacy of modified vaccinia Ankara (MVA) against Dryvax® challenge in vaccinia-naïve and vaccinia-immune individuals. *Vaccine* **25**, 1513–1525.

Pembroke, T., Rees, I., Gallagher, K., Jones, E., Mizen, P., Navruzov, T., Freedman, A., Fielding, C., Humphreys, I. R., Wang, E. C. Y., Gallimore, A. M. and Godkin, A. (2012). Rapid early innate control of hepatitis C virus during IFN-α treatment compromises adaptive CD4+ T-cell immunity. *Eur. J. Immunol.* **42**, 2383–2394.

Penaloza-MacMaster, P., Provine, N. M., Blass, E. and Barouch, D. H. (2015). CD4 T Cell Depletion Substantially Augments the Rescue Potential of PD-L1 Blockade for Deeply Exhausted CD8 T Cells. *J. Immunol.* **195**, 1054–1063.

Penna, A., Pilli, M., Zerbini, A., Orlandini, A., Mezzadri, S., Sacchelli, L., Missale, G. and Ferrari, C. (2007). Dysfunction and functional restoration of HCV-specific CD8 responses in chronic hepatitis C virus infection. *Hepatology* **45**, 588–601.

Perotti, M., Mancini, N., Diotti, R. A., Tarr, A. W., Ball, J. K., Owsianka, A.,

Adair, R., Patel, A. H., Clementi, M. and Burioni, R. (2008). Identification of a broadly cross-reacting and neutralizing human monoclonal antibody directed against the hepatitis C virus E2 protein. *J. Virol.* **82**, 1047–1052.

Pestka, J. M., Zeisel, M. B., Bläser, E., Schürmann, P., Bartosch, B., Cosset, F. L., Patel, A. H., Meisel, H., Baumert, J. and Viazov, S. (2007). Rapid induction of virus-neutralizing antibodies and viral clearance in a single-source outbreak of hepatitis C. *Proc. Natl. Acad. Sci.* **104**, 6025.

Peters, P. J., Borst, J., Oorschot, V., Fukuda, M., Krähenbühl, O., Tschopp, J., Slot, J. W. and Geuze, H. J. (1991). Cytotoxic T lymphocyte granules are secretory lysosomes, containing both perforin and granzymes. *J. Exp. Med.* **173**, 1099–1109.

Picker, L. J. (2014). Are effector memory T cells the key to an effective HIV/AIDS vaccine? *EMBO Rep.* **15**, 820–821.

Porter, D. W., Thompson, F. M., Berthoud, T. K., Hutchings, C. L., Andrews, L., Biswas, S., Poulton, I., Prieur, E., Correa, S., Rowland, R., Lang, T., Williams, J., Gilbert, S. C., Sinden, R. E., Todryk, S. and Hill, A. V. S. (2011). A human Phase I/IIa malaria challenge trial of a polyprotein malaria vaccine. *Vaccine* **29**, 7514–7522.

Post, J. J., Pan, Y., Freeman, A. J., Harvey, C. E., White, P. A., Palladinetti, P., Haber, P. S., Marinos, G., Levy, M. H. and Kaldor, J. M. (2004). Clearance of hepatitis C viremia associated with cellular immunity in the absence of seroconversion in the hepatitis C incidence and transmission in prisons study cohort. *J. Infect. Dis.* **189**, 1846–1855.

Pratt, W. B., Morishima, Y., Peng, H.-M. and Osawa, Y. (2010). Proposal for a role of the Hsp90/Hsp70-based chaperone machinery in making triage decisions when proteins undergo oxidative and toxic damage. *Exp. Biol. Med. (Maywood).* **235**, 278–289.

Precopio, M. L., Betts, M. R., Parrino, J., Price, D. A., Gostick, E., Ambrozak, D. R., Asher, T. E., Douek, D. C., Harari, A., Pantaleo, G., Bailer, R., Graham, B. S., Roederer, M. and Koup, R. A. (2007). Immunization with vaccinia virus induces polyfunctional and phenotypically distinctive CD8(+) T cell responses. *J. Exp. Med.* **204**, 1405–1416.

Pronker, E. S., Weenen, T. C., Commandeur, H., Claassen, E. H. J. H. M. and Osterhaus, A. D. M. E. (2013). Risk in Vaccine Research and Development Quantified. *PLoS One* **8**, e57755.

Protzer, U., Maini, M. K. and Knolle, P. a. (2012). Living in the liver: hepatic infections. *Nat. Rev. Immunol.* **12**, 201–213.

Puig, M., Mihalik, K., Tilton, J. C., Williams, O., Merchlinsky, M., Connors, M., Feinstone, S. M. and Major, M. E. (2006). CD4+ immune escape and

subsequent T-cell failure following chimpanzee immunization against hepatitis C virus. *Hepatology* **44**, 736–745.

Pybus, O. G., Barnes, E., Taggart, R., Lemey, P., Markov, P. V, Rasachak, B., Syhavong, B., Phetsouvanah, R., Sheridan, I., Humphreys, I. S., Lu, L., Newton, P. N. and Klenerman, P. (2009). Genetic history of hepatitis C virus in East Asia. *J. Virol.* **83**, 1071–1082.

Quigley, M., Pereyra, F., Nilsson, B., Porichis, F., Fonseca, C., Eichbaum, Q., Julg, B., Jesneck, J. L., Brosnahan, K., Imam, S., Russell, K., Toth, I., Piechocka-Trocha, A., Dolfi, D., Angelosanto, J., Crawford, A., Shin, H., Kwon, D. S., Zupkosky, J., Francisco, L., Freeman, G. J., Wherry, E. J., Kaufmann, D. E., Walker, B. D., Ebert, B. and Haining, W. N. (2010). Transcriptional analysis of HIV-specific CD8+ T cells shows that PD-1 inhibits T cell function by upregulating BATF. *Nat. Publ. Gr.* **16**, 1147–1151.

Quinn, K. M., Da Costa, A., Yamamoto, A., Berry, D., Lindsay, R. W. B., Darrah, P. A., Wang, L., Cheng, C., Kong, W.-P., Gall, J. G. D., Nicosia, A., Folgori, A., Colloca, S., Cortese, R., Gostick, E., Price, D. A., Gomez, C. E., Esteban, M., Wyatt, L. S., Moss, B., Morgan, C., Roederer, M., Bailer, R. T., Nabel, G. J., Koup, R. A. and Seder, R. A. (2013). Comparative analysis of the magnitude, quality, phenotype, and protective capacity of simian immunodeficiency virus gag-specific CD8+ T cells following human-, simian-, and chimpanzee-derived recombinant adenoviral vector immunization. *J. Immunol.* **190**, 2720–2735.

Quinn, K. M., Zak, D. E., Costa, A., Yamamoto, A., Kastenmuller, K., Hill, B. J., Lynn, G. M., Darrah, P. a, Lindsay, R. W. B., Wang, L., Cheng, C., Nicosia, A., Folgori, A., Colloca, S., Cortese, R., Gostick, E., Price, D. a, Gall, J. G. D., Roederer, M., Aderem, A. and Seder, R. a (2015). Antigen expression determines adenoviral vaccine potency independent of IFN and STING signaling. *J. Clin. Invest.* **125**, 1–18.

Raghavan, M., Del Cid, N., Rizvi, S. M. and Peters, L. R. (2008). MHC class I assembly: out and about. *Trends Immunol.* **29**, 436–443.

Ramirez, J. C., Finke, D., Esteban, M., Kraehenbuhl, J. P. and Acha-Orbea, H. (2003). Tissue distribution of the Ankara strain of vaccinia virus (MVA) after mucosal or systemic administration. *Arch. Virol.* **148**, 827–839.

Ramírez, J. C., Gherardi, M. M. and Esteban, M. (2000). Biology of attenuated modified vaccinia virus Ankara recombinant vector in mice: virus fate and activation of B- and T-cell immune responses in comparison with the Western Reserve strain and advantages as a vaccine. *J. Virol.* **74**, 923–933.

Randall, R. E. and Goodbourn, S. (2008). Interferons and viruses: an interplay between induction, signalling, antiviral responses and virus countermeasures. *J. Gen. Virol.* **89**, 1–47.

Rao, R. R., Li, Q., Odunsi, K. and Shrikant, P. A. (2010). The mTOR Kinase Determines Effector versus Memory CD8+ T Cell Fate by Regulating the Expression of Transcription Factors T-bet and Eomesodermin. *Immunity* **32**, 67–78.

Rehermann, B., Chang, K. M., McHutchison, J. G., Kokka, R., Houghton, M. and Chisari, F. V (1996). Quantitative analysis of the peripheral blood cytotoxic T lymphocyte response in patients with chronic hepatitis C virus infection. *J. Clin. Invest.* **98**, 1432–1440.

Reyes-Sandoval, A., Berthoud, T., Alder, N., Siani, L., Gilbert, S. C., Nicosia, A., Colloca, S., Cortese, R. and Hill, A. V. S. (2010). Prime-Boost Immunization with Adenoviral and Modified Vaccinia Virus Ankara Vectors Enhances the Durability and Polyfunctionality of Protective Malaria CD8+ T-Cell Responses. *Infect. Immun.* **78**, 145–153.

Reyes-Sandoval, A., Wyllie, D. H., Bauza, K., Milicic, A., Forbes, E. K., Rollier, C. S. and Hill, A. V. S. (2011). CD8+ T effector memory cells protect against liver-stage malaria. *J. Immunol.* **187**, 1347–1357.

Reyes-Sandoval, A., Rollier, C. S., Milicic, A., Bauza, K., Cottingham, M. G., Tang, C.-K., Dicks, M. D., Wang, D., Longley, R. J., Wyllie, D. H. and Hill, A. V. S. (2012). Mixed vector immunization with recombinant adenovirus and MVA can improve vaccine efficacy while decreasing antivector immunity. *Mol. Ther.* **20**, 1633–1647.

Ribeiro-dos-Santos, P., Turnbull, E. L., Monteiro, M., Legrand, A., Conrod, K., Baalwa, J., Pellegrino, P., Shaw, G. M., Williams, I., Borrow, P. and Rocha, B. (2012). Chronic HIV infection affects the expression of the 2 transcription factors required for CD8 T-cell differentiation into cytolytic effectors. *Blood* **119**, 4928–38.

Richter, K., Brocker, T. and Oxenius, A. (2012). Antigen amount dictates CD8+ T-cell exhaustion during chronic viral infection irrespective of the type of antigen presenting cell. *Eur. J. Immunol.* **42**, 2290–2304.

Ringner, M. (2008). What is principal component analysis? *Nat. Biotechnol.* **26**, 303–304.

Rizza, P., Capone, I., Moretti, F., Proietti, E. and Belardelli, F. (2011). IFN-α as a vaccine adjuvant: recent insights into the mechanisms and perspectives for its clinical use. *Expert Rev. Vaccines* **10**, 487–498.

Roche, P. A. and Furuta, K. (2015). The ins and outs of MHC class II-mediated antigen processing and presentation. *Nat. Rev. Immunol.* **15**, 203–216.

Rock, K. L. (2006). Exiting the outside world for cross-presentation. *Immunity* **25**, 523–525.

Rock, K. L., Gramm, C., Rothstein, L., Clark, K., Stein, R., Dick, L., Hwang, D. and Goldberg, A. L. (1994). Inhibitors of the proteasome block the degradation of most cell proteins and the generation of peptides presented on MHC class I molecules. *Cell* **78**, 761–771.

Rock, K. L., York, I. a and Goldberg, A. L. (2004). Post-proteasomal antigen processing for major histocompatibility complex class I presentation. *Nat. Immunol.* **5**, 670–677.

Roederer, M., Nozzi, J. L. and Nason, M. C. (2011). SPICE: Exploration and analysis of post-cytometric complex multivariate datasets. *Cytom. Part A* **79A**, 167–174.

Rollier, C. S., Paranhos-Baccala, G., Verschoor, E. J., Verstrepen, B. E., Drexhage, J. A. R., Fagrouch, Z., Berland, J.-L., Komurian-Pradel, F., Duverger, B., Himoudi, N., Staib, C., Meyr, M., Whelan, M., Whelan, J. A., Adams, V. A., Larrea, E., Riezu, J. I., Lasarte, J. J., Bartosch, B., Cosset, F.-L., Spaan, W. J. M., Diepolder, H. M., Pape, G. R., Sutter, G., Inchauspe, G. and Heeney, J. L. (2007). Vaccine-induced early control of hepatitis C virus infection in chimpanzees fails to impact on hepatic PD-1 and chronicity. *Hepatology* **45**, 602–613.

Rollier, C. S., Reyes-Sandoval, A., Cottingham, M. G., Ewer, K. and Hill, A. V. S. (2011). Viral vectors as vaccine platforms: deployment in sight. *Curr. Opin. Immunol.* **23**, 377–382.

Romagnoli, P. and Germain, R. N. (1995). Inhibition of invariant chain (Ii)-calnexin interaction results in enhanced degradation of Ii but does not prevent the assembly of alpha beta Ii complexes. *J. Exp. Med.* **182**, 2027–2036.

Rong, L., Dahari, H., Ribeiro, R. M. and Perelson, A. S. (2010). Rapid Emergence of Protease Inhibitor Resistance in Hepatitis C Virus. *Sci. Transl. Med.* **2**, 30ra32.

Rosario, M., Bridgeman, A., Quakkelaar, E. D., Quigley, M. F., Hill, B. J., Knudsen, M. L., Ammendola, V., Ljungberg, K., Borthwick, N., Im, E.-J., McMichael, A. J., Drijfhout, J. W., Greenaway, H. Y., Venturi, V., Douek, D. C., Colloca, S., Liljeström, P., Nicosia, A., Price, D. a, Melief, C. J. M. and Hanke, T. (2010). Long peptides induce polyfunctional T cells against conserved regions of HIV-1 with superior breadth to single-gene vaccines in macaques. *Eur. J. Immunol.* **40**, 1973–84.

Rosen, H. (2002). Frequencies of HCV-specific effector CD4+ T cells by flow cytometry: Correlation with clinical disease stages. *Hepatology* **35**, 190–198.

Roychoudhuri, R., Lefebvre, F., Honda, M., Pan, L., Ji, Y., Klebanoff, C. A., Nichols, C. N., Fourati, S., Hegazy, A. N., Goulet, J.-P., Gattinoni, L., Nabel, G. J., Gilliet, M., Cameron, M., Restifo, N. P., Sékaly, R. P. and Flatz, L.

(2014). Transcriptional profiles reveal a stepwise developmental program of memory CD8(+) T cell differentiation. *Vaccine*.

Ruhl, M., Chhatwal, P., Strathmann, H., Kuntzen, T., Bankwitz, D., Skibbe, K., Walker, A., Heinemann, F. M., Horn, P. A., Allen, T. M., Hoffmann, D., Pietschmann, T. and Timm, J. (2012). Escape from a dominant HLA-B*15-restricted CD8+ T cell response against hepatitis C virus requires compensatory mutations outside the epitope. *J. Virol.* **86**, 991–1000.

Sacks-Davis, R., Aitken, C. K., Higgs, P., Spelman, T., Pedrana, A. E., Bowden, S., Bharadwaj, M., Nivarthi, U. K., Suppiah, V., George, J., Grebely, J., Drummer, H. E. and Hellard, M. (2013). High rates of hepatitis C virus reinfection and spontaneous clearance of reinfection in people who inject drugs: a prospective cohort study. *PLoS One* **8**, e80216.

Sacks-Davis, R., Grebely, J., Dore, G. J., Osburn, W., Cox, A. L., Rice, T. M., Spelman, T., Bruneau, J., Prins, M., Kim, A. Y., McGovern, B. H., Shoukry, N. H., Schinkel, J., Allen, T. M., Morris, M., Hajarizadeh, B., Maher, L., LLOYD, A. R., Page, K., Hellard, M. and group, I. study (2015). Hepatitis C Virus Reinfection and Spontaneous Clearance of Reinfection-the InC3 Study. *J. Infect. Dis.* **212**, 1407–1419.

Sáez-Cirión, A., Bacchus, C., Hocqueloux, L., Avettand-Fenoel, V., Girault, I., Lecuroux, C., Potard, V., Versmisse, P., Melard, A., Prazuck, T., Descours, B., Guergnon, J., Viard, J.-P., Boufassa, F., Lambotte, O., Goujard, C., Meyer, L., Costagliola, D., Venet, A., Pancino, G., Autran, B., Rouzioux, C. and Group, the A. V. S. (2013). Post-Treatment HIV-1 Controllers with a Long-Term Virological Remission after the Interruption of Early Initiated Antiretroviral Therapy ANRS VISCONTI Study. *PLoS Pathog.* **9**, e1003211.

Sällberg, M., Frelin, L. and Weiland, O. (2009). DNA vaccine therapy for chronic hepatitis C virus (HCV) infection: immune control of a moving target. *Expert Opin. Biol. Ther.* **9**, 805–815.

Sallusto, F., Lenig, D., Förster, R., Lipp, M. and Lanzavecchia, A. (1999). Two subsets of memory T lymphocytes with distinct homing potentials and effector functions. *Nature* **401**, 708–712.

Sallusto, F., Geginat, J. and Lanzavecchia, A. (2004). C entralM emory andE ffectorM emoryT C ellS ubsets: Function, Generation, and Maintenance. *Annu. Rev. Immunol.* **22**, 745–763.

Sallusto, F., Lanzavecchia, A., Araki, K. and Ahmed, R. (2010). From Vaccines to Memory and Back. *Immunity* **33**, 451–463.

Sandoval, I. V and Bakke, O. (1994). Targeting of membrane proteins to endosomes and lysosomes. *Trends Cell Biol.* **4**, 292–297.

Saric, T., Chang, S. C., Hattori, A., York, I. A., Markant, S., Rock, K. L.,

Tsujimoto, M. and Goldberg, A. L. (2002). An IFN-gamma-induced aminopeptidase in the ER, ERAP1, trims precursors to MHC class I-presented peptides. *Nat. Immunol.* **3**, 1169–1176.

Schirren, C. A., Zachoval, R., Gerlach, J. T., Ulsenheimer, A., Gruener, N. H., Diepolder, H. M., Baretton, G., Schraut, W., Rau, H.-G., Nitschko, H., Pape, G. R. and Jung, M.-C. (2003). Antiviral treatment of recurrent hepatitis C virus (HCV) infection after liver transplantation: association of a strong, multispecific, and long-lasting CD4+ T cell response with HCV-elimination. *J. Hepatol.* **39**, 397–404.

Schreiber, J., Moreno, C., Garcia, B. G., Louvet, A., Trepo, E., Henrion, J., Thabut, D., Mathurin, P. and Deltenre, P. (2012). Meta-analysis: the impact of IL28B polymorphisms on rapid and sustained virological response in HCV-2 and -3 patients. *Aliment. Pharmacol. Ther.* **36**, 353–362.

Schroder, K., Hertzog, P. J., Ravasi, T. and Hume, D. A. (2004). Interferon-gamma: an overview of signals, mechanisms and functions. *J. Leukoc. Biol.* **75**, 163–189.

Schulze zur Wiesch, J., Ciuffreda, D., Lewis-Ximenez, L., Kasprowicz, V., Nolan, B. E., Streeck, H., Aneja, J., Reyor, L. L., Allen, T. M., Lohse, A. W., McGovern, B., Chung, R. T., Kwok, W. W., Kim, A. Y. and Lauer, G. M. (2012). Broadly directed virus-specific CD4+ T cell responses are primed during acute hepatitis C infection, but rapidly disappear from human blood with viral persistence. *J. Exp. Med.* **209**, 61–75.

Scott, N., McBryde, E., Vickerman, P., Martin, N. K., Stone, J., Drummer, H. and Hellard, M. (2015). The role of a hepatitis C virus vaccine: modelling the benefits alongside direct-acting antiviral treatments. *Bmc Med.* **13**,.

Seddiki, N., Santner-Nanan, B., Martinson, J., Zaunders, J., Sasson, S., Landay, A., Solomon, M., Selby, W., Alexander, S. I., Nanan, R., Kelleher, A. and de St Groth, B. F. (2006). Expression of interleukin (IL)-2 and IL-7 receptors discriminates between human regulatory and activated T cells. *J. Exp. Med.* **203**, 1693–1700.

Seder, R. A., Darrah, P. A. and Roederer, M. (2008). T-cell quality in memory and protection: implications for vaccine design. **8**, 247–258.

Seeff, L. B. and Hoofnagle, J. H. (2002). National Institutes of Health Consensus Development Conference Statement: Management of hepatitis C: 2002—June 10-12, 2002. *Hepatology* **36**, s3–s20.

Semmo, N. (2006). Maintenance of HCV-specific T-cell responses in antibody-deficient patients a decade after early therapy. *Blood* **107**, 4570–4571.

Semmo, N., Day, C. L., Ward, S. M., Lucas, M., Harcourt, G., Loughry, A. and Klenerman, P. (2005). Preferential loss of IL-2-secreting CD4+ T helper

cells in chronic HCV infection. *Hepatology* **41**, 1019–1028.

Serti, E., Chepa-Lotrea, X., Kim, Y. J., Keane, M., Fryzek, N., Liang, T. J., Ghany, M. and Rehermann, B. (2015). Successful Interferon-Free Therapy of Chronic Hepatitis C Virus Infection Normalizes Natural Killer Cell Function. *Gastroenterology* **149**, 190–200.e2.

Sevilla, L. M., Comstock, S. S., Swier, K. and Miller, J. (2004). Endoplasmic Reticulum-Associated Degradation-Induced Dissociation of Class II Invariant Chain Complexes Containing a Glycosylation-Deficient Form of p41. *J. Immunol.* **173**, 2586–2593.

Shastri, N., Susan Schwab, and and Serwold, T. (2003). PRODUCING NATURE'S GENE-CHIPS: The Generation of Peptides for Display by MHC Class I Molecules. *dx.doi.org*.

Sheehy, S. H., Duncan, C. J. A., Elias, S. C., Choudhary, P., Biswas, S., Halstead, F. D., Collins, K. A., Edwards, N. J., Douglas, A. D., Anagnostou, N. A., Ewer, K. J., Havelock, T., Mahungu, T., Bliss, C. M., Miura, K., Poulton, I. D., Lillie, P. J., Antrobus, R. D., Berrie, E., Moyle, S., Gantlett, K., Colloca, S., Cortese, R., Long, C. A., Sinden, R. E., Gilbert, S. C., Lawrie, A. M., Doherty, T., Faust, S. N., Nicosia, A., Hill, A. V. S. and Draper, S. J. (2012). ChAd63-MVA-vectored blood-stage malaria vaccines targeting MSP1 and AMA1: assessment of efficacy against mosquito bite challenge in humans. *Mol. Ther.* **20**, 2355–2368.

Shiffman, M. L., Sterling, R. K., Contos, M., Hubbard, S., Long, A., Luketic, V. A., Stravitz, R. T., Fuchs, M. and Sanyal, A. J. (2014). Long term changes in liver histology following treatment of chronic hepatitis C virus. *Ann. Hepatol.* **13**, 340–349.

Shin, E.-C., Seifert, U., Kato, T., Rice, C. M., Feinstone, S. M., Kloetzel, P.-M. and Rehermann, B. (2006). Virus-induced type I IFN stimulates generation of immunoproteasomes at the site of infection. *J. Clin. Invest.* **116**, 3006–14.

Shin, H., Blackburn, S. D., Blattman, J. N. and Wherry, E. J. (2007). Viral antigen and extensive division maintain virus-specific CD8 T cells during chronic infection. *J. Exp. Med.* **204**, 941–9.

Shin, E. C., Capone, S., Cortese, R., Colloca, S., Nicosia, A., Folgori, A. and Rehermann, B. (2008). The Kinetics of Hepatitis C Virus-Specific CD8 T-Cell Responses in the Blood Mirror Those in the Liver in Acute Hepatitis C Virus Infection. *J. Virol.* **82**, 9782–9788.

Shoukry, N. H., Grakoui, A., Houghton, M., Chien, D. Y., Ghrayeb, J., Reimann, K. A. and Walker, C. M. (2003). Memory CD8+ T Cells Are Required for Protection from Persistent Hepatitis C Virus Infection. *J. Exp. Med.* **197**, 1645–1655.

Sicard, C., Shek, N., White, D., Bowers, R. J., Brown, R. S. and Brennan, J. D.

(2014). A rapid and sensitive fluorimetric β-galactosidase assay for coliform detection using chlorophenol red-β-D-galactopyranoside. *Anal. Bioanal. Chem.* **406**, 5395–403.

Sidharthan, S., Kohli, A., Sims, Z., Nelson, A., Osinusi, A., Masur, H. and Kottilil, S. (2015). Utility of Hepatitis C Viral Load Monitoring on Direct-Acting Antiviral Therapy. *Clin. Infect. Dis.* **60**, 1743–1751.

Simmonds, P. (2001). The origin and evolution of hepatitis viruses in humans. *J. Gen. Virol.* **82**, 693–712.

Simmonds, P. (2004). Genetic diversity and evolution of hepatitis C virus--15 years on. *J. Gen. Virol.* **85**, 3173–3188.

Simmonds, P., Holmes, E. C., Cha, T. A., Chan, S. W., McOmish, F., Irvine, B., Beall, E., Yap, P. L., Kolberg, J. and Urdea, M. S. (1993). Classification of hepatitis C virus into six major genotypes and a series of subtypes by phylogenetic analysis of the NS-5 region. *J. Gen. Virol.* **74 (Pt 11**, 2391–2399.

Simmonds, P., Bukh, J., Combet, C., Deléage, G., Enomoto, N., Feinstone, S., Halfon, P., Inchauspe, G., Kuiken, C., Maertens, G., Mizokami, M., Murphy, D. G., Okamoto, H., Pawlotsky, J.-M., Penin, F., Sablon, E., Shin-I, T., Stuyver, L. J., Thiel, H.-J., Viazov, S., Weiner, A. J. and Widell, A. (2005). Consensus proposals for a unified system of nomenclature of hepatitis C virus genotypes. In *Hepatology (Baltimore, Md.)*, pp. 962–973. Centre for Infectious Diseases, University of Edinburgh, Summerhall, Edinburgh, United Kingdom. Peter.Simmonds@ed.ac.uk.

Smith, C., Elhassen, D., Gras, S., Wynn, K. K., Dasari, V., Tellam, J., Tey, S.-K., Rehan, S., Liu, Y. C., Rossjohn, J., Burrows, S. R. and Khanna, R. (2012). Endogenous antigen presentation impacts on T-box transcription factor expression and functional maturation of CD8+ T cells. *Blood* **120**, 3237–3245.

Snyder, C. M., Cho, K. S., Bonnett, E. L., van Dommelen, S., Shellam, G. R. and Hill, A. B. (2008). Memory inflation during chronic viral infection is maintained by continuous production of short-lived, functional T cells. *Immunity* **29**, 650–659.

Soderholm, J., Ahlen, G., Kaul, A., Frelin, L., Alheim, M., Barnfield, C., Liljeström, P., Weiland, O., Milich, D. R., Bartenschlager, R. and Sallberg, M. (2006). Relation between viral fitness and immune escape within the hepatitis C virus protease. *Gut* **55**, 266–274.

Soghoian, D. Z. and Streeck, H. (2010). Cytolytic CD4(+) T cells in viral immunity. *Expert Rev. Vaccines* **9**, 1453–1463.

Sorensen, M. R., Holst, P. J., Pircher, H., Christensen, J. P. and Thomsen, A. R. (2009). Vaccination with an adenoviral vector encoding the tumor antigen

directly linked to invariant chain induces potent CD4(+) T-cell-independent CD8(+) T-cell-mediated tumor control. *Eur. J. Immunol.* **39**, 2725–2736.

Sorensen, M. R., Holst, P. J., Steffensen, M. A., Christensen, J. P. and Thomsen, A. R. (2010). Adenoviral vaccination combined with CD40 stimulation and CTLA-4 blockage can lead to complete tumor regression in a murine melanoma model. *Vaccine* **28**, 6757–6764.

Sourisseau, M., Goldman, O., He, W., Gori, J. L., Kiem, H.-P., Gouon-Evans, V. and Evans, M. J. (2013). Hepatic cells derived from induced pluripotent stem cells of pigtail macaques support hepatitis C virus infection. *Gastroenterology* **145**, 966–969.e7.

Spaan, M., Claassen, M. A. A., Hou, J., Janssen, H. L. A., de Knegt, R. J. and Boonstra, A. (2015). The Intrahepatic T Cell Compartment Does Not Normalize Years After Therapy-Induced Hepatitis C Virus Eradication. *J. Infect. Dis.* **212**, 386–390.

Spada, E. (2004). Multispecific T cell response and negative HCV RNA tests during acute HCV infection are early prognostic factors of spontaneous clearance. *Gut* **53**, 1673–1681.

Spangenberg, H. C., Viazov, S., Kersting, N., Neumann-Haefelin, C., McKinney, D., Roggendorf, M., von Weizsacker, F., Blum, H. E. and Thimme, R. (2005). Intrahepatic CD8+ T-cell failure during chronic hepatitis C virus infection. *Hepatology* **42**, 828–837.

Spencer, A. J., Cottingham, M. G., Jenks, J. a, Longley, R. J., Capone, S., Colloca, S., Folgori, A., Cortese, R., Nicosia, A., Bregu, M. and Hill, A. V. S. (2014). Enhanced Vaccine-Induced CD8+ T Cell Responses to Malaria Antigen ME-TRAP by Fusion to MHC Class II Invariant Chain. *PLoS One* **9**, e100538.

Sponaas, A., Carstens, C. and Koch, N. (1999). C-terminal extension of the MHC class II-associated invariant chain by an antigenic sequence triggers activation of naive T cells. *Gene Ther.* **6**, 1826–1834.

Sridhar, S., Begom, S., Bermingham, A., Hoschler, K., Adamson, W., Carman, W., Bean, T., Barclay, W., Deeks, J. J. and Lalvani, A. (2013). Cellular immune correlates of protection against symptomatic pandemic influenza. *Nat. Publ. Gr.* **19**, 1305–1312.

Stamataki, Z., Coates, S., Abrignani, S., Houghton, M. and McKeating, J. A. (2011). Immunization of Human Volunteers With Hepatitis C Virus Envelope Glycoproteins Elicits Antibodies That Cross-Neutralize Heterologous Virus Strains. *J. Infect. Dis.* **204**, 811–813.

Stanley, D. A., Honko, A. N., Asiedu, C., Trefry, J. C., Lau-Kilby, A. W., Johnson, J. C., Hensley, L., Ammendola, V., Abbate, A., Grazioli, F., Foulds, K. E., Cheng, C., Wang, L., Donaldson, M. M., Colloca, S., Folgori, A., Roederer,

M., Nabel, G. J., Mascola, J., Nicosia, A., Cortese, R., Koup, R. A. and Sullivan, N. J. (2014). Chimpanzee adenovirus vaccine generates acute and durable protective immunity against ebolavirus challenge. *Nat. Med.* **20**, 1126–1129.

Starlets, D., Gore, Y., Binsky, I., Haran, M., Harpaz, N., Shvidel, L., Becker-Herman, S., Berrebi, A. and Shachar, I. (2006). Cell-surface CD74 initiates a signaling cascade leading to cell proliferation and survival. *Blood* **107**, 4807–4816.

Steffensen, M. A., Jensen, B. A. H., Holst, P. J., Bassi, M. R., Christensen, J. P. and Thomsen, A. R. (2012). Pre-Existing Vector Immunity Does Not Prevent Replication Deficient Adenovirus from Inducing Efficient CD8 T-Cell Memory and Recall Responses. *PLoS One* **7**, e34884.

Steffensen, M. A., Holst, P. J., Steengaard, S. S., Jensen, B. A. H., Bartholdy, C., Stryhn, A., Christensen, J. P. and Thomsen, A. R. (2013). Qualitative and quantitative analysis of adenovirus type 5 vector-induced memory CD8 T cells: not as bad as their reputation. *J. Virol.* **87**, 6283–6295.

Sturm, N., Thélu, M.-A., Camous, X., Dimitrov, G., Ramzan, M., Dufeu-Duchesne, T., Bonorino, P., Guillermet, C., Brambilla, E., Arvers, P., Pernollet, M., Leroy, V., Zarski, J. P., Marche, P. N. and Jouvin-Marche, E. (2010). Characterization and role of intra-hepatic regulatory T cells in chronic hepatitis C pathogenesis. *J. Hepatol.* **53**, 25–35.

Sulkowski, M. S., Gardiner, D. F., Rodriguez-Torres, M., Reddy, K. R., Hassanein, T., Jacobson, I., Lawitz, E., Lok, A. S., Hinestrosa, F., Thuluvath, P. J., Schwartz, H., Nelson, D. R., Everson, G. T., Eley, T., Wind-Rotolo, M., Huang, S.-P., Gao, M., Hernandez, D., McPhee, F., Sherman, D., Hindes, R., Symonds, W., Pasquinelli, C., Grasela, D. M. and Group, A. S. (2014). Daclatasvir plus sofosbuvir for previously treated or untreated chronic HCV infection. *N. Engl. J. Med.* **370**, 211–221.

Sumida, S. M., Truitt, D. M., Kishko, M. G., Arthur, J. C., Jackson, S. S., Gorgone, D. A., Lifton, M. A., Koudstaal, W., Pau, M. G., Kostense, S., Havenga, M. J. E., Goudsmit, J., Letvin, N. L. and Barouch, D. H. (2004). Neutralizing antibodies and CD8+ T lymphocytes both contribute to immunity to adenovirus serotype 5 vaccine vectors. *J. Virol.* **78**, 2666–2673.

Suryaprasad, A. G., White, J. Z., Xu, F., Eichler, B.-A., Hamilton, J., Patel, A., Hamdounia, S. B., Church, D. R., Barton, K., Fisher, C., Macomber, K., Stanley, M., Guilfoyle, S. M., Sweet, K., Liu, S., Iqbal, K., Tohme, R., Sharapov, U., Kupronis, B. A., Ward, J. W. and Holmberg, S. D. (2014). Emerging Epidemic of Hepatitis C Virus Infections Among Young Non-Urban Persons who Inject Drugs in the United States, 2006–2012. *Clin. Infect. Dis.* **59**, ciu643–1419.

Swadling, L., Klenerman, P. and Barnes, E. (2013). Ever closer to a

prophylactic vaccine for HCV. *Expert Opin. Biol. Ther.* **13**, 1109–1124.

Swadling, L., Capone, S., Antrobus, R. D., Brown, A., Richardson, R., Newell, E. W., Halliday, J., Kelly, C., Bowen, D., Fergusson, J., Kurioka, A., Ammendola, V., Del Sorbo, M., Grazioli, F., Esposito, M. L., Siani, L., Traboni, C., Hill, A., Colloca, S., Davis, M., Nicosia, A., Cortese, R., Folgori, A., Klenerman, P. and Barnes, E. (2014). A human vaccine strategy based on chimpanzee adenoviral and MVA vectors that primes, boosts, and sustains functional HCV-specific T cell memory. *Sci. Transl. Med.* **6**, 261ra153–261ra153.

Szabo, S. J., Kim, S. T., Costa, G. L., Zhang, X., Fathman, C. G. and Glimcher, L. H. (2000). A Novel Transcription Factor, T-bet, Directs Th1 Lineage Commitment. *Cell* **100**, 655–669.

Takaki, A. A., Wiese, M. M., Maertens, G. G., Depla, E. E., Seifert, U. U., Liebetrau, A. A., Miller, J. L. J. L., Manns, M. P. M. P. and Rehermann, B. B. (2000a). Cellular immune responses persist and humoral responses decrease two decades after recovery from a single-source outbreak of hepatitis C. *Nat. Med.* **6**, 578–582.

Takaki, A., Wiese, M., Maertens, G., Depla, E., Seifert, U., Liebetrau, A., Miller, J. L., Manns, M. P. and Rehermann, B. (2000b). Cellular immune responses persist and humoral responses decrease two decades after recovery from a single-source outbreak of hepatitis C. *Nat. Med.* **6**, 578–582.

Takemoto, N., Intlekofer, A. M., Northrup, J. T., Wherry, E. J. and Reiner, S. L. (2006). Cutting Edge: IL-12 inversely regulates T-bet and eomesodermin expression during pathogen-induced CD8+ T cell differentiation. *J. Immunol.* **177**, 7515–7519.

Tatsis, N. and ERTL, H. (2004). Adenoviruses as vaccine vectors. *Mol. Ther.* **10**, 616–629.

Tatsis, N., Fitzgerald, J. C., Reyes-Sandoval, A., Harris-McCoy, K. C., Hensley, S. E., Zhou, D., Lin, S. W., Bian, A., Xiang, Z. Q., Iparraguirre, A., Lopez-Camacho, C., Wherry, E. J. and Ertl, H. C. J. (2007). Adenoviral vectors persist in vivo and maintain activated CD8+ T cells: implications for their use as vaccines. *Blood* **110**, 1916–1923.

Terrault, N. A., Dodge, J. L., Murphy, E. L., Tavis, J. E., Kiss, A., Levin, T. R., Gish, R. G., Busch, M. P., Reingold, A. L. and Alter, M. J. (2013). Sexual transmission of hepatitis C virus among monogamous heterosexual couples: The HCV partners study. *Hepatology* **57**, 881–889.

Thibault, P. A. and Wilson, J. A. (2014). Transient replication of Hepatitis C Virus sub-genomic RNA in murine cell lines is enabled by miR-122 and varies with cell passage. *PLoS One* **9**, e89971.

Thimme, R., Oldach, D., Chang, K. M., Steiger, C., Ray, S. C. and Chisari, F. V (2001). Determinants of viral clearance and persistence during acute hepatitis C virus infection. *J. Exp. Med.* **194**, 1395–1406.

Thimme, R., Bukh, J., Spangenberg, H. C., Wieland, S., Pemberton, J., Steiger, C., Govindarajan, S., Purcell, R. H. and Chisari, F. V (2002). Viral and immunological determinants of hepatitis C virus clearance, persistence, and disease. *Proc. Natl. Acad. Sci.* **99**, 15661–15668.

Thomas, D. L. (2013). Global control of hepatitis C: where challenge meets opportunity. *Nat. Med.* **19**, 850–858.

Tilton, J. C., Luskin, M. R., Johnson, A. J., Manion, M., Hallahan, C. W., Metcalf, J. A., McLaughlin, M., Davey, R. T. and Connors, M. (2007). Changes in Paracrine Interleukin-2 Requirement, CCR7 Expression, Frequency, and Cytokine Secretion of Human Immunodeficiency Virus-Specific CD4+ T Cells Are a Consequence of Antigen Load. *J. ….*

Timm, J., Lauer, G. M., Kavanagh, D. G., Sheridan, I., Kim, A. Y., Lucas, M., Pillay, T., Ouchi, K., Reyor, L. L., zur Wiesch, J. S., Gandhi, R. T., Chung, R. T., Bhardwaj, N., Klenerman, P., Walker, B. D. and Allen, T. M. (2004). CD8 epitope escape and reversion in acute HCV infection. *J. Exp. Med.* **200**, 1593–1604.

Tobery, T. W. and Siliciano, R. F. (1997). Targeting of HIV-1 antigens for rapid intracellular degradation enhances cytotoxic T lymphocyte (CTL) recognition and the induction of de novo CTL responses in vivo after immunization. *J. Exp. Med.* **185**, 909–920.

Toebes, M., Coccoris, M., Bins, A., Rodenko, B., Gomez, R., Nieuwkoop, N. J., van de Kasteele, W., Rimmelzwaan, G. F., Haanen, J. B. A. G., Ovaa, H. and Schumacher, T. N. M. (2006). Design and use of conditional MHC class I ligands. *Nat. Med.* **12**, 246–251.

Tohme, R. A. and Holmberg, S. D. (2012). Transmission of Hepatitis C Virus Infection Through Tattooing and Piercing: A Critical Review. *Clin. Infect. Dis.* **54**, 1167–1178.

Topalian, S. L., Hodi, F. S., Brahmer, J. R., Gettinger, S. N., Smith, D. C., McDermott, D. F., Powderly, J. D., Carvajal, R. D., Sosman, J. A., Atkins, M. B., Leming, P. D., Spigel, D. R., Antonia, S. J., Horn, L., Drake, C. G., Pardoll, D. M., Chen, L., Sharfman, W. H., Anders, R. A., Taube, J. M., McMiller, T. L., Xu, H., Korman, A. J., Jure-Kunkel, M., Agrawal, S., McDonald, D., Kollia, G. D., Gupta, A., Wigginton, J. M. and Sznol, M. (2012). Safety, activity, and immune correlates of anti-PD-1 antibody in cancer. *N. Engl. J. Med.* **366**, 2443–2454.

Tortorella, D., Gewurz, B. E., Furman, M. H., Schust, D. J. and Ploegh, H. L. (2000). Viral subversion of the immune system. *Annu. Rev. Immunol.* **18**,

861–926.

Tricot, S., Meyrand, M., Sammicheli, C., Elhmouzi-Younes, J., Corneau, A., Bertholet, S., Malissen, M., Le Grand, R., Nuti, S., Luche, H. and Cosma, A. (2015). Evaluating the efficiency of isotope transmission for improved panel design and a comparison of the detection sensitivities of mass cytometer instruments. *Cytometry. A* **87**, 357–68.

Tsvetkov, P., Reuven, N. and Shaul, Y. (2009). Ubiquitin-independent p53 proteasomal degradation. *Cell Death Differ.* **17**, 103–108.

Urbani, S., Boni, C., Missale, G., Elia, G., Cavallo, C., Massari, M., Raimondo, G. and Ferrari, C. (2002). Virus-specific CD8+ lymphocytes share the same effector-memory phenotype but exhibit functional differences in acute hepatitis B and C. *J. Virol.* **76**, 12423–12434.

Urbani, S., Amadei, B., Fisicaro, P., Tola, D., Orlandini, A., Sacchelli, L., Mori, C., Missale, G. and Ferrari, C. (2006). Outcome of acute hepatitis C is related to virus-specific CD4 function and maturation of antiviral memory CD8 responses. *Hepatology* **44**, 126–139.

Utzschneider, D. T., Legat, A., Fuertes Marraco, S. A., Carrié, L., Luescher, I., Speiser, D. E. and Zehn, D. (2013). T cells maintain an exhausted phenotype after antigen withdrawal and population reexpansion. *Nat. Immunol.* **14**, 603–610.

Van Den Berg, C., Smit, C., Van Brussel, G., Coutinho, R. and Prins, M. (2007). Full participation in harm reduction programmes is associated with decreased risk for human immunodeficiency virus and hepatitis C virus: evidence from the Amsterdam Cohort Studies among drug users. *Addiction* **102**, 1454–1462.

Verstrepen, B. E., Depla, E., Rollier, C. S., Mares, G., Drexhage, J. A. R., Priem, S., Verschoor, E. J., Koopman, G., Granier, C., Dreux, M., Cosset, F.-L., Maertens, G. and Heeney, J. L. (2011). Clearance of genotype 1b hepatitis C virus in chimpanzees in the presence of vaccine-induced E1-neutralizing antibodies. *J. Infect. Dis.* **204**, 837–844.

Vidalin, O., Tanaka, E., Spengler, U., Trépo, C. and Inchauspé, G. (1999). Targeting of hepatitis C virus core protein for MHC I or MHC II presentation does not enhance induction of immune responses to DNA vaccination. *DNA Cell Biol.* **18**, 611–621.

Vignali, D. A. A., Collison, L. W. and Workman, C. J. (2008). How regulatory T cells work. *Nat. Rev. Immunol.* **8**, 523–532.

Viola, A. and Lanzavecchia, A. (1996). T cell activation determined by T cell receptor number and tunable thresholds. *Science (80-.).* **273**, 104–106.

von Delft, A., Humphreys, I. S., Brown, A., Pfafferott, K., Lucas, M., Klenerman, P., Lauer, G. M., Cox, A. L., Gaudieri, S. and Barnes, E. (2015). The broad assessment of HCV genotypes 1 and 3 antigenic targets reveals limited cross-reactivity with implications for vaccine design. *Gut* gutjnl–2014–308724.

von Hahn, T., Yoon, J. C., Alter, H., Rice, C. M., Rehermann, B., Balfe, P. and McKeating, J. A. (2007). Hepatitis C Virus Continuously Escapes From Neutralizing Antibody and T-Cell Responses During Chronic Infection In Vivo. *Gastroenterology* **132**, 667–678.

Voutsas, I. F., Gritzapis, A. D., Mahaira, L. G., Salagianni, M., von Hofe, E., Kallinteris, N. L. and Baxevanis, C. N. (2007). Induction of potent CD4(+) T cell-mediated antitumor responses by a helper HER-2/neu peptide linked to the Ii-Key moiety of the invariant chain. *Int. J. Cancer* **121**, 2031–2041.

Wahid, A. and Dubuisson, J. (2013). Virus-neutralizing antibodies to hepatitis C virus. *J. Viral Hepat.* **20**, 369–376.

Walker, C. M. and Grakoui, A. (2015). Hepatitis C virus: why do we need a vaccine to prevent a curable persistent infection? *Curr. Opin. Immunol.* **35**, 137–143.

Walters, K.-A., Syder, A. J., Lederer, S. L., Diamond, D. L., Paeper, B., Rice, C. M. and Katze, M. G. (2009). Genomic Analysis Reveals a Potential Role for Cell Cycle Perturbation in HCV-Mediated Apoptosis of Cultured Hepatocytes. *PLoS Pathog.* **5**, (1).

Wandeler, G., Gsponer, T., Bregenzer, A., Guenthard, H. F., Clerc, O., Calmy, A., Stoeckle, M., Bernasconi, E., Furrer, H., Rauch, A. and Study, S. H. I. V. C. (2012). Hepatitis C Virus Infections in the Swiss HIV Cohort Study: A Rapidly Evolving Epidemic. *Clin. Infect. Dis.* **55**, 1408–1416.

Ward, S. M., Fox, B. C., Brown, P. J., Worthington, J., Fox, S. B., Chapman, R. W., Fleming, K. A., Banham, A. H. and Klenerman, P. (2007). Quantification and localisation of FOXP3+ T lymphocytes and relation to hepatic inflammation during chronic HCV infection. *J. Hepatol.* **47**, 316–324.

Wedemeyer, H., He, X. S., Nascimbeni, M., Davis, A. R., Greenberg, H. B., Hoofnagle, J. H., Liang, T. J., Alter, H. and Rehermann, B. (2002). Impaired effector function of hepatitis C virus-specific CD8+ T cells in chronic hepatitis C virus infection. *J. Immunol.* **169**, 3447–3458.

Weinberger, E. E., Isakovic, A., Scheiblhofer, S., Ramsauer, C., Reiter, K., Hauser-Kronberger, C., Thalhamer, J. and Weiss, R. (2013). The influence of antigen targeting to sub-cellular compartments on the anti-allergic potential of a DNA vaccine. *Vaccine* **31**, 6113–6121.

Weng, N., Araki, Y. and Subedi, K. (2012). The molecular basis of the memory T

cell response: differential gene expression and its epigenetic regulation. *Nat. Rev. Immunol.* **12**, 306–315.

Wherry, E. J. (2011). T cell exhaustion. *Nat. Immunol.* **12**, 492–499.

Wherry, E. J. and Ahmed, R. (2004). Memory CD8 T-cell differentiation during viral infection. *J. Virol.* **78**, 5535–5545.

Wherry, E. J., Teichgräber, V., Becker, T. C., Masopust, D., Kaech, S. M., Antia, R., von Andrian, U. H. and Ahmed, R. (2003a). Lineage relationship and protective immunity of memory CD8 T cell subsets. *Nat. Immunol.* **4**, 225–234.

Wherry, E. J., Blattman, J. N., Murali-Krishna, K., van der Most, R. and Ahmed, R. (2003b). Viral persistence alters CD8 T-cell immunodominance and tissue distribution and results in distinct stages of functional impairment. *J. Virol.* **77**, 4911–4927.

Wherry, E. J., Blattman, J. N. and Ahmed, R. (2005). Low CD8 T-Cell Proliferative Potential and High Viral Load Limit the Effectiveness of Therapeutic Vaccination. *J. Virol.* **79**, 8960–8968.

White, B., Madden, A., Prins, M., Hellard, M., Wand, H., Dore, G. J., Page, K. and Maher, L. (2014). Assessing the feasibility of hepatitis C virus vaccine trials: results from the Hepatitis C Incidence and Transmission Study-community (HITS-c) vaccine preparedness study. *Vaccine* **32**, 5460–5467.

Willinger, T., Freeman, T., Hasegawa, H., McMichael, A. J. and Callan, M. F. C. (2005). Molecular signatures distinguish human central memory from effector memory CD8 T cell subsets. *J. Immunol.* **175**, 5895–5903.

Wölfl, M., Rutebemberwa, A., Mosbruger, T., Mao, Q., Li, H., Netski, D., Ray, S. C., Pardoll, D., Sidney, J., Sette, A., Allen, T., Kuntzen, T., Kavanagh, D. G., Kuball, J., Greenberg, P. D. and Cox, A. L. (2008). Hepatitis C virus immune escape via exploitation of a hole in the T cell repertoire. *J. Immunol.* **181**, 6435–6446.

Wüest, T., Both, G. W., Prince, A. M., Hofmann, C. and Löser, P. (2004). Recombinant ovine atadenovirus induces a strong and sustained T cell response against the hepatitis C virus NS3 antigen in mice. *Vaccine* **22**, 2717–2721.

Xu, X., Chen, H., Cao, X. and Ben, K. (2007). Efficient infection of tree shrew (Tupaia belangeri) with hepatitis C virus grown in cell culture or from patient plasma. *J. Gen. Virol.* **88**, 2504–12.

Yamaguchi, N., Tokushige, K., Yamauchi, K. and Hayashi, N. (2000). Humoral immune response in Japanese acute hepatitis patients with hepatitis C virus infection. *Can. J. Gastroenterol.* **14**, 593–598.

Ye, L., Liu, X., Rout, S. N., Li, Z., Yan, Y., Lu, L., Kamala, T., Nanda, N. K., Song, W., Samal, S. K. and Zhu, X. (2008). The MHC class II-associated invariant chain interacts with the neonatal Fc gamma receptor and modulates its trafficking to endosomal/lysosomal compartments. *J. Immunol.* **181**, 2572–2585.

Youil, R., Toner, T. J., Su, Q., Chen, M., Tang, A., Bett, A. J. and Casimiro, D. (2002). Hexon gene switch strategy for the generation of chimeric recombinant adenovirus. *Hum. Gene Ther.* **13**, 311–320.

Yu, N., Li, X., Song, W., Li, D., Yu, D., Zeng, X., Li, M., Leng, X. and Li, X. (2012). CD4(+)CD25(+)CD127(low/-) T Cells: A More Specific Treg Population in Human Peripheral Blood. *Inflammation* **35**, 1773–1780.

Zabaleta, A., D'Avola, D., Echeverria, I., Llopiz, D., Silva, L., Villanueva, L., Riezu-Boj, J. I., Larrea, E., Pereboev, A., Lasarte, J. J., Rodriguez-Lago, I., Iñarrairaegui, M., Sangro, B., Prieto, J. and Sarobe, P. (2015). Clinical testing of a dendritic cell targeted therapeutic vaccine in patients with chronic hepatitis C virus infection. *Mol. Ther. Methods Clin. Dev.* **2**, 15006.

Zajac, A. J., Blattman, J. N., Murali-Krishna, K., Sourdive, D. J., Suresh, M., Altman, J. D. and Ahmed, R. (1998). Viral immune evasion due to persistence of activated T cells without effector function. *J. Exp. Med.* **188**, 2205–2213.

Zak, D. E., Andersen-Nissen, E., Peterson, E. R., Sato, A., Hamilton, M. K., Borgerding, J., Krishnamurty, A. T., Chang, J. T., Adams, D. J., Hensley, T. R., Salter, A. I., Morgan, C. A., Duerr, A. C., De Rosa, S. C., Aderem, A. and McElrath, M. J. (2012). Merck Ad5/HIV induces broad innate immune activation that predicts $CD8^+$ T-cell responses but is attenuated by preexisting Ad5 immunity. *Proc. Natl. Acad. Sci. U. S. A.* **109**, E3503–12.

Zhang, X., Dou, J. and Germann, M. W. (2009). Characterization of the cellular immune response in hepatitis C virus infection. *Med. Res. Rev.* **29**, 843–866.

Zheng, H., Jin, B., Henrickson, S. E., Perelson, A. S., von Andrian, U. H. and Chakraborty, A. K. (2008). How Antigen Quantity and Quality Determine T-Cell Decisions in Lymphoid Tissue. *Mol. Cell. Biol.* **28**, 4040–4051.

Zinkernagel, R. M. and Hengartner, H. (2006). Protective "immunity" by pre-existent neutralizing antibody titers and preactivated T cells but not by so-called "immunological memory". *Immunol. Rev.* **211**, 310–319.

Zuckerman, J. N. (2006). Protective efficacy, immunotherapeutic potential, and safety of hepatitis B vaccines. *J. Med. Virol.* **78**, 169–177.

Zwart, W., Peperzak, V., de Vries, E., Keller, A. M., van der Horst, G., Veraar, E. A. M., Geumann, U., Janssen, H., Janssen, L., Naik, S. H., Neefjes, J. and

Borst, J. (2010). The invariant chain transports TNF family member CD70 to MHC class II compartments in dendritic cells. *J. Cell Sci.* **123**, 3817–3827.